ibvt
Institut für Bioverfahrenstechnik

Technische Universität Braunschweig

Band 76
ibvt-Schriftenreihe

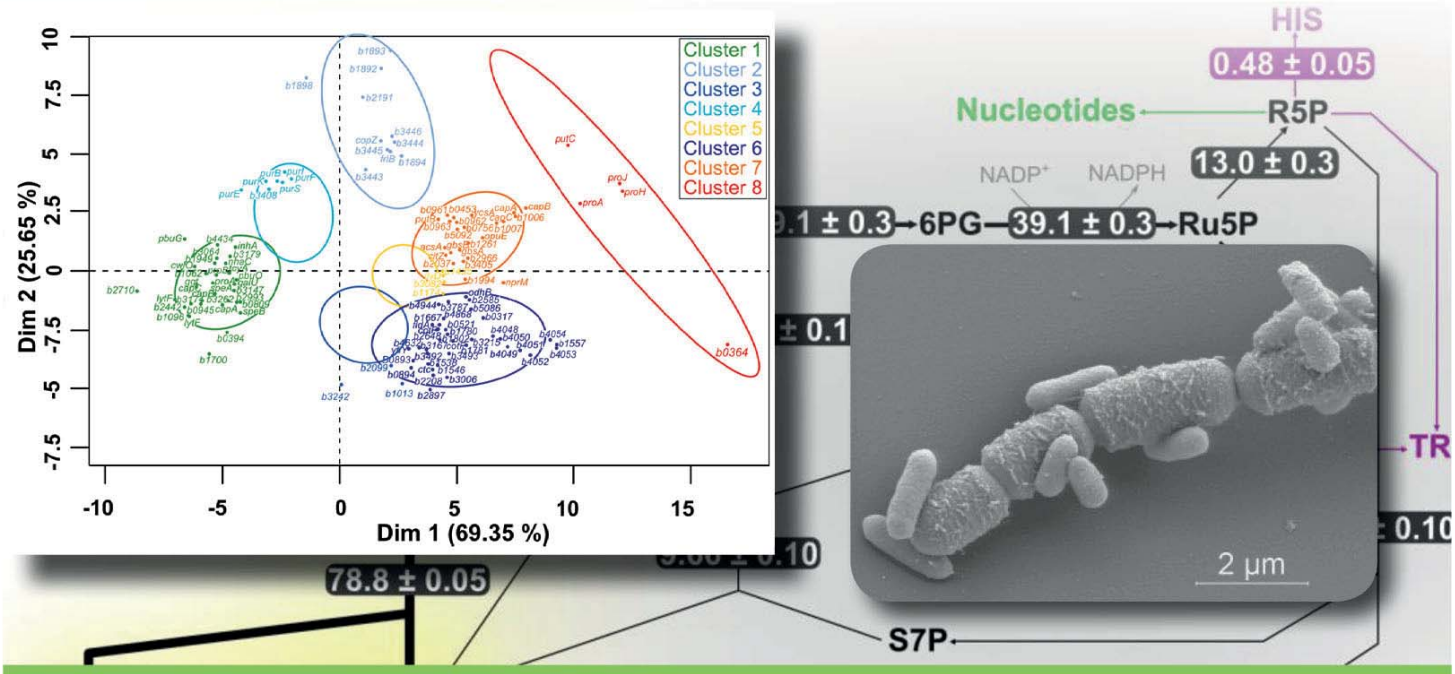


# Systems biology of stress in *Bacillus megaterium* and its potential applications

**Thibault Godard**

Cuvillier-Verlag

**ibvt-Schriftenreihe**
Schriftenreihe des Institutes für Bioverfahrenstechnik
der Technischen Universität Braunschweig

Herausgegeben von Prof. Dr. Rainer Krull

Band 76

**Cuvillier-Verlag**
**Göttingen, Deutschland**

Herausgeber
Prof. Dr. Rainer Krull
Institut für Bioverfahrenstechnik
TU Braunschweig
Rebenring 56, 38106 Braunschweig
www.ibvt.de

**Hinweis**: Obgleich alle Anstrengungen unternommen wurden, um richtige und aktuelle Angaben in diesem Werk zum Ausdruck zu bringen, übernehmen weder der Herausgeber, noch der Autor oder andere an der Arbeit beteiligten Personen eine Verantwortung für fehlerhafte Angaben oder deren Folgen. Eventuelle Berichtigungen können erst in der nächsten Auflage berücksichtigt werden.

**Bibliographische Informationen der Deutschen Nationalbibliothek**
Die Deutsche Nationalbibliothek verzeichnet diese Publikation in der Deutschen Nationalbibliographie; detaillierte bibliographische Daten sind im Internet über *http://dnb.d-nb.de* abrufbar.
1. Aufl. – Göttingen: Cuvillier, 2016


Nonnenstieg 8, 37075 Göttingen
Telefon: 0551-54724-0
Telefax: 0551-54724-21
www.cuvillier.de



1. Auflage, 2016
Gedruckt auf säurefreiem Papier

ISBN 978-3-7369-9336-5
eISBN 978-3-7369-8336-6
ISSN 1431-7230

# Systems biology of stress in *Bacillus megaterium* and its potential applications

Bei der Fakultät für Maschinenbau

der Technischen Universität Carolo-Wilhelmina zu Braunschweig

zur Erlangung der Würde eines Doktor-Ingenieurs (Dr.-Ing.)

eingereichte Dissertation

von Herrn Dipl.-Ing. Thibault Godard

aus Creil - Frankreich

eingereicht am: 19.06.2015

mündliche Prüfung am: 24.09.2015

Prüfungsvorsitzender: Prof. Dr. Georg Garnweitner

1. Referent: Prof. Dr. Rainer Krull

2. Referent: Prof. Dr. Dieter Jahn

## Danksagung

Bei der Anfertigung dieser Arbeit am Institut für Bioverfahrenstechnik der TU Braunschweig haben mich eine Vielzahl von Personen unterstützt und somit das Zusammentragen der nötigen experimentellen Daten ermöglicht. Bei meinem Doktorvater Prof. Dr. Rainer Krull möchte ich mich für die Übernahme des Referats und sein fachliches Interesse an meiner Arbeit bedanken. Herrn Prof. Dr. Dieter Jahn und Prof. Dr. Georg Garnweitner danke ich für die Übernahme des Korreferats und die Bereitschaft zur Übernahme des Prüfungsvorsitzes. Bei Herrn Prof. Dr. Christoph Wittmann bedanke ich mich für die Überlassung des Themas, die Betreuung in den ersten Jahren und die Möglichkeit mit der Universität Namur über ein zweites Projekt zu kooperieren.

Mein besonderer Dank gilt Dr. Rebekka Biedendieck vom Institut für Mikrobiologie der TU Braunschweig für ihre Hilfe bei der Durchführung und Auswertung der Microarrays, ihre stets gute Laune und Ansprechbarkeit aber vor allem für ihre aktive Betreuung meiner Promotion bis zur Ziellinie. Danke für das ausführliche Korrekturlesen und die vielen wissenschaftlichen und weniger fachlichen Diskussionen. Deine persönlichen Ratschläge haben mich in schwierigen Zeiten mit Energie aufgepumpt und genug Gründe geliefert, diese Arbeit zu Ende zu bringen. Ebenso möchte ich mich bei meinem “Osmo-Partner”, Dr. Michael Kohlstedt, für die sinnvollen Vorschläge bei der Planung und Auswertung meiner Experimente sowie für sein stets offenes Ohr und die zahlreichen Ratschläge fürs Leben bedanken. Unsere französischen Plaudereien und die Ausflüge mit den anderen Doppeldiplomanden werde ich in Erinnerung behalten.

Bei allen Mitarbeitern des Instituts bedanke ich mich für die tolle Arbeitsatmosphäre, die lustigen Party- und Laborerlebnisse sowie für die Unterstützung bei der Durchführung meiner Experimente. Besonderen Dank möchte ich hier an Dr. Claudia Korneli ausprechen für die Einführung in die Welt der Biotechnologie und die konstruktive Zusammenarbeit während meiner Diplomarbeit. Ohne dich hätte ich mich sicherlich nicht für eine Promotion in diesem Wissenschaftsbereich entschieden. Besonders danken möchte ich auch Rudolf Schäfer, Georg Richter und Dr. André Luis Rodrigues für ihre Hilfe bei dem Sampling und der Messung von intrazellulären Metaboliten. Danke für eure Zeit und euren Enthusiasmus! Ihr habt eindeutig zu dem Erfolg dieser Arbeit beigetragen. Bei meinen Bürokolleginnen, Dr. Sarah Schiefelbein und Katrin Bartsch, möchte ich mich ebenso für die stets angenehme Büroatmosphäre, die fachlichen aber manchmal auch sinnlosen Diskussionen bedanken. Die schöne Zeit mit euch im Büro werde ich im Gedächtnis behalten.

Ebenfalls möchte ich mich ganz herzlich bei meinen Bachelor-Studenten Melanie Wall, Thilo Duensing und Mauro Torres bedanken. Vielen Dank für euer Engagement! Es hat mir Spaß gemacht mit euch im Labor zu arbeiten und eure Ergebnisse haben diese Arbeit maßgeblich bereichert.

Außerhalb der Technischen Universität Braunschweig haben auch andere Personen zu meiner wissenschaftlichen Weiterentwicklung beigetragen. Ein großer Dank gilt insbesondere Dr. Daniela Zühlke vom Institut für Mikrobiologie der Ernst-Moritz-Arndt-Universität Greifswald für ihre Hilfe bei

der Vermessung der Proteomproben und ihre Zeit zur Beantwortung aller meiner technischen Fragen. Bei Dr. Thibault Barbier vom Institut für Mikrobiologie und Molekularbiologie der Universität Namur möchte ich mich ebenso für die gute Zusammenarbeit und die interessanten Gespräche im Rahmen unserer Kooperation über die Aufklärung des Zusammenhangs zwischen Pathogenität und Metabolismus von *Brucella* spp. bedanken.

Für die finanzielle Unterstützung im Rahmen des Sonderforschungsbereichs SFB 578 „*Vom Gen zu Produkt*" bedanke ich mich ganz herzlich bei der Deutschen Forschungsgemeinschaft (DFG).

Zuletzt möchte ich mich noch bei meiner Familie und meinen Freunden bedanken. Ihr habt nicht immer verstanden, warum ich mich für die Promotion entschieden habe aber habt mich trotzdem auf diesem langen Weg unterstützt, selbst wenn das Ende oftmals in weiter Ferne schien. Es tut mir leid, dass mich manche während der letzten Jahre nicht so oft zu Gesicht bekommen haben, aber die wenigen Augenblicke, die wir zusammen verbracht haben, haben für die notwendige Ablenkung gesorgt und mir die Kraft zum Weitermachen gegeben.

Thibault Godard Braunschweig, im September 2015

# Publications

Partial results of this work have been published in advance. This was authorized by the Department of Mechanical Engineering of the Technische Universität Braunschweig, Institute of Biochemical Engineering represented by Prof. Dr. habil. Rainer Krull.

### Peer-reviewed Journals

Korneli C., David F., **Godard T.**, Franco-Lara E. (2011) - Influence of fructose and oxygen gradients on fed-batch recombinant protein production using *Bacillus megaterium*. Eng. Life Sci. 11:338-349.

Korneli C., Bolten C.J., **Godard T.**, Franco-Lara E., Wittmann, C. (2012) - Debottlenecking recombinant protein production in *Bacillus megaterium* under large scale conditions - targeted precursor feeding designed from metabolomics. Biotechnol. Bioeng. 109:1538-1550.

Barbier T., Collard F., Zungia-Ripa A., Moriyon I., **Godard T.**, Becker J., Wittmann C., van Schaftingen E., Letesson JJ. (2014) - Erythritol feeds the pentose phosphate pathway via three new isomerases leading to D-erythrose-4-phosphate in *Brucella*. Proc. Nat. Acad. Sci. 111(50) : 17815-17820.

### Conference contributions

Korneli C., **Godard T.**, Franco-Lara E. (2010) Kulturheterogenität von *Bacillus megaterium* ist eine Funktion der angewandten Fed-Batch-Strategie. Vortrags- und Diskussionstagung „Bioprozessorientiertes Anlagedesign“, 10. – 12. Mai, Nürnberg, Germany.

Korneli C., Bolten C.J., **Godard T.**, Franco-Lara E., Wittmann C. (2011) Recombinant protein production by *Bacillus megaterium* – Overcoming transient substrate limitation by targeted precursor feeding. Annual Meeting of the VAAM, 03. – 06. April, Karlsruhe, Germany.

**Godard, T.**, Torres, M., Wall, M., Zühlke D., Riedel K., Rohde M., Wittmann C, Jahn D., Biedendieck R. (2014) System-wide analysis of stress-adaptation in *Bacillus megaterium* and its applications. Annual Meeting of the VAAM, 05. – 08. October, Dresden, Germany.

**Godard, T.**, Wall, M., Zühlke D., Riedel K., Jahn D., Biedendieck R. (2014) Systems biology of osmoadaptation in *Bacillus megaterium* and its potential applications - Proceedings of the BRICS forum, 17-18. März, Braunschweig, Germany.

## Summary

For many years now, *Bacillus megaterium* has been successfully developed as a host for production, secretion and purification of recombinant proteins. The g/L-scale for intra- as well as for extracellular recombinant products has already been reached. Generally, once a producer has been genetically designed, optimal process parameters are established to maximise its potential for industrial production. Despite this upstream work, bacterial cells are constantly exposed to various kinds of stress during the whole production process, including e.g. mechanical induced stress, high nutrient or product concentrations and variations of temperature, medium composition or oxygen availability. To date, the impact of these conditions on cellular activity is only slightly understood but the recent development of systems biology now provides precious tools for characterising cellular behaviour of stressed cells.

In this context, the main objective of this work was to investigate more deeply the impact of harsh cultivation temperatures (between 15 and 45°C) and osmotic stress (mimicked using up to 1.8 M NaCl) on the metabolism of the wild-type *B. megaterium* DSM319 during unlimited growth. To this end, a holistic study including transcriptome, proteome, metabolome and fluxome analyses was performed. After analysing the data from each of these techniques separately, they were combined together to offer an integrated picture of cellular adaptation and to find underlying genetic targets for the development of more robust production hosts.

Interestingly, while both stress conditions resulted in disruption of redox balance, decreased biomass yields and reduced substrate uptake rates, the flux distribution within the central carbon and energy metabolism as well as the levels of the corresponding mRNAs and proteins were only locally affected. On the contrary, significant modulation of metabolite pools was observed and might constitute a key mechanism to compensate for loss of enzyme activity and maintain or adjust metabolic fluxes under stressful conditions. In addition, specific responses occurring at every biological level were detected in both cases. In particular, exposure at high and low temperature triggered the production of so-called heat and cold shock proteins, respectively, whose functions support sustained growth under these adverse conditions. Under ionic osmotic stress, on the other hand, the whole metabolic machinery was reorganised towards production of the osmoprotectant proline using an alternative pathway only active under this condition. Notably, relative fluxes through the pentose phosphate pathway and tricarboxylic acid cycle were increased to provide the indispensable precursors NADPH and glutamate, respectively.

More surprisingly, although *B. megaterium* has long been known for its capacity to produce the biopolymer polyhydroxybutyric acid (PHB), a positive correlation between intracellular PHB content and salt concentration could be demonstrated for the first time. As neither the concentration of the enzymes involved in the classical PHB-pathway nor that of their related mRNAs significantly increased, these proteins were systematically overproduced in new plasmid strains, resulting in an up to 75 % higher PHB content. Finally, *in silico* modelling using elementary flux mode analysis was applied and highlighted new genetic targets for the further improvement of PHB production in *B. megaterium*

.

## Zusammenfassung

*Bacillus megaterium* wird bereits seit mehreren Jahren als bakterieller Wirt für die Produktion, Sekretion und Reinigung von rekombinanten Proteinen erfolgreich eingesetzt. Mittlerweile ist der g/L-Maßstab für intra- sowie extrazelluläre rekombinante Produkte erreicht. Nach der gentechnischen Entwicklung eines neuen bakteriellen Produktionssystems werden in der Regel optimale Kultivierungsbedingungen ermittelt, um die bestmögliche Ausbeute zu erreichen. Dabei können jedoch Stressbedingungen wie z.B. mechanisch induzierte Beanspruchung, hohe Substrat- oder Produktkonzentrationen sowie Schwankungen der Sauerstoffverfügbarkeit, Mediumtemperatur und -zusammensetzung entstehen, die sich nicht vermeiden lassen und die Produktivität herabsetzen.
In diesem Zusammenhang bestand das Hauptziel dieser Arbeit darin, die Auswirkungen von unterschiedlichen Temperaturen zwischen 15 und 45°C und von osmotischem Stress (bis 1.8 M NaCl) auf den Metabolismus von *B. megaterium* DSM319 während des exponentiellen Wachstums zu untersuchen. Zu diesem Zweck wurden im Rahmen eines ganzheitlichen Ansatzes Transkriptom-, Proteom-, Metabolom- sowie Fluxomanalysen durchgeführt. Zunächst wurden die Datensätze der Omics-Techniken einzeln statistisch analysiert und anschließend zusammengeführt, um so ein gesamtes Bild des Adaptationsprozesses wiedergeben und mögliche genetische Targets für die Entwicklung stressbeständigerer Produktionsbakterien identifizieren zu können.
Während beide Stressbedingungen zur Beeinträchtigung des Redox-Zustandes und Verminderung der Biomasseausbeute und Substrataufnahmerate führten, blieben im Zentralstoffwechsel sowohl die Flussverteilung als auch die entsprechende Genexpression zum Großteil unbeeinflusst. Im Gegensatz dazu wurde eine stressbedingte Veränderung der Metabolitkonzentrationen beobachtet, die dem Organismus wahrscheinlich eine energiesparende Lösung bietet, um den Aktivitätsverlust von Enzymen auszugleichen und metabolische Flüsse aufrechtzuerhalten oder strategisch anzupassen. Zusätzlich wurden spezifische Stressantworten ausgelöst, die auf jeder einzelnen untersuchten biologischen Ebene erkennbar waren. Insbesondere wurde bei extremen Temperaturen die Produktion von sogenannten „heat shock“- und „cold shock“-Proteinen verstärkt, die die Aufrecherhaltung des Wachstums unter diesen widrigen Bedingungen ermöglichen. Unter osmotischem Stress wurde dagegen der komplette Stoffwechsel umgestellt, sodass ausreichende Mengen des kompatiblen Soluts Prolin produziert werden konnten. Dies gelang unter anderem durch die Aktivierung eines osmo-spezifischen Prolin-Synthesewegs und die Steigerung der relativen Flüsse durch den Pentose-Phosphat-Weg und den Zitratzyklus zur Bereitstellung der notwendigen Vorläufer Glutamat und NADPH.
Obwohl die Fähigkeit von *B. megaterium* zur Produktion des Biopolymers Polyhydroxybuttersäure (PHB) lange bekannt ist, zeigten die hier vorgestellten Ergebnisse zum ersten Mal eine positive Korrelation zwischen steigender Salzkonzentration und intrazellulärem PHB-Gehalt. Die Konzentrationen von Transkripten und Proteinen, die an der PHB-Synthese beteiligt sind, änderten sich hingegen kaum mit steigendem Salzgehalt. So wurden die Proteine PhaA, PhaB, PhaC, PhaR und PhaP in Plasmidstämmen systematisch überproduziert, wodurch die PHB-Produktion um bis zu 75 % gesteigert wurde. Schließlich konnten unter Einsatz eines Modellierungstools neue genetische Targets für die Weiteroptimierung dieser Produktion aufgedeckt werden.

# Table of contents

# 1 Introduction and aim of the study

*Bacillus megaterium* is a rod-shaped Gram-positive soil bacterium, which was first discovered in 1884 by Anton de Bary [1, 2]. It got its name from the Greek “megatherium” for “big beast” because of its enormous size of up to 2.5 x 2.5 x 10 µm$^3$ (**Fig. 1.1**). Within the bacterial kingdom, these remarkable dimensions have propelled it to model organism of choice for single-cell analysis and investigation of cell structures and protein localisation [3, 4]. Cell wall synthesis, sporulation, bacteriophages and biochemistry of Gram-positive bacteria have been, for instance, widely studied using *B. megaterium* [5-8]. Besides its main natural habitat, the soil, its proficiency to metabolise a large range of carbon sources and its high osmotic tolerance has enabled *B. megaterium* to colonise varied ecological niches such as sea, industrial wastewaters and food products like honey or dry meat. This versatility and its ability to produce a large range of industrially relevant products have progressively made it an essential bacterial cell factory.

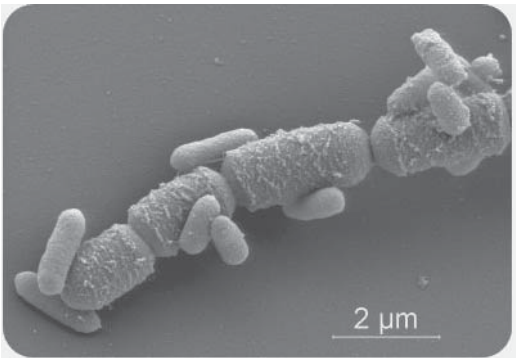


**Figure 1.1: Scanning electronic microscope (SEM) pictures of *B. megaterium* (2.5 x 2.5 x 10 µm$^3$) and *E. coli* (0.5 x 0.5 x 2 µm$^3$)** (M. Rohde; Helmholtz-Zentrum für Infektionsforschung GmbH, Braunschweig, 2006).

A decisive step towards the widespread use of *B. megaterium* in the industry is undoubtedly the introduction and development of a xylose inducible promoter system for heterologous plasmid-based protein production by Rygus and Hillen (**Fig. 1.2**) [9]. The natural system consists of the genes *xylA*, *xylB* and *xylT* encoding xylose isomerase, xylulokinase and xylose permease, respectively [10]. Divergently to these genes, the gene *xylR* encodes the repressor XylR regulated by $P_{xylA}$. In the absence of xylose, the repressor binds the operator regions $O_L$ and $O_R$ of the promoter $P_{xylA}$ and transcription of all genes downstream cannot be initiated. On the contrary, upon addition of xylose, the repressor protein XylR binds the xylose, undergoes a conformational modification and can no longer bind the operator regions. As a consequence, RNA-polymerase mediated transcription of the *xyl*-operon is derepressed and increased by 150 times in comparison to the inhibited state. Apart from this main control system, two additional mechanisms regulate the expression of the xylose operon when glucose is present. On the one hand, glucose enhances the binding affinity of the catabolite control protein A (CcpA) for the catabolite repression DNA-element *cre* located in the gene *xylA* and thereby hinders the proper transcription of the whole operon. On

the other hand, assimilation of extracellular glucose generates significant intracellular amounts of its phosphorylated counterpart glucose-6-monophosphate, which can outcompete xylose in binding repressor protein XylR and thus prevent operon transcription. Overall, these two mechanisms account for a 14 times lower transcription level in the presence of glucose. The catabolite responsive element was therefore subsequently removed on the corresponding vector system to obtained a system suited for recombinant protein production using glucose as carbon source and xylose as inducer [11]. Later, further optimisation of the promoter, the ribosome-binding site and untranslated 5' mRNA region (5'UTR) resulted in an up to 12-fold improvement of the system global efficiency [12].

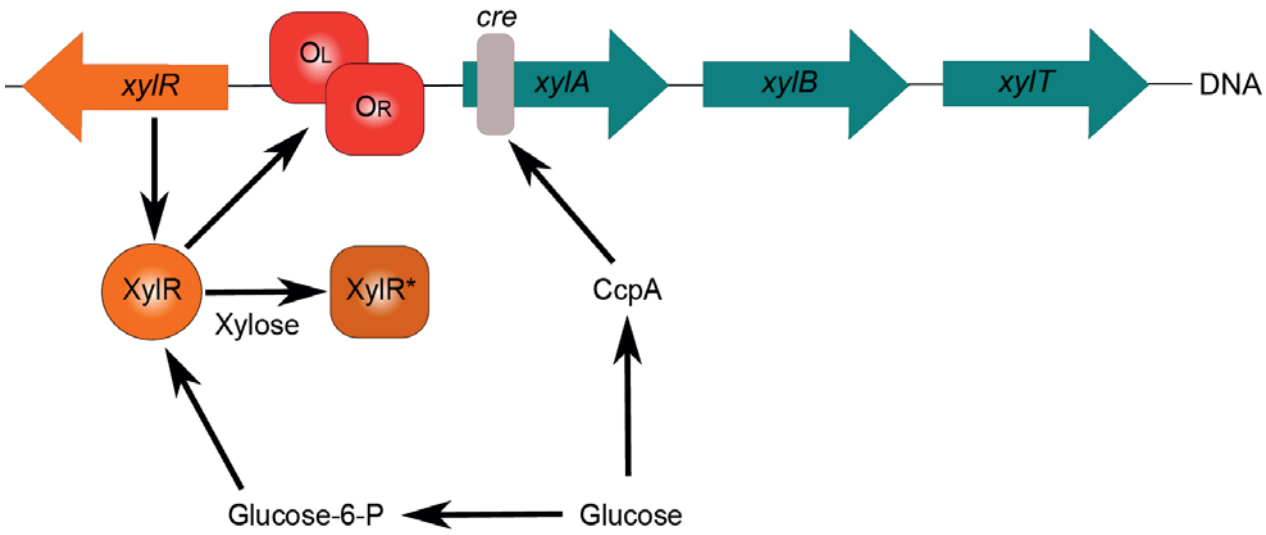


**Figure 1.2: Regulation of the xylose-operon in *B. megaterium* – CcpA**: catabolite control protein A, ***cre***: catabolite response element, **$O_L$/$O_R$**: operator region of the xyl-promoter, ***xylA***: xylose isomerase gene, ***xylB***: xylulokinase gene, ***xylR***: xylose repressor gene, **XylR**: active xylose repressor protein, **XylR***: inactive xylose repressor protein

In addition to its stable plasmid replication system, *B. megaterium* presents several other advantages in comparison with traditional industrial workhorses such as *Escherichia coli* or *Bacillus subtilis*. Firstly, it exhibits a high secretion capacity combined with the lack of an outer membrane [13]. So secreted products can directly be collected from the supernatant. Secondly, whereas several alkaline proteases are produced by *B. subtilis*, none of them were found in *B. megaterium* and produced exoenzymes accordingly show a remarkable stability [14]. Thirdly, the lack of endotoxins in *B. megaterium* and its non-pathogen status makes it an ideal production host for pharmaceutical and food applications, for which safety issues often impose expensive downstream processing otherwise.

At first, only unaltered wild-type strains were used for the production of a limited number of compounds comprising vitamin $B_{12}$, α- and β-amylases, xylanase, penicillin G acylase and polyhydroxybutyrate (PHB) but the introduction of the plasmid-based expression system has widen the product spectrum to varied recombinant proteins and sophisticated compounds such as

antibody fragments, glycosyltransferase (levansucrase, dextransucrase) and the green fluorescent protein (GFP). The latter being a particularly useful model protein for assessing the promoter efficiency or for monitoring the impact of process parameters on recombinant production [15, 16].

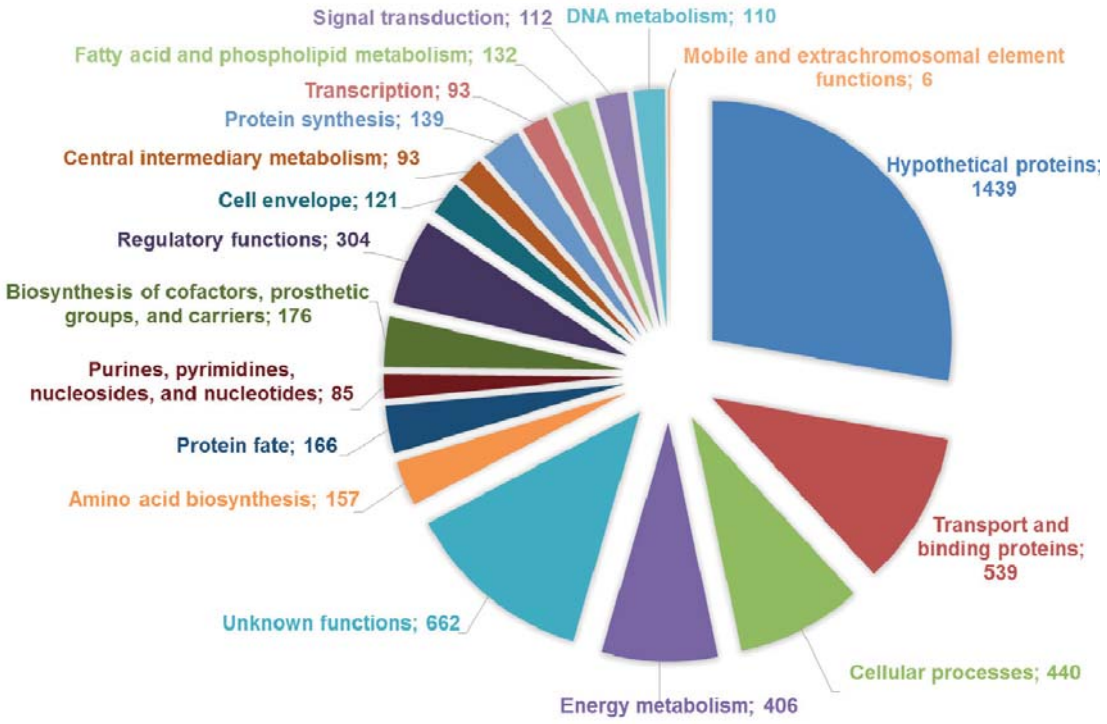


**Figure 1.3: Classification of genes from *B. megaterium* DSM319 into TIGR role categories –** Functions were attributed according to the sequencing of its complete genome by Eppinger et al. [17].

Recently, the sequencing of the complete genome of three different strains and the fast development of dedicated omics-techniques have furthermore laid the foundations for an in-depth understanding of its metabolic behaviour and opened up new possibilities towards its rational genetic modification (**Fig. 1.3**) [17-20]. This system-wide approach should in term enable the elucidation of all metabolic and regulatory steps involved in the production of a given substance and predict subtle targets for metabolic engineering.

This study takes place in this context of continual improvement of *B. megaterium* as a production host and was set out to get a better comprehension of its metabolic behaviour and of regulatory mechanisms involved in response to two industrially relevant issues, namely temperature and osmotic stress. Taking advantage of the recent technical developments of systems biology, system-wide response to these two adverse conditions shall be assessed for the first time in this organism in a multi-omics study including transcriptome, proteome, metabolome and fluxome analyses. For the latter, condition-specific macromolecular biomass compositions shall be determined and corresponding precursor demands integrated in a brand new model. Results obtained from the different omics-techniques shall then be analysed separately, combined together and with gathered physiological data to provide a functional understanding of metabolic adaptation of cells responding to temperature (between 15 and 45°C) and osmotic stress (mimicked with up to

1.8 M NaCl). Finally, potential genetic targets shall be identified using generated data sets and implemented to further optimise robustness and production characteristics of *B. megaterium*.

# 2 Theoretical background

## 2.1 Systems biology and omics technologies

### 2.1.1 Systems biology and its recent development

Life is a complex, multifaceted and evolutive process involving sophisticated and fascinating mechanisms such as tissue regeneration, immune response or thermal homeostasis. It is unfortunately an imperfect one as well, in which dysfunctions such as cell degeneration, hormonal disorders or memory loss may occur. In recent years, it has become obvious that no matter how meaningful the breakthroughs within the single fields of biology are, they will never be able to address this complexity and provide viable healthcare solutions if considered separately. Of course, it is in the first place of crucial importance to know of which biological components (genes, proteins, transcripts, metabolites, pathways) a living organism disposes and what the possible interactions between them are. However, since life is not static, it is even more important to unravel global regulation networks orchestrating those interactions *in vivo* and defining how biological components actually function together as a whole. From these considerations, systems biology emerged as a science willing to remodel the classical and segmented approach of biology into a highly interdisciplinary and informational one, where interaction and control dynamics between single biological layers would also be assessed (**Fig. 2.1**).

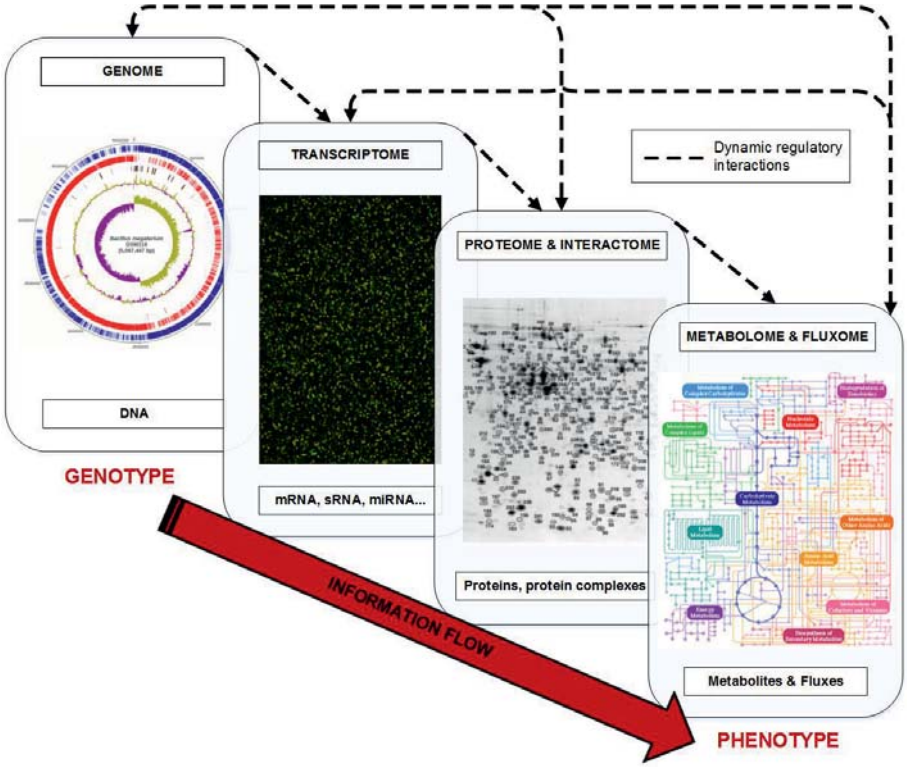


**Figure 2.1: Architecture of cellular systems and interactions among the different functional layers –** Dashed lines represent dynamic regulatory interactions between molecular species. Figure was adapted from [21] and [22].

Such a functional and system-wide comprehension was only made conceivable by the parallel fast development of high-throughput omics-technologies and advanced computational methods, which enabled the acquisition and processing of large amounts of experimental data. Indeed, to comprehend the global regulation of biological structures, systems biology systematically perturb organisms in various ways and records their reaction at different organisational levels, including gene expression and protein production, modification of metabolite pools and pathway utilisation. Collected data are afterwards integrated in global *in silico* models containing all known and hypothesised regulatory systems and contribute to their iterative refining by corroborating or rejecting initial model assumptions. As the generated data and underlying biological interplays are far too substantial and complex for human brains to deal with, computers arise progressively as the cornerstone of this new approach. They provide scientists with numerous databases indexing uncovered metabolic pathways, genetic information and interaction patterns but also with simulation tools able to confirm, discard or even suggest hypothesis that would otherwise not necessary be apparent to human beings [23]. Moreover, they are intensively employed in effective experimental design, thereby avoiding irrelevant analysis and reducing laboratory efforts needed to address specific issues. Another critical turning point for the boom of systems biology was the rapid development of automated and standardized genetic tools achieved within the framework of the human genome project (HGP), paving the way to fast sequencing, systematic gene deletion, insertion and mutagenesis [24]. After that, systems' perturbation could be performed not only by changing abiotic conditions but also through targeted modification of organisms' intrinsic capabilities and scientists could easily manipulate organisms to resolve specific regulatory pathways.

Although systems biology has already extended our knowledge of cell function and physiology in many ways, several barriers still prevent it from reaching its full potential. Firstly, measurement accuracy and coverage of actual devices remain insufficient to supply enough information for the complete determination of metabolic and regulatory properties of cellular systems. Development of even more efficient computational methods could partly compensate this problem but further technical advancements are inevitable. Secondly, the access to high-throughput and computational technologies is still limited due to their price and/or the level of expertise their operation requires. As institutes are usually specialized in only one or two domains, they cannot perform a system-wide analysis alone. Hence, the creation of solid research networks regrouping teams with complementary skills seems to be a prerequisite to widen the actual scope of systems biology. Lastly, no efficient pooling of collected omics-data has been implemented so far and information exchange between researchers at a global level is not trivial. Overcoming these challenges depends to a large extent on breakthroughs in other area such as computer science, biochemical engineering, physics or chemistry. Thus, systems biology arises as a strong driving force for scientific innovation.

In spite of still being in its infancy, systems biology has proven to be a promising area of research with a broad range of applications in both academic and industrial fields. Far beyond the single

understanding of life and its evolution, unravelling regulatory mechanisms gives us the keys to predict how genetic manipulations and induced metabolic interferences will affect phenotypes. Consequently, in the future, systems biology will undoubtedly play a central role in developing more effective therapeutic treatments with minimal side effects or also in improving bacterial cell factories. These new industrial workhorses will no longer be generated by random mutagenesis but rather rationally designed to be less stress-sensitive and less inclined to unnecessary by-products secretion, revolutionizing our common conception of bioprocess design in which production process must be adapted to bacteria and not the opposite [25, 26].

### 2.1.2 Genomics and Transcriptomics

Thanks to the fast progress of sequencing techniques achieved over the last three decades, genomes can now easily, swiftly and cheaply be sequenced. With more than a new bacterial genome completely sequenced every month, biological research has moved to a post-genomic era, where the gathered genetic information has to be organised into functional structures to depict the global dynamics of living cells [27, 28]. In this context, the identification and quantification of the complete set of transcripts present in a cell under given physiological conditions, referred to as transcriptomics, has proved to be a powerful approach to gain new insights into gene functionality and their regulation [29]. Historically, gene expression has first been locally analysed using Northern blot, where RNA transcripts from samples are first separated by electrophoresis and subsequently hybridised with labelled complementary probes [30]. Later, the discovery of reverse transcriptase, which converts mRNA into its complementary DNA (cDNA), has enabled the development of real-time reverse transcription polymerase chain reaction (qRT-PCR), the most sensitive technique presently available for quantifying RNA [31, 32]. However, qRT-PCR is a gene-specific procedure and monitoring gene expression levels at the genome scale with this technique would require a great deal of time and effort.

On the contrary, DNA microarray, a technology developed approximately thirty years ago, offers a straightforward and reliable way to identify and quantify the expression levels of a hundred thousand of genes simultaneously [33, 34]. To this end, DNA probes specific to parts of every single gene sequence of the investigated organism are either mechanically deposited or in-situ synthesised in the grid cells of a glass, plastic or nylon chip [35]. In parallel, RNA transcripts from given samples are purified, directly labelled or reverse-transcribed to their more stable cDNAs and labelled afterwards with fluorescent dyes. Subsequently, these labelled cDNA transcripts are hybridised to their DNA counterparts immobilised on the surface of the chip. After removing unbound transcripts by washing the array slide, labelled strands are excited using dye-specific wavelengths. The light emitted from each grid spot is captured in a scanner by a photo-multiplier tube (PMT) and converted into a digital image [36]. After algorithmic post-processing of this image including grid alignment for gene identification, spot characterisation (size, intensity, quality and outlier removal), background correction and intensity normalisation, the expression of a given gene is obtained from its corresponding spot intensities. Most of the time, microarray analyses are used

for direct comparison of gene expression between two samples (experimental vs. reference) and carried out as double-channel experiments, meaning that transcripts originated from samples are labelled with distinctive dyes (e.g. cyanines cy3 and cy5), hybridised on the same chip and their relative expression levels obtained by scanning the array at two wavelengths (e.g. red and green for cy3 and cy5, respectively) (**Fig. 2.2**) [37]. Since it is cheaper and does not need to be corrected for batch effects, this approach is often preferred to single-channel experiments, for which samples to compare are hybridised separately on two arrays using a single dye. However, if numerous samples need to be compared and thus the use of different microarrays is inevitable, single-channel experiments can be preferred to prevent aberrant samples from contaminating data derived from others and to get rid of eventual dye-related artefacts. It is therefore essential to choose the most appropriate experimental design with respect to the addressed biological issue to maximise the output of the analysis [34]. In this respect, it is also of outmost importance to define the number and nature of replicates needed to reach statistical relevance. While technical replicates tend to become superfluous as technology progresses, at least 3 to 5 biological replicates should be used for cDNA microarrays [38-40].

After completion of the microarray experiments, a tremendous quantity of information is available and the main challenge for researchers is to make sense out of these data. First, measured expression levels are normalised using either internal standards or statistical parameters such as standard deviation, mean and median values inter and intra arrays to improve comparability of microarrays [41]. To facilitate pattern discovery, data complexity is then drastically reduced by applying statistical filters that only retain genes whose regulation is significantly modified under the evaluated conditions. Typically, a cut-off value for gene expression is arbitrarily set and the pertinence of the resulting candidate selection is statistically assessed using various tests such as Student or Welch's t-tests, analysis of variance (ANOVA) and the false discovery rate (FDR) [42-46]. Finally, once the significance of the data is established, different clustering algorithms (hierarchical, k-means, SOM) can be applied to regroup genes with similar behaviours and unravel new regulation patterns [27, 47]. Alternatively, principal component analysis (PCA) can also be performed to reduce the dimension of the data set and classify genes according to their coordinates in a simpler system retaining the characteristic variability of the original data set [48]. Afterwards, presumed candidates highlighted from transcriptome analysis must be further validated both technically by qRT-PCR and functionally using reverse genetics, i.e. observing the effects of targeted gene deletion, overexpression or point mutation on the final phenotype [49-51].

Despite being a very powerful technology, microarrays, just like other hybridisation techniques, presents some drawbacks and do not capture the entire complexity of the transcriptome. First, DNA probes may be subject to cross-hybridisation with transcripts presenting sequences similar to the targeted one, thus affecting signal reliability [52]. Second, the abundance measurement is relative and its dynamic range is inherently limited upwards by signal saturation and downwards by background noise, reaching at most a hundred fold [53].

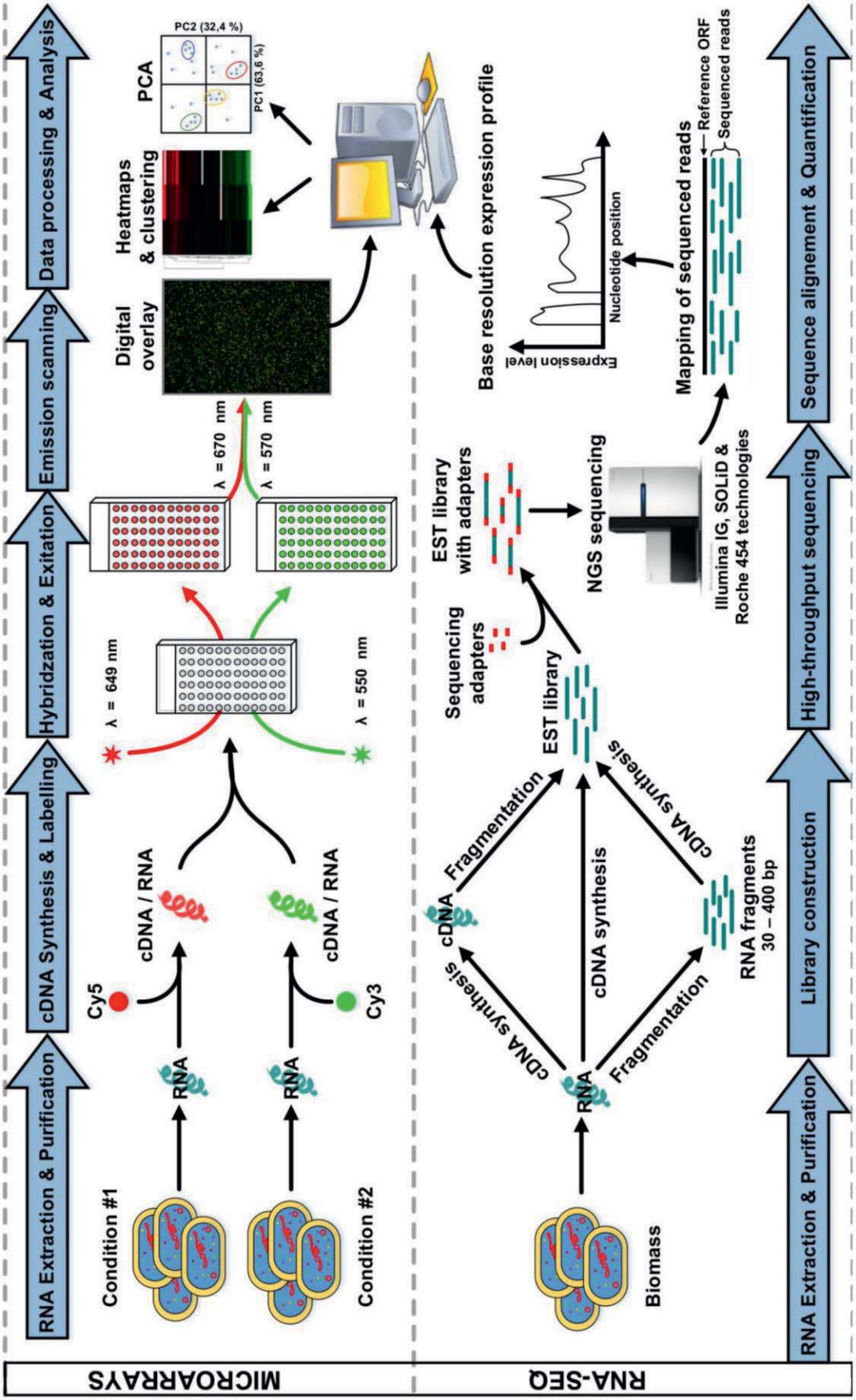


**Figure 2.2: Analytical workflows for microarray- and RNA-seq-based transcriptome analysis** – Central steps in microarray analysis include labelling of RNA extracted from two samples or of the corresponding cDNA with different cyanides, mixing and hybridisation of labelled samples on a designed array, excitation at dye-specific wavelengths and, finally, scanning of the array (upper part). For RNA-seq, an EST library is constructed by fragmentation and absolute transcript quantification is performed by high-throughput sequencing using next-generation sequencers (lower part). Regardless of the applied technique, generated data are post-processed using statistical methods such as analysis of variance, setting of cut-off values, principal component analysis (PCA) or hierarchical clustering to identify significant regulation. **cDNA**: complementary DNA; **Cy**: Cyanide; **EST**: expression sequence tag; **NGS**: Next-generation sequencing; **PCA**: principal component analysis. Figure was adapted from [53].

Furthermore, this technology relies on the knowledge of the genome under investigation and is therefore not generally applicable to non-model organisms. Even though many efforts have been devoted to increase the number and specificity of DNA probes, account for cross-hybridisation via mismatch probes and correction models or resolve labelling effects, saturation problems and alternative intramolecular folding, the future of transcriptome analysis might be somewhere else [54-58].

In fact, RNA-seq, a recently developed high-throughput technology based on next generation sequencing techniques, overcomes most of these limitations and is predicted to outperform microarray technology in the coming years [53, 59, 60]. To put it briefly, RNA samples are first cleared from abundant interfering ribosomal RNA, converted into their double-stranded complementary DNA (cDNA) and subsequently fragmented into small reads (30-400 bp) with DNase I [61]. Finally, those reads are ligatured with amplification adapters and massively parallel sequenced for absolute quantification and identification through mapping onto the reference genome if available (Fig. 2.2). There are ensuing benefits in terms of transcripts identification and quantification. First of all, the sequencing procedure enables the detection and characterisation of both known and unknown sequences with a single base accuracy and consequently single nucleotide polymorphisms as well as transcription boundaries and connections between exons can be resolved [53, 62]. Of particular interest is the possibility to study biological functions of intra- and intergenic non-coding RNA or particular transcription features such as directionality and allelic expression [61, 63]. From a technical point of view, this method is moreover less inclined to batch variation or background noise and the resulting reproducibility, sensitivity and dynamic range are therefore much greater than for microarrays, covering accurately expression levels up to 8000 fold [53, 64, 65]. Hence, RNA-seq is a very promising technology for uncovering complete transcriptomes but it currently still suffers a lack of hindsight compared to microarrays. So existing technical limitations or bias will probably only become clear as this technique spreads widely throughout scientific community.

### 2.1.3 Proteomics

Although transcriptome analysis gives a detailed and comprehensive overview of gene expression under given environmental conditions, detected mRNA transcripts are only intermediates between genes and proteins. On the contrary, proteins undertake the majority of cellular functions from catalysis to gene regulation, including nucleotides and amino acid recycling, signal transduction and structure stabilisation. Because of post-transcriptional regulations and protease activity, their concentrations can hardly be inferred from their transcript levels and must be assessed directly using dedicated methods and equipment [66, 67].

Proteomics deals with this specific issue and aims first and foremost at developing new analytical and computational techniques to detect, identify and quantify the whole set of proteins in a given sample, namely its proteome [68]. However, the scope of proteomics is much wider and also

includes the identification of post-translational modifications (PTM) and the detailed characterisation of protein localisation, interactions and structures that are essential to fully comprehend their biological functions [69, 70]. Although the field is still developing quickly, well-established approaches using various separation and quantification techniques are presently available and have been recently reviewed in detail [71, 72]. Historically, proteins were first separated according to their molar mass (MM) and isoelectric point (pI) by 1D/2D-sodium dodecyl sulfate (SDS)-polyacrylamide gel electrophoresis, subsequently stained with varied dyes, quantified using digital imaging and finally identified by GC-MS (**Fig. 2.3**) [73, 74]. This classical workflow is still well-suited for differential proteomics, the comparison of two protein samples, in particular after the development of difference gel electrophoresis (DIGE). In this method, proteins from two samples to compare are separately stained with two distinct cyanine-based dyes, then mixed and separated on a single gel, overcoming thereby the problem of gel variability inherent to the comparison of classical SDS-polyacrylamide gels [75, 76]. Despite great improvements of gel resolution through optimisation of buffer systems and gel compositions, this approach only enables a coverage of up to 50 % of the whole proteome, thus remaining inappropriate for global proteomics [77]. Indeed, only the more abundant non-hydrophobic proteins can be properly extracted from gels, whereas those presenting low natural abundances ($10^3$ – $10^4$) cannot even be detected [69, 78]. Moreover, proteins with extreme pI (> 11 or < 3) or MM (> 200 kDa or < 10 kDa) can hardly be separated and conversely other proteins produce multiple spots or trains because of PTMs, making the subsequent identification and quantification difficult, if not impossible. Lastly, involved staining dyes and solvents for solubilisation of membrane proteins are often incompatible with GC-MS-measurements [71]. For these reasons, the use of off-gel chromatographic separation techniques and MS-based quantification methods have grown in importance in modern proteomics, whereas gel electrophoresis is mainly applied as a pre-fractionation step to reduce the degree of complexity of protein or peptide solutions to analyse.

Since the creation of the first mass spectrometer by Aston in 1919, a lot of progress has been made and soft ionisation methods such as matrix-assisted laser desorption/ionisation (MALDI) and electrospray ionization (ESI) have enabled the measurement of intact proteins and peptides [79, 80]. However, the direct analysis of undamaged proteins or so called “top-down” strategy still requires high experimental efforts and the measurement of their constitutive peptides, namely the “bottom-up” strategy, remains in practice the method of choice for protein identification [81]. Here, protein samples are first enzymatically digested with a sequence-specific endoprotease like trypsin and resulting peptides are separated and fragmented in various ways in mass spectrometers (selected (SRM) or multiple (MRM) reaction monitoring) (Fig. 2.3). Their characteristic MS-fragmentation patterns are then used to identify the corresponding proteins and their eventual PTMs by comparing with theoretical mass spectra stored in databases (Fig. 2.3). Hence, this approach requires both high resolution mass spectrometers capable of performing exact mass determination over a wide dynamic range and powerful computational tools able to reconstruct proteins from their basic peptides.

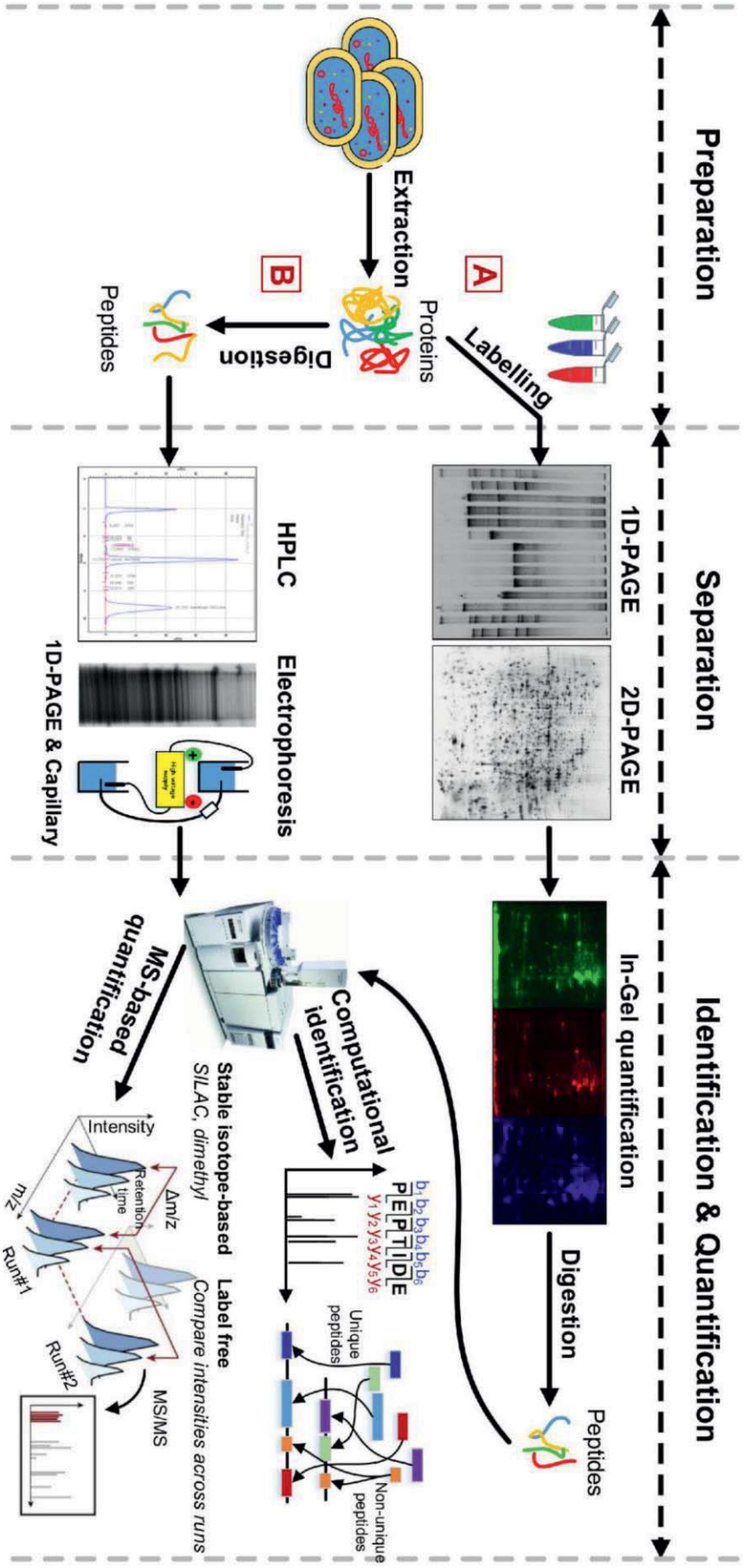


**Figure 2.3: Analytical workflow for protein- (A) and peptide-based (B) proteomics** – In the protein-based approach, extracted proteins are stained with different dyes for each sample, separated by gel electrophoresis and resulting colour intensities enable relative quantification. When used dyes are compatible, proteins can subsequently be extracted from gel, digested and submitted to GC-MS for identification. For peptide-based proteomics, proteins are first digested to peptides which are subsequently separated by HPLC or electrophoresis and finally identified and quantified by GC-MS using computational methods. Figure adapted from [1] and [3].

In addition to protein identification, the ongoing improvements of MS-proteomics and computational methods have now enabled their relative and absolute quantification on the basis of their peptide mass spectra. For relative quantification, the typical strategy relies on distinctive isotope tagging of proteins or peptides to compare. Indeed, as labelling does not affect physical properties, labelled and unlabelled peptides will be separated, ionised and fragmented in exactly the same way.
However, in the final MS-spectrum, the mass shift caused by the labelling will enable peptide differentiation. The labelling can be integrated directly into peptides or proteins by numerous chemical and enzymatic reactions (isobaric tag for relative and absolute quantitation (iTRAQ), isotope-coded affinity tag (ICAT), isotope-coded protein label (ICPL), enzyme mediated oxygen substitution (EMOS), acid mediated oxygen substitution (AMOS)) or, alternatively, it can be incorporated during growth on isotopically enriched medium ($^{13}C$, $^{15}N$) or medium containing amino acid isotopes (stable isotope labelling by amino acids in cell culture (SILAC)) [82-84].
In most cases, this technique remains costly and label-free techniques based on algorithmic calculations have therefore gained interest in the past decades. They correlate protein quantity either with the intensity of mass spectra or with the number of peptides sequenced for a given protein (spectral counting). At the moment, these techniques are still limited in term of accuracy and mobilised great computational efforts. Nevertheless, with the development of effective algorithms to deconvolute and normalise MS spectra, they will undoubtedly become privileged methods in the future. Absolute quantification of proteins requires the use of internal standards (labelled or not) that are incorporated whether prior to or after protein digestion. Most of the time, the standard is a labelled version of the protein to quantify (protein standard for absolute quantification (PSAQ)) or a labelled peptide originating from this protein (absolute quantification of proteins (AQUA)) [85, 86]. Since the chemical synthesis of labelled proteins or peptides is very expensive, these techniques are often restricted to a small number of proteins in the framework of a targeted proteome analysis. To overcome this limitation, the QconCAT approach design a chimeric gene encoding selected signature peptides of all proteins to quantify and concatenating them into an artificial labelled protein. The purified chimeric protein is finally added to samples and enzymatic digestion generates automatically the labelled standard peptides necessary for absolute quantification [87-89].

### 2.1.4 Metabolomics

Since their introduction, genomic, transcriptomic and proteomic technologies have been successfully associated to gain new insights into the functional behaviour of biological systems [90-95]. This combination, however, has also rapidly started to show its limits and investigation of metabolites emerges as an essential counterpart to bridge the gap between genome and phenotype [96]. In fact, sequenced genome usually comprises 30-40% of genes encoding proteins with unknown functions or whose function was automatically attributed according to structural similarities, regardless of the potential biochemical significance of slight architectural differences [17, 97]. Moreover, whereas metabolite pools greatly depends on enzyme concentrations [98, 99], variations

in cell transcriptome and proteome do not necessary lead to altered phenotype, suggesting the existence of higher and post-translational regulation mechanisms [100-102]. As metabolites are further down the line from genome to phenotype and the connection nodes of all anabolic and catabolic reactions, their investigation arises quite naturally as the next step towards uncovering new gene functions, interactions, metabolic pathways and regulatory systems.

All metabolites synthesised by an organism under given physiological conditions constitute its metabolome [103]. Depending on the organism, it can encompass up to 200,000 metabolites varying significantly in their chemical nature and concentrations (from pM to mM) [104]. This diversity promises to be a very rich source of information but also makes the simultaneous identification and quantification of all metabolites, referred to as metabolomics, one of the biggest challenges of modern biochemistry. Indeed, no adequate measurement and sampling procedure have been developed so far to adequately recover and quantify the whole metabolome. Instead, modern techniques combining separation by gas (GC) or liquid chromatography (LC) with detection using mass spectrometry (MS), nuclear magnetic resonance (NMR) or infrared spectrometry (IR) have been employed for specific purposes, namely metabolite fingerprinting, target analysis and profiling (**Fig. 2.4**) [105, 106].

Metabolite fingerprinting aims at clustering different samples without quantifying, identifying or even separating metabolites, but only by using their characteristic measurement spectrum as discriminatory criterion. In clinical diagnosis, it is a systematic method for processing many samples and rapidly differentiating between healthy and diseased patient afterwards [107, 108]. Metabolite target analysis, for its part, is restricted to a small group of known compounds related to a given gene or specifically affected by a given abiotic perturbation. For this approach, metabolites of interest are extracted from samples using highly selective preparation and separation techniques.

Finally, metabolic profiling intends to identify and quantify different sets of defined metabolites such as amino acids, carbohydrates or those involved in a specific pathway in order to apprehend its function. This approach is often applied in pharmacology to trace the fate of administrated drugs and understand their effects. Thus, the current techniques are either too selective or not specific enough to reach a temporal separation of all metabolites. To extend the number of metabolites detected, composite metabolite profiling, a new approach involving simultaneous measurement of sample fractions with different systems, has been introduced. However, the additional spatial separation comes at a cost and the impact of other critical issues such as sample storage, measurement drift, matrix effects, sampling procedure and metabolite extraction on the subsequent quantification remains furthermore uncharacterised, underlining the need for suitable data normalisation methods [109]. The scope of metabolomics is huge and goes far beyond the single understanding of life. Indeed, unravelling functions of orphan genes or understanding interactions between metabolites and other biological components would for sure reveal new therapeutic targets and promising drugs. Moreover, the pharmaceutical industry is always on the lookout for new biomarker metabolites that make the spotting of health conditions easier. In addition, in the food industry, there is a growing interest for the discovery of new bioactive molecules and their incorporation in our everyday diet for promoting health and preventing diseases (functional food).

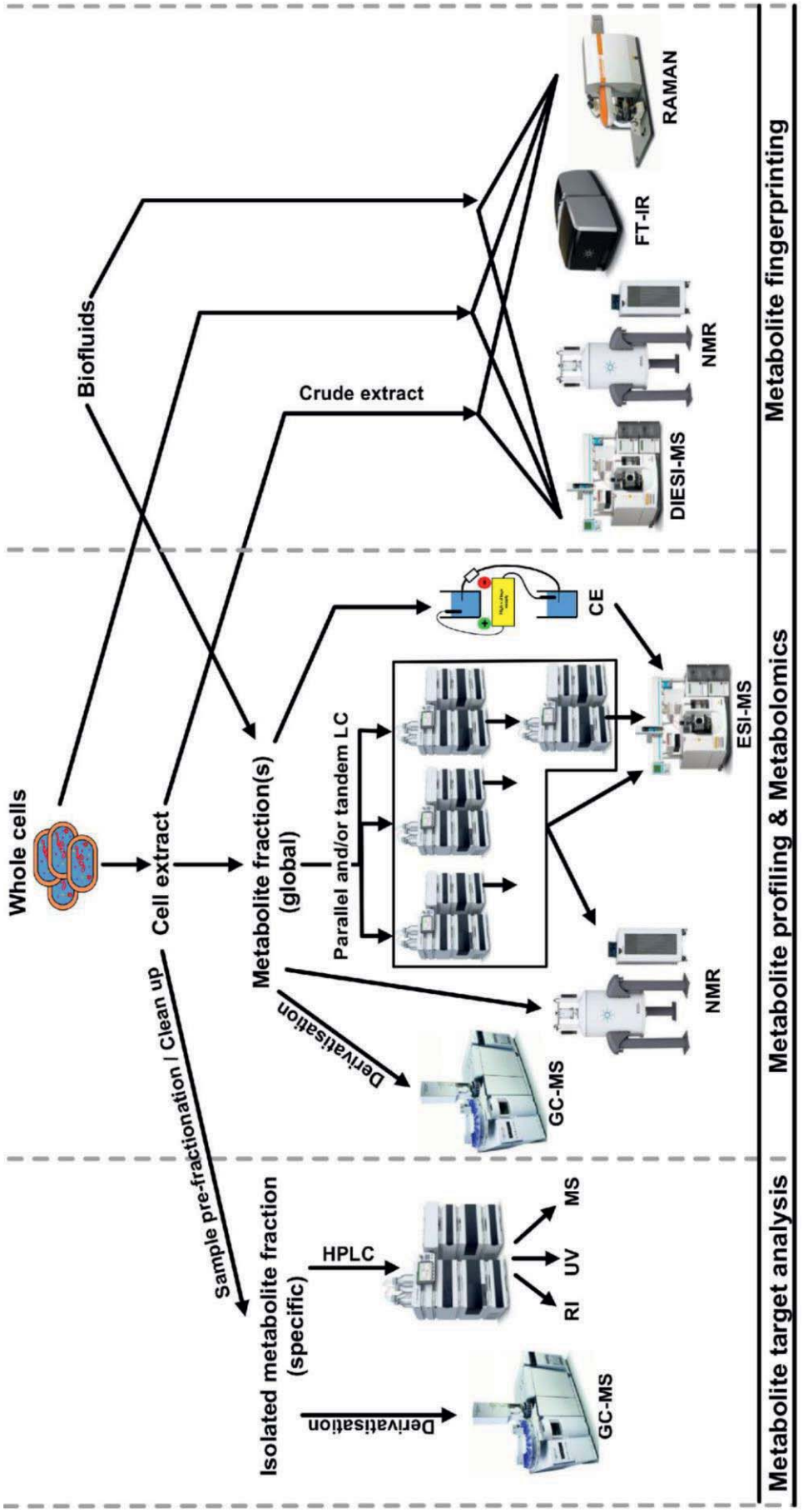


**Figure 2.4: General strategies for metabolome analysis** – Depending on the intended goal different approaches and equipments are used. Metabolite target analysis is focused on the quantification of a small and very specific group of known metabolites. Metabolite profiling aims at identifying and quantifying different sets of metabolites to unravel their metabolic function. Finally, metabolite fingerprinting only aims at clustering samples without identifying or quantifying metabolites by finding characteristic features in their measurement spectra. **CE**: capillary electrophoresis, **DIESI**: direct-infusion electron spray ionisation, **ESI**: electron spray ionisation, **FT-IR**: Fourrier transform infrared spectrometry, **GC**: Gas chromatography, **HPLC**: High-performance liquid chromatography **MS**: mass spectrometry **NMR**: nuclear magnetic resonance **RAMAN**: Raman spectroscopy **RI**: refraction index detection, **UV**: ultraviolet detection. Figure adapted from [110].

### 2.1.5 Fluxomics

In the course of cellular activity, metabolites are constantly converted into others through complex and nested pathways, resulting ultimately in energy and biomass production. The final output of all nonlinear regulatory and metabolic interactions between genome, proteome, transcriptome and metabolome is metabolic fluxes (i.e. biochemical conversion rates) through those different pathways. As such, these fluxes characterise global cell physiology and observed phenotype. In fact, whereas fluxome - all metabolic fluxes - depicts directly system dynamics, other omics-data gave the necessary backdrop to understand this final outcome. This complementarity of fluxomics with other omics-techniques to fully portray the complexity of regulatory interactions and quantify post-transcriptional and post-translational effects has been underlined in recent studies, which interestingly revealed severe discrepancies between actual flux distribution and predictions based on transcriptome and metabolome data [111-113].

Since metabolic fluxes are time-dependent variables, they cannot be quantified directly. Instead, they must be inferred from measurable quantities or physical properties using mathematical models based on stoichiometry, mass balance, thermodynamic, enzyme kinetic or isotopic labelling. Among actual techniques, flux balance analysis (FBA) and $^{13}C$ metabolic flux analysis ($^{13}C$-MFA) clearly stand out by their exhaustive characterisation and widespread use [114]. Given the stoichiometry of metabolic reactions, the early developed FBA method enables the estimation of intracellular fluxes in large user-defined metabolic networks (over 1000 reactions) solely from known biosynthetic requirements and extracellular fluxes (uptake and production rates). As such models are fundamentally underdetermined, several additional assumptions on thermodynamic, gene regulation and energy balance are made to narrow down feasible solutions [115, 116]. Fluxes are furthermore calculated to meet a given objective function, e.g. maximal product or biomass formation. Hence, FBA rather estimates optimal flux distribution for a given performance than actually determines *in vivo* flux distribution and its output relevance depends considerably on the correctness of formulated hypotheses. Moreover, the lack of information about intracellular activity prevents FBA from solving biologically relevant parallel and cyclic reactions. Nevertheless, it was successfully applied to predict biomass and production yields, growth rates, and lethal or profitable gene deletion in various microorganisms [117-119].

To overcome FBA limitations and rigorously evaluate *in vivo* flux distribution, a new working framework was offered by $^{13}C$-MFA [120, 121]. In this approach, microorganisms are fed with $^{13}C$-labelled substrates and labelled atoms are progressively incorporated into newly synthesised metabolites as the carbon source gets metabolised. Depending on the tracer chosen and the biosynthetic routes taken, $^{13}C$-atoms are found at different positions of metabolite backbones, resulting in various positional isotopic isomers (isotopomers). Once steady-state is reached, metabolite pools and their final isotopomer distribution are stable and characteristic of a unique flux distribution. For eight key intermediates of the central carbon metabolism (CCM), this final labelling pattern can be derived from either mass spectrometry (MS) or nuclear magnetic resonance (NMR) measurements of about 10-15 proteinogenic amino acids collected from hydrolysed biomass (**Fig. 2.5**).

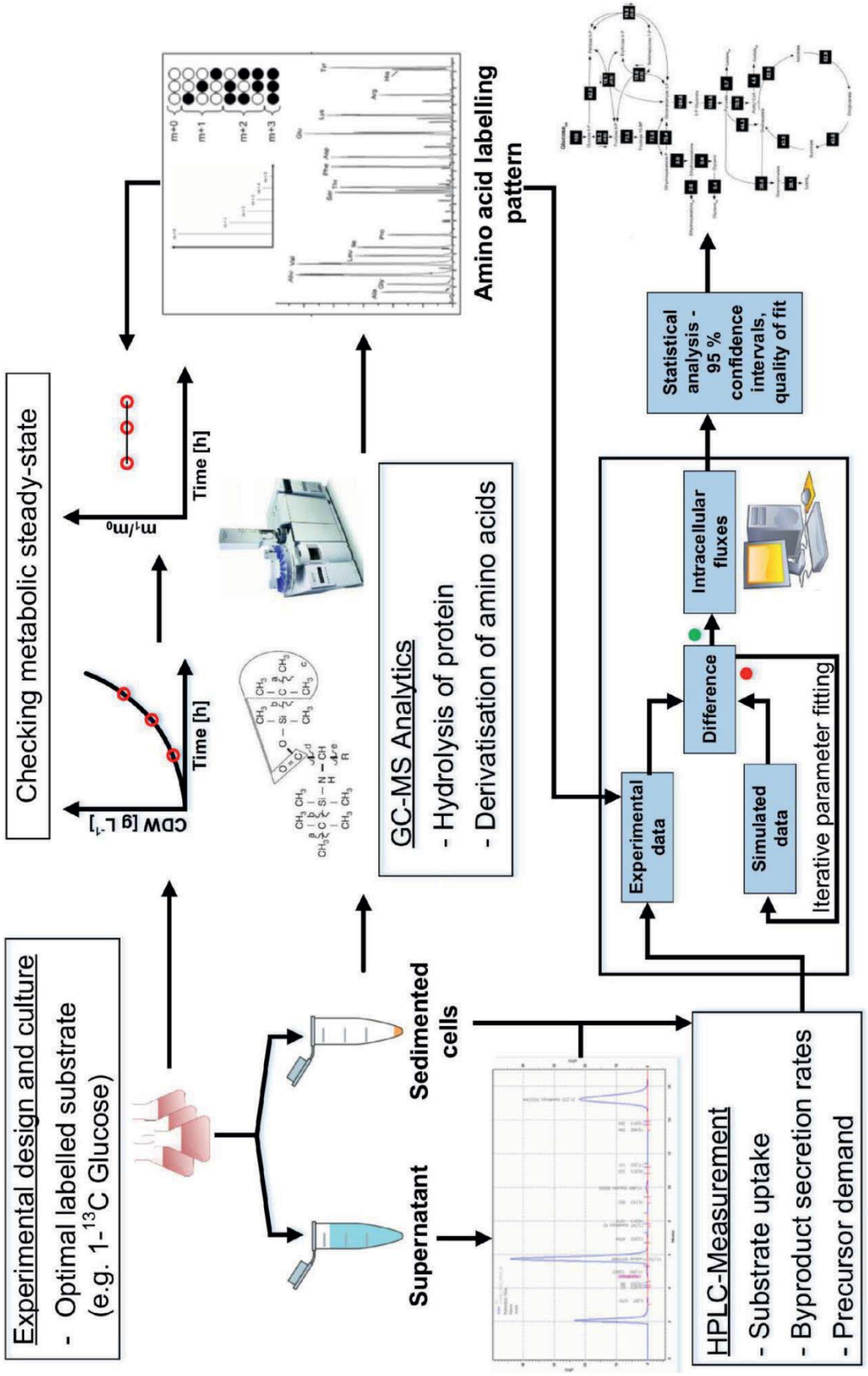


**Figure 2.5: Analytical workflow for metabolic flux analysis (MFA)** – Typical workflow for $^{13}C$ MFA includes (1) the choice of a labelled substrate suited for solving a given flux problem, (2) tracer experiments with this substrate, (3) measurement of resulting $^{13}C$ labelling patterns of amino acid, extracellular fluxes and biosynthetic requirements and (4) computational calculation of fluxes using an *in silico* model representing the studied network and integrating all these data. Figure adapted from [122].

Whereas NMR measurement presents the advantage to detect the exact position of incorporated labelled atoms (positional isotopomers), MS measurement can only distinguish isotopomers according to their mass (mass isotopomers) and must afterwards be coupled with computational methods to resolve flux partitioning. However, thanks to its far higher sensitivity and practicability, MS is applied more often for flux analysis in research. As data gained from both techniques are complementary, they should ideally be combined together whenever possible to refine flux calculation. For absolute flux calculation, obtained isotopic data are incorporated in *in silico* models listing all reactions with corresponding carbon atom transition and containing biosynthetic precursor demand and extracellular fluxes. Computational flux estimation relies on an iterative fitting procedure whereby free fluxes are varied until the deviation between simulated and measured isotopomer distributions satisfies a set minimisation criterion [123] (Fig. 2.5). Moreover, most software tools also incorporate additional algorithms to assess afterwards the statistical relevance and robustness of resulting fluxes and can be used to compare different network topologies [124-126]. As the goodness of fit greatly depends on the adequacy of the chosen substrate for solving a specific reaction network, other design tools have been developed in parallel in order to optimise the $^{13}$C-tracer used [127]. Nonetheless, the applicability of $^{13}$C-MFA is still confined to small systems of 50-100 reactions and thus mostly restricted to calculation of fluxes within the CCM. Alternatively, specific $^{13}$C-labelling data can be used to perform metabolic flux ratio (METAFoR) analysis, which, regardless of physiological activity, locally investigate the relative contribution of converging pathways to the labelling observed in a particular metabolite. Though this method is restricted to the resolution of 10-15 flux ratios of the CCM, the determined flux ratios can be used as additional constraints in other MFA approaches to calculate absolute fluxes in bigger reaction networks [128, 129].

A prerequisite for both FBA and $^{13}$C-MFA calculations is the existence of a metabolic and isotopic steady-state and the temporal stability of flux distribution [130]. In the nature, microorganisms must constantly cope with quickly changing conditions, adjusting their metabolism accordingly and alternating between growth and non-growth periods [131]. To adequately describe this dynamical behaviour and extend metabolic flux analysis to non-stationary systems and non-growing cells, two alternatives have recently been proposed. In the first, labelling information is directly obtained from intermediary metabolites, which in contrast to their derived amino acids reach isotopic steady-state within a few minutes due to their small pool sizes and high turnover rate [132]. For the second, time-dependent metabolite pool sizes and labelling patterns must be monitored during the first minute following perturbation and fluxes are subsequently calculated by solving a system of differential equations [133-135]. Both methods are very promising but technical progress is still needed to increase measurement coverage, develop rapid sampling procedures and algorithms requiring less computational effort for solving complex differential equations systems [136]. Complementary to these approaches, metabolic control analysis (MCA) evaluates how variations in enzyme concentration and activity affect flux intensity and distribution, thus providing an effective tool to understand dynamic adaptation and find key or limiting enzymes of specific pathways [137, 138].

Although some improvements are required, metabolic flux analysis can already be considered as a mature technique. Still, until now, it has been greatly undervalued and under-utilised in both research and industry in contrast to other omics approaches [21]. Indeed, its actual scope has been mostly restricted to verifying afterwards the benefits of introduced genetic modifications, while it should on the contrary participate actively to the upstream genetic design. Such a rational approach would enable *in silico* predictions of unintended and detrimental side effects resulting from modifications such as higher by-products secretion, slow growth or cell death, which in term hampered productivity [114]. In the last decade, some studies have moreover confirmed the promising potential of fluxome for revealing non-trivial optimisation targets and overcoming bottlenecks for enhanced production of amino acids and alcohols in *E. coli*, *Corynebacterium glutamicum* and other bacteria [139, 140]. Other recent studies revealed on the other hand the potential of fluxomics for unravelling new pathways or assigning new biological functions to known pathways, making it an indispensable tool to capture the whole complexity of living organisms [111, 141-144].

## 2.2 Stress emergence and response in bacteria

### 2.2.1 Living in hostile environments

In their natural habitats, all living organisms are constantly experiencing modifications in the physical state and biochemical composition of their ecological niches. To face stressful changes such as temperature and osmotic shock or nutrient limitations, organisms have developed complex and interconnected regulation networks that operate at the transcriptome, proteome and metabolome levels [145]. Among those mechanisms, a widespread and well-characterised stress response in Gram-positive bacteria involves a huge stimulon under direct control of the alternative sigma factor B ($\sigma^B$) [146-148]. As this $\sigma^B$-stimulon is rapidly induced by most stress stimuli and comprises more than 150 genes, it is thought to provide cells with a rather non-specific protection, allowing them to survive all kind of low-intensity stresses and prepare specific response. Despite lots of efforts, the function of many $\sigma^B$-dependent genes is still unknown but encoded proteins encompass, inter alia, stabilising and repairing proteins, detoxifying transporters, regulators and proteases and offer cells a survival strategy other than sporulation.
Under stressful conditions, up to one third of the protein synthesis machinery can be burden with the expression of $\sigma^B$-dependent genes and this regulon must therefore remain tightly controlled. The control over $\sigma^B$ and its regulon requires seven regulatory genes present in the $\sigma^B$-operon and relies on partner-switching between the corresponding proteins (**Fig. 2.6**).

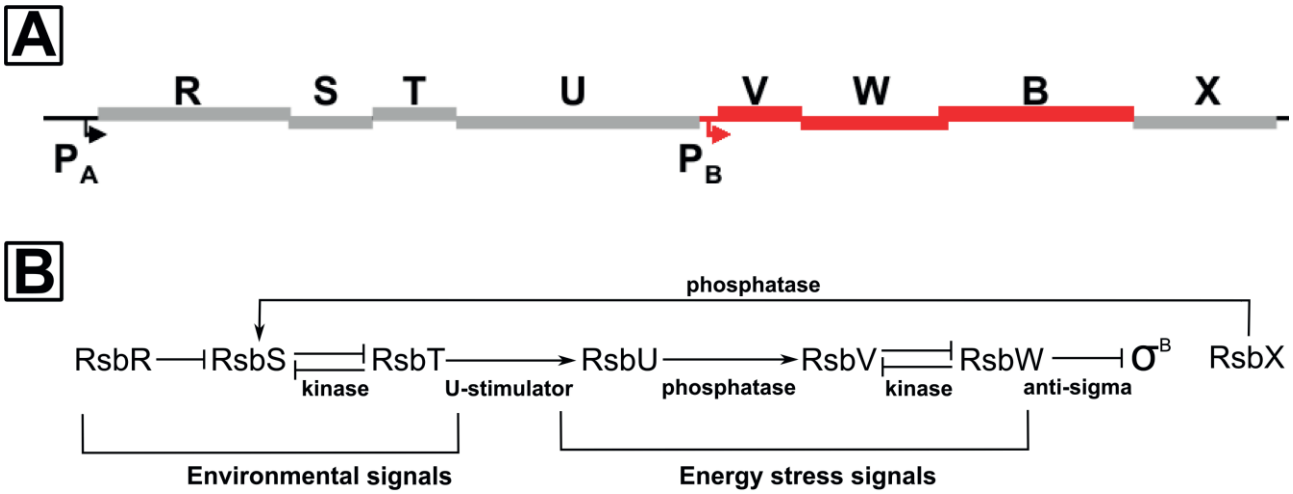


**Figure 2.6: Organisation of genes encoding proteins involved in activation of the $\sigma_B$-regulon (A) and its regulation by coupled partner-switching modules (B) –** Normal arrows indicate activation while T-head arrows display inhibition. Two modules can be identified and each consists of three elements: a PP2C serine phosphatase (RsbX or RsbU), an antagonist protein (RsbS or RsbV) and a switch protein that is also a serine protein kinase (RsbT or RsbW). The first module is involved in the activation of the $\sigma_B$-regulon in response to environmental stress while the second is required for its activation in response to energy stress and environmental stress signal conveyed from the first module via interactions between switch protein kinase RsbT and phosphatase RsbU. Transcription is initiated at two distinct promoter regions by the $\sigma^A$-factor ($\mathbf{P_A}$) and the $\sigma^B$-factor ($\mathbf{P_B}$), respectively. The first promoter is responsible for the basal level expression of the eight genes of the sigB operon while the latter is responsible for the autoregulation of the downstream half of this operon. Figure was adapted from [149] and [150].

In a nutshell, according to the phosphorylation state of certain regulatory proteins, complexes are formed or dissembled and the resulting reaction cascade leads to active or inactive $\sigma^B$ [149-151]. Under balanced growth condition, RsbV is in its phosphorylated form (RsbV~P) and $\sigma^B$ and RsbS are in complex with RsbW and RsbT, respectively. Hence, the whole $\sigma^B$-regulon is silenced. When a physical stress emerges, kinase activity of RsbT is enhanced leading to phosphorylation of RsbS and dismantling of their complex. Free RsbT activates RsbU, which in turn dephosphorylates RsbV~P. Consequently, RsbW is forced to switch partner from $\sigma^B$ to RsbV, thus leading to the release of $\sigma^B$ and induction of its regulon. Yet magnitude of this induction is also restricted by RsbX, an RsbS~P phosphatase, which ensures a feedback regulation by counteracting the kinase effect of RsbT. In case of starvation, the drop in cellular ATP mediates alone the dephopsphorylation of RsbV~P leading to expression of the $\sigma^B$-regulon. Depending on the nature and intensity of the stress, specific proteins that are co-regulated with $\sigma^B$ or whose expression falls under the control of other global regulators, also come into play and make the elucidation of global regulation networks a very fastidious task.

More generally, the capability of sensing specific stimuli and inducing the expression of appropriate genes in response to a given stress relies on sophisticated mechanisms that transduced environmental stimuli into biological signals which can subsequently be interpreted by cells. Most of the time, membrane proteins and embedded enzymes as well as carriers, channels and receptors are needed in order to transfer the external information across the membrane into the cytoplasm where it can be processed. The best characterised of these mechanisms are two-component systems (TCS) which consist of membrane bound histidine kinases associated with response regulators (**Fig. 2.7**).

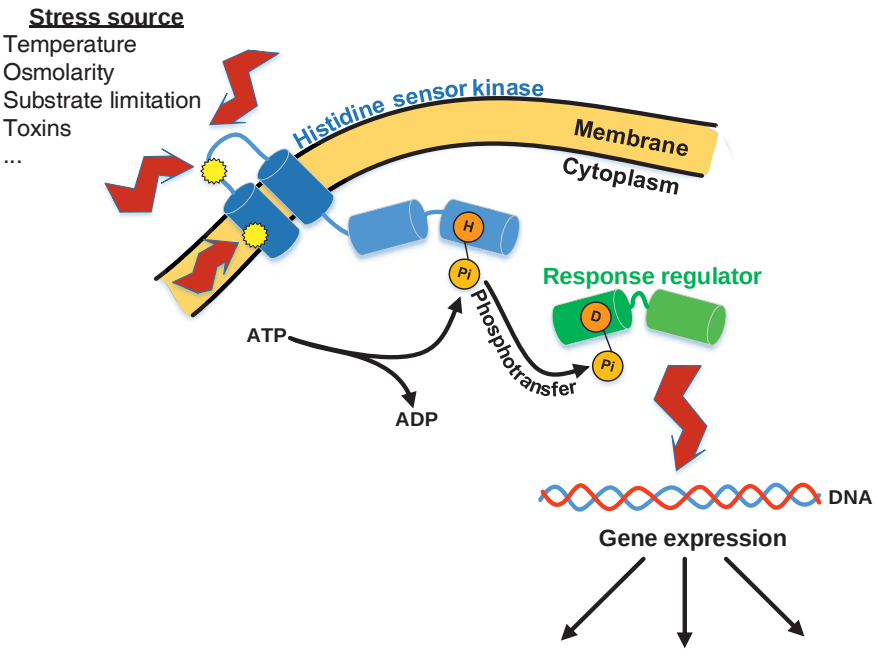


**Figure 2.7: Stress sensing and signal transduction by two-component regulatory systems in bacteria –** Stress stimuli are perceived by the input domain (dark blue) of a sensor histidine kinase embed in the membrane and leads to autophosphorylation of its transmitter domain (light blue) at a conserved histidine residue. The phosphoryl group is then transferred to an aspartate residue in the receiver domain (dark green) of the response regulator, inducing conformational change and activation of its output domain (light green) which binds to DNA and alters gene expression. Figure adapted from [152].

Shortly, physical stimuli induce a conformational change of the kinase perception domain, which in turn leads to autophosphorylation of the transmitter domain at a histidine residue. Subsequently, the phosphor group is transferred to the receiver domain of a response regulator which undergoes a conformational change as well. This modification enables it to interact with target molecules such as DNA regulatory binding sites and finally trigger expression of given genes.
Since little is currently known about adaptation processes in *B. megaterium*, the following two chapters will principally present bacterial adaptation to osmotic and temperature stress as known for *B. subtilis* and other well-characterised prokaryotes.

### 2.2.2 From cold to heat - Survival mechanisms in bacteria

Although *B. megaterium* is a typical mesophilic bacterium, its presence in niches such as soil and seawater implies an exposure to very different and fluctuating temperatures. As a few degree deviation from optimal growth temperature is sufficient to disrupt the well-run cellular machinery, cells must have evolved adequate adaptation mechanisms to sustain growth and survival at otherwise adverse temperatures [153]. While heat shock response has already been well documented for many organisms from insects to bacteria and appears to be quite universal, very little is known about mechanisms that enable growth at low temperatures [154-156].
One of the first consequences of a temperature increase is the aggregation of mRNA with cytosolic proteins leading fatally to a global slowdown of RNA translation. At the same time, emergence of unfolded and denatured proteins quickly steps up and eventually triggers an appropriate response to restore balanced proteostasis [157-159].
This heat-specific response is based on the expression of several heat stress proteins (HSPs), whose features help reducing deleterious effects of high temperatures. The major group of HSPs consists of molecular chaperones and chaperonins that prevent protein aggregation, assist protein folding and refold damaged proteins. A second class of HSPs regroups proteases and other proteins implicated in the degradation of irreparably denatured proteins. The third important class comprises RNA/DNA modifying enzymes and attend to fix DNA damages and processing failure caused for instance by methylation of ribosomal RNA. Remaining HSPs can be divided in regulators, transporters and metabolic enzymes, whose role is to reorganise pathway utilisation to fulfil new requirements imposed by stress. Even though the global regulation network of HSPs has not been fully elucidated yet, certain control elements common to several Gram-positive bacteria have been brought into light [158, 160-163].
Under normal growth conditions for example, expression of genes encoding chaperones is repressed by the HrcA regulator, which binds to a DNA element called CIRCE (**C**ontrolling **I**nverted **R**epeat of **C**haperone **E**xpression) and present upstream of the so-called class I heat shock genes. In contrast, the accumulation of unfolded proteins under heat stress initiates the repressor release and thus transcription of genes encoding for class I heat proteins [162-164]. Another repressor called CtsR (**C**lass **t**hree **s**tress gene **r**epressor) binds in a similar way to promoter regions of some heat shock genes controlling the expression of genes encoding class III heat proteins [160, 161, 165].

Some other HSPs designated as class II heat proteins simply belong to the general stress $\sigma^B$-regulon and are not only heat specific but also involved in protection against various stresses [149, 166, 167]. In *B. subtilis*, a heat inducible gene named *htpG* was furthermore recently reclassified as class IV heat shock gene since Versteeg et al. have proven that its $\sigma_A$-dependent induction under heat stress rely on a yet unknown transcriptional activator [168]. Though not clear, its induction mechanism stands as an exception among heat shock genes because it responds to absolute temperature rather than heat shock and cytoplasmic accumulation of misfolded proteins [169]. The existence of other genes inducible by the same mechanism is probable but has not been reported yet. Finally, some HSPs have not been related to any known regulons yet and their expression patterns remain to be clarified. Members of each of these groups common to *B. subtilis* and *E. coli* can be taken from **Tab. 2.1**.

**Table 2.1: Genes with major functions in heat and cold stress responses in *B. subtilis* and *E. coli* which have homologues in *B. megaterium* genome –** Comparative genome analysis was performed using the MegaBac database (MegaBac v9, http://megabac.tu-bs.de/) [17, 18, 149, 162, 166, 170, 171]. Regulators of most genes involved in cold response remain unknown until now and are therefore not indicated in this figure.

| Heat Stress | | |
|---|---|---|
| **Regulator** | **Gene** | **Gene product** |
| HrcA | *hrcA* | Heat-inducible transcription repressor HrcA |
| | *grpE* | Co-chaperone GrpE – Activation of DnaA |
| | *dnaK* | Chaperone protein DnaK – Protein quality control |
| | *dnaJ* | Chaperone protein DnaJ - Protein quality control |
| | *groEL* | 60 kDA chaperonin – Protein folding and re-folding |
| | *groES* | 10 kDA chaperonin – Protein folding and re-folding |
| $\sigma_B$ | *dps* | DNA-protecting protein |
| | *ctc* | 50S ribosomal protein L25 – General stress protein |
| | *csbD* | General stress protein |
| | *trxA* | Thioredoxin – Protection of proteins against oxidative stress |
| | *ydaG* | General stress protein 26 |
| CtsR | *clpP* | ATP-dependent protease – proteolytic subunit ClpP |
| | *clpE* | ATP-dependent protease –subunit ClpE |
| | *clpC* | ATP-dependent protease – subunit ClpC |
| Unknown | *clpX* | ATP-dependent protease – subunit ClpX |
| | *htpG* | Chaperone protein HtpG |
| | *htrA* | Serine protease HtrA – Protein quality control |
| | *lonA* | ATP-dependent protease LonA – Protein quality control |
| | *ftsH* | Cell division protease FtsH – Cell division, sporulation initiation |

| Cold Stress | |
|---|---|
| **Gene** | **Gene product** |
| *cspB* | Cold shock protein |
| *cspC* | Cold shock protein |
| *cspD* | Cold shock protein |
| *cspE* | Cold shock protein – RNA chaperone / Transcriptional antitermination |
| *des* | Fatty acid desaturase – Cell wall modification |
| *gyrA* | DNA-gyrase A subunit – DNA binding / cleaving / joining |
| *gyrB* | DNA-gyrase B subunit – DNA binding / cleaving / joining |
| *dps* | DNA-protecting protein |
| *infA* | Translation initiation factor IF-3 |
| *infB* | Translation initiation factor IF-2 |
| *infC* | Translation initiation factor IF-3 |
| *nusA* | Transcription termination factor NusA |
| *pnp* | Polynucleotide phosphorylase (PNPase) - 3'-5' exoribonuclease R |
| *rnr* | 3'-5' exoribonuclease R |
| *rbfA* | Ribosomal binding factor A – Processing of 16S RNA at low temperature |
| *recA* | General recombination and DNA repair |
| *dnaA* | Chromosomal replication initiator |
| *tig* | Trigger factor - protein folding |

At low temperature, bacteria have to cope with problems of a somewhat different nature. Along with slight protein misfolding, stabilisation of DNA and RNA secondary structures impairs the proper functioning of ribosomes and fatally reduces transcription and translation efficiency [155, 170, 172].

Besides, cells must cope with reduced substrate uptake and reaction kinetics, which affect substantially the global energy supply and threaten their survival [173]. In response, bacteria produce a large cocktail of specific proteins designated by analogy with heat shock proteins (HSPs) as cold shock proteins (CSPs) and whose function is to fix those life-challenging issues. Interestingly, expression of general stress proteins is partially, if not totally, suppressed under cold stress conditions in *B. subtilis*, in which cold shock response appears to be very specific [174, 175]. This idea is reinforced by the rare expression of CSPs in relation to other stresses and confirms the existence of global regulation networks. Another striking fact in *B. subtilis* and *E. coli* is that cold stress genes are distributed all over the genomic DNA and do not seem to be clustered in well-organised operons. Mechanisms governing their induction and regulation remain mostly nebulous but recent evidences suggest that they are operating at both the transcriptional and post-transcriptional level. In fact, some CSPs exhibit a nucleic acid binding domain and possibly stabilise the RNA-polymerase/DNA complex, thus improving transcription of targeted genes. CspA and CspB, two such CSPs from *E. coli* and *B. subtilis,* respectively, were also found to activate transcription of several cold shock genes and probably act as major regulators of the cold stress response. Moreover, it has been proposed that the mRNAs encoding CSPs undergo a conformational change with decreasing temperatures, thus increasing their stability and enabling a better translation in comparison to other mRNAs [176-178].

According to Wang et al. [179] and Dorman et al. [180], the DNA supercoiling state should be taken into account as well when trying to resolve the regulation of gene expression after a cold or osmotic shock. They suggest that the increase in negative DNA supercoiling implemented by DNA gyrases could have a role in stress signalling and trigger or prevent gene expression by operating structural modifications on some twist-sensitive promoters. From a post-transcriptional perspective now, studies demonstrated that CSP-mRNA lifespan is strongly improved at low temperatures and accounts to a greater extent than transcriptional modifications for the observed increase in CSP concentrations. Moreover, a unique sequence present in some CSPs' mRNAs and located downstream of the start codon is presumed to enhance translation initiation. Depending on their functions, CSPs can be categorised into RNA chaperones, RNA helicases and exoribonucleases. While the first group endeavours to facilitate transcription and translation by melting RNA secondary structures, supporting antitermination, assisting correct RNA folding, or speeding up annealing steps, the last two stimulate RNA unwinding and degradation. Helicases are furthermore implicated in the biosynthesis of cold-adapted ribosomes and their ability to process cold-sensitive mRNA.

Apart from disrupting protein synthesis and metabolic activity, change in ambient temperature also deeply affects membrane physical state and functions. Indeed, the membrane fluidity, which refers to the viscosity of its phospholipid bilayer and characterises its ability to let molecules diffuse through, is a temperature dependent parameter [181-183]. At high temperatures on the one hand, decrease of the molecular order leads to membrane fluidisation and exposes cell to death by disintegration of its lipid bilayer. On the other hand, drops in temperatures endanger cell viability as

well because they enhance membrane stiffening, restraining thereby incoming nutrient transport and secretion of toxic compounds. Fluidity must therefore be kept within acceptable boundaries and survival of organisms at unfavourable temperatures depends largely on their capacity to adjust membrane fluidity. Though the involved perception mechanism could not be apprehended in its wholeness yet, fluidity fluctuations seems to be closely implicated in stress sensing and thus, in the outbreak of stress protein expression [153, 183]. Conversely, some produced stress proteins are designed to modify membrane fatty acid composition and correct fluidity deviation. Typical mechanisms to compensate for fluidity interferences in bacteria rely on alteration of fatty acid saturation grade, incorporation of branched fatty acids and modification of their composition (anteiso vs. iso). In the late 60's, Fulco et al. [184] demonstrated that a drop in temperature activates fatty acid desaturation in *B. megaterium* 14581, enabling partial recovery of membrane fluidity. Even though these results were extended to other bacteria and organisms later, the reaction steps needed for desaturation vary significantly among them [185, 186]. In *B. megaterium* and *B. subtilis*, the sole gene *des*, which is closely regulated by the two component system DesKR, seems to orchestrate desaturation [187]. Increased membrane fluidity can also be achieved by integration of anteiso fatty acids in the membrane but this might require an increased supply of the precursor isoleucine, which is only given when cells are grown on complex medium [186, 188]. On the contrary, adaptation to high temperatures necessitates a high saturation grade and could be correlated with an increased iso fatty acid content for several *B. megaterium* strains cultivated on complex medium [189].

### 2.2.3 Osmo-adaptation in moderate halophile bacteria

Over the year, seasonal and daily weather variations affect soil conditions by modifying water availability and thereby the molar concentration of osmotically active compounds (osmolytes), also referred to as osmolarity [Osmol $L^{-1}$]. Depending on climatic and environmental conditions, a positive or negative osmolarity gradient arises between intra- and extracellular milieu and water starts diffusing across the cytoplasmic membrane. Since water is essential for almost every cellular processes from protein folding to genetic information processing, bacteria must be able to swiftly restore water balance in order to survive. Unfortunately, they do not own any active transport system for water and the only way to reduce osmolarity gradients and maintain a suitable cell volume relies on active import or secretion of diverse osmolytes. After rainfall, soil osmolarity drops drastically and the resulting gradient forces water to diffuse from the environment into the cell. As a strong water influx disturb metabolic activity and can ultimately lead to cell burst, bacteria open some mechanosensitive channels to unspecifically release intracellular compounds in their immediate vicinity and restore osmotic balance. This channel opening is thought to be triggered by the increasing pressure exerted against the cytoplasmic membrane, namely the turgor pressure. Under normal conditions, this pressure is the driving force for cell expansion and division. As such, it must always remain within a controlled range.

In contrast, periods of drought lead to increased water activity in soils and to a passive water diffusion from the cell inner to the hypertonic environment, commonly described as plasmolysis [190-192]. Because of this loss of water, cellular volume shrinks and intracellular concentrations of some compounds might eventually get toxic. To avoid cell dehydration and sustain effective metabolic activity under hypertonic conditions, bacteria have developed several strategies according to their living habitats and genetic background. The *salt-in strategy* provides an energetically favourable alternative to deal with the sudden increase of osmotic pressure and is based on the import of various ions such as $K^+$ and $Cl^-$ into the cytoplasm by proton-motive force (PMF) and the removal of concomitant cytotoxic sodium ions, using a $Na^+/H^+$-antiporter [193, 194]. Although this solution is common among halophilic bacteria and archaea flourishing in saline habitats, ion accumulation usually lowers intracellular pH to otherwise non-physiological values and implies irreversible restructuring of the enzymatic machinery [195, 196].

Indeed, protein stability, solubility and activity at high ionic strengths is only achieved through integration of acidic and slightly hydrophobic amino acids into proteins, which would afterwards denature under normal conditions [195]. For this reason, non-halophilic bacteria and other organisms, which are exposed to a wider range of osmotic conditions and unable to afford such a proteomic readjustment, only use it as a short-term answer before implementing a more convenient solution called the *salt-out strategy.* In this second phase, salts are progressively replaced with imported or *de novo* synthesised organic osmolytes, known as compatible solutes or osmoprotectants (**Fig. 2.8**). Unlike $K^+$ or $Cl^-$, compatible solutes do not interfere with intracellular physiology and accumulate to high cytoplasmic concentrations for the purpose of reducing intracellular water activity [194]. In addition to their role in compensating osmolarity gradients, osmoprotectants also act as chemical chaperones and help stabilising proteins, nucleic acids and membranes. They encompass a large number of chemical compounds including sugars, amino acids, polyoles and their derivatives such as betaine and ectoine. Recently, there was a growing industrial interest for their protecting and stabilising properties that make them suited for applications in many fields such as cosmetics, health care and biotechnology [197-200].

Among the *Bacillus* spp., the short-term response is highly conserved and relies on the uptake of potassium ions using high affinity transport systems KtrAB and KtrCD and glutamate as counterion to maintain electric neutrality (Fig. 2.8) [201, 202]. On the contrary, the long-term adaptation of *Bacillus* sp. largely depends on the availability of compatible solutes in the surrounding environment and the intrinsic genetic capabilities of each species. In fact, for energetic reasons, *Bacillus* sp. prefers importing compatible solutes or their advanced precursor like choline from their environment whenever possible. To this end, they own various specific ABC-transporters, among which OpuABCDE are important members (Fig. 2.8). If not available in their surroundings, compatible solutes have to be *de novo* synthesised and vary a lot among *Bacillus* sp.. While *B. subtilis*, *B. licheniformis* and *B. megaterium* accumulate proline, *B. cereus* and *B. thuringiensis* rather synthesise glutamate and *B. pasteurii* and *B. alcalophilus* preferentially produce ectoine [203].

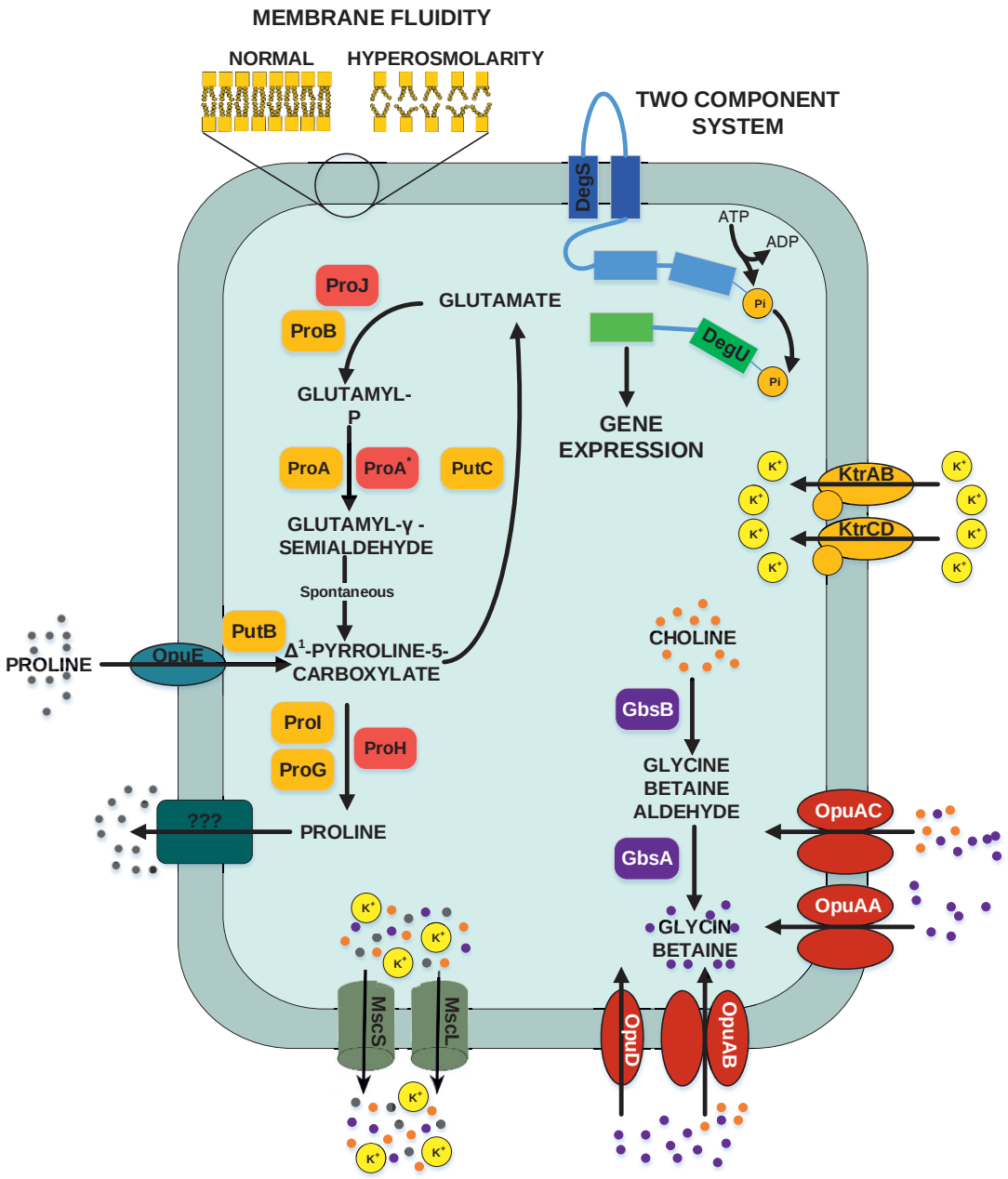


**Figure 2.8: Provisional synthetic overview of the osmotic stress response in *B. megaterium* inferred from genetic context and comparison with *B. subtilis* and *B. licheniformis*** – Depending on their function, proteins have been attributed different font colours: light red for synthesis of proline as an osmoprotectant, orange for proline synthesis and utilisation for biosynthetic purposes, purple for synthesis of glycine betaine from choline, red for choline and glycine betaine transporters, dark turquoise for proline transporters, grey for mechanosensitive channels MscS and MscL, olive green for potassium transporters, dark pine green for unknown proline exporter, dark blue for the input domain of the sensing histidine kinase, light blue for the transmitter domain of the histidine kinase, dark green for the receiver domain of the sensing histidine kinase and light green for the output domain of the response regulator. **DegS**: two-component sensor histidine kinase, **DegU**: two-component response regulator, **GbsA**: glycine betaine-aldehyde dehydrogenase, **GbsB**: choline dehydrogenase, **KtrAB**: high affinity potassium transporter KtrA-KtrB, **KtrCD**: low affinity potassium transporter KtrC-KtrD, **MscL**: large conductance mechanosensitive channel protein, **MscS**: small conductance mechanosensitive channel protein, **ProA**: glutamate-5-semialdehyde dehydrogenase, **ProA***: glutamate-5-semialdehyde dehydrogenase **ProB**: glutamate 5-kinase, **ProG**: 1-pyrroline-5-carboxylate dehydrogenase, **ProH**: pyrroline-5-carboxylate reductase, **ProI**: pyrroline-5-carboxylate reductase, **ProJ**: glutamate 5-kinase, **PutB**: proline dehydrogenase, **Opu**: glycine betaine ABC transporter, **OpuAB**: glycine betaine ABC transporter, **OpuD**: glycine betaine transporter.

Based on these findings and *in silico* analysis of its genome sequence, one can easily predict that the stress behaviour of *B. megaterium* might be very similar to that of *B. subtilis* and *B. licheniformis*. In those strains two distinct biosynthetic pathways exist for proline biosynthesis from the precursor glutamate. Although the reaction sequence is always catalysed by glutamate-5-kinase, glutamate-5-semialdehyde dehydrogenase and pyrroline-5-carboxylate reductase, the genes encoding these enzymes and the underlying transcriptional control differs significantly for both routes, thereby reflecting their completely different physiological functions.
On the one hand, an anabolic pathway composed of ProB-ProA-ProI is tightly controlled by a T-Box system and by the probable allosteric feedback inhibition by proline on expression of *proB* ensuring that this route is only induced when cells are starving for proline [204, 205]. A second route ProJ-ProA*-ProH, on the other hand, is induced in an osmolarity-dependent manner and enables the proline overproduction needed under sustained osmotic stress [206]. Surprisingly, whereas *B. licheniformis* uses an osmotically inducible homologous enzyme of ProA for osmoprotection, *B. subtilis* only disposes of the anabolic version, whose standard activity seems nevertheless sufficient for protection purposes [207]. In *B. megaterium*, two versions of *proA* are annotated but data about their functions in anabolism and osmoprotection are still lacking. All inferred mechanisms involved in transport and production of compatible solutes in *B. megaterium* are summarised in the provisional overview presented in Fig. 2.8.
Just as temperature variations, hyper- and hypoosmotic conditions deeply alter membrane composition and physical proprieties as well [183]. In-depth research is still missing on this matter but early studies revealed a cell shrinkage at high ionic strength in *B. megaterium* and *E. coli*, which could be imputed to electrostatic wall contraction [192, 208]. More recently, a decreased fluidity and an increased hydrophobicity of membranes experiencing hyperosmotic stress have been reported for *B. subtilis* and *S. cerevisiae* [209, 210]. To compensate for this loss of fluidity, bacteria and yeasts might use the same mechanisms as for temperature adaptation, that is to say fatty acid desaturation and incorporation of cyclic or anteiso fatty acids [211, 212]. The observed hydrophobicity together with a higher diglucosyl-diglyceride content also tends to indicate that lipoteichoic acids have a key role in adaptation of bacteria to high ionic strength [212]. In *E. coli*, *B. subtilis* and *S. aureus*, another striking modification in response to osmotic stress is a high cardiolipin enrichment of phospholipids at the expense of phosphatidylglycerol [210, 213, 214]. Though the function of cardiolipin in osmotic response is not clearly understood yet, many studies postulate that it might increase the order on membrane surface, undertake a major role in active transport but also behave like a barrier against external high ionic strength [214-216].

## 2.3 Polyhydroxyalkanoates and their synthesis in *Bacillus megaterium*

### 2.3.1 Bio-based economy and industrial relevance of biopolymers

In recent years, the progressive depletion of existing fossil resources (gas, oil and coal) has become evident. Hence, the resulting increase of their prices has pushed industrial actors to start looking for renewable and environmentally friendly alternatives. This dynamic is all the more sustained since eco-consciousness and public awareness on global warming have emerged and led to some governments undertaking tax measures to reduce our ecological footprint and our dependence upon fossil resources, which currently provide 80 % of the steadily increasing global energy demand [217]. In this context, a particular attention has been given to the development of biofuels and bio-based products in replacement of typical petrochemical products, whose demand in fast-developing countries such as China or India is rapidly increasing [218]. However, their part in the global chemical industry (7 % of sales) remains anecdotal so far, not only because of technical and economic aspects but also due to political and societal reluctance towards genetically modified organisms (GMOs) and a strong influence of oil lobbies [219]. Nevertheless, the bio-based economy sector is currently flourishing quickly in Europe, being 22 trillion EUR worth and employing 9 % of the global workforce [220].

Among usual petrochemical products, 155 million tons of plastics are produced yearly, consuming approximately 10 % of the global oil supply [221]. At first not economically viable, the large-scale production of bioplastics is now conceivable thanks to the increasing price gap between bio-feedstock and oil. It is expected to reach 1.1 million tons in 2015 and grow by 400 % by 2017 [222] [220]. Bioplastics are natural or semi-synthetic polymers which can be formed in their soft state, and retain a given shape after hardening [223]. From a technical point of view, their large diversity of chemical and physical properties enable them to replace almost every conventional plastics in fields ranging from packaging, electronics and coating to cosmetics, biomaterials and textiles. They include, among others, polyesters such as polylactic acids (PLAs) and polyhydroxyalkanoates (**PHAs**), polyolefines (bio-polyethylene (bio-PE) and bio-polypropylene (bio-PP)), polyamides (PAs), polysaccharides and their blends with usual petrochemical polymers [224]. Contrary to common beliefs, there is no implicit connection between bio-based and biodegradable plastics. Indeed, some biopolymers are durable (e.g. bio-PE) whereas some petrochemical plastics might not be (polybutylene succinate (PBS), polycaprolactone (PCL)) [225]. In the framework of sustainable development, there is nowadays a growing interest for biodegradable biopolymers that can be produced and fully degraded by bacteria. Their nontoxicity furthermore enables their assimilation by mammalian, plants and bacteria without impacting the food chain, thus presenting both a neutral carbon balance and a health benefit [226, 227]. This interest is reinforced by the fact that global biochemical production would only mobilise a small part of all available arable land (3-4 %) and therefore never compete with food production, underlining the possibility of a complete independence from fossil oil [220].

### 2.3.2 *Bacillus megaterium* as a working horse for PHA production

Polyhydroxyalkanoates (PHAs) are linear insoluble polyesters of hydroxyalkanoic acid monomers ($10^3$-$10^4$ units) synthesised by certain microorganisms and plants in response to various environmental stresses [228, 229]. Within the cell, they accumulate as granules with a size varying from 200 to 500 µm and a molecular mass comprised between 50 and 1.000 kDa [230, 231]. Their cellular functions are not fully understood yet but they are commonly thought to serve as carbon and energy storage and also seem to undertake a key role in maintaining redox balance [232]. Depending on size (1 to 14 carbons) and nature of the alkyl group in the R-position of their monomer, they can be categorised into small or medium side chain polyhydroxyalkanoates (ssc-PHAs and msc-PHAs) and their biosynthesis as well as their physical and mechanical properties differs accordingly [233]. Whereas ssc-PHAs primarily necessitate acetyl-CoA as precursor, the synthesis of msc-PHAs derives mostly from fatty acid biosynthesis and degradation pathways (**Fig. 2.9**). To date, more than 150 varieties of PHAs have been documented and the potential of PHAs for industrial applications is almost unlimited since original biopolymers with novel properties can be obtained by incorporating new natural or unnatural substituents into the alkyl side chains using bacterial pathway diversity or chemistry [234].

This diversity is exemplified in Fig. 2.9 and **Tab. A.1**, indicating the formation pathways of some usual ssc-PHA copolymers such as P(3HB-4HB), P(3HB-3HV), P(3HB-3HH) and their corresponding physical properties, respectively. Besides their application as replacement for conventional plastics, PHAs have been recently in focus for their biocompatibility which makes them suitable for biomedical and biotechnological applications. Their use as drug delivery systems is also currently under evaluation [235-237]. In addition, they are proposed as a new source of small precursor molecules such as β-hydroxy acids, 2-alkenoic acids, β-hydroxyalkanols, β-amino acids or β-hydroxyacid esters that can be obtained from their monomers after hydrolysis and are extensively used in industry [231].

Although PHAs were first discovered in the form of polyhydroxybutanoate (PHB) in *B. megaterium*, the physiology and genetic underlying PHA synthesis in this organism remains poorly characterised in comparison with other natural producers such as *Cupriavidus necator*, *Pseudomonas* spp. or some methylobacteria, in which metabolic engineering has already been successfully applied to develop bacterial cell factories [238-243]. Substantial progress was only achieved more than seventy years after the initial discovery when McCool et al. characterised the 7,917-bp coding regions of PHB associated proteins and elucidated their respective functions and localisations [244]. This region comprises a cluster of 5 genes *phaP*,-*Q*,-*R*,-*B*,-*C* organised in two operons *phaQP* and *phaRBC*, with the latter being divergently transcribed. This one-of-a-kind gene cluster is remarkably dissimilar to those previously described and interestingly does not include a gene encoding the ketoacyl-coA thiolase necessary for the first reaction of the PHB pathway, namely the conversion of 2 acetyl-CoA into acetoactyl-CoA (Fig. 2.9) [231, 244].

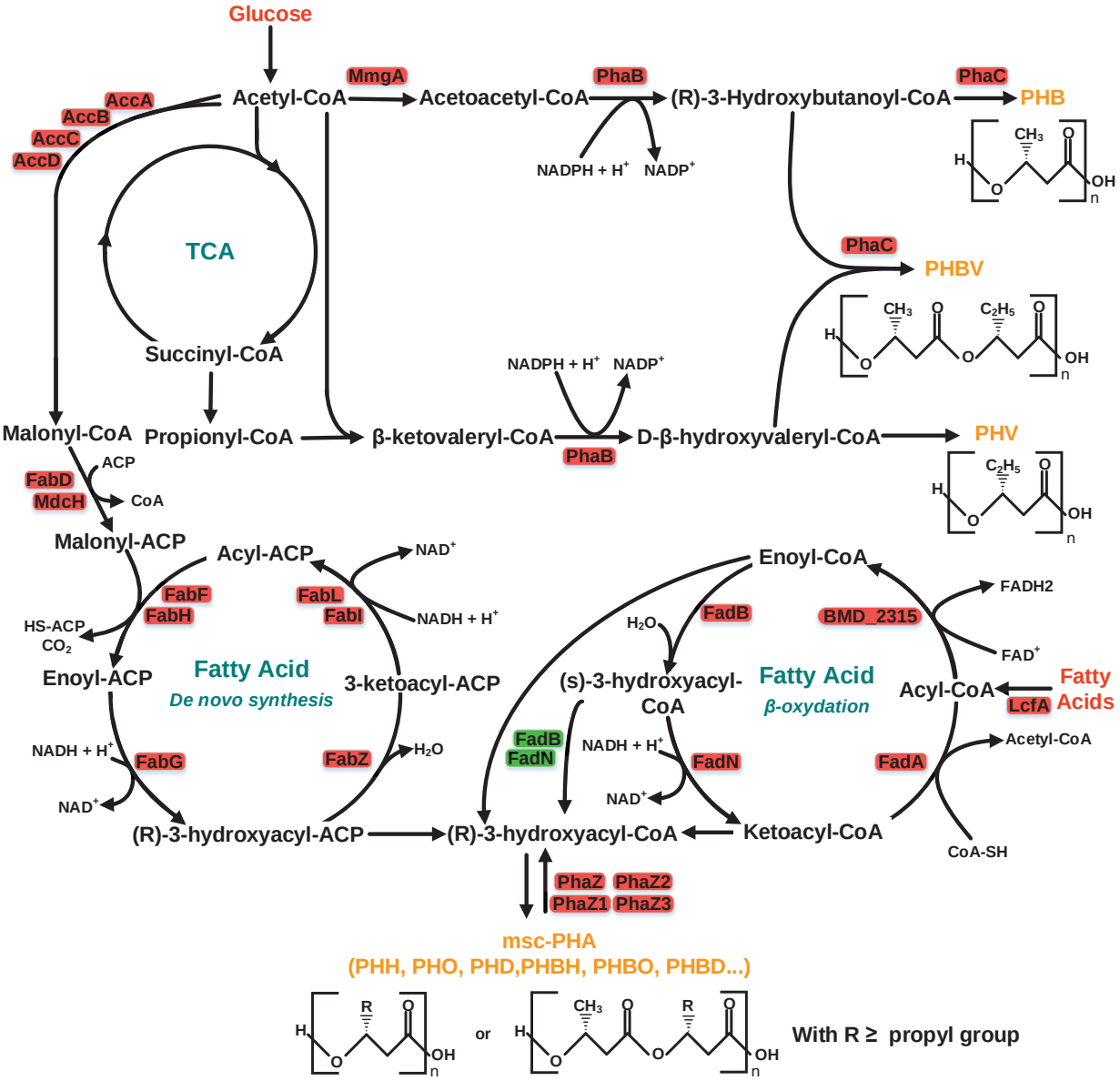


**Figure 2.9: Bacterial synthesis pathways of PHAs –** Enzymes catalysing the different reaction steps in *B. megaterium* were retrieved from KEGG database (http://www.genome.jp/kegg/) and are indicated next to the corresponding arrows. Enzymes with known functions are highlighted in red and those with supposed functions in green. Although *B. megaterium* seems to possess all enzymes required for synthesis of middle side chain PHAs (msc-PHAs), it has never been reported so far in this organism. **TCA**: tricarboxylic acid cycle, **PHB**: poly-β-hydroxybutyrate, **PHBV**: poly(3-hydroxybutyric acid-co-3-hydroxyvaleric acid), **PHH**: polyhydroxyhexanoic acid, **PHO**: polyhydroxyoctanoic acid, **PHD**: polyhydroxydecanoic acid, **PHBH**: poly(3-hydroxybutyric acid-co-3-hydroxyhexanoic acid), **PHBO**: poly(3-hydroxybutyric acid-co-3-hydroxyhexanoic acid), **PHBD:** poly(3-hydroxybutyric acid-co-3-hydroxydecanoic acid), **msc-PHA**: middle side chain polyhydroxyalkanoate.

This singularity is also reflected in the encoded proteins which, though they undertake similar functions, do not share much structural homology with known PHB associated proteins [4, 245]. Within the *phaRBC* operon, the genes *phaR* and *phaC* were shown to encode two essential subunits of a unique heterodimeric PHA synthase responsible for the final polymerisation step, while the gene product of *phaB* is a NADPH-dependant reductase supplying the necessary

hydroxyalkanoic acid monomers [4, 246]. In the second operon, PhaQ was identified as a DNA-binding protein interacting with the promoter region and negatively regulating its own expression and that of gene phaP encoding a phasin [245]. Phasins are low molecular mass proteins (14-24 kDa) that are not necessary for PHA synthesis but bind granules and promote PHA production by accelerating the synthesis rate, stabilising nascent granules and regulating tightly their size and shape (surface to volume ratio) [247]. Based on the functional analogy between PhaQ from *B. megaterium* and PhaR, the negative regulator of PhaP accumulation in *C. necator*, it is reasonable to think that PhaQ also binds preferentially PHB granules and only represses *phaQP*-expression under conditions not permissive for PHB synthesis or once PHB granules have reached their final size and their surface is completely covered with phasins [235, 248]. Since their products have somehow antagonist roles, it is however surprising to have *phaP* and *phaQ* co-transcribed in *B. megaterium*. To explain this rather unusual combination, Lee et al. suggested the existence of a posttranscriptional regulation involving the degradation of the *phaQ*-transcript in PHB accumulating bacteria, thus allowing differential synthesis of these proteins [245].

In addition to PHA synthase and phasins, the PHB accumulation is also function of the concentration and activity of several PHA depolymerases (PhaZ,-Z1,-Z2,-Z3), which are responsible for the degradation of granules. Moreover, other regulation elements such as sigma factors or concentrations of key intermediates of the central carbon metabolism are likely to exist and have to be brought into light using a system wide approach [231].

Industrially, the production of PHA plastics started in the 80's with the synthesis of a P(3HB-3HV) copolymer in *Cupriavidus metallidurans* using a two stage fermentation and is driven by the cooperation between industry and academic research since then [249-251]. However, it remains five to ten times more expensive than the production of common petrochemical plastics and will only become competitive with the development of industrial workhorses able to grow faster, metabolise cheap substrates and accumulate high levels of PHB all at once [252]. For this, precise knowledge of both bacterial physiology and PHA metabolism regulation must first be gained in order to determine optimal cultivation conditions and define targets for metabolic engineering [253]. The increasing number of published works on these key topics tends to indicate that efficient production processes will be available soon (**Fig. 2.10**). Now, other challenges such as the optimisation of PHA recovery and the construction of dedicated facilities able to process the extracted raw material into products should be tackled [221, 254, 255]. In *B. megaterium*, little effort has been dedicated to constructing PHA cell factories so far and production still relies on wild-type strains showing exceptional natural performances. On the contrary, a lot of attention has been paid to the impact of cultivation parameters such as temperature, pH, oxygen level or C-N ratio on PHA yield and more surprisingly the down-processing question has already been addressed by Hori et al. [256] who constructed a self-disruptive strain able to release intracellular PHB into the culture broth after substrate exhaustion [257-260]. Given the fact that natural producers are often hard to lyse, this unique recovery system could, in addition to its short generation time and its greater growth temperature flexibility, confer *B. megaterium* another

significant advantage over other producing bacteria [261]. Hence, all pieces are falling into place and should ensure a great future for the production of PHAs in *B. megaterium*.

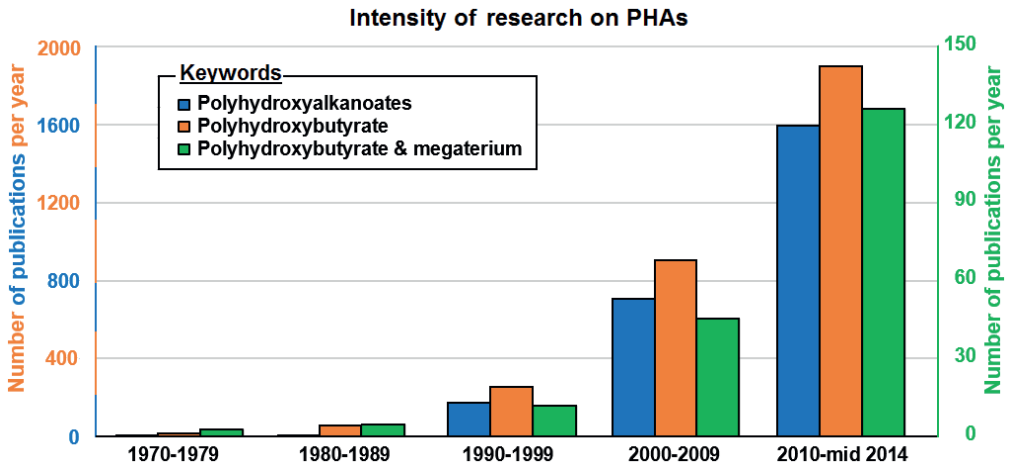


**Figure 2.10: Activity of the research on polyhydroxyalkanoates (PHAs) since 1970 –** The number of scientific publications indexed in Google scholar was used as characteristic indicator for ten years periods from 1970 to 2015. Three different keywords were used for the search: “Polyhydroxyalkanoates” (●), “Polyhydroxybutyrate” (●) and “Polyhydroxybutyrate and *megaterium*” (●).

# 3 Materials and methods

## 3.1 Strains and plasmids

In this work, *Bacillus megaterium* DSM319 was used as model organism to study the impact of osmotic and temperature stress on cell metabolism. Further, it was used as host for several engineered plasmids, striving to improve the production of polyhydroxybutyrate (PHB) in this organism (**Tab. 3.1**). It was obtained from the German collection of microorganisms and cell cultures (DSMZ, Braunschweig, Germany) and stored in M9 minimal medium supplemented with glycerol (20 % v/v) at -80°C.

**Table 3.1: Strains and plasmids used in this work**

| Strain | Description | Reference |
|---|---|---|
| *Bacillus megaterium* DSM319 | Wild type | DSMZ Braunschweig (Braunschweig,Germany) |
| *Escherichia coli* DH10B | F mcrA Δ*(mrr-hsd*RMS-*mcr*BC*)* Φ80d*lacZ*ΔM15 Δ*lac*X74 *deo*R *rec*A1 *end*A1*araD139* Δ*(ara,leu)*7697 *gal*U *gal*K Δ*rps*L *nup*G | Gibco life technologies (Darmstadt, Germany) |

| Plasmid | Specification(s) | Reference |
|---|---|---|
| p3STOP1623hp | Shuttle vector for recombinant production of target proteins driven by the optimised xylose-inducible promoter; $P_{xylA\_opt.}$-mcs | Stammen et al. [12] |
| pRBBm214 | *phaQP* introduced into p3STOP1623hp via SpeI and SacI; $P_{xylA\_opt}$-*phaQP* | This work |
| pRBBm215 | *phaRBC* introduced into p3STOP1623hp via SpeI and SacI; $P_{xylA\_opt}$-*phaRBC* | This work |
| pRBBm216 | *phaQP* introduced into pRBBm215 via SpeI/AvrII and BamHI; $P_{xylA\_opt}$-*phaRBCQP* | This work |
| pRBBm217 | *proHJA* introduced into p3STOP1623hp via SpeI/AvrII and SphI; $P_{xylA\_opt}$-*proHJA* | This work |

## 3.2 Chemicals

All Chemicals used for standard media preparation were obtained from Sigma-Aldrich (Steinheim, Germany) Merck KGaA (Darmstadt, Germany), Carl Roth GmbH (Karlsruhe, Germany). For flux analysis experiments, the labelled compounds were however obtained from Eurisotop® (Saint-Aubin, France).

## 3.3 Growth media

For every cultivation with *B. megaterium* strains, M9 minimal medium derived from Harwood and Cutting (1990) was used and its composition only slightly varied for experiments on osmotic stress and cultivations with plasmid strains (**Tab. 3.2**) [262]. In the first case, additional sodium chloride (0, 0.3, 0.6, 0.9, 1.2 and 1.8 M NaCl) was supplemented to the standard M9 minimal medium to simulate different osmolarities, while in the second inducer xylose and antibiotic tetracycline were added to a final concentration of 5 g $L^{-1}$ and 10 mg $L^{-1}$, respectively. Furthermore, glucose start concentration was adjusted to 20 g $L^{-1}$ for cultivations with strains containing plasmids carrying genes involved in PHB synthesis (pRBBm214, pRBBm215, pRBBm216).

**Table 3.2: Composition of the M9 minimal medium used in this work –** NaCl concentration was varied to simulate different osmolarities. Autoclaved ultrapure water was used as solvent and stock solutions containing salts were autoclaved (121°C, 20 min). Other stock solutions were sterile filtered (Minisart® NML Syringe filters, 0.2 µm pore size, Sartorius stedim, Göttingen, Germany).

| Component | Concentration [g $L^{-1}$] |
|---|---|
| Glucose | 5.00 |
| $KH_2PO_4$ | 3.00 |
| $NH_4Cl$ | 1.00 |
| $Na_2HPO_4$ | 6.70 |
| $FeCl_3$ | $8.11 \cdot 10^{-3}$ |
| $CaCl_2$ | $11.10 \cdot 10^{-3}$ |
| 3,4 DHB | $30.05 \cdot 10^{-3}$ |
| $MgSO_4$ | $120.21 \cdot 10^{-3}$ |
| $ZnCl_2$ | $17.00 \cdot 10^{-4}$ |
| $MnCl_2 \cdot 4H_2O$ | $10.00 \cdot 10^{-4}$ |
| $NaMoO_4 \cdot 2H_2O$ | $60.00 \cdot 10^{-5}$ |
| $CoCl_2$ | $32.80 \cdot 10^{-5}$ |
| $CuCl_2 \cdot 2H_2O$ | $43.00 \cdot 10^{-5}$ |
| NaCl | 0.5 to 105.692 |

## 3.4 Cultivation techniques

### 3.4.1 Shake flasks

For cultivation in shake flasks, a glycerol stock was used as inoculum for a 10 mL pre-culture in M9 minimal medium (100 mL baffled shake flasks). This pre-culture was incubated at 37°C and 230 $min^{-1}$ (Multitron, Infors AG, Bottmingen, Switzerland – 5 cm shaking diameter) until its optical density ($OD_{600nm}$) reached 4, whereafter cells were harvested by centrifugation (13000 $min^{-1}$, 4°C, 5 min, Microcentrifuge 5415R, Eppendorf AG, Hamburg, Germany), washed with fresh medium and used to inoculate at least three biological replicates to an initial $OD_{600nm}$ of 0.1. Each of these replicates consisted of a 500 mL baffled shake flask containing 50 mL M9 minimal medium.

### 3.4.2 Bioreactors

For PHB and proline production, batch reactor cultivations were performed in a parallelised 1 L-bioreactor system (DASGIP®, Jülich, Germany) with a working volume of 700 mL. To have a sufficient inoculum volume, cells from 50 mL shake flask cultures carried as described above were first collected at an $OD_{600nm}$ of 4 and used as inoculum for 1 L-shake flasks containing 100 mL M9 minimal medium ($OD_{600nm}$ = 0.1). Finally, once the optical density of these cultures reached 4, appropriate volumes of cell suspensions were centrifuged and sedimented cells used to inoculate bioreactors to an initial $OD_{600nm}$ of 0.1. Stirrer speed and aeration rate were set at 400 $min^{-1}$ and 6 L $h^{-1}$, respectively, and progressively increased during cultivation using the DASGIP® proprietary control software to maintain dissolved oxygen concentration at around 30 % saturation. In addition, temperature was kept constant at 37°C and pH was adjusted to 7.01 during the whole cultivation using 2 M NaOH. The online measurement of dissolved oxygen concentration and pH relied on an optic sensor Visiferm DO (Hamilton Messtechnik GmbH, Höchst, Germany) and a pH-electrode InPro3250 (Mettler-Toledo GmbH, Gießen, Germany), respectively. To avoid foam formation, sterile-filtered Ucolub (FRAGOL, Mülheim, Germany) was furthermore occasionally added to the growth medium.

## 3.5 Analytical techniques

### 3.5.1 Biomass determination

Cell concentration was recorded as optical density at 600 nm ($OD_{600nm}$) (Libra S11, Biochrome, Cambridge, UK) and converted afterwards in its corresponding biomass concentration using established correlations. Correlation factors between optical density ($OD_{600nm}$) and biomass concentration for the different cultivation conditions were determined gravimetrically. To this end, nylon filters (0.45 µm, Whatman, Dassel, Germany) were first washed with ultrapure water and dried at 105°C until constant weight. Finally, their mass was determined on an analytical balance

(BP210D, Sartorius, Göttingen, Germany). They were then used to filter weighed volumes of cell suspension at given optical densities (duplicate measurements). In order to remove the medium from the cells, the filters were first washed with a sodium chloride solution of same osmolarity as the medium and with ultrapure water directly after. Finally, filters were dried at 105°C once again and cell dry weight was calculated as the difference between filter masses before and after filtration [263]. As reported in **Fig. 3.1**, this study revealed a discrepancy between the correlation factor for cells grown on salty M9 minimal media (0.1917 $g_{CDW}$ $L^{-1}$) and its counterpart factor for cells grown on standard M9 minimal medium (0.2173 $g_{CDW}$ $L^{-1}$). On the contrary, cultivation temperature doesn't seem to impact the correlation factor (0.2154 $g_{CDW}$ $L^{-1}$).

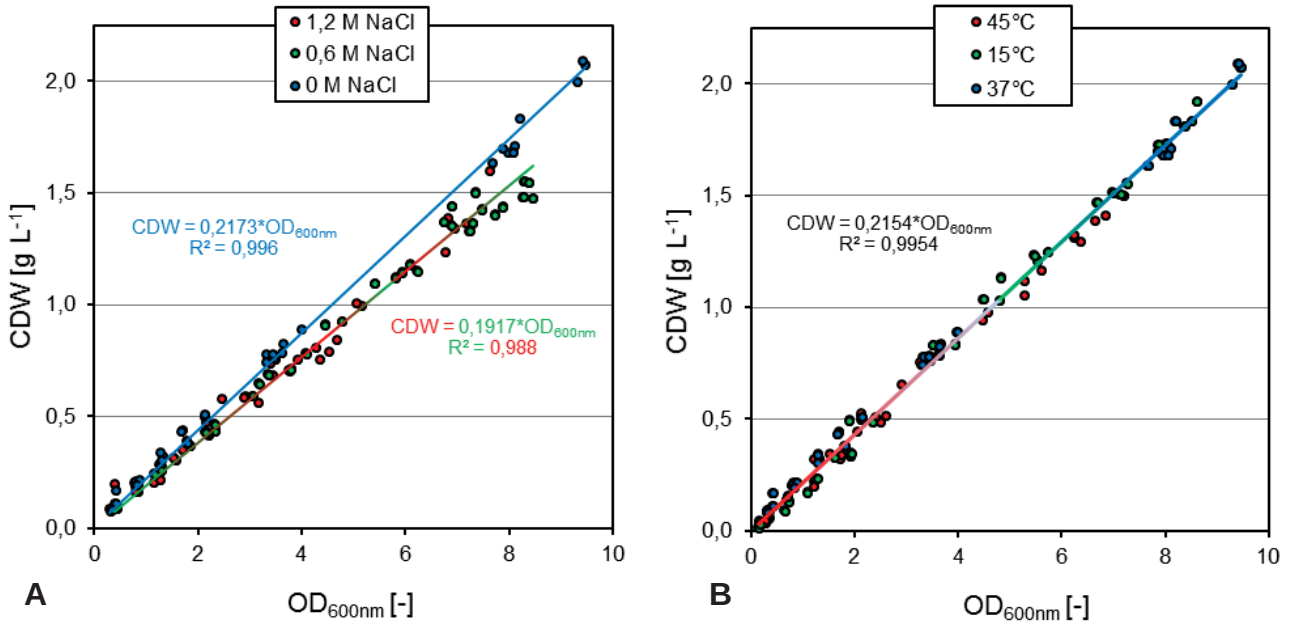


**Figure 3.1: Correlation of optical density ($OD_{600nm}$) and cell dry weight for *B. megaterium* DSM319 grown on M9 minimal medium at different salinities (A) and temperatures (B)**. Optical density was measured photometrically at 600 nm and corresponding cell dry weight was determined gravimetrically by filtering given volumes of cell suspension.

### 3.5.2 Sugars and organics acids

Glucose was quantified enzymatically using a YSI 2700 SELECT™Biochemistry Analyzer (YSI incorporated, Yellow Springs, Ohio, USA), whereas fructose concentrations were determined by HPLC (Hitachi LaChrom Elite, Krefeld, Germany), working with a Metacarb 87C column (300 x 7.8 mm, Varian Inc, Paolo Alto, CA, USA) as the stationary and ultrapure water as the mobile phase. Measurement was operated at 85°C with an isocratic flow of 0.6 mL $min^{-1}$. Substances were detected using their characteristic refractive indices.

For organic acid measurement, the same LaChrom EliteHPLC system was equipped with an Aminex HPX 87H column (300 x 7.8 mm, Bio-Rad, Hercules, CA, USA) at 45°C as stationary phase. A constant 0.5 mL $min^{-1}$ flow of 12 mM $H_2SO_4$ was used as mobile phase. The detection was achieved by UV absorbance at 210 nm.

## 3.6 Transcriptomics

### 3.6.1 Sampling and RNA processing

For transcriptome analysis a culture volume equivalent to 25 $OD_{600nm}$ was sampled in the exponential phase ($OD_{600nm}$ = 4), quickly transfer to ice-cold killing buffer to stop cell metabolism and centrifuged for 5 min at 7500 $min^{-1}$ and 4°C (Biofuge stratos, Heraeus, Hanau, Germany). Killing buffer was then discarded and sedimented cells were immediately frozen in liquid nitrogen and stored at -80°C. Afterwards, sedimented cells were resuspended in 1 mL of lysis buffer and mechanically disrupted with soda-lime glass beads (20 % v/v, 0.038-0.045 mm, Worf Glaskugeln GmbH, Mainz, Germany) in a FastPrep®-24 (3 x 1 min, 6.5 m $s^{-1}$, 4°C, MP Biomedical, Santa Ana, CA, USA) (**Tab. 3.3**).

**Table 3.3: Solutions required for isolation and purification of RNA used in transcriptome analyses –** Ultrapure water was used as solvent and all solutions were autoclaved twice (121°C, 20 min)

| Component | Concentration [mM] |
|---|---|
| **Killing Buffer** | |
| Tris-HCl (pH 7.5) | 20.0 |
| $MgCl_2$ | 5.0 |
| $NaN_3$ | 20.0 |
| **RNA lysis buffer** | |
| Sodium acetate (pH 7.5) | 150.0 |
| Guanidinium thiocyanate | 4.0 |
| *N*-Lauroylsarcosine sodium | 17.0 |
| **10 x DNase buffer** | |
| Sodium acetate (pH 4.5) | 200.0 |
| $MgCl_2$ | 100.0 |
| NaCl | 100.0 |
| **RNA storage buffer** | |
| $Na_2PO_4$ (pH 4.5) | 200.0 |
| EDTA (pH 8.0) | 1.0 |

RNA isolation involved a phenolic extraction with 1 mL Roti-phenol:chloroform:isoamylalcohol (50:48:2), followed by another phase separation with 1 mL chloroform:isoamylalcohol (48:2). After RNA precipitation with 700 µL of 3 M sodium acetate and 1 mL of isopropanol, the precipitated RNA was resuspended in 180 µL of RNA storage buffer and treated for 30 min at 37°C with 30 units of DNase I (Invitrogen, Carlsbad, California, USA) dissolved in 20 µL of 10x DNase buffer (Tab. 3.3).

Purification of the obtained RNA was performed with the innuPREP RNA mini kit following the instructions of the distributor from step 5 (Analytik Jena AG, Jena, Germany). Finally, RNA concentration was determined with a NanoDrop 1000™ (Thermo Fisher Scientific, Waltham, MA, USA) and corresponding RNA integrity number (RIN) was assessed using a bioanalyzer 2100 and RNA 6000 Nano kit (Agilent technologies, Waldbronn, Germany).

### 3.6.2 Microarray analysis

Microarrays were prepared with RNA originating from 4 biological replicates, whose RIN were equal to or greater than 9, and designed for dual labelling. First, 1 µg of RNA from reference and evaluated condition were labelled with two different dyes using the "USL Fluorescent labeling kit" according the supplied instructions (Kreatech, Amsterdam, The Netherlands). After labelling, RNA concentration and dye incorporation rate were determined with the NanoDrop 1000™ for every samples.

For RNA fragmentation and hybridisation, the "Gene Expression Hybridization Kit" from Agilent technologies (Waldbronn, Germany) was used. First, 300 ng labelled RNA from both reference and tested conditions were mixed together and completed with 5 µL of 10 x blocking agent and water to a final volume of 24 µL. Then, 1 µL of 25 x fragmentation buffer was added and the reaction mix was incubated at 60°C for 30 min. Immediately, reaction mixes were supplemented with 25 µL of 2 x hybridisation buffer and placed on ice. Finally, samples were loaded on an Agilent microarray slide (8 x 15 K custom made) comprising 2-3 60 bp DNA probes for each gene of *B. megaterium*. Hybridisation took place for 17 h at 65°C and 10 $min^{-1}$ in a hybridisation oven (Agilent technologies, Waldbronn, Germany). After that, array slides were washed with the gene expression wash buffer kit (Agilent technologies, Waldbronn, Germany). Prepared microarrays were finally scanned using the Agilent C scanner associated to its proprietary softwares Scan Control 8.4.1 and Feature Extraction 10.7.3.1. Generated data were post-processed in R with Bioconductor for statistical analysis, including an estimation of measurement relevance using analysis of variance (ANOVA) and eliminating aberrant values from the analysis (adjusted p-values > 0.5).

## 3.7 Proteomics

Proteome measurements only focused on changes in intracellular protein concentrations, i.e. modification of extracellular proteome was not examined.

### 3.7.1 Protein extraction and quantification

Cells from 3 biological replicates were collected in the mid-exponential phase by centrifugation of complete cell suspensions (50 mL) for 10 min at 7500 $min^{-1}$ and 4°C (Biofuge stratos, Heraeus, Hanau, Germany). Sedimented cells were washed three times with TE-Buffer (10 mM TRIS, 1 mM EDTA, pH 8) to avoid contamination with extracellular proteins. Intracellular proteins were then extracted by mechanical cell disruption in a FastPrep®-24 (3 x 1 min, 6.5 m $s^{-1}$,

4°C, MP Biomedical, Santa Ana, CA, USA) using soda-lime glass beads (20 % v/v, 0.038-0.045 mm, Worf Glaskugeln GmbH, Mainz, Germany). Finally, protein concentration in the extracts was determined using the commercial Roti® Nanoquant solution (Carl Roth GmbH, Karlsruhe, Germany) and following the supplier's guidelines.

### 3.7.2 Protein digestion and purification

Prior to measurement by LC-IMS$^e$, proteins were digested with trypsin and further prepared by stage tip purification. To do so, 100 µg extract were first incubated at 60°C for 45 min with tetraethylammonium bromide (TEAB, Sigma-Aldrich, Steinheim, Germany), tris(2-carboxyethyl)phosphine (TCEP, Life Technologies GmbH, Darmstadt, Germany), sterile filtered water and the RapidGest commercial solution (Waters, Eschborn, Germany) according to the pipetting scheme presented in **Tab. 3.4**. Thereafter, 2 µL of 500 mM Iodoacetamide (IAA, Sigma-Aldrich, Steinheim, Germany) were added to the 100 µL preparation and the solution was incubated in the dark at room temperature for another 15 min. In the meantime, 20 µg of proteomics grade trypsin (Promega, Madison, WI, USA) was dissolved in 100 µL of activation buffer provided by the supplier and activated at 37°C for 15 min as well. Trypsin digestion was then initiated by adding 2.5 µL of activated trypsin to the treated protein extracts and carried out for 5 h at 37°C and 900 $min^{-1}$. Lastly, the RapidGest solution was eliminated from the treated extracts by precipitation for 45 min at 37°C and pH < 2 with 2 µL of trifluoroacetic acid (TFA, Applichem, Darmstadt, Germany) and subsequent centrifugation (3 x 10 min, 4°C, 13200 $min^{-1}$, Microcentrifuge 5415R, Eppendorf AG, Hamburg, Germany).

**Table 3.4: Pipetting scheme for incubation of protein extract prior to digestion with trypsin – IAA**: Iodoacetamide, 1 mg in 10.8 µL of 50 mM TEAB; **RapidGest:** 1 vial (1 mg) in 200 µL of 50 mM TEAB (conc. 0.5 %); **TCEP**: tris(2-carboxyethyl)phosphine, 1 mg in 7 µL of 50 mM TEAB; **TEAB**: tetraethylammonium bromide.

| Protein extract | RapidGest | 1 M TEAB | Water | TCEP | IAA |
|---|---|---|---|---|---|
| 100 µg | 20 µL | 5 µL | 75 µL | 1 µL | 2 µL |

For stage tip purification, the C18 material was added to the column and the tip was cut 5 mm under the material (Luma C-18 3 µ 100 A, Eppendorf AG, Hamburg, Germany). The material was successively washed 3 times with MS-Water (buffer A, 0.1 % acetic acid) and twice with acetonitrile (buffer B, 0.1 % acetic acid) by column centrifugation (5 min, 13200 $min^{-1}$, 4°C, Microcentrifuge 5415R, Eppendorf AG, Hamburg, Germany). The stage tip was then equilibrated with buffer A and the protein extract loaded onto the column. Subsequently, the column was centrifuged once and washed twice with 100 µL of buffer A (5 min, 13200 $min^{-1}$, 4°C, Microcentrifuge 5415R, Eppendorf AG, Hamburg, Germany). The purified protein solution was eluted in a weighed vial using 30 µL of buffer B and completed with 20 µl of $H_2O$ afterwards.

Solution was finally evaporated to 10 µL in a Speedvac (Thermo Fisher Scientific, Waltham, MA, USA), the volume determined gravimetrically and 5 µL yeast alcohol dehydrogenase were supplemented (ADH, 1 pmol $\mu L^{-1}$, Waters, Eschborn, Germany). Sample volume was expanded to 100 µL by addition of sterile filtered water and stored at -80°C until LC-IMS$^e$ measurement.

### 3.7.3 Protein identification and quantification by LC-IMS$^e$

Peptide separation, identification and quantification were completed using a NanoACQUITY™ UPLC™-System (Waters, Milford, MA, USA) coupled to a synapt-G2 mass spectrometer (Waters, Milford, MA, USA). Samples were first loaded at a flow rate of 0.3 µL $min^{-1}$ onto the column (nanoACQUITY™ UPLC™ column, BEH130 C18, 1.7 µm, 75 µm / 200 mm, Waters Milford, MA, USA) with a mixture of 99.9 % (v/v) ultrapure water (Buffer A, 0.1 % (v/v) acetic acid) and 99.9 % (v/v) acetonitrile (Buffer B, 0.1% (v/v) acetic acid), whose composition was incrementally modified to achieve peptide separation (**Tab. 3.5**). Separated peptides were then transferred to the mass spectrometer and ionised by electrospray ionisation (ESI). Detection of the generated ions was finally carried out in "resolution mode" for masses ranging from 50 to 2000 Da and [Glu1]-fibrinopeptide B (GluFib, m/z 785.8426 Da, Sigma, 500 fmol $\mu L^{-1}$ in 50 % (v/v) acetonitrile, 0.1 % (v/v) formic acid) was furthermore infused at a flow rate of 0.5 µL $min^{-1}$ through the fluidics-system of the mass spectrometer every 30 s to perform lock mass gap correction.

**Table 3.5: Method used for the separation of peptides by liquid chromatography (LC) –** Composition of the mobile phase was varied during measurement to achieved separation by gradient elution. **Buffer A**: 99.9 % (v/v) ultrapure water, 0.1 % (v/v) acetic acid; **Buffer B**: 99.9 % (v/v) acetonitrile, 0.1% (v/v) acetic acid. Curve parameters: 8 = convex profile, 6 = linear profile.

| Time [min] | Buffer A [%] | Buffer B [%] | Flow rate [µL·$min^{-1}$] | Curve |
|---|---|---|---|---|
| 0 | 99 | 1 | 0.3 | |
| 31 | 95 | 5 | 0.3 | 8 (convex) |
| 102 | 82 | 18 | 0.3 | 6 (linear) |
| 124 | 74 | 26 | 0.3 | 6 (linear) |
| 140 | 1 | 99 | 0.3 | 6 (linear) |
| 150 | 1 | 99 | 0.3 | 6 (linear) |
| 150.10 | 99 | 1 | 0.3 | 6 (linear) |
| **Stop time** | 165 min | | | |

For data collection, a series of scan measurements were successively performed with low and high energies, increasing progressively the high energy from 25 to 45 V per scan time. Moreover, the ion mobility function was activated, allowing the selection of peptides not only according to their m/z ratio but also on the basis of their rotational cross sections and leading to a considerable increase of the protein identification and quantification rate. Other relevant MS parameters applied are summarised in **Tab. 3.6**.

**Table 3.6: Parameters used for the measurement of peptides by ion mobility spectrometry-mass spectrometry (IMSe) – ESI**: electrospray ionisation; **CE**: collision energy; **IMS**: ion mobility spectrometer.

| Parameter | Setting |
|---|---|
| **Polarity** | positive |
| **Ionisation technique** | ESI |
| **Scan range** | 50 – 2000 Da |
| **Scan time** | 1 s |
| **Low collision energy** | |
| ***Trap CE*** | off |
| ***Transfer CE*** | off |
| **High collision energy** | |
| ***Trap CE*** | off |
| ***Transfer CE*** | Ramp von 25 auf 45 eV |
| **Sample cone-voltage** | 28 V |
| **IMS Wave velocity** | Start 1000 V; End 400 V |
| **IMS Wave height** | 40 V |
| **Capillary voltage** | 2.4 kV |
| **Measurement time** | 150 min |

**Table 3.7: Parameters for IMSe-data processing (left) and peptide identification (right)**

| Parameter | Setting |
|---|---|
| **Peak width** | automatic |
| **MS TOF resolution** | automatic |
| **Lock mass 2-x charge** | 785.8426 |
| **Lock mass window** | 0.25 Da |
| **Limit for low energy scan** | 200 counts |
| **Limit for high energy scan** | 20 counts |
| **Intensity limit** | 750 counts |

| Parameter | Setting |
|---|---|
| **Peptide mass deviation** | automatic |
| **Fragment mass deviation** | automatic |
| **Fragment ions pro peptide** | 1 |
| **Fragment ions pro protein** | 5 |
| **Peptide pro protein** | 1 |
| **Digestion enzyme** | trypsin |
| **Missed cleavage sites** | 2 |
| **False-positive-rate (FDR)** | 5 % |
| **Calibration protein** | ADH1_YEAST |
| **Constant modification** | Carbamidomethyl at cysteine |
| **Variable modifications** | Deamidation of asparagine and glutamine; oxidation of methionine; N-terminal pyrrolidone carboxylic acid |

Collected data were then imported in the ProteinLynx Global Server 2.5.3-Software (PLGS, Waters, Milford, MA, USA) and further processed with the Apex3D-Algorithmus (**Tab. 3.7** - left).

Peptide sequence identification was then performed with the „ion accounting“ algorithm using a randomized *B. megaterium* DSM319 data base comprising all employed laboratory contaminants and the sequence of yeast alcohol dehydrogenase (Tab. 3.7 - right). To ensure statistical relevance, the data were strictly filtered in that only proteins found in at least 2 of 3 biological replicates and 2 of 3 of the corresponding technical replicates were selected for quantification. Subsequently, the determined concentrations were averaged over technical replicates and submitted to a student's t-test ($p < 0.01$) to estimate the significance of detected modifications of protein concentrations.

## 3.8 Metabolomics

In this work, metabolome analyses were restricted to intracellular metabolites of the central carbon metabolism, energy carriers and reducing equivalents. Quantification was carried out based on a differential measurement, where the intracellular metabolome was estimated as the difference between total broth metabolome and extracellular metabolome [264].

### 3.8.1 Sampling and extraction procedure

Prior to sampling, tubes containing 5 mL of pre-cooled methanol (60 % v/v) were prepared for the subsequent quenching of cellular metabolism. Once cultures reached the mid-exponential phase, 1 mL of broth was removed from shake flasks and immediately transferred into a quenching tube within 10 s. In parallel, 1 mL of broth was fast filtered (0.2 µm, Sartorius, Göttingen, Germany) into another quenching tube. Both quenched solutions were then stored in liquid nitrogen until extraction. To guarantee an accurate determination of metabolite concentrations later, dilution volumes for $OD_{600nm}$-measurements as well as volumes of quenching solution, withdrawn and filtered cell suspensions were determined gravimetrically using analytical balances (BP210D, Sartorius, Göttingen, Germany).
Extraction of intracellular metabolites was performed by boiling 500 µL of cell extract with 2.5 mL of 75 % (v/v) ethanol (100°C, 2 min). Moreover, 100 µL of labelled cell extract from *Corynebacterium glutamicum* was added and used as internal standard to correct for metabolite degradation during the extraction process. Extracts were then cooled on ice and freeze-dried under vacuum overnight (Alpha 1-4 Ld, Martin Christ Gefriertrocknungsanlagen GmbH, Osterode am Harz, Deutschland). Finally, lyophilised extracts were resuspended in ultrapure water and cell debris discarded by centrifugation (5 min, 13000 $min^{-1}$, 4°C, Microcentrifuge 5415R, Eppendorf AG, Hamburg, Germany). Supernatants were stored at -80°C until measurement.

### 3.8.2 Quantification by LC-MS/MS

Metabolites originated from three biological replicates were firstly separated by ion exclusion chromatography using a liquid chromatography system (LC, Agilent 1290, Agilent Technologies, Waldbronn, Germany) equipped with a reverse phase column (VisionHT C18 HL,

100 mm × 2 mm I.D., 1.5 µm, Grace, Columbia, MD, United States) and subsequently quantified with a triple quadrupole mass spectrometer (QTRAP 5500, AB Sciex, Darmstadt, Germany) equipped with a TurboIonSpray source. 10 µL of sample was injected to the column and metabolite separation was performed at 50°C using a mixture of 6 mM of aqueous tributylamine solution (Eluent A, adjusted to pH 6.2 with acetic acid) and aqueous acetonitrile solution (50 % v/v) supplemented with 6 mM of tributylamine (Eluent B, adjusted to pH 6.2 with acetic acid) as mobile phase. Composition of this mobile phase was gradually varied along the measurement (**Tab. 3.8**).

**Table 3.8: Gradient profile applied for separation of intracellular metabolites by liquid chromatography –** Composition of the mobile phase was varied during measurement to achieved separation by gradient elution. **Eluent A**: 6 mM aqueous tributylamine, pH 6.2; **Eluent B**: 50% v/v aqueous acetonitrile supplemented with 6 mM tributylamine, pH 6.2.

| Time [min] | Eluent A [% v/v] | Eluent B [% v/v] |
|---|---|---|
| 0.0 | 95.0 | 5.0 |
| 2.0 | 95.0 | 5.0 |
| 22.0 | 10.0 | 90.0 |
| 23.0 | 95.0 | 5.0 |
| 28.0 | 95.0 | 5.0 |

Separated compounds were then introduced at a flow rate of 350 µL $min^{-1}$ into the mass spectrometer (MS) via the turbo ion spray source and detection was completed by multiple reaction monitoring (MRM) with the MS operating in its negative ionisation mode. Besides, the MS was run in unit resolution in order to achieve the best possible selectivity and sensitivity. Regarding the other key MS-parameters, the entrance potential (EP) was set at -10 V, the dwell time was fixed at 5 ms for all transitions, the auxiliary gas temperature was adjusted to 550°C and the source dependent parameters were set as follows: ion spray voltage -4500 V, nebuliser gas (GS1) auxiliary gas (GS2), curtain gas (CUR) and collision gas CAD 60, 60, 35 medium, respectively.

## 3.9 Fluxomics

### 3.9.1 Sampling and labelling analyses of proteinogenic amino acids

In order to restrain sample contamination with unlabelled cells and ensure a biomass labelling grade superior to 99.5 %, both precultures and main cultures were carried out with labelled substrate. Cells were harvested at different sample times along the exponential phase ($OD_{600nm}$ = 2, 4, 6) to prepare 2 mg of sedimented cells by centrifugation (13200 $min^{-1}$, 4°C, 5 min, Microcentrifuge 5415R, Eppendorf AG, Hamburg, Germany). Collected cells were washed twice with matching NaCl solutions and protein hydrolysis was then performed at 105°C for 22 h with

100 µL of 6 M HCl. Cell debris was discarded from hydrolysates afterwards using Ultra-MC centrifugal filter units (Merck KGaA, Darmstadt, Germany).
After collecting hydrolysates from 3 biological replicates, steady state values of proteinogenic amino acid labelling were determined by GC-MS [265]. Prior to measurement, hydrolysates were dried under a nitrogen stream and amino acids were turned into their t-butyl-di-methyl-silyl derivates by incubation at 80°C for 30 min with 50 µL of N-methyl-N-tert-butyldimethylsilyl-trifluoracetamide (MBDSTFA) and 50 µL of 0.1 % pyridine in dimethylformamide (DMF). Derivatised samples were then injected into a GC-MS system for labelling pattern determination (Agilent 7890A and MSD 5979C, Agilent Technologies, Waldbronn Germany). Amino acid separation was performed using Agilent HP5MS capillary column (5 % phenyl-methyl-siloxane diphenypolysiloxane, 30 m x 250 µm) with 1 mL $min^{-1}$ helium as carrier gas and following temperature profile: 120°C for 2 min, 8°C $min^{-1}$ up to 200°C and 10°C $min^{-1}$ until 325°C is reached. Finally, amino acids were ionised by electron ionisation (70 eV), fragmented and detected using a triple quadrupole detector with inlet, interface and quadrupole temperatures set at 250, 280 and 230°C, respectively [266].
Each labelling analysis comprised one measurement in scan mode to check for isobaric fragment overlays. Relative fractions of relevant mass isotopomers were then determined in duplicate in selective ion monitoring (SIM) mode [266]. Steady state labelling pattern was therefore calculated as mean value of 18 measurements for every investigated conditions (3 biological replicates, 3 samples, 2 technical duplicates).

### 3.9.2 Metabolic network and flux calculation

Metabolic reaction network was constructed based on previous flux analysis studies and greatly refined and extended using the KEGG and Metacyc databases and genomic data [17, 267]. Moreover, the inappropriate *E. coli*'s precursor demand, which was used until now, was replaced with a freshly determined one specific to *B. megaterium* and varying in accordance to the studied cultivation conditions (section 3.10, section 4.1.1.2 and **Tab. A.2**) [267, 268]. The final model comprises all major central pathways such as glycolysis (EMP), pentose phosphate pathway (PPP), tricarboxylic acid cycle (TCA) and anaplerotic reactions but also pathways specific to polyhydroxybutyrate (PHB) and proline biosynthesis. Exhausting listing of all included reactions can be found in **Tab. A.3**.
Flux calculation and statistical analysis were implemented in Matlab using the open source software OpenFlux [269]. Required input data were gathered in an excel-sheet containing all reactions with corresponding atom transitions, labelling data, biomass yield and known secretion rates. Labelling data were then automatically corrected for natural isotopes by applying correction matrices and fluxes were finally estimated within a confidence interval of 95 % using a Monte Carlo computational algorithm [269, 270].

## 3.10 Biomass composition and specific precursor demand

As emphasised previously, knowledge of the biomass composition and its specific precursor demand is a prerequisite for the development of a suitable model for flux analysis. Moreover, many studies demonstrated that this composition is a function of miscellaneous parameters such as temperature, pH or medium composition, and thus its determination could provide new insights in cell physiology [210, 271-274].

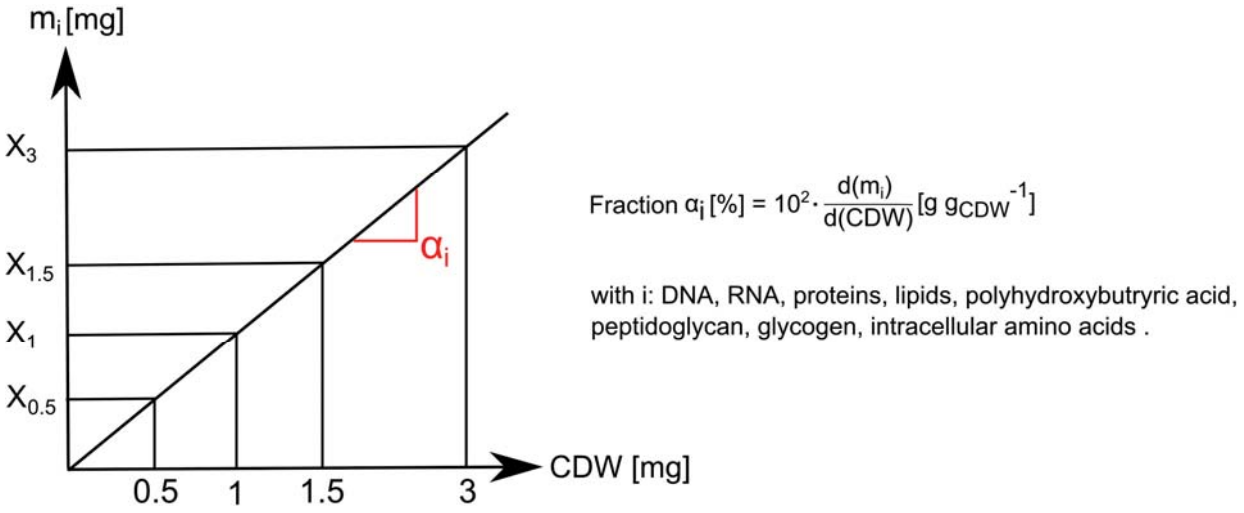


**Figure 3.2: Differential determination of mass fractions of cellular components –** Proteins, DNA, RNA, glycogen, polyhydroxybutyric acid, lipids, peptidoglycan and intracellular amino acids were extracted from different amounts of sedimented cells and their mass quantified. These masses were then plotted against used cell dry weights and the slope of the obtained straight line was taken as fraction $\alpha_i$ of the cell component i in the biomass.

In this work, its determination was carried out for every condition under examination, namely for different medium osmolarities and temperatures (**Fig. A.1**). To do so, 0.5 to 4 mg of sedimented cells were prepared and used for determination of the fraction $\alpha_i$ [%] of each biomass component i (DNA, RNA, protein...) using a trivial differential calculus as described above (**Fig. 3.2**) .

### 3.10.1 Protein content and its amino acid composition

Proteins were extracted from cells as described for proteome analysis (3.7.1) and total content was subsequently assessed using several methods found in common literature, namely Waddell's method, the bicinchoninic acid assay (BCA assay) and a spectrometric measurement at 205 nm [275-277].

For Waddell's method, the absorbance of cell extracts was determined at 215 and 225 nm using a spectrometer V-650 (Jasco, Easton, MD, USA) and the corresponding protein concentration was evaluated using the following equation [278]:

$$\text{Protein concentration [mg L}^{-1}] = (A_{215nm} - A_{225nm}) \cdot 144.$$

The BCA assay was implemented as directed by distributors (BCA protein assay kit, Pierce, Rockford, IL,USA) using bovine serum albumin (BSA) as standard [279].

To limit possible buffer interferences with the measurement, sedimented cells were disrupted with water. Accuracy and variability of the quantification at 205 nm were first tested with several pure protein solutions (BSA, lysozyme, pepsin). As presented in **Fig. 3.3**, absorbance at 205 nm behaves in a very linear and similar manner over a wide concentration range (0 to 80 µg $mL^{-1}$) for the evaluated proteins. Hence, it was assumed that with this method, amino acid composition of proteins has only a very restricted influence on protein determination. Quantification of protein concentration in cell extracts was thus performed with the calibration curve in Fig. 3.3, taking a correlation factor of 37.195 µg $mL^{-1}$ per 1 $A_{205nm}$.

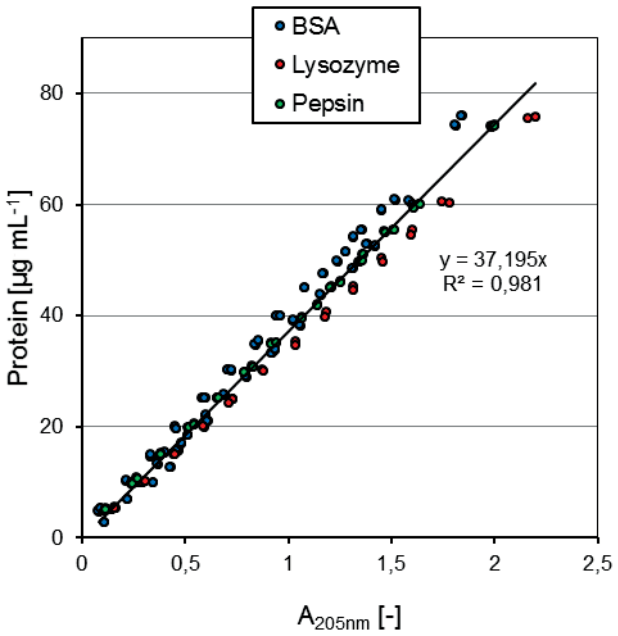


**Figure 3.3: Correlation of protein concentration and absorbance at 205 nm –** Three different proteins were used for the determination: (●) bovine serum albumin (BSA), (●) lysozyme and (●) pepsin. Absorbance was measured using a spectrometer V-650 (Jasco Easton, MD, USA)

Amino acid composition of proteins was evaluated by hydrolysing sedimented cells at 105°C for 24 h and 48 h, respectively, with 6 M HCl supplemented with 0.1% phenol to reduce losses of sensitive residues [280]. Hydrolysates were subsequently evaporated under a nitrogen stream and resuspended in 200 µM α-aminobutyrate, the latter serving as internal standard. Amino acid concentrations in the prepared samples were finally measured by fluorescence detection using an Agilent 1200 HPLC system (Agilent technologies, Waldbronn, Germany) equipped with a reverse phase column Gemini 5µ C18 110 A (150 x 4.6 mm, Phenomenex, Aschaffenburg, Germany) as stationary phase. Separation of the different proteinogenic amino acids relied on a gradual change of the mobile phase composition throughout the measurement, mixing differently eluent A (40 mM $NaH_2PO_4$, pH 7.8) and eluent B (45 % methanol, 45 % acetonitrile, 10 % water) according to a well-defined gradient profile (Tab. 3.9). Moreover, column separation was operated at 40°C with a flow rate of 1 mL $min^{-1}$. In addition, a pre-column (Gemini C18, MAX, RP, 4 x 3 mm, Phenomenex, Aschaffenburg, Germany) was used to increase column life time. Fluorescence detection was achieved through pre-column derivatisation with o-phtalaldehyde (OPA) and 9-fluorenylmethyloxycarbonyl (FMOC) and modification of the excitation and emission wavelength as described in greater detail in **Tab. 3.9** [281]. To account for amino acid losses during hydrolysis,

amino acid composition of proteins was calculated on the basis of the HPLC measurement and then extrapolated to the theoretical concentrations using the previously determined protein content. Here, the percentage of losses was assumed to be the same for every amino acids, except for cysteine, methionine and tryptophan, for which fractions were taken from the literature [268].

**Table 3.9: Method used for separation and quantification of amino acids –** Composition of the mobile phase was varied during measurement to achieved separation by gradient elution. **Eluent A**: 40 mM $NaH_2PO_4$, pH 7.8; **Eluent B**: 45 % methanol, 45 % acetonitrile, 10 % water.

| Time [min] | Eluent A [%] | Eluent B [%] | Excitation λ [nm] | Emission λ [nm] |
|---|---|---|---|---|
| 0 | 100 | 0.0 | 340 | 450 |
| 40.5 | 59.5 | 40.5 | 340 | 450 |
| 41 | 39 | 61 | 340 | 450 |
| 43 | 39 | 61 | 266 | 305 |
| 57.5 | 0.0 | 100 | 266 | 305 |
| 59.5 | 0.0 | 100 | 340 | 450 |
| 60.5 | 25.0 | 75.0 | 340 | 450 |
| 61.5 | 50.0 | 50.0 | 340 | 450 |
| 62.5 | 75.0 | 25.0 | 340 | 450 |
| 63.5 | 100.0 | 0.0 | 340 | 450 |
| 65.5 | 100.0 | 0.0 | 340 | 450 |

### 3.10.2 DNA

To extract DNA content, cell walls were first enzymatically digested in 560 µL of DNA lysis buffer for 30 min (30°C, 350 $min^{-1}$, Thermomixer comfort, Eppendorf AG, Hamburg, Germany) and additionally subjected to mechanical disruption with soda-lime glass beads (20 % v/v, 0.038-0.045 mm, Worf Glaskugeln GmbH, Mainz, Germany) in a FastPrep®-24 (3 x 1 min, 6.5 m $s^{-1}$, 4°C, MP Biomedical, Santa Ana, CA, USA) (**Tab. 3.10**).

**Table 3.10: Composition of DNA lysis buffer (pH 8 adjusted with 6 M NaOH) –** Final solution was sterile filtered (Minisart® NML Syringe filters, 0.2 µm pore size, Sartorius stedim, Göttingen, Germany).

| Component | Concentration [g $L^{-1}$] |
|---|---|
| Tris | 3.03 |
| EDTA | 1.31 |
| Sucrose | 102.70 |
| Lysozyme | $0.50 \cdot 10^{-3}$ |

Extracts were then centrifuged for 5 min at 13200 $min^{-1}$ and 4°C (Microcentrifuge 5415R, Eppendorf AG, Hamburg, Germany) and supernatants were collected and treated for RNA digestion with 140 µL RES solution containing 60 µg $L^{-1}$ of RNase ("Plasmid DNA purification",

Macherey-Nagel, Düren, Germany). Subsequently, the DNA underwent a two-step purification comprising a first separation with 700 µL Roti-phenol-chloroform-isoamylalcohol and a second with 700 µL of chloroform. Both separations were supported by a 10 min centrifugation at 13200 $min^{-1}$ and 4°C (Microcentrifuge 5415R, Eppendorf AG, Hamburg, Germany). The next step involved DNA precipitation with 65 µL of 3 M sodium acetate (pH 5.5) and 1.3 mL of ice-cold pure ethanol. After centrifugation, the supernatants were carefully discarded and precipitated DNA could finally be washed with 70 % ethanol, dried in a vacuum concentrator 5301 (Eppendorf AG, Hamburg, Germany) and solved in 100 µL of ultrapure water. DNA concentration was determined with a NanoDrop 1000™ (Thermo Fisher Scientific, Waltham, MA, USA).

### 3.10.3 RNA

Prior to RNA quantification, sedimented cells were washed once with 1 mL of 700 mM $HClO_4$ and subsequently digested for 80 min at 37°C and 300 $min^{-1}$ (Thermomixer comfort, Eppendorf AG, Hamburg, Germany) with 1 mL of 300 mM KOH. After digestion, cell extracts were cooled on ice and neutralised with 100 µL of 3 M $HClO_4$. Supernatants were then collected (13200 $min^{-1}$, 4°C, 5 min, Microcentrifuge 5415R, Eppendorf AG, Hamburg, Germany) and cell debris washed twice with 450 µL of 500 mM $HClO_4$ to collect remaining RNA and remove precipitate of $KClO_4$ [282]. Supernatants from the washing steps and from the alkaline digestion were finally brought together and as for DNA, intracellular RNA content was quantified by spectrometric measurement at 260 nm with a NanoDrop 1000™ (Thermo Fisher Scientific, Waltham, MA, USA).

### 3.10.4 Polyhydroxybutyric acid (PHB)

To determine PHB content, sedimented cells were hydrolysed for 30 min at 100°C with 1 mL of 2 M NaOH, thus turning PHB granules consecutively into 3-hydroxybutyrate monomers and crotonic acid. Hydrolysates were then neutralised with 1 mL of 2 M HCl and cell debris discarded via centrifugation (13200 $min^{-1}$, 4°C, 5 min, Microcentrifuge 5415R, Eppendorf AG, Hamburg, Germany). Finally, crotonic acid concentration in the supernatant could be quantified with the same HPLC system and configuration as for organic acids (section 3.5.2). Calibration series were obtained by applying the same procedure to pure PHB and diluting the stock solution with water afterwards [283].

### 3.10.5 Intracellular amino acids and potassium

For amino acid quantification, samples with a volume equivalent to 6 $OD_{600nm}$ were taken along the exponential phase and filtered on cellulose nitrate filters (0.2 µm, Sartorius AG, Göttingen, Germany). To avoid contamination with extracellular amino acids, the surrounding medium was removed by washing the filters with a NaCl solution whose concentration matched the ionic strength of the culture medium. Filters were then placed in closed caps with 2 mL of 200 µM of α-aminobutyric acid (ABU) and left for 15 min in boiling water to extract intracellular

metabolites. Lastly, extracts were cooled on ice for 5 min, cell debris discarded by centrifugation (5 min, 13200 $min^{-1}$, 4°C, Microcentrifuge 5415R, Eppendorf AG, Hamburg, Germany) and free amino acid were quantified by HPLC as reported previously in section 3.10.1.
Using the same extraction protocol, intracellular potassium could be quantified with a Dionex-ICS 2000 HPLC system (Thermo Fischer Scientific, Waltham, MA, USA) equipped with a Dionex IonPac CS16 cation-exchange column (3 x 250 mm, Thermo Fischer Scientific, Waltham, MA, USA) and a Dionex CERS 500 suppressor (2 mm, Thermo Fischer Scientific, Waltham, MA, USA). Separation was operated at a column temperature of 40°C using ultrapure water at a constant flow of 0.5 mL $min^{-1}$ as mobile phase. Furthermore, a Dionex IonPac CG16 guard column (3 x 50 mm, Thermo Fischer Scientific, Waltham, MA, USA) was installed to protect analytical column from sample impurities.

### 3.10.6 Lipid fraction and its composition

To estimate the lipid fraction and its composition, 400 mg of biomass obtained from eight biological replicates were freeze-dried (Alpha 1-4 LD, Martin Christ Gefriertrocknungsanlagen GmbH, Osterode am Harz, Germany) und underwent a lipid extraction according to a modified Folch method, involving a chloroform/methanol/acidified salt solution (2:1:0.8) [284]. A fraction from the total lipid extract was used for total lipid fatty acid quantification, whereas the remaining volume was further divided into two fractions for the extraction of polar and non-polar lipids. Non polar lipid were separated by one dimensional thin layer chromatography (1D–TLC) using solvent mix isohexane / diethyl ether / formic acid (75:25:2). Fractions were then removed and a C21:0 internal standard was added before esterification.
In order to separate polar lipid species, another fraction of the total lipid extract was submitted to two dimensional thin layer chromatography (2D–TLC). The implemented solvent system involved chloroform / methanol / water (65:25:4) for the first migration direction and chloroform / methanol / acetic acid / water (80:12:15:4) for the second. Moreover, total lipid extracts were supplemented with C17:0 phosphatidylethanolamine as internal standard before separation. Polar lipid fractions were finally removed from the TLC-plate.
All collected fractions were converted to fatty acid methyl esters (FAME) and subsequently quantified according to the AOCS official method Ce 1b-89 [285]. First, the different fractions were transferred into a screw-cap tube containing 0.5 mg of C23:0 methyl ester internal standard and saponification was performed with 1.5 mL of 500 mM alcoholic sodium hydroxide (100°C, 5 min). The solutions were then cooled, completed with 2 mL of 12 % (w/w) boron trifluoride ($BF_3$) in methanol and incubated anew for 30 min at 100°C. After incubation, the samples were cooled again and the methyl ester extraction was achieved by addition of 1 mL of isooctane and 5 mL of saturated NaCl (360 g $mL^{-1}$). The tubes were gently vortexed and rested until phase separation. The upper isooctane layer was then carefully collected and the bottom phase extracted once again. Finally, corresponding isooctane layers were brought together and concentrated to a final volume of 1 mL under a nitrogen stream.

The concentrates were either stored at -20°C or directly subjected to GC-analysis (**Tab. 3.11**).

**Table 3.11: GC parameters used for the analysis of fatty acid methyl esters**

| Parameter | Setting |
|---|---|
| **Detector temperature** | 300°C |
| **Detector mode** | Constant make up flow |
| **Hydrogen flow** | 40 mL $min^{-1}$ |
| **Air flow** | 450 mL $min^{-1}$ |
| **Make up flow** | 45 mL $min^{-1}$ |
| **Make up gas** | Helium (He) |
| **Injector temperature** | 230°C |
| **Injector mode** | Split |
| **Split ratio** | 50:1 |
| **Injection volume** | 1 mL |
| **Temperature programme** | 170°C for 3 min<br>170-220 at 4°C $min^{-1}$<br>220°C for 10 min |

### 3.10.7 Peptidoglycan layer

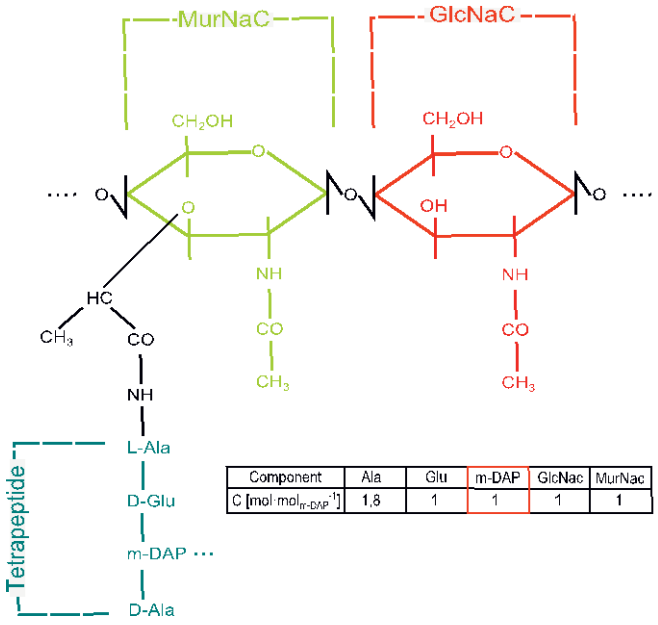


**Figure 3.4: Peptidoglycan monomer and its molar composition – glcNaC:** *N*-acetylglucosamine; **m-DAP:** meso-diaminopimelate; **MurNac**: *N*-acetylmuramic acid

Besides the lipid bilayer, peptidoglycan layer is the second major component of bacterial cell envelopes and also determines the cell shape. It is a polymer in which chains of covalently bound molecules of *N*-acetylglucosamine (glcNac) and *N*-acetylmuramic acid (murNAc) are crosslinked together by two tetrapetides containing mostly L-alanine, D-glutamic acid, *meso*-diaminopimelic acid and D-alanine. The repeating monomer unit in *B. megaterium* can be taken from **Fig. 3.4** [286, 287]. In *B. megaterium*, meso-diaminopimelate (m-DAP) can only be integrated in peptidoglycan or converted to lysine. Hence, considering the molar composition of monomer units and knowing the m-DAP content, the global peptidoglycan content and its corresponding precursor demand can be deduced. In this study, m-DAP concentration was determined from the same biomass hydrolysates as for amino acid composition (section 3.10.1) and corrected using the same percentage of losses. Measurement was carried out by HPLC as described in the section 3.8.1.

### 3.10.8 Glycogen

Glycogen was enzymatically isolated from the cytosol with lysozyme and converted to glucose with amyloglycosidase (59.9 U $mg^{-1}$, Sigma-Aldrich (Fluka), Steinheim, Germany). To this end, sedimented cells were resuspended in 500 µL lysis buffer (**Tab. 3.12**) and incubated at 37°C and 400 $min^{-1}$ for 3 hours (Thermomixer comfort, Eppendorf AG, Hamburg, Germany). Finally, cell extracts were centrifuged (13200 $min^{-1}$, 5 min, 4°C, Microcentrifuge 5415R, Eppendorf AG, Hamburg, Germany) and glucose concentration was determined as described in section 3.5.2.

**Table 3.12: Composition of the lysis buffer used for extraction of glycogen and its enzymatic conversion to glucose –** Final solution was sterile filtered (Minisart® NML Syringe filters, 0.2 µm pore size, Sartorius stedim, Göttingen, Germany).

| Component | Concentration [g $L^{-1}$] |
|---|---|
| Tris | 3.15 |
| Lysozyme | $3.00 \cdot 10^{-2}$ |
| Amyloglucosidase | 1.00 |

## 3.11 Genetic engineering

### 3.11.1 Isolation of genomic DNA from *B. megaterium*

First, a colony from *B. megaterium* DSM319 was used to inoculate 10 mL of LB-medium in a 100 mL shake flask, which was then incubated overnight for 15 h at 37°C and 150 $min^{-1}$ (Multitron, Infors AG, Bottmingen, Switzerland – 5 cm shaking diameter). Then, cells were harvested by centrifugation, the LB-Medium discarded and genomic DNA was extracted and purified using buffers and spin columns from the JETQuick Plasmid-miniprep kit (Genomed GmbH, Löhne, Germany). For this, sedimented cells were resuspended in 250 µL of buffer G1 supplemented with 200 ng lysozyme and cell disruption was carried out for 10 min at 37°C and 750 $min^{-1}$. Following cell lysis, 250 µL of buffer G2 was added to the extract, mixed thoroughly and neutralised with 350 µL of buffer G3. After centrifugation (13200 $min^{-1}$, 5 min, 4°C, Microcentrifuge 5415R, Eppendorf AG, Hamburg, Germany), the supernatant was added onto a Minispin column, which was subsequently centrifuged (13200 $min^{-1}$, 5 min, 4°C, Microcentrifuge 5415R, Eppendorf AG, Hamburg, Germany). Collected fluid was discarded and nucleases were inactivated by addition of 500 µL of buffer GX, followed by a new centrifugation of the column (13200 $min^{-1}$, 1 min, 4°C, Microcentrifuge 5415R, Eppendorf AG, Hamburg, Germany). Recovery tube was emptied, the column filled up with 500 µL buffer G4 and centrifuged for one minute twice. To remove residual ethanol originating from buffer G4, the column was dried for 3 min at 70°C. Genomic DNA was finally eluted from the column with 30 µL of preheated ultrapure water at 70°C and stored in aliquots at -80°C.

### 3.11.2 DNA amplification by polymerase chain reaction (PCR)

In the framework of this thesis, several genes related to PHB and proline biosynthesis were amplified. For each gene, oligonucleotide primers (**Tab. 3.13**) were designed and obtained from Life Technologies (Darmstadt, Germany). Before starting the PCR reaction, the lid and the PCR-machine were preheated at 105 and 98°C, respectively. The reaction mix was then prepared following the pipetting schema from **Tab. 3.14** and included the specific Phusion™ polymerase (Finnzymes, Espoo Finland), which exhibits a proofreading function preventing amplification errors. Lastly, the reaction was initiated and performed according to the temperature programme presented in **Tab. 3.15**.

**Table 3.13: Primers used for amplification of genes involved in polyhydroxybutyrate (PHB) and osmo-dependent proline synthesis –** Restriction sites are indicated in italics.

| Name and direction | Sequence |
|---|---|
| Primer_phaP_rev | acat*gagctccctagg*ttattttacaactgcatattg |
| Primer_phaQ_for | acat*actagt*caaggaggtgaatgAacaatggaaaacaaattctctttttttcg |
| Primer_phaR_for | acat*actagt*caaggaggtgaatgAacaAtggaacagcaaaaagtatttg |
| Primer_phaC_rev | acatga*gctccctagg*ttatttagagcgtttttctag |
| Primer_proH_for | tatca*cctagga*tggatcaaaaacaaaaagttgc |
| Primer_proA*_rev | tatc*agcatgc*ttatcgagtttgtccgtttcc |
| SeqpXylA_for | aagttggtgtttttgaagc |
| SeqpMM1520_rev | gtttgcgcattcacagttctcc |

**Table 3.14: Composition of PCR mix for DNA amplification**

| Component | Amount / Concentration |
|---|---|
| Template, gen. DNA (*B. megaterium* DSM319) | 200 ng |
| 5 x Phusion™ HF Reaction Buffer | 4 µL |
| Primers | 10 pmol each |
| dNTPs | 200 µM |
| Phusion™ polymerase | 400 mU |
| $H_2O_{dei}$ | ad 20 µL |

**Table 3.15: PCR temperature programme for DNA amplification**

| Temperature | Time | Cycle | Phase |
|---|---|---|---|
| 98°C | 30 s | 1 | DNA denaturation |
| 98°C | 10 s | | DNA denaturation |
| 55°C | 20 s | 30 | Primer annealing |
| 72°C | 80-100 s | | Elongation |
| 72°C | 10 min | 1 | Final elongation |

### 3.11.3 DNA digestion and fragment separation by gel electrophoresis

Generated PCR products were purified using the QIAquick PCR purification kit (Quiagen, Hilden, Germany) following the instructions except that DNA was eluted with water at 70°C. Purified PCR products were subsequently digested overnight at 37°C with appropriate restriction enzymes purchased from New England Biolabs (NEB, Ipswic, MA, USA) and subsequently separated by gel electrophoresis. To this end, PCR products as well as the commercial GeneRuler™ DNA ladder mix (Thermo Fischer Scientific, Waltham, MA, USA) were loaded on a gel composed of 1 % (w/v) agarose in TAE buffer (40 mM TRIS-acetate, 1 mM EDTA, pH 8), which was then subjected to an electric field of 100 V. After 45 min electrophoresis, DNA fragments migrated separately on the gel with a velocity proportional to the negative logarithm of their length and the gel was finally dyed for 30 min with GelStar™ Nucleic Acid Gelstain (Lonza, Cologne, Germany).

### 3.11.4 Purification of DNA fragments and ligation reaction

After the staining, DNA detection was performed on a blue light Transilluminator™ (Life Technologies, Darmstadt, Germany). DNA fragments of interest were detected, excised from the gel with a scalpel and purified with the QIAquick Gel Extraction Kit (Qiagen, Hilden, Germany) following the supplier's protocol, except that DNA was eluted with water at 70°C. For the ligation reaction, insert and vector were added in a ratio of 5:1 and the mix was completed to an end volume of 20 µL with 200 U T4 ligase and 10x buffer (NEB, Ipswich, MA, USA). Reaction mix was finally incubated for 1 h at 17°C and the ligation solution was further used for transformation of competent *E. coli* cells.

### 3.11.5 Production and transformation of competent *E. coli* cells using $CaCl_2$

*E. coli* DH10B cells from a single colony were used as inoculum for a culture tube containing 5 mL of LB-medium, incubated overnight (37°C, 200 $min^{-1}$) and finally harvested by centrifugation (13200 $min^{-1}$, 4°C, 5 min, Microcentrifuge 5415R, Eppendorf AG, Hamburg, Germany). Cell pellet was then resuspended in fresh LB-medium and used to inoculate a 100 mL main culture with a start optical density $OD_{600nm}$ of 0.01. Culture was incubated at 37°C and 250 $min^{-1}$ (Multitron, Infors AG, Bottmingen, Switzerland – 5 cm shaking diameter) and cells were collected by centrifugation (7500 $min^{-1}$, 4°C, 5 min, Biofuge stratos, Heraeus, Hanau, Germany) once it reached an optical density of 0.8. After removal of the supernatant, 10 mL resuspension buffer (10 mM $CaCl_2$, 10 % (w/v) glycerol) was added and cell suspension was thoroughly vortexed and incubated on ice for 15 min. Lastly, competent cells were collected by centrifugation, resupended in the same buffer and stored in aliquots at -80° until transformation.
For the transformation, 50 µL of competent *E. coli* cells were mixed with 5 µL of the ligation solution (section 3.11.4). Subsequently, cell suspension was successively placed on ice for 20 min,

incubated at 42°C for 45 s and cooled down on ice for 2 min. Cells were then regenerated by incubation in 300 µL LB-medium at 37°C and 750 $min^{-1}$ for one hour. Halfway through regeneration, resistance was furthermore induced by adding ampicillin to an end concentration of 100 µg $mL^{-1}$. Finally, transformed cells were streak out on a LB agar plate with the same ampicillin concentration and incubated overnight at 37°C.

### 3.11.6 Preparation of plasmid DNA from *E.coli*

Plasmid DNA from *E. coli* was prepared following two alternative protocols. To obtain high plasmid DNA for analysis, 5.5 mL of LB-Medium containing 100 µg $mL^{-1}$ ampicillin was inoculated with an *E. coli* DH10B colony carrying the plasmid of interest and incubated overnight at 37°C and 200 $min^{-1}$. Bacterial cells were then collected by centrifugation (13200 $min^{-1}$, 4°C, 5 min, Microcentrifuge 5415R, Eppendorf AG, Hamburg, Germany) and resuspended in 300 µL of buffer B1 (**Tab. 3.16**). Subsequently, the cell suspension was supplemented with 300 µL of buffer B2 and incubated for 2 min at room temperature. Proteins were then precipitated by adding 300 µL of buffer B3 and further eliminated by centrifugation (13200 $min^{-1}$, 30 min, Microcentrifuge 5415R, Eppendorf AG, Hamburg, Germany). The supernatant was transferred to a new tube and the addition of 600 µL isopropanol conduced to DNA precipitation. Precipitated DNA was collected by centrifugation (13000 $min^{-1}$, 15 min, Microcentrifuge 5415R, Eppendorf AG, Hamburg, Germany) and washed with 400 µL of 70 % (v/v) ethanol. Ethanol was afterwards evaporated to dryness at 75°C in a thermoblock (Thermomixer comfort, Eppendorf AG, Hamburg, Germany) and DNA pellet was resuspended and dissolved at 70°C in 50 µL of ultrapure water.
The second protocol involved the use of the mini Prep Kit (QIAgen, Hilden, Germany) and was carried out according to the supplier's instructions to obtain high quality plasmid DNA. This purified plasmid DNA was sent to GATC Biotech AG (Konstanz, Germany) for sequencing to verify the DNA fragments of interest. Sequencing reactions was carried out using primers seqpXylA_for and seqpMM1520_rev, respectively, and sequencing results were analysed with an in-house software (DNA Star, GATC Biotech, Konstanz, Germany). The plasmid DNA could either be directly used for protoplast transformation of *B. megaterium* or stored at -20°C for a long period of time.

**Table 3.16: Buffer solutions for plasmid DNA preparation –** All solutions were autoclaved (121°C, 20 min)

| | |
|---|---|
| **Buffer B1** | 50 mM Tris-HCl, pH = 8 |
| | 10 mM EDTA, pH = 8 |
| | 100 mg $L^{-1}$ RNAse A |
| **Buffer B2** | 200 mM NaOH |
| | 1 % (w/v) SDS |
| **Buffer B3** | 3 M $CH_3COOK$, pH = 5.5 |

### 3.11.7 Production and transformation of *B. megaterium* protoplasts

A flask containing 50 mL of LB medium was inoculated with a single colony of *B. megaterium* DSM319 and incubated overnight at 37°C and 100 $min^{-1}$ (Multitron, Infors AG, Bottmingen, Switzerland – 5 cm shaking diameter). On the next day, 1 mL from this culture was used as inoculum for a 50 mL main culture, which was incubated at 37°C and 250 $min^{-1}$ (Multitron, Infors AG, Bottmingen, Switzerland – 5 cm shaking diameter). Once this culture reached an $OD_{600nm}$ of 1, cells were separated from the LB medium by centrifugation (3,000 x g, 10 min, RT, Biofuge stratos, Heraeus, Hanau, Germany), resuspended in 5 mL fresh SMMP solution and transferred to a 15 mL tube. Subsequently, 100 µg $mL^{-1}$ of lysozyme was added and the suspension was finally incubated for 20 min at 37°C. Protoplast formation and quality was assessed using a microscope. Thereafter, protoplasts were collected by soft centrifugation (1,300 x g, 10 min, RT, Biofuge stratos, Heraeus, Hanau, Germany). Lastly, protoplasts were washed once with 5 mL of SMMP solution and resuspended in 5 mL of SMMP. The protoplast suspension was supplemented with 750 µL of 87 % (v/v) glycerol and stored in 500 µL aliquots at -80°C.
For protoplast transformation, one 500 µL of aliquot was carefully mixed with 5 µg plasmid DNA and added to 1.5 mL PEG-P solution in a 15 mL tube (**Tab. 3.17**).

**Table 3.17: Composition of PCR mix for DNA amplification –** Autoclaved ultrapure water was used as solvent and prepared stock solutions were either autoclaved (121°C, 20 min) or sterile filtered (Minisart® NML Syringe filters, 0.2 µm pore size, Sartorius stedim, Göttingen, Germany).

| Solution | Component | Concentration [g $L^{-1}$] |
|---|---|---|
| **SMMP** | Antibiotic medium n°3 | |
| | *Difco, BD, Heidelberg, Germany* | 17.50 |
| **SMM (pH 6.5)** | Maleic acid | 0.58 |
| | $MgCl_2 \cdot 6H_2O$ | 1.02 |
| | NaOH | 0.40 |
| | Sucrose | 42.79 |
| **PEG-P** | PEG 6000 in 1 x SMM (pH 6.5) | 400.00 |
| **CR5 top-agar** | L-proline | 6.00 |
| | D-glucose | 10.00 |
| | Sucrose | 103.00 |
| | MOPS | 6.50 |
| | NaOH | 0.60 |
| | Agar | 4.00 |
| | Casamino acids | 0.20 |
| | Yeast extract | 10.00 |
| | $K_2SO_4$ | 0.23 |
| | $MgCl_2 \cdot 6H_2O$ | 9.22 |
| | $KH_2PO_4$ | $46.08 \cdot 10^{-3}$ |
| | $CaCl_2$ | 2.03 |

The solution was then incubated for 2 min at room temperature, supplemented with 5 mL SMMP solution and gently mixed. Protoplasts were collected by centrifugation (1,300 x g, 10 min, RT, Biofuge stratos, Heraeus, Hanau, Germany) and resuspended anew in 500 µL of SMMP solution. This cell suspension was first incubated for 45 min at 30°C without shaking and then for 45 min more at 30°C and 300 $min^{-1}$. The suspension was completed with 2.5 mL pre-heated CR5-Topagar, mixed gently and plated on a LB agar plate containing 10 µg $mL^{-1}$ of tetracycline (Tab. 3.17). After an overnight incubation at 30°C, colonies found on the plate were streak out on a new LB-agar plate containing 10 µg $mL^{-1}$ tetracycline and incubated at 37°C for up to 24 h as well.

# 4 Results and discussion

## 4.1 System-wide analysis of adaptation to harsh temperatures

*B. megaterium*, like other soil bacteria, is exposed to daily and seasonal temperature variations and its survival relies on its capacity to adapt rapidly to these changing conditions. Besides improving basic knowledge of bacterial life, comprehending mechanisms involved in adaptation to cold and heat is of particular interest because several present biotechnological issues are temperature-related. In particular, enzyme stability is still the limiting factor in many current bioprocesses and development of enzymes whose activity is less affected by temperature is a central objective of modern biotechnology [288]. Cold-adapted enzymes are for instance appealing for simultaneously reducing energy consumption and increasing efficiency of bioremediation and laundry processes [289]. In the food industry, they would further reduced contamination risks during enzymatic modification of products. Moreover, use of cold-adapted enzymes would increase performance and viability of processes where stability of substrate or products is enhanced at low temperature (e.g. deoxyviolacein) [290, 291]. Heat-adapted enzymes, on the other hand, are interesting for modifying reaction equilibrium and minimising side reactions [292, 293]. In addition, biotechnological production using heat-adapted bacteria also minimises the risks of contamination by others microorganisms, thus reducing sterilisation costs.

In this work, adaptation to cold and heat was investigated by culturing *B. megaterium* at temperature between 15 and 45°C. To unravel relevant adaptive mechanisms, cells originating from at least three biological replicates were furthermore collected within the exponential phase at 15, 37 and 45°C, respectively, and used for transcriptome, proteome, metabolome and fluxome analyses using 37°C as reference.

### 4.1.1 Physiological modifications induced by cold and heat stress in *B. megaterium*

At first, the impact of temperature on cellular metabolism was assessed by determining all relevant growth parameters ($\mu$, $Y_{X/S}$, $Y_{P/S}$, $q_S$) and secretion rates of organic acids at temperatures ranging from 15°C to 45°C using shake flask experiments. Additionally, cells were collected within the exponential phase to determine the macromolecular composition of *B. megaterium* at 15, 37 and 45, respectively. This encompassed the evaluation of protein, DNA, RNA, fatty acid, intracellular amino acid, polyhydroxybutyric acid (PHB), glycogen and peptidoglycan contents.

### 4.1.1.1 Growth characteristics and by-product secretion

Bacterial growth is the result of a succession of interconnected biochemical reactions. Hence, its temperature dependence can be described by a modified Arrhenius equation, in which activation energy is replaced by specific growth rate μ [294]. Plotting $\mu = f(T^{-1})$, determination of a linear domain corresponding to physiological growth temperatures is possible [295].

#### *Extreme temperatures have detrimental effects on cell growth and physiology*

For *B. megaterium* DSM319 growing in M9 minimal medium, the modified Arrhenius plot indicates that the physiological domain approximately lies between 15 and 42°C, being in good accordance with previous studies carried out with other *B. megaterium* strains (**Fig. A.2**) [294, 296]. Within this temperature range, biomass yield remained largely constant while specific growth rate increased with temperature (**Tab. 4.1**) [297].

**Table 4.1: Physiological data for *B. megaterium* DSM319 growing at different temperatures on M9 minimal medium** – Bold numbers indicate maximal yield observed for each measured organic acids.

| Parameter | Unit | 15°C | 25°C | 30°C | 37°C | 45°C |
|---|---|---|---|---|---|---|
| μ | $h^{-1}$ | 0.15 ± 0.00 | 0.60 ± 0.01 | 0.87 ± 0.01 | 1.19 ± 0.02 | 0.65 ± 0.01 |
| $Y_{X/S}$ | $g_{CDW}$ $mol^{-1}$ | 71.2 ± 0.7 | 88.5 ± 1.9 | 88.9 ± 1.2 | 79.5 ± 1.2 | 50.0 ± 1.0 |
| $q_s$ | mmol $g_{CDW}^{-1}$ $h^{-1}$ | 2.1 ± 0.0 | 6.8 ± 0.2 | 9.8 ± 0.2 | 15.0 ± 0.3 | 13.1 ± 0.3 |
| $Y_{Acetate / S}$ | mmol $mol^{-1}$ | 422 ± 5 | 479 ± 25 | 494 ± 18 | 669 ± 26 | **958 ± 17** |
| $Y_{Pyruvate / S}$ | mmol $mol^{-1}$ | **154.0 ± 4.6** | 91.9 ± 2.6 | 73.6 ± 2.4 | 6.37 ± 0.3 | 0 ± 0 |
| $Y_{Lactate / S}$ | mmol $mol^{-1}$ | 1.8 ± 0.1 | 2.5 ± 0.2 | 3.0 ± 0.5 | 4.4 ± 0.3 | **15.0 ± 0.6** |
| $Y_{Succinate / S}$ | mmol $mol^{-1}$ | 4.2 ± 0.5 | 11.9 ± 0.6 | 16.2 ± 2.2 | 60.8 ± 2.7 | **99.7 ± 2.2** |
| $Y_{Oxoglutarate / S}$ | mmol $mol^{-1}$ | **26.2 ± 1.1** | 3.1 ± 0.1 | 8.0 ± 0.2 | 9.7 ± 0.4 | 10.9 ± 0.3 |

On the contrary, at temperatures above or below this range, growth was impaired because either the enzymatic or the transport machinery was disrupted and cells had to developed adequate strategies to survive. This was the case for cultivations at 45°C, where the positive effects of temperature on kinetics were abolished and unbalanced growth took place (Tab. 4.1). At this temperature, protein aggregation, denaturation and/or degradation prevailed and led to a strong reduction of specific growth rate. Moreover, absorbed glucose was preferentially converted to acetate and other organic acids by overflow reactions, resulting thereby in a significant drop in biomass yield and pH levels (Fig. 4.1 and Tab. 4.1).

Despite standing closer to the range of physiological temperatures in the modified Arrhenius plot, 15°C triggered evident metabolic perturbations as well (Fig. A.2). Indeed, as a consequence of membrane stiffening and the associated loss of substrate affinity with decreasing temperatures, the glucose uptake was very low and restricted growth as well as biomass production (**Fig. 4.1** and Tab 4.1) [173]. To compensate for this, *B. megaterium* DSM319 activated various

mechanisms including for instance a targeted desaturation of membrane fatty acids (see section 4.1.1.2).

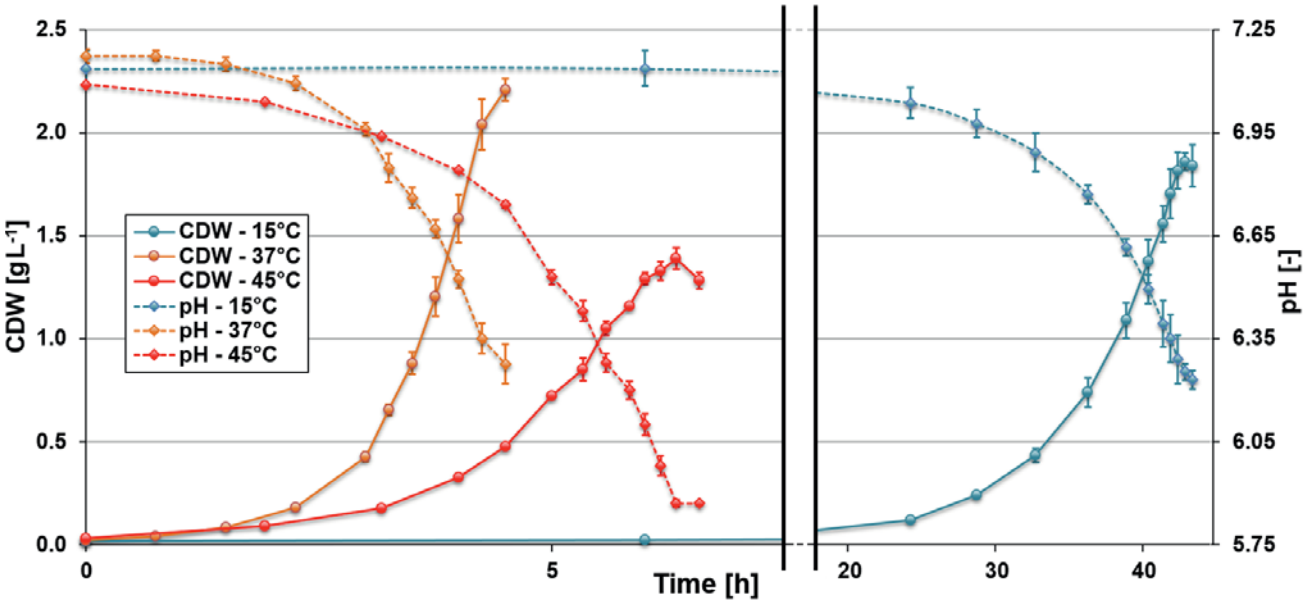


**Figure 4.1: Time course of biomass and medium pH for cultivations of *B. megaterium* DSM319 grown at different temperatures in M9 minimal medium** – Solid and dotted lines represent biomass and pH profiles at 15°C (blue), 37°C (orange) and 45°C (red), respectively.

### *Cellular redox state affects activity of the Pox route and secretion of acetate at 45°C*

The production of acidic by-products when glucose is in excess has long been documented for cells growing aerobically at 37°C [298, 299] and is mainly due to a discrepancy between intracellular glucose availability and growth requirements [300]. However, since the incoming glycolytic flux at 45°C was slightly decreased compared to 37°C, the higher acetate yield at this temperature must result from other metabolic aspects (Tab. 4.1). Interestingly, as determined from the transcriptome and proteome analyses, this increase in acetate concentration compared to 37°C coincided with a 10-fold increased production of pyruvate oxidase (Pox) and a 3.5-fold stronger expression of the corresponding gene *bmd_1311* at 45°C (**Fig. 4.2**). In that sense, Wittmann et al. [301] have suggested that increased acetate accumulation at 42°C in *E. coli* could be imputed to the utilisation of the Pox route to circumvent the limiting pyruvate dehydrogenase (Pdh) when the incoming glycolytic flux is high [302, 303].

The intensifying acetate secretion with increasing temperature and glucose uptake detected between 15 and 45°C as well as the slightly higher concentrations of acetate kinase (AckA) and phosphate acetyltransferase (Pta) recorded at 45°C also support this hypothesis (Tab. 4.1 and Fig. 4.2). Furthermore, the transcriptome and proteome data suggest that the enhanced acetate secretion ensuing from this shift was at least partly due to the lack of increased recycling by acetyl-CoA synthase (Fig. 4.2). As mentioned previously, the glycolytic flux at 45°C was slightly lower compared to 37°C and cannot account for the stronger activation of the Pox route. On the

contrary, a clue might be given by Moreau [304] who indicates that *E. coli* cells shift pathway utilisation from Pdh ($NAD^+$ dependent) to Pox ($NAD^+$ independent) to actively reduce oxidative stress by limiting the production of NADH, whose oxidation by NADH dehydrogenases produces $H_2O_2$ and other reactive oxygen species. In accordance with these results, Vemuri et al. [305] have demonstrated that acetate production is positively correlated with the redox ratio ($NADH/NAD^+$). Moreover, it is known that high NADH concentrations and reactive oxygen species (ROS) inhibit or damage Pdh and could thus foster a rerouting of the carbon flux towards acetate under oxidative or reductive stress [306-308]. Considering the high glycolytic flux, redox ratio and NADH dehydrogenase levels detected in *B. megaterium* grown at 45°C, it is reasonable to assume that the redox state of cells induced this shift from Pdh to Pox for both bypassing the Pdh and reducing ROS production (Tab. 4.1 and **Tab. 4.2**). The transcriptome data further suggest that this shift was mediated by the global regulator SigB which certainly controls the expression of gene *bmd_1131* encoding Pox, thus supporting recent prediction obtained by the BacillusRegNet database [309]. Paradoxically, conversion of pyruvate by Pox also generates $H_2O_2$ but studies in *Streptococcus pneumonia* have shown that this activity confers increased resistance against higher concentrations of $H_2O_2$ [310].

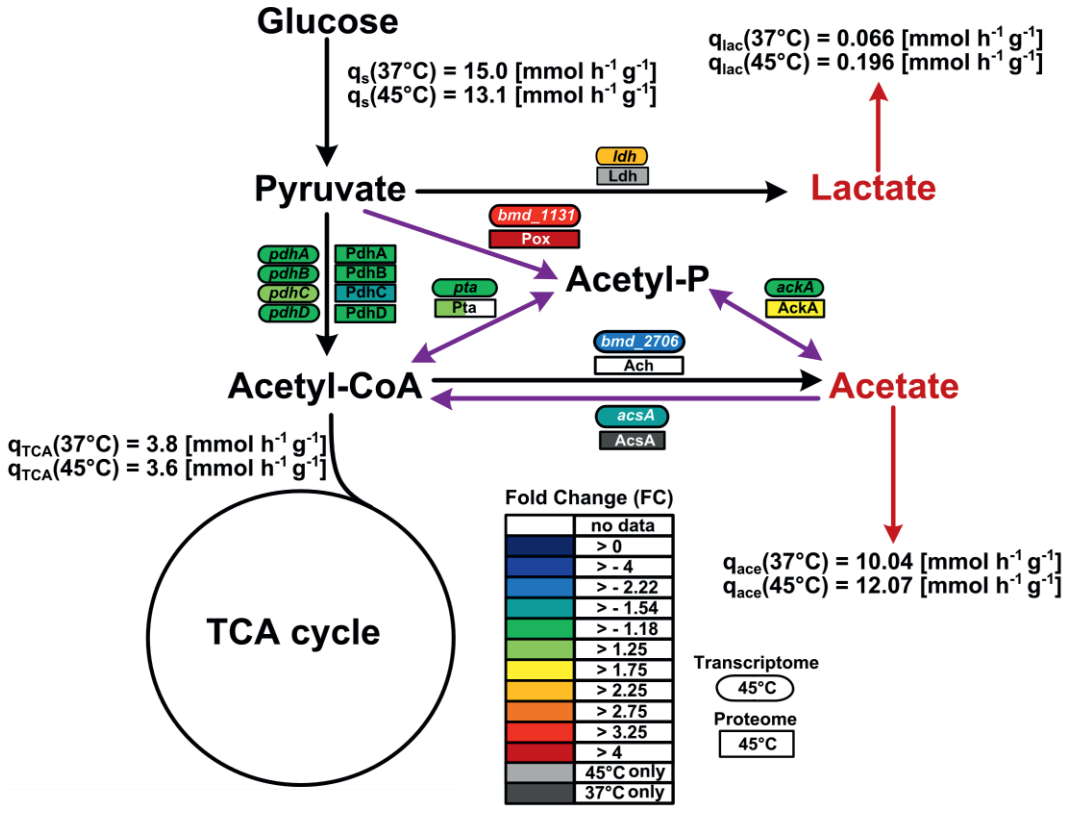


**Figure 4.2: Pox route and overflow metabolism in *B. megaterium* DSM319 growing at 45°C compared to 37° in M9 minimal medium –** Purple arrows correspond to reactions of the Pox route while red arrows indicate organic acid secretion. Gene expression was determined by microarray analysis using purified RNA samples obtained from four biological replicates and is indicated as fold change compared to expression at 37°C. Intracellular proteins were identified and quantified by proteome analysis using LC-IMS$^e$. **Ach**: acetyl-CoA hydrolase; **AckA**: acetate kinase; **AcsA**: acetyl-CoA synthetase; **Ldh**: lactate dehydrogenase; **Pdh**: pyruvate dehydrogenase; **Pox**: pyruvate oxidase; **Pta**: phosphate acetyltransferase.

**Table 4.2: Energy charge and redox state values of *B. megaterium* growing at different temperatures.**

| | Range | 15 °C | 37 °C | 45 °C |
|---|---|---|---|---|
| Adenylate energy charge (AEC) | > 0.7 | 0.8805 | 0.8336 | 0.8358 |
| NADH/$NAD^+$ | < 0.1 | 0.0071 | 0.0079 | 0.0244 |
| NADPH/$NADP^+$ | < 1.4 | 0.8068 | 0.5162 | 0.5736 |

### *Lactate production and recycling is apparently mediated by the redox ratio at 45°C*

The redox ratio might furthermore be responsible for the high induction of the expression of the gene encoding lactate dehydrogenase (*ldh*) and for the higher lactate concentration observed at 45°C (Tab 4.1 and Fig. 4.2). Indeed, synthesis of lactate from pyruvate is accompanied by the oxidation of NADH to $NAD^+$ and could be an additional way to fight against oxidative stress while recycling $NAD^+$ necessary for the glycolysis at the same time (4.1.3.1). Previous works on oxidative stress as well as the detected emergence of lactate dehydrogenase (Ldh) in the intracellular protein fraction of cells grown at 45°C support this hypothesis (Fig. 4.2) [311-313]. In addition, an up to 8-fold stronger expression of *bmd_1224, bmd_1225* and *bmd_1226*, three genes whose products are similar to proteins involved in lactate utilization in *B. subtilis*' (LutABC - previously YvfV, YvfW and YvbY), was observed (**Tab. A.4**) [314]. The function of those genes must be further investigated and confirmed for *B. megaterium*. Nevertheless, it could be speculated that these proteins are also involved in lactate consumption and used to recycle lactate at 45°C. The 1.75-fold increased expression of *lctP*, a gene encoding a lactate permease, would possibly back up this hypothesis. In *B. subtilis*, it is not clear whether the conversion of lactate to pyruvate by these enzymes is coupled to the reduction of $NAD^+$. If not, it could form together with Ldh a cycle for efficiently adjusting NADH to $NAD^+$-ratio under stressful conditions.

### *Enhanced utilisation of PTS-systems results in strong secretion of pyruvate at 15°C*

A striking feature that underlines the suboptimal metabolic activity at 15°C is the 24-fold increased production yield for pyruvate compared to 37°C (Tab. 4.1). Given the poor efficiency of glucose transport at low temperature, it is tempting to assume that conversion of phosphoenolpyruvate to pyruvate was intensified at 15°C to improve glucose uptake by phosphotransferase systems (PTS) and that despite the very small glucose uptake, a bottleneck appeared at the pyruvate node. In addition, activity of the pyruvate dehydrogenase should be significantly reduced at low temperatures, favouring the emergence of such a bottleneck. Other results from metabolic flux analysis supporting this theory for *B. megaterium* are discussed in section 4.1.2.

Interestingly, despite this apparent waste of carbon through pyruvate secretion, the Pox route was not transcriptionally activated at 15°C. In this context, the fact that the redox ratio (NADH/$NAD^+$)

remained quite normal and the absolute glycolytic flux very low, tends to confirm that those parameters are key regulators of this route. In contrast to heat, the reduced acetate production at 15°C corroborates, to a certain extent, the postulate that increased acetate secretion is a side effect of the utilization of this route (Tab 4.1 and 4.2) [315]. Further, the conversion of glucose to 2-oxoglutarate was 2.7-fold increased at 15°C and might suggest that accumulation of pyruvate and 2-oxoglutarate at this temperature is supported by a dysfunction of the dihydrolipoamide dehydrogenase, an enzymatic component (E3) that is common to both pyruvate dehydrogenase and 2-oxoglutarate dehydrogenase (Tab. 4.1).

### 4.1.1.2 Cellular composition and membrane alterations

Cellular composition is highly variable and a function of growth medium (complex or minimal) and physical parameters such as temperature, pH and pressure, that affects nutrient supply and growth rate. **Fig 4.3** shows the modification of the protein, DNA, RNA, fatty acid, intracellular amino acid, PHB, glycogen and peptidoglycan contents as determined for *B. megaterium* growing in M9 minimal medium at 15, 37 and 45°C, respectively.

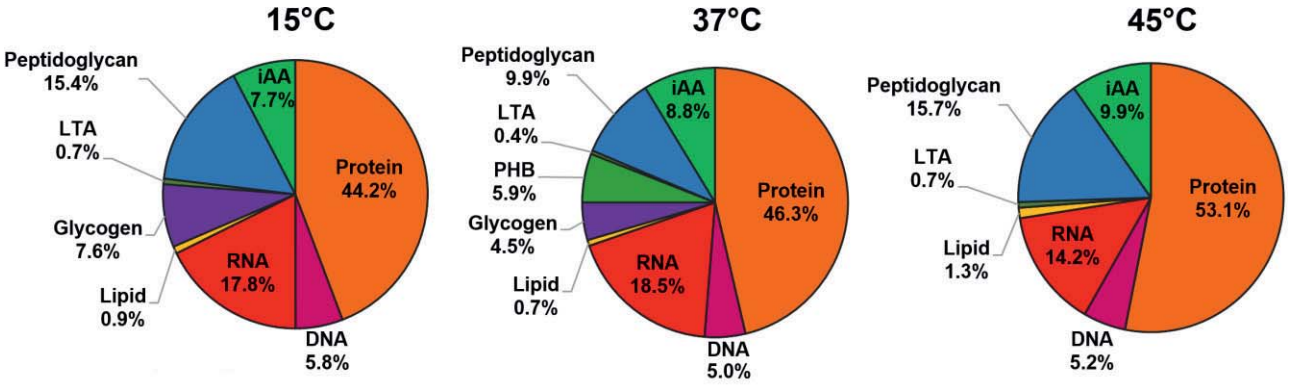


**Figure 4.3: Macromolecular composition of *B. megaterium* DSM319 growing in M9 minimal medium at 15, 37 and 45°C, respectively –** Protocols used for the determination of each cellular component are described in section 3.10. **DNA:** deoxyribonucleic acid, **iAA:** intracellular amino acids, **LTA:** lipoteichoic acids, **PHB:** polyhydroxybutyrate, **RNA:** ribonucleic acid.

#### *DNA, RNA and proteins*

As expected, DNA content in *B. megaterium* grown at different temperatures was hardly altered and took values between 5-6 % of the biomass at all three temperatures. Despite the slower growth rate at 15°C, both the RNA and protein contents remained mostly unchanged compared to their values at 37°C with around 18 and 45 % of cell biomass, respectively, which certainly bodes for a strong production of cold shock proteins [155, 271]. On the contrary, a notable reduction of RNA content to 14.2 % was registered at 45°C and is in good agreement with the up to 3-fold lower expression levels observed for genes from the purines and pyrimidines pathways and up to 4.5-fold reduced concentrations for the corresponding enzymes (**Tab. A.5**). The

expression of many genes coding for ribosomal proteins was also up to 3-fold repressed at 45°C but did not affect their final concentration which even increases to 53 %, suggesting a large significance of post-transcriptional events at this temperature.

### *Storage compounds*

With regard to storage compounds, glycogen accumulation was inversely proportional to temperature (7.6, 4.5 and 0 %), while reserves of polyhydroxybutyrate (PHB) were directly depleted when growth temperature deviates from its optimum (5.9 % at 37°C) (Fig. 4.3).
The depletion of glycogen storage at 45°C correlated with the 2-fold reduced expression of genes from its synthesis pathway and 3.5-fold stronger expression of *amyL*, a gene encoding an α-amylase responsible for glycogen degradation (Tab. A.4). At 15°C, on the contrary, the enhanced glycogen synthesis probably responded to a limited glucose uptake and a slightly higher adenylate energy charge inducing nutrient storage (Tab. 4.1 and 4.2). Such a re-routing of carbon towards glycogen synthesis at low temperature in combination with a global metabolic slow-down has also been reported for *Propionibacterium freudenreichii*, a Gram-positive food bacterium, and proposed as molecular basis for a long-term survival in the cold [316].
The depletion of PHB at 45°C was imputable to a fast glucose metabolisation into organic acids, a up to 4-fold lower level of enzymes involved in its synthesis (PhaRBC, MmgA) and a 3-fold reduced concentration of phasin PhaP (Tab. A.5). Surprisingly, while the low concentration of PhaP was in accordance with the reduced transcript concentration measured for operon *phaQP* at 45°C, translational or post-translational events seems to regulate the activity of PhaRBC because the levels of the corresponding transcripts were not affected at this temperature. At 15°C, despite a higher energy charge, the ATP pool was strongly reduced because of the low glucose uptake and cells certainly preferred accumulating glycogen instead of PHB as its storage requires less maintenance energy (Tab. 4.1 and 4.2). Moreover, glycogen can be formed and consumed a lot faster than PHB stockpiles [317, 318]. However, the exact mechanism to restrict PHB accumulation at 15°C is less clear than at 45°C because expression levels of the involved genes were somehow contradictory and proteome data at this temperature are still lacking. In fact, at 15°C, a slight reduction of *phaRBC* transcript concentrations in combination with a strong induction of *phaQP* expression was observed compared to 37°C (Tab. A.4). Probably, the regulation operates on translation of *phaRBC* transcript or protein stability while PhaP and PhaQ could undertake other functions under conditions non-permissive for PHB accumulation. Recent studies have proposed that PhaP is involved in resistance against environmental stress and reduces the expression of typical heat shock genes such as *groEL*, *groES*, *dnaK* and *dps* [319]. Considering that expression of all these genes is strongly repressed at 15°C, PhaP could undertake a similar role under cold stress in *B. megaterium* (Tab. A.4).

### *Membrane and fatty acid profile: the* B. megaterium *exception?*

The plasma membrane, which acts as an interface between the external and internal environments of the cell, is presumably considered one of the primary sensors modulating gene expression in response to both heat and cold stress [320-322]. Indeed, temperature stimuli modify its structural organisation and fluidity, leading to expression of specific genes to cope with stress and restore fluidity to a physiological level by adjusting the distribution of fatty acids within the membrane [152, 181, 183].

In *B. megaterium* DSM319, additionally to an apparent thickening of cell wall, such a complete remodelling of fatty acid composition was also observed upon temperature shifts, with a 5.6-fold increase of desaturated fatty acids at 15°C and a 2.6-fold increase in the global percentage of anteiso fatty acids at 45°C being the two most blatant modifications compared to 37°C (**Fig. 4.4**).

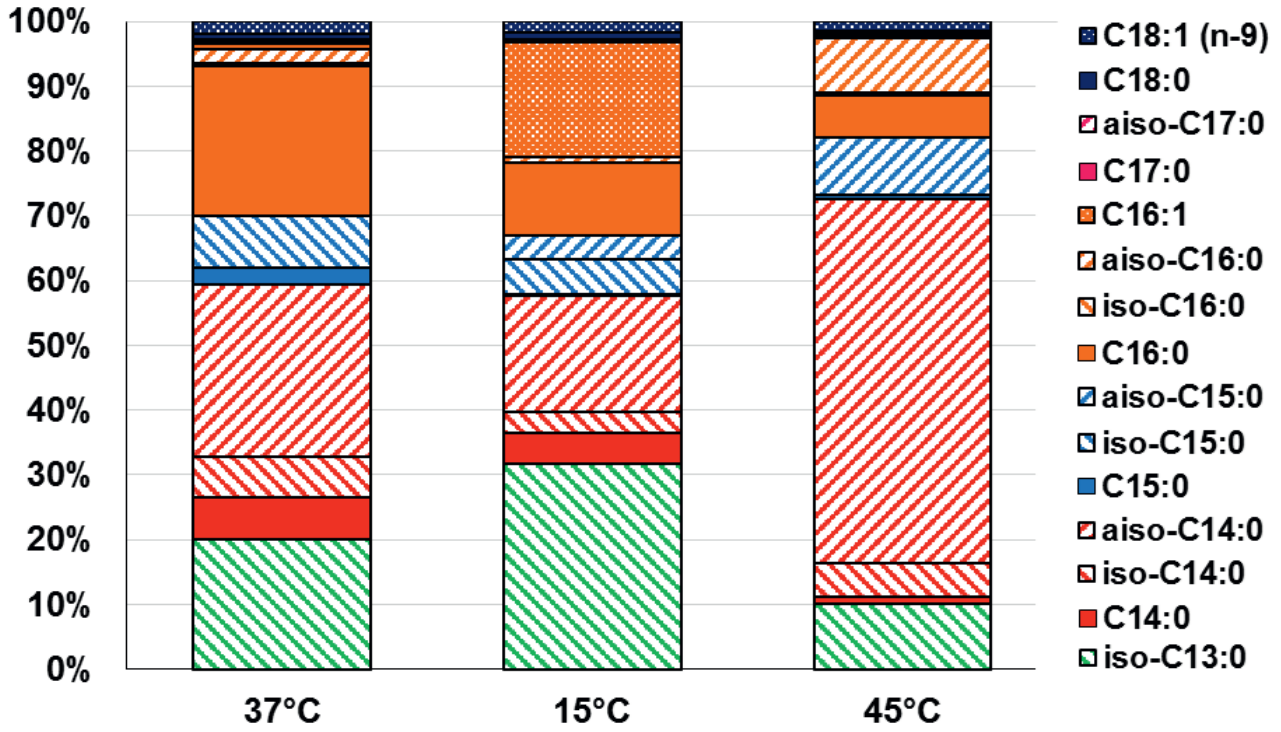


**Figure 4.4: Fatty acid profile of *B. megaterium* DSM319 cells growing at 15, 37 and 45°C, respectively** – Fatty acid are designated using the number of carbon atoms within their straight-chain. A colour is attributed to each chain length: green (C13), red (C14), light blue (C15), orange (C16), pink (C17) and dark blue (C18). Uniformly coloured, dotted, filled with backslashes and filled with slashes areas represent non-branched saturated, unsaturated fatty acid, saturated branched-iso and saturated branched-anteiso fatty acids, respectively.

While desaturation of fatty acids is a well-described mechanism to restore membrane fluidity upon cold shock, it is generally described as a short-term adaptive solution. Incorporation of branched chain anteiso fatty acids, which similarly to unsaturated fatty acids have a lower-melting point, is commonly considered as the long-term strategy to adjust fluidity at low temperature [95, 185, 323-325]. Hence, the high level of desaturation supported by a sustained induction of *des* expression as well as the poor content of anteiso fatty acids measured in *B. megaterium* at 15°C are quite

surprising (Fig. 4.4 and Tab. A.4). Possibly, synthesis of anteiso fatty acids is energetically less favourable than desaturation at 15°C because the low nutrient uptake and the restrictions imposed by the use of a M9 minimal medium restrict the *de novo* synthesis of the precursor isoleucine.
Supporting this point, previous works have proved that overexpression of *des* and the resulting desaturation compensate isoleucine deficiency and allow normal growth at low temperature in *B. subtilis* mutant strains [188]. Still, recent works of Budde et al. [95], Beranova et al. [325] and Suutari and Laakso [326] have shown that, even in minimal medium, the extent of desaturation as well as the expression level of *des* in *B. subtilis* remain almost unchanged under these conditions and confirm that, as suggested by others, adaptive behaviours of *B. subtilis* and *B. megaterium* at this temperature present some intrinsic differences. In *B. megaterium* growing at 15°C, the on-going desaturation is even more disconcerting since the operon *desKR*, whose products are exclusive regulators of *des* transcription in *B. subtilis*, presented normal expression patterns, thus suggesting the existence of either an additional induction mechanism or a post-translational regulation (Fig. 4.4 and Tab. A.4) [181, 187, 327].
Besides this flagrant desaturation, *B. megaterium* had also recourse to a shortening of fatty acids to restore fluidity by reducing van der Waals interactions within the membrane [328, 329]. As a result, the percentage of iso-C13:0 fatty acids at 15°C rose at the expense of other long-chain branched fatty acids and participated to a global lowering of the anteiso/iso fatty acid ratio. This situation is in complete contradiction with previous findings in *B. subtilis* and other mesophilic bacteria and further supports the hypothesis that cold adaptation in *B. megaterium* growing in minimal medium differs from standard considerations [326, 330]. At 45°C, the content of anteiso-fatty acids increased by 2.6-fold to reach 70 % of total fatty acids and contradicts the conventional paradigm on how membrane adaptation is achieved at high temperature in *Bacillus* sp. Indeed, low-melting anteiso-fatty acids are generally considered as fluidising agents and thought to be characteristic of cold adapted cells while, on the other hand, saturated and iso-fatty acids are expected to increase in heat adapted cells [325, 331, 332]. Interestingly, studies coming to this conclusion, including one with *B. megaterium*, were carried out using complex media. Hence, medium composition might be a major effector of biological possibilities offered for fluidity adjustment [189, 333-336]. In that sense, the precursor valine became limiting in *B. megaterium* DSM319 growing in M9 minimal medium at 45°C, making *de novo* synthesis of the main iso-fatty acids (C13:0 and C15:0) impossible or energetically unfavourable (**Tab. A.6**). In *B. subtilis* growing at 40°C on glycerol in minimal medium, a similar accumulation of anteiso fatty acids has been observed and did not affect greatly membrane fluidity. It is therefore highly plausible that anteiso fatty acids are not only cold specific as presently thought [325].
To sum up, these results highlight the limited and dated comprehension of modulation of membrane composition. Further, they show the versatility of solutions implemented by biological systems to solve a given problem depending on environmental and genetic parameters. As membrane structure affects gene expression and transport processes such as product secretion or virus penetration, more efforts need to be devoted to the complete characterisation of their interactions and to the development of cell membrane engineering if more efficient cell factories and improved health prevention methods are to be developed [332, 337].

### 4.1.2 Adaptation of *B. megaterium* carbon core metabolism during sustained temperature stress

In the attempt to apprehend the implications of temperature on cellular activity, a particular attention has been paid to the regulation of the central carbon metabolism because it provides the cell with energy, reducing equivalents and building blocks indispensable for biosynthetic reactions and successful adaptation. To this end, stable isotope batch cultivations with 1-$^{13}$C glucose and a mixture of 50 % U-$^{12}$C / 50 % U-$^{13}$C glucose were first performed to determine the flux distribution within the whole central carbon metabolism (CCM) of cells growing at 15, 37 and 45°C, respectively. For flux analysis, steady-state labelling patterns of 10 proteinogenic amino acids were measured by GC-MS and integrated in a mathematical representation of *B. megaterium* central carbon metabolism containing temperature-dependent precursor demands derived from the macromolar compositions (Tab. A.2). The obtained models were subsequently used for estimating *in vivo* pathway activity under the studied conditions with the open source software OpenFLUX (Tab. A.3) [269]. Calculated fluxes can be found in **Tab. A.7** and **Tab. A.8** while cooresponding measured and simulated labelling patterns are listed in **Tab. A.9** and **Tab. A.10**. Finally, transcriptome, proteome and metabolome data were integrated in the interpretation of the fluxome analyses.

#### *Flux homeostasis within the central carbon metabolism relies on flux switch points*

Results from flux analysis showed that *B. megaterium* DSM319 metabolised glucose using both the glycolysis and the pentose phosphate pathway (PPP) at all three temperatures (**Fig. 4.5 and Fig. 4.6**). With some specific exceptions, the relative distribution of fluxes remained rather stable, indicating that utilisation of central catabolic routes was not significantly affected by temperature stress. Given the key metabolic functions fulfilled by the carbon core metabolism, this robustness is not very surprising and surely constitutes the basis for surviving environmental and genetic perturbations [338-340]. How this flux homeostasis is achieved is still open to debate but evidence is mounting that flux regulation is operated at several biological levels from transcriptome to metabolome and includes genetic redundancy, allosteric interactions and targeted activation of alternative pathways [21, 338, 341, 342]. In *B. megaterium* DSM319, flux distribution at the anaplerotic node was significantly modified under both cold and heat stress and this node seems to operate as a switch ensuring optimal carbon and energy flow within the carbon core metabolism as proposed by others [144, 343].

Contrary to *B. subtilis*, *B. megaterium* disposes of both a pyruvate carboxylase (PycA) and a phosphoenolpyruvate carboxylase (PepC) for replenishing the tricarboxylic acid cycle (TCA), a coexistence that surely provides cells with an enhanced flexibility to cope with a wide range of substrates and environmental conditions as proposed for *C. glutamicum* [144]. In fact, oxaloacetate (OAA) was mainly synthesised from phosphoenolpyruvate (PEP) at 37 and 45°C while conversion of pyruvate by PycA was preferred at 15°C, directly expending the ATP formed by dephosphorylation of PEP (Fig. 4.5 and 4.6).

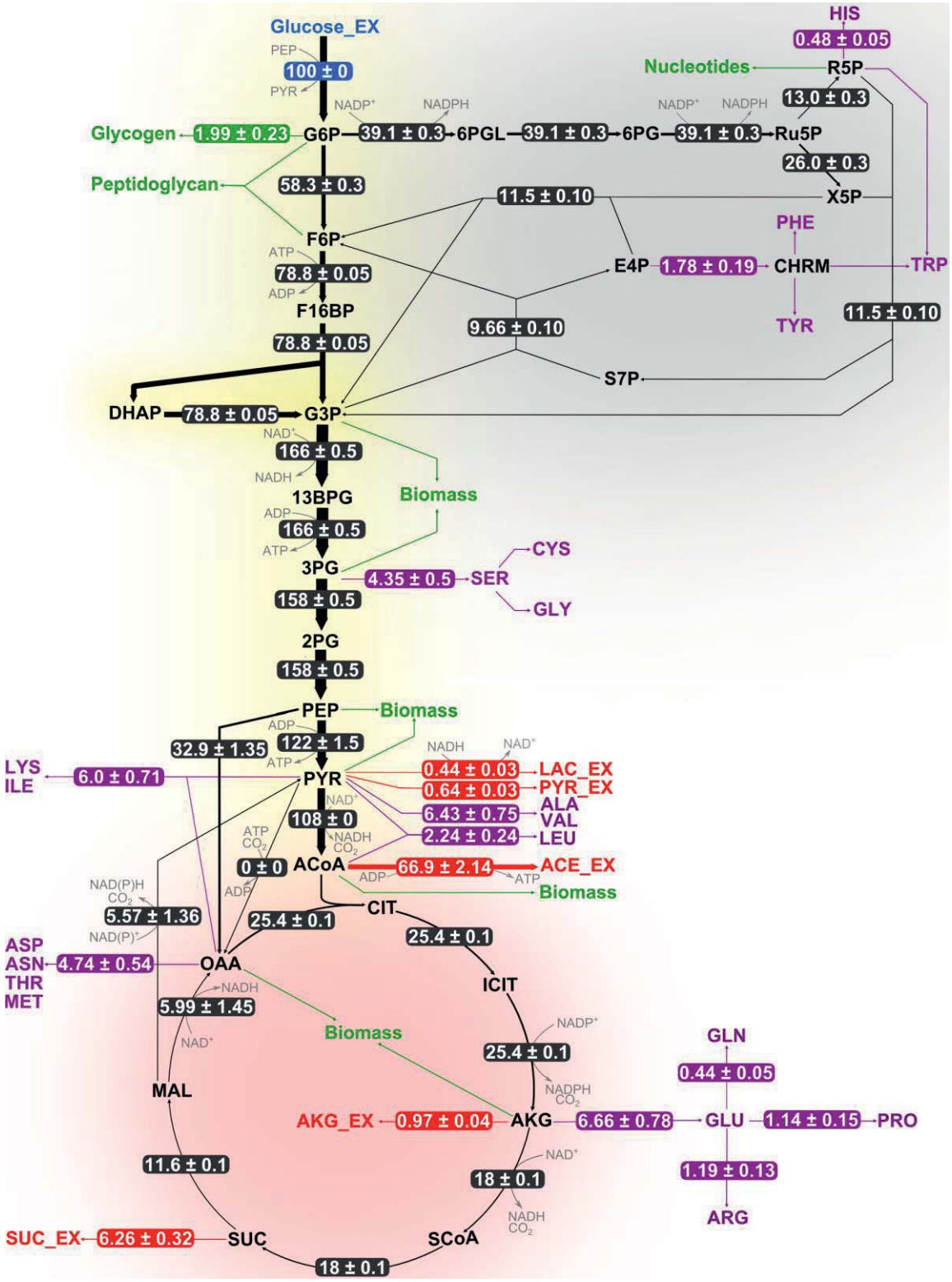


**Fig 4.5: Flux distribution within the central carbon metabolism of *B. megaterium* DSM319 growing at 37°C in M9 minimal medium –** Fluxes were determined combining labelling data sets from experiments with 100% 1-$^{13}$C glucose and with a mixture of 50 % U-$^{12}$C / 50 % U-$^{13}$C glucose, respectively. They are given as relative values (%) after normalisation with the glucose uptake rate. Fluxes to amino acids (purple) and secretion of organic acids (red) are issued from measurements and were not simulated. Green arrows represent precursor withdrawal for the synthesis of biomass compounds.

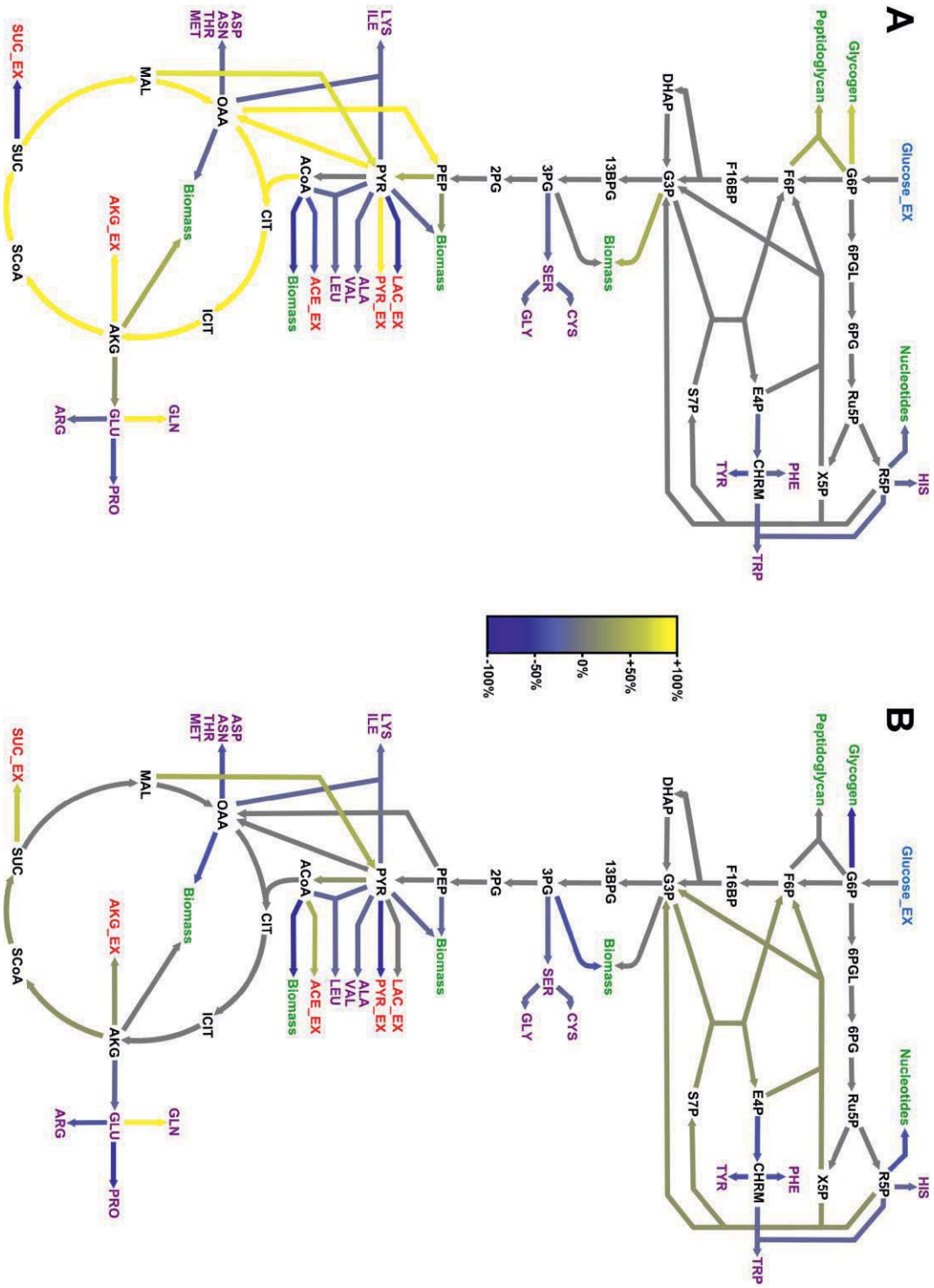


**Fig. 4.6: Adaptation of carbon core metabolism to harsh temperatures –** Change (%) in relative flux distribution in cells growing at 15°C **(A)** and 45°C **(B)** compared to cells growing at 37°C (Fig.4.5).

### *Energy excess at low temperature is actively dissipated by futile cycles*

As a matter of fact, anaplerotic routes were particularly active at 15°C and pyruvate carboxylase further formed a futile cycle in combination with pyruvate kinase (Pyk) and PEP carboxykinase (PckA) as well as the so-called “pyruvate shunt” bypassing malate dehydrogenase (Mdh) with malic enzyme (MalE), both leading to net consumption of one additional ATP-mole per turn (Fig. 4.6) [344]. Since the adenylate energy charge (AEC) was pretty high at this temperature in *B. megaterium*, this apparent unnecessary dissipation of several ATP-moles may in fact be involved in reducing an established ATP-excess (Fig. 4.6 and Tab. 4.2). A similar fine-tuning of energy levels by channelling TCA flux towards anaplerotic reactions has already been reported for bacteria growing slowly or experiencing severe limitations and is supported by the fact that aerobic bacteria do not optimise their ATP yield per se [345-348]. At 15°C, this excess, also indicated by a 2-fold increase of the ATP-to-AMP ratio, was certainly the result of an undue utilisation of the TCA cycle while cell metabolic activity was strongly reduced because of cells’ inability to efficiently import glucose (Tab 4.1).

To deal with this issue, cells actually possess various safeguard systems. A high AEC inhibits for instance several enzymes of the TCA cycle and certainly triggered the observed repression of the corresponding genes at 15°C [306, 349, 350]. Despite the implementation of those countermeasures, relative fluxes through the TCA cycle nevertheless increased at 15°C, illustrating well the complexity of regulation of pathway utilisation which remained largely independent from gene expression and protein concentration under temperature stress (Fig. 4.6, **Fig. 4.7B and Fig 4.7C**). Regarding this surprising conclusion, the presented data are consistent with recent works in *E. coli* and *B. subtilis* stating that magnitude of relative fluxes through the TCA cycle are inversely proportional to the glucose uptake rate, irrespective of external glucose concentration [344, 351, 352]. This trend was, however, not conserved up to the level of absolute fluxes because of the important disparity between glucose uptake at 15 and 37°C (Tab. 4.1 and Fig. 4.6).

Another collateral consequence of this discrepancy between catabolic supply and anabolic requirements was a 1.6-fold increase of the NADPH-to-NADP ratio which was apparently not corrected by enhanced consumption in futile cycles consuming NADPH and may have even been reinforced by the activation of the pyruvate shunt (Tab. 4.2).

In addition, the activation of the PckA route at 15°C could serve an increased regeneration of PEP to boost the limiting glucose transport by PTS-systems with the detected high pyruvate secretion as side effect. Similar findings have been made in *E. coli* and *B. subtilis* in which a novel pathway coupling the glyoxylate shunt to PckA leads to regeneration of one PEP for each oxidised glucose molecule and allows buffering of NADPH production [346, 353]. Even though the results from flux and metabolome analysis confirmed that the glyoxylate shunt was not active at all three temperatures in *B. megaterium* DSM319 growing exponentially on glucose, a PEP recycling by PckA remains a genuine possibility [144].

**Fig. 4.7: Correlation plot of normalised gene expression ratios, protein concentrations and flux intensity in *B. megaterium* growing at 45°C in M9 minimal medium** – Elements have been attributed a colour according to the pathway they belong to: green for glycolysis, red for the tricarboxylic acid cycle, orange for the pentose phosphate pathway and blue for the pyruvate node. The grey box includes elements that are not significantly regulated. The logarithmic values of the fold change were used and accordingly translated to obtain a zero-centred representation.

**A** - Genes expression and intracellular protein concentrations

**B** - Metabolic fluxes and intracellular protein concentrations

**C** - Metabolic fluxes and gene expression

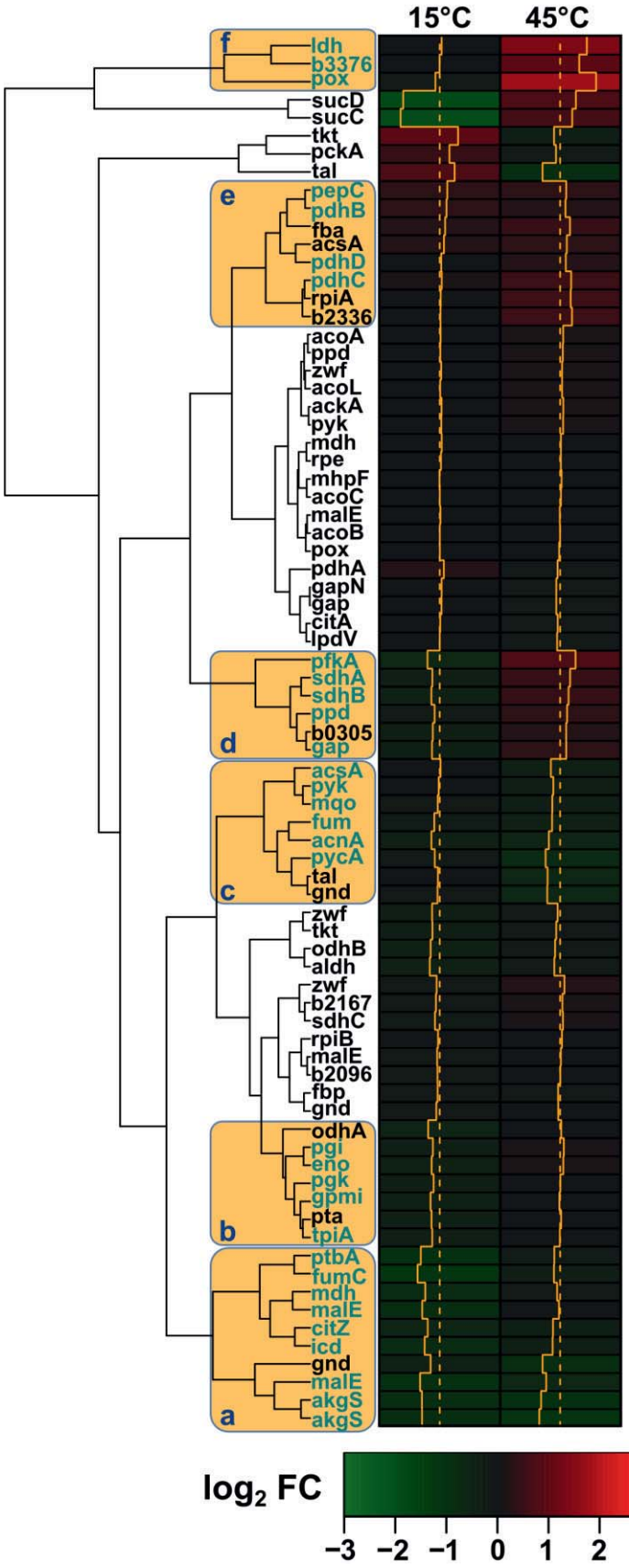


**Fig. 4.8: Hierarchical clustering of gene expression ratios of 77 selected genes of the central carbon metabolism of *B. megaterium* DSM319.** Expression is indicated as $\log_2$ fold change ($\log_2$ FC) compared to expression at 37°C. Six main regulation clusters can be identified:

**a** - Genes coding for enzymes from the TCA and involved in glucose uptake

**b** - Genes coding for glycolytic enzymes

**c** - Genes coding for enzymes at the interface between glycolysis and TCA

**d** - Genes encoding key enzymes from the glycolysis or the TCA

**e** - Genes coding for enzymes of the pyruvate node

**f** - Genes involved in overflow metabolism

### *Gene regulation within the carbon core metabolism (CCM) is operated in a modular fashion*

Despite not being strongly altered, expression levels of genes from the CCM allowed a clustering which reveals the modular organisation of regulation (Fig. 4.7 and **Fig. 4.8**). Genes encoding enzymes of the PTS-system and TCA cycle formed, for instance, a functional group (a) (Fig. 4.8). Both gene expression and relative distribution of fluxes within this pathway seems therefore closely related to the glucose uptake rate, albeit in antagonistic ways. Besides this first cluster, five additional modules of genes whose expression was co-regulated could be detected and mainly regrouped genes from the glycolysis (b), genes at the interface between the glycolysis and the TCA cycle (c), genes being part of the glycolysis or the TCA cycle (d), genes operating at the pyruvate node (e) and finally, genes involved in overflow metabolism (f) (Fig. 4.8). In addition, two small clusters including genes encoding succinyl-CoA synthetase (SucD/C), on the one hand, and transaldolase (Tal), transketolase (Tkt) and PckA on the other hand, were regulated significantly in opposite directions at both temperatures (Fig. 4.8).

The cluster analysis also indicated that genes from the PPP were not uniformly regulated and that despite a high NADPH-to-NADP ratio at 15°C, no transcriptional countermeasure was undertaken to modify flux partition at the G6P node under these conditions where the demand for both NADPH and building blocks such as ribulose-5-Phosphate (R5P) and erythrose-4-Phosphate (E4P) for biosynthetic purposes was decreased (Fig. 4.6). Such a decoupling of flux distribution within the CCM from biosynthetic demand has also been observed in *B. subtilis* and robustness is apparently favoured over optimal energy and cofactor yields to maintain cells in a state that allows rapid response to environmental variations [339]. Moreover, the distinct mismatch between transcript and protein concentrations at 45°C underlines the limited contribution of the sole transcriptome to fully apprehend metabolic adaptation and the need for phosphoproteomics to bridge this gap (Fig. **4.7A**) [354, 355].

### *Modulation of metabolite pools enables fine tuning of absolute flux intensity*

Apart from a strong drop in fluxes to biomass and a notable waste of carbon through increased secretion of organic acids, the relative and absolute flux distributions at 45°C remained almost identical compared to 37°C (Fig. 4.6 and **Fig. 4.9**).

**Fig. 4.9 : Integrated view of the response of the central carbon metabolism of *B. megaterium* ▶ DSM319 to temperature stress –** Bar plots represent intracellular metabolite concentrations in µmol $g_{CDW}^{-1}$ . Transcriptome and proteome data are indicated as the determined fold change (FC) compared to the reference temperature (37°C).

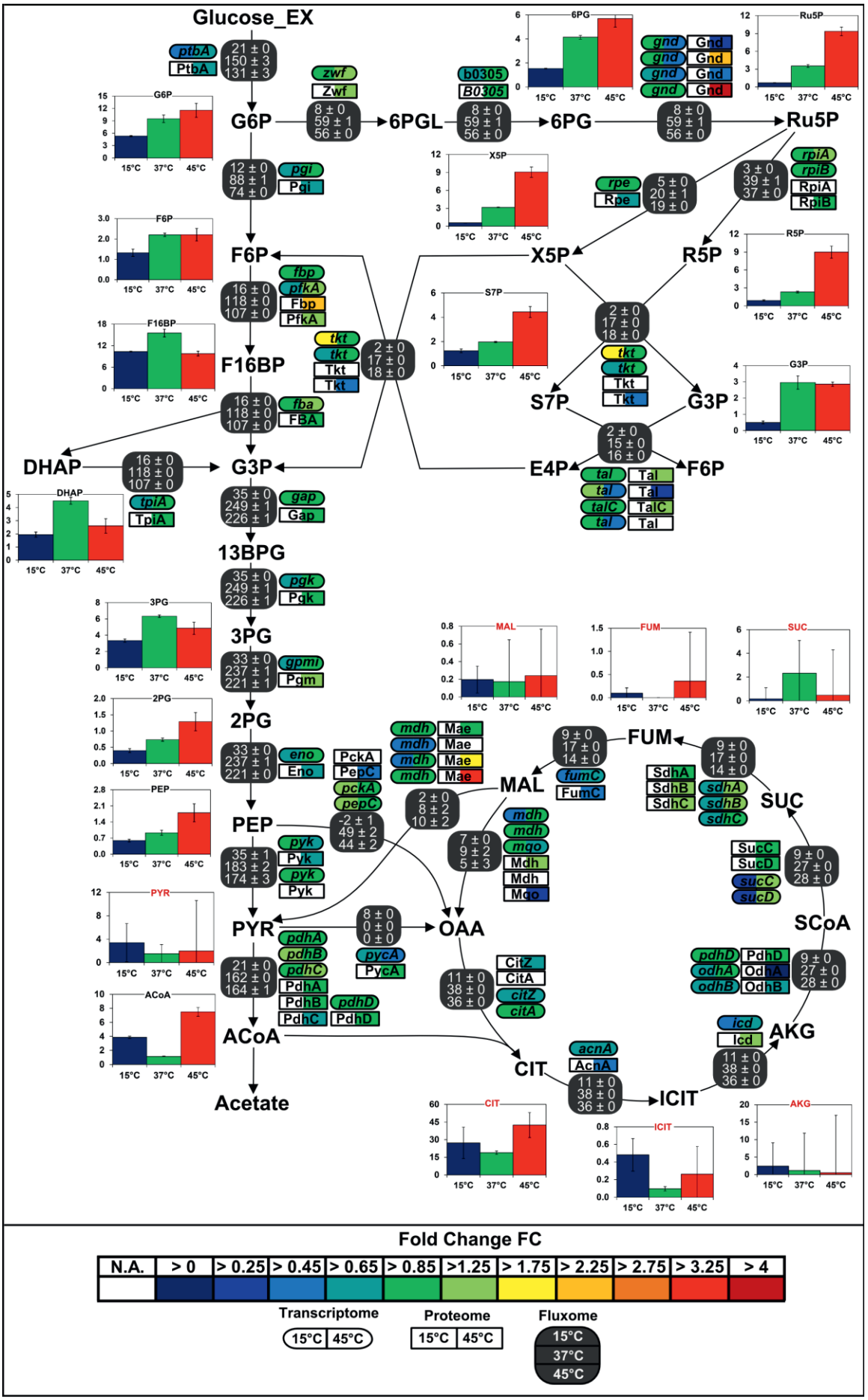

The only relevant difference identified was an increased utilisation of the pentose phosphate pathway and the anaplerotic route catalysed by malic enzyme, two metabolic routes involved in balancing of NADPH [352]. Taking a closer look at the corresponding absolute fluxes, it becomes obvious that cells devoted more resources to keep these fluxes constant at 45°C, increasing the intracellular concentration of malic enzyme and phosphogluconate dehydrogenase to drive this strategy (Fig. 4.9). This modification is likely pertaining to the key role of NADPH for scavenging ROS as will be discussed in section 4.1.3.2.

This robustness of absolute fluxes is surprising since many enzymes of the CCM are known to experience a significant loss of activity at temperatures above 40°C, which was only rarely compensated by increasing their intracellular concentrations at 45°C (Fig. 4.9) [356].

When integrating the gained metabolome data into the global analysis, it became obvious that most intracellular metabolite pools were increased when temperature rises to 45°C and certainly counterbalance the loss of activity. To better apprehend this effect, conversion rates within the CCM were supposed to follow a conventional Michaelis-Menten kinetic (**Fig. 4.10**). In this instance, for a given enzyme concentration, the loss of activity induced by temperature results in a reduced conversion rate at any substrate concentration (Fig. 4.10 - red and orange curves).

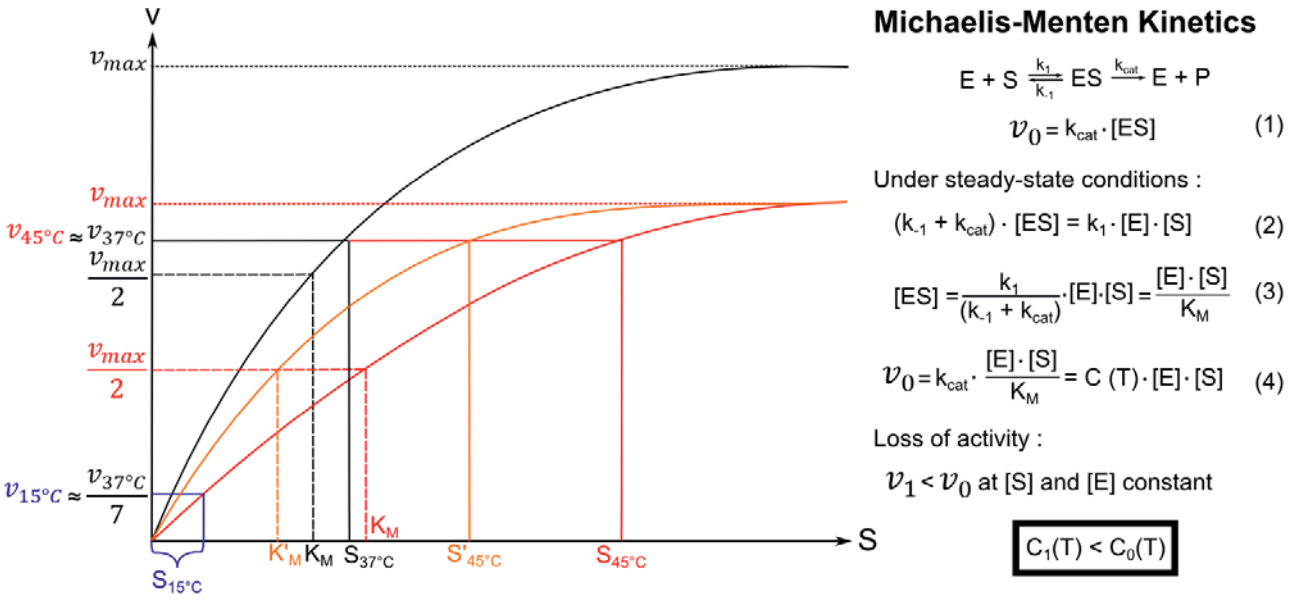


**Figure 4.10: Michaelis-Menten kinetics applied to our fluxome and metabolome data for a given enzyme concentration $E_0$** – Black curve represents the unaffected kinetics at 37°C, orange curve pictures kinetics for a reduced enzyme activity and $K_M$ (increased affinity) at 45°C and red curve depicts kinetics for a reduced activity and increased $K_M$ (reduced affinity) at 45°C. Blue bracket indicates the domain of substrate concentration for which the conversion rate at 15°C is achieved, depending on the effect of low temperature on kinetics (black, orange and red curves). Equations (1) to (4) describe the dependence of conversion rate on temperature, substrate and enzyme concentration for reactions following the Michaelis-Menten kinetics.

Hence, upon heat stress, metabolite pools needed to be increased to maintain the same conversion rate, regardless of whether the Michaelis-Menten constant $K_M$ got bigger (red) or smaller (orange). A bigger $K_M$ seems, however, more likely because enzyme affinity tends to decrease with temperature as well [356]. On the contrary, the absolute fluxes at 15°C were approximately seven times lower and as a result, metabolite pools did not need to be as big as those at 37°C, irrespective of the effect of temperature on enzyme activity (Fig. 4.9 and Fig. 4.10 - blue line). Nevertheless, normalising the pool sizes with their corresponding fluxes indicates that the metabolite concentration needed to support a given flux was often higher at 15°C compared to 37°C. Hence, together with the reduced transcription of most genes from the CCM at this temperature, it suggests a shift from a protein-based to a metabolite-based regulation of flux, which might aim at reducing protein synthesis when nutrient supply is low.

The progressive increase of pool size with rising temperature was also observed for energy molecules, cofactors and most amino acids, certainly affecting the nature and extent of allosteric interactions within the CCM. However, the existence of metabolites such as fructose-1,6-biphosphate or 3-phosphoglycertate, for which the temperature-dependent pattern of pool size diverted strongly from the rule presented above, suggests that some enzymes do act as key regulators and/or are subject to strict allosteric regulations. Nonetheless, this strong variability of metabolite pool sizes and the lack of sharp modifications at the transcriptome and proteome levels at 45°C suggest that flux regulation within the CCM is mostly operated at the metabolite level (Fig. 4.8 and 4.9). Since temperature follows circadian rhythms, such a regulation could prevent energy waste due to temperature-dependent production and degradation of proteins.

Naturally, regulation of fluxes is far more complex than a simple adjustment of metabolite levels and rather results from the concerted action of gene expression, activity modulation via allosteric effects and enzyme saturation [357]. Hence, further data concerning kinetics of enzymes at all three temperatures would be necessary to affine our analysis and address this question in more depth using mathematical models such as metabolic control analysis or regulation analysis [357, 358].

### 4.1.3 Global adaptation to harsh temperatures

Robustness and modularity of the CCM represent only two strategies to survive extreme temperatures. Adaptation further requires specific elements dedicated to coping with deleterious effects of temperature on cellular functions. Hence, the transcriptome and proteome data were further analysed to unravel mechanisms specific to cold and heat stress. Nevertheless, it is difficult to define exactly the involved regulation structures without working with mutant strains and further studies will be required to confirm findings and suggestions made in this study.

#### 4.1.3.1 Statistical approach to temperature stress

In order to find a meaningful interpretation path across the large data sets resulting from the transcriptome and proteome analyses, several statistical methods were combined to reduced data complexity and spot interesting patterns.

##### *Adaptation to cold is highly specific and differs greatly from other stress responses*

As a first step to apprehending the impact of heat and cold stress on cell metabolism, the extent of modification of gene expression under both conditions were compared using Venn diagrams (**Fig. 4.11**) [359].

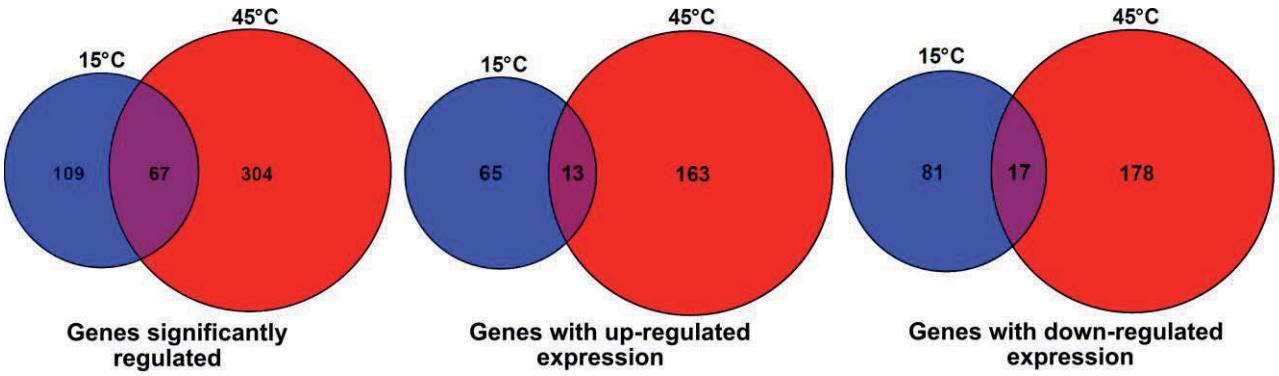


**Figure 4.11: Comparison of transcriptome data from *B. megaterium* cultured at 15 and 45°C, respectively.** Gene expression was determined by microarray analysis using purified RNA samples obtained from four biological replicates. For a given gene, expression at 15 and 45°C was considered significantly modified when the fold change compared to 37°C was greater than 1.75 (up-regulation) or lower than 0.57 (down-regulation), respectively.

While survival at both 15 and 45°C relied on a stronger expression of specific sets of genes, the extent of disruption of gene expression compared to 37°C was about twice lower at 15°C than at 45°C, with only 176 genes significantly regulated. Hence, cold response appears to be either far more specific or less pronounced. The poor correlation found between genes whose expression is enhanced under cold stress and those more strongly expressed under heat and

osmotic stress is rather in favour of the first hypothesis (data not shown). In particular, only a few genes were involved in cross-protection against both high and low temperature and the repression operated under both conditions differed greatly as well (Fig. 4.11).

### *Genes particularly affected by cold and heat belong to specific functional categories*

To visualise which metabolic functions were most affected by temperature, our transcriptome data were subsequently submitted to gene set enrichment analysis (GSEA) and used to construct Voronoi treemaps (**Fig 4.12** and **Tab. A.11**) [360-362].

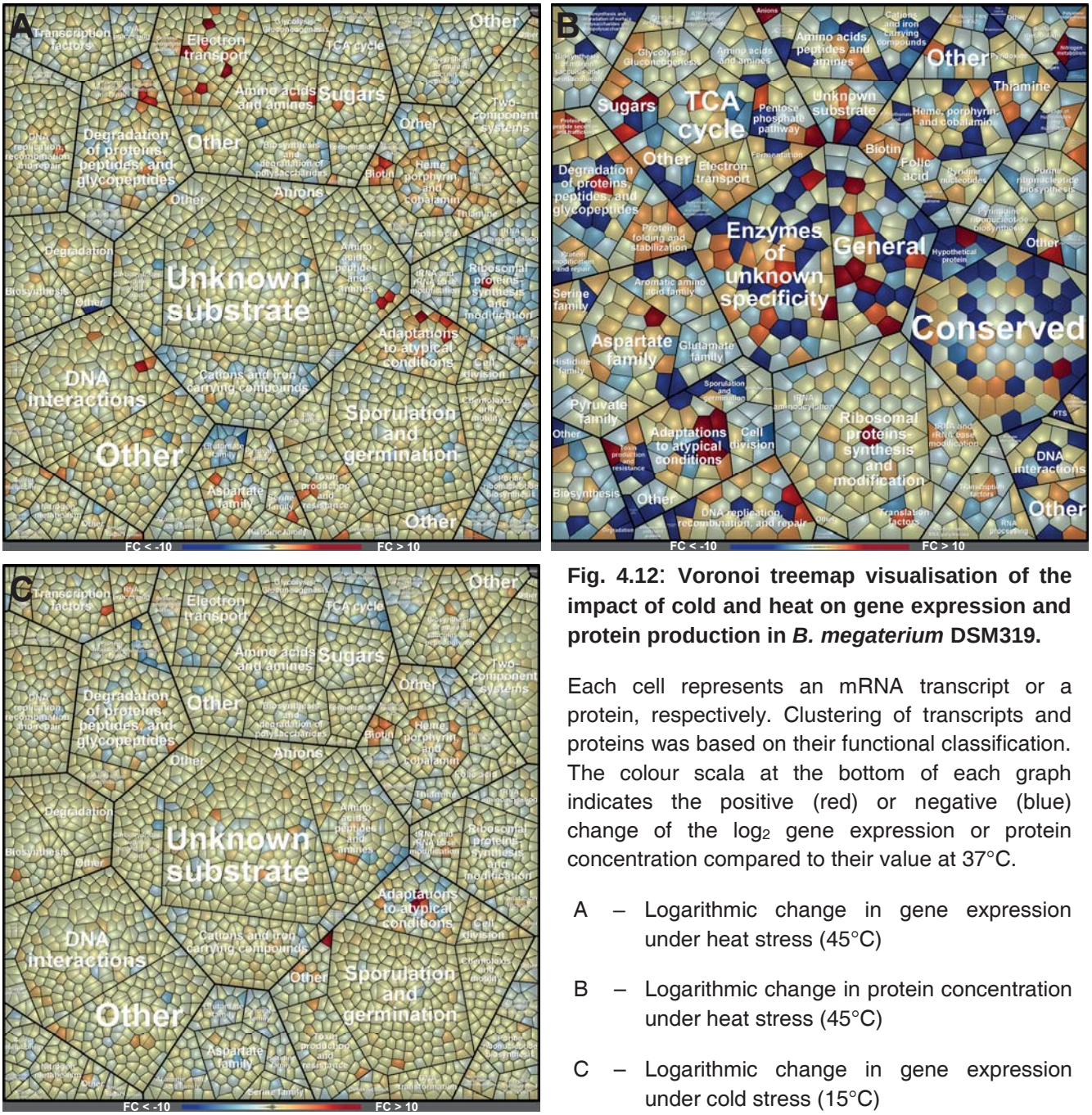


**Fig. 4.12: Voronoi treemap visualisation of the impact of cold and heat on gene expression and protein production in *B. megaterium* DSM319.**

Each cell represents an mRNA transcript or a protein, respectively. Clustering of transcripts and proteins was based on their functional classification. The colour scala at the bottom of each graph indicates the positive (red) or negative (blue) change of the $\log_2$ gene expression or protein concentration compared to their value at 37°C.

A – Logarithmic change in gene expression under heat stress (45°C)

B – Logarithmic change in protein concentration under heat stress (45°C)

C – Logarithmic change in gene expression under cold stress (15°C)

Voronoi representation of proteome data at 45°C furthermore revealed that concentration of a lot of proteins with unknown function ("Unknown specificity" and "General" in Fig. 4.12B) was strongly affected both positively and negatively. Hence, some of them might undertake key regulatory functions while a lot of them get rapidly degraded at this temperature.
Functional categories deeply afflicted at both 15 and 45°C included, among others, elements involved in the electron transport chain, adaptation to atypical conditions, biotin synthesis, amino acid synthesis, DNA protection and reparation as well as protein synthesis, stabilisation and degradation. However, genes within these categories were often regulated in opposite direction at both temperatures. In addition, expression of a lot of genes involved in RNA synthesis and processing was strongly reduced at 45°C (Fig. 4.12A).
Finally, comparison of Voronoi representations of proteome and transcriptome data at 45°C also revealed that the mismatch between transcript and protein levels observed within the CCM is a general rule under heat stress (Fig. 4.12A and B).

### *Principal component analysis (PCA), a powerful tool for data reduction and analysis*

GSEA and Voronoi treemaps are a useful screening tool to detect global modifications and reduce the number of genes that need to be closely analysed. However, the provided information is only poorly structured and fails to fully capture the relation among genes and the temperature dependence of their regulation. To further investigate these two aspects, a principal component analysis (PCA) was performed on the transcriptome data originating from both temperatures using the FactomineR module from R (**Fig. 4.13**) [363]. PCA is a statistical method aiming at reducing the dimension of a given data set to describe, as faithfully as possible, the relation existing among the i individuals and the k variables of this set by building synthetic two-dimensional representations that summarise the central information, namely the circles of correlation and the graphs of individuals [48, 364]. This method is particularly powerful when dimensions of individuals and/or variables are greater than three and can't be picture with standard methods. To construct these two graphs, the experimental observations for the variables of interest first undergo an orthogonal transformation converting them into a new set of values of linearly uncorrelated variables, the principal components (PC). This transformation is defined in such a way that the first principal component accounts for the greatest variability in the data and each of the following have the next largest possible variance every time. The axis system consisting of the first and the second principal component offers therefore the best planar representation of the experimental observation, that is, the best graph of individuals. Alternatively, the relation among observations can be refined afterwards using another set of principal components. The circle of correlations, on the other hand, describes the relationship between variables and calculated principal components and variables among them. It is constructed by gathering the coordinates of every individual for each principal component in separated vectors.

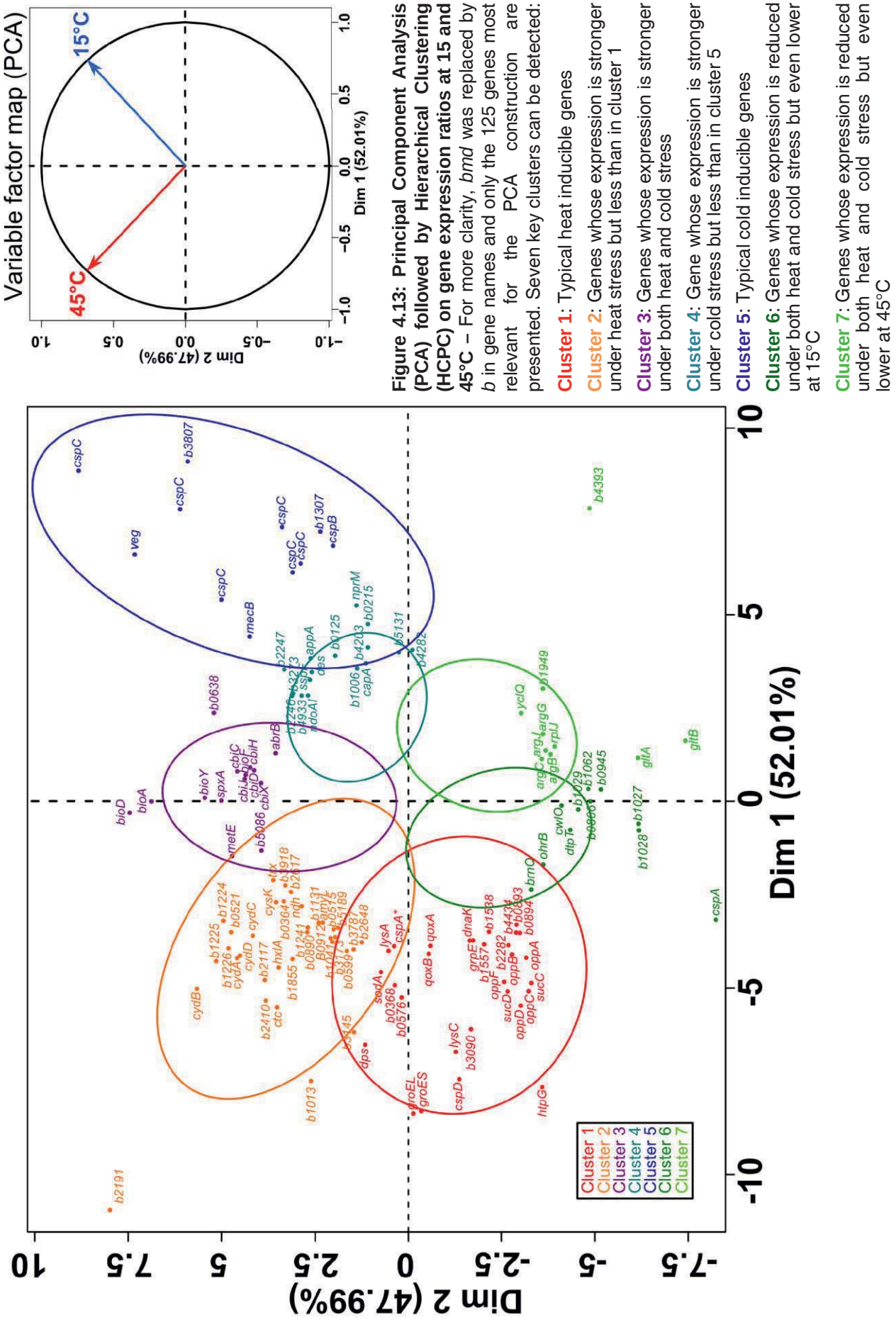


**Figure 4.13: Principal Component Analysis (PCA) followed by Hierarchical Clustering (HCPC) on gene expression ratios at 15 and 45°C** – For more clarity, *bmd* was replaced by *b* in gene names and only the 125 genes most relevant for the PCA construction are presented. Seven key clusters can be detected:

**Cluster 1**: Typical heat inducible genes

**Cluster 2**: Genes whose expression is stronger under heat stress but less than in cluster 1

**Cluster 3**: Genes whose expression is stronger under both heat and cold stress

**Cluster 4**: Gene whose expression is stronger under cold stress but less than in cluster 5

**Cluster 5**: Typical cold inducible genes

**Cluster 6**: Genes whose expression is reduced under both heat and cold stress but even lower at 15°C

**Cluster 7**: Genes whose expression is reduced under both heat and cold stress but even lower at 45°C

### *Typical heat and cold stress genes are regulated antagonistically at both temperatures*

In this study, the data set consists of more than 5000 individuals, the genes, but only two variables, cold and heat, and the first two principal components (dimensions) are therefore sufficient to properly explain 100 % of the data. In the circle of correlations, the variable cold (15°C) takes a high value on the x-axis and y-axis, indicating that it is positively correlated with both the first and second principal component. Correlation with the first component implies that genes having high expression level under cold stress are situated in the right part of the graph of individuals while genes with low expression levels are in the left part. The second dimension allows refinement of this first discrimination between genes. It points out that genes whose expression is most strongly up-regulated at 15°C are located in the upper right part of the graph of individuals while genes whose expression is heavily down-regulated are in the lower left part. Conducting a similar analysis on the variable corresponding to heat stress reveals that a significant proportion of genes having high expression levels at 15°C tend to show low levels of expression at 45°C, and vice versa. Thus, as observed in *B. subtilis,* transcriptional modifications operated under these conditions in *B. megaterium* DSM319 were also often antagonistic (Fig. 4.11 and Fig 4.13) [175]. In fact, more than 55 % of the 67 genes whose expression was significantly modified under both conditions showed opposite expression patterns. In comparison, this percentage remained below 20 % when comparing regulation at 45°C and under osmotic stress, underlying the specificity of cold stress once again.

Coupling the PCA results with a hierarchical clustering and restricting the analysis to the 125 most relevant genes for the PCA construction, we could group the genes whose expression was the most affected by temperature stress into seven characteristic clusters. Taking the previous considerations into account and using the paragons of each cluster, one can easily capture how genes from a given cluster are regulated at both temperature and to a certain extent what they have in common. For instance, transcription of genes from cluster one (red) was strongly up-regulated at 45°C and strongly down-regulated at 15°C, indicating that those genes are typical heat stress genes. On the contrary, cluster 3 (purple) is located in the middle of the upper part of the graph and includes genes whose transcription was up-regulated under both cold and heat conditions. Logically, many genes encoding typical heat and cold shock proteins (*cspC*, *htpG*,*groEL/ES*…) form distinct clusters but, interestingly, some genes encoding cold shock proteins (*cspD*, *cspA*) cluster with typical heat shock genes and challenge their conventional designation in *B. megaterium*.

### 4.1.3.2 Specific response to heat

Little is known about the heat stress response in *B. megaterium* and comparing our data with previous works on *B. subtilis* and other bacteria, this study will try to describe for the first time the corresponding heat stimulon.

#### *Adaptation of* B. megaterium *to high temperature relies on the expression of heat specific regulons indispensable for DNA, RNA and protein homeostasis*

Our transcriptome analysis revealed that the expression of 380 genes was significantly modified - at least 1.75-fold up- or down-regulated - in *B. megaterium* DSM319 growing at 45°C (> 7% of its genome). As expected, expression of many genes homologous to genes from regulons known to be particularly induced by heat in other *Bacillus* sp., such as the CtsR, HrcA and $\sigma_B$-regulons, were found among the 181 genes whose expression was significantly induced at this temperature (**Tab. 4.3**) [162]. However, only a few members of the $\sigma_B$-regulon had higher expression levels at 45°C, suggesting that most of this regulon is only induced transiently in response to heat stress, as proposed by Helmann et al. (2001) in *B. subtilis* [166]. Putative members whose expression was significantly increased regroup principally class III heat genes (*clpE*, *clpP*, *clpC*) which are under dual control of SigB and CtsR in other *Bacillus* sp., and genes coding for diverse general stress proteins (*ctc*, *bmd_2117*, *bmd_5086* and *bmd_1013*). Since the concentrations of SigB and most proteins of the $\sigma_B$-regulon were not increased at 45°C, the strong expression of the latter four genes indicates that additional regulators have still to be found. Similarly, functions and regulation mechanisms of many uncharacterised proteins produced at 45°C need to be clarified.

The proteome data further confirmed that heat response in *B. megaterium* recruits characteristic elements common to all *Bacillus* sp. and most mesophilic bacteria. Indeed, many members of the HrcA- and CtsR-regulons, which regroup various proteases (ClpCEP), chaperones (GroEL, GroES, DnaK, DnaJ) and quality control proteins (RadA, DisA), were present in higher concentration at 45°C. Hence, long-term adaptation at this temperature relies mostly on the maintenance of DNA, RNA and protein homeostasis using large sets of stabilising, repairing and recycling proteins.

The absence of HrcA in the protein fraction at 45°C as well as higher concentrations of MscAB, two modulator proteins essential for the ClpCP-dependent degradation of CtsR, suggest that the expression of these two heat regulons in *B. megaterium* could rely on an effective degradation of the corresponding repressor proteins when temperature rises and denatured proteins accumulates [365]. In agreement with others studies on *B. subtilis* and *B. licheniformis*, the increased expression of the HrcA-dependent heptacistronic *dnaK*-operon was however limited to its first three members *hrcA*, *grpE*, and *dnaK* in *B. megaterium* [158, 166].

**Table 4.3: Gene expression levels and protein concentrations of elements typically involved in heat stress response in *B. megaterium* DSM319 growing at 45°C –** Data are given as fold change (FC) of transcript or protein concentrations compared to their values at 37°C. Proteins that could not be quantified by the proteome approach are designated with "n.d.". Similarly, "37°C" and "45°C" indicates that protein was only detected at 37 and 45°C, respectively. Red and blue bold numbers indicate significant increases (> 1.75) and decreases (< -1.75) of gene expression and/or protein concentrations, respectively.

| Locus Tag | Name | Description | Transcriptome FC | Proteome FC |
|---|---|---|---|---|
| | | **HrcA Regulon** | | |
| *bmd_0260* | *groES* | 60 kDa chaperonin | **5.93** | **2.53** |
| *bmd_0261* | *groEL* | 10 kDa chaperonin | **6.31** | **2.40** |
| *bmd_4547* | *rimO* | Ribosomal protein S12 methylthiotransferase | -1.02 | **-2.00** |
| *bmd_4548* | *rsmE* | Ribosomal RNA small subunit methyltransferase E | -1.02 | n.d. |
| *bmd_4549* | *prmA* | Ribosomal protein L11 methyltransferase | -1.01 | **-2.17** |
| *bmd_4550* | *dnaJ* | Chaperone protein DnaJ | -1.14 | 1.23 |
| *bmd_4551* | *dnaK* | Chaperone protein DnaK | 1.60 | **1.92** |
| *bmd_4552* | *grpE* | Co-chaperone GrpE | 1.57 | **2.69** |
| *bmd_4553* | *hrcA* | Heat-inducible transcription repressor HrcA | 1.49 | 37°C |
| | | **CtsR Regulon** | | |
| *bmd_0102* | *ctsR* | Transcriptional repressor of class III stress genes protein | **1.83** | n.d. |
| *bmd_0103* | *mcsA* | Modulator of CstR activity | **2.10** | 45°C |
| *bmd_0104* | *mcsB* | Modulator of CstR activity | 1.67 | **11.64** |
| *bmd_0105* | *clpC* | ATP-dependent Clp protease ATP-binding subunit ClpC | **1.93** | **3.14** |
| *bmd_0106* | *radA* | DNA repair protein RadA | 1.2 | 37°C |
| *bmd_0107* | *disA* | DNA integrity scanning protein DisA | 1.32 | **2.66** |
| *bmd_1249* | *clpE* | ATP-dependent Clp protease, ATP-binding subunit ClpE | **2.73** | **2.85** |
| *bmd_3096* | *clpP* | ATP-dependent Clp protease, proteolytic subunit ClpP | **1.97** | n.d. |
| *bmd_3798* | *clpP* | ATP-dependent Clp protease, proteolytic subunit ClpP | 1.00 | n.d. |
| *bmd_4675* | *lonA* | ATP-dependent protease LonA | -1.03 | 1.42 |
| *bmd_4677* | *clpX* | ATP-dependent Clp protease, ATP-binding subunit ClpX | -1.33 | -1.00 |
| *bmd_4715* | *trx* | Thioredoxin | **3.60** | **1.76** |
| *bmd_5044* | *clpP* | ATP-dependent Clp protease, proteolytic subunit ClpP | **2.10** | **2.41** |
| | | **Unknown Regulation** | | |
| *bmd_0077* | | Small heat shock protein | -1.26 | **2.08** |
| *bmd_0091* | *hslO* | Chaperonin HslO | -1.14 | 1.62 |
| *bmd_0368* | | Intracellular protease, PfpI family | **3.26** | **6.48** |
| *bmd_0687* | *clpB* | ATP-dependent chaperone ClpB | 1.51 | **3.11** |
| *bmd_1362* | | Zn-dependent protease | 1.79 | 1.56 |
| *bmd_2385* | *htpG* | Chaperone protein HtpG (Class IV heat shock protein) | **2.49** | **3.34** |
| *bmd_3006* | | ThiJ/PfpI family protein | 2.02 | **4.93** |
| *bmd_3728* | | CAAX amino terminal protease family protein | 1.70 | n.d. |
| *bmd_4185* | *hslU* | Heat shock protein HslVU, ATPase subunit HslU | -1.59 | **1.82** |
| *bmd_4186* | *hslV* | ATP-dependent protease HslV | -1.74 | 37°C |

As reported for other bacteria, the class IV heat shock gene *htpG* showed a higher expression level in *B. megaterium* as well and the concentration of the encoded chaperone protein was 3.3-fold higher at 45°C [168, 366]. By contrast, neither a stronger expression of the putative gene *htrA* nor of the operon *cssRS* encoding its supposed regulators was noticed. Since Voigt et al. [158] and Darmon et al. [367] have observed a progressive decrease in the induction of CssRS-dependent genes with increasing exposure time in *B. licheniformis*, these class V heat shock genes are probably only involved in the short-term response to heat stress. In addition to these major and well-described systems, other proteases from the PfpI family (*bmd_0368* and *bmd_3006*) were produced in large amounts in response to heat stress (Tab. 4.3).

### *Production of DNA-protecting elements is mostly regulated post-transcriptionally*

Regarding DNA protection, the most striking difference was the 5.6-fold increased expression of *dps*, a gene encoding a protective DNA binding element whose concentration was 11-fold increased at 45°C (Tab. A.4 and Tab. A.5) [368]. Similarly to the four general stress genes previously mentioned, this gene is part of the $\sigma_B$-regulon in *B. subtilis* and its high expression at 45°C in *B. megaterium* confirms the existence of a more complex regulation.

In many bacteria, a large regulon encoding DNA repairing proteins is regulated by the LexA repressor [369]. In *B. megaterium*, the expression of genes homologous to those belonging to the LexA regulon in *B. subtilis* was not affected by heat but the concentration of several of their products was strongly increased, implying the existence of post-transcriptional and/or post-translational effects increasing translation rate and/or transcript and protein stability (Tab. A.5). This pattern seems to be characteristic of many elements involved in DNA homeostasis and was also observed for topoisomerases TopA and TopB, DNA polymerases PolX and PolC, excinulease UvrA, repair factor RecF and Mfd, tyrosine recombinase XerD and others (Tab. A.5).

Whether all these elements belong to a unique regulon or interact together in a global scheme in *B. megaterium* under heat stress is still unclear. It is however very tempting to make a link between the 5-fold increased production of topoisomerase I (TopA) and the 3.4-fold higher expression level of the gene *bmd_0576*, coding for a DNA-binding protein HU sharing 70 % homology with the heat-stable protein HBsU from *B. subtilis* [370]. Indeed, besides being involved in DNA recombination and repair, HU proteins similar to HBsU have been shown to modulate the relaxing activity of topoisomerase I in *E. coli* in order to maintain DNA supercoiling into physiological boundaries [371, 372]. Here again, further studies are required to confirm the exact function undertaken by this HU protein in *B. megaterium* (Tab. A.4).

## B. megaterium *cells exposed to high temperatures suffered from a pronounced reductive stress generating reactive oxygen species (ROS)*

Redox processes are common to all living organisms, in which they undertake key functions in cellular homeostasis and signalling but also deeply affect all aspects of cellular function, metabolism and structure [373]. Hence, variations in redox ratios ($NADH/NAD^+$ and $NADPH/NADP^+$) are of paramount importance to apprehend underlying metabolic activities and gene regulations.
In *B. megaterium* DSM319, the high NADH-to-$NAD^+$ ratio at 45°C suggests that cells suffer from a marked reductive stress (Tab. 4.2) [374, 375]. According to Ying et al. [376], this high redox ratio was responsible for the enhanced production of NADH-dependent dehydrogenases and oxidases observed, which in turn can generate free radicals and peroxides by inducing iron release from ferritin and electron leakage from the respiratory chain (**Tab. 4.4**).

**Table 4.4: Gene expression levels and protein concentrations of elements involved in ROS production and scavenging in *B. megaterium* DSM319 growing at 45°C –** Data are given as fold change (FC) of transcript or protein concentrations compared to their values at 37°C. Proteins that could not be quantified by the proteome approach are designated with "n.d.". Similarly, "37°C" and "45°C" indicates that protein was only detected at 37 and 45°C, respectively. Red bold numbers indicate significant increases of gene expression and/or protein concentration, respectively.

| Locus Tag | Name | Description | Transcriptome FC | Proteome FC |
|---|---|---|---|---|
| *bmd_0358* | *msrA* | Peptide methionine sulfoxide reductase MsrA | 1.34 | n.d. |
| *bmd_0552* | *thiO* | Glycine oxidase | 1.51 | **1.80** |
| *bmd_0890* | *hxlB* | 6-phospho-3-hexuloisomerase | **3.91** | 37°C |
| *bmd_0891* | *hxlA* | 3-hexulose-6-phosphate synthase | **5.90** | 1.34 |
| *bmd_0892* | *hxlR* | HTH-type transcriptional activator hxlR | **3.04** | n.d. |
| *bmd_1201* | *msrAB* | Peptide methionine sulfoxide reductase MsrA/MsrB | **2.91** | 37°C |
| *bmd_1314* | | Putative 2-cys peroxiredoxin | **1.82** | 1.33 |
| *bmd_1855* | | Cytochrome P450 | **5.17** | **11.83** |
| *bmd_1948* | | Thioredoxin | 1.41 | 37°C |
| *bmd_1995* | | Cytochrome P450 | 1.07 | n.d. |
| *bmd_2003* | *msrAB* | Peptide methionine sulfoxide reductase MsrA/MsrB | -1.01 | n.d. |
| *bmd_2035* | | Cytochrome P450 | 1.01 | n.d. |
| *bmd_2091* | *sodC* | Copper/zinc superoxide dismutase | -1.29 | n.d. |
| *bmd_2711* | | Superoxide dismutase | -1.00 | n.d. |
| *bmd_3040* | | Catalase | -1.02 | n.d. |
| *bmd_3213* | | Manganese catalase | 1.06 | n.d. |
| *bmd_3215* | | Manganese catalase | -1.01 | n.d. |
| *bmd_3874* | | Cytochrome P450 | 1.60 | n.d. |
| *bmd_4502* | *sodA* | Superoxide dismutase [Mn] | **3.29** | -1.28 |
| *bmd_4715* | *trx* | Thioredoxin | **3.60** | 1.76 |
| *bmd_4781* | *tpx* | Thiol peroxidase (Thioredoxin peroxidase) | 1.48 | 0.75 |
| *bmd_4815* | | Thioredoxin | 1.05 | 2.40 |
| *bmd_4938* | *sodC* | Copper/zinc superoxide dismutase | -1.04 | n.d. |
| *bmd_5050* | *trxB* | Thioredoxin-disulfide reductase | **1.77** | **1.76** |
| *bmd_5226* | *katA* | Catalase | 1.12 | -1.09 |

The fast decrease of pH-value as well as a 5-fold stronger expression of a gene encoding cytochrome P450 (*bmd_1855)*, a hemoprotein principally acting as monooxygenase and a proven source of highly reactive oxygen species (ROS), also tend to indicate a marked tendency to produce ROS at 45°C (Fig. 4.1 and Tab. 4.4) [377-379]. Such a connection between heat and ROS production has already been reported for others microorganisms including *S. cerevisiae* and *E. coli* and is further supported by the up to 3-fold increased expression of members of the PerR regulon, which in *B. subtilis* responds to peroxide stress and includes *perR*, *fur*, *katA*, *spx*, *hemAXCDBL* and *ahpC* (cf. Tab. 4.5 and Tab. 4.6) [380]. As in *B. subtilis*, the discrepancies found in expression levels of putative regulon members in *B. megaterium* seem to confirm that the affinity of PerR, the global regulator, for the different members is modulated by the nature of the bond metal ions [381-383].
Since the expression of *hxlAB*, encoding two enzymes implicated in formaldehyde detoxification in *B. subtilis*, and of *hxlR*, which encodes their regulator, was between 3 and 6-fold up-regulated at 45°C, it seems that ROS produced at 45°C further reacted with proteins and lipids and generated reactive aldehydes via carbonylation (Tab. 4.4) [384-386]. In this context, it is particularly interesting to note that the protease encoded by *bmd_0368* whose concentration was 6.5-fold increased at 45°C, shares more than 64 % homology with the YraA protein from *B. subtilis*, a cysteine proteinase involved in the degradation of thiol-containing proteins and responding to aldehyde stress [387].

### *Enhanced production of elements involved in redox balance and oxygen utilization restricts ROS generation*

In *B. subtilis* and other bacteria, the disruption of redox balance further leads to inhibition of Rex, a transcriptional repressor of genes involved in response to oxygen limitation [388]. Upon NADH increase, Rex dissociates indeed faster from DNA and transcription can be initiated [389]. In *B. megaterium* DSM319, the expression of genes encoding respiratory cytochrome bd oxidase (*cydABDC*) and lactate dehydrogenase (*ldh*), five members of the Rex-regulon in *B. subtilis*, was up to 10-fold increased at 45°C and leaded to larger concentrations of both proteins (Tab. A.4 and Tab. A.5). The first protein ensuring a more efficient oxygen usage while the second recycles the excess of NADH to restore balance [390, 391]. Hence, the Rex-regulon seems to be conserved in *B. megaterium* and induced in response to the high $NADH/NAD^+$- ratio at 45°C. This could be confirmed by the 3.6-fold increased expression of *ndh* which suggests that the regulatory loop composed of Rex and NADH dehydrogenase Ndh proposed by Gyan et al. [389] for the maintenance of the $NADH/NAD^+$-ratio was also active in *B. megaterium* growing at 45°C. Two additional NADH dehydrogenases might be part of this loop as well because expression of their encoding genes, namely *bmd_2191* and *bmd_1241*, was respectively 69-fold and 4-fold higher at 45°C (Tab. A.4).

This overlap between hypoxia and oxidative stress responses was further confirmed by the 2.3-fold increased expression of *resDE*, an operon encoding a two-component signal transduction system inducing several genes inter alia in response to oxygen limitation (Tab. A.4) [392-394]. Since other transcriptional regulators of the ResD regulon (*phoP* and *nsrR*, respectively) were not differentially expressed, its enhanced transcription at 45°C in *B. megaterium* probably only relied on the oxygen-dependent regulator ResD. In *B. subtilis*, this regulon includes genes that are primordial for heme A (*ctaAB)* and cytochrome c biosynthesis (*resABC, cydABCD and qoxABCD)* but also in DNA synthesis and repair (*nrdF* and *nrdE*) [395-398]. In *B. megaterium*, the expression of *qoxABCD* was increased by 2 at 45°C and, together with the enhanced production of other terminal cytochrome oxidase and NADH dehydrogenases, reflects a global acceleration of the electron transport chain. Such an acceleration seems reasonable since a better conversion of oxygen to water undoubtedly decreases its availability for ROS production.
As indicated by the 2.6- and 3-fold increased expression of the $H_2O_2$-inducible *nrdE* and *nrdF,* synthesis of ribonucleotide reductases (RNR) was also enhanced at 45°C and surely served the production of deoxyribonucleotides (dNTPs), which are necessary to repair DNA damages caused by reactive oxygen species and ensure genetic fidelity [399, 400]. In relation to that, a 3.6-fold increase in the concentration of a protein similar to flavodoxin (*bmd_3911*), an electron carrier needed for the reductive activation of RNR, occurred at 45°C (Tab. A.5).

### *SpxA orchestrates the response against reductive stress at 45°C in* B. megaterium

Surprisingly, the concentrations of most enzymes typically involved in ROS scavenging such as superoxide dismutases, catalases and peroxiredoxins were not significantly increased in *B. megaterium* DSM319 growing at 45°C and, *sodA* excepted, only few of the encoding genes had higher expression levels (Tab. 4.4 and **Fig. 4.14**) [401].
On the contrary, an increased expression of genes related to thiol-specific stress response was observed and their products may, as proposed by Björnstedt et al. [402] and Shibata et al. [403], fully replace conventional scavenging and repair systems at 45°C in *B. megaterium* (Tab. 4.4). Among them, the thioredoxin (Trx) / thioredoxin reductase (TrxB) system emerges as a key mechanism to reduce both $H_2O_2$ and protein disulphide bonds resulting from oxidative damages (Fig. 4.14) [404-407]. An enhanced production of this class of heat-stable redox proteins in response to high temperature has also been described by Scharf et al. [408] in *B. subtilis* and the characterised induction mechanism involves two promoters responding to $\sigma^B$- and $\sigma^A$-factor, respectively. Moreover, genes encoding thioredoxins and thioredoxin reductases belong to a larger regulon responding to thiol-specific oxidative stress, comprising over a hundred of genes and having Spx as main regulator [409-412]. Although SpxA, its homologue in *B. megaterium* DSM319, could not be detected in the proteome at 45°C, the expression of its coding gene *spxA (bmd_0714)* was 3-fold up-regulated at 45°C and it could therefore undertake the same regulatory function. The parallel 2.9-fold increased transcription of *msrAB* (*bmd_1201*), a gene encoding a methionine

sulfoxide reductase involved in restoring protein function after oxidative damage and whose homologues belong to the same regulon in *B. subtilis*, is also in favour of this conclusion [413, 414]. In accordance with observations of Nakano et al. [410], a reduced expression of supposedly SpxA-dependent genes whose products are involved in central pathways such as purine (*pur*), pyrimidine (*pyr*) and amino acid metabolism was noticed, probably explaining the reduced growth rate at this temperature.

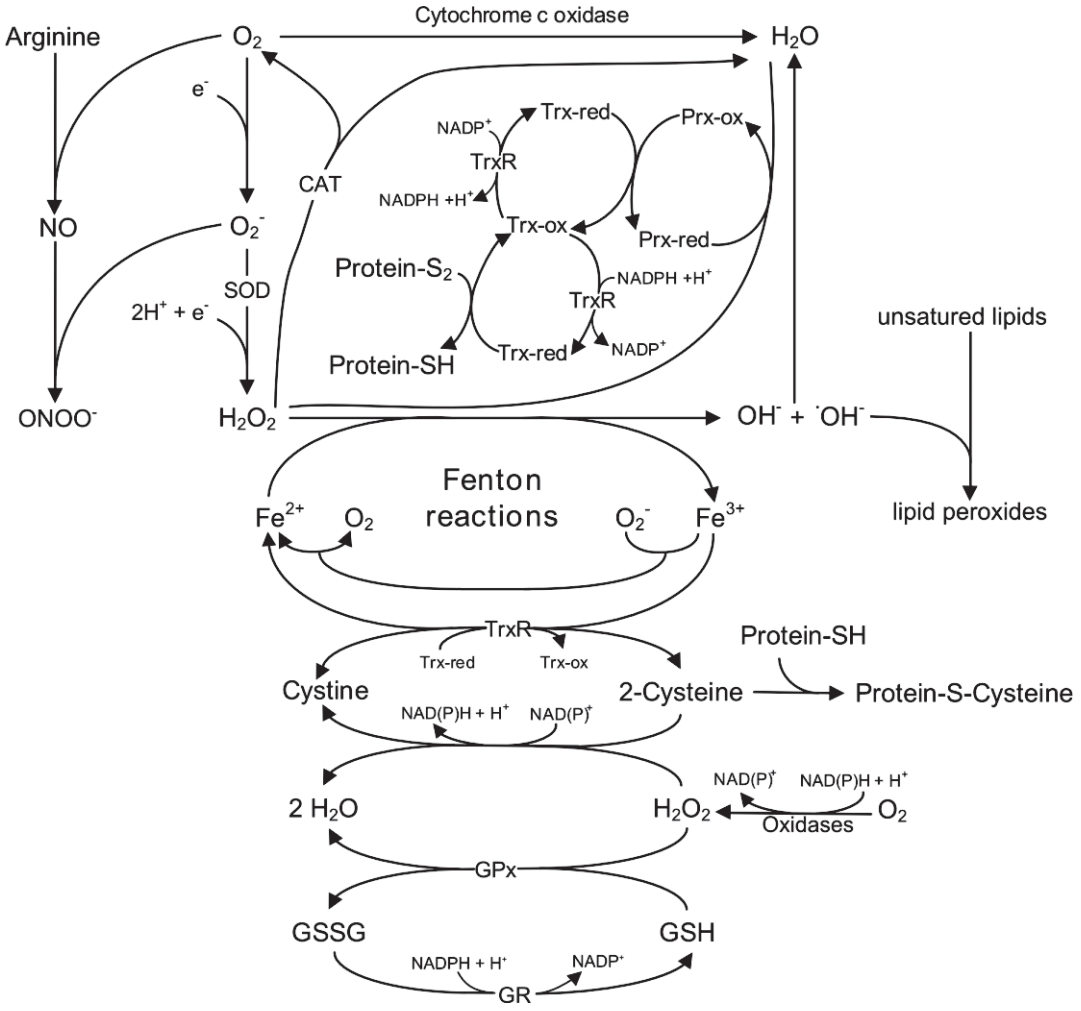


**Figure 4.14: Typical pathways for superoxide, peroxide and reactive oxygen species (ROS) production and scavenging in bacteria - CAT**: catalase, **GPX**: glutathione peroxidase, **GR**: glutathione reductase **GSH**: glutathione, **GSSG**: glutathione disulfide, **Prx-ox**: oxidized peroxiredoxin, **Prx-red**: reduced peroxiredoxin, **SOD**: superoxide dismutase, ***TrxR***: thioredoxin reductase, **Trx-ox**: oxidized thioredoxin, **Trx-red**: reduced thioredoxin.

### *Control of ROS formation requires strict regulation of cysteine and arginine pools*

In many organisms, glutathione constitutes the first line of defence against oxidative damages, reducing disulfide bonds and scavenging $H_2O_2$ to water. However, similarly to *B. subtilis* and many Gram-positive bacteria, *B. megaterium* seems to lack the genes necessary for glutathione synthesis.

In many *Bacillus* sp., cysteine undertakes its function and protects thiol-containing proteins from oxidative damages via S-cysteinylation [409, 415]. The 4-fold increase in expression of *cysK*, a gene encoding a cysteine synthase, and the 2.2-fold higher concentration of Ytkp, another cysteine synthase, are a priori in favour of a similar role in *B. megaterium* (Tab. A.4 and Tab. A.5).
Since cysteine, unlike glutathione, presents the big drawback to reduce $Fe^{3+}$ to $Fe^{2+}$ via cystine formation and can be recycled by thioredoxin afterwards, its activity certainly needs to be regulated to limit damages caused by the so-called Fenton reactions that convert lightly toxic hydrogen peroxide ($H_2O_2$) into highly toxic hydroxyl radicals ($^{\cdot}HO$) (cf. Fig. 4.14) [401]. In that sense, the increased expression of *cydABDC* is furthermore interesting because, apart from being essential for functional cytochromes bd and c, the heterodimeric transmembrane cysteine/glutathione exporter encoded by *cydDC* is required for maintenance of the optimal redox balance in *E. coli* and could operate an adjustment of cysteine concentrations in *B. megaterium* (Tab. A.4) [416, 417]. In *B. subtilis*, Gusarov and Nudler [418] have proposed an additional control mechanism involving inactivation of thioredoxin-mediated cysteine recycling by nitric oxide (NO) produced from arginine. This hypothesis is in good accordance with previous observations from Hellmann et al. [166] reporting an enhanced expression of all genes from the arginine pathway under heat stress. By contrast, gene expression within the arginine biosynthetic pathway was 3-fold reduced and enzyme concentrations were halved at 45°C in *B. megaterium,* thus hardly supporting the existence of such a mechanism. On the contrary, this reduced activity of the arginine pathway could reflect a strategy to restrain the formation of NO, which can also react with superoxide $O_2^-$ to produce highly reactive peroxinitrite ($ONO_2^-$). The 2-fold lowered expression of genes involved in arginine import (*artMPQ*) reinforces this idea (Tab. A.4).

### *Iron metabolism is adjusted to limit deleterious effects of Fenton reactions*

With respect to ROS production by Fenton chemistry, intracellular iron level is naturally a parameter that must be kept under tight control. In that sense, the up to 3-fold reduced expression of several genes encoding putative ferrichrome transporters (*yclNOPQ*) and the lower concentrations of other iron uptake systems (YfiY and YusV) at 45°C probably aim at reducing free iron pool (**Tab. 4.5**). The 2-fold reduction of the expression of genes *nikABCDE* involved in acquisition of nickel, a metal ion known to positively modulate the iron pool size and induce oxidative damages on DNA and lipids by Fenton reactions, seems to confirm this protective strategy [419, 420]. However, the repression operated on iron uptake systems is surprising since the expression of *fur* (*bmd_4385*), which encodes the major ferric uptake regulator, was 1.7-fold lower at 45°C and the protein was absent from the proteome, implying the existence of other transcription regulators similar to the FsrA sRNA in *B. subtilis* (cf. Tab. 4.5) [421].
Reactive oxygen species furthermore degrade hemoproteins and Fe-S proteins, releasing free hemes and iron ions that in turn participate in ROS generation [401, 422]. In that sense, the 3.4-fold increased expression of gene *bmd_0599,* encoding a monooxygenase similar to the

*B. subtilis* HmoB (60% identity), suggests that *B. megaterium*, like other bacteria, actively degrades free hemes in presence of peroxides (Tab. A.4) [423, 424].

On the other hand, transcription of several genes involved in tetrapyrrole biosynthesis, with among them *hemA*, *hemC* and *hemD* whose alter ego belongs to the Rex-regulon in *B. subtilis*, was up to 2.4-fold increased at 45°C and might compensate hemoprotein degradation [425]. Such an acceleration of heme turnover would enable a reduction of both intracellular iron and free heme concentrations without affecting their metabolic functions. However, the enzyme concentrations determined by the proteome analysis were only occasionally increased.

**Table 4.5: Gene expression levels and protein concentrations of elements involved in Fe-S cluster assembly and iron and nickel homeostasis in *B. megaterium* DSM319 growing at 45°C –** Data are given as fold change (FC) of transcript or protein concentrations compared to their values at 37°C. Proteins that could not be quantified by the proteome approach are designated with "n.d.". Similarly, "37°C" and "45°C" indicates that protein was only detected at 37 and 45°C, respectively. Red and blue bold numbers indicate significant increases and decreases of gene expression and/or protein concentrations, respectively.

| Locus Tag | Name | Description | Transcriptome FC | Proteome FC |
|---|---|---|---|---|
| *bmd_0417* | *perR* | Peroxide resistance regulation protein | -1.17 | 1.71 |
| *bmd_1507* | *fhuG* | Ferrichrome import ABC transporter | -1.03 | n.d. |
| *bmd_1508* | *fhuB* | Ferrichrome import ABC transporter | -1.01 | n.d. |
| *bmd_1509* | *fhuD* | Ferrichrome import ABC transporter | -1.36 | **1.97** |
| *bmd_1510* | *fhuC* | Ferrichrome import ABC transporter | -1.30 | n.d. |
| *bmd_1538* | | Ferritin-like protein | 1.35 | **1.75** |
| *bmd_1702* | *nikA* | Nickel import ABC transporter, nickel-binding protein | **-1.99** | 1.08 |
| *bmd_1703* | *nikB* | Nickel import ABC transporter, nickel-binding protein | **-1.83** | n.d. |
| *bmd_1704* | *nikC* | Nickel import ABC transporter, nickel-binding protein | **-1.86** | n.d. |
| *bmd_1705* | *nikD* | Nickel import ABC transporter, nickel-binding protein | **-2.13** | n.d. |
| *bmd_1706* | *nikE* | Nickel import ABC transporter, nickel-binding protein | **-2.05** | 37°C |
| *bmd_3216* | yclQ | Putative ferrichrome import ABC transporter | **-3.35** | -1.17 |
| *bmd_3217* | *yclP* | Putative ferrichrome import ABC transporter | **-2.79** | -1.61 |
| *bmd_3218* | *yclO* | Putative ferrichrome import ABC transporter | **-2.11** | n.d. |
| *bmd_3219* | *yclN* | Putative ferrichrome import ABC transporter | **-2.42** | n.d. |
| *bmd_4048* | | Siderophore biosynthesis protein | -1.16 | 1.74 |
| *bmd_4051* | | Siderophore biosynthesis protein | -1.11 | n.d. |
| *bmd_4052* | | Siderophore biosynthesis protein | -1.16 | n.d. |
| *bmd_4385* | *fur* | Ferric uptake regulation protein | -1.63 | 37°C |
| *bmd_4857* | *dps* | DNA-protecting protein | **5.58** | **11.25** |
| *bmd_4976* | *sufB* | FeS assembly protein SufB | -1.52 | -1.49 |
| *bmd_4977* | *iscU* | SUF system FeS assembly protein | **-1.79** | -1.44 |
| *bmd_4978* | *sufS* | Cysteine desulfurase SufS | **-2.03** | -1.32 |
| *bmd_4979* | *sufD* | FeS assembly protein SufD | **-2.22** | -1.57 |
| *bmd_4980* | *sufC* | FeS assembly ATPase SufC | **-2.21** | -1.46 |
| *bmd_4997* | *yusV* | Putative ferrichrome import ABC transporter | -1.12 | 37°C |
| *bmd_4998* | *yfhA* | Putative ferrichrome import ABC transporter | -1.26 | n.d. |
| *bmd_4999* | *yfiZ* | Putative ferrichrome import ABC transporter | -1.42 | n.d. |
| *bmd_5000* | *yfiY* | Putative ferrichrome import ABC transporter | **-2.34** | **-2.13** |

In contrast, expression of genes sufB, *sufC*, *sufD*, *sufS* and *iscU*, which encode a group of scaffold proteins involved in Fe-S cluster synthesis, was 2-fold lower at 45°C. Given the central metabolic functions of Fe-S proteins and since these genes are typically induced to replace degraded clusters under oxidative stress, this finding is quite unexpected (cf. Fig.4.5) [426-428].
In addition, the enhanced release of ferrous iron resulting from the degradation of free hemes and Fe-S proteins is counterbalanced by its recapture by two ferritin-like proteins encoded by *dps* and *bmd_1538* whose concentration was increased by 11.25 and 1.75, respectively (cf. Tab. 4.5) [429]. Indeed, apart from its DNA protecting properties, Dps has, like other ferritins, the ability to store iron and convert reactive $Fe^{2+}$ into more stable $Fe^{3+}$, a ferroxidase activity that is coupled to the reduction of hydrogen peroxide into water in *E. coli* and increases the relevance of this protein for tackling the ROS problem [430-433].

### *Biotinylation synergises with methionine sulfoxidation to scavenge produced ROS*

The most striking and unexpected finding in *B. megaterium* growing at 45°C was the up to 5.7-fold increased expression of genes from the biotin synthesis and transport pathways and the high concentrations observed for the corresponding enzymes (Tab. 4.6). Interestingly, Li et al. [434] have demonstrated that the shift from a biotin-rich to a biotin-free medium increases ROS production in human cells and proposed a model in which biotinylation, the covalent binding of biotin to proteins, acts in combination with methionine sulfoxidation, the oxidation of methionine residues, as an active ROS scavenging system. Indeed, the authors have observed a strong proneness to biotinylation among heat shock proteins (HSPs) and as almost 100 % of these biotinylated HSPs also displayed various degree of methionine sulfoxidation, they suggest that biotin serves as tagging system and favours the successive formation and reduction of methionine sulfoxides in HSPs. Hence, the concomitant high expression of genes involved in biotin and methionine sulfoxide reductase MsrAB synthesis at 45°C could support the existence of this novel scavenging system in *B. megaterium* and other bacteria. To our knowledge, the role of methionine sulfoxidation and its implication in gene regulation and defences against oxidative damages has already been reviewed in details for several organisms but a possible link with biotin under heat stress is completely new [435-438].
With regards to methionine, a stronger activity of its synthesis pathways was observed at 45°C and perhaps cells specifically produce methionine-enriched proteins for scavenging ROS according to the model presented above. In particular, a 19-fold higher concentration of methionine synthase MetE and a 4-fold increased expression of *lysC*, which encodes an aspartate kinase, were detected at this temperature (Tab. A.5). In *E. coli*, studies have furthermore proved that the slow growth under heat and oxidative stress is principally due to a reduced methionine availability related to the inactivation of key enzymes of this pathway and can, in the first case, be restored upon methionine supplementation [439, 440]. The cobalamin-independent methionine synthase MetE tends, for instance, to aggregate at high temperature and is rapidly inactivated by acetate and ROS [439, 441].

**Table 4.6: Gene expression levels and protein concentrations of elements involved in biotin and heme metabolism in *B. megaterium* DSM319 growing at 45°C –** Data are given as fold change (FC) of transcript or protein concentrations compared to their values at 37°C. Proteins that could not be quantified with our proteome approach are designated with "n.d.". Similarly, "37°C" and "45°C" indicates that protein was only detected at 37 and 45°C, respectively. Red and blue bold numbers indicate significant increases and decreases of gene expression and/or protein concentrations, respectively.

| Locus Tag | Name | Description | Transcriptome FC | Proteome FC |
|---|---|---|---|---|
| *bmd_0460* | *bioB* | Biotin synthase | **1.77** | **-2.72** |
| *bmd_0537* | *bioY* | Biotin biosynthesis protein BioY | 1.13 | **-2.48** |
| *bmd_0599* | | Monooxygenase | **3.37** | **2.87** |
| *bmd_0601* | *hemE* | Uroporphyrinogen decarboxylase | 1.34 | 1.07 |
| *bmd_0602* | *hemH* | Ferrochelatase | **2.03** | -1.04 |
| *bmd_0603* | *hemG* | Protoporphyrinogen oxidase | 1.63 | 37°C |
| *bmd_0828* | *bioY* | Biotin biosynthesis protein BioY | **3.32** | n.d. |
| *bmd_0829* | *bioD* | Dethiobiotin synthase | **5.68** | **2.57** |
| *bmd_0830* | *bioA* | adenosylmethionine-8-amino-7-oxononanoate transaminase | **4.67** | **2.06** |
| *bmd_1742* | | DinB family protein | 1.02 | n.d. |
| *bmd_2483* | *bioY* | Biotin biosynthesis protein BioY | -1.19 | n.d. |
| *bmd_3693* | *bioF* | 8-amino-7-oxononanoate synthase | **2.33** | **2.48** |
| *bmd_3694* | *bioH* | Biotin biosynthesis protein BioH | **1.87** | n.d. |
| *bmd_3695* | *bioC* | Biotin biosynthesis protein BioC | 1.72 | n.d. |
| *bmd_3961* | *hemG* | Protoporphyrinogen oxidase | 1.66 | 37°C |
| *bmd_4667* | *hemL* | Glutamate-1-semialdehyde-2,1-aminomutase | **2.14** | 1.41 |
| *bmd_4668* | *hemB* | Delta-aminolevulinic acid dehydratase | **1.91** | **2.44** |
| *bmd_4669* | *hemD* | Uroporphyrinogen-III synthase | **1.82** | n.d. |
| *bmd_4670* | *hemC* | Porphobilinogen deaminase | **2.35** | -1.31 |
| *bmd_4671* | *hemX* | Uroporphyrin-III C-methyltransferase | **1.97** | n.d. |
| *bmd_4672* | *hemA* | Glutamyl-tRNA reductase | **2.39** | 45°C |
| *bmd_4912* | *sirC* | Precorrin-2 dehydrogenase | 1.42 | 37°C |
| *bmd_4913* | *sirB* | Sirohydrochlorin ferrochelatase | **1.78** | **-1.84** |
| *bmd_4914* | *sirA* | Uroporphyrin-III C-methyltransferase | **2.30** | n.d. |

Hence, the heat inducibility of *metE* expression, also reported in *C. albicans,* as well as the higher enzyme concentration could compensate its reduced activity and avoid methionine auxotrophy at 45°C [442]. A similar reasoning applies to genes *lysC*, *patB*, *metC* and *metB*.

On the contrary, the production of cobalamin-dependent methionine synthase MetH was reduced by a factor of 4 and tends to confirm that, as seen in *E. coli*, this enzyme only drives the reaction under anaerobic conditions when cob(I)alamin is not oxidised to inactive cob(II)alamin (Tab. A.5) [441, 443]. Interestingly, expression of genes from the cobalamin synthesis pathway was 2-fold increased in average and a replacement of inactive cobalamin-dependent enzyme could take place at 45°C. Alternatively, vitamin $B_{12}$ could undertake a role in ROS defences in *B. megaterium* since cobalamin derivatives have recently been shown to efficiently scavenge reactive oxygen and nitrogen species *in vitro* [444].

#### 4.1.3.3 Specific response to low temperatures

While the response to an abrupt drop in growth temperature has been well documented for model organisms such as *E. coli* and *B. subtilis*, little is known about the long-term adaptation to cold temperatures in mesophilic bacteria [445, 446]. In that sense, this study investigating the adaptive behaviour of *B. megaterium* growing at 15°C can be regarded as a pioneering work in this field. Since no proteome data could be obtained at 15°C, the analysis presented here is, however, only based on results from transcriptome analysis.

##### *Cold adaptation in* B. megaterium *and* B. subtilis *differs from one another*

When comparing the gene expression data from *B. megaterium* DSM319 growing in the cold with literature data for its counterpart *B. subtilis*, several differences are to be noted. The first and most striking one is the non-induction of the SigB-operon and, consequently, of the SigB-regulon in *B. megaterium* growing at 15°C. Indeed, results from transcriptome and proteome studies indicate that the general stress regulon is strongly induced under cold stress in *B. subtilis* and a $\sigma_B$-mutant is hardly, if at all, able to grow at low temperature [95, 148, 447, 448]. This disparity probably explains the lower number of genes whose expression is at least 1.75-fold increased in *B. megaterium* (only 65 against 279 for *B. subtilis*) and could indicate a better robustness under chill stress, sparing resources for other cellular functions. Considering these results, it would be particularly interesting to test whether SigB is indeed dispensable for growth at 15°C in *B. megaterium* or whether, despite not being strongly induced, it still plays a key role in cold acclimatisation.
Similarly, the expression of putative regulons involved in early sporulation and governed by alternative sigma factors SigE, SigF and SigG did not seem to be induced in *B. megaterium*, contrary to findings in *B. subtilis*. This was possibly due to the 2.2-fold increase in expression of *abrB* whose product AbrB negatively controls a larger regulon including transition state genes from the SigF-, SigG and SigH-regulons, thus enabling sustained growth at low temperature (Tab. A.4) [449]. In addition, a lot of metabolic pathways including fatty acid biosynthesis and degradation, translational apparatus, chemotaxis and motility, and purine synthesis which are affected by low temperatures in *B. subtilis*, did not show significant alterations in *B. megaterium*, at least at the transcriptional level [95, 450].

##### *Maintenance of RNA integrity and translation efficiency is a central issue at 15°C*

Despite these intrinsic differences, both bacteria also share some common elements indispensable for dealing with typical cold-related issues such as the impairment of translation processes caused by ribosome inactivation and stabilisation of mRNA secondary structures [154, 295]. Among them, cold shock proteins (CSPs) form a large family of well-conserved proteins sharing a common cold-shock domain (“cold box”) and performing many functions at low

temperature including translation initiation, destabilisation of RNA secondary structures and antitermination [155, 174, 451]. In *B. megaterium*, fourteen genes encoding CSPs have been annotated so far and among them eight showed up to almost 18-fold higher expression levels at 15°C compared to 37°C, underlining the utmost importance of this family for long-term acclimatisation (**Tab. 4.7**). This strong and sustained expression is, however, quite surprising since the increased production of these proteins has been imputed to post-transcriptional events in *B. subtilis* and *E. coli*, in which expression of the corresponding genes is only moderately induced in adapted cells [95, 171, 327, 452].

RNA helicases usually constitute a second central pillar for restoring proper translation at low temperature but only one gene (*bmd_0215*) encoding a protein homologous to CsdA from *E. coli* and CshA from *B. subtilis* and *B. cereus* was 2.6-fold more strongly expressed at 15°C in *B. megaterium* [175, 453]. In these bacteria, this helicase is indispensable for survival at low temperature and apparently works cooperatively with some cold shock proteins to rescue misfolded mRNA and maintain correct translation initiation [453-455]. As a matter of fact, deletion of CsdA and CshA, respectively, results in a reduction of ribosomal units and a cold-sensitive phenotype [456, 457]. Apart from easing translation processes by unwinding RNA duplexes, recent studies have furthermore revealed that this protein is an integral part of the RNA degradosome of *B. subtilis* and *E. coli* at low temperature, interacting with PNPase and various RNase to break down RNA [458-460]. Hence, it is tempting to hypothesise that helicases CsdA and CshA undertake a pivotal role in RNA homeostasis at low temperature, signalling whether mRNA should be fixed or dismantled and thus favouring indirectly the production of specific proteins over others.

Still in relation with RNA processing, expression of the gene *bipA* encoding a GTPase sharing 85.8 % homology with a GTP-binding elongation factor from *B. subtilis* (YlaG) was increased 2-fold at 15°C in *B. megaterium* and could, as its homologue in *B. subtilis* and another GTPase in *E. coli*, be involved in correct ribosome assembly and improvement of translation efficiency under cold stress [327, 461]. Finally, the 1.8-fold higher expression of *rluB*, a gene encoding a pseudouridine synthase, could indicate a role of isomerisation of uridine to pseudouridine (Ψ) in the post-transcriptional increase of mRNA stability and translation efficiency during growth in the cold [462-465].

### *Transcription and protein homeostasis is not greatly affected in cold-adapted* B. megaterium *DSM319*

According to Le Chatelier's principle, while the entropy of a system rises upon a strong temperature increase and inevitably leads to protein denaturation, a drop in temperature generally results in a better protein stability. However, proper folding and stability of a wide range of proteins appears to be limited when temperature dips below a certain threshold because different physicochemical interactions take over and perturb the previously favourable thermodynamic state [154, 289, 466, 467]. In *B. megaterium*, genes encoding most chaperones belong to diverse heat stress regulons and as such their expression was 2 to 4-fold repressed at 15°C (Tab. 4.7).

**Table 4.7: Gene expression level of cold-induced elements in *B. megaterium* DSM319 growing at 15 and 45°C –** Data are given as fold change (FC) of transcript concentrations compared to their values at 37°C. Red and blue bold numbers indicate significant increases and decreases of gene expression, respectively.

| Locus Tag | Name | Description | Transcriptome FC | |
|---|---|---|---|---|
| | | ***Cold Shock Proteins (CSPs)*** | **15°C** | **45°C** |
| *bmd_0987* | *cspB* | Cold shock protein | **4.27** | **-2.94** |
| *bmd_1404* | *cspA* | Cold shock protein | **-6.39** | **-3.10** |
| *bmd_1450* | *cspD* | Cold shock protein | **-4.19** | **3.91** |
| *bmd_1682* | *cspA* | Cold shock protein | **-1.76** | **2.60** |
| *bmd_1730* | *cspC* | Cold shock protein | **9.75** | -1.47 |
| *bmd_2695* | *cspC* | Cold shock protein | **4.53** | **-1.97** |
| *bmd_2698* | *cspC* | Cold shock protein | **4.55** | **-2.18** |
| *bmd_2791* | *cspC* | Cold shock protein | -1.24 | **2.26** |
| *bmd_2794* | *cspC* | Cold shock protein | **5.48** | -1.09 |
| *bmd_3204* | *cspB* | Cold shock protein | -1.54 | -1.16 |
| *bmd_3402* | *cspC* | Cold shock protein | **5.78** | **-2.42** |
| *bmd_3404* | *cspC* | Cold shock protein | **17.93** | -1.01 |
| *bmd_3482* | *cspE* | Cold shock protein | -1.04 | 1.04 |
| *bmd_3807* | | Cold shock protein | **11.62** | **-2.04** |
| | | ***Protein, DNA and RNA homeostasis*** | **15°C** | **45°C** |
| *bmd_0005* | *gyrB* | DNA gyrase, B subunit | 1.43 | -1.00 |
| *bmd_0006* | *gyrA* | DNA gyrase, A subunit | 1.37 | 1.06 |
| *bmd_0215* | *cshA* | ATP-dependent RNA helicase | **2.60** | **-2.27** |
| *bmd_0345* | | ATP-dependent RNA helicase | -1.07 | -1.56 |
| *bmd_0763* | *dbpA* | ATP-dependent RNA helicase | 1.48 | -1.13 |
| *bmd_1340* | *bipA* | GTPase | **2.02** | **-1.88** |
| *bmd_1409* | *yprA* | ATP-dependent RNA helicase | -1.08 | 1.05 |
| *bmd_1447* | *rnhA* | RNase H | 1.54 | -1.01 |
| *bmd_2285* | | Bacillolysin precursor (neutral protease) | **2.96** | **-2.37** |
| *bmd_2792* | | ATP-dependent RNA helicase | 1.16 | -1.08 |
| *bmd_4132* | *pnp* | Polynucleotide phosphorylase | 1.40 | -1.65 |
| *bmd_4358* | *rluB* | Pseudouridine synthase | **1.83** | -1.19 |
| *bmd_4521* | | ATP-dependent RNA helicase, DEAD/DEAH box family | 1.34 | -1.16 |
| *bmd_4677* | *clpX* | ATP-dependent Clp protease, ATP-binding subunit ClpX | 1.41 | -1.33 |
| *bmd_5044* | *clpP* | ATP-dependent Clp protease, proteolytic subunit ClpP | **1.82** | **2.10** |
| | | ***Competence regulation & defences against bacteriophage*** | **15°C** | **45°C** |
| *bmd_0054* | *abrB* | Transition state regulatory protein AbrB | **2.21** | 1.66 |
| *bmd_0061* | *veg* | Control of biofilm formation | **9.77** | 1.17 |
| *bmd_0125* | | 16S rRNA m(2)G 1207 methyltransferase | **2.61** | -1.54 |
| *bmd_0221* | *ndoAI* | Antitoxin EndoAI (EndoA inhibitor) | **2.47** | -1.03 |
| *bmd_0222* | *ndoA* | Endoribonuclease EndoA | **2.32** | 1.09 |
| *bmd_0349* | | Conserved hypothetical protein | **-2.21** | -1.13 |

**Table 4.7 (continued)**

| Locus Tag | Name | Description | Transcriptome FC | |
|---|---|---|---|---|
| | | ***Competence regulation & defences against bacteriophage*** | **15°C** | **45°C** |
| *bmd_0350* | | Conserved hypothetical protein | -1.23 | -1.06 |
| *bmd_0351* | | Conserved hypothetical protein | -1.19 | -1.01 |
| *bmd_0352* | | Conserved hypothetical protein | -1.18 | 1.01 |
| *bmd_0353* | | Conserved hypothetical protein | -1.34 | -1.06 |
| *bmd_0699* | *appD* | Oligopeptide ABC transporter, ATP-binding protein AppD | 1.56 | 1.03 |
| *bmd_0700* | *appF* | Oligopeptide ABC transporter, ATP-binding protein AppF | 1.63 | 1.01 |
| *bmd_0701* | *appA* | Oligopeptide ABC transporter, binding protein AppA | **2.70** | -1.21 |
| *bmd_0702* | *appB* | Oligopeptide ABC transporter, permease protein AppB | **2.05** | -1.10 |
| *bmd_0703* | *appC* | Oligopeptide ABC transporter, permease protein AppC | **1.72** | -1.11 |
| *bmd_0706* | *oppA* | Oligopeptide ABC transporter, oligopeptide-binding protein | **-3.31** | 1.26 |
| *bmd_0707* | *oppB* | Oligopeptide ABC transporter, permease protein | **-3.06** | 1.34 |
| *bmd_0708* | *oppC* | Oligopeptide ABC transporter, permease protein | **-3.78** | 1.42 |
| *bmd_0709* | *oppD* | Oligopeptide ABC transporter, ATP-binding protein | **-3.97** | 1.73 |
| *bmd_0710* | *oppF* | Oligopeptide ABC transporter, ATP-binding protein | **-3.33** | 1.66 |
| *bmd_0714* | *spxA* | Competence regulatory protein Spx | **2.27** | **3.05** |
| *bmd_0719* | *mecA* | Competence-associated adapter protein | 1.52 | **1.95** |
| *bmd_0832* | | Integral membrane protein | **2.13** | -1.01 |
| *bmd_1003* | *capB* | Capsule biosynthesis protein CapB | **2.16** | -1.63 |
| *bmd_1004* | *capC* | Capsule biosynthesis protein CapC | **1.98** | -1.34 |
| *bmd_1005* | *capA* | Capsule biosynthesis protein CapA | **2.21** | **-1.78** |
| *bmd_1137* | *comK* | Competence transcription factor K | 1.03 | 1.04 |
| *bmd_1924* | | Methyltransferase | **1.81** | -1.01 |
| *bmd_4341* | *mecB* | Negative regulator of genetic competence | **4.13** | -1.04 |
| *bmd_4482* | *spxA* | Regulatory protein Spx | **1.80** | 1.25 |
| *bmd_4759* | *fxsA* | FxsA cytoplasmic membrane protein | **1.82** | -1.22 |
| *bmd_5108* | *degU* | Two-component response regulator DegU | 1.54 | -1.32 |
| | | ***Other cold induced proteins (CIPs)*** | **15°C** | **45°C** |
| *bmd_0417* | *perR* | Peroxide operon regulator | **1.80** | -1.17 |
| *bmd_0638* | | Conserved hypothetical protein | **3.45** | **1.88** |
| *bmd_0990* | | 2-cys peroxiredoxin | **2.07** | **-1.79** |
| *bmd_1211* | *phaP* | Polyhydroxyalkanoic acid inclusion protein PhaP | **1.94** | **-1.85** |
| *bmd_1212* | *phaQ* | Poly-beta-hydroxybutyrate-responsive repressor | **1.94** | -1.54 |
| *bmd_1307* | | Protein of unknown function (DUF1797) | **4.79** | **-2.97** |
| *bmd_1474* | *des* | Fatty acid desaturase | **2.88** | -1.31 |
| *bmd_2091* | *sodC* | Copper/zinc superoxide dismutase | 1.49 | -1.29 |
| *bmd_4715* | *trx* | Thioredoxin | 1.28 | **3.6** |
| *bmd_4933* | | General stress protein 13 | **2.53** | 1.00 |

Even the transcription of *ppiB*, a cold-induced gene encoding an isomerase involved in protein folding in *B. subtilis*, was not particularly induced in *B. megaterium* [468]. Hence, either protein stability is improved or production of chaperones relies on post-transcriptional events at this temperature. Similarly, only few genes involved in protein degradation were more strongly expressed at 15°C, with among them those encoding neutral protease bacillolysin (*bmd_2285*) and the ClpPX proteolytic complex showing a 3-fold, 1.4-fold and 1.8-fold increased transcription, respectively (Tab. 4.7) [469]. It is difficult to come to a conclusion without proteome data but at first sight, protein homeostasis seems to be a secondary problem, if at all.
The alteration of transcription is also a commonly reported effect of low temperatures and a direct consequence of temperature-induced modifications of DNA structure [470]. In fact, DNA gyrases generate an increase in DNA negative supercoiling and expression of genes essential for survival under these conditions is sustainably triggered via twist-sensitive promoters while transcription of others is impaired [180, 471, 472]. Contrary to observations after cold shock in *B. subtilis* and *E. coli*, expression of genes *gyrA* and *gyrB* encoding DNA gyrases in *B. megaterium* was not significantly increased and do not support a marked modification of DNA structure at 15°C (Tab. 4.7) [327, 473]. Naturally, proteome data would be necessary to confirm this conclusion but the 6.7-fold reduced expression of *cspA*, whose product is a positive regulator of *gyrA* expression in *E. coli*, is in good agreement with this hypothesis. Moreover, the 2.5-fold reduced expression of gene *bmd_0576* encoding a DNA binding protein HU also suggests that DNA supercoiling is not greatly modified once cells are adapted (Tab. A.4). Indeed, Mizushima et al. [470] have proposed that both DNA gyrases and DNA binding HU proteins contribute to increasing negative supercoiling under cold stress and showed that in mutants unable to produce the latter proteins, the increase of DNA supercoiling was partially inhibited. In accordance with this, none of these genes were reported as strongly induced in works from Budde et al. [95] on cold acclimatisation in *B. subtilis*.

### *The cold-induced metabolic slow-down impacts cellular redox potential*

As mentioned previously, acclimatisation to low and high temperatures relies on very distinct systems and only thirteen genes had a significantly higher expression under both conditions. Interestingly, this group comprises ten genes involved in biotin and cobalamin synthesis in combination with *spxA* (*bmd_0714*). Considering that expression of the hydrogen peroxide-responsive gene *perR* was 1.8-fold enhanced at 15°C, the presented data therefore suggest the emergence of a $H_2O_2$-mediated stress and support the idea that cobalamin and biotin are involved in reducing oxidative damages at both temperatures (Tab. 4.7). Surprisingly, expression of genes encoding methionine sulfoxide reductases and genes belonging to the Spx-regulon in *B. subtilis* was, however, not particularly induced at 15°C in *B. megaterium*. Hence, their regulation and the exact function of biotin in *B. megaterium* require further clarifications [95, 413]. Since the NADH/$NAD^+$-ratio at 15°C remained close to its most physiological value, it is also not clear how peroxides can be produced at this temperature. Perhaps the higher oxygen solubility

at low temperature combined with an extremely high NADPH/$NADP^+$-ratio foster $H_2O_2$-generation through leakages from the electron transport chain and activity of cytochrome P450 or a yet unknown NADPH-oxidase (cf. Tab. 4.2) [376, 474, 475]. Still, with the exception of a peroxiredoxin (*bmd_0990*) whose encoding gene was 2-fold more expressed at 15°C, none other ROS scavenging system seems active and the production of highly reactive oxygen species from $H_2O_2$ is certainly excluded. Here again, it is also of high interest to see that peroxiredoxins involved in $H_2O_2$ reduction at 15 and 45°C showed inversed induction patterns and are seemingly temperature specific (cf. Tab. 4.4 and Tab. 4.7). Paradoxically, the high NADPH/$NADP^+$-ratio that might contribute to $H_2O_2$ formation provides the reductive power necessary for recycling compounds involved in ROS scavenging such as cysteine, peroxiredoxin and thioredoxin and probably restricts the production of ROS at 15°C [376]. As hydrogen peroxide is also a powerful intracellular signalling messenger, it is possible that cells adjust its concentration to a certain threshold level using peroxiredoxin in order to induce targeted genes useful under these conditions [476, 477].

### *Expression of genes supposedly involved in natural competence regulation is significantly altered at 15°C*

In contrast to other *Bacillus* sp., *B. megaterium* has never been reported to develop natural competence so far. Nevertheless, its recent genome sequencing has revealed that this organism possesses homologues to all genes involved in competence acquisition and regulation in *B. subtilis* and lots of efforts are therefore currently dedicated to elucidating the mechanisms governing the expression of competence related genes [17, 478, 479]. In this respect, expression of *mecB* and *abrB*, two genes coding for negative regulators of the competence transcription factor ComK in *B. subtilis*, was increased by a factor of 4 and 2.2, respectively, in *B. megaterium* growing at 15°C (cf. Tab. 4.7). In *B. subtilis*, ComK is the main activator of genes involved in DNA binding, uptake and recombination and is actively degraded by a complex composed of ClpP, MecA and MecB, a member of the ClpC ATPase family [480-482]. Considering that expression of *clpP* and *mecA* had also slightly higher expression levels at 15°C, degradation of ComK by this complex could be conserved in *B. megaterium* (cf. Tab. 4.7). Interestingly, results from Nakano et al. [483] have furthermore proposed that the presence of Spx enhances ComK binding to ClpP-MecA and the increased transcription of both *spx*A genes (*bmd_0714 and bmd_4482*) at 15°C is in good agreement with their putative role in degrading ComK. The negative regulator AbrB, on the other hand, operates at the transcriptional level by binding the promoter of comK [484]. In *B. megaterium*, however, expression of *comK* was not significantly altered at 15°C and the role of AbrB in competence regulation must be further studied.

Another finding possibly related to competence is the 3.5-fold reduced expression measured at 15°C for the *opp* operon, encoding a membrane-anchored oligopeptide transporter involved in modulation of the activity of sporulation and competence genes in response to environmental

stress in *B. subtilis* and other Gram-positive bacteria (cf. Tab. 4.7) [485]. As a matter of fact, deletion of one or several of the *opp* genes results in a drastic reduction in competence acquisition and inhibits sporulation in these organisms [486-488]. The underlying mechanism in *B. subtilis* is complex and recruits two signalling peptides, PhrC and PhrA, which trigger phosphorylation of ComA and enable activation of *srfA*, a central activator of competence genes [489]. In *B. megaterium*, no peptides similar to PhrC and PhrA or gene equivalent to *srfA* have been found so far and this absence could eventually contribute to the general lack of competence in this organism. In this context, it seems important to point out that the *opp*-operon was, on the contrary, 3.5-fold more expressed in *B. subtilis* adapted to 15°C [95]. Although these observations are still insufficient to grasp whether *B. megaterium* can indeed develop competence or not, they at least bring some new elements to the current reflection.

### *At low temperature, B. megaterium activates specific mechanisms to ensure conservation of DNA integrity*

Consistent with the modifications operated on competence-related genes, several genes involved in protection against bacteriophages showed higher expression levels at 15°C (cf. Tab. 4.7). Bacteriophages are ubiquitous viruses injecting their DNA or RNA genome into cells for replication at the expense of the host. In nature, they outnumber bacteria by a factor 10 and since their proliferation within the cytoplasm ultimately leads to cell lysis, bacteria have evolved a broad range of resistance strategies aiming mostly at preventing bacteriophage adhesion to cell wall, blocking genome injection or cutting phage nucleic acid [490, 491]. In *B. megaterium*, expression of operon *capABC*, which encodes a system producing bacterial γ-poly-glutamic acid capsules, and of *veg*, a gene involved in biofilm formation, was 2-fold and 9.8-fold increased at 15°C, respectively (cf. Tab. 4.7) [492]. Hence, as described for other *Bacillus* spp., *B. megaterium* apparently builds an extracellular chemical barrier that cannot be easily hydrolysed by phages and prevent their adhesion by obstructing phage-specific receptors [493-495]. Gene *bmd_0382*, whose expression was 2-fold increased at 15°C and which encodes a protein 45 % similar to *B. subtilis* YjbE, might also contribute to the synthesis of a protective matrix since its homologue in *E. coli* seems involved in exopolysaccharide and biofilm synthesis [496, 497]. Given the very different genomic context in these organisms, further investigation is, however, required to assess the exact function of this gene.

As phage receptors have only been poorly characterised in *Bacillus* spp. so far, less is known about defences acting on them directly. Similarly, no superinfection exclusion systems (Sie), a structure consisting of membrane-associated or anchored proteins and blocking the entry of certain phage DNAs, has been characterised in *Bacillus* spp. yet and they are rather thought to be produced by prophages to help their host struggling with other bacteriophages. On the contrary, a typical restriction-modification (R-M) system consisting of endoribonuclease EndoA (*ndoA*) and two methyltransferases (*bmd_1924* and *bmd_0125*) seems to be turned on (up to 2.61-fold enhanced expression) and certainly degrade foreign nucleic acids at 15°C in *B. megaterium* (cf. Tab. 4.7).

While the latter two ensure methylation of restriction sites in both the genome and transcripts of the host cell, the first cleaves non methylated intruding DNA or RNA. Along with the 2.3-fold higher expression of *ndoA*, a 2.5-fold increase in transcript concentration was also noticed for *ndoAI*, the gene encoding its inhibitor and indicates that activity of EndoA at 15°C is also strictly regulated to prevent toxic damages on host genome in case of methyltransferase denaturation.
Finally, the expression of *fxsA*, encoding a transmembrane protein whose homologous protein seems to inhibit phage exclusion in *E. coli*, was also 1.8-fold higher at 15°C (cf. Tab. 4.7) [498, 499]. Phage exclusion, also called abortive infection (Abi), is the triggering of cell lysis in response to an infection with bacteriophages in order to avoid their proliferation and contamination of other cells. In that sense, this increased *fxsA* expression certainly prevents cell death when other bacteriophage defences are active, considering phage exclusion as a last resort [500].
Since the presented transcriptome data originate from four different replicates and since cells have always presented the same growth characteristics (μ, $Y_{X/S}$, $Y_{P/S}$) over dozens of cultivations, the expression of all these genes at low temperature is probably not due to an infection but rather corresponds to a preventive measure to preserve DNA integrity. In fact, the risk of contamination by bacteriophages rises exponentially with exposure time and is therefore higher at low temperature when bacteria have a long generation time.

## 4.2 System-wide analysis of adaptation to osmotic stress

As a typical soil bacterium, *B. megaterium* is exposed in its habitat to life-threatening environmental modifications caused, among other things, by circadian and seasonal variations. Fluctuations in water availability are no exception and cells have, for instance, to endure hyper- and hypo-osmotic episodes during drought and rainy periods, respectively. Comprehending the nested survival responses elicited by alteration of osmolarity is of particular interest for biotechnological applications since *B. megaterium* and other industrial workhorses are readily confronted to this issue in bioreactors where fed substrate and expected product concentrations are particularly high and affect water efflux, in turn reducing bacterial overall performance [501].
Based on its available genome sequence, the present study assesses the response of *B. megaterium* DSM319 to sustained moderate and severe osmotic stress by combining physiological and multi-omics data, thus providing new insights in the involved cellular mechanisms and enabling a comparison with other *Bacillus* sp. [17].

### 4.2.1 Impact of ionic osmotic stress on cellular physiology in *B. megaterium*

To assess the impact of osmotic stress on *B. megaterium*'s physiology, the growth profile and product yields for organic acids were determined from shake flask experiments at 37°C in M9 minimal medium supplemented with up to 1.8 M NaCl. In addition, transcripts, intracellular proteins and metabolites produced during exponential phase ($OD_{600nm}$ = 5) were identified and quantified combining microarrays, LC-MS and HPLC-measurements.

### *Resistance of* B. megaterium *against salt stress and its adverse effects*

The physiological aftermaths of high salinities in *B. megaterium* were not different from those observed in other *Bacillus sp..* They included growth delay, up to 40 % reduction of biomass yield as well as an up to 5-fold decreased growth rate as a consequence of reduced substrate uptake (**Tab. 4.8**) [207, 502, 503]. However, contrary to other studied *Bacillus sp.*, *B. megaterium* was still able to grow reproducibly in M9 minimal medium supplemented with 1.8 M NaCl. Moreover, at equivalent NaCl-concentrations, detrimental consequences on physiology were less pronounced than in other members of this genus. This higher robustness was also reflected in the up to 5-fold reduction of the number of genes whose expression was significantly altered under salt stress in *B. megaterium* compared to *B. cereus, B. subtilis* or *B. licheniformis* [92, 207, 503].

**Table 4.8: Physiological data for *B. megaterium* DSM319 growing on M9 minimal medium supplemented with different NaCl-concentrations (0, 0.3, 0.6, 0.9, 1.2 and 1.8 M).** Bold numbers indicate maximal yield observed for each measured organic acids.

| Parameter | Unit | 0 M | 0.3 M | 0.6 M | 0.9 M | 1.2 M | 1.8 M |
|---|---|---|---|---|---|---|---|
| $\mu$ | $h^{-1}$ | 1.19 ± 0.02 | 0.88 ± 0.01 | 0.69 ± 0.01 | 0.57 ± 0.01 | 0.39 ± 0.00 | 0.24 ± 0.00 |
| $Y_{X/S}$ | $g_{CDW}$ $mol^{-1}$ | 83.1 ± 1.1 | 77.2 ± 0.9 | 74.6 ± 1.1 | 70.7 ± 1.3 | 67.3 ± 0.9 | 58.7 ± 0.7 |
| $q_s$ | mmol $g_{CDW}^{-1}$ $h^{-1}$ | 14.4 ± 0.3 | 11.5 ± 0.2 | 9.3 ± 0.2 | 8.0 ± 0.2 | 5.8 ± 0.1 | 4.0 ± 0.1 |
| $Y_{Acetate/S}$ | mmol $mol^{-1}$ | **669 ± 21** | 526 ± 24 | 490 ± 19 | 422 ± 41 | 346 ± 26 | 253 ± 22 |
| $Y_{Pyruvate/S}$ | mmol $mol^{-1}$ | 6.4 ± 0.3 | 7.6 ± 0.4 | 2.9 ± 0.1 | 1.7 ± 0.1 | 2.2 ± 0.2 | **20.1 ± 1.6** |
| $Y_{Lactate/S}$ | mmol $mol^{-1}$ | 4.4 ± 0.3 | 3.6 ± 0.2 | 8.3 ± 0.4 | 15.0 ± 0.6 | 20.3 ± 0.6 | **37.7 ± 2.0** |
| $Y_{Succinate/S}$ | mmol $mol^{-1}$ | **62.6 ± 3.2** | 22.7 ± 1.0 | 14.7 ± 0.7 | 13.4 ± 0.6 | 10.0 ± 0.4 | 5.8 ± 0.6 |
| $Y_{Oxoglutarate/S}$ | mmol $mol^{-1}$ | **9.7 ± 0.4** | 2.3 ± 0.1 | 1.3 ± 0.1 | 0.7 ± 0.1 | 1.2 ± 0.1 | 1.6 ± 0.1 |

As for heat stress, increasing ionic osmotic stress furthermore disrupted redox state and resulted in up to 8.6-fold higher lactate yields, thus supporting the notion that lactate synthesis serves redox balancing by recycling $NAD^+$ (Tab. 4.8 and **Tab. 4.9**). In that sense, recent studies have underlined the central role of lactate dehydrogenase in redox homeostasis and resistance to environmental stress in *Enterococcus faecalis* and *Staphylococcus aureus* [504, 505].

**Table 4.9: Energy charge and redox state values of *B. megaterium*.**

| | Range | 0 M | 0.6 M | 1.2 M |
|---|---|---|---|---|
| Adenylate energy charge (AEC) | > 0.7 | 0.8336 | 0.7659 | 0.8612 |
| $NADH/NAD^+$ | < 0.1 | 0.0079 | 0.0260 | 0.0191 |
| $NADPH/NADP^+$ | < 1.4 | 0.5162 | 0.4330 | 1.0551 |

Surprisingly, neither the transcription of the gene encoding lactate dehydrogenase (*ldh*) nor the production of the corresponding enzyme was significantly enhanced by salt in *B. megaterium*, suggesting that lactate synthesis was either allosterically regulated or performed by a yet unknown protein under these conditions. Similarly, the 2.5-fold higher expression of the gene encoding pyruvate oxidase Pox (*bmd_1131*) in cells exposed to more than 1.2 M NaCl tends to confirm that activation of Pox route is closely related to cell redox state as observed at 45°C (Tab. 4.9 and **Fig. 4.15**) [304]. However, despite the high NADH-to-$NAD^+$ ratio, *bmd_1131* was not differentially expressed when 0.6 M NaCl was supplemented to the medium. Since most genes involved in scavenging of reactive oxygen species (ROS) showed a similar expression pattern, we suggest that ROS level is the actual signal activating the Pox route while disruption of redox ratio only promotes the emergence of these compounds [376].

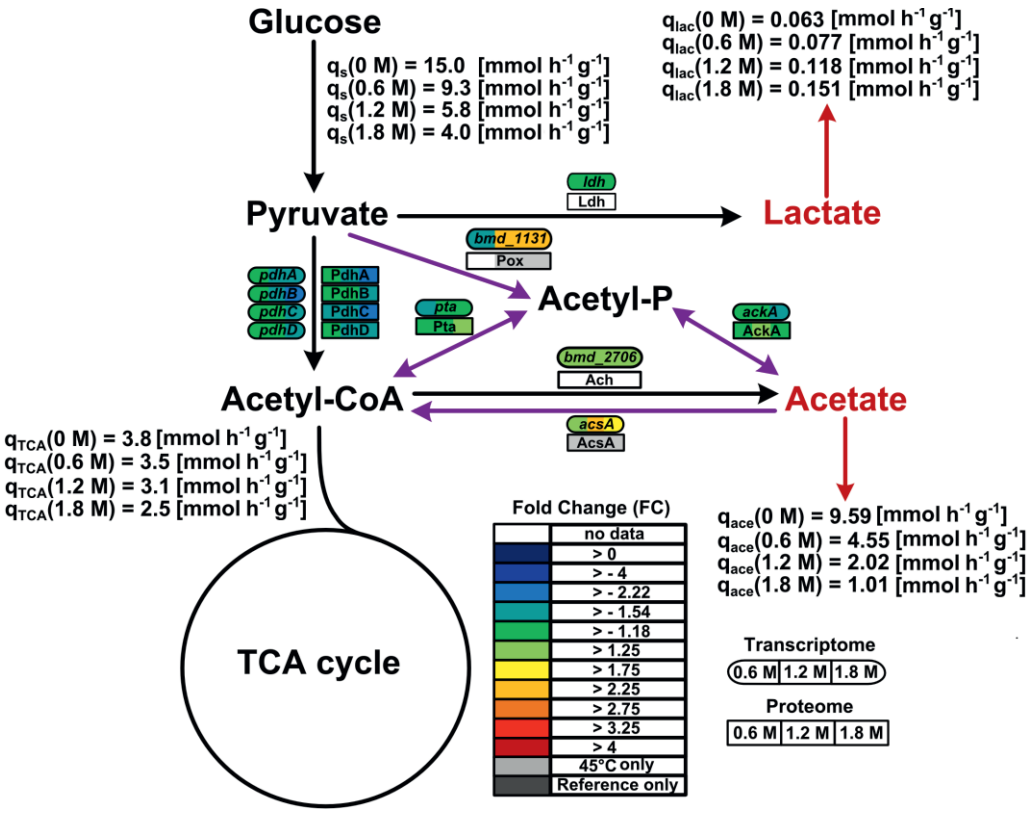


**Figure 4.15: Pox route and overflow metabolism in *B. megaterium* DSM319 growing in M9 minimal medium supplemented with different NaCl concentrations** – Purple arrows correspond to reactions of the Pox route while red arrows indicate organic acid secretions. Gene expression was determined by microarray analysis using purified RNA samples obtained from four biological replicates. Intracellular proteins were identified and quantified by proteome analysis using LC- $IMS^e$ for cells originating from four replicates as well. Values are indicated as fold change compared to expression in cells grown at 37°C in M9 minimal medium without additional NaCl supplementation (**Reference**). **Ach**: acetyl-CoA hydrolase; **AckA**: acetate kinase; **AcsA**: acetyl-CoA synthetase; **Ldh**: lactate dehydrogenase; **Pdh**: pyruvate dehydrogenase; **Pox**: pyruvate oxidase; **Pta**: phosphate acetyltransferase.

### *Metabolic adjustments at high salinity aim at fine-tuning of the intracellular proline pool*

Interestingly, the conversion of glucose to organic acids other than lactate was significantly reduced at elevated medium osmolarities. More particularly, in good accordance with findings in *B. subtilis*, secretion of acetate strongly dropped despite the apparent utilisation of the Pox route (cf. Tab. 4.8 and Fig. 4.15) [502]. Two important factors can explain this discrepancy compared to the situation at high temperature. First, the absolute glycolytic flux was at least twice lower than at 45°C and limited intensity of flux diversion towards overflow reactions. Second, responding to an up to 2.7-fold increased expression of *acsA*, cells started producing acetyl-coA synthetase (AcsA) that efficiently redirected produced acetate towards the TCA cycle under osmotic stress [303].
On the contrary, intracellular concentrations of several amino acids and in particular of the compatible solute proline gradually increased with medium osmolarity (**Fig. 4.16**). Hence, it seems that cells tended to avoid carbon wastage through secretion and rather converted acetate into acetyl-CoA to meet the physiological constraints imposed by osmotic stress.

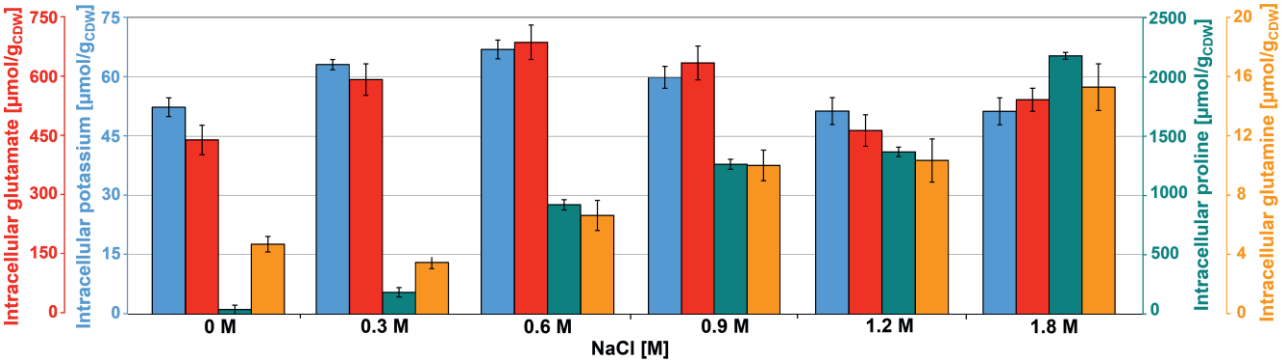


**Figure 4.16: Intracellular concentration of potassium (●), glutamate (●), glutamine (●) and proline (●) for cultivations of *B. megaterium* DSM319 in M9 minimal medium supplemented with different NaCl concentrations.**

Since proline accumulated intracellularly to concentrations of over 2200 µmol $g_{CDW}^{-1}$ at 1.8 M NaCl and because *B. megaterium* DSM319 does not possess the genes for the *de novo* synthesis of other osmoprotectants such as ectoine, glycine betaine or trehalose, we assume that it is the major osmoprotectant in this organism (Fig. 4.16). Nevertheless, the up to 3-fold stronger expression of *gbsA* and *gbsB* under osmotic stress, two genes involved in the last steps of glycine betaine biosynthesis, tends to indicate that, as observed in *B. subtilis*, this compatible solute can also be synthesised if the precursor choline is supplied to the medium [506-508]. Surprisingly, with the exception of *ousA* whose expression was 3-fold increased, transcription of genes encoding osmoprotectant transporters (*opuAA* to *AC, opuD*) was, however, not particularly modified in *B. megaterium* under hypertonic conditions (**Tab. A.12** and **Tab. A.13**) [509].

Alternatively, other amino acids presenting high solubility such as serine, alanine and glycine might serve as secondary compatible solutes or help coping with osmotic stress because their intracellular concentrations also increased with increasing salt concentrations (Tab. A.6). Their role in protein hydration and stabilisation has for instance been reviewed in details before [510-512].

### *Glutamate undertakes a pivotal role in adaptation to mild and severe salt stress*

As in *B. subtilis* and many other bacteria, glutamate was the most abundant metabolite in the cytosol of *B. megaterium* under standard conditions with a concentration of 450 µmol $g_{CDW}^{-1}$ (cf. Fig. 4.16) [513, 514]. Together with glutamine, it is a central metabolite linking carbon metabolism to nitrogen metabolism and a major precursor for the *de novo* synthesis of proline [206, 515]. Consequently, its intracellular pool has to be tightly controlled under osmotic stress when it is massively consumed to fulfil proline biosynthetic requirements. While glutamine pool increased concomitantly with proline pool, intracellular glutamate pool reached its maximum at 0.6 M NaCl and gradually returned to its initial value at 1.2 M NaCl. Interestingly, this concentration pattern matched perfectly the profile of intracellular potassium and reveals the two-sided nature of adaptation to salt stress. At moderate NaCl-concentrations (≤ 0.6 M NaCl), cells seems to use glutamate as counterion to import potassium for adjusting turgor pressure and its intracellular concentration was accordingly increased [516, 517]. In *B. megaterium*, this import could be performed by the conserved uptake systems KtrAB and KtrCD as described in *B. subtilis* but expression of the corresponding genes was not significantly modified under salt stress and protein concentration could not be grasped by our proteome approach because these are membrane proteins [202].

On the contrary, for concentrations above 0.6 M NaCl, this solution was completely replaced by proline synthesis, probably because the potassium concentration would otherwise become cytotoxic, and both the glutamate and potassium pools were progressively reduced. Responding to the larger demand for proline, the intracellular concentration of glutamate however increased slightly again at 1.8 M NaCl. The importance of glutamate as main precursor for proline synthesis was also highlighted by the progressive reduction of its release in the culture broth with increasing salinities (**Tab. A.14**).

Curiously, despite the need to adjust turgor pressure and export toxic compounds under osmotic stress, the expression of genes encoding mechanosensitive channels (*mscL, mscS*) but also sodium transporters (*mrpABCDGEF*) was, however, not influenced by salt in *B. megaterium* [518]. Hence, it is not clear how potassium is exported under these conditions [92, 519].

Still, these results indicate that the choice of an adaptation mechanism is not only a function of stress duration but also seems to depend on its intensity. Contrary to classical scientific consensus, accumulation of potassium might play a central role in long-term adaptation of moderate halotolerant bacteria under mild salt stress [201].

### 4.2.2 Adaptation of *Bacillus megaterium* carbon core metabolism during sustained osmotic stress

To get a better insight into physiological adjustments observed under osmotic stress, flux distribution within the central carbon metabolism of cells growing in M9 minimal medium with up to 1.8 M NaCl was determined by metabolic flux analysis as described for temperature (4.1.2). Condition-specific precursor demands and measured steady-state labelling patterns of amino acids used for estimating fluxes at the different NaCl concentrations can be find in Appendix (Tab. A.2, Tab. A.9 and Tab. A.10). Precursor demands were determined from the macromolecular compositions at 0, 0.6 and 1.2 M NaCl, respectively, and subsequently extrapolated from these values for other NaCl concentrations. They were notably affected by the 3-fold increase of the amino acid content caused by glutamate and proline production at both 0.6 M and 1.2 M NaCl (Fig. 4.16 and Tab. A.6). Other major alterations of the macromolecular content included a reduction of RNA content proportional to added NaCl concentrations (18.5 , 14.9 and 12.5 % of biomass) and a 2- and 5-fold increased PHB content at 0.6 M and 1.2 M, respectively (5.87 %, 14.36% and 29.54 % of biomass) (Fig. A.1). The latter was quite unexpected and will be discussed in details in section 4.3.

#### *Flux distribution is strategically rearranged to fulfil requirements specific to osmotic stress*

Comparison between flux distributions in non-stressed cells and cells exposed to mild (≤ 0.6 M NaCl) and severe osmotic stress (> 0.6 M NaCl) (Fig. 4.5, **Fig. 4.17**, Tab. A.7 and Tab. A.8) revealed a progressive intensification of relative fluxes through the TCA cycle with increasing salt concentrations and a massive rerouting of carbon from 2-oxoglutarate towards glutamate and proline synthesis. This was achieved by reducing the precursor drain for the synthesis of biomass compounds, organic and amino acids upstream and downstream from the 2-oxoglutarate node. In particular, carbon fuelling the TCA cycle was preferentially recycled to oxaloacetate by malate dehydrogenase and re-injected into the cycle, probably explaining why flux repartition at the anaplerotic node was not particularly altered despite the increasing utilisation of 2-oxoglutarate for proline biosynthesis.

Similarly, relative flux through the pentose phosphate pathway (PPP) increased proportionally to the imposed osmotic burden and exceeded by far the anabolic demand, resulting in a strengthened carbon channelling back to glycolysis intermediates. Since three moles NADPH are expended to synthesise one mole proline from 2-oxoglutarate, this marked increase certainly provided cells with the reducing power required for this conversion. However, it appeared that NADPH supply already outstripped biosynthetic demand by more than 20 % under normal conditions and the increased PPP fluxes under salt stress only accentuated this discrepancy, generating an 86 % NADPH excess at 1.2 M NaCl (**Fig. 4.18**). As a matter of fact, intracellular NADPH pool increased with salt concentrations and could trigger the observed enhancement of polyhydroxybutryate (PHB) synthesis from acetyl-CoA as will be discussed later (see section 4.2.4).

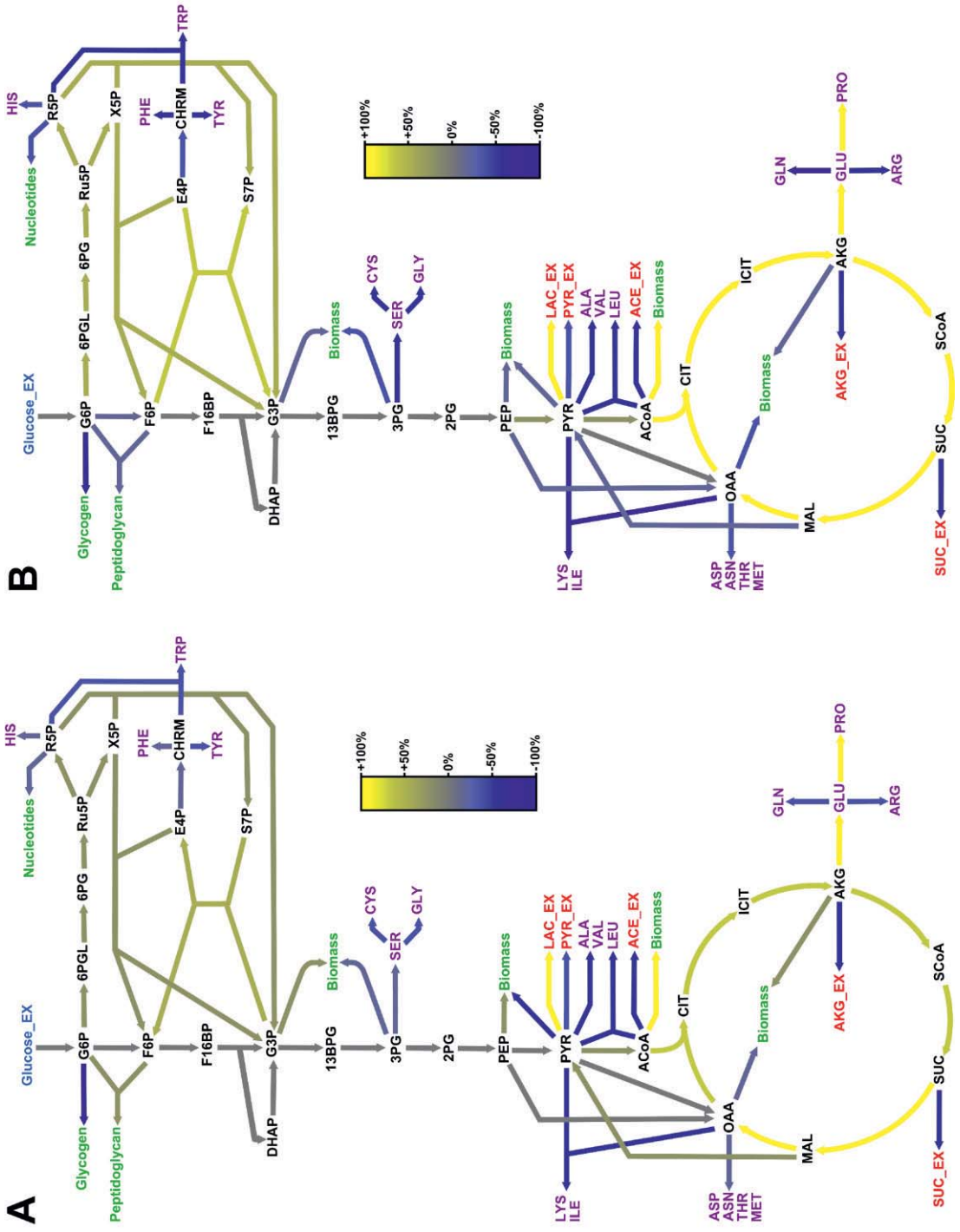


**Figure 4.17: Adaptation of carbon core metabolism to changing osmolarity** – Change (%) in relative flux distribution in cells growing at 37°C with 0.6 M **(A)** and 1.2 M NaCl **(B)** compared to cells growing at 37°C in normal M9 minimal medium (Fig. 4.5).

Such an imbalance between NADPH supply and demand has previously been reported for slow-growing bacteria and transhydrogenation cycle have been proposed as a mean to maintain redox balance [352, 520]. The up to 2.5-fold reduced expression of *gapN*, a gene coding a NADP-dependent glyceraldehyde-3-phosphate dehydrogenase, and the increased activity of several malic enzymes (*bmd_2037*, *bmd_4764*) whose cofactors are still unknown might for instance reflect the existence of similar cycles under severe salt stress in *B. megaterium*. In contrast, relative fluxes through the glycolysis remained approximately constant and surely participated to the maintenance of a high energy level even under stressful conditions, as indicated by the measured adenylate energy charge.

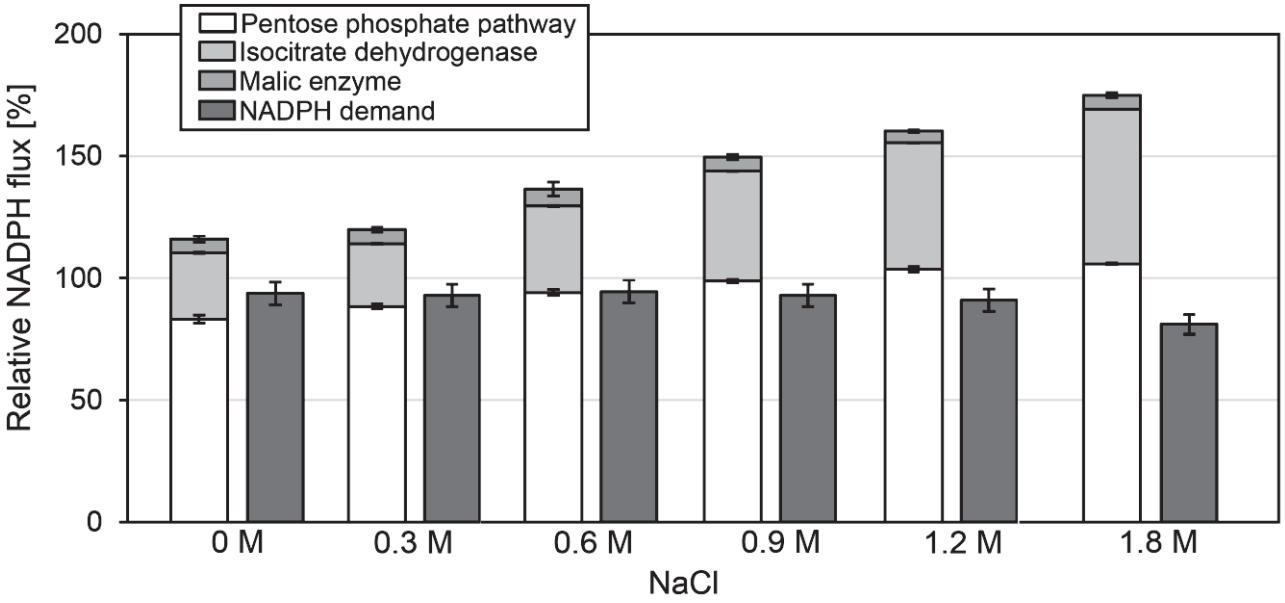


**Fig. 4.18: Comparison between NADPH supply and demand in cells growing at 37°C in M9 minimal medium supplemented with up to 1.8 M NaCl.** Biosynthetic NADPH demand was calculated from biomass composition at the respective NaCl concentration. NADPH supply was derived from flux analysis results.

Together, the combined increases of fluxes through the TCA cycle and PPP resulted in an up to 70 % stronger $CO_2$ release under osmotic stress and partly explain the reduction of biomass yield observed when sodium chloride was added to the medium (cf. Tab. 4.8). This situation was furthermore reinforced by the concomitant reduction of $CO_2$ fixation by phosphoenolpyruvate carboxylase under the same conditions (cf. Fig. 4.17).

### *Reorganisation of flux distribution is supported by targeted transcriptional modifications*

As highlighted by the hierarchical clustering performed on expression of genes belonging to the extended central carbon metabolism, rerouting of carbon fluxes towards proline synthesis under osmotic stress was fostered by altered expression of key genes (**Fig. 4.19**). Notably, our transcriptome data enabled discrimination between two sets of genes involved in the synthesis of proline from glutamate.

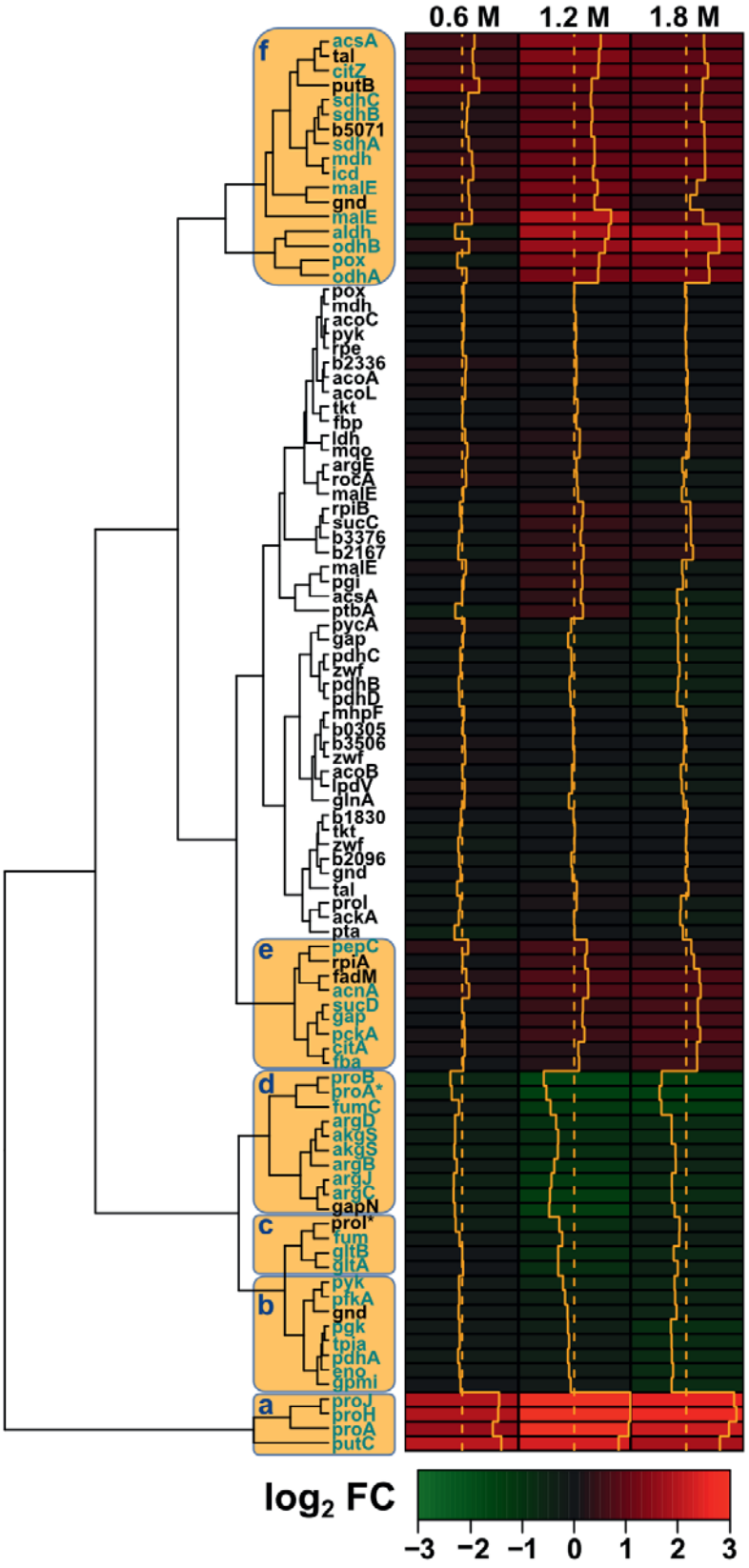


**Figure 4.19: Hierarchical clustering of gene expression of 97 selected genes of the central carbon, proline and arginine metabolism of *B. megaterium* DSM319.** Expression is indicated as fold change (FC) compared to expression at 37°C. Six main regulation clusters can be identified:

**a** - Genes coding for enzymes involved in proline biosynthesis under osmotic stress

**b** - Genes coding for glycolytic enzymes

**c** - Genes with unexpectedly low transcription level under salt stress

**d** - Genes encoding key enzymes of the arginine and anabolic proline metabolism

**e** - Genes coding for enzymes of the glycolysis, TCA cycle and junction of these two pathways

**f** - Genes encoding enzymes from the TCA cycle or involved in overflow metabolism

Whereas the expression of the first set composed of *proH-proJ-proA** was 4- and 10-fold enhanced at 0.6 M and 1.2 M NaCl, respectively, genes from the second set include *proB*, *proA* and *proI* and had their expression up to 3-fold reduced under osmotic stress. As concentrations

of the respective proteins behaved the same way, these results suggest that *proHJA** encodes a biosynthetic route for the unbridled synthesis of proline as an osmoprotectant, while *proBA* and *proI* are responsible for the anabolic proline production and negatively regulated by proline itself. The existence of two distinctive genes encoding glutamate-5-semialdehyde dehydrogenase reductase, namely the anabolic *proA* (*bmd_5523*) and osmo-inducible *proA** (*bmd_2245*), is of particular interest and indicates a strict separation between synthesis of proline for anabolic and protective purposes. In that sense, genetic organisation of proline synthesis in *B. megaterium* is similar to that in *B. licheniformis* and differs from that in *B. subtilis*, for which both routes are curiously interlinked by the unique γ-glutamylphosphate reductase ProA [206, 207]. Under severe osmotic stress, the increased flux towards proline biosynthesis was furthermore favoured by the 2-fold repression operated on expression of genes from the arginine biosynthesis pathway (*arg*), resulting in reduced concentrations of the corresponding enzymes (Fig. 4.19, Tab A.12 and Tab. A.13). Similarly, concentration of most enzymes converting glutamate and glutamine into intermediates of the purine, pyrimidine, and amino sugar metabolism were 2- to 5-fold reduced and the transcription of the corresponding genes was accordingly repressed (Tab. A.12 and Tab. A.13). On the contrary, expression of genes encoding D-amino-acid transaminase (*dat*) was increased and concentration of the corresponding enzyme up to 5-fold higher in hypertonic medium, certainly enabling an increased synthesis of glutamate, the main precursor of proline.

In addition, responding to the increased demand for osmoprotection, expression of several genes of the TCA cycle was up to 3-fold higher in stressed cells and might compensate the loss of activity induced by salt and, to a lesser extent, contribute to the increased flux deflection from glycolysis to proline biosynthesis (**Fig. 4.20**) [502]. On the other hand, metabolite pools from acetyl-CoA to 2-oxoglutarate got bigger with increasing salt concentration and certainly drove this rerouting in *B. megaterium* by enabling the conservation of a similar absolute flux despite the lower enzyme activity as explained for temperature (see section 4.1.2). Indeed, absolute flux through the TCA cycle was kept quite high while absolute glycolytic flux was reduced 1.6 and 2.6-fold when 0.6 and 1.2 M NaCl were added, respectively. Contrasting with previous findings in *B. subtilis*, enzyme concentrations and gene expression of elements downstream of 2-oxoglutarate were also higher under osmotic stress in *B. megaterium*, which coincided well with the increased carbon recycling revealed by flux analysis [92, 502, 521].

**Figure 4.20: Integrated view of the response of the central carbon metabolism of *B. megaterium* DSM319 to ionic osmotic stress –** Transcriptome and proteome data are indicated as the determined fold change compared to cultivation at 37°C in M9 minimal medium without NaCl supplementation. Gene expression was determined by microarray analysis using purified RNA samples obtained from four biological replicates. Intracellular proteins were identified and quantified by proteome analysis using LC-IMS$^{e}$ for cells originating from four replicates as well. Bar plots represent intracellular metabolite concentrations in µmol gCDW$^{-1}$. Intracellular metabolite concentrations were determined by LC-MS/MS using a differential method, i.e. subtracting extracellular metabolite concentration from the global metabolite concentration. ►

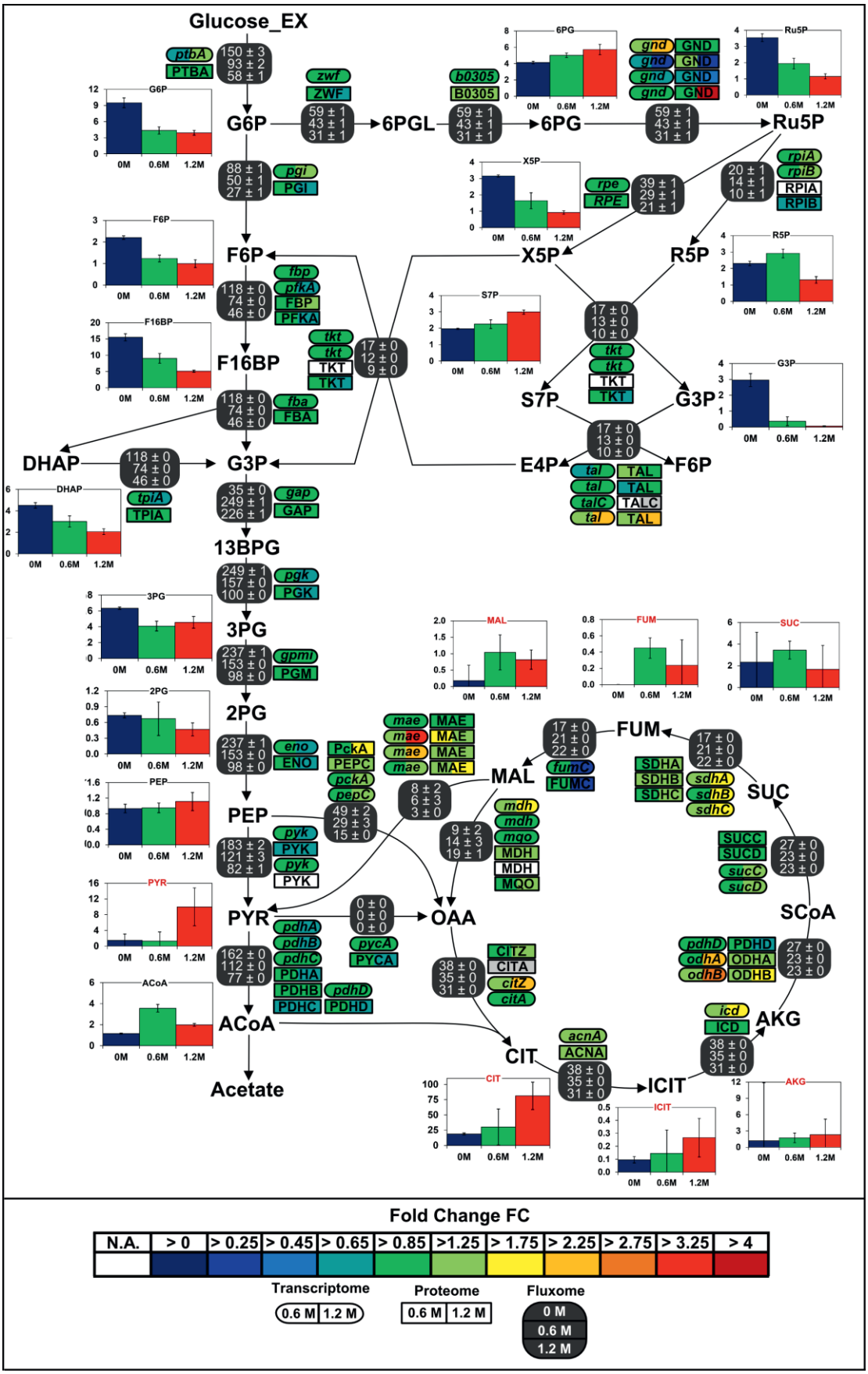

### *Hierarchical clustering reveals the emergence of regulation modules within the central carbon metabolism (CCM)*

Interestingly, most transcriptional changes observed in the presence of 0.6 to 1.8 M NaCl appeared to be operated in a structured way. In fact, several clusters of genes whose expression was co-regulated can be clearly distinguished. Among them, three clusters are composed of genes discussed above, namely (a) genes involved in the synthesis of proline in response to osmotic stress, (d) genes from the arginine and anabolic proline metabolism and (f) genes from the TCA cycle. In addition, two other clusters regroup genes from (b) the glycolysis on the one hand and (e) miscellaneous genes belonging either to the TCA cycle, the glycolysis or anaplerotic reactions on the other hand (cf. Fig. 4.19). This coordinated adjustment of gene expression of central modules probably facilitates the fine-tuning of cell energetic status and precursor supply indispensable for adaptation.
Combining expression patterns under temperature and osmotic stress, the modular regulation of genes from the glycolysis and TCA cycle becomes even more obvious (**Fig. A.3**). On the contrary, genes from the pentose phosphate pathway (PPP) are distributed all over the classification tree and do not seem to be regulated in a coordinated manner. Given the notable increase of relative flux towards the PPP under osmotic stress, the lack of a concerted and unilateral regulation of gene expression within this pathway is quite surprising but in good accordance with results from Kohlstedt et al. [502]. Since the concentration of 6-phosphoglycerate (6PG) increased gradually while that of ribulose-5-phosphate (Ru5P) was progressively reduced with increasing salt concentration, this increased flux diversion may be achieved by reducing the mass-action ratio of the reaction catalysed by phosphogluconate dehydrogenase (*gnd*) to favour 6PG conversion (cf. Fig. 4.20) [522]. In any case, concentrations of most enzymes from this pathway were not significantly increased under osmotic stress and cannot account for this rerouting. This discrepancy between metabolic fluxes and gene regulation is illustrated in **Fig. 4.21C**.
Independently from the previous functional modules, a final cluster (c) comprises genes encoding glutamate synthase (*gltA*, *gltB*) and fumarate hydratase (*fumC*) whose expression was up to 2.5-fold reduced in *B. megaterium* growing at NaCl concentrations above 0.6 M. Accordingly, concentrations of the corresponding proteins were up to 3-fold reduced under these conditions. Given the increased glutamate demand for proline synthesis and the major function of fumarase within the TCA cycle, these modifications are quite surprising and it is highly probable that *B. megaterium* disposes of additional isoenzymes active under stressful conditions. In that sense, YerD, a putative ferredoxin-dependent glutamate synthase, has been proposed as possible isoenzyme replacing GltAB under salt stress in *B. subtilis* [92, 502, 521]. Despite the only up to 1.8-fold higher expression of its encoding gene at concentrations above 0.6 M NaCl, YerD could undertake a similar role under salt and heat stress in *B. megaterium*. In fact, expression of this gene was 2-fold stronger at 45°C when expression of *gltA* and *gltB* was 5.3- and 7.7-fold lower, respectively (Fig. 4.19 and Tab. A.4). Interestingly, expression of *gltA* and *gltB* was also reduced under osmotic stress in *B. licheniformis* and furthermore up to 2.5-fold lower under cold stress in this study, so the encoded protein seems stress sensitive (cf. Fig. 4.19 and Tab A.4) [207].

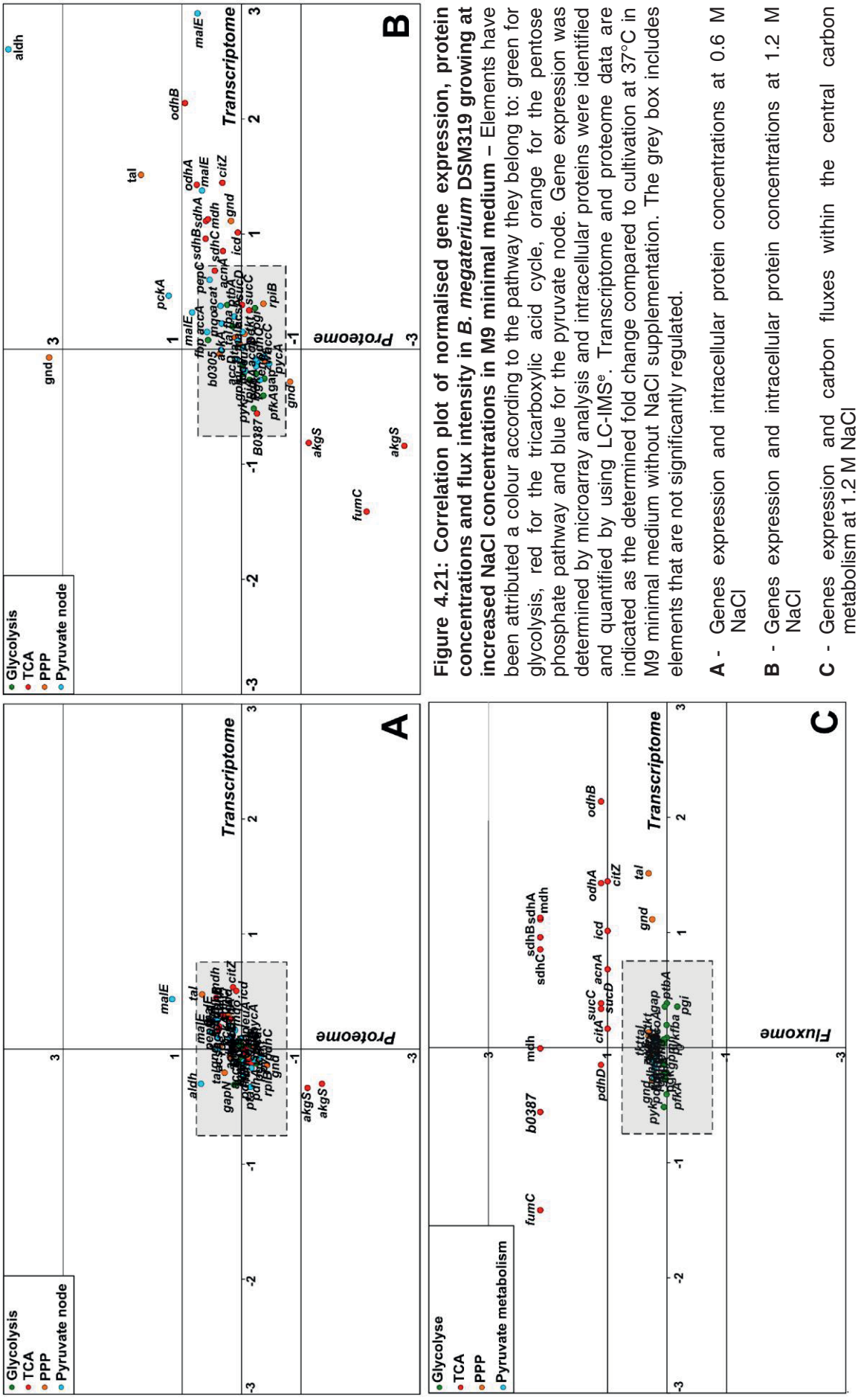


**Figure 4.21: Correlation plot of normalised gene expression, protein concentrations and flux intensity in *B. megaterium* DSM319 growing at increased NaCl concentrations in M9 minimal medium** – Elements have been attributed a colour according to the pathway they belong to: green for glycolysis, red for the tricarboxylic acid cycle, orange for the pentose phosphate pathway and blue for the pyruvate node. Gene expression was determined by microarray analysis and intracellular proteins were identified and quantified by using LC-IMS$^e$. Transcriptome and proteome data are indicated as the determined fold change compared to cultivation at 37°C in M9 minimal medium without NaCl supplementation. The grey box includes elements that are not significantly regulated.

**A** - Genes expression and intracellular protein concentrations at 0.6 M NaCl

**B** - Genes expression and intracellular protein concentrations at 1.2 M NaCl

**C** - Genes expression and carbon fluxes within the central carbon metabolism at 1.2 M NaCl

Finally, compared to heat stress, a linaear relation can be noticed between transcript and corresponding protein concentrations under osmotic stress and the impact of protein degradation and post-transcriptional events seems less pronounced than at 45°C (**Fig. 4.21B**)

### 4.2.3 Specific responses elicited by sustained osmotic stress

As for heat stress survival at high salt concentrations is very complex and additionally requires specific elements to cope with vital issues. To get a better understanding of hyperosmotic stress in *B. megaterium*, transcriptome and proteome data obtained from cultivations with 0.6, 1.2 and 1.8 M NaCl were analysed following the same statistical approach as for temperature stress, i.e. combining Venn diagrams, Voronoi representations and principal component analysis (see 4.1.3.1).

#### *Adaptation relies on the regulation of a core group of genes and proteins whose size increases with salt concentration*

As underlined previously, addition of 0.6 M NaCl seems to be a physiological threshold above which adaptive behaviour of *B. megaterium* is modified, with a reduction of potassium import and the activation of the Pox route as main new features. In that sense, gene expression was only significantly altered for 43 genes at 0.6 M NaCl while more than 300 genes were differently expressed at higher NaCl concentration (**Fig. 4.22**).

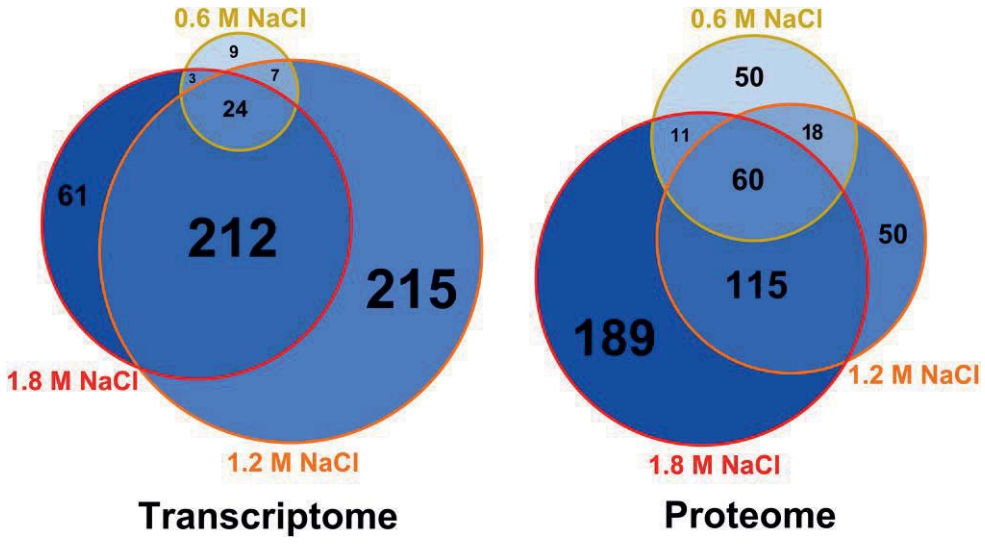


**Figure 4.22: Weighed Venn diagrams of the number of transcripts and proteins whose concentration was significantly altered in *B. megaterium* growing in M9 minimal medium with 0.6, 1.2 and 1.8 M NaCl, respectively.** A gene or a transcript was considered significantly regulated when its concentration was either 1.75-fold higher or lower compared to 0 M NaCl. Gene expression was determined by microarray analysis and intracellular proteins were identified and quantified by proteome analysis using LC-IMS$^{e}$.

Among them, 212 were common to both 1.2 M and 1.8 M NaCl. Hence, a separation can be made between mild (≤ 0.6 M NaCl) and severe (> 0.6 M NaCl) salt stress, which is confirmed by the circle of correlations from the PCA analysis and the related gene clustering (**Fig. 4.23**).

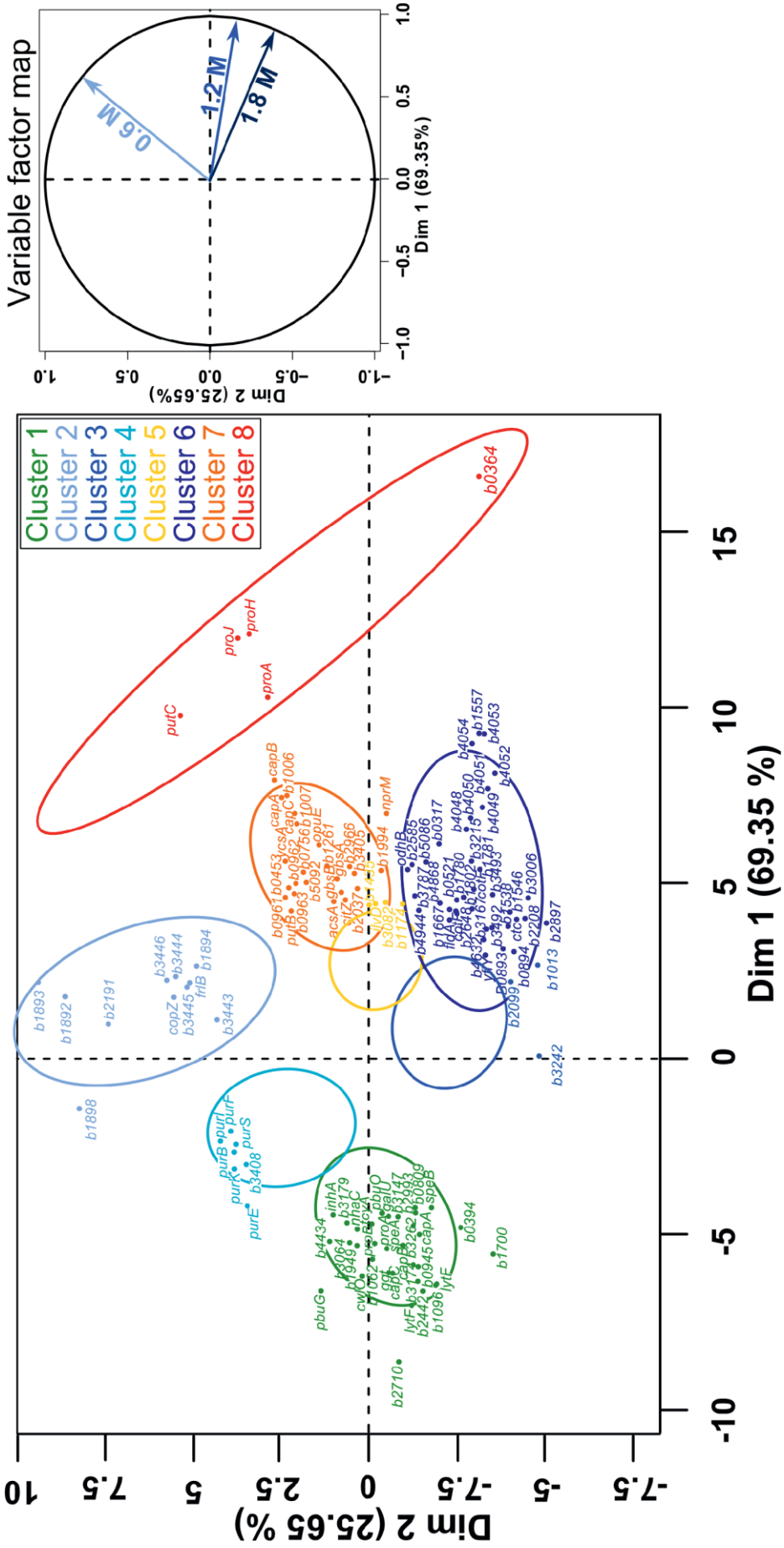


**Figure 4.23: Principal Component Analysis (PCA) followed by Hierarchical Clustering (HCPC) on gene expression ratios in *B. megaterium* DSM319 grown in M9 medium supplemented with 0.6, 1.2 and 1.8 M NaCl.** For more clarity, *bmd* was replaced by B in gene names and only the 125 genes most relevant for the PCA construction are presented. **Cluster 1**: Genes whose expression is down-regulated under both mild (0.6 M NaCl) and severe salt stress (1.2 M and 1.8 M NaCl); **Cluster 2**: Gene whose expression is only stronger under mild stress; **Cluster 3**: Genes whose expression is slightly reduced at 0.6 M NaCl and slightly increased under severe salt stress; **Cluster 4**: Genes whose expression is slightly up-regulated at 0.6 M NaCl and strongly down-regulated under severe salt stress; **Cluster 5**: Genes whose expression is slightly up-regulated under both mild and severe salt stress; **Cluster 6**: Genes whose expression is specifically up-regulated under severe salt stress; **Cluster 7**: Genes whose expression is up-regulated under both mild and severe salt stress; **Cluster 8**: Genes involved in proline synthesis.

In addition, four genes encoding distinctive two-component systems (*bmd_1892 / 1893* and *bmd_3442 / 3443*) responded specifically to mild salt stress and might orchestrate an exclusive feedback response (Fig. 4.23 – Cluster 2).

As a matter of fact, expression of several of their neighbouring genes (*bmd_1894* to *1896* and *bmd_3444* to *3446*) was also only increased at 0.6 M NaCl, thus suggesting the existence of transcriptional units. In particular, increased transcription of *copZ*, *copA* and *bmd_1894*, whose product shares 40 % homology with *B. subtilis*' CsoR regulator, may indicate an intensified scavenging of intracellular copper under these conditions [523-525]. Other induced genes encode an ABC transporter (*bmd_3446*) and two putative membrane proteins (*bmd_3444* and *bmd_3445*) whose functions need to be clarified. Nevertheless, 55 % of the 43 genes differently expressed under mild salt stress were shared with severe salt stress and their regulation seems therefore crucial for adaptation. This core group consists mainly of genes with functions in proline synthesis (*putB*, *putC*, *proH*, *proJ*, *proA*) and transport (*opuE* - *bmd_1401*) whose expression was up to 10.4-fold increased (Fig. 4.23 - Cluster 8) and others involved in cell wall metabolism (*lytF*, *bmd_2442*, *bmd_1096*, *bmd_3174*) which were, on the contrary, up to 4.4-fold less strongly expressed under osmotic stress (Fig. 4.23 - Cluster 1) [509]. Interestingly, it also includes a pentacistronic operon (*bmd_1003* to *1007*) which contains *capABC*, three genes responsible for the synthesis of a poly-y-glutamate capsule acting as a virulence factor in *B. anthracis* (Fig. 4.23 - Cluster 7) [494, 495]. Synthesis and function of such a chemical barrier in the context of osmotic stress has not been reported yet and curiously, expression of the other operon encoding CapABC (*bmd_1092* to *1095*) was up to 3-fold reduced under salt stress (Fig. 4.23 - Cluster 1). Hence, further attention should be devoted to the elucidation of the exact function of this operon, especially because its expression was also increased under cold stress (see section 4.1.3.3).

Despite a restricted modification of gene expression, 139 proteins had already significantly altered concentrations – at least 1.75-fold higher or lower – under mild salt stress. This number then increased proportionally to the supplemented salt concentration, reaching 375 proteins at 1.8 M NaCl and revealing a large core set of 60 proteins systematically more produced in presence of salt (cf. Fig. 4.22). As spotted using Voronoi representations, this central set was moreover completed by so-called "on-proteins", that is, proteins only produced in cells exposed to salt stress (**Fig. 4.24**). Besides products of genes mentioned above, this group comprises several NAD dependent epimerases / hydratases (Bmd_0685, GalE, Mro, Bmd_2433, Bmd_2930 Bmd_3943) whose concentrations increased up to 29-fold upon addition of NaCl (**Fig. A.4** and Tab. A.13). In plants and rice, these proteins modulate cell wall biosynthesis to confer cells a better resistance against osmotic stress [526-529].

Finally, several oxidoreductases (BMD_0912, BMD_0989, BMD_1041, BMD_2681, BMD_3119, BMD_3139, BMD_3288, BMD_3473, BMD_3493), peptidases and proteases (BMD_0331, InhA, BMD_3039, PepQ, BMD_4817, CtpB, BMD_5202) are also part of this core group of proteins and their increased concentrations certainly contribute to a reduction of damages resulting from the salt-induced perturbation of redox state and to the alteration of cell wall (Tab. 4.9 and Fig. A.4)[530].

### *Severe salt stress triggers general stress response and production of proteins involved in protection against oxidative damages*

When cells were cultured at NaCl concentrations higher than 0.6 M, expression of the $\sigma_B$-operon (*rsbV*, *rsbW*, *rsbX*, *sigB*) was only up to 1.8 fold higher but concentration of several of its products increased up to 3-fold at 1.8 M NaCl, suggesting the activation of the general stress response under acute salt stress. In accordance with this conclusion, predicted members of the SigB-regulon (*bmd_1994*, *bmd_1557*, *bmd_1546*, *bmd_1131*, *bmd_1041*, *dps*, *bmd_5086*, *bmd_3493*, *bmd_3215, gbsB, gbsA*) were between 2.2- and 12-fold more strongly expressed and concentration of the corresponding proteins up to 57-fold higher at concentration above 0.6 M NaCl (Tab. A.12, Tab. A.13 and Fig. A.4) [92, 149, 309, 521].

Similarly, concentration of the regulator of the peroxide regulon PerR was 2.6- and 4.6-fold increased at 1.2 M and 1.8 M NaCl, respectively, thus confirming the production of reactive oxygen species (ROS) under severe salt stress. The increased production of NADH dehydrogenase YutJ (BMD_4957), iron-binding protein Dps (BMD_4857), 2-cys peroxiredoxin (BMD_0990), redox regulator Rex (BMD_0255), several cytochromes P450 (BMD_1855, BMD_2035, BMD_3874) as well as the up to 4-fold induction of gene encoding a manganese catalase (*bmd_3215*) provides further evidence of the emergence of oxidative damages and the implementation of adequate countermeasures (Fig. 4.23 – Cluster 6) (Tab. A.12 and Tab. A.13) [376, 377, 389, 431, 476]. However, contrary to the situation at 45°C, outbreak of thiol-specific oxidative damages can certainly be excluded because expression of genes involved in repairing them (*spxA*, *trxA*, *trxB*, *msrA*, *msrAB*) was not significantly modified under salt stress [410, 413].

Interestingly, concentrations of several flaxodoxins (BMD_3384, BMD_3385, BMD_3911) were also between 2- and 6.6-fold increased at concentrations above 0.6 M NaCl and others were even specifically produced under these conditions (EtfA and EtfB). Curiously, expression of the corresponding genes was, however, not particularly higher. Conversely, expression of *fldA*, which encodes another flavodoxin, was up to 4-fold higher under severe salt stress but the protein was absent from the proteome. Flavodoxins have already been reported to replace ferredoxins, their isofunctional analogues, and participate in repair activities during iron starvation and oxidative stress [531-534]. Indeed, ferredoxins see their functions compromised under stressful conditions because the Fe-S cluster they bear as prosthetic group gets damaged by diverse reactive species [535].

In this regard, expression of genes involved in synthesis and reparation of Fe-S clusters (*sufB*, *iscU*, *sufS*, *sufD*, *sufC*) was approximately 2-fold stronger and concentration of their products was accordingly higher under severe salt stress (Tab. A12 and Tab. A.13) [521]. Surprisingly, despite the catalytic role of iron in ROS generation, transcription of numerous genes encoding proteins involved in iron acquisition such as siderophores (*bmd_4048*, *bmd_4051*, *bmd_4052*) and ferrichromes (*fhuD*, *fhuC*, *yclQ*, *yclP*, *yclO*, *yclN*, *yusV*, *yfhA*, *yfiZ*, *yfiY*) was between 2- and 15-fold up-regulated and their products present in up to 12-fold larger amounts at concentrations above

0.6 M NaCl (Fig 4.23 – Cluster 6) [401]. Together with the increased production of flavodoxins, this result tends to confirm that high-salinity is also causing iron limitation [521, 531, 536].

### *Increased salt concentrations also impact RNA, amino acid and cell wall metabolisms*

Voronoi representations of transcriptome and proteome data reveal the existence of many other metabolic disruptions under severe salt stress (Fig. 4.24). In particular, progressive reduction of concentrations of several ribosomal proteins (RplW, RpsN, RpsO, RpsT, RpmA, RplT), translation factors (BipA, PrfC, PrfB) and proteins from the purine and pyrimidine metabolisms (PurEKBCSQLFMNHD, PyrK, PyrAA, PyrAB, PyrC, PyrB, PyrG) with increasing salt concentrations denotes a major downturn in RNA synthesis and processing activities consistent with the measured reduction of RNA content (Fig. A.2, Fig. A.4 and Tab. A.13). In this regard, decrease in concentrations of enzymes involved in synthesis of purines and pyrimidines was supported by the 2 to 2.5-fold reduced expression of genes encoding them and proteins from the connected histidine biosynthesis pathway (*hisG*, *hisZ*, *hisI*, *hisA*, *hisF*, *hisH*, *hisB*, *hisK*, *hisD*) (Fig. 4.23 – Cluster 4).

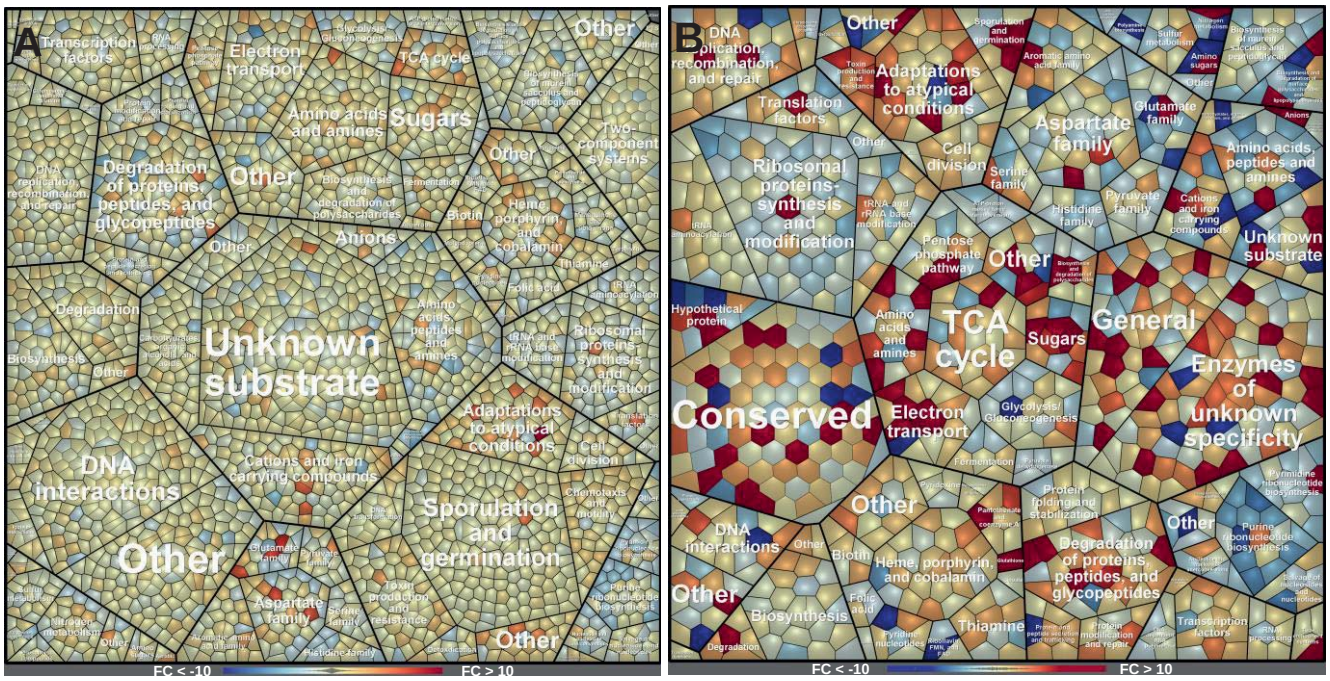


**Figure 4.24: Voronoi treemap visualisation of the impact of 1.8 M NaCl on gene expression and protein production in *B. megaterium* DSM319.** Gene expression was determined by microarray analysis and intracellular proteins were identified and quantified by proteome analysis using LC-IMS$^e$. Each cell represents an mRNA transcript **(A)** or a protein **(B)**, respectively. Clustering of transcripts and proteins was based on their functional classification. The colour scale at the bottom of each graph indicates the positive (red) or negative (blue) change of the $\log_2$ gene expression **(A)** or protein concentration **(B)** compared to their value in a medium where no additional NaCl was supplemented.

In addition, besides proline, arginine and histidine metabolisms, synthesis and transport of several other amino acids were deeply affected at NaCl concentrations above 0.6 M. Notably, genes encoding methionine ABC transporters (*met*, *metN*, *metQ*, *metP*, *tcyC*, *tcyB*, *tcyA*) and involved in methionine salvage (*mtnA*, *mtnK*, *mtnE*, *mtnW*, *mtnX*, *mtnB*, *mtnD*) had approximately 2-fold decreased expression levels while concentration of methionine synthase MetE and cystathionine beta-lyase PatB was, on the contrary, at least 2-fold increased.
Similarly, concentration of enzymes involved in tryptophan (BMD_2992, TrpA, TrpB, TrpC) and cysteine synthesis (YtkP) were 2 to 2.5-fold and 4-fold increased under severe salt stress, respectively (Tab. A.13). Given the reactivity of reactive oxygen and nitrogen species towards methionine, cysteine and tryptophan residues, all these modifications might be related to the emergence of oxidative damages under severe salt stress [415, 537-539]. Likewise, the up to 5-fold higher concentrations of enzymes from the pantothenate pathway (PanB, PanC, PanD) could help prevent oxidative damages (Fig. A.4 and Tab. A.13) [540].
In accordance with works from Steil et al. [509] in *B. subtilis*, expression of several genes encoding protein associated to the cell wall or involved in peptidoglycan, murein and polysaccharide synthesis (*bmd_0452*, *bmd_1096*, *ponA*, *cwlO*, *yocH*, *lytF*, *lytE*, *bmd_1114*, *bmd_1117* to *1120*, *bmd_3174*) was 2.5 to 5-fold reduced at concentration above 0.6 M NaCl. Most of the corresponding proteins also had reduced concentrations under these conditions, with the exception of the binding protein YocH which was, despite the 3-fold reduced expression, present in 12- and 19-fold larger amounts at 1.2 M and 1.8 M NaCl, respectively (cf. Fig 4.24 and Tab. A.14) [502, 509].
Hence, *B. megaterium*'s cell envelop might also experience major changes under strong hypertonic stress. As a matter of fact, cell shape was strongly modified in the presence of sodium chloride and cell wall certainly underwent an electrostatic contraction affecting its structure and properties as described by others (**Fig. 4.25**) [192, 208]. Moreover, the percentage of odd-numbered iso-fatty acids (iso C13:0 and iso C15:0) incorporated into the cell wall was gradually increased in cells exposed to higher NaCl-concentrations and probably responded to a reduction of membrane fluidity at higher osmolarities (data not shown) [541].

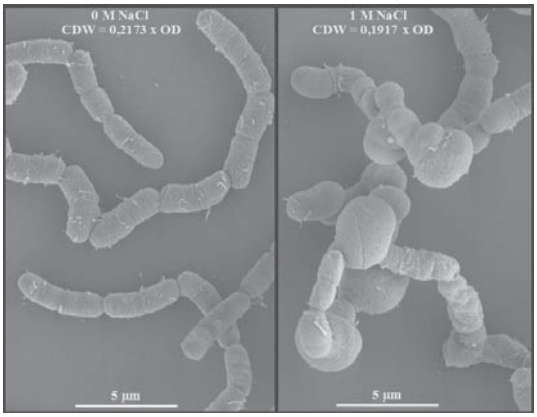


**Figure 4.25: Salt-induced modifications of cell morphology in *Bacillus megaterium* DSM319.** Left picture show cell morphology in LB-medium and right picture its alteration when 1 M NaCl was supplemented to the same medium. Pictures were captured by means of electron microscopy (M. Rohde; HZI, Braunschweig, 2007).

On the contrary, expression of genes involved in chemotaxis and motility was not repressed as in *B. subtilis* [502]. Several genes encoding flagellar components (*fliK*, *fliJ*, *fliI*, *fliH*, *fliM*) were even approximatively 2-fold more strongly expressed under severe salt stress (Tab. A.12).
Finally, expression of numerous genes encoding uncharacterised proteins (*bmd_0317*, *bmd_0364*, *bmd_0521*, *bmd_0893*, *bmd_0894*, *bmd_3006*, *bmd_1667*, *bmd_1780*, *bmd_1802*, *bmd_2897*, *bmd_3167*, *bmd_3492 bmd_3787*, *bmd_4632*, *bmd_4868*, *bmd_4944*) was between 2.5 and 51-fold stronger under severe hyperosmotic conditions. Some of them furthermore seem involved in protection against both temperature and high salt concentrations (*bmd_0521*, *bmd_3006*, *bmd_3167, bmd_3787*, *bmd_4632*, *bmd_4944*) (Fig. 4.23 – Cluster 6). Homologues of certain of these proteins were found in others *Bacillus* spp. and encode other uncharacterised proteins but also exported protein YkoJ (BMD_0317), an inhibitor of cells separation enzyme (BMD_0521), peptidase YraA (BMD_3006) as well as general stress proteins YflH (BMD_3167, BMD_0894), YjgB (BMD_3787) and YsnF (BMD_4632). Elucidating the exact function of all these proteins would definitely improve our understanding of adaptation to stress and possibly provide new genetic targets for strain improvements.

### 4.2.4 Biotechnological production of osmotically relevant compounds

In the course of the study on osmotic stress in *B. megaterium*, a clear dependence of proline and polyhydroxybutyric acid (PHB) biosynthesis on supplemented NaCl concentration has been unravelled (cf. Fig. 4.16 and section 4.2.2). Since both compounds are gaining increasing attention for their promising industrial applications, the mechanisms triggering their synthesis under salt stress will be analysed in further detail in this section to find potential genetic targets for developing production workhorses [221, 542, 543].

#### *Enhancement of the osmo-dependent pathway as a first step towards industrial proline production?*

Proline is mainly used in the food and pharmaceutical industry. More recently, it has come into focus because of its role as an organic catalyst in asymmetric synthesis, a process which introduces one or more new elements of chirality in a substrate and leads to formation of unequal amounts of stereoisomeric products [544]. Since enantiomeric products have different properties, the possibility of favouring the production of one over the other is particularly interesting for drug and food additive development [545, 546].
As highlighted before, the massive synthesis of intracellular proline under osmotic stress relies on the usage of an alternative production pathway which is not negatively affected by high proline concentration. This pathway consists of glutamate-5-kinase ProJ (BMD_2244), gamma-glutamyl phosphate reductase ProA* (BMD_2245) and pyrroline-5-carboxylate reductase ProH (BMD_2243) (see section 4.2.2). Hence, the first working hypothesis was that enhancement of this pathway

under normal conditions, i.e. in the absence of high NaCl concentrations, would result in the release of proline into the medium. To test it, DNA fragments corresponding to the three genes encoding these enzymes were amplified by PCR using appropriate primers and subsequently inserted into plasmid p3STOP1623hp equipped with an optimized xylose inducible promoter controlling expression of the introduced genes (cf. Fig. 1.2, Tab. 3.1 and Tab. 3.13) [12]. Finally, *B. megaterium* DSM319 was transformed with this constructed plasmid (pRBBm217) and the three genes were overexpressed in cultivations with normal M9 minimal medium supplemented with 5 g $L^{-1}$ xylose. Surprisingly, this overexpression did not affect proline secretion nor the proline and glutamate intracellular pools compared to the wild type. Probably, the enzymes of the osmo-dependent pathway ProJ-ProA*-ProH are only active under osmotic stress.
Interestingly, the collected transcriptome data underline that expression of genes encoding 1-pyrroline-5-carboxylate dehydrogenase (*putC*) and proline oxidase (*putB*), which convert proline back to glutamate, was between 2 and 5-fold increased under osmotic stress. Similarly, expression of the gene encoding the proline transporter OpuE (*bmd_1401*) was up to 3.9-fold higher under salt stress. Despite its strong intracellular accumulation, proline was not secreted under these conditions which, together with the previous observations, indicate that cells might tightly control their proline intracellular pool and actively recycle this compound to avoid carbon wastage. Consequently, proline accumulation and secretion under normal conditions could also be restricted by an effective recycling.
Either way, further investigations on gene regulation and activity of the osmo-dependent proteins under normal conditions need to be carried out in this new plasmid strain (pRBBm217) to better comprehend this quite surprising situation. A potentially meaningful next step would be the development of a Δ*putC*Δ*putB* knockout strain unable to convert proline back to glutamate and including plasmid pRBBm216. However, existences of other genes encoding 1-pyrroline-5-carboxylate dehydrogenase (rocA) and proline oxidase (fadM, bmd_5071) as well as the existence of other metabolic pathways for proline utilisation make it difficult to predict the outcome of such a modification.

### *Bacterial milking: proof of concept of a potential alternative for proline production*

To assess the possibility of producing high amounts of proline by bacterial milking as described by others [547-549]. For this, secretion potential of *B. megaterium* was evaluated by abruptly transferring cells ($OD_{600nm}$ = 7) from M9 minimal medium supplemented with 1.5 M NaCl to normal M9 minimal medium containing only 0.5 g $L^{-1}$ NaCl. This osmotic down-shock triggered a quick release of metabolites into the medium via mechanosensitive channels to restore osmotic equilibrium and extracellular concentration of proline increased from 25 mg $L^{-1}$ (5 mg $g_{glucose}^{-1}$) to approximately 200 mg $L^{-1}$ (40 g $g_{glucose}^{-1}$). Hence, implementation of a high cell density continuous culture recruiting a two-compartement system identical to that of Fallet et al. [547] for ectoine production should enable high extracellular proline titers and space-time yields. Further, optimisation of production parameters by central composite design and response surface methodology would make this process even more competitive compared to known producers [550-555].

### *Salt stress as a mean to investigate regulation of polyhydroxybutyric acid (PHB) production in* B. megaterium

While proline production in response to increased osmolarity was likely given the strong genetic similarities between *B. megaterium* and *B. subtilis*, linear correlation between salt concentration and polyhydroxybutyric acid (PHB) content is quite unexpected and offers a valuable way to investigate the underlying mechanisms (**Fig. 4.26**). PHB is generally produced when an essential nutrient other than the C-source (N, P, $O_2$) becomes limiting and enables the intracellular storage of excess carbon and reducing power under these conditions. When substrate is exhausted, this polymer can be degraded back to acetyl-CoA and (S)-3-hydroxybutyl-CoA, respectively, to fuel TCA and β-oxidation cycles for energy production [556]. Moreover, several studies indicate that its accumulation has beneficial effects on resistance against heavy metals, temperature, phenol, ethanol and peroxide stress but the involved mechanisms are not fully understood yet [556-560]. Regarding salt stress, a potential role has only been mentioned for nitrogen-fixing bacteria of the *Rhizobia* family so far and involves balancing of the osmotic burden by incorporating reduced carbon into PHB [561, 562]. However, several *B. megaterium* strains producing large amounts of PHB have also been isolated from salty environments recently [563-565]. The reasons for this enhanced production remains unclear so far but recent studies have proposed that production of PHB and related phasins could help coping with abiotic stress and confer bacteria a better tolerance to osmotic stress [319, 556, 566, 567].

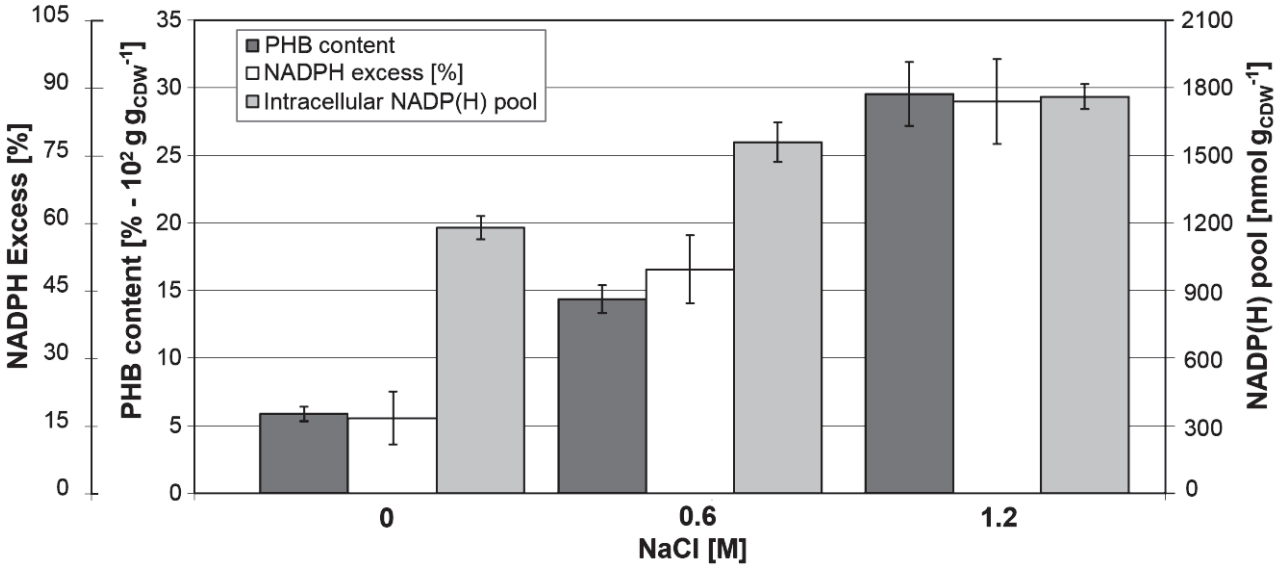


**Figure 4.26: Relationship between PHB content and NADPH production in *B. megaterium* DSM319 growing at 37°C in M9 minimal medium supplemented with up to 1.2 M NaCl.** NADPH excess was calculated using the ratio between NADPH supply derived from flux analysis and biosynthetic NADPH demand estimated from biomass composition at the respective NaCl concentrations. Global NADP(H) pool represents the sum of NADP and NADPH pools as determined by LC-MS-measurements.

In this work, fluxome data reveal a strong correlation between increase in PHB content and cellular NADPH excess when medium is supplemented with NaCl. Similarly, probably responding to a stronger NADPH-demand for proline synthesis, the global NADP(H) pool increased from 1400 to 2100 nmol $g_{cdw}^{-1}$ in cells cultivated with 1.2 M NaCl. Hence, just as increased conversion of pyruvate to lactate probably modulated NADH-to-$NAD^+$ ratio, PHB accumulation could act as redox regulator mitigating NADPH-to-$NADP^+$ ratio under these conditions, as proposed by Wang et al. [232]. In this case, its accumulation under salt stress could be a side effect of proline synthesis and the concomitant enhanced NADPH production [568].

Despite a 2.4-fold higher PHB content, no significant regulation of transcripts and proteins involved in PHB synthesis was observed in cells grown with 0.6 M NaCl (**Tab. 4.10**) [4, 244, 245]. Similarly, the PHB content was increased by 500 % at 1.2 M NaCl but, with the exception of PhaR subunit of the PHA synthase whose concentration was 2.3-fold higher, neither the concentrations of enzymes catalysing the conversion of acetyl-CoA to PHB (MmgA, PhaB, PhaC) nor the expression of genes encoding them were positively affected.

**Table 4.10: Gene expression levels and protein concentrations of elements involved in PHB synthesis and degradation in *B. megaterium* DSM319 growing in M9 minimal medium supplemented with 0.6 and 1.2 M NaCl, repectively**. Data are given as fold change (FC) of transcript or protein concentrations compared to their values in normal M9 minimal medium. Proteins that could not be quantified with our proteome approach are designated with "n.d.". Similarly, "0.6 M" and "1.2 M" indicates that the protein was only detected for cells grown with 0.6 M and 1.2 M NaCl, respectively. Red bold numbers indicate a significant increased gene expression.

| Locus Tag | Name | Description | Transcriptome 0.6 / 1.2 M | Proteome 0.6 / 1.2 M |
|---|---|---|---|---|
| | | ***Polyhydroxybutyric acid synthesis*** | | |
| *bmd_1211* | *phaP* | Polyhydroxyalkanoic acid inclusion protein PhaP | 1.31 / **2.25** | 1.32 / **1.81** |
| *bmd_1212* | *phaQ* | Poly-beta-hydroxybutyrate-responsive repressor | 1.10 / **1.77** | 0.6 M / n.d. |
| *bmd_1214* | *phaR* | Polyhydroxyalkanoic acid synthase, PhaR subunit | 1.17 / 1.31 | 1.66 / **2.24** |
| *bmd_1215* | *phaB* | Acetoacetyl-CoA reductase | 1.17 / 1.28 | -1.05 / -1.16 |
| *bmd_1216* | *phaC* | Polyhydroxyalkanoic acid synthase, PhaC subunit | 1.23 / 1.34 | 1.35 / 1.32 |
| *bmd_2333* | | Acetyl-CoA acetyltransferase | 1.09 / 1.03 | n.d. / n.d. |
| *bmd_2484* | | Acetyl-CoA acetyltransferase | 1.19 / 1.42 | 0.6 M / 1.2 M |
| *bmd_4393* | | Acetyl-CoA acetyltransferase | 1.11 / 1.38 | 1.16 / 1.35 |
| *bmd_5171* | *mmgA* | Acetyl-CoA acetyltransferase | 1.35 / 1.38 | n.d. / n.d. |
| | | ***Polyhydroxybutyric acid degradation*** | | |
| *bmd_0477* | *phaZ1* | Poly(3-hydroxybutyrate) depolymerase | 1.15 / 1.10 | n.d. / n.d. |
| *bmd_1841* | *phaZ3* | Poly(3-hydroxybutyrate) depolymerase | -1.16 / -1.25 | n.d. / n.d. |
| *bmd_2166* | | 3-hydroxybutyrate dehydrogenase | 1.09 / **2.81** | 0.6 M / 1.2 M |
| *bmd_2297* | | 3-hydroxybutyrate dehydrogenase | -1.13 / -1.22 | 0.6 M / 1.2 M |
| *bmd_3024* | *phaZ* | Poly(3-hydroxybutyrate) depolymerase | 1.04 / 1.68 | n.d. / n.d. |
| *bmd_3395* | *phaZ2* | Poly(3-hydroxybutyrate) depolymerase | -1.11 / -1.13 | n.d. / n.d. |
| *bmd_4391* | *scoB* | 3-oxoacid CoA-transferase subunit B | 1.34 / **1.95** | **1.76** / 1.50 |
| *bmd_4392* | *scoA* | 3-oxoacid CoA-transferase subunit A | 1.32 / **1.82** | 0.6 M / 1.2 M |

At this concentration, however, expression of gene encoding the phasin PhaP was 2.3-fold stronger and concentration of the corresponding protein 1.8-fold higher than in cells grown in standard M9 minimal medium. Since phasins are known stimulators of PHB production favouring increased accumulation by reducing granule size, this slight modification could contribute to the enhanced formation of PHB stockpiles at 1.2 M NaCl (2.3.2) [247].
Still, the mismatch between alteration of protein concentration and modification of PHB content is significant enough to predict that other mechanisms are at work. In this context, forthcoming works should for instance assess whether activity of those enzymes whose concentration remains largely unaffected is increased under salt stress, and if so, identify the corresponding mechanisms. Eventually, new elements involved in PHB metabolism might still be hidden in the plethora of uncharacterized proteins whose concentration increased steeply when sodium chloride was added.

### *First steps towards the development of a genetically engineered PHB producing strain*

Since no significant increase in expression of genes involved in PHB synthesis and in concentrations of the corresponding proteins was observed in *B. megaterium* under salt stress, we decided to assess if PHB production would be improved if those genes were overexpressed. To this end, new plasmids containing operons *phaRBC* (pRBBm214) and *phaPQ* (pRBBm215) were constructed by amplifying corresponding DNA fragments and subsequently inserting them into the same plasmid p3STOP1623hp as described before. Cells were then transformed with the new plasmids and batch cultivations in M9 minimal medium supplemented with 0.6 M NaCl were carried out in triplicates using a DASGIP® bioreactor system. Addition of 0.6 M NaCl was meant to support initial PHB accumulation while minimizing the detrimental effects of salt on growth rate compared to 1.2 M NaCl. Because nitrogen limitation has been shown to foster PHA accumulation in some bacteria, glucose initial concentration was furthermore adjusted to 20 g $L^{-1}$ to reach this state at the end of the growth phase [569-572].
Compared to cultivations with the wild-type strain, growth characteristics remained largely unaffected by these plasmids while PHB formation reached 32 % (+ 75 %) and 27.5 % (+ 50 %) of biomass in strains carrying pRBBm214 and pRBBm215, respectively (**Tab. 4.11**). On the other hand, as reported by others, PHB accumulation was solely growth-associated in *B. megaterium* and, in this study, nearly 37 % of the carbon supplied during stationary phase was directly converted to acetate (17 %) and α-ketoglutaric acid (20 %) [258, 573, 574]. Since biomass remains nearly constant once stationary phase is reached and cells have already amassed enough proline to cope with salt stress at this stage, accumulation of α-ketoglutaric acid might be a direct consequence of medium osmolarity. Indeed, presence of salt probably prevents complete rewiring of the metabolism and carbon might still be preferentially directed towards α-ketoglutaric acid in anticipation of growth resumption, causing accumulation and secretion of this metabolite. This process is probably strengthened by the lack of nitrogen which restricts conversion of α-ketoglutaric acid into glutamate. Interestingly, no acetate was excreted by the wild-type strain once stationary

phase had been reached and increased secretion in strains modified for improved PHB production might indicate a stronger accumulation of the precursor acetyl-CoA in these mutants (data not shown). Finally, expecting a cumulative effect, a plasmid containing both *phaPQ* and *phaRBC* operons was constructed (pRBBm216). However, overexpression of all 5 genes did not improve the PHB content which remained similar to that in the wild-type strain (16-18 % of cell dry weight). All together, these findings underlines the complexity of the regulation of PHB synthesis and the need for a better understanding of physiological states triggering production as well as of interactions between the different elements involved.

**Table 4.11: Comparison of PHB production using different microorganisms and cultivation techniques.** [1]predictions based on observed growth rate, PHB content and biomass concentrations achieved in fed-batch cultivation by others [563, 575], [2]pH stat, [3]exponential feeding, [4]intermittent feeding.

| Substrate | | Microorganism | Productivity | PHB | Ref. |
|---|---|---|---|---|---|
| Carbon | Titer [g $L^{-1}$] | | [g $L^{-1}$ $h^{-1}$] | [%] | |
| **Batch** | | | | | |
| CSL | 40 | *B. megaterium* ATCC 6748 | 0.016 | 43.0 | [576] |
| Glucose | 20 | *B. megaterium* DSM 319 | 0.030 | 18.3 | This work |
| Glucose | 20 | *B. megaterium* DSM 319 pRBBm216 | 0.036 | 16.7 | This work |
| Molasse | 20 | *B. megaterium* | 0.040 | 59.0 | [577] |
| Glucose | 20 | *B. megaterium* DSM 319 pRBBm215 | 0.051 / 0.230[1] | 27.5 | This work |
| Glucose | 20 | *B. megaterium* DSM 319 pRBBm214 | 0.060 / 0.270[1] | 32.0 | This work |
| Sucrose | 12 | *B.megaterium* | 0.080 | 27.5 | [573] |
| Glycerol | 20 | *Recombinant E. coli* | 0.096 | 60.0 | [578] |
| Sucrose | 20 | *Azotobacter vinelandii* OP | 0.130 | 83 | [579] |
| Glucose | 27.5 | *Alcaligenes eutrophus DSM545* | 0.15 | 43 | [580] |
| Sugarcane | 20 | *Pseudomonas fluorescens A2AJ* | 0.230 | 70.0 | [581] |
| Molasse | 60 | *B. megaterium BA-019* | 0.730 | 27 | [260] |
| **Fed-batch** | | | | | |
| Glycerol | 20 | *B. megaterium* | 0.088 | 60.0 | [582] |
| Molasse | 32.6 | *B. megaterium uyuni S29* | 0.250 | 29.7 | [563] |
| Molasse | 6.12 | *B. megaterium uyuni S29* | 0.450 | 69.2 | [563] |
| Methanol | N/A | *M. extorquens* | 0.600 | 40.0 | [241] |
| Glucose | ca. 80 | *B. megaterium* DSM 319 pRBBm215 | 0.810 | 27.5 | Predicted[1] |
| Glucose | ca. 80 | *B. megaterium* DSM 319 pRBBm214 | 0.940 | 32.0 | Predicted[1] |
| Molasse | 26.5 | *Recombinant E. coli* | 1.000 | 80.0 | [239] |
| Tapioca | 20 | *Alcaligenes eutrophus* | 1.040 | 58.0 | [583] |
| Molasse[2] | 20 | *B. megaterium BA-019* | 1.270 | 42.0 | [584] |
| Molasse[3] | 60 | *B. megaterium BA-019* | 1.300 | 43.0 | [260] |
| Molasse[4] | 60 | *B. megaterium BA-019* | 1.730 | 46.0 | [260] |
| Soybean oil | 40 | *Cupriavidus necator* | 2.500 | 81.0 | [568] |

### *Finding meaningful genetic targets for the improvement of PHB production in* B. megaterium

The fast nitrogen depletion imposed in the performed batch cultivations caused an early growth arrest resulting in relatively low productivities compared to other reported batch cultivations (Tab. 4.11). Nevertheless, the relatively high specific growth rate ($\mu \approx 0.65\ h^{-1}$) and PHB content, 28 and 32 % of cell dry weight respectively, observed for strains carrying pRBBm214 and pRBBm215 growing in M9 minimal medium supplemented with 0.6 M NaCl offers good perspectives for the production in *B. megaterium*. Indeed, since PHB synthesis seems growth associated higher biomass concentrations and PHB content could surely be achieved if sufficient nitrogen concentrations are provided. As a matter of fact, biomass concentrations as high as 33.5 g $L^{-1}$ have been reached by others during fed-batch cultivations with *B. megaterium*. Hence, implementation of a similar strategy with these two plasmid strains should enable production of PHB at a rate close to 1 g $L^{-1}$ $h^{-1}$, thus already competing with most current producers [563, 575]. Moreover, although PHB content has been strongly increased in these two strains, it remains far below the up to 60 % of biomass reported for other *B. megaterium* strains, suggesting that there is still room for improvement. Applying elementary flux mode analysis (EFMA) as described by Melzer et al. (2009) to a simple network regrouping reactions from the carbon core metabolism of *B. megaterium* and extended to proline and PHB synthesis pathways confirms that achieved contents lie in the lower range of its metabolic capability (**Fig. 4.27** and **Tab. A.15**) [585]. Within the solution space described by the 997 elementary modes observed, most modes are located on the axes and correspond to extreme cases where biomass or PHB is exclusively produced.

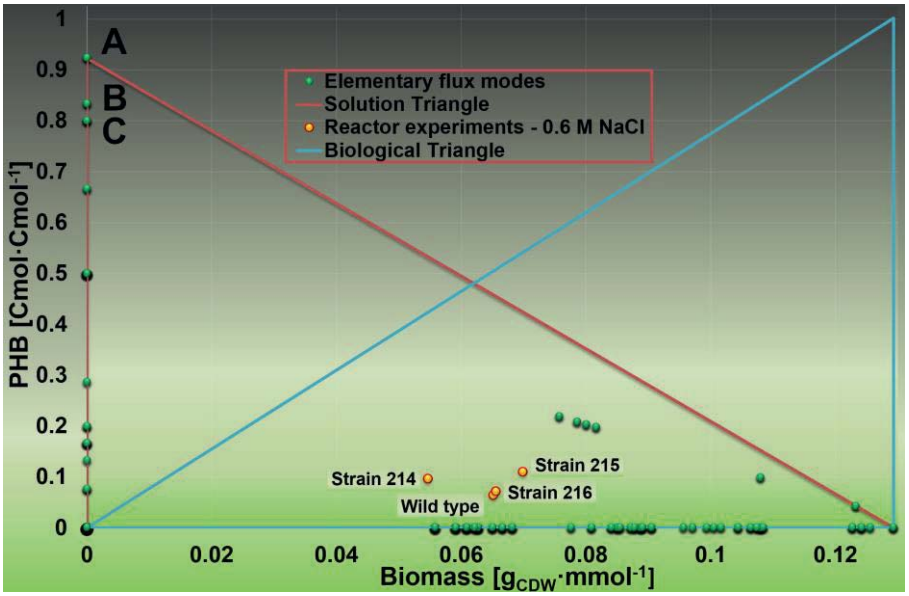


**Figure 4.27: Elementary modes for PHB and biomass production in *B. megaterium* growing on glucose.** The solution space of elementary modes, represented by green dots, consists of the interior and sides of the red triangle. This space is further reduced to its intersection with the space of biologically possible solutions, i.e. when PHB content do not exceed 100 % of biomass, represented by the blue triangle. Yellow dots indicate the performance in the wild-type and modified strains. A, B and C indicate modes with the three highest theoretical yields.

Since PHB is an intracellular compound, the latter are biologically impossible but of particular interest because the corresponding flux distributions enable fast detection of pathways indispensable for efficient PHB production. In particular, modes giving rise to the highest PHB yields (> 0.8 $Cmol_{PHB}$ $Cmol^{-1}$) reveal that enhancement of PHB production can be achieved in three distinct ways (Fig. 4.27 and **Fig. 4.28**). Basically, all strategies aim at providing cells with increased amounts of NADPH and acetyl-CoA, the two precursor molecules indispensable for PHB synthesis, but they recruit different pathways to reach that objective [586].

The first (A) and second strategies (B) strive to reduce flux through the TCA cycle to increase acetyl-CoA availability but while this is accompanied with an enhancement of flux through the NADPH-producing pentose phosphate pathway (PPP) for the second one, the first strategy proposes a balanced flux distribution between PPP and glycolysis similar to that observed *in vivo* at 0.6 M NaCl. The third strategy (C) favours glycolysis over PPP to provide cells with higher amounts of acetyl-CoA while NADPH supply is ensured by the TCA cycle. To improve this supply and maintain a high flux from pyruvate to acetyl-CoA, malate dehydrogenase is furthermore bypassed using NADPH-dependent malic enzyme. Overall, these results are in good accordance with previous works in *E. coli*, showing that overexpression of genes encoding glucose-6-phosphate dehydrogenase (*zwf*) and 6-phosphogluconate (*gnd*) or of those coding for triose phosphate isomerase (*tpiA*) and fructose-bisphosphate aldolase (*fbaA*) results in higher PHB contents [587, 588]. Interestingly, overexpression of the first two genes in *E. coli* furthermore resulted in a 6-fold higher NADPH-to-NADP ratio which tends to confirm the regulatory role of redox state in PHB biosynthesis.

All three strategies furthermore highlight the pyruvate dehydrogenase complex as a central amplification target towards improving PHB production. In that sense, enhancement of the combined operation of pyruvate oxidase (Pox) and acetyl-CoA synthethase (AcsA) as observed under salt stress could complement pyruvate dehydrogenase and represent an effective way to increase acetyl-CoA supply by reducing both pyruvate and acetate secretion (4.2.1). Although the flux design analysis indicate that the first strategy (A) would probably yield the highest PHB content, involved genetic modifications could also affect growth and drastically reduce the resulting production rate. In that sense, optimisation strategy obtained by statistical analysis of modes describing combined production of biomass and PHB in *B. megaterium* is more similar to strategy (C) (Fig. 4.28C and **Fig. 4.29**). Nevertheless, all three strategies have to be tested *in vivo* to find the solution offering the best possible compromise between enhanced PHB synthesis and sustained growth under chosen conditions [586]. Further, although no depolymerases or (R)-3-hydroxybutanoic acid monomers could be detected, 3-hydroxybutyrate dehydrogenase (BMD_2166) and 3-oxoacid CoA-transferase (ScoA, ScoB) are specifically produced under salt stress and expression of the corresponding genes is up to 2.8-fold higher at 1.2 M NaCl. Hence, PHB degradation might occur simultaneously with synthesis and restrict PHB accumulation, thus providing another angle of attack for optimising production (Tab. 4.10).

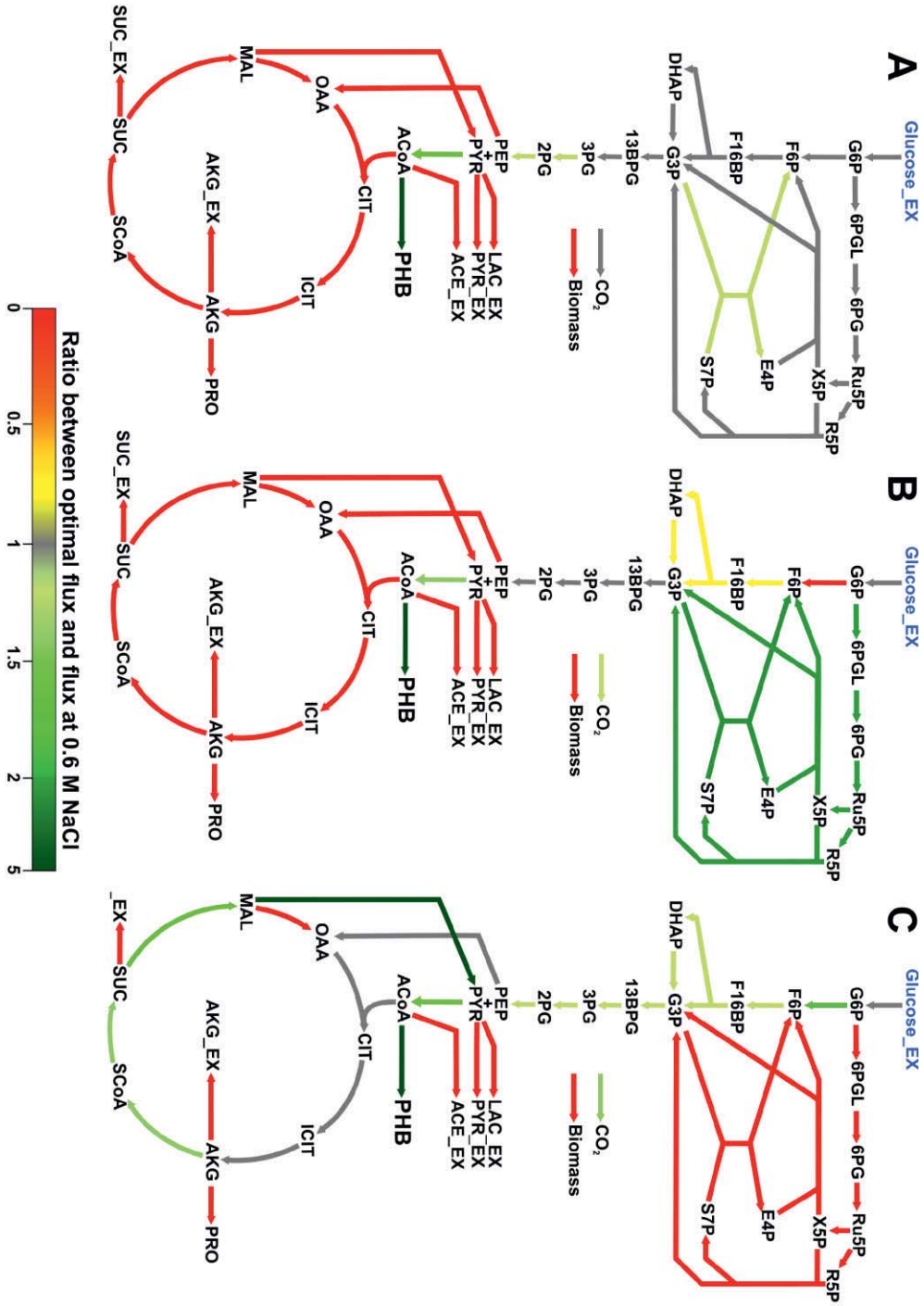


**Figure 4.28: Model-based flux design for polyhydroxybutyric acid (PHB) production in *B. megaterium* growing on glucose.** The ratio between flux values obtained from elementary flux mode analysis for the three highest theoretical production yields (0.8, 0.83 and 0.92 Cmol Cmol$^{-1}$) and the experimental flux distribution determined for *B. megaterium* growing in M9 minimal medium supplemented with 0.6 M NaCl is expressed by colour and described three different optimisation strategies (**A**, **B**, **C**) (Fig. 4.27). For each strategy, pathways in green need to be amplified while those in red should be attenuated to improve PHB production.

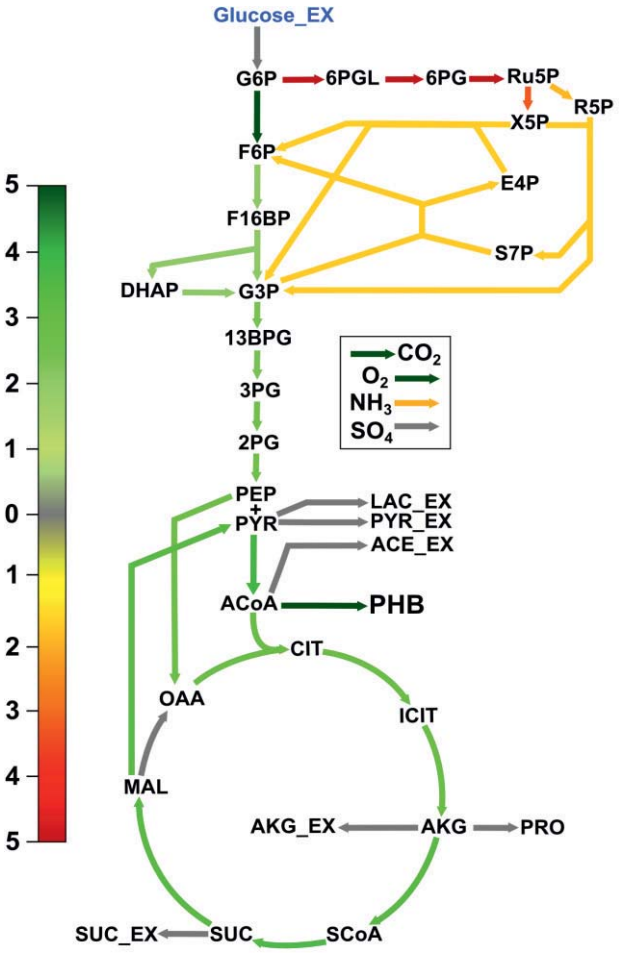


**Figure 4.29 *In silico* target prediction for superior polyhydroxybutyric acid (PHB) production in *B. megaterium* growing on glucose.** Flux correlation to the target flux (PHB production) was obtained from elementary flux mode analysis using only modes enabling simultaneous production of biomass and PHB as observed experimentally for *B. megaterium* growing in M9 minimal medium. Obtained correlation factors were then mapped onto the central carbon metabolism and represented using the colour scale situated left from the network. Hence, green arrows and red arrows indicate amplification and deletion targets, respectively. For organic acid secretions, no correlation was found because fluxes always had a value of null for the selected modes (grey arrows).

Regardless of these genetic considerations, central importance of medium composition and process parameters such as oxygen availability, pH, temperature and C/N-ratio in providing cells with a metabolic state supportive of PHB production has already been stressed in different studies and requires further examination in *B. megaterium* as well [257-260, 584, 589]. For instance, even though addition of salt triggers PHB accumulation in the first place, the related production of the osmoprotectant proline drains acetyl-CoA and NADPH molecules, thus restricting polymer synthesis. Hence, a medium with standard salinity should be preferred once exact mechanisms activating PHB accumulation are known, thus enabling faster growth and higher space-time-yields.

Metabolome data of the first part of this chapter indicate that intracellular acetyl-CoA concentration increases from 1159 nmol $g_{CDW}^{-1}$ at 37°C to 7502 nmol $g_{CDW}^{-1}$ at 45°C, being 2-fold higher as in medium supplemented with 0.6 M NaCl (cf. Fig. 4.20). Given the role of acetyl-CoA accumulation in promoting PHB synthesis, a cultivation combining both temperature and salt stress could be a meaningful process-oriented approach for increasing PHB content in *B. megaterium*. In the end, comprehension of PHB accumulation process and subsequent production optimisation will only be achieved through collection of large sets of transcriptome, metabolome, proteome and fluxome data characterising PHB production under various conditions in different strains.

# 5. Conclusion

With a product portfolio growing from year to year, *Bacillus megaterium* is progressively emerging as a major industrial workhorse. However, laconic comprehension of its metabolic behaviour still restricts the detection of bottlenecks limiting performance of current production processes. In this work, emphasis was therefore placed on the investigation and functional understanding of regulatory mechanisms triggered during exposure to different temperatures and osmolarities, two parameters affecting production efficiency of industrial reactors, with the ultimate goal of uncovering related issues and find adequate targets for strain improvement.

To this end, metabolic response of *B. megaterium* to these two stress conditions was characterised for the first time using a systems biology approach combining whole genome expression, intracellular proteome, intra- and extracellular metabolite concentrations as well as *in vivo* fluxes within the central carbon metabolism. The resulting data set is by far the most exhaustive collected for this organism to date and appropriate statistical analysis had to be applied to reduce its complexity and identify stress-specific phenomena. In general, environmental stress led to impaired growth, alteration of biomass composition and production of elements specifically involved in coping with challenges characteristic of applied stressor.

As in other microorganisms, responses to high and low temperature were quite antagonistic and relied on the production of so-called heat and cold shock proteins, respectively, which are indispensable for protein, DNA and RNA homeostasis. Under cold stress, improving translation efficiency and mRNA stability was the main concern but enhanced expression of genes involved in defences against bacteriophages suggest that conservation of DNA integrity constitutes another important feature. Further, membrane stiffening restrained glucose uptake and was partly compensated by desaturation of fatty acids and intensified activity of PTS systems as suggested by strongly increased pyruvate secretions. In addition, relative flux through the citric acid cycle steeply increased to provide cells with energy despite the poor carbon supply, resulting in a higher energetic state (AEC) and dissipation of ATP through futile cycles at the anaplerotic node.

A central issue spotted under all studied stress conditions is the disruption of redox homeostasis, which in turn triggered various mechanisms aiming at restricting the associated production of reactive oxygen species (ROS) and restoring balance. This issue was particularly pronounced at 45°C where several known and presumed systems scavenging ROS, preventing their formation or repairing oxidative damages were identified. At this temperature and also under salt stress, deviation of the $NADH/NAD^+$ ratio from its physiological value was furthermore moderated by enhanced activity of the lactate dehydrogenase and pyruvate oxidase. Adaptation to high temperature was also characterised by the production of DNA protecting elements, numerous stabilising chaperones and proteases that counterbalance heat-induced denaturation of genetic material and proteins.

Interestingly, absolute fluxes within the central carbon metabolism were not greatly affected by detrimental effects of heat on protein activity and global kinetics was maintained by increasing

metabolite pools rather than protein concentrations. As a matter of fact, expression of genes and concentration of proteins from the central carbon metabolism were, with some exceptions, not greatly affected by any environmental stressor and cannot account alone for the modifications observed in flux distribution under cold and osmotic stress. Hence, in some cases, modification of metabolite concentrations may offer a simple and less costly alternative for redirecting fluxes toward certain pathways.

Finally, adaptation to ionic osmotic stress in *B. megaterium* was mainly centred on the massive *de novo* synthesis of the compatible solute proline and recruits an osmo-dependent pathway to fulfil this requirement. This strategy was evidenced by higher transcript and protein concentrations within this pathway and confirmed by the reorganisation of flux distribution towards proline production. In addition, relative fluxes through the pentose phosphate pathway and citric acid cycle were significantly increased to supply the cofactor NADPH required for proline synthesis. As a consequence, NADPH was present in large excess in cells under osmotic stress and apparently triggered accumulation of the storage compound polyhydroxybutyric acid (PHB), a highly promising biopolymer. By overexpressing genes encoding proteins involved in PHB synthesis from acetyl-coA, its production was improved by up to 75 % compared to the wild type, reaching a maximal PHB content of 32 % in M9 minimal medium supplemented with 0.6 M NaCl. Finally, *in silico* analysis using elementary flux mode analysis (EFMA) predicted a far better potential for this organism and enabled the detection of distinct genetic targets for the development of superior producing strains able to outperform current producers.

# 6. Outlook

Although biotechnological production using *B. megaterium* is long established and has in recent years benefited from the development of efficient expression systems for recombinant protein production, the impact of various kinds of stress occurring in bioreactors on cellular activity is only poorly understood and still restricts the potential of this bacterium. In that sense, the present study on temperature and osmotic stress is part of a broader effort to unravel gene and protein functions as well as regulatory mechanisms governing relations between the different biological layers in this organism, from gene expression to observed carbon flux distribution. Hence, similar multi-omics studies investigating the behaviour of *B. megaterium* under other conditions need to be carried out to identify recurring patterns characteristic of given regulation systems and find key genetic targets that are most likely to result in significant improvement of production performance.
According to the results presented in this work, biotin and cobalamin synthesis might constitute such targets and further efforts should be dedicated to analysing the effect of a genetic enhancement of their synthesis pathways and of their supplementation in cultures on strain resilience. Similarly, elucidating functions of unknown proteins whose concentration increased the most under both temperature and osmotic stress will certainly deliver other interesting biotechnological targets and should be considered a priority.
In addition, study on osmotic stress revealed the capacity of *B. megaterium* to accumulate large amounts of intracellular proline when exposed to high salt concentrations and release it after osmotic down-shock. Hence, *B. megaterium* could be used to produce proline industrially using bacterial milking and the feasibility of such a process should be further assessed. Moreover, discovery of an osmo-dependent pathway which is not negatively regulated by proline concentrations offers interesting perspectives towards overproduction of proline in mutant strains. However, particular attention should first be paid to clarifying the regulation mechanisms involved in activation of this metabolic road because overexpression of the corresponding genes in cells growing at normal osmolarities did not affect production.
Finally, this work gave some new insights in the production of the biopolymer polyhydroxybutyric acid (PHB) in *B. megaterium* and further experiments need to focus on the comprehension of metabolic conditions favouring its accumulation and relations between the different elements involved. This study has underlined the central role of NADPH excess in this process but target modifications beneficial for PHB production found by *in silico* modelling have not been implemented yet. Among them, combined overexpression of genes encoding pyruvate dehydrogenase complex (*pdh*), NADPH-dependent malic enzyme and isocitrate dehydrogenase (*icd*) seems worth exploring. Alternatively, another approach would consist in the overexpression of genes coding for glucose-6-phosphate dehydrogenase (*zwf*) and 6-phosphogluconate dehydrogenase (*gnd*). In any case, the development of appropriate cultivation medium and process parameters fostering PHB accumulation using statistical tools such as central composite design and response surface methodology seems an indispensable prerequisite.

# 7. Abbreviations and symbols

## 7.1 Abbreviations

| | | | |
|---|---|---|---|
| 13BPG | 1,3-bisphosphoglycerate | GAP | glyceraldehyde 3-phosphate |
| 2PG | 2-phosphoglycerate | GC | gas chromatography |
| 3PG | 3-phosphoglycerate | glcNAC | N-Acétylglucosamine |
| 6PG | 6-phosphogluconate | GLN | glutamine |
| 6PGL | 6-phosphogluconolactone | GLU | glutamate |
| ABU | α-aminobutyric acid | GLY | glycine |
| ACE | acetate | GPx | glutathione peroxidase |
| ACoA | acetyl-CoA | GR | glutathione reductase |
| ADP | adenosine diphosphate | GSEA | gene set enrichment analysis |
| AEC | adenylate energy charge | GSH | glutathione |
| AKG | 2-oxoglutarate | GSSG | glutathione disulfide |
| ALA | alanine | GTP | guanosine-5'-triphosphate |
| AMP | adenosine monophosphate | HCPC | hierarchical clustering on principal components |
| ANOVA | analysis of variance | HPLC | high-performance liquid chromatography |
| ARG | arginine | HSP | heat shock protein |
| ASN | asparagine | iAA | intracellular amino acid |
| ASP | aspartate | ICIT | isocitrate |
| ATP | adenosine triphosphate | IEA | international energy agency |
| BSA | bovine serum albumin | ILE | isoleucine |
| CAT | catalase | IMS | ion mobility spectrometry |
| CCM | central carbon metabolism | LAC | lactate |
| cDNA | complementary deoxyribonucleic acid | LB | lysogeny broth |
| CE | capillary electrophoresis | LC | liquid chromatography |
| CHRM | chorismate | LEU | leucine |
| CIT | citrate | LTA | lipoteichoic acid |
| CSP | cold shock protein | LYS | lysine |
| CtsR | class three heat gene regulator | MAL | malate |
| CYS | cysteine | MCA | metabolic control analysis |
| DHAP | dihydroxyacetone phosphate | mcl-PHA | medium chain length polyhydroxyalkanoate |
| DNA | deoxyribonucleic acid | MET | methionine |
| dNTP | nucleoside triphosphate | METAFoR | metabolic flux ratio analysis |
| E4P | erythrose 4-phosphate | MFA | metabolic flux analysis |
| EDTA | ethylenediaminetetraacetic acid | mRNA | messenger ribonucleic acid |
| EFMA | elementary flux mode analysis | MS | mass spectrometry |
| EMP | Embden–Meyerhof–Parnas pathway | NAD(H) | nicotinamide adenine dinucleotide |
| ESI | electrospray ionisation | NADP(H) | nicotinamide adenine dinucleotide phosphate |
| EST | expression sequence tag | NMR | nuclear magnetic resonance |
| F16BP | fructose-1,6-biphosphate | OAA | oxaloacetate |
| F6P | fructose-6-phosphate | $OD_{600nm}$ | optical density at 600 nm |
| FBA | flux balance analysis | OPA | o-phtalaldehyde |
| FC | fold change | PC | principal component |
| FMOC | 9-fluorenylmethyloxycarbonyl | PCA | principal component analysis |
| G6P | glucose-6-phosphate | PCR | polymerase chain reaction |

| | |
|---|---|
| PEP | phosphoenolpyruvate |
| PHA | polyhydroxyalkanoate |
| PHB | poly-β-hydroxybutyrate |
| PHE | phenylalanine |
| PPP | pentose phosphate pathway |
| PRO | proline |
| Prx | peroxiredoxin |
| PTM | post-transcriptional modification |
| PTS | phosphotransferase system |
| PYR | pyruvate |
| qRT-PCR | real-time reverse transcription polymerase chain reaction |
| R5P | ribose-5-phosphate |
| RIN | RNA integrity number |
| RNA | ribonucleic acid |
| ROS | reactive oxygen species |
| RT | room temperature |
| Ru5P | ribulose-5-phosphate |
| S7P | sedoheptulose 7-phosphate |
| scl-PHA | short chain lenght polyhydroxyalkanoate |
| SCoA | succinyl-CoA |
| SDS | sodium dodecyl sulfate |
| SER | serine |
| SOD | superoxide dismutase |
| SOM | self-organizing map |
| SUC | succinate |
| TAE | tris base, acetic acid and EDTA |
| TCA | tricarboxylic acid cycle |
| TCEP | tris(2-carboxyethyl)phosphin |
| TCS | two-component system |
| TE | tris EDTA |
| TEAB | tetraethylammonium bromide |
| THR | threonine |
| TIGR | the institute for genomic research |
| TLC | thin layer chromatography |
| TOF | time-of-flight |
| Tris | tris(hydroxymethyl)aminomethane |
| TRP | tryptophan |
| Trx | thioredoxin |
| TrxR | thioredoxin reductase |
| TYR | tyrosine |
| UPLC | ultra-high performance liquid chromatography |

## 7.2 Symbols

| | | |
|---|---|---|
| μ | growth rate | [$h^{-1}$] |
| A | absorption | [-] |
| C | concentration or carbon | [g $L^{-1}$] |
| CDW | cell dry weight | [g $L^{-1}$] |
| DO | dissolved oxygen | [%] |
| E | enzyme concentration | [g $L^{-1}$] |
| $k_1$, $k_{-1}$ | reaction constant for substrate binding and unbinding | [$s^{-1}$] |
| $k_{CAT}$ | reaction constant for product conversion | [L $mol^{-1}$ $s^{-1}$] |
| $K_M$ | Michaelis-Menten constant | [g $L^{-1}$] |
| OD | optical density | [-] |
| $q_S$ | glucose uptake rate | [mol $h^{-1}$] |
| $R^2$ | coefficient of determination | [-] |
| S | substrate | [g $L^{-1}$] |
| T | temperature | [°C] |
| t | time | [h] |
| v | reaction rate | [mol $h^{-1}$] |
| $Y_{X/S}$ | biomass yield | [g $mol^{-1}$] |
| $Y_{P/S}$ | product yield | [g $mol^{-1}$] |
| λ | wavelength | [nm] |
| $\sigma^B$ | RNA polymerase sigma factor sigma B | |

# 8. References


1. Vary, P.S., Biedendieck, R., Fuerch, T., Meinhardt, F., Rohde, M., Deckwer, W.D., and Jahn, D., Bacillus megaterium--*from simple soil bacterium to industrial protein production host.* Applied microbiology and biotechnology, 2007. **76**(5): p. 957-67.
2. De Bary, A., *Vergleichende Morphologie und Biologie der Pilze, Mycetozoen und Bakterien*. 1884, Leipzig: Whilhelm Engelmann.
3. Hrafnsdottir, S., Nichols, J.W., and Menon, A.K., *Transbilayer movement of fluorescent phospholipids in* Bacillus megaterium *membrane vesicles.* Biochemistry, 1997. **36**(16): p. 4969-78.
4. McCool, G.J. and Cannon, M.C., *PhaC and PhaR are required for polyhydroxyalkanoic acid synthase activity in* Bacillus megaterium*.* Journal of bacteriology, 2001. **183**(14): p. 4235-43.
5. Clarke, N.A., *Studies on the host-virus relationship in a lysogenic strain of* Bacillus megaterium*. II. The growth of* Bacillus megaterium *in synthetic medium.* Journal of bacteriology, 1952. **63**(2): p. 187-92.
6. Robinow, C.F., *Observations on the nucleus of resting and germinating spores of* Bacillus megaterium*.* Journal of bacteriology, 1953. **65**(4): p. 378-82.
7. De Carlo, M.R., Sarles, W.B., and Knight, S.G., *Lysogenicity of* Bacillus megaterium*.* Journal of bacteriology, 1953. **65**(1): p. 53-5.
8. Levinson, H.S. and Sevag, M.G., *Manganese and the proteolytic activity of spore extracts of* Bacillus megaterium *in relation to germination.* Journal of bacteriology, 1954. **67**(5): p. 615-6.
9. Rygus, T. and Hillen, W., *Inducible high-level expression of heterologous genes in* Bacillus megaterium *using the regulatory elements of the xylose-utilization operon.* Applied microbiology and biotechnology, 1991. **35**(5): p. 594-599.
10. Schmiedel, D., Kintrup, M., and Hillen, W., *Regulation of expression, genetic organization and substrate specificity of xylose uptake in* Bacillus megaterium*.* Molecular microbiology, 1997. **23**(5): p. 1053-1062.
11. Malten, M., Hollmann, R., Deckwer, W.D., and Jahn, D., *Production and secretion of recombinant* Leuconostoc mesenteroides *dextransucrase DsrS in* Bacillus megaterium*.* Biotechnology and bioengineering, 2005. **89**(2): p. 206-18.
12. Stammen, S., Muller, B.K., Korneli, C., Biedendieck, R., Gamer, M., Franco-Lara, E., and Jahn, D., *High-yield intra- and extracellular protein production using* Bacillus megaterium*.* Applied and environmental microbiology, 2010. **76**(12): p. 4037-46.
13. Vary, P.S., *Prime time for Bacillus megaterium.* Microbiology, 1994. **140 ( Pt 5)**: p. 1001-13.
14. Bolhuis, A., Tjalsma, H., Smith, H.E., de Jong, A., Meima, R., Venema, G., Bron, S., and van Dijl, J.M., *Evaluation of bottlenecks in the late stages of protein secretion in* Bacillus subtilis*.* Applied and environmental microbiology, 1999. **65**(7): p. 2934-2941.
15. Korneli, C., Bolten, C.J., Godard, T., Franco-Lara, E., and Wittmann, C., *Debottlenecking recombinant protein production in* Bacillus megaterium *under large-scale conditions--targeted precursor feeding designed from metabolomics.* Biotechnology and bioengineering, 2012. **109**(6): p. 1538-50.
16. Korneli, C., David, F., Biedendieck, R., Jahn, D., and Wittmann, C., *Getting the big beast to work—systems biotechnology of* Bacillus megaterium *for novel high-value proteins.* Journal of biotechnology, 2013. **163**(2): p. 87-96.
17. Eppinger, M., Bunk, B., Johns, M.A., Edirisinghe, J.N., Kutumbaka, K.K., Koenig, S.S., Creasy, H.H., Rosovitz, M.J., Riley, D.R., Daugherty, S., Martin, M., Elbourne, L.D., Paulsen, I., Biedendieck, R., Braun, C., Grayburn, S., Dhingra, S., Lukyanchuk, V., Ball, B., Ul-Qamar, R., Seibel, J., Bremer, E., Jahn, D., Ravel, J., and Vary, P.S., *Genome sequences of the biotechnologically important* Bacillus megaterium *strains QM B1551 and DSM319.* Journal of bacteriology, 2011. **193**(16): p. 4199-213.

18. Biedendieck, R., Borgmeier, C., Bunk, B., Stammen, S., Scherling, C., Meinhardt, F., Wittmann, C., and Jahn, D., *Systems biology of recombinant protein production using* Bacillus megaterium*.* Methods in enzymology, 2011. **500**: p. 165-95.
19. Liu, L., Li, Y., Zhang, J., Zou, W., Zhou, Z., Liu, J., Li, X., Wang, L., and Chen, J., *Complete genome sequence of the industrial strain* Bacillus megaterium *WSH-002.* Journal of bacteriology, 2011. **193**(22): p. 6389-6390.
20. Arya, G., Petronella, N., Crosthwait, J., Carrillo, C.D., and Shwed, P.S., *Draft genome sequence of* Bacillus megaterium *type strain ATCC 14581.* Genome announcements, 2014. **2**(6): p. e01124-14.
21. Kohlstedt, M., Becker, J., and Wittmann, C., *Metabolic fluxes and beyond-systems biology understanding and engineering of microbial metabolism.* Applied microbiology and biotechnology, 2010. **88**(5): p. 1065-75.
22. Kuntumalla, S., Braisted, J.C., Huang, S.T., Parmar, P.P., Clark, D.J., Alami, H., Zhang, Q., Donohue-Rolfe, A., Tzipori, S., Fleischmann, R.D., Peterson, S.N., and Pieper, R., *Comparison of two label-free global quantitation methods, APEX and 2D gel electrophoresis, applied to the* Shigella dysenteriae *proteome.* Proteome science, 2009. **7**: p. 22.
23. Ideker, T., Galitski, T., and Hood, L., *A new approach to decoding life: systems biology.* Annual review of genomics and human genetics, 2001. **2**(1): p. 343-372.
24. Rowen, L., Lasky, S., and Hood, L., *Deciphering genomes through automated large-scale sequencing.* Methods in Microbiology, 1999. **28**: p. 155-191.
25. Sasano, Y., Haitani, Y., Ohtsu, I., Shima, J., and Takagi, H., *Proline accumulation in baker's yeast enhances high-sucrose stress tolerance and fermentation ability in sweet dough.* International journal of food microbiology, 2012. **152**(1-2): p. 40-3.
26. Sasano, Y., Watanabe, D., Ukibe, K., Inai, T., Ohtsu, I., Shimoi, H., and Takagi, H., *Overexpression of the yeast transcription activator Msn2 confers furfural resistance and increases the initial fermentation rate in ethanol production.* Journal of bioscience and bioengineering, 2012. **113**(4): p. 451-5.
27. Clarke, J.D. and Zhu, T., *Microarray analysis of the transcriptome as a stepping stone towards understanding biological systems: practical considerations and perspectives.* The Plant journal : for cell and molecular biology, 2006. **45**(4): p. 630-50.
28. Debouck, C. and Goodfellow, P.N., *DNA microarrays in drug discovery and development.* Nature genetics, 1999. **21**(1 Suppl): p. 48-50.
29. Chen, W., Provart, N.J., Glazebrook, J., Katagiri, F., Chang, H.S., Eulgem, T., Mauch, F., Luan, S., Zou, G., Whitham, S.A., Budworth, P.R., Tao, Y., Xie, Z., Chen, X., Lam, S., Kreps, J.A., Harper, J.F., Si-Ammour, A., Mauch-Mani, B., Heinlein, M., Kobayashi, K., Hohn, T., Dangl, J.L., Wang, X., and Zhu, T., *Expression profile matrix of* Arabidopsis *transcription factor genes suggests their putative functions in response to environmental stresses.* The Plant cell, 2002. **14**(3): p. 559-74.
30. McLachlan, G., Do, K.-A., and Ambroise, C., *Analyzing microarray gene expression data*. Vol. 422. 2005: John Wiley & Sons.
31. Czechowski, T., Bari, R.P., Stitt, M., Scheible, W.R., and Udvardi, M.K., *Real-time RT-PCR profiling of over 1400* Arabidopsis *transcription factors: unprecedented sensitivity reveals novel root-and shoot-specific genes.* The Plant Journal, 2004. **38**(2): p. 366-379.
32. Schmittgen, T.D., Lee, E.J., and Jiang, J., *High-throughput real-time PCR*, in *Molecular Beacons: Signalling Nucleic Acid Probes, Methods, and Protocols*. 2008, Springer. p. 89-98.
33. Zhu, T., *Global analysis of gene expression using GeneChip microarrays.* Current opinion in plant biology, 2003. **6**(5): p. 418-25.
34. Mehta, J.P., *Microarray Analysis of mRNAs: Experimental Design and Data Analysis Fundamentals*, in *Gene Expression Profiling*. 2011, Springer. p. 27-40.
35. Lockhart, D.J., Dong, H., Byrne, M.C., Follettie, M.T., Gallo, M.V., Chee, M.S., Mittmann, M., Wang, C., Kobayashi, M., Horton, H., and Brown, E.L., *Expression monitoring by*

*hybridization to high-density oligonucleotide arrays.* Nature biotechnology, 1996. **14**(13): p. 1675-80.
36. Zhang, A., *Advanced analysis of gene expression microarray data*. Vol. 104. 2006: World Scientific Singapore.
37. Patterson, T.A., Lobenhofer, E.K., Fulmer-Smentek, S.B., Collins, P.J., Chu, T.M., Bao, W., Fang, H., Kawasaki, E.S., Hager, J., Tikhonova, I.R., Walker, S.J., Zhang, L., Hurban, P., de Longueville, F., Fuscoe, J.C., Tong, W., Shi, L., and Wolfinger, R.D., *Performance comparison of one-color and two-color platforms within the MicroArray Quality Control (MAQC) project.* Nature biotechnology, 2006. **24**(9): p. 1140-50.
38. Meyers, B.C., Galbraith, D.W., Nelson, T., and Agrawal, V., *Methods for transcriptional profiling in plants. Be fruitful and replicate.* Plant physiology, 2004. **135**(2): p. 637-52.
39. Pavlidis, P., Li, Q., and Noble, W.S., *The effect of replication on gene expression microarray experiments.* Bioinformatics, 2003. **19**(13): p. 1620-7.
40. Lee, M.L., Kuo, F.C., Whitmore, G.A., and Sklar, J., *Importance of replication in microarray gene expression studies: statistical methods and evidence from repetitive cDNA hybridizations.* Proceedings of the National Academy of Sciences of the United States of America, 2000. **97**(18): p. 9834-9.
41. Yeung, K.Y., Medvedovic, M., and Bumgarner, R.E., *From co-expression to co-regulation: how many microarray experiments do we need?* Genome biology, 2004. **5**(7): p. R48.
42. Reiner, A., Yekutieli, D., and Benjamini, Y., *Identifying differentially expressed genes using false discovery rate controlling procedures.* Bioinformatics, 2003. **19**(3): p. 368-75.
43. Schena, M., Shalon, D., Davis, R.W., and Brown, P.O., *Quantitative monitoring of gene expression patterns with a complementary DNA microarray.* Science, 1995. **270**(5235): p. 467-70.
44. DeRisi, J.L., Iyer, V.R., and Brown, P.O., *Exploring the metabolic and genetic control of gene expression on a genomic scale.* Science, 1997. **278**(5338): p. 680-6.
45. Kerr, M.K., Martin, M., and Churchill, G.A., *Analysis of variance for gene expression microarray data.* Journal of computational biology : a journal of computational molecular cell biology, 2000. **7**(6): p. 819-37.
46. Stekel, D., *Microarray bioinformatics*. 2003: Cambridge University Press.
47. Eisen, M.B., Spellman, P.T., Brown, P.O., and Botstein, D., *Cluster analysis and display of genome-wide expression patterns.* Proceedings of the National Academy of Sciences, 1998. **95**(25): p. 14863-14868.
48. Jolliffe, I., *Principal component analysis*. 2002: Wiley Online Library.
49. Alonso, J.M., Stepanova, A.N., Leisse, T.J., Kim, C.J., Chen, H., Shinn, P., Stevenson, D.K., Zimmerman, J., Barajas, P., and Cheuk, R., *Genome-wide insertional mutagenesis of* Arabidopsis thaliana*.* Science, 2003. **301**(5633): p. 653-657.
50. Wang, D., Weaver, N.D., Kesarwani, M., and Dong, X., *Induction of protein secretory pathway is required for systemic acquired resistance.* Science, 2005. **308**(5724): p. 1036-1040.
51. Glazebrook, J., Chen, W., Estes, B., Chang, H.S., Nawrath, C., Métraux, J.P., Zhu, T., and Katagiri, F., *Topology of the network integrating salicylate and jasmonate signal transduction derived from global expression phenotyping.* The Plant Journal, 2003. **34**(2): p. 217-228.
52. Okoniewski, M.J. and Miller, C.J., *Hybridization interactions between probesets in short oligo microarrays lead to spurious correlations.* BMC bioinformatics, 2006. **7**(1): p. 276.
53. Wang, Z., Gerstein, M., and Snyder, M., *RNA-Seq: a revolutionary tool for transcriptomics.* Nature reviews. Genetics, 2009. **10**(1): p. 57-63.
54. Lipshutz, R.J., Fodor, S.P., Gingeras, T.R., and Lockhart, D.J., *High density synthetic oligonucleotide arrays.* Nature genetics, 1999. **21**: p. 20-24.
55. Mei, R., Hubbell, E., Bekiranov, S., Mittmann, M., Christians, F.C., Shen, M.-M., Lu, G., Fang, J., Liu, W.-M., and Ryder, T., *Probe selection for high-density oligonucleotide arrays.* Proceedings of the National Academy of Sciences, 2003. **100**(20): p. 11237-11242.

56. Zhang, L., Miles, M.F., and Aldape, K.D., *A model of molecular interactions on short oligonucleotide microarrays.* Nature biotechnology, 2003. **21**(7): p. 818-821.
57. Binder, H., Kirsten, T., Loeffler, M., and Stadler, P.F., *Sensitivity of microarray oligonucleotide probes: variability and effect of base composition.* The Journal of Physical Chemistry B, 2004. **108**(46): p. 18003-18014.
58. Binder, H., Kirsten, T., Hofacker, I.L., Stadler, P.F., and Loeffler, M., *Interactions in oligonucleotide hybrid duplexes on microarrays.* The Journal of Physical Chemistry B, 2004. **108**(46): p. 18015-18025.
59. Shendure, J., *The beginning of the end for microarrays?* Nat Methods, 2008. **5**(7): p. 585-7.
60. Mardis, E.R., *Next-generation DNA sequencing methods.* Annual review of genomics and human genetics, 2008. **9**: p. 387-402.
61. Costa, V., Angelini, C., De Feis, I., and Ciccodicola, A., *Uncovering the complexity of transcriptomes with RNA-Seq.* BioMed research international, 2010. **2010**.
62. Kogenaru, S., Qing, Y., Guo, Y., and Wang, N., *RNA-seq and microarray complement each other in transcriptome profiling.* BMC genomics, 2012. **13**: p. 629.
63. Jacquier, A., *The complex eukaryotic transcriptome: unexpected pervasive transcription and novel small RNAs.* Nature Reviews Genetics, 2009. **10**(12): p. 833-844.
64. Marioni, J.C., Mason, C.E., Mane, S.M., Stephens, M., and Gilad, Y., *RNA-seq: an assessment of technical reproducibility and comparison with gene expression arrays.* Genome research, 2008. **18**(9): p. 1509-1517.
65. 't Hoen, P.A.C., Ariyurek, Y., Thygesen, H.H., Vreugdenhil, E., Vossen, R.H., de Menezes, R.X., Boer, J.M., van Ommen, G.-J.B., and den Dunnen, J.T., *Deep sequencing-based expression analysis shows major advances in robustness, resolution and inter-lab portability over five microarray platforms.* Nucleic acids research, 2008. **36**(21): p. e141-e141.
66. Schwanhausser, B., Busse, D., Li, N., Dittmar, G., Schuchhardt, J., Wolf, J., Chen, W., and Selbach, M., *Global quantification of mammalian gene expression control.* Nature, 2011. **473**(7347): p. 337-42.
67. Guo, Y., Xiao, P., Lei, S., Deng, F., Xiao, G.G., Liu, Y., Chen, X., Li, L., Wu, S., and Chen, Y., *How is mRNA expression predictive for protein expression? A correlation study on human circulating monocytes.* Acta biochimica et biophysica Sinica, 2008. **40**(5): p. 426-436.
68. Wilkins, M.R., Gasteiger, E., Sanchez, J.C., Appel, R.D., and Hochstrasser, D.F., *Protein identification with sequence tags.* Current biology : CB, 1996. **6**(12): p. 1543-4.
69. Tyers, M. and Mann, M., *From genomics to proteomics.* Nature, 2003. **422**(6928): p. 193-7.
70. Anderson, N.L. and Anderson, N.G., *Proteome and proteomics: new technologies, new concepts, and new words.* Electrophoresis, 1998. **19**(11): p. 1853-1861.
71. Hein, M.Y., Sharma, K., Cox, J., and Mann, M., *Proteomic analysis of cellular systems.* Handbook of Systems Biology, 2012: p. 3-25.
72. Deracinois, B., Flahaut, C., Duban-Deweer, S., and Karamanos, Y., *Comparative and quantitative global proteomics approaches: an overview.* Proteomes, 2013. **1**(3): p. 180-218.
73. O'Farrell, P.H., *High resolution two-dimensional electrophoresis of proteins.* Journal of biological chemistry, 1975. **250**(10): p. 4007-4021.
74. Görg, A., Weiss, W., and Dunn, M.J., *Current two-dimensional electrophoresis technology for proteomics.* Proteomics, 2004. **4**(12): p. 3665-3685.
75. Lilley, K.S. and Friedman, D.B., *All about DIGE: quantification technology for differential-display 2D-gel proteomics.* Expert review of proteomics, 2004. **1**(4): p. 401-9.
76. Minden, J.S., Dowd, S.R., Meyer, H.E., and Stuhler, K., *Difference gel electrophoresis.* Electrophoresis, 2009. **30 Suppl 1**: p. S156-61.
77. Zhou, S., Bailey, M.J., Dunn, M.J., Preedy, V.R., and Emery, P.W., *A quantitative investigation into the losses of proteins at different stages of a two-dimensional gel electrophoresis procedure.* Proteomics, 2005. **5**(11): p. 2739-2747.

78. Petrak, J., Ivanek, R., Toman, O., Cmejla, R., Cmejlova, J., Vyoral, D., Zivny, J., and Vulpe, C.D., *Deja vu in proteomics. A hit parade of repeatedly identified differentially expressed proteins.* Proteomics, 2008. **8**(9): p. 1744-1749.
79. Karas, M. and Hillenkamp, F., *Laser desorption ionization of proteins with molecular masses exceeding 10,000 daltons.* Analytical chemistry, 1988. **60**(20): p. 2299-2301.
80. Fenn, J.B., Mann, M., Meng, C.K., Wong, S.F., and Whitehouse, C.M., *Electrospray ionization for mass spectrometry of large biomolecules.* Science, 1989. **246**(4926): p. 64-71.
81. Breuker, K., Jin, M., Han, X., Jiang, H., and McLafferty, F.W., *Top-down identification and characterization of biomolecules by mass spectrometry.* Journal of the American Society for Mass Spectrometry, 2008. **19**(8): p. 1045-1053.
82. Ross, P.L., Huang, Y.N., Marchese, J.N., Williamson, B., Parker, K., Hattan, S., Khainovski, N., Pillai, S., Dey, S., and Daniels, S., *Multiplexed protein quantitation in* Saccharomyces cerevisiae *using amine-reactive isobaric tagging reagents.* Molecular & cellular proteomics, 2004. **3**(12): p. 1154-1169.
83. Mann, M., *Functional and quantitative proteomics using SILAC.* Nature reviews Molecular cell biology, 2006. **7**(12): p. 952-958.
84. Ong, S.-E., Blagoev, B., Kratchmarova, I., Kristensen, D.B., Steen, H., Pandey, A., and Mann, M., *Stable isotope labeling by amino acids in cell culture, SILAC, as a simple and accurate approach to expression proteomics.* Molecular & cellular proteomics, 2002. **1**(5): p. 376-386.
85. Brun, V., Dupuis, A., Adrait, A., Marcellin, M., Thomas, D., Vandenesch, F., and Garin, J., *Isotope-labeled protein standards toward absolute quantitative proteomics.* Molecular & Cellular Proteomics, 2007. **6**(12): p. 2139-2149.
86. Gerber, S.A., Rush, J., Stemman, O., Kirschner, M.W., and Gygi, S.P., *Absolute quantification of proteins and phosphoproteins from cell lysates by tandem MS.* Proceedings of the National Academy of Sciences, 2003. **100**(12): p. 6940-6945.
87. Beynon, R.J., Doherty, M.K., Pratt, J.M., and Gaskell, S.J., *Multiplexed absolute quantification in proteomics using artificial QCAT proteins of concatenated signature peptides.* Nature methods, 2005. **2**(8): p. 587-589.
88. Simpson, D.M. and Beynon, R.J., *QconCATs: design and expression of concatenated protein standards for multiplexed protein quantification.* Analytical and bioanalytical chemistry, 2012. **404**(4): p. 977-89.
89. Brownridge, P.J., Harman, V.M., Simpson, D.M., and Beynon, R.J., *Absolute multiplexed protein quantification using QconCAT technology*, in *Quantitative Methods in Proteomics*. 2012, Springer. p. 267-293.
90. Mostertz, J., Scharf, C., Hecker, M., and Homuth, G., *Transcriptome and proteome analysis of* Bacillus subtilis *gene expression in response to superoxide and peroxide stress.* Microbiology, 2004. **150**(2): p. 497-512.
91. Stingele, S., Stoehr, G., Peplowska, K., Cox, J., Mann, M., and Storchova, Z., *Global analysis of genome, transcriptome and proteome reveals the response to aneuploidy in human cells.* Molecular systems biology, 2012. **8**(1).
92. Hahne, H., Mader, U., Otto, A., Bonn, F., Steil, L., Bremer, E., Hecker, M., and Becher, D., *A comprehensive proteomics and transcriptomics analysis of* Bacillus subtilis *salt stress adaptation.* Journal of bacteriology, 2010. **192**(3): p. 870-82.
93. Lee, J.-H., Lee, D.-E., Lee, B.-U., and Kim, H.-S., *Global analyses of transcriptomes and proteomes of a parent strain and an L-threonine-overproducing mutant strain.* Journal of bacteriology, 2003. **185**(18): p. 5442-5451.
94. Yoon, S.H., Han, M.J., Lee, S.Y., Jeong, K.J., and Yoo, J.S., *Combined transcriptome and proteome analysis of* Escherichia coli *during high cell density culture.* Biotechnology and bioengineering, 2003. **81**(7): p. 753-767.
95. Budde, I., Steil, L., Scharf, C., Volker, U., and Bremer, E., *Adaptation of* Bacillus subtilis *to growth at low temperature: a combined transcriptomic and proteomic appraisal.* Microbiology, 2006. **152**(Pt 3): p. 831-53.

96. Fiehn, O., *Metabolomics–the link between genotypes and phenotypes.* Plant molecular biology, 2002. **48**(1-2): p. 155-171.
97. Blattner, F.R., Plunkett, G., 3rd, Bloch, C.A., Perna, N.T., Burland, V., Riley, M., Collado-Vides, J., Glasner, J.D., Rode, C.K., Mayhew, G.F., Gregor, J., Davis, N.W., Kirkpatrick, H.A., Goeden, M.A., Rose, D.J., Mau, B., and Shao, Y., *The complete genome sequence of* Escherichia coli K-12*.* Science, 1997. **277**(5331): p. 1453-62.
98. Raamsdonk, L.M., Teusink, B., Broadhurst, D., Zhang, N., Hayes, A., Walsh, M.C., Berden, J.A., Brindle, K.M., Kell, D.B., and Rowland, J.J., *A functional genomics strategy that uses metabolome data to reveal the phenotype of silent mutations.* Nature biotechnology, 2001. **19**(1): p. 45-50.
99. Kell, D. and Mendes, P., *Snapshots of Systems*, in *Technological and Medical Implications of Metabolic Control Analysis*, Cornish-Bowden, A. and Cárdenas, M., Editors. 2000, Springer Netherlands. p. 3-25.
100. Ryan, D. and Robards, K., *Metabolomics: The greatest omics of them all?* Analytical chemistry, 2006. **78**(23): p. 7954-8.
101. Weckwerth, W., *Metabolomics in systems biology.* Annual review of plant biology, 2003. **54**: p. 669-89.
102. ter Kuile, B.H. and Westerhoff, H.V., *Transcriptome meets metabolome: hierarchical and metabolic regulation of the glycolytic pathway.* FEBS letters, 2001. **500**(3): p. 169-71.
103. Oliver, S.G., Winson, M.K., Kell, D.B., and Baganz, F., *Systematic functional analysis of the yeast genome.* Trends in biotechnology, 1998. **16**(9): p. 373-8.
104. Dunn, W.B., Bailey, N.J., and Johnson, H.E., *Measuring the metabolome: current analytical technologies.* The Analyst, 2005. **130**(5): p. 606-25.
105. Dettmer, K., Aronov, P.A., and Hammock, B.D., *Mass spectrometry-based metabolomics.* Mass spectrometry reviews, 2007. **26**(1): p. 51-78.
106. Lenz, E.M. and Wilson, I.D., *Analytical strategies in metabonomics.* Journal of proteome research, 2007. **6**(2): p. 443-458.
107. Kim, K.-R., Park, H.-G., Paik, M.-J., Ryu, H.-S., Oh, K.S., Myung, S.-W., and Liebich, H.M., *Gas chromatographic profiling and pattern recognition analysis of urinary organic acids from uterine myoma patients and cervical cancer patients.* Journal of Chromatography B: Biomedical Sciences and Applications, 1998. **712**(1): p. 11-22.
108. Kimura, M., Yamamoto, T., and Yamaguchi, S., *Automated metabolic profiling and interpretation of GC/MS data for organic acidemia screening: a personal computer-based system.* The Tohoku journal of experimental medicine, 1999. **188**(4): p. 317-334.
109. Brazma, A. and Vilo, J., *Gene expression data analysis.* FEBS letters, 2000. **480**(1): p. 17-24.
110. Goodacre, R., Vaidyanathan, S., Dunn, W.B., Harrigan, G.G., and Kell, D.B., *Metabolomics by numbers: acquiring and understanding global metabolite data.* Trends in biotechnology, 2004. **22**(5): p. 245-52.
111. Krömer, J.O., Sorgenfrei, O., Klopprogge, K., Heinzle, E., and Wittmann, C., *In-depth profiling of lysine-producing* Corynebacterium glutamicum *by combined analysis of the transcriptome, metabolome, and fluxome.* Journal of bacteriology, 2004. **186**(6): p. 1769-1784.
112. Hua, Q., Joyce, A.R., Palsson, B.Ø., and Fong, S.S., *Metabolic characterization of* Escherichia coli *strains adapted to growth on lactate.* Applied and environmental microbiology, 2007. **73**(14): p. 4639-4647.
113. Fong, S.S., Nanchen, A., Palsson, B.O., and Sauer, U., *Latent pathway activation and increased pathway capacity enable* Escherichia coli *adaptation to loss of key metabolic enzymes.* Journal of Biological Chemistry, 2006. **281**(12): p. 8024-8033.
114. Feng, X., Page, L., Rubens, J., Chircus, L., Colletti, P., Pakrasi, H.B., and Tang, Y.J., *Bridging the gap between fluxomics and industrial biotechnology.* BioMed research international, 2011. **2010**.
115. Orth, J.D., Thiele, I., and Palsson, B.O., *What is flux balance analysis?* Nature biotechnology, 2010. **28**(3): p. 245-8.

116. Stephanopoulos, G., Aristidou, A.A., and Nielsen, J., *Metabolic engineering: principles and methodologies*. 1998: Academic press.
117. Feist, A.M., Zielinski, D.C., Orth, J.D., Schellenberger, J., Herrgard, M.J., and Palsson, B.O., *Model-driven evaluation of the production potential for growth-coupled products of* Escherichia coli*.* Metabolic engineering, 2010. **12**(3): p. 173-86.
118. Dikicioglu, D., Pir, P., Onsan, Z.I., Ulgen, K.O., Kirdar, B., and Oliver, S.G., *Integration of metabolic modeling and phenotypic data in evaluation and improvement of ethanol production using respiration-deficient mutants of* Saccharomyces cerevisiae*.* Applied and environmental microbiology, 2008. **74**(18): p. 5809-5816.
119. Blazeck, J. and Alper, H., *Systems metabolic engineering: Genome-scale models and beyond.* Biotechnology journal, 2010. **5**(7): p. 647-659.
120. Wiechert, W., *13C metabolic flux analysis.* Metabolic engineering, 2001. **3**(3): p. 195-206.
121. Wiechert, W., Mollney, M., Petersen, S., and de Graaf, A.A., *A universal framework for 13C metabolic flux analysis.* Metabolic engineering, 2001. **3**(3): p. 265-83.
122. Kiefer, P., Heinzle, E., Zelder, O., and Wittmann, C., *Comparative metabolic flux analysis of lysine-producing* Corynebacterium glutamicum *cultured on glucose or fructose.* Applied and environmental microbiology, 2004. **70**(1): p. 229-239.
123. Wiechert, W., Siefke, C., de Graaf, A.A., and Marx, A., *Bidirectional reaction steps in metabolic networks: II. Flux estimation and statistical analysis.* Biotechnology and bioengineering, 1997. **55**(1): p. 118-35.
124. Antoniewicz, M.R., Kelleher, J.K., and Stephanopoulos, G., *Determination of confidence intervals of metabolic fluxes estimated from stable isotope measurements.* Metabolic engineering, 2006. **8**(4): p. 324-37.
125. Araúzo-Bravo, M.J. and Shimizu, K., *An improved method for statistical analysis of metabolic flux analysis using isotopomer mapping matrices with analytical expressions.* Journal of biotechnology, 2003. **105**(1): p. 117-133.
126. Yang, J., Wongsa, S., Kadirkamanathan, V., Billings, S., and Wright, P., *Metabolic flux distribution analysis by 13C-tracer experiments using the Markov chain-Monte Carlo method.* Biochemical Society transactions, 2005. **33**(6): p. 1421.
127. Millard, P., Sokol, S., Letisse, F., and Portais, J.C., *IsoDesign: A software for optimizing the design of 13C-metabolic flux analysis experiments.* Biotechnology and bioengineering, 2014. **111**(1): p. 202-208.
128. Suthers, P.F., Burgard, A.P., Dasika, M.S., Nowroozi, F., Van Dien, S., Keasling, J.D., and Maranas, C.D., *Metabolic flux elucidation for large-scale models using 13C labeled isotopes.* Metabolic engineering, 2007. **9**(5): p. 387-405.
129. Zamboni, N., Fischer, E., and Sauer, U., *FiatFlux--a software for metabolic flux analysis from 13C-glucose experiments.* BMC bioinformatics, 2005. **6**: p. 209.
130. Giersch, C., *Mathematical modelling of metabolism.* Current opinion in plant biology, 2000. **3**(3): p. 249-53.
131. Nöh, K., Grönke, K., Luo, B., Takors, R., Oldiges, M., and Wiechert, W., *Metabolic flux analysis at ultra short time scale: isotopically non-stationary 13C labeling experiments.* Journal of biotechnology, 2007. **129**(2): p. 249-267.
132. Winden, W.A., Dam, J.C., Ras, C., Kleijn, R.J., Vinke, J.L., Gulik, W.M., and Heijnen, J.J., *Metabolic-flux analysis of* Saccharomyces cerevisiae *CEN. PK113-7D based on mass isotopomer measurements of 13C-labeled primary metabolites.* FEMS yeast research, 2005. **5**(6-7): p. 559-568.
133. Wahl, S.A., Nöh, K., and Wiechert, W., *13C labeling experiments at metabolic nonstationary conditions: an exploratory study.* BMC bioinformatics, 2008. **9**(1): p. 152.
134. Nöh, K., Wahl, A., and Wiechert, W., *Computational tools for isotopically instationary 13 C labeling experiments under metabolic steady state conditions.* Metabolic engineering, 2006. **8**(6): p. 554-577.
135. Yuan, J., Bennett, B.D., and Rabinowitz, J.D., *Kinetic flux profiling for quantitation of cellular metabolic fluxes.* Nature protocols, 2008. **3**(8): p. 1328-1340.

136. Dauner, M., *From fluxes and isotope labeling patterns towards in silico cells.* Current opinion in biotechnology, 2010. **21**(1): p. 55-62.
137. Wildermuth, M.C., *Metabolic control analysis: biological applications and insights.* Genome biology, 2000. **1**(6): p. REVIEWS1031.
138. Fell, D. and Cornish-Bowden, A., *Understanding the control of metabolism*. Vol. 2. 1997: Portland press London.
139. Becker, J., Klopprogge, C., Herold, A., Zelder, O., Bolten, C.J., and Wittmann, C., *Metabolic flux engineering of L-lysine production in* Corynebacterium glutamicum*--over expression and modification of G6P dehydrogenase.* Journal of biotechnology, 2007. **132**(2): p. 99-109.
140. Iwatani, S., Yamada, Y., and Usuda, Y., *Metabolic flux analysis in biotechnology processes.* Biotechnology letters, 2008. **30**(5): p. 791-9.
141. Krömer, J.O., Wittmann, C., Schröder, H., and Heinzle, E., *Metabolic pathway analysis for rational design of L-methionine production by* Escherichia coli *and* Corynebacterium glutamicum*.* Metabolic engineering, 2006. **8**(4): p. 353-369.
142. Krömer, J.O., Heinzle, E., Schröder, H., and Wittmann, C., *Accumulation of homolanthionine and activation of a novel pathway for isoleucine biosynthesis in* Corynebacterium glutamicum *McbR deletion strains.* Journal of bacteriology, 2006. **188**(2): p. 609-618.
143. Nanchen, A., Schicker, A., and Sauer, U., *Nonlinear dependency of intracellular fluxes on growth rate in miniaturized continuous cultures of* Escherichia coli*.* Applied and environmental microbiology, 2006. **72**(2): p. 1164-1172.
144. Sauer, U. and Eikmanns, B.J., *The PEP-pyruvate-oxaloacetate node as the switch point for carbon flux distribution in bacteria.* FEMS microbiology reviews, 2005. **29**(4): p. 765-94.
145. Bulyk, M. and Walhout, A.J.M., *Gene Regulatory Network*, in *Handbook of Systems Biology: Concepts and Insights*, Walhout, A.J.M., Vidal, M., and Dekker, J., Editors. 2012, Elsevier Inc. p. 65-88.
146. de Been, M., Francke, C., Siezen, R.J., and Abee, T., *Novel sigmaB regulation modules of Gram-positive bacteria involve the use of complex hybrid histidine kinases.* Microbiology, 2011. **157**(Pt 1): p. 3-12.
147. Hecker, M., Pané-Farré, J., and Uwe, V., *SigB-dependent general stress response in* Bacillus subtilis *and related gram-positive bacteria.* Annu. Rev. Microbiol., 2007. **61**: p. 215-236.
148. Price, C.W., Fawcett, P., Ceremonie, H., Su, N., Murphy, C.K., and Youngman, P., *Genome-wide analysis of the general stress response in* Bacillus subtilis*.* Molecular microbiology, 2001. **41**(4): p. 757-774.
149. Hecker, M. and Völker, U., *General stress response of* Bacillus subtilis *and other bacteria.* Advances in microbial physiology, 2001. **44**: p. 35-91.
150. Kang, C.M., Vijay, K., and Price, C.W., *Serine kinase activity of a* Bacillus subtilis *switch protein is required to transduce environmental stress signals but not to activate its target PP2C phosphatase.* Molecular microbiology, 1998. **30**(1): p. 189-96.
151. Kang, C.M., Brody, M.S., Akbar, S., Yang, X., and Price, C.W., *Homologous pairs of regulatory proteins control activity of* Bacillus subtilis *transcription factor sigma(b) in response to environmental stress.* Journal of bacteriology, 1996. **178**(13): p. 3846-53.
152. Krämer, R., *Bacterial stimulus perception and signal transduction: response to osmotic stress.* The Chemical Record, 2010. **10**(4): p. 217-229.
153. Vigh, L., Maresca, B., and Harwood, J.L., *Does the membrane's physical state control the expression of heat shock and other genes?* Trends in biochemical sciences, 1998. **23**(10): p. 369-374.
154. Phadtare, S., *Recent developments in bacterial cold-shock response.* Current issues in molecular biology, 2004. **6**(2): p. 125-36.
155. Weber, M.H. and Marahiel, M.A., *Bacterial cold shock responses.* Science progress, 2003. **86**(Pt 1-2): p. 9-75.

156. Morimoto, R.I., *Regulation of the heat shock transcriptional response: cross talk between a family of heat shock factors, molecular chaperones, and negative regulators.* Genes & development, 1998. **12**(24): p. 3788-3796.
157. Richter, K., Haslbeck, M., and Buchner, J., *The heat shock response: life on the verge of death.* Molecular cell, 2010. **40**(2): p. 253-66.
158. Voigt, B., Schroeter, R., Jurgen, B., Albrecht, D., Evers, S., Bongaerts, J., Maurer, K.H., Schweder, T., and Hecker, M., *The response of* Bacillus licheniformis *to heat and ethanol stress and the role of the SigB regulon.* Proteomics, 2013. **13**(14): p. 2140-61.
159. Becker, J. and Craig, E.A., *Heat-shock proteins as molecular chaperones.* European journal of biochemistry / FEBS, 1994. **219**(1-2): p. 11-23.
160. Derre, I., Rapoport, G., and Msadek, T., *CtsR, a novel regulator of stress and heat shock response, controls clp and molecular chaperone gene expression in gram-positive bacteria.* Molecular microbiology, 1999. **31**(1): p. 117-31.
161. Elsholz, A.K., Michalik, S., Zuhlke, D., Hecker, M., and Gerth, U., *CtsR, the Gram-positive master regulator of protein quality control, feels the heat.* The EMBO journal, 2010. **29**(21): p. 3621-9.
162. Hecker, M., Schumann, W., and Volker, U., *Heat-shock and general stress response in* Bacillus subtilis*.* Molecular microbiology, 1996. **19**(3): p. 417-28.
163. Selby, K., Lindstrom, M., Somervuo, P., Heap, J.T., Minton, N.P., and Korkeala, H., *Important role of class I heat shock genes hrcA and dnaK in the heat shock response and the response to pH and NaCl stress of group I* Clostridium botulinum strain ATCC 3502*.* Applied and environmental microbiology, 2011. **77**(9): p. 2823-30.
164. Schulz, A. and Schumann, W., *hrcA, the first gene of the* Bacillus subtilis *dnaK operon encodes a negative regulator of class I heat shock genes.* Journal of bacteriology, 1996. **178**(4): p. 1088-93.
165. Derre, I., Rapoport, G., Devine, K., Rose, M., and Msadek, T., *ClpE, a novel type of HSP100 ATPase, is part of the CtsR heat shock regulon of* Bacillus subtilis*.* Molecular microbiology, 1999. **32**(3): p. 581-93.
166. Helmann, J.D., Wu, M.F., Kobel, P.A., Gamo, F.J., Wilson, M., Morshedi, M.M., Navre, M., and Paddon, C., *Global transcriptional response of* Bacillus subtilis *to heat shock.* Journal of bacteriology, 2001. **183**(24): p. 7318-28.
167. van Schaik, W., Tempelaars, M.H., Wouters, J.A., de Vos, W.M., and Abee, T., *The alternative sigma factor* sigmaB *of* Bacillus cereus*: response to stress and role in heat adaptation.* Journal of bacteriology, 2004. **186**(2): p. 316-25.
168. Versteeg, S., Escher, A., Wende, A., Wiegert, T., and Schumann, W., *Regulation of the* Bacillus subtilis *heat shock gene* htpG *is under positive control.* Journal of bacteriology, 2003. **185**(2): p. 466-74.
169. Versteeg, S., Mogk, A., and Schumann, W., *The* Bacillus subtilis htpG *gene is not involved in thermal stress management.* Molecular & general genetics : MGG, 1999. **261**(3): p. 582-8.
170. Barria, C., Malecki, M., and Arraiano, C.M., *Bacterial adaptation to cold.* Microbiology, 2013. **159**(Pt 12): p. 2437-43.
171. Kaan, T., Homuth, G., Mader, U., Bandow, J., and Schweder, T., *Genome-wide transcriptional profiling of the* Bacillus subtilis *cold-shock response.* Microbiology, 2002. **148**(Pt 11): p. 3441-55.
172. Farewell, A. and Neidhardt, F.C., *Effect of temperature on in vivo protein synthetic capacity in* Escherichia coli*.* Journal of bacteriology, 1998. **180**(17): p. 4704-10.
173. Nedwell, D.B., *Effect of low temperature on microbial growth: lowered affinity for substrates limits growth at low temperature.* FEMS microbiology ecology, 1999. **30**(2): p. 101-111.
174. Graumann, P. and Marahiel, M.A., *Some like it cold: response of microorganisms to cold shock.* Archives of microbiology, 1996. **166**(5): p. 293-300.
175. Graumann, P., Schroder, K., Schmid, R., and Marahiel, M.A., *Cold shock stress-induced proteins in* Bacillus subtilis*.* Journal of bacteriology, 1996. **178**(15): p. 4611-9.

176. Giuliodori, A.M., Brandi, A., Gualerzi, C.O., and Pon, C.L., *Preferential translation of cold-shock mRNAs during cold adaptation.* Rna, 2004. **10**(2): p. 265-76.
177. Giuliodori, A.M., Di Pietro, F., Marzi, S., Masquida, B., Wagner, R., Romby, P., Gualerzi, C.O., and Pon, C.L., *The* cspA *mRNA is a thermosensor that modulates translation of the cold-shock protein CspA.* Molecular cell, 2010. **37**(1): p. 21-33.
178. Gualerzi, C.O., Giuliodori, A.M., and Pon, C.L., *Transcriptional and post-transcriptional control of cold-shock genes.* Journal of molecular biology, 2003. **331**(3): p. 527-39.
179. Wang, J.C., *Cellular roles of DNA topoisomerases: a molecular perspective.* Nature reviews. Molecular cell biology, 2002. **3**(6): p. 430-40.
180. Dorman, C.J., *Flexible response: DNA supercoiling, transcription and bacterial adaptation to environmental stress.* Trends in microbiology, 1996. **4**(6): p. 214-6.
181. Mansilla, M.C., Cybulski, L.E., Albanesi, D., and de Mendoza, D., *Control of membrane lipid fluidity by molecular thermosensors.* Journal of bacteriology, 2004. **186**(20): p. 6681-8.
182. Zhang, Y.M. and Rock, C.O., *Membrane lipid homeostasis in bacteria.* Nature reviews. Microbiology, 2008. **6**(3): p. 222-33.
183. Los, D.A. and Murata, N., *Membrane fluidity and its roles in the perception of environmental signals.* Biochimica et biophysica acta, 2004. **1666**(1-2): p. 142-57.
184. Fulco, A.J., *The biosynthesis of unsaturated fatty acids by* bacilli*. I. Temperature induction of the desaturation reaction.* The Journal of biological chemistry, 1969. **244**(3): p. 889-95.
185. Aguilar, P.S. and de Mendoza, D., *Control of fatty acid desaturation: a mechanism conserved from bacteria to humans.* Molecular microbiology, 2006. **62**(6): p. 1507-14.
186. Hashimoto, K., Yoshizawa, A.C., Saito, K., Yamada, T., and Kanehisa, M., *The repertoire of desaturases for unsaturated fatty acid synthesis in 397 genomes.* Genome Informatics, 2006. **17**(1): p. 173-183.
187. Albanesi, D., Mansilla, M.C., and de Mendoza, D., *The membrane fluidity sensor DesK of* Bacillus subtilis *controls the signal decay of its cognate response regulator.* Journal of bacteriology, 2004. **186**(9): p. 2655-63.
188. Weber, M.H., Klein, W., Muller, L., Niess, U.M., and Marahiel, M.A., *Role of the* Bacillus subtilis *fatty acid desaturase in membrane adaptation during cold shock.* Molecular microbiology, 2001. **39**(5): p. 1321-9.
189. Rilfors, L., Wieslander, A., and Stahl, S., *Lipid and protein composition of membranes of* Bacillus megaterium *variants in the temperature range 5 to 70 degrees C.* Journal of bacteriology, 1978. **135**(3): p. 1043-52.
190. Kempf, B. and Bremer, E., *Uptake and synthesis of compatible solutes as microbial stress responses to high-osmolality environments.* Archives of microbiology, 1998. **170**(5): p. 319-330.
191. Korber, D.R., Choi, A., Wolfaardt, G.M., and Caldwell, D.E., *Bacterial plasmolysis as a physical indicator of viability.* Applied and environmental microbiology, 1996. **62**(11): p. 3939-47.
192. Marquis, R.E., *Salt-induced contraction of bacterial cell walls.* Journal of bacteriology, 1968. **95**(3): p. 775-81.
193. Empadinhas, N. and da Costa, M.S., *Osmoadaptation mechanisms in prokaryotes: distribution of compatible solutes.* International microbiology : the official journal of the Spanish Society for Microbiology, 2008. **11**(3): p. 151-61.
194. Held, C., Neuhaus, T., and Sadowski, G., *Compatible solutes: Thermodynamic properties and biological impact of ectoines and prolines.* Biophysical chemistry, 2010. **152**(1-3): p. 28-39.
195. Oren, A., *Microbial life at high salt concentrations: phylogenetic and metabolic diversity.* Saline systems, 2008. **4**: p. 2.
196. Ventosa, A., Nieto, J.J., and Oren, A., *Biology of moderately halophilic aerobic bacteria.* Microbiology and molecular biology reviews : MMBR, 1998. **62**(2): p. 504-44.
197. Graf, R., Anzali, S., Buenger, J., Pfluecker, F., and Driller, H., *The multifunctional role of ectoine as a natural cell protectant.* Clinics in dermatology, 2008. **26**(4): p. 326-33.

198. Takagi, H., *Proline as a stress protectant in yeast: physiological functions, metabolic regulations, and biotechnological applications.* Applied microbiology and biotechnology, 2008. **81**(2): p. 211-23.
199. Pastor, J.M., Salvador, M., Argandona, M., Bernal, V., Reina-Bueno, M., Csonka, L.N., Iborra, J.L., Vargas, C., Nieto, J.J., and Canovas, M., *Ectoines in cell stress protection: uses and biotechnological production.* Biotechnology advances, 2010. **28**(6): p. 782-801.
200. Oren, A., *Industrial and environmental applications of halophilic microorganisms.* Environmental technology, 2010. **31**(8-9): p. 825-834.
201. Whatmore, A.M., Chudek, J.A., and Reed, R.H., *The effects of osmotic upshock on the intracellular solute pools of* Bacillus subtilis*.* Journal of general microbiology, 1990. **136**(12): p. 2527-35.
202. Holtmann, G., Bakker, E.P., Uozumi, N., and Bremer, E., *KtrAB and KtrCD: two K+ uptake systems in* Bacillus subtilis *and their role in adaptation to hypertonicity.* Journal of bacteriology, 2003. **185**(4): p. 1289-98.
203. Kuhlmann, A.U. and Bremer, E., *Osmotically regulated synthesis of the compatible solute ectoine in* Bacillus pasteurii *and related* Bacillus spp*.* Applied and environmental microbiology, 2002. **68**(2): p. 772-83.
204. Grundy, F.J. and Henkin, T.M., *tRNA as a positive regulator of transcription antitermination in* B. subtilis*.* Cell, 1993. **74**(3): p. 475-482.
205. Brill, J., Hoffmann, T., Putzer, H., and Bremer, E., *T-box-mediated control of the anabolic proline biosynthetic genes of* Bacillus subtilis*.* Microbiology, 2011. **157**(4): p. 977-987.
206. Brill, J., Hoffmann, T., Bleisteiner, M., and Bremer, E., *Osmotically controlled synthesis of the compatible solute proline is critical for cellular defense of* Bacillus subtilis *against high osmolarity.* Journal of bacteriology, 2011. **193**(19): p. 5335-46.
207. Schroeter, R., Hoffmann, T., Voigt, B., Meyer, H., Bleisteiner, M., Muntel, J., Jurgen, B., Albrecht, D., Becher, D., Lalk, M., Evers, S., Bongaerts, J., Maurer, K.H., Putzer, H., Hecker, M., Schweder, T., and Bremer, E., *Stress responses of the industrial workhorse* Bacillus licheniformis *to osmotic challenges.* PloS one, 2013. **8**(11): p. e80956.
208. Koch, A.L., *Shrinkage of growing* Escherichia coli *cells by osmotic challenge.* Journal of bacteriology, 1984. **159**(3): p. 919-24.
209. Laroche, C., Beney, L., Marechal, P.A., and Gervais, P., *The effect of osmotic pressure on the membrane fluidity of* Saccharomyces cerevisiae *at different physiological temperatures.* Applied microbiology and biotechnology, 2001. **56**(1-2): p. 249-54.
210. Lopez, C.S., Heras, H., Ruzal, S.M., Sanchez-Rivas, C., and Rivas, E.A., *Variations of the envelope composition of* Bacillus subtilis *during growth in hyperosmotic medium.* Current microbiology, 1998. **36**(1): p. 55-61.
211. Machado, M.C., López, C.S., Heras, H., and Rivas, E.A., *Osmotic response in* Lactobacillus casei ATCC 393*: biochemical and biophysical characteristics of membrane.* Archives of biochemistry and biophysics, 2004. **422**(1): p. 61-70.
212. Lopez, C.S., Heras, H., Garda, H., Ruzal, S., Sanchez-Rivas, C., and Rivas, E., *Biochemical and biophysical studies of* Bacillus subtilis *envelopes under hyperosmotic stress.* International journal of food microbiology, 2000. **55**(1-3): p. 137-42.
213. Romantsov, T., Stalker, L., Culham, D.E., and Wood, J.M., *Cardiolipin controls the osmotic stress response and the subcellular location of transporter ProP in* Escherichia coli*.* The Journal of biological chemistry, 2008. **283**(18): p. 12314-23.
214. Kanemasa, Y., Yoshioka, T., and Hayashi, H., *Alteration of the phospholipid composition of* Staphylococcus aureus *cultured in medium containing NaCl.* Biochimica et biophysica acta, 1972. **280**(3): p. 444-50.
215. Romantsov, T., Guan, Z., and Wood, J.M., *Cardiolipin and the osmotic stress responses of bacteria.* Biochimica et biophysica acta, 2009. **1788**(10): p. 2092-100.
216. Hoch, F.L., *Cardiolipins and biomembrane function.* Biochimica et biophysica acta, 1992. **1113**(1): p. 71-133.
217. (IEA), I.E.A., *Key World Energy Statistics 2014*. 2014, International Energy Agency. p. 82.

218. Rudolf, J.C. *Less than 50 years of oil left, HSBC warns*. 2014; Available from: http://green.blogs.nytimes.com/2011/03/30/less-than-50-years-of-oil-left-hsbc-warns/.
219. Claassen, V. and Silvertand, M. *DSM in motion: driving focused growth*. in *UBS Biomaterials Conference*. 2011. Frankfurt am Main.
220. Bioplastics, E., *Bioplastics facts and figures*, Bioplastics, E., Editor. 2013, European Bioplastics. p. 6.
221. Bernard, M., *Industrial Potential of Polyhydroxyalkanoate Bioplastic: A Brief Review.* USURJ: University of Saskatchewan Undergraduate Research Journal, 2014. **1**(1).
222. Metabolix. 2015; Available from: http://www.metabolix.com/.
223. Foundation, C.H. *Science of Plastics*. 2013 [cited 2015 17 Juni]; Available from: http://www.chemheritage.org/discover/online-resources/conflicts-in-chemistry/the-case-of-plastics/all-science-of-plastics.aspx.
224. Rehm, B.H., *Bacterial polymers: biosynthesis, modifications and applications.* Nature reviews. Microbiology, 2010. **8**(8): p. 578-92.
225. Tokiwa, Y., Calabia, B.P., Ugwu, C.U., and Aiba, S., *Biodegradability of plastics.* International journal of molecular sciences, 2009. **10**(9): p. 3722-42.
226. Forni, D., Bee, G., Kreuzer, M., and Wenk, C., *Novel biodegradable plastics in sheep nutrition, 1: Effects of untreated plastics on digestibility and metabolic energy and nitrogen utilization.* Journal of Animal Physiology and Animal Nutrition (Germany), 1999.
227. Snell, K.D. and Peoples, O.P., *PHA bioplastic: A value-added coproduct for biomass biorefineries.* Biofuels, Bioproducts and Biorefining, 2009. **3**(4): p. 456-467.
228. de Smet, M.J., Eggink, G., Witholt, B., Kingma, J., and Wynberg, H., *Characterization of intracellular inclusions formed by* Pseudomonas oleovorans *during growth on octane.* Journal of bacteriology, 1983. **154**(2): p. 870-8.
229. Rehm, B.H., *Polyester synthases: natural catalysts for plastics.* The Biochemical journal, 2003. **376**(Pt 1): p. 15-33.
230. Reddy, C., Ghai, R., and Kalia, V.C., *Polyhydroxyalkanoates: an overview.* Bioresource technology, 2003. **87**(2): p. 137-146.
231. Madison, L.L. and Huisman, G.W., *Metabolic engineering of poly(3-hydroxyalkanoates): from DNA to plastic.* Microbiology and molecular biology reviews : MMBR, 1999. **63**(1): p. 21-53.
232. Wang, W., Hollmann, R., Furch, T., Nimtz, M., Malten, M., Jahn, D., and Deckwer, W.D., *Proteome analysis of a recombinant* Bacillus megaterium *strain during heterologous production of a glucosyltransferase.* Proteome science, 2005. **3**: p. 4.
233. Hazer, B. and Steinbuchel, A., *Increased diversification of polyhydroxyalkanoates by modification reactions for industrial and medical applications.* Applied microbiology and biotechnology, 2007. **74**(1): p. 1-12.
234. Steinbüchel, A. and Valentin, H.E., *Diversity of bacterial polyhydroxyalkanoic acids.* FEMS microbiology letters, 1995. **128**(3): p. 219-228.
235. Pötter, M. and Steinbüchel, A., *Poly (3-hydroxybutyrate) granule-associated proteins: impacts on poly (3-hydroxybutyrate) synthesis and degradation.* Biomacromolecules, 2005. **6**(2): p. 552-560.
236. Murueva, A.V., Shishatskaya, E.I., Kuzmina, A.M., Volova, T.G., and Sinskey, A.J., *Microparticles prepared from biodegradable polyhydroxyalkanoates as matrix for encapsulation of cytostatic drug.* Journal of materials science. Materials in medicine, 2013. **24**(8): p. 1905-15.
237. Shrivastav, A., Kim, H.Y., and Kim, Y.R., *Advances in the applications of polyhydroxyalkanoate nanoparticles for novel drug delivery system.* BioMed research international, 2013. **2013**: p. 581684.
238. Floccari, M.E., López, N.I., Méndez, B.S., Fürst, U.P., and Steinbüchel, A., *Isolation and partial characterization of* Bacillus megaterium *mutants deficient in poly (3-hydroxybutyrate) synthesis.* Canadian journal of microbiology, 1995. **41**(13): p. 77-79.
239. Liu, F., Li, W., Ridgway, D., Gu, T., and Shen, Z., *Production of poly-β-hydroxybutyrate on molasses by recombinant* Escherichia coli*.* Biotechnology letters, 1998. **20**(4): p. 345-348.

240. Park, S.J., Ahn, W.S., Green, P.R., and Lee, S.Y., *Production of Poly (3-hydroxybutyrate-co-3-hydroxyhexanoate) by Metabolically Engineered* Escherichia coli *strains.* Biomacromolecules, 2001. **2**(1): p. 248-254.
241. Bourque, D., Pomerleau, Y., and Groleau, D., *High-cell-density production of poly-β-hydroxybutyrate (PHB) from methanol by* Methylobacterium extorquens*: production of high-molecular-mass PHB.* Applied microbiology and biotechnology, 1995. **44**(3-4): p. 367-376.
242. Poblete-Castro, I., Rodriguez, A.L., Lam, C.M.C., and Kessler, W., *Improved production of medium-chain-length Polyhydroxyalkanotes in glucose-based fed-batch cultivations of metabolically engineered* Pseudomonas putida *strains.* Journal of microbiology and biotechnology, 2013.
243. Lemoigne, M., *Produits de dehydration et de polymerisation de l'acide ß-oxobutyrique.* Bull. Soc. Chim. Biol., 1926. **8**: p. 770-782.
244. McCool, G.J. and Cannon, M.C., *Polyhydroxyalkanoate inclusion body-associated proteins and coding region in* Bacillus megaterium*.* Journal of bacteriology, 1999. **181**(2): p. 585-92.
245. Lee, T.R., Lin, J.S., Wang, S.S., and Shaw, G.C., *PhaQ, a new class of poly-beta-hydroxybutyrate (phb)-responsive repressor, regulates* phaQ *and* phaP *(phasin) expression in* Bacillus megaterium *through interaction with PHB.* Journal of bacteriology, 2004. **186**(10): p. 3015-21.
246. Valappil, S.P., Boccaccini, A.R., Bucke, C., and Roy, I., *Polyhydroxyalkanoates in Gram-positive bacteria: insights from the genera* Bacillus *and* Streptomyces*.* Antonie van Leeuwenhoek, 2007. **91**(1): p. 1-17.
247. York, G.M., Stubbe, J., and Sinskey, A.J., *New insight into the role of the PhaP phasin of* Ralstonia eutropha *in promoting synthesis of polyhydroxybutyrate.* Journal of bacteriology, 2001. **183**(7): p. 2394-2397.
248. Pötter, M., Müller, H., Reinecke, F., Wieczorek, R., Fricke, F., Bowien, B., Friedrich, B., and Steinbüchel, A., *The complex structure of polyhydroxybutyrate (PHB) granules: four orthologous and paralogous phasins occur in* Ralstonia eutropha*.* Microbiology, 2004. **150**(7): p. 2301-2311.
249. Shah, A.A., Hasan, F., Hameed, A., and Ahmed, S., *Biological degradation of plastics: a comprehensive review.* Biotechnology advances, 2008. **26**(3): p. 246-65.
250. Chen, G.Q., *A microbial polyhydroxyalkanoates (PHA) based bio- and materials industry.* Chemical Society reviews, 2009. **38**(8): p. 2434-46.
251. Bohlmann, G.M., *General characteristics, processability, industrial applications and market evolution of biodegradable polymers.* Handbook of biodegradable polymers, 2005: p. 183-218.
252. Suriyamongkol, P., Weselake, R., Narine, S., Moloney, M., and Shah, S., *Biotechnological approaches for the production of polyhydroxyalkanoates in microorganisms and plants - a review.* Biotechnology advances, 2007. **25**(2): p. 148-75.
253. Yamane, T., *Yield of poly-D(-)-3-hydroxybutyrate from various carbon sources: a theoretical study.* Biotechnology and bioengineering, 1993. **41**(1): p. 165-70.
254. Wellisch, M., Jungmeier, G., Karbowski, A., Patel, M.K., and Rogulska, M., *Biorefinery systems–potential contributors to sustainable innovation.* Biofuels, bioproducts and biorefining, 2010. **4**(3): p. 275-286.
255. Narayan, R. *Biobased and biodegradable polymer materials: rationale, drivers, and technology exemplars*. in *American Chemical Society Symposium Ser*. 2006.
256. Hori, K., Kaneko, M., Tanji, Y., Xing, X.H., and Unno, H., *Construction of self-disruptive* Bacillus megaterium *in response to substrate exhaustion for polyhydroxybutyrate production.* Applied microbiology and biotechnology, 2002. **59**(2-3): p. 211-6.
257. Faccin, D.J.L., Martins, I., Cardozo, N.S.M., Rech, R., Ayub, M.A.Z., Alves, T.L.M., Gambetta, R., and Resende Secchi, A., *Optimization of C: N ratio and minimal initial carbon source for poly (3-hydroxybutyrate) production by* Bacillus megaterium*.* Journal of chemical technology and biotechnology, 2009. **84**(12): p. 1756-1761.

258. Faccin, D.J.L., Rech, R., Secchi, A.R., Cardozo, N.S.M., and Ayub, M.A.Z., *Influence of oxygen transfer rate on the accumulation of poly (3-hydroxybutyrate) by* Bacillus megaterium*.* Process Biochemistry, 2013. **48**(3): p. 420-425.
259. Bora, L., *Polyhydroxybutyrate accumulation in* Bacillus megaterium *and optimization of process parameters using response surface methodology.* Journal of Polymers and the Environment, 2013. **21**(2): p. 415-420.
260. Kanjanachumpol, P., Kulpreecha, S., Tolieng, V., and Thongchul, N., *Enhancing polyhydroxybutyrate production from high cell density fed-batch fermentation of* Bacillus megaterium BA-019*.* Bioprocess and biosystems engineering, 2013. **36**(10): p. 1463-1474.
261. Thirumala, M. and Reddy, S.V., *Production of PHA by recombinant organisms.* International Journal of Life Sciences Biotechnology and Pharma Research, 2012. **1**(2): p. 22.
262. Harwood, C.R. and Cutting, S.M., *Chemically defined growth media and supplements*, in *Molecular biological methods for Bacillus*, Harwood, C.R. and Cutting, S.M., Editors. 1990, Wiley: Chichester, United Kingdom.
263. Sonnleitner, B., Locher, G., and Fiechter, A., *Biomass determination.* Journal of biotechnology, 1992. **25**(1-2): p. 5-22.
264. Taymaz-Nikerel, H., de Mey, M., Ras, C., ten Pierick, A., Seifar, R.M., van Dam, J.C., Heijnen, J.J., and van Gulik, W.M., *Development and application of a differential method for reliable metabolome analysis in* Escherichia coli*.* Analytical biochemistry, 2009. **386**(1): p. 9-19.
265. Wittmann, C., *Metabolic flux analysis using mass spectrometry.* Advances in biochemical engineering/biotechnology, 2002. **74**: p. 39-64.
266. Wittmann, C., Hans, M., and Heinzle, E., *In vivo analysis of intracellular amino acid labelings by GC/MS.* Analytical biochemistry, 2002. **307**(2): p. 379-82.
267. Fürch, T., Wittmann, C., Wang, W., Franco-Lara, E., Jahn, D., and Deckwer, W.-D., *Effect of different carbon sources on central metabolic fluxes and the recombinant production of a hydrolase from* Thermobifida fusca *in* Bacillus megaterium*.* Journal of biotechnology, 2007. **132**(4): p. 385-394.
268. Neidhardt, F.C., Ingraham, J.L., and Schaechter, M., *Physiology of the bacterial cell: a molecular approach.* 1990.
269. Quek, L.-E., Wittmann, C., Nielsen, L.K., and Krömer, J.O., *OpenFLUX: efficient modelling software for 13C-based metabolic flux analysis.* Microbial cell factories, 2009. **8**(1): p. 25.
270. van Winden, W.A., Wittmann, C., Heinzle, E., and Heijnen, J.J., *Correcting mass isotopomer distributions for naturally occurring isotopes.* Biotechnology and bioengineering, 2002. **80**(4): p. 477-9.
271. Dauner, M. and Sauer, U., *Stoichiometric growth model for riboflavin-producing* Bacillus subtilis*.* Biotechnology and bioengineering, 2001. **76**(2): p. 132-143.
272. Hu, Q., *Environmental Effects on Cell Composition.* Handbook of microalgal culture: biotechnology and applied phycology, 2004: p. 83.
273. Neidhardt, F.C., *Effects of environment on the composition of bacterial cells.* Annual Reviews in Microbiology, 1963. **17**(1): p. 61-86.
274. Tempest, D., Meers, J., and Brown, C., *Influence of environment on the content and composition of microbial free amino acid pools.* Journal of general microbiology, 1970. **64**(2): p. 171-185.
275. Waddell, W.J., *A simple ultraviolet spectrophotometric method for the determination of protein.* The Journal of laboratory and clinical medicine, 1956. **48**(2): p. 311-4.
276. Tombs, M.P., Souter, F., and Maclagan, N.F., *The spectrophotometric determination of protein at 210 millimicrons.* The Biochemical journal, 1959. **73**: p. 167-71.
277. Goldfarb, A.R., Saidel, L.J., and Mosovich, E., *The ultraviolet absorption spectra of proteins.* The Journal of biological chemistry, 1951. **193**(1): p. 397-404.
278. Wolf, P., *A critical reappraisal of Waddell's technique for ultraviolet spectrophotometric protein estimation.* Analytical biochemistry, 1983. **129**(1): p. 145-55.

279. Smith, P.K., Krohn, R.I., Hermanson, G.T., Mallia, A.K., Gartner, F.H., Provenzano, M.D., Fujimoto, E.K., Goeke, N.M., Olson, B.J., and Klenk, D.C., *Measurement of protein using bicinchoninic acid.* Analytical biochemistry, 1985. **150**(1): p. 76-85.
280. Fountoulakis, M. and Lahm, H.W., *Hydrolysis and amino acid composition of proteins.* Journal of chromatography. A, 1998. **826**(2): p. 109-34.
281. Krömer, J.O., Fritz, M., Heinzle, E., and Wittmann, C., *In vivo quantification of intracellular amino acids and intermediates of the methionine pathway in* Corynebacterium glutamicum*.* Analytical biochemistry, 2005. **340**(1): p. 171-3.
282. Benthin, S., Nielsen, J., and Villadsen, J., *A simple and reliable method for the determination of cellular RNA content.* Biotechnology Techniques, 1991. **5**(1): p. 39-42.
283. Sharma, L. and Mallick, N., *Accumulation of poly-beta-hydroxybutyrate in* Nostoc muscorum*: regulation by pH, light-dark cycles, N and P status and carbon sources.* Bioresource technology, 2005. **96**(11): p. 1304-10.
284. Folch, J., Lees, M., and Sloane Stanley, G.H., *A simple method for the isolation and purification of total lipides from animal tissues.* The Journal of biological chemistry, 1957. **226**(1): p. 497-509.
285. AOCS, *Official method 991.39*, in *Official methods and recommended practices of the AOCS.* Firestone, D., Editor. 1999: AOCS, Champaign, IL.
286. Van Heijenoort, J., Elbaz, L., Dezelee, P., Petit, J.F., Bricas, E., and Ghuysen, J.M., *Structure of the meso-diaminopimelic acid containing peptidoglycans in* Escherichia coli B *and* Bacillus megaterium KM*.* Biochemistry, 1969. **8**(1): p. 207-13.
287. Vollmer, W., Blanot, D., and de Pedro, M.A., *Peptidoglycan structure and architecture.* FEMS microbiology reviews, 2008. **32**(2): p. 149-67.
288. Illanes, A., *Stability of biocatalysts.* Electronic Journal of Biotechnology, 1999. **2**: p. nd-nd.
289. Marshall, C.J., *Cold-adapted enzymes.* Trends in biotechnology, 1997. **15**(9): p. 359-64.
290. Rodrigues, A.L., Trachtmann, N., Becker, J., Lohanatha, A.F., Blotenberg, J., Bolten, C.J., Korneli, C., de Souza Lima, A.O., Porto, L.M., Sprenger, G.A., and Wittmann, C., *Systems metabolic engineering of* Escherichia coli *for production of the antitumor drugs violacein and deoxyviolacein.* Metabolic engineering, 2013. **20**: p. 29-41.
291. Vera, A., Gonzalez-Montalban, N., Aris, A., and Villaverde, A., *The conformational quality of insoluble recombinant proteins is enhanced at low growth temperatures.* Biotechnology and bioengineering, 2007. **96**(6): p. 1101-6.
292. Somkuti, G. and Holsinger, V., *Microbial technologies in the production of low-lactose dairy foods/Tecnologías microbiológicas para la elaboración de productos lácteos con bajo contenido en lactosa.* Food Science and Technology International, 1997. **3**(3): p. 163-169.
293. Mozhaev, V.V., *Mechanism-based strategies for protein thermostabilization.* Trends in biotechnology, 1993. **11**(3): p. 88-95.
294. Mohr, P.W. and Krawiec, S., *Temperature characteristics and Arrhenius plots for nominal psychrophiles, mesophiles and thermophiles.* Journal of general microbiology, 1980. **121**(2): p. 311-7.
295. Hébraud, M. and Potier, P., *Cold shock response and low temperature adaptation in psychrotrophic bacteria.* Journal of molecular microbiology and biotechnology, 1999. **1**(2): p. 211-219.
296. Strnadova, M., Prasad, R., Kučerová, H., and Chaloupka, J., *Effect of temperature on growth and protein turnover in* Bacillus megaterium*.* Journal of basic microbiology, 1986. **26**(5): p. 289-298.
297. Bisht, S.C., Mishra, P.K., and Joshi, G.K., *Proteomic response of Himalayan psychotrophic bacterium* Pseudomonas lurida NPRP15*.* International Journal of Bioassays, 2015. **4**(05): p. 3888-3895.
298. Anderson, K.W., Grulke, E., and Gerhardt, P., *Microfiltration culture process for enhanced production of rDNA receptor Cells of* Escherichia coli*.* Nature biotechnology, 1984. **2**(10): p. 891-896.

299. Brown, T., Jones-Mortimer, M., and Kornberg, H., *The enzymic interconversion of acetate and acetyl-coenzyme A in* Escherichia coli*.* Journal of general microbiology, 1977. **102**(2): p. 327-336.
300. El-Mansi, E. and Holms, W., *Control of carbon flux to acetate excretion during growth of* Escherichia coli *in batch and continuous cultures.* Journal of general microbiology, 1989. **135**(11): p. 2875-2883.
301. Wittmann, C., Weber, J., Betiku, E., Krömer, J., Bohm, D., and Rinas, U., *Response of fluxome and metabolome to temperature-induced recombinant protein synthesis in* Escherichia coli*.* Journal of biotechnology, 2007. **132**(4): p. 375-84.
302. Rinas, U., Kracke-Helm, H.-A., and Schügerl, K., *Glucose as a substrate in recombinant strain fermentation technology.* Applied microbiology and biotechnology, 1989. **31**(2): p. 163-167.
303. Li, M., Ho, P.Y., Yao, S., and Shimizu, K., *Effect of lpdA gene knockout on the metabolism in* Escherichia coli *based on enzyme activities, intracellular metabolite concentrations and metabolic flux analysis by 13C-labeling experiments.* Journal of biotechnology, 2006. **122**(2): p. 254-266.
304. Moreau, P.L., *Diversion of the metabolic flux from pyruvate dehydrogenase to pyruvate oxidase decreases oxidative stress during glucose metabolism in nongrowing* Escherichia coli *cells incubated under aerobic, phosphate starvation conditions.* Journal of bacteriology, 2004. **186**(21): p. 7364-8.
305. Vemuri, G.N., Altman, E., Sangurdekar, D.P., Khodursky, A.B., and Eiteman, M.A., *Overflow metabolism in* Escherichia coli *during steady-state growth: transcriptional regulation and effect of the redox ratio.* Applied and environmental microbiology, 2006. **72**(5): p. 3653-61.
306. Berg, J.M. and Tymoczko, J.L., *Stryer Biochemie*. 2012: Spektrum.
307. Cabiscol, E., Piulats, E., Echave, P., Herrero, E., and Ros, J., *Oxidative stress promotes specific protein damage in* Saccharomyces cerevisiae*.* The Journal of biological chemistry, 2000. **275**(35): p. 27393-8.
308. Martin, E., Rosenthal, R.E., and Fiskum, G., *Pyruvate dehydrogenase complex: metabolic link to ischemic brain injury and target of oxidative stress.* Journal of neuroscience research, 2005. **79**(1-2): p. 240-7.
309. Misirli, G., Hallinan, J., Rottger, R., Baumbach, J., and Wipat, A., *BacillusRegNet: a transcriptional regulation database and analysis platform for* Bacillus *species.* Journal of integrative bioinformatics, 2014. **11**(2): p. 244.
310. Pericone, C.D., Park, S., Imlay, J.A., and Weiser, J.N., *Factors contributing to hydrogen peroxide resistance in* Streptococcus pneumoniae *include pyruvate oxidase (SpxB) and avoidance of the toxic effects of the Fenton reaction.* Journal of bacteriology, 2003. **185**(23): p. 6815-6825.
311. Karamichos, D., Hutcheon, A., Rich, C., Trinkaus-Randall, V., Asara, J., and Zieske, J., *In vitro model suggests oxidative stress involved in keratoconus disease.* Scientific reports, 2014. **4**.
312. Jovanovic, P., Zoric, L., Stefanovic, I., Dzunic, B., Djordjevic-Jocic, J., Radenkovic, M., and Jovanovic, M., *Lactate dehydrogenase and oxidative stress activity in primary open-angle glaucoma aqueous humour.* Bosnian journal of basic medical sciences / Udruzenje basicnih mediciniskih znanosti = Association of Basic Medical Sciences, 2010. **10**(1): p. 83-8.
313. Lieberman, M., Marks, A.D., Smith, C.M., and Marks, D.B., *Marks' Essential Medical Biochemistry*. 2006: Lippincott Williams & Wilkins.
314. Chai, Y., Kolter, R., and Losick, R., *A widely conserved gene cluster required for lactate utilization in* Bacillus subtilis *and its involvement in biofilm formation.* Journal of bacteriology, 2009. **191**(8): p. 2423-30.
315. Pronk, J.T., Yde Steensma, H., and Van Dijken, J.P., *Pyruvate metabolism in* Saccharomyces cerevisiae*.* Yeast, 1996. **12**(16): p. 1607-33.
316. Dalmasso, M., Aubert, J., Even, S., Falentin, H., Maillard, M.B., Parayre, S., Loux, V., Tanskanen, J., and Thierry, A., *Accumulation of intracellular glycogen and trehalose by*

Propionibacterium freudenreichii *under conditions mimicking cheese ripening in the cold.* Applied and environmental microbiology, 2012. **78**(17): p. 6357-64.
317. Beun, J.J., Dircks, K., Van Loosdrecht, M.C., and Heijnen, J.J., *Poly-beta-hydroxybutyrate metabolism in dynamically fed mixed microbial cultures.* Water research, 2002. **36**(5): p. 1167-80.
318. Dircks, K., Beun, J.J., van Loosdrecht, M., Heijnen, J.J., and Henze, M., *Glycogen metabolism in aerobic mixed cultures.* Biotechnology and bioengineering, 2001. **73**(2): p. 85-94.
319. de Almeida, A., Catone, M.V., Rhodius, V.A., Gross, C.A., and Pettinari, M.J., *Unexpected stress-reducing effect of PhaP, a poly(3-hydroxybutyrate) granule-associated protein, in* Escherichia coli*.* Applied and environmental microbiology, 2011. **77**(18): p. 6622-9.
320. Török, Z., Crul, T., Maresca, B., Schütz, G.J., Viana, F., Dindia, L., Piotto, S., Brameshuber, M., Balogh, G., and Péter, M., *Plasma membranes as heat stress sensors: from lipid-controlled molecular switches to therapeutic applications.* Biochimica et Biophysica Acta (BBA)-Biomembranes, 2014. **1838**(6): p. 1594-1618.
321. Rowbury, R.J., *Temperature effects on biological systems: introduction.* Science progress, 2003. **86**(1-2): p. 1-7.
322. Inaba, M., Suzuki, I., Szalontai, B., Kanesaki, Y., Los, D.A., Hayashi, H., and Murata, N., *Gene-engineered rigidification of membrane lipids enhances the cold inducibility of gene expression in* Synechocystis*.* Journal of Biological Chemistry, 2003. **278**(14): p. 12191-12198.
323. Sakamoto, T. and Murata, N., *Regulation of the desaturation of fatty acids and its role in tolerance to cold and salt stress.* Current opinion in microbiology, 2002. **5**(2): p. 208-10.
324. Klein, W., Weber, M.H., and Marahiel, M.A., *Cold shock response of* Bacillus subtilis*: isoleucine-dependent switch in the fatty acid branching pattern for membrane adaptation to low temperatures.* Journal of bacteriology, 1999. **181**(17): p. 5341-9.
325. Beranova, J., Jemiola-Rzeminska, M., Elhottova, D., Strzalka, K., and Konopasek, I., *Metabolic control of the membrane fluidity in* Bacillus subtilis *during cold adaptation.* Biochimica et biophysica acta, 2008. **1778**(2): p. 445-53.
326. Suutari, M. and Laakso, S., *Unsaturated and branched chain-fatty acids in temperature adaptation of* Bacillus subtilis *and* Bacillus megaterium*.* Biochimica et biophysica acta, 1992. **1126**(2): p. 119-24.
327. Beckering, C.L., Steil, L., Weber, M.H., Volker, U., and Marahiel, M.A., *Genomewide transcriptional analysis of the cold shock response in* Bacillus subtilis*.* Journal of bacteriology, 2002. **184**(22): p. 6395-402.
328. Russell, N.J., *Bacterial membranes: the effects of chill storage and food processing. An overview.* International journal of food microbiology, 2002. **79**(1-2): p. 27-34.
329. Berg, J.M., Tymoczko, J.L., and Stryer, L., *Fatty Acids Are Key Constituents of Lipids.* 2002.
330. Zhu, K., Ding, X., Julotok, M., and Wilkinson, B.J., *Exogenous isoleucine and fatty acid shortening ensure the high content of anteiso-C15:0 fatty acid required for low-temperature growth of* Listeria monocytogenes*.* Applied and environmental microbiology, 2005. **71**(12): p. 8002-7.
331. Koga, Y., *Thermal adaptation of the archaeal and bacterial lipid membranes.* Archaea, 2012. **2012**: p. 789652.
332. Kaneda, T., *Iso- and anteiso-fatty acids in bacteria: biosynthesis, function, and taxonomic significance.* Microbiological reviews, 1991. **55**(2): p. 288-302.
333. Kaneda, T., *Fatty acids of the genus* Bacillus*: an example of branched-chain preference.* Bacteriological reviews, 1977. **41**(2): p. 391-418.
334. Oshima, M. and Miyagawa, A., *Comparative studies on the fatty acid composition of moderately and extremely thermophilic bacteria.* Lipids, 1974. **9**(7): p. 476-80.
335. Prado, A., da Costa, M.S., Laynez, J., and Madeira, V.M., *Physical properties of membrane lipids isolated from a thermophilic eubacterium (*Thermus sp.*).* Advances in experimental medicine and biology, 1988. **238**: p. 47-58.

336. Weerkamp, A. and Heinen, W., *The effect of nutrients and precursors on the fatty acid composition of two thermophilic Bacteria.* Archiv fur Mikrobiologie, 1972. **81**(4): p. 350-60.
337. Chen, R.R., *Permeability issues in whole-cell bioprocesses and cellular membrane engineering.* Applied microbiology and biotechnology, 2007. **74**(4): p. 730-8.
338. Stelling, J., Sauer, U., Szallasi, Z., Doyle, F.J., 3rd, and Doyle, J., *Robustness of cellular functions.* Cell, 2004. **118**(6): p. 675-85.
339. Fischer, E. and Sauer, U., *Large-scale in vivo flux analysis shows rigidity and suboptimal performance of* Bacillus subtilis *metabolism.* Nature genetics, 2005. **37**(6): p. 636-40.
340. Dauner, M., Sonderegger, M., Hochuli, M., Szyperski, T., Wuthrich, K., Hohmann, H.P., Sauer, U., and Bailey, J.E., *Intracellular carbon fluxes in riboflavin-producing* Bacillus subtilis *during growth on two-carbon substrate mixtures.* Applied and environmental microbiology, 2002. **68**(4): p. 1760-71.
341. Blank, L.M., Kuepfer, L., and Sauer, U., *Large-scale 13C-flux analysis reveals mechanistic principles of metabolic network robustness to null mutations in yeast.* Genome biology, 2005. **6**(6): p. R49.
342. Tang, Y.J., Martin, H.G., Dehal, P.S., Deutschbauer, A., Llora, X., Meadows, A., Arkin, A., and Keasling, J.D., *Metabolic flux analysis of* Shewanella spp. *reveals evolutionary robustness in central carbon metabolism.* Biotechnology and bioengineering, 2009. **102**(4): p. 1161-9.
343. Nicolas, C., Kiefer, P., Letisse, F., Krömer, J., Massou, S., Soucaille, P., Wittmann, C., Lindley, N.D., and Portais, J.C., *Response of the central metabolism of* Escherichia coli *to modified expression of the gene encoding the glucose-6-phosphate dehydrogenase.* FEBS letters, 2007. **581**(20): p. 3771-6.
344. Dauner, M., Storni, T., and Sauer, U., Bacillus subtilis *metabolism and energetics in carbon-limited and excess-carbon chemostat culture.* Journal of bacteriology, 2001. **183**(24): p. 7308-17.
345. Sauer, U., Lasko, D.R., Fiaux, J., Hochuli, M., Glaser, R., Szyperski, T., Wuthrich, K., and Bailey, J.E., *Metabolic flux ratio analysis of genetic and environmental modulations of* Escherichia coli *central carbon metabolism.* Journal of bacteriology, 1999. **181**(21): p. 6679-88.
346. Fischer, E. and Sauer, U., *A novel metabolic cycle catalyzes glucose oxidation and anaplerosis in hungry* Escherichia coli*.* The Journal of biological chemistry, 2003. **278**(47): p. 46446-51.
347. Emmerling, M., Dauner, M., Ponti, A., Fiaux, J., Hochuli, M., Szyperski, T., Wuthrich, K., Bailey, J.E., and Sauer, U., *Metabolic flux responses to pyruvate kinase knockout in* Escherichia coli*.* Journal of bacteriology, 2002. **184**(1): p. 152-64.
348. Petersen, S., de Graaf, A.A., Eggeling, L., Mollney, M., Wiechert, W., and Sahm, H., *In vivo quantification of parallel and bidirectional fluxes in the anaplerosis of* Corynebacterium glutamicum*.* The Journal of biological chemistry, 2000. **275**(46): p. 35932-41.
349. Ohné, M., *Regulation of the dicarboxylic acid part of the citric acid cycle in* Bacillus subtilis*.* Journal of bacteriology, 1975. **122**(1): p. 224-34.
350. Biedendieck, R., Bunk, B., Fürch, T., Franco-Lara, E., Jahn, M., and Jahn, D., *Systems biology of recombinant protein production in* Bacillus megaterium, in *Biosystems Engineering I*. 2010, Springer. p. 133-161.
351. Heyland, J., Fu, J., and Blank, L.M., *Correlation between TCA cycle flux and glucose uptake rate during respiro-fermentative growth of* Saccharomyces cerevisiae*.* Microbiology, 2009. **155**(Pt 12): p. 3827-37.
352. Rühl, M., Le Coq, D., Aymerich, S., and Sauer, U., *13C-flux analysis reveals NADPH-balancing transhydrogenation cycles in stationary phase of nitrogen-starving* Bacillus subtilis*.* The Journal of biological chemistry, 2012. **287**(33): p. 27959-70.
353. Liao, J.C., Hou, S.Y., and Chao, Y.P., *Pathway analysis, engineering, and physiological considerations for redirecting central metabolism.* Biotechnology and bioengineering, 1996. **52**(1): p. 129-40.

354. Schilling, O., Frick, O., Herzberg, C., Ehrenreich, A., Heinzle, E., Wittmann, C., and Stulke, J., *Transcriptional and metabolic responses of* Bacillus subtilis *to the availability of organic acids: transcription regulation is important but not sufficient to account for metabolic adaptation.* Applied and environmental microbiology, 2007. **73**(2): p. 499-507.
355. Chubukov, V., Uhr, M., Le Chat, L., Kleijn, R.J., Jules, M., Link, H., Aymerich, S., Stelling, J., and Sauer, U., *Transcriptional regulation is insufficient to explain substrate-induced flux changes in* Bacillus subtilis*.* Molecular systems biology, 2013. **9**: p. 709.
356. Szasz, G., *The effect of temperature on enzyme activity and on the affinity of enzymes to their substrates.* Zeitschrift fur klinische Chemie und klinische Biochemie, 1974. **12**(4): p. 166-70.
357. Rossell, S., van der Weijden, C.C., Lindenbergh, A., van Tuijl, A., Francke, C., Bakker, B.M., and Westerhoff, H.V., *Unraveling the complexity of flux regulation: a new method demonstrated for nutrient starvation in* Saccharomyces cerevisiae*.* Proceedings of the National Academy of Sciences of the United States of America, 2006. **103**(7): p. 2166-71.
358. Fell, D.A., *Enzymes, metabolites and fluxes.* Journal of experimental botany, 2005. **56**(410): p. 267-72.
359. Chen, H. and Boutros, P.C., *VennDiagram: a package for the generation of highly-customizable Venn and Euler diagrams in R.* BMC bioinformatics, 2011. **12**: p. 35.
360. Bernhardt, J., Funke, S., Hecker, M., and Siebourg, J. *Visualizing Gene Expression Data via Voronoi Treemaps*. in *ISVD*. 2009.
361. Otto, A., Bernhardt, J., Meyer, H., Schaffer, M., Herbst, F.-A., Siebourg, J., Mäder, U., Lalk, M., Hecker, M., and Becher, D., *Systems-wide temporal proteomic profiling in glucose-starved* Bacillus subtilis*.* Nature communications, 2010. **1**: p. 137.
362. Subramanian, A., Tamayo, P., Mootha, V.K., Mukherjee, S., Ebert, B.L., Gillette, M.A., Paulovich, A., Pomeroy, S.L., Golub, T.R., and Lander, E.S., *Gene set enrichment analysis: a knowledge-based approach for interpreting genome-wide expression profiles.* Proceedings of the National Academy of Sciences of the United States of America, 2005. **102**(43): p. 15545-15550.
363. Lê, S., Josse, J., and Husson, F., *FactoMineR: an R package for multivariate analysis.* Journal of statistical software, 2008. **25**(1): p. 1-18.
364. Husson, F., Lê, S., and Pagès, J., *Exploratory multivariate analysis by example using R*. 2010: CRC press.
365. Krüger, E., Zuhlke, D., Witt, E., Ludwig, H., and Hecker, M., *Clp-mediated proteolysis in Gram-positive bacteria is autoregulated by the stability of a repressor.* The EMBO journal, 2001. **20**(4): p. 852-63.
366. Schumann, W., *The* Bacillus subtilis *heat shock stimulon.* Cell stress & chaperones, 2003. **8**(3): p. 207-17.
367. Darmon, E., Noone, D., Masson, A., Bron, S., Kuipers, O.P., Devine, K.M., and van Dijl, J.M., *A novel class of heat and secretion stress-responsive genes is controlled by the autoregulated CssRS two-component system of* Bacillus subtilis*.* Journal of bacteriology, 2002. **184**(20): p. 5661-71.
368. Antelmann, H., Engelmann, S., Schmid, R., Sorokin, A., Lapidus, A., and Hecker, M., *Expression of a stress- and starvation-induced* dps/pexB*-homologous gene is controlled by the alternative sigma factor sigmaB in* Bacillus subtilis*.* Journal of bacteriology, 1997. **179**(23): p. 7251-6.
369. Butala, M., Zgur-Bertok, D., and Busby, S.J., *The bacterial LexA transcriptional repressor.* Cellular and molecular life sciences : CMLS, 2009. **66**(1): p. 82-93.
370. Ghodsi, S., Gharavi, S., and Ghadam, P., *Cloning the hbs gene from* Bacillus subtilis *and expression of the HBsu protein in* Escherichia coli*.* Iranian journal of microbiology, 2010. **2**(3): p. 152.
371. Kamashev, D., Balandina, A., Mazur, A.K., Arimondo, P.B., and Rouviere-Yaniv, J., *HU binds and folds single-stranded DNA.* Nucleic acids research, 2008. **36**(3): p. 1026-1036.

372. Bensaid, A., Almeida, A., Drlica, K., and Rouviere-Yaniv, J., *Cross-talk between topoisomerase I and HU in* Escherichia coli*.* Journal of molecular biology, 1996. **256**(2): p. 292-300.
373. de Castro Fernandes, D., Bonatto, D., and Laurindo, F.R., *The evolving concept of oxidative stress*, in *Studies on Cardiovascular Disorders*. 2010, Springer. p. 1-41.
374. Charles, R.L., Burgoyne, J.R., and Eaton, P., *Mechanisms of redox signaling in cardiovascular disease*, in *Studies on Cardiovascular Disorders*. 2010, Springer. p. 43-60.
375. Lipinski, B., *Evidence in support of a concept of reductive stress.* The British journal of nutrition, 2002. **87**(1): p. 93-4; discussion 94.
376. Ying, W., *NAD+/NADH and NADP+/NADPH in cellular functions and cell death: regulation and biological consequences.* Antioxidants & redox signaling, 2008. **10**(2): p. 179-206.
377. Lewis, D.F.V., *Oxidative stress: the role of cytochromes P450 in oxygen activation.* Journal of Chemical Technology and Biotechnology, 2002. **77**(10): p. 1095-1100.
378. Dostalek, M., Hardy, K.D., Milne, G.L., Morrow, J.D., Chen, C., Gonzalez, F.J., Gu, J., Ding, X., Johnson, D.A., Johnson, J.A., Martin, M.V., and Guengerich, F.P., *Development of oxidative stress by cytochrome P450 induction in rodents is selective for barbiturates and related to loss of pyridine nucleotide-dependent protective systems.* The Journal of biological chemistry, 2008. **283**(25): p. 17147-57.
379. Maurer, L.M., Yohannes, E., Bondurant, S.S., Radmacher, M., and Slonczewski, J.L., *pH regulates genes for flagellar motility, catabolism, and oxidative stress in* Escherichia coli K-12*.* Journal of bacteriology, 2005. **187**(1): p. 304-319.
380. Davidson, J.F., Whyte, B., Bissinger, P.H., and Schiestl, R.H., *Oxidative stress is involved in heat-induced cell death in* Saccharomyces cerevisiae*.* Proceedings of the National Academy of Sciences, 1996. **93**(10): p. 5116-5121.
381. Privalle, C.T. and Fridovich, I., *Induction of superoxide dismutase in* Escherichia coli *by heat shock.* Proceedings of the National Academy of Sciences, 1987. **84**(9): p. 2723-2726.
382. Faulkner, M.J. and Helmann, J.D., *Peroxide stress elicits adaptive changes in bacterial metal ion homeostasis.* Antioxidants & redox signaling, 2011. **15**(1): p. 175-89.
383. Fuangthong, M., Herbig, A.F., Bsat, N., and Helmann, J.D., *Regulation of the* Bacillus subtilis fur *and* perR *genes by PerR: not all members of the PerR regulon are peroxide inducible.* Journal of bacteriology, 2002. **184**(12): p. 3276-86.
384. Yurimoto, H., Hirai, R., Matsuno, N., Yasueda, H., Kato, N., and Sakai, Y., *HxlR, a member of the DUF24 protein family, is a DNA-binding protein that acts as a positive regulator of the formaldehyde-inducible* hxlAB *operon in* Bacillus subtilis*.* Molecular microbiology, 2005. **57**(2): p. 511-519.
385. Kato, N., Yurimoto, H., and Thauer, R.K., *The physiological role of the ribulose monophosphate pathway in bacteria and archaea.* Bioscience, biotechnology, and biochemistry, 2006. **70**(1): p. 10-21.
386. Grimsrud, P.A., Xie, H., Griffin, T.J., and Bernlohr, D.A., *Oxidative stress and covalent modification of protein with bioactive aldehydes.* The Journal of biological chemistry, 2008. **283**(32): p. 21837-41.
387. Nguyen, T.T., Eiamphungporn, W., Mader, U., Liebeke, M., Lalk, M., Hecker, M., Helmann, J.D., and Antelmann, H., *Genome-wide responses to carbonyl electrophiles in* Bacillus subtilis*: control of the thiol-dependent formaldehyde dehydrogenase AdhA and cysteine proteinase YraA by the MerR-family regulator YraB (AdhR).* Molecular microbiology, 2009. **71**(4): p. 876-94.
388. Wang, E., Bauer, M.C., Rogstam, A., Linse, S., Logan, D.T., and von Wachenfeldt, C., *Structure and functional properties of the* Bacillus subtilis *transcriptional repressor Rex.* Molecular microbiology, 2008. **69**(2): p. 466-78.
389. Gyan, S., Shiohira, Y., Sato, I., Takeuchi, M., and Sato, T., *Regulatory loop between redox sensing of the NADH/NAD(+) ratio by Rex (YdiH) and oxidation of NADH by NADH dehydrogenase Ndh in* Bacillus subtilis*.* Journal of bacteriology, 2006. **188**(20): p. 7062-71.

390. Larsson, J.T., Rogstam, A., and von Wachenfeldt, C., *Coordinated patterns of cytochrome bd and lactate dehydrogenase expression in* Bacillus subtilis*.* Microbiology, 2005. **151**(Pt 10): p. 3323-35.
391. Winstedt, L., Yoshida, K.-I., Fujita, Y., and von Wachenfeldt, C., *Cytochrome bd Biosynthesis in* Bacillus subtilis*: Characterization of the* cydABCD *Operon.* Journal of bacteriology, 1998. **180**(24): p. 6571-6580.
392. Nakano, M.M. and Hulett, F.M., *Adaptation of* Bacillus subtilis *to oxygen limitation.* FEMS microbiology letters, 1997. **157**(1): p. 1-7.
393. Nakano, M.M., Geng, H., Nakano, S., and Kobayashi, K., *The nitric oxide-responsive regulator NsrR controls ResDE-dependent gene expression.* Journal of bacteriology, 2006. **188**(16): p. 5878-5887.
394. Nakano, M.M., *Induction of ResDE-dependent gene expression in* Bacillus subtilis *in response to nitric oxide and nitrosative stress.* Journal of bacteriology, 2002. **184**(6): p. 1783-7.
395. Zhang, X. and Hulett, F.M., *ResD signal transduction regulator of aerobic respiration in* Bacillus subtilis*: ctaA promoter regulation.* Molecular microbiology, 2000. **37**(5): p. 1208-1219.
396. Härtig, E., Hartmann, A., Schätzle, M., Albertini, A.M., and Jahn, D., *The* Bacillus subtilis nrdEF *genes, encoding a class Ib ribonucleotide reductase, are essential for aerobic and anaerobic growth.* Applied and environmental microbiology, 2006. **72**(8): p. 5260-5265.
397. Yu, W.-B., Gao, S.-H., Yin, C.-Y., Zhou, Y., and Ye, B.-C., *Comparative transcriptome analysis of* Bacillus subtilis *responding to dissolved oxygen in adenosine fermentation.* PloS one, 2011. **6**(5): p. e20092.
398. Puri-Taneja, A., Schau, M., Chen, Y., and Hulett, F.M., *Regulators of the* Bacillus subtilis cydABCD *operon: identification of a negative regulator, CcpA, and a positive regulator, ResD.* Journal of bacteriology, 2007. **189**(9): p. 3348-3358.
399. Gon, S. and Beckwith, J., *Ribonucleotide reductases: influence of environment on synthesis and activity.* Antioxidants & redox signaling, 2006. **8**(5-6): p. 773-780.
400. Cotruvo, J.A., Jr. and Stubbe, J., *An active dimanganese(III)-tyrosyl radical cofactor in* Escherichia coli *class Ib ribonucleotide reductase.* Biochemistry, 2010. **49**(6): p. 1297-309.
401. Galaris, D. and Pantopoulos, K., *Oxidative stress and iron homeostasis: mechanistic and health aspects.* Critical reviews in clinical laboratory sciences, 2008. **45**(1): p. 1-23.
402. Björnstedt, M., Xue, J., Huang, W., Akesson, B., and Holmgren, A., *The thioredoxin and glutaredoxin systems are efficient electron donors to human plasma glutathione peroxidase.* Journal of Biological Chemistry, 1994. **269**(47): p. 29382-29384.
403. Shibata, E., Ejima, K., Nanri, H., Toki, N., Koyama, C., Ikeda, M., and Kashimura, M., *Enhanced protein levels of protein thiol/disulphide oxidoreductases in placentae from pre-eclamptic subjects.* Placenta, 2001. **22**(6): p. 566-572.
404. Koharyova, M. and Kolarova, M., *Oxidative stress and thioredoxin system.* General physiology and biophysics, 2008. **27**(2): p. 71-84.
405. Spector, A., Yan, G.Z., Huang, R.R., McDermott, M.J., Gascoyne, P.R., and Pigiet, V., *The effect of $H_2O_2$ upon thioredoxin-enriched lens epithelial cells.* The Journal of biological chemistry, 1988. **263**(10): p. 4984-90.
406. Holmgren, A., *Thioredoxin and glutaredoxin systems.* The Journal of biological chemistry, 1989. **264**(24): p. 13963-6.
407. Holmgren, A., *Antioxidant function of thioredoxin and glutaredoxin systems.* Antioxidants & redox signaling, 2000. **2**(4): p. 811-20.
408. Scharf, C., Riethdorf, S., Ernst, H., Engelmann, S., Volker, U., and Hecker, M., *Thioredoxin is an essential protein induced by multiple stresses in* Bacillus subtilis*.* Journal of bacteriology, 1998. **180**(7): p. 1869-77.
409. Zuber, P., *Management of oxidative stress in* Bacillus*.* Annual review of microbiology, 2009. **63**: p. 575-97.
410. Nakano, S., Kuster-Schock, E., Grossman, A.D., and Zuber, P., *Spx-dependent global transcriptional control is induced by thiol-specific oxidative stress in* Bacillus subtilis*.*

Proceedings of the National Academy of Sciences of the United States of America, 2003. **100**(23): p. 13603-8.
411. Larsson, J.T., Rogstam, A., and von Wachenfeldt, C., *YjbH is a novel negative effector of the disulphide stress regulator, Spx, in* Bacillus subtilis*.* Molecular microbiology, 2007. **66**(3): p. 669-84.
412. Zuber, P., *Function and Control of the Spx-Family of Proteins Within the Bacterial Stress Response*. 2013: Springer.
413. You, C., Sekowska, A., Francetic, O., Martin-Verstraete, I., Wang, Y., and Danchin, A., *Spx mediates oxidative stress regulation of the methionine sulfoxide reductases operon in* Bacillus subtilis*.* BMC microbiology, 2008. **8**: p. 128.
414. Moskovitz, J., *Methionine sulfoxide reductases: ubiquitous enzymes involved in antioxidant defense, protein regulation, and prevention of aging-associated diseases.* Biochimica et biophysica acta, 2005. **1703**(2): p. 213-9.
415. Hochgräfe, F., Mostertz, J., Pother, D.C., Becher, D., Helmann, J.D., and Hecker, M., *S-cysteinylation is a general mechanism for thiol protection of* Bacillus subtilis *proteins after oxidative stress.* The Journal of biological chemistry, 2007. **282**(36): p. 25981-5.
416. Yamashita, M., Shepherd, M., Booth, W.I., Xie, H., Postis, V., Nyathi, Y., Tzokov, S.B., Poole, R.K., Baldwin, S.A., and Bullough, P.A., *Structure and Function of the Bacterial Heterodimeric ABC Transporter CydDC stimulation of ATPase activity by thiol and heme compounds.* Journal of Biological Chemistry, 2014. **289**(33): p. 23177-23188.
417. Pittman, M.S., Robinson, H.C., and Poole, R.K., *A bacterial glutathione transporter (*Escherichia coli *CydDC) exports reductant to the periplasm.* The Journal of biological chemistry, 2005. **280**(37): p. 32254-61.
418. Gusarov, I. and Nudler, E., *NO-mediated cytoprotection: instant adaptation to oxidative stress in bacteria.* Proceedings of the National Academy of Sciences of the United States of America, 2005. **102**(39): p. 13855-60.
419. Doreswamy, K., Shrilatha, B., and Rajeshkumar, T., *Nickel-Induced Oxidative Stress in Testis of Mice: Evidence of DNA Damage and Genotoxic Effects.* Journal of andrology, 2004. **25**(6): p. 996-1003.
420. Lloyd, D.R. and Phillips, D.H., *Oxidative DNA damage mediated by copper(II), iron(II) and nickel(II) fenton reactions: evidence for site-specific mechanisms in the formation of double-strand breaks, 8-hydroxydeoxyguanosine and putative intrastrand cross-links.* Mutation research, 1999. **424**(1-2): p. 23-36.
421. Gaballa, A., Antelmann, H., Aguilar, C., Khakh, S.K., Song, K.B., Smaldone, G.T., and Helmann, J.D., *The* Bacillus subtilis *iron-sparing response is mediated by a Fur-regulated small RNA and three small, basic proteins.* Proceedings of the National Academy of Sciences of the United States of America, 2008. **105**(33): p. 11927-32.
422. Nagababu, E. and Rifkind, J.M., *Heme degradation by reactive oxygen species.* Antioxidants & redox signaling, 2004. **6**(6): p. 967-978.
423. Park, S., Kim, D., Jang, I., Oh, H.B., and Choe, J., *Structural and biochemical study of* Bacillus subtilis *HmoB in complex with heme.* Biochemical and biophysical research communications, 2014. **446**(1): p. 286-91.
424. Gaballa, A. and Helmann, J.D., Bacillus subtilis *Fur represses one of two paralogous haem-degrading monooxygenases.* Microbiology, 2011. **157**(Pt 11): p. 3221-31.
425. Wang, E., Bauer, M.C., Rogstam, A., Linse, S., Logan, D.T., and Von Wachenfeldt, C., *Structure and functional properties of the* Bacillus subtilis *transcriptional repressor Rex.* Molecular microbiology, 2008. **69**(2): p. 466-478.
426. Riboldi, G.P., Bierhals, C.G., de Mattos, E.P., Frazzon, A.P., d'Azevedo, P.A., and Frazzon, J., *Oxidative stress enhances the expression of sulfur assimilation genes: preliminary insights on the* Enterococcus faecalis *iron-sulfur cluster machinery regulation.* Memorias do Instituto Oswaldo Cruz, 2014. **109**(4): p. 408-13.
427. Albrecht, A.G., Netz, D.J., Miethke, M., Pierik, A.J., Burghaus, O., Peuckert, F., Lill, R., and Marahiel, M.A., *SufU is an essential iron-sulfur cluster scaffold protein in* Bacillus subtilis*.* Journal of bacteriology, 2010. **192**(6): p. 1643-51.

428. Mihara, H. and Esaki, N., *Bacterial cysteine desulfurases: their function and mechanisms.* Applied microbiology and biotechnology, 2002. **60**(1-2): p. 12-23.
429. Varghese, S., Wu, A., Park, S., Imlay, K.R., and Imlay, J.A., *Submicromolar hydrogen peroxide disrupts the ability of Fur protein to control free-iron levels in* Escherichia coli*.* Molecular microbiology, 2007. **64**(3): p. 822-30.
430. Harrison, P.M. and Arosio, P., *The ferritins: molecular properties, iron storage function and cellular regulation.* Biochimica et biophysica acta, 1996. **1275**(3): p. 161-203.
431. Ishikawa, T., Mizunoe, Y., Kawabata, S., Takade, A., Harada, M., Wai, S.N., and Yoshida, S., *The iron-binding protein Dps confers hydrogen peroxide stress resistance to* Campylobacter jejuni*.* Journal of bacteriology, 2003. **185**(3): p. 1010-7.
432. Lim, A.C., Mak, K.C., Ng, N.U., and Ng, T., *Multiple modes of protection against hydrogen peroxide-induced oxidative damage in stationary and exponential phase* Escherichia coli *by DNA-binding protein (Dps).* J. Exp. Microbiol. Immunol, 2007. **11**: p. 86-92.
433. Zhao, G., Ceci, P., Ilari, A., Giangiacomo, L., Laue, T.M., Chiancone, E., and Chasteen, N.D., *Iron and hydrogen peroxide detoxification properties of DNA-binding protein from starved cells. A ferritin-like DNA-binding protein of* Escherichia coli*.* The Journal of biological chemistry, 2002. **277**(31): p. 27689-96.
434. Li, Y., Malkaram, S.A., Zhou, J., and Zempleni, J., *Lysine biotinylation and methionine oxidation in the heat shock protein HSP60 synergize in the elimination of reactive oxygen species in human cell cultures.* The Journal of nutritional biochemistry, 2014. **25**(4): p. 475-482.
435. Drazic, A., Miura, H., Peschek, J., Le, Y., Bach, N.C., Kriehuber, T., and Winter, J., *Methionine oxidation activates a transcription factor in response to oxidative stress.* Proceedings of the National Academy of Sciences of the United States of America, 2013. **110**(23): p. 9493-8.
436. Luo, S. and Levine, R.L., *Methionine in proteins defends against oxidative stress.* FASEB journal : official publication of the Federation of American Societies for Experimental Biology, 2009. **23**(2): p. 464-72.
437. Abulimiti, A., Qiu, X., Chen, J., Liu, Y., and Chang, Z., *Reversible methionine sulfoxidation of* Mycobacterium tuberculosis *small heat shock protein Hsp16.3 and its possible role in scavenging oxidants.* Biochemical and biophysical research communications, 2003. **305**(1): p. 87-93.
438. Müller, A. and Leichert, L., *Redox Proteomics*, in *Oxidative Stress and Redox Regulation*, Jakob, U. and Reichmann, D., Editors. 2013, Springer Netherlands. p. 157-186.
439. Hondorp, E.R. and Matthews, R.G., *Oxidative stress inactivates cobalamin-independent methionine synthase (MetE) in* Escherichia coli*.* PLoS biology, 2004. **2**(11): p. e336.
440. Ron, E.Z. and Davis, B.D., *Growth rate of* Escherichia coli *at elevated temperatures: limitation by methionine.* Journal of bacteriology, 1971. **107**(2): p. 391-396.
441. Mordukhova, E.A. and Pan, J.G., *Evolved cobalamin-independent methionine synthase (MetE) improves the acetate and thermal tolerance of* Escherichia coli*.* Applied and environmental microbiology, 2013. **79**(24): p. 7905-15.
442. Burt, E.T., O'Connor, C., and Larsen, B., *Isolation and identification of a 92-kDa stress induced protein from* Candida albicans*.* Mycopathologia, 1999. **147**(1): p. 13-20.
443. González, J.C., Peariso, K., Penner-Hahn, J.E., and Matthews, R.G., *Cobalamin-independent methionine synthase from* Escherichia coli*: a zinc metalloenzyme.* Biochemistry, 1996. **35**(38): p. 12228-12234.
444. Birch, C.S., Brasch, N.E., McCaddon, A., and Williams, J.H., *A novel role for vitamin B(12): Cobalamins are intracellular antioxidants in vitro.* Free radical biology & medicine, 2009. **47**(2): p. 184-8.
445. Graumann, P.L. and Marahiel, M.A., *Cold shock response in* Bacillus subtilis*.* Journal of molecular microbiology and biotechnology, 1999. **1**(2): p. 203-9.
446. Yamanaka, K., *Cold shock response in* Escherichia coli*.* Journal of molecular microbiology and biotechnology, 1999. **1**(2): p. 193-202.

447. Brigulla, M., Hoffmann, T., Krisp, A., Volker, A., Bremer, E., and Volker, U., *Chill induction of the SigB-dependent general stress response in* Bacillus subtilis *and its contribution to low-temperature adaptation.* Journal of bacteriology, 2003. **185**(15): p. 4305-14.
448. Méndez, M.B., Orsaria, L.M., Philippe, V., Pedrido, M.E., and Grau, R.R., *Novel roles of the master transcription factors Spo0A and σB for survival and sporulation of* Bacillus subtilis *at low growth temperature.* Journal of bacteriology, 2004. **186**(4): p. 989-1000.
449. Liu, B., Zhang, Y., and Zhang, W., *RNA-seq-based analysis of cold shock response in* Thermoanaerobacter tengcongensis*, a Bacterium Harboring a Single Cold Shock Protein Encoding Gene.* PloS one, 2014. **9**(3): p. e93289.
450. Aizawa, S.-I., Zhulin, I.B., Marquez-Magana, L., and Ordal, G.W., *Chemotaxis and motility.* Bacillus subtilis *and its closest relatives: from genes to cells*. ASM Press, Washington, DC, 2002: p. 437-452.
451. Weber, M.H. and Marahiel, M.A., *Coping with the cold: the cold shock response in the Gram-positive soil bacterium* Bacillus subtilis*.* Philosophical transactions of the Royal Society of London. Series B, Biological sciences, 2002. **357**(1423): p. 895-907.
452. Yamanaka, K. and Inouye, M., *Selective mRNA degradation by polynucleotide phosphorylase in cold shock adaptation in* Escherichia coli*.* Journal of bacteriology, 2001. **183**(9): p. 2808-16.
453. Pandiani, F., Brillard, J., Bornard, I., Michaud, C., Chamot, S., Nguyen-the, C., and Broussolle, V., *Differential involvement of the five RNA helicases in adaptation of* Bacillus cereus ATCC 14579 *to low growth temperatures.* Applied and environmental microbiology, 2010. **76**(19): p. 6692-7.
454. Hunger, K., Beckering, C.L., Wiegeshoff, F., Graumann, P.L., and Marahiel, M.A., *Cold-induced putative DEAD box RNA helicases CshA and CshB are essential for cold adaptation and interact with cold shock protein B in* Bacillus subtilis*.* Journal of bacteriology, 2006. **188**(1): p. 240-8.
455. Ando, Y. and Nakamura, K., Bacillus subtilis *DEAD protein YdbR possesses ATPase, RNA binding, and RNA unwinding activities.* Bioscience, biotechnology, and biochemistry, 2006. **70**(7): p. 1606-1615.
456. Charollais, J., Dreyfus, M., and Iost, I., *CsdA, a cold-shock RNA helicase from* Escherichia coli*, is involved in the biogenesis of 50S ribosomal subunit.* Nucleic acids research, 2004. **32**(9): p. 2751-9.
457. Lehnik-Habrink, M., Rempeters, L., Kovacs, A.T., Wrede, C., Baierlein, C., Krebber, H., Kuipers, O.P., and Stulke, J., *DEAD-Box RNA helicases in* Bacillus subtilis *have multiple functions and act independently from each other.* Journal of bacteriology, 2013. **195**(3): p. 534-44.
458. Prud'homme-Généreux, A., Beran, R.K., Iost, I., Ramey, C.S., Mackie, G.A., and Simons, R.W., *Physical and functional interactions among RNase E, polynucleotide phosphorylase and the cold-shock protein, CsdA: evidence for a 'cold shock degradosome'.* Molecular microbiology, 2004. **54**(5): p. 1409-1421.
459. Carpousis, A.J., *The RNA degradosome of* Escherichia coli*: an mRNA-degrading machine assembled on RNase E.* Annual review of microbiology, 2007. **61**: p. 71-87.
460. Lehnik-Habrink, M., Pfortner, H., Rempeters, L., Pietack, N., Herzberg, C., and Stulke, J., *The RNA degradosome in* Bacillus subtilis*: identification of CshA as the major RNA helicase in the multiprotein complex.* Molecular microbiology, 2010.
461. Inoue, K., Alsina, J., Chen, J., and Inouye, M., *Suppression of defective ribosome assembly in a rbfA deletion mutant by overexpression of Era, an essential GTPase in* Escherichia coli*.* Molecular microbiology, 2003. **48**(4): p. 1005-16.
462. Charette, M. and Gray, M.W., *Pseudouridine in RNA: what, where, how, and why.* IUBMB life, 2000. **49**(5): p. 341-351.
463. Hamma, T. and Ferré-D'Amaré, A.R., *Pseudouridine synthases.* Chemistry & biology, 2006. **13**(11): p. 1125-1135.
464. Schwartz, S., Bernstein, D.A., Mumbach, M.R., Jovanovic, M., Herbst, R.H., Leon-Ricardo, B.X., Engreitz, J.M., Guttman, M., Satija, R., Lander, E.S., Fink, G., and Regev, A.,

*Transcriptome-wide mapping reveals widespread dynamic-regulated pseudouridylation of ncRNA and mRNA.* Cell, 2014. **159**(1): p. 148-62.
465. Karikó, K., Muramatsu, H., Welsh, F.A., Ludwig, J., Kato, H., Akira, S., and Weissman, D., *Incorporation of pseudouridine into mRNA yields superior nonimmunogenic vector with increased translational capacity and biological stability.* Molecular therapy : the journal of the American Society of Gene Therapy, 2008. **16**(11): p. 1833-40.
466. Privalov, P.L., *Cold denaturation of proteins.* Critical reviews in biochemistry and molecular biology, 1990. **25**(4): p. 281-305.
467. Becktel, W.J. and Schellman, J.A., *Protein stability curves.* Biopolymers, 1987. **26**(11): p. 1859-1877.
468. Göthel, S.F., Scholz, C., Schmid, F.X., and Marahiel, M.A., *Cyclophilin and trigger factor from* Bacillus subtilis *catalyze in vitro protein folding and are necessary for viability under starvation conditions.* Biochemistry, 1998. **37**(38): p. 13392-13399.
469. Sen, M., Maillard, R.A., Nyquist, K., Rodriguez-Aliaga, P., Presse, S., Martin, A., and Bustamante, C., *The ClpXP protease unfolds substrates using a constant rate of pulling but different gears.* Cell, 2013. **155**(3): p. 636-46.
470. Mizushima, T., Kataoka, K., Ogata, Y., Inoue, R., and Sekimizu, K., *Increase in negative supercoiling of plasmid DNA in* Escherichia coli *exposed to cold shock.* Molecular microbiology, 1997. **23**(2): p. 381-6.
471. Grau, R., Gardiol, D., Glikin, G.C., and Mendoza, D., *DNA supercoiling and thermal regulation of unsaturated fatty acid synthesis in* Bacillus subtilis*.* Molecular microbiology, 1994. **11**(5): p. 933-941.
472. Schröder, W., Bernhardt, J., Marincola, G., Klein-Hitpass, L., Herbig, A., Krupp, G., Nieselt, K., and Wolz, C., *Altering gene expression by aminocoumarins: the role of DNA supercoiling in* Staphylococcus aureus*.* BMC genomics, 2014. **15**(1): p. 291.
473. Jones, P.G., Krah, R., Tafuri, S.R., and Wolffe, A.P., *DNA gyrase, CS7.4, and the cold shock response in* Escherichia coli*.* Journal of bacteriology, 1992. **174**(18): p. 5798-802.
474. Munro, A.W., Lindsay, J.G., Coggins, J.R., Kelly, S.M., and Price, N.C., *NADPH oxidase activity of cytochrome P-450 BM3 and its constituent reductase domain.* Biochimica et biophysica acta, 1995. **1231**(3): p. 255-64.
475. Yousefi-Nejad, M., Manesh, H.N., and Khajeh, K., *Proteomics of early and late cold shock stress on thermophilic bacterium,* Thermus sp. GH5*.* Journal of proteomics, 2011. **74**(10): p. 2100-11.
476. Rhee, S.G., Kang, S.W., Jeong, W., Chang, T.S., Yang, K.S., and Woo, H.A., *Intracellular messenger function of hydrogen peroxide and its regulation by peroxiredoxins.* Current opinion in cell biology, 2005. **17**(2): p. 183-9.
477. Veal, E.A., Day, A.M., and Morgan, B.A., *Hydrogen peroxide sensing and signaling.* Molecular cell, 2007. **26**(1): p. 1-14.
478. Lammers, M., Nahrstedt, H., and Meinhardt, F., *The* Bacillus megaterium comE *locus encodes a functional DNA uptake protein.* Journal of basic microbiology, 2004. **44**(6): p. 451-458.
479. Kovács, Á.T., Smits, W.K., Mirończuk, A.M., and Kuipers, O.P., *Ubiquitous late competence genes in* Bacillus *species indicate the presence of functional DNA uptake machineries.* Environmental microbiology, 2009. **11**(8): p. 1911-1922.
480. Hamoen, L.W., Van Werkhoven, A.F., Bijlsma, J.J., Dubnau, D., and Venema, G., *The competence transcription factor of* Bacillus subtilis *recognizes short A/T-rich sequences arranged in a unique, flexible pattern along the DNA helix.* Genes & development, 1998. **12**(10): p. 1539-1550.
481. Persuh, M., Mandic-Mulec, I., and Dubnau, D., *A MecA paralog, YpbH, binds ClpC, affecting both competence and sporulation.* Journal of bacteriology, 2002. **184**(8): p. 2310-2313.
482. Msadek, T., Kunst, F., and Rapoport, G., *MecB of* Bacillus subtilis*, a member of the ClpC ATPase family, is a pleiotropic regulator controlling competence gene expression and*

*growth at high temperature.* Proceedings of the National Academy of Sciences, 1994. **91**(13): p. 5788-5792.
483. Nakano, M.M., Nakano, S., and Zuber, P., *Spx (YjbD), a negative effector of competence in* Bacillus subtilis*, enhances ClpC–MecA–ComK interaction.* Molecular microbiology, 2002. **44**(5): p. 1341-1349.
484. Hamoen, L.W., Kausche, D., Marahiel, M.A., van Sinderen, D., Venema, G., and Serror, P., *The* Bacillus subtilis *transition state regulator AbrB binds to the -35 promoter region of comK.* FEMS microbiology letters, 2003. **218**(2): p. 299-304.
485. Monnet, V., *Bacterial oligopeptide-binding proteins.* Cellular and Molecular Life Sciences CMLS, 2003. **60**(10): p. 2100-2114.
486. LeDeaux, J.R., Solomon, J.M., and Grossman, A.D., *Analysis of non-polar deletion mutations in the genes of the* spo0K *(*opp*) operon of* Bacillus subtilis*.* FEMS microbiology letters, 1997. **153**(1): p. 63-69.
487. Lazazzera, B.A., Solomon, J.M., and Grossman, A.D., *An exported peptide functions intracellularly to contribute to cell density signaling in* B. subtilis*.* Cell, 1997. **89**(6): p. 917-925.
488. Rudner, D.Z., LeDeaux, J.R., Ireton, K., and Grossman, A.D., *The* spo0K *locus of* Bacillus subtilis *is homologous to the oligopeptide permease locus and is required for sporulation and competence.* Journal of bacteriology, 1991. **173**(4): p. 1388-1398.
489. Lazazzera, B.A., Kurtser, I.G., McQuade, R.S., and Grossman, A.D., *An autoregulatory circuit affecting peptide signaling in* Bacillus subtilis*.* Journal of bacteriology, 1999. **181**(17): p. 5193-5200.
490. Labrie, S.J., Samson, J.E., and Moineau, S., *Bacteriophage resistance mechanisms.* Nature Reviews Microbiology, 2010. **8**(5): p. 317-327.
491. Hill, C., Garvey, P., and Fitzgerald, G., *Bacteriophage-host interactions and resistance mechanisms, analysis of the conjugative bacteriophage resistance plasmid pNP40.* Le Lait, 1996. **76**(1-2): p. 67-79.
492. Sonenshein, A.L., Hoch, J.A., and Losick, R., Bacillus subtilis *and other gram-positive bacteria: biochemistry, physiology, and molecular genetics.* 1993.
493. Sutherland, I.W., Hughes, K.A., Skillman, L.C., and Tait, K., *The interaction of phage and biofilms.* FEMS microbiology letters, 2004. **232**(1): p. 1-6.
494. Kimura, K. and Itoh, Y., *Characterization of poly-γ-glutamate hydrolase encoded by a bacteriophage genome: possible role in phage infection of* Bacillus subtilis *encapsulated with poly-γ-glutamate.* Applied and environmental microbiology, 2003. **69**(5): p. 2491-2497.
495. Makino, S., Uchida, I., Terakado, N., Sasakawa, C., and Yoshikawa, M., *Molecular characterization and protein analysis of the cap region, which is essential for encapsulation in* Bacillus anthracis*.* Journal of bacteriology, 1989. **171**(2): p. 722-30.
496. Ferrieres, L., Aslam, S.N., Cooper, R.M., and Clarke, D.J., *The yjbEFGH locus in* Escherichia coli K-12 *is an operon encoding proteins involved in exopolysaccharide production.* Microbiology, 2007. **153**(4): p. 1070-1080.
497. Miajlovic, H., Cooke, N.M., Moran, G.P., Rogers, T.R., and Smith, S.G., *Response of extraintestinal pathogenic* Escherichia coli *to human serum reveals a protective role for Rcs-regulated exopolysaccharide colanic acid.* Infection and immunity, 2014. **82**(1): p. 298-305.
498. Cheng, X., Wang, W., and Molineux, I.J., *F exclusion of bacteriophage T7 occurs at the cell membrane.* Virology, 2004. **326**(2): p. 340-352.
499. Wang, W.-F., Cheng, X., and Molineux, I.J., *Isolation and identification of fxsA, an* Escherichia coli *gene that can suppress F exclusion of bacteriophage T7.* Journal of molecular biology, 1999. **292**(3): p. 485-499.
500. Stern, A. and Sorek, R., *The phage-host arms race: shaping the evolution of microbes.* BioEssays : news and reviews in molecular, cellular and developmental biology, 2011. **33**(1): p. 43-51.

501. Schweder, T., Kruger, E., Xu, B., Jurgen, B., Blomsten, G., Enfors, S.O., and Hecker, M., *Monitoring of genes that respond to process-related stress in large-scale bioprocesses.* Biotechnology and bioengineering, 1999. **65**(2): p. 151-9.
502. Kohlstedt, M., Sappa, P.K., Meyer, H., Maaß, S., Zaprasis, A., Hoffmann, T., Becker, J., Steil, L., Hecker, M., and Dijl, J.M., *Adaptation of* Bacillus subtilis *carbon core metabolism to simultaneous nutrient limitation and osmotic challenge: a multi-omics perspective.* Environmental microbiology, 2014. **16**(6): p. 1898-1917.
503. den Besten, H.M., Mols, M., Moezelaar, R., Zwietering, M.H., and Abee, T., *Phenotypic and transcriptomic analyses of mildly and severely salt-stressed* Bacillus cereus ATCC 14579 *cells.* Applied and environmental microbiology, 2009. **75**(12): p. 4111-9.
504. Rana, N.F., Sauvageot, N., Laplace, J.M., Bao, Y., Nes, I., Rince, A., Posteraro, B., Sanguinetti, M., and Hartke, A., *Redox balance via lactate dehydrogenase is important for multiple stress resistance and virulence in* Enterococcus faecalis*.* Infection and immunity, 2013. **81**(8): p. 2662-8.
505. Richardson, A.R., Libby, S.J., and Fang, F.C., *A nitric oxide–inducible lactate dehydrogenase enables* Staphylococcus aureus *to resist innate immunity.* Science, 2008. **319**(5870): p. 1672-1676.
506. Boch, J., Kempf, B., Schmid, R., and Bremer, E., *Synthesis of the osmoprotectant glycine betaine in* Bacillus subtilis*: characterization of the* gbsAB *genes.* Journal of bacteriology, 1996. **178**(17): p. 5121-9.
507. Kappes, R.M., Kempf, B., Kneip, S., Boch, J., Gade, J., Meier-Wagner, J., and Bremer, E., *Two evolutionarily closely related ABC transporters mediate the uptake of choline for synthesis of the osmoprotectant glycine betaine in* Bacillus subtilis*.* Molecular microbiology, 1999. **32**(1): p. 203-16.
508. Nau-Wagner, G., Opper, D., Rolbetzki, A., Boch, J., Kempf, B., Hoffmann, T., and Bremer, E., *Genetic control of osmoadaptive glycine betaine synthesis in* Bacillus subtilis *through the choline-sensing and glycine betaine-responsive GbsR repressor.* Journal of bacteriology, 2012. **194**(10): p. 2703-14.
509. Steil, L., Hoffmann, T., Budde, I., Volker, U., and Bremer, E., *Genome-wide transcriptional profiling analysis of adaptation of* Bacillus subtilis *to high salinity.* Journal of bacteriology, 2003. **185**(21): p. 6358-70.
510. Galinski, E., *Compatible solutes of halophilic eubacteria: molecular principles, water-solute interaction, stress protection.* Experientia, 1993. **49**(6-7): p. 487-496.
511. Shahjee, H.M., Banerjee, K., and Ahmad, F., *Comparative analysis of naturally occurring L-amino acid osmolytes and their D-isomers on protection of* Escherichia coli *against environmental stresses.* Journal of biosciences, 2002. **27**(5): p. 515-520.
512. Arakawa, T. and Timasheff, S., *The stabilization of proteins by osmolytes.* Biophysical journal, 1985. **47**(3): p. 411.
513. Bolten, C.J., Kiefer, P., Letisse, F., Portais, J.-C., and Wittmann, C., *Sampling for metabolome analysis of microorganisms.* Analytical chemistry, 2007. **79**(10): p. 3843-3849.
514. Commichau, F.M., Gunka, K., Landmann, J.J., and Stulke, J., *Glutamate metabolism in* Bacillus subtilis*: gene expression and enzyme activities evolved to avoid futile cycles and to allow rapid responses to perturbations of the system.* Journal of bacteriology, 2008. **190**(10): p. 3557-64.
515. Gunka, K. and Commichau, F.M., *Control of glutamate homeostasis in* Bacillus subtilis*: a complex interplay between ammonium assimilation, glutamate biosynthesis and degradation.* Molecular microbiology, 2012. **85**(2): p. 213-24.
516. Epstein, W., *The roles and regulation of potassium in bacteria.* Progress in nucleic acid research and molecular biology, 2003. **75**: p. 293-320.
517. McLaggan, D., Naprstek, J., Buurman, E.T., and Epstein, W., *Interdependence of K+ and glutamate accumulation during osmotic adaptation of* Escherichia coli*.* Journal of Biological Chemistry, 1994. **269**(3): p. 1911-1917.

518. Kajiyama, Y., Otagiri, M., Sekiguchi, J., Kosono, S., and Kudo, T., *Complex formation by the* mrpABCDEFG *gene products, which constitute a principal Na+/H+ antiporter in* Bacillus subtilis*.* Journal of bacteriology, 2007. **189**(20): p. 7511-4.
519. Hoffmann, T., Boiangiu, C., Moses, S., and Bremer, E., *Responses of* Bacillus subtilis *to hypotonic challenges: physiological contributions of mechanosensitive channels to cellular survival.* Applied and environmental microbiology, 2008. **74**(8): p. 2454-2460.
520. Fuhrer, T. and Sauer, U., *Different biochemical mechanisms ensure network-wide balancing of reducing equivalents in microbial metabolism.* Journal of bacteriology, 2009. **191**(7): p. 2112-21.
521. Höper, D., Bernhardt, J., and Hecker, M., *Salt stress adaptation of* Bacillus subtilis*: a physiological proteomics approach.* Proteomics, 2006. **6**(5): p. 1550-62.
522. Hess, B. and Brand, K., *Enzyme and metabolite profiles.* Control of energy metabolism, 1965. **111**.
523. Corbett, D., Schuler, S., Glenn, S., Andrew, P.W., Cavet, J.S., and Roberts, I.S., *The combined actions of the copper-responsive repressor CsoR and copper-metallochaperone CopZ modulate CopA-mediated copper efflux in the intracellular pathogen* Listeria monocytogenes*.* Molecular microbiology, 2011. **81**(2): p. 457-72.
524. Banci, L., Bertini, I., Ciofi-Baffoni, S., Del Conte, R., and Gonnelli, L., *Understanding copper trafficking in bacteria: interaction between the copper transport protein CopZ and the N-terminal domain of the copper ATPase CopA from* Bacillus subtilis*.* Biochemistry, 2003. **42**(7): p. 1939-49.
525. Radford, D.S., Kihlken, M.A., Borrelly, G.P., Harwood, C.R., Le Brun, N.E., and Cavet, J.S., *CopZ from* Bacillus subtilis *interacts in vivo with a copper exporting CPx-type ATPase CopA.* FEMS microbiology letters, 2003. **220**(1): p. 105-112.
526. Rösti, J., Barton, C.J., Albrecht, S., Dupree, P., Pauly, M., Findlay, K., Roberts, K., and Seifert, G.J., *UDP-glucose 4-epimerase isoforms UGE2 and UGE4 cooperate in providing UDP-galactose for cell wall biosynthesis and growth of* Arabidopsis thaliana*.* The Plant Cell Online, 2007. **19**(5): p. 1565-1579.
527. Kim, S.-K., Kim, D., Kim, B.-G., Jeon, Y., Hong, B., and Ahn, J.-H., *Cloning and characterization of the UDP glucose/galactose epimerases of* Oryza sativa*.* J. Korean Soc. Appl. Biol. Chem., 2009. **52**(4): p. 315-320.
528. Rabbani, M.A., Maruyama, K., Abe, H., Khan, M.A., Katsura, K., Ito, Y., Yoshiwara, K., Seki, M., Shinozaki, K., and Yamaguchi-Shinozaki, K., *Monitoring expression profiles of rice genes under cold, drought, and high-salinity stresses and abscisic acid application using cDNA microarray and RNA gel-blot analyses.* Plant physiology, 2003. **133**(4): p. 1755-1767.
529. Seifert, G.J., Barber, C., Wells, B., Dolan, L., and Roberts, K., *Galactose biosynthesis in Arabidopsis: genetic evidence for substrate channeling from UDP-D-galactose into cell wall polymers.* Current Biology, 2002. **12**(21): p. 1840-1845.
530. Wang, W., Sun, J., Hollmann, R., Zeng, A.P., and Deckwer, W.D., *Proteomic characterization of transient expression and secretion of a stress-related metalloprotease in high cell density culture of* Bacillus megaterium*.* Journal of biotechnology, 2006. **126**(3): p. 313-24.
531. Zurbriggen, M.D., Tognetti, V.B., and Carrillo, N., *Stress-inducible flavodoxin from photosynthetic microorganisms. The mystery of flavodoxin loss from the plant genome.* IUBMB life, 2007. **59**(4-5): p. 355-60.
532. Giro, M., Carrillo, N., and Krapp, A.R., *Glucose-6-phosphate dehydrogenase and ferredoxin-NADP(H) reductase contribute to damage repair during the* soxRS *response of* Escherichia coli*.* Microbiology, 2006. **152**(Pt 4): p. 1119-28.
533. Pomposiello, P.J., Bennik, M.H., and Demple, B., *Genome-wide transcriptional profiling of the* Escherichia coli *responses to superoxide stress and sodium salicylate.* Journal of bacteriology, 2001. **183**(13): p. 3890-902.
534. Tognetti, V.B., Palatnik, J.F., Fillat, M.F., Melzer, M., Hajirezaei, M.-R., Valle, E.M., and Carrillo, N., *Functional replacement of ferredoxin by a cyanobacterial flavodoxin in tobacco confers broad-range stress tolerance.* The Plant Cell Online, 2006. **18**(8): p. 2035-2050.

535. Singh, K.P., Zaidi, A., Anwar, S., Bimal, S., Das, P., and Ali, V., *Reactive oxygen species regulates expression of iron–sulfur cluster assembly protein IscS of* Leishmania donovani*.* Free Radical Biology and Medicine, 2014. **75**: p. 195-209.
536. Hoffmann, T., Schutz, A., Brosius, M., Volker, A., Volker, U., and Bremer, E., *High-salinity-induced iron limitation in* Bacillus subtilis*.* Journal of bacteriology, 2002. **184**(3): p. 718-27.
537. Peyrot, F. and Ducrocq, C., *Potential role of tryptophan derivatives in stress responses characterized by the generation of reactive oxygen and nitrogen species.* Journal of pineal research, 2008. **45**(3): p. 235-246.
538. Levine, R.L., Berlett, B.S., Moskovitz, J., Mosoni, L., and Stadtman, E.R., *Methionine residues may protect proteins from critical oxidative damage.* Mechanisms of ageing and development, 1999. **107**(3): p. 323-332.
539. Yamakura, F. and Ikeda, K., *Modification of tryptophan and tryptophan residues in proteins by reactive nitrogen species.* Nitric Oxide, 2006. **14**(2): p. 152-161.
540. Wojtczak, L. and Slyshenkov, V.S., *Protection by pantothenic acid against apoptosis and cell damage by oxygen free radicals-the role of glutathione.* BioFactors, 2003. **17**(1): p. 61-73.
541. Kaneda, T., *Iso-and anteiso-fatty acids in bacteria: biosynthesis, function, and taxonomic significance.* Microbiological reviews, 1991. **55**(2): p. 288-302.
542. Bach, T.M.H. and Takagi, H., *Properties, metabolisms, and applications of L-proline analogues.* Applied microbiology and biotechnology, 2013. **97**(15): p. 6623-6634.
543. Gröger, H. and Wilken, J., *The application of l-proline as an enzyme mimic and further new asymmetric syntheses using small organic molecules as chiral catalysts.* Angewandte Chemie International Edition, 2001. **40**(3): p. 529-532.
544. List, B., *Proline-catalyzed asymmetric reactions.* Tetrahedron, 2002. **58**(28): p. 5573-5590.
545. McConathy, J. and Owens, M.J., *Stereochemistry in Drug Action.* Primary care companion to the Journal of clinical psychiatry, 2003. **5**(2): p. 70-73.
546. Armstrong, D.W., Chang, C.D., and Li, W.Y., *Relevance of enantiomeric separations in food and beverage analyses.* Journal of agricultural and food chemistry, 1990. **38**(8): p. 1674-1677.
547. Fallet, C., Rohe, P., and Franco-Lara, E., *Process optimization of the integrated synthesis and secretion of ectoine and hydroxyectoine under hyper/hypo-osmotic stress.* Biotechnology and bioengineering, 2010. **107**(1): p. 124-133.
548. Sauer, T. and Galinski, E.A., *Bacterial milking: a novel bioprocess for production of compatible solutes.* Biotechnology and bioengineering, 1998. **57**(3): p. 306-313.
549. Frings, E., Sauer, T., and Galinski, E.A., *Production of hydroxyectoine: high cell-density cultivation and osmotic downshock of* Marinococcus strain M52*.* Journal of biotechnology, 1995. **43**(1): p. 53-61.
550. Bergmann, S., David, F., Franco-Lara, E., Wittmann, C., and Krull, R., *Ectoine production by* Alkalibacillus haloalkaliphilus*—Bioprocess development using response surface methodology and model-driven strategies.* Engineering in Life Sciences, 2013. **13**(4): p. 399-407.
551. Jensen, J. and Wendisch, V.F., *Ornithine cyclodeaminase-based proline production by* Corynebacterium glutamicum*.* Microbial cell factories, 2013. **12**: p. 63.
552. Myers, R.H., Montgomery, D.C., and Anderson-Cook, C.M., *Response surface methodology: process and product optimization using designed experiments*. Vol. 705. 2009: John Wiley & Sons.
553. Kato, J., Horie, S., Komatsubara, S., Kisumi, M., and Chibata, I., *Production of L-proline by* Kurthia catenaforma*.* Applied microbiology, 1968. **16**(8): p. 1200-1206.
554. Sugiura, M. and Kisumi, M., *Proline-hyperproducing strains of* Serratia marcescens*: enhancement of proline analog-mediated growth inhibition by increasing osmotic stress.* Applied and environmental microbiology, 1985. **49**(4): p. 782-786.
555. Yoshinaga, F., Konishi, S., Okumura, S., and Katsuya, N., Studies on the fermentative production of L-proline*.* The Journal of General and Applied Microbiology, 1966. **12**(3): p. 219-228.

556. Wang, Q., Yu, H., Xia, Y., Kang, Z., and Qi, Q., *Complete PHB mobilization in* Escherichia coli *enhances the stress tolerance: a potential biotechnological application.* Microbial cell factories, 2009. **8**: p. 47.
557. Nair, I.C., Pradeep, S., Ajayan, M., Jayachandran, K., and Shashidhar, S., *Accumulation of intracellular polyhydroxybutyrate in* alcaligenes sp. d2 *under phenol stress.* Applied biochemistry and biotechnology, 2009. **159**(2): p. 545-552.
558. Zhao, Y.H., Li, H.M., Qin, L.F., Wang, H.H., and Chen, G.-Q., *Disruption of the polyhydroxyalkanoate synthase gene in* Aeromonas hydrophila *reduces its survival ability under stress conditions.* FEMS microbiology letters, 2007. **276**(1): p. 34-41.
559. Obruca, S., Marova, I., Svoboda, Z., and Mikulikova, R., *Use of controlled exogenous stress for improvement of poly (3-hydroxybutyrate) production in* Cupriavidus necator*.* Folia microbiologica, 2010. **55**(1): p. 17-22.
560. Kamnev, A.A., Tugarova, A.V., and Antoniuk, L.P., *Endophytic and epiphytic strains of* Azospirillum brazilense *respond differently to heavy metal stress.* Mikrobiologiia, 2007. **76**(6): p. 908-11.
561. Arora, N., Singhal, V., and Maheshwari, D., *Salinity-induced accumulation of poly-β-hydroxybutyrate in* rhizobia *indicating its role in cell protection.* World Journal of Microbiology and Biotechnology, 2006. **22**(6): p. 603-606.
562. Natarajan, K., Kishore, L., and Babu, C., *Sodium chloride stress results in increased poly-β-hydroxybutyrate production in* Rhizobium DDSS 69*.* Microbios, 1995. **82**(331): p. 95-107.
563. Rodríguez-Contreras, A., Koller, M., Miranda-de Sousa Dias, M., Calafell-Monfort, M., Braunegg, G., and Marqués-Calvo, M.S., *High production of poly (3-hydroxybutyrate) from a wild* Bacillus megaterium *Bolivian strain.* Journal of applied microbiology, 2013. **114**(5): p. 1378-1387.
564. Salgaonkar, B., Mani, K., and Braganca, J., *Characterization of polyhydroxyalkanoates accumulated by a moderately halophilic salt pan isolate* Bacillus megaterium strain H16*.* Journal of applied microbiology, 2013. **114**(5): p. 1347-1356.
565. López, J.A., Naranjo, J.M., Higuita, J.C., Cubitto, M.A., Cardona, C.A., and Villar, M.A., *Biosynthesis of PHB from a new isolated* Bacillus megaterium *strain: outlook on future developments with endospore forming bacteria.* Biotechnology and bioprocess engineering, 2012. **17**(2): p. 250-258.
566. Woo, S., Subramanian, P., Ramasamy, K., Joe, M.M., and Sa, T., *EPS Production, PHB Accumulation and Abiotic Stress Endurance of Plant Growth Promoting* Methylobacterium *Strains Grown in a High Carbon Concentration.* Korean J. Soil Sci. Fert, 2012. **45**(4): p. 572-581.
567. Ayub, N.D., Pettinari, M.J., Ruiz, J.A., and Lopez, N.I., *A polyhydroxybutyrate-producing* Pseudomonas sp. *isolated from Antarctic environments with high stress resistance.* Current microbiology, 2004. **49**(3): p. 170-4.
568. Anderson, A.J. and Dawes, E.A., *Occurrence, metabolism, metabolic role, and industrial uses of bacterial polyhydroxyalkanoates.* Microbiological reviews, 1990. **54**(4): p. 450-72.
569. Poblete-Castro, I., Escapa, I.F., Jäger, C., Puchalka, J., Lam, C.M.C., Schomburg, D., Prieto, M.A., and dos Santos, V.A.M., *The metabolic response of P. putida KT2442 producing high levels of polyhydroxyalkanoate under single-and multiple-nutrient-limited growth: Highlights from a multi-level omics approach.* Microbial cell factories, 2012. **11**(1): p. 34.
570. Ward, A.C., Rowley, B.I., and Dawes, E.A., *Effect of oxygen and nitrogen limitation on poly-β-hydroxybutyrate biosynthesis in ammonium-grown* Azotobacter beijerinckii*.* Journal of general microbiology, 1977. **102**(1): p. 61-68.
571. Wang, F. and Lee, S.Y., *Poly (3-Hydroxybutyrate) Production with high productivity and high polymer content by a fed-batch culture of* Alcaligenes latus *under nitrogen limitation.* Applied and environmental microbiology, 1997. **63**(9): p. 3703-3706.
572. Ramsay, B.A., Saracovan, I., Ramsay, J.A., and Marchessault, R.H., *Effect of nitrogen limitation on long-side-chain poly-beta-hydroxyalkanoate synthesis by* Pseudomonas resinovorans*.* Applied and environmental microbiology, 1992. **58**(2): p. 744-6.

573. Omar, S., Rayes, A., Eqaab, A., Voß, I., and Steinbüchel, A., *Optimization of cell growth and poly (3-hydroxybutyrate) accumulation on date syrup by a* Bacillus megaterium *strain.* Biotechnology letters, 2001. **23**(14): p. 1119-1123.
574. Faccin, D.J.L., Corrêa, M.P., Rech, R., Ayub, M.A.Z., Secchi, A.R., and Cardozo, N.S.M., *Modeling P (3HB) production by* Bacillus megaterium*.* Journal of Chemical Technology and Biotechnology, 2012. **87**(3): p. 325-333.
575. Korneli, C., David, F., Godard, T., and Franco-Lara, E., *Influence of fructose and oxygen gradients on fed-batch recombinant protein production using* Bacillus megaterium*.* Engineering in life sciences, 2011. **11**(4): p. 338-349.
576. Chaijamrus, S. and Udpuay, N., *Production and characterization of polyhydroxybutyrate from molasses and corn steep liquor produced by* Bacillus megaterium ATCC 6748*.* Agricultural Engineering International: CIGR Journal, 2008.
577. Gouda, M.K., Swellam, A.E., and Omar, S.H., *Production of PHB by a* Bacillus megaterium *strain using sugarcane molasses and corn steep liquor as sole carbon and nitrogen sources.* Microbiological research, 2001. **156**(3): p. 201-207.
578. Mahishi, L., Tripathi, G., and Rawal, S., *Poly (3-hydroxybutyrate)(PHB) synthesis by recombinant* Escherichia coli *harbouring* Streptomyces aureofaciens *PHB biosynthesis genes: effect of various carbon and nitrogen sources.* Microbiological research, 2003. **158**(1): p. 19-27.
579. García, A., Segura, D., Espín, G., Galindo, E., Castillo, T., and Peña, C., *High production of poly-β-hydroxybutyrate (PHB) by an* Azotobacter vinelandii *mutant altered in PHB regulation using a fed-batch fermentation process.* Biochemical Engineering Journal, 2014. **82**: p. 117-123.
580. Beaulieu, M., Beaulieu, Y., Melinard, J., Pandian, S., and Goulet, J., *Influence of ammonium salts and cane molasses on growth of* Alcaligenes eutrophus *and production of polyhydroxybutyrate.* Applied and environmental microbiology, 1995. **61**(1): p. 165-169.
581. Jiang, Y., Song, X., Gong, L., Li, P., Dai, C., and Shao, W., *High poly (β-hydroxybutyrate) production by* Pseudomonas fluorescens A2a5 *from inexpensive substrates.* Enzyme and microbial technology, 2008. **42**(2): p. 167-172.
582. Naranjo, J.M., Posada, J.A., Higuita, J.C., and Cardona, C.A., *Valorization of glycerol through the production of biopolymers: the PHB case using* Bacillus megaterium*.* Bioresource technology, 2013. **133**: p. 38-44.
583. Kim, B.S. and Chang, H.N., *Control of glucose feeding using exit gas data and its application to the production of PHB from tapioca hydrolysate by* Alcaligenes eutrophus*.* Biotechnology techniques, 1995. **9**(5): p. 311-314.
584. Kulpreecha, S., Boonruangthavorn, A., Meksiriporn, B., and Thongchul, N., *Inexpensive fed-batch cultivation for high poly(3-hydroxybutyrate) production by a new isolate of* Bacillus megaterium*.* Journal of bioscience and bioengineering, 2009. **107**(3): p. 240-5.
585. Melzer, G., Esfandabadi, M.E., Franco-Lara, E., and Wittmann, C., *Flux Design: In silico design of cell factories based on correlation of pathway fluxes to desired properties.* BMC systems biology, 2009. **3**: p. 120.
586. Smolke, C., *The metabolic pathway engineering handbook: tools and applications*. Vol. 2. 2009: CRC press.
587. Lim, S.-J., Jung, Y.-M., Shin, H.-D., and Lee, Y.-H., *Amplification of the NADPH-related genes* zwf *and* gnd *for the oddball biosynthesis of PHB in an* E. coli *transformant harboring a cloned phbCAB operon.* Journal of bioscience and bioengineering, 2002. **93**(6): p. 543-549.
588. Lee, S.H., Kang, K.-H., Kim, E.Y., Chae, T.U., Oh, Y.H., Hong, S.H., Song, B.K., Jegals, J., Park, S.J., and Lee, S.Y., *Metabolic engineering of* Escherichia coli *for enhanced biosynthesis of poly (3-hydroxybutyrate) based on proteome analysis.* Biotechnology letters, 2013. **35**(10): p. 1631-1637.
589. Grothe, E., Moo-Young, M., and Chisti, Y., *Fermentation optimization for the production of poly (β-hydroxybutyric acid) microbial thermoplastic.* Enzyme and microbial technology, 1999. **25**(1): p. 132-141.

590. Akaraonye, E., Keshavarz, T., and Roy, I., *Production of polyhydroxyalkanoates: the future green materials of choice.* Journal of Chemical Technology and Biotechnology, 2010. **85**(6): p. 732-743.

**Table A.1: Comparison of the physical properties of some specific PHAs with common synthetic polymers** [590] – **3HD**: 3-hydroxydecanoic acid, **3HH**:3-hydroxyhexanoic acid, **3HV**: 3-hydroxyvaleric acid, **mcl**: middle chain length, **P(3HB)**: poly-3-hydroxybutyric acid, **P(4HB):** poly-4-hydroxybutric acid, **PP**: polypropylene, **PS**: polystryrene, **scl**: small chain length.

| | Melting Temperature (°C) | Glass transition temperature (°C) | Young's modulus (Gpa) | Elongation to break (%) | Tensile strength (Mpa) |
|---|---|---|---|---|---|
| P(3HB) | 180 | 4 | 3.5 | 5 | 40 |
| P(4HB) | 53 | -48 | 149 | 1000 | 104 |
| P(3HB-co-20% 3HV) | 145 | -1 | 1.2 | 50 | 20 |
| P(3HB-co-16% 4HB) | 150 | -7 | - | 444 | 26 |
| P(3HB-co-10% 3HHx) | 127 | -1 | - | 400 | 21 |
| P(3HB-co-06% 3HD) | 130 | -8 | - | 680 | 17 |
| Polypropylene (PP) | 176 | -10 | 1.7 | 400 | 34.5 |
| Polystyrene (PS) | 240 | 100 | 3.1 | - | 50 |

| Properties | scl-PHAs | mcl-PHAs | PP |
|---|---|---|---|
| Cristallinity | 40-80 | 20-40 | 70 |
| Metling point | 53-80 | 30-80 | 176 |
| Density | 1.25 | 1.05 | 0.91 |
| Tensile strength | 43-04 | 20 | 34 |
| Glass transition temperature | -148-4 | -40-150 | -10 |
| Extension to break | 6-1000 | 300-450 | 400 |
| UV light resistant | Good | Good | Poor |
| Solvent resistant | Poor | Poor | Good |
| Biodegradability | Good | Good | None |

**Table A.2: Precursor demand [µmol $g_{CDW-1}$] for the wild-type *B. megaterium* growing in M9 minimal medium at 15°C, 45°C and 37°C in presence of up to 1.8 M NaCl.** Condition specific precursor demands were derived from the determined cell macromolar compositions (Fig. 4.3, 4.4 and Fig. A.1). ***** Pecursor demand for cells growing at 37°C in M9 minimal medium supplemented with 0.3, 0.9 and 1.8 M NaCl were extrapolled from data at 0, 0.6 and 1.2 M NaCl.

| | Precursor metabolites from central metabolism [µmol $g_{CDW}^{-1}$] | | | | | | | | | | | CO2 | Other metabolites [µmol $g_{CDW}^{-1}$] | | | | | |
|---|---|---|---|---|---|---|---|---|---|---|---|---|---|---|---|---|---|---|
| | G6P | F6P | R5P | E4P | GAP | 3PG | PEP | Pyr | AcCoA | α-KG | OAA | | ATP | NADH | NADPH | 1-C | $NH_4^+$ | S |
| 0 M NaCl | 342 | 91 | 830 | 225 | 192 | 910 | 470 | 2511 | 1925 | 859 | 1731 | -1652 | 13505 | -2382 | 11256 | 197 | 8493 | 104 |
| 0.3 M NaCl | 237 | 101 | 749 | 193 | 214 | 792 | 408 | 2103 | 3267 | 1370 | 1406 | -1434 | 12121 | -2593 | 12020 | 198 | 18015 | 92 |
| 0.6 M NaCl | 109 | 108 | 709 | 174 | 228 | 727 | 373 | 1829 | 3706 | 1877 | 1156 | -1184 | 11509 | -1926 | 12646 | 200 | 7575 | 76 |
| 0.9 M NaCl | 100 | 99 | 642 | 154 | 209 | 644 | 329 | 1623 | 5168 | 1931 | 1043 | -1059 | 10763 | -3028 | 13135 | 193 | 16987 | 71 |
| 1.2 M NaCl | 89 | 88 | 578 | 133 | 187 | 564 | 286 | 1398 | 6443 | 1973 | 899 | -902 | 9946 | -1511 | 13487 | 186 | 6436 | 62 |
| 1.8 M NaCl | 102 | 122 | 385 | 60 | 259 | 290 | 140 | 474 | 9716 | 3208 | 176 | -496 | 8093 | -3681 | 13779 | 172 | 15445 | 39 |
| 15°C | 564 | 142 | 822 | 177 | 301 | 858 | 387 | 2269 | 608 | 1188 | 1524 | -1417 | 13369 | -2193 | 9993 | 211 | 8465 | 93 |
| 45°C | 146 | 144 | 715 | 235 | 306 | 932 | 504 | 3000 | 763 | 1005 | 1898 | -2013 | 13193 | -2353 | 12445 | 103 | 8999 | 129 |

**Table A.3: Biochemical reaction network used for flux calculation with OpenFlux.** All reactions are listed with their corresponding stoichiometry (rxnEQ), carbon atom transition (cTrans) and type. Reactions marked with an "X" indicate reactions set as free fluxes for the simulation.

| rxnID | rxnEQ | cTrans | Type | | |
|---|---|---|---|---|---|
| R01 | GLC_EX = GLC6P | abcdef = abcdef | F | | **PTS** |
| R02 | GLC6P = F6P | abcdef = abcdef | F | | |
| R03 | F6P = GLC6P | abcdef = abcdef | F | | |
| R04 | F6P = F16BP | abcdef = abcdef | F | | **EMP** |
| R05 | F16BP = DHAP + G3P | abcdef = abc + def | F | | |
| R06 | DHAP = G3P | abc = cba | F | | |
| R07 | GLC6P = P5P + CO2 | abcdef = bcdef + a | F | X | |
| R08 | P5P + P5P = S7P + G3P | abcde + fghij = fgabcde + hij | FR | | |
| R09 | S7P + G3P = P5P + P5P | fgabcde + hij = abcde + fghij | R | X | |
| R10 | S7P + G3P = E4P + F6P | abcdefg + hij = defg + abchij | FR | | **PPP** |
| R11 | E4P + F6P = S7P + G3P | defg + abchij = abcdefg + hij | R | X | |
| R12 | E4P + P5P = F6P + G3P | abcd + efghi = efabcd + ghi | FR | | |
| R13 | F6P + G3P = E4P + P5P | efabcd + ghi = abcd + efghi | R | X | |
| R14 | G3P = 3PG | abc = abc | FR | | |
| R15 | 3PG = G3P | abc = abc | R | X | **EMP** |
| R16 | 3PG = PEP | abc = abc | F | | |
| R17 | PEP = PYR | abc = abc | F | | |
| R18 | PYR = ACCOA + CO2 | abc = bc + a | F | | |
| R19 | ACCOA + OAA = AKG + CO2 | ab + cdef = fedba + c | F | | |
| R20 | AKG = 0.5 SUC + 0.5 SUC + CO2 | abcde = 0.5 bcde + 0.5 edcb + a | F | | **TCA** |
| R21 | SUC = MAL | abcd = abcd | F | | |
| R22 | MAL = OAA | abcd = abcd | F | | |
| R23 | PYR + CO2 = OAA | abc + d = abcd | F | X | **PEP-** |
| R24 | MAL = PYR + CO2 | abcd = abc + d | F | X | **PYR-** |
| R25 | OAA = PEP + CO2 | abcd = abc + d | F | X | **OAA** |
| R26 | PEP + CO2 = OAA | abc + d = abcd | F | X | **node** |
| R27 | CO2 = CO2_EX | a = a | FR | | **CO2** |
| R28 | CO2_EX = CO2 | a = a | R | X | |
| R29 | AKG = AKG_EX | | B | | |
| R30 | PYR = PYR_EX | | B | | |
| R31 | SUC = SUC_EX | | B | | **Organic acids** |
| R32 | PYR = LAC_EX | | B | | |
| R33 | ACCOA = ACETAT_EX | | B | | |
| R34 | GLC6P = GLC6P_B | | B | | |
| R35 | F6P = F6P_B | | B | | |
| R36 | P5P = P5P_B | | B | | |
| R37 | E4P = E4P_B | | B | | |
| R38 | G3P = G3P_B | | B | | |
| R39 | 3PG = 3PG_B | abc = abc | F | | |
| R40 | PEP = PEP_B | | B | | |
| R41 | PYR = PYR_B | | B | | |
| R42 | OAA = OAA_B | | B | | **Biomass** |
| R43 | ACCOA = ACCOA_B | | B | | |
| R44 | AKG = AKG_B | | B | | |
| R45 | MTHF = MTHF_B | | B | | |
| R46 | 3PG_B = 3PG_BT | | B | | |
| R47 | 0.205 VALX + 0.065 TYRX + 0.098 PHEX + 0.137 SER + 0.434 ALAX + 0.268 GLYX + 0.242 LYSX + 0.158 THR + 0.151 ASPX + 0.343 GLUX = BIOMASS | | B | | |
| R48 | 3PG_B = SER | abc = abc | F | | |
| R49 | SER = GLYX + MTHF | abc = ab + c | FR | | |
| R50 | GLYX + MTHF = SER | ab + c = abc | R | X | |
| R51 | E4P + PEP = SHKM | abcd + efg = efgabcd | S | | |
| R52 | SHKM + PEP = CHRM | abcdefg + hij = abcdefghij | S | | |
| R53 | CHRM = PHEX + CO2 | abcdefghij = hijbcdefg + a | S | | |
| R54 | CHRM = TYRX + CO2 | abcdefghij = hijbcdefg + a | S | | **Amino acids** |
| R55 | PYR + PYR = VALX + CO2 | abc + def = abefc + d | S | | |
| R56 | PYR = ALAX | abc = abc | S | | |
| R57 | OAA + PYR = 0.5 LYSX + 0.5 LYSX + 0.5 CO2 + 0.5 CO2 | abcd + efg = 0.5 abcdfg + 0.5 efgdcb + 0.5 e + 0.5 a | S | | |
| R58 | OAA = THR | abcd = abcd | S | | |
| R59 | OAA = ASPX | abcd = abcd | S | | |
| R60 | AKG = GLUX | abcde = abcde | S | | |
| R61 | ACCOA + ACCOA = HB | ab + cd = abcd | S | | **PHB** |

**Table A.4: Gene expression levels in *B. megaterium* DSM319 grown at 15°C and 45°C.** Data are given as fold change (FC) of transcript concentrations compared to their values at 37°C. They were obtained from microarray experiments carried out using four biological replicates for each cultivation condition. Only genes whose expression was at least 1.75-fold up- (**red**) or down-regulated (**blue**) with a p-value < 0.05 at 15 and/or 45°C were considered as significantly regulated and listed.

| Gene product | Gene ID | Gene symbol | 15°C | 45°C |
|---|---|---|---|---|
| Pyridoxine biosynthesis lyase PdxS | *bmd_0015* | *pdxS* | - | 1.37 |
| Glutamine amidotransferase subunit PdxT | *bmd_0016* | *pdxT* | - | 1.32 |
| Transition state regulatory protein AbrB | *bmd_0054* | *abrB* | **2.21** | 1.66 |
| Control of biofilm formation | *bmd_0061* | *veg* | **9.76** | 1.17 |
| Small acid-soluble spore protein F | *bmd_0062* | *sspF* | **2.63** | - |
| Septation protein SpoVG | *bmd_0066* | *spoVG* | 1.59 | - |
| 50S ribosomal protein L25/general stress protein Ctc | *bmd_0069* | *ctc* | - | **7.58** |
| Cysteine synthase A | *bmd_0092* | *cysK* | 1.15 | **4.06** |
| Firmicute transcriptional repressor of class III stress genes (CtsR) protein | *bmd_0102* | *ctsR* | - | **1.83** |
| Heat shock - Cstr acitivity | *bmd_0103* | *mcsA* | - | **2.09** |
| ATP-dependent Clp protease ATP-binding subunit ClpC | *bmd_0105* | *clpC* | - | **1.93** |
| 50S ribosomal protein L10 | *bmd_0123* | *rplJ* | - | - |
| 50S ribosomal protein L7/L12 | *bmd_0124* | *rplL* | - | - |
| 16S rRNA m(2)G 1207 methyltransferase | *bmd_0125* | | **2.61** | - |
| 50S ribosomal protein L7Ae | *bmd_0128* | *rplGB* | 1.09 | - |
| 30S ribosomal protein S12 | *bmd_0129* | *rpsL* | - | - |
| 30S ribosomal protein S7 | *bmd_0130* | *rpsG* | - | - |
| Translation elongation factor G (EF-G) | *bmd_0131* | *fusA* | - | - |
| 30S ribosomal protein S10 | *bmd_0133* | *rpsJ* | - | - |
| 50S ribosomal protein L3 | *bmd_0134* | *rplC* | - | - |
| 50S ribosomal protein L4 | *bmd_0135* | *rplD* | - | - |
| 50S ribosomal protein L23 | *bmd_0136* | *rplW* | - | - |
| 50S ribosomal protein L2 | *bmd_0137* | *rplB* | - | - |
| 30S ribosomal protein S19 | *bmd_0138* | *rpsS* | - | - |
| 50S ribosomal protein L22 | *bmd_0139* | *rplV* | 1.01 | - |
| 30S ribosomal protein S3 | *bmd_0140* | *rpsC* | - | - |
| 50S ribosomal protein L16 | *bmd_0141* | *rplP* | - | - |
| 50S ribosomal protein L29 | *bmd_0142* | *rpmC* | - | - |
| 30S ribosomal protein S17 | *bmd_0143* | *rpsQ* | - | - |
| 50S ribosomal protein L14 | *bmd_0144* | *rplN* | - | - |
| 50S ribosomal protein L24 | *bmd_0145* | *rplX* | - | - |
| 50S ribosomal protein L5 | *bmd_0146* | *rplE* | - | - |
| 30S ribosomal protein S14 | *bmd_0147* | *rpsN* | - | - |
| 30S ribosomal protein S8 | *bmd_0148* | *rpsH* | - | - |
| 50S ribosomal protein L6 | *bmd_0149* | *rplF* | - | - |
| 50S ribosomal protein L18 | *bmd_0150* | *rplR* | - | - |
| 30S ribosomal protein S5 | *bmd_0151* | *rpsE* | - | - |
| 50S ribosomal protein L30 | *bmd_0152* | *rpmD* | - | - |
| 50S ribosomal protein L15 | *bmd_0153* | *rplO* | 1.03 | - |
| Preprotein translocase, SecY subunit | *bmd_0154* | *secY* | 1.03 | - |
| Adenylate kinase | *bmd_0155* | *adk* | 1.03 | - |
| Translation initiation factor IF-1 | *bmd_0157* | *infA* | - | - |
| tRNA pseudouridine synthase A | *bmd_0165* | *truA* | 1.19 | - |
| ATP-dependent RNA helicase | *bmd_0215* | | **2.60** | - |
| Antitoxin EndoAI (EndoA inhibitor) | *bmd_0221* | *ndoAI* | **2.47** | - |
| Endoribonuclease EndoA | *bmd_0222* | *ndoA* | **2.32** | 1.09 |
| 10 kDa chaperonin | *bmd_0260* | *groES* | - | **5.93** |
| 60 kDa chaperonin | *bmd_0261* | *groEL* | - | **6.31** |
| Hypoxanthine/guanine permease | *bmd_0266* | *pbuG* | - | - |
| Phosphoribosylaminoimidazole carboxylase, catalytic subunit | *bmd_0271* | *purE* | - | - |
| Phosphoribosylaminoimidazole carboxylase, ATPase subunit | *bmd_0272* | *purK* | - | - |
| Adenylosuccinate lyase | *bmd_0273* | *purB* | 1.04 | - |
| Phosphoribosylaminoimidazole-succinocarboxamide synthase | *bmd_0274* | *purC* | 1.02 | - |
| Phosphoribosylformylglycinamidine synthase, purS protein | *bmd_0275* | *purS* | 1.06 | - |
| Phosphoribosylformylglycinamidine synthase I | *bmd_0276* | *purQ* | 1.02 | - |
| Phosphoribosylformylglycinamidine synthase II | *bmd_0277* | *purL* | 1.01 | - |
| Amidophosphoribosyltransferase | *bmd_0278* | *purF* | 1.06 | - |
| Phosphoribosylformylglycinamidine cyclo-ligase | *bmd_0279* | *purM* | 1.07 | - |
| Phosphoribosylglycinamide formyltransferase | *bmd_0280* | *purN* | - | - |
| Bifunctional purine biosynthesis protein PurH | *bmd_0281* | *purH* | - | - |
| Putative nickel transporter | *bmd_0328* | | 1.27 | **1.91** |
| Conserved hypothetical protein | *bmd_0349* | | - | - |
| Conserved hypothetical protein | *bmd_0355* | | **2.13** | - |
| Conserved hypothetical protein | *bmd_0364* | | 1.19 | **3.46** |
| Intracellular protease, PfpI family | *bmd_0368* | | - | **3.26** |
| Phenolic acid decarboxylase (PAD) | *bmd_0380* | *PadC* | - | **2.33** |
| Peroxide operon regulator | *bmd_0417* | *perR* | **1.80** | - |
| Proton/sodium-glutamate symport protein | *bmd_0453* | | **1.88** | 1.42 |
| Biotin synthase | *bmd_0460* | *bioB* | - | **1.77** |
| Putative exported cell wall-binding protein | *bmd_0478* | *yocH* | 1.41 | - |
| Conserved hypothetical protein | *bmd_0515* | | - | **3.67** |

| Gene product | Gene ID | Gene symbol | 15°C | 45°C |
|---|---|---|---|---|
| Conserved hypothetical protein | *bmd_0518* | | **1.96** | 1.26 |
| Conserved hypothetical protein | *bmd_0521* | | 1.33 | **6.24** |
| L-lactate permease | *bmd_0523* | *lctP* | 1.10 | **1.75** |
| L-lactate dehydrogenase | *bmd_0524* | *ldh* | 1.07 | **2.52** |
| Thiazole biosynthesis protein ThiG | *bmd_0554* | *thiG* | - | **2.07** |
| Adenylyltransferase ThiF | *bmd_0555* | *thiF* | - | **2.18** |
| Phosphomethylpyrimidine kinase | *bmd_0556* | *thiD* | - | **2.11** |
| Enoyl-CoA hydratase / isomerase family protein | *bmd_0575* | | - | - |
| DNA-binding protein HU | *bmd_0576* | | - | **3.37** |
| Monooxygenase | *bmd_0599* | | - | **3.37** |
| Ferrochelatase | *bmd_0602* | *hemH* | - | **2.03** |
| Conserved hypothetical protein | *bmd_0638* | | **3.45** | **1.88** |
| Conserved hypothetical protein | *bmd_0668* | | - | **1.98** |
| N-acetyl-gamma-glutamyl-phosphate reductase | *bmd_0678* | *argC* | - | - |
| Arginine biosynthesis bifunctional protein ArgJ | *bmd_0679* | *argJ* | - | - |
| Acetylglutamate kinase | *bmd_0680* | *argB* | - | - |
| Acetylornithine aminotransferase | *bmd_0681* | *argD* | - | - |
| Carbamoyl-phosphate synthase, small subunit | *bmd_0682* | *carA* | - | - |
| Carbamoyl-phosphate synthase, large subunit | *bmd_0683* | *carB* | - | - |
| Ornithine carbamoyltransferase | *bmd_0684* | *argF* | - | - |
| Oligopeptide ABC transporter, oligopeptide-binding protein AppA | *bmd_0701* | *appA* | **2.70** | - |
| Oligopeptide ABC transporter, permease protein AppB | *bmd_0702* | *appB* | **2.05** | - |
| Oligopeptide ABC transporter, oligopeptide-binding protein OppA | *bmd_0706* | *oppA* | - | 1.26 |
| Oligopeptide ABC transporter, permease protein OppB | *bmd_0707* | *oppB* | - | 1.34 |
| Oligopeptide ABC transporter, permease protein OppC | *bmd_0708* | *oppC* | - | 1.42 |
| Oligopeptide ABC transporter, ATP-binding protein OppD, frameshift | *bmd_0709* | | - | 1.73 |
| Oligopeptide ABC transporter, ATP-binding protein OppF | *bmd_0710* | *oppF* | - | 1.66 |
| Competence regulatory protein Spx | *bmd_0714* | *spxA* | **2.27** | **3.05** |
| Competence-associated adapter protein | *bmd_0719* | *mecA* | 1.52 | **1.95** |
| Globin-like protein | *bmd_0725* | | - | **1.76** |
| 6-phosphogluconate dehydrogenase (decarboxylating) | *bmd_0753* | *gnd* | - | - |
| Conserved hypothetical protein | *bmd_0757* | | - | **2.67** |
| Sodium:solute symporter family | *bmd_0806* | | - | - |
| Amino acid permease | *bmd_0809* | | - | - |
| O-acetylhomoserine sulfhydrylase | *bmd_0817* | | - | **1.89** |
| Amino acid permease | *bmd_0827* | | 1.01 | - |
| Biotin biosynthesis protein BioY | *bmd_0828* | *bioY* | **2.48** | **3.32** |
| Dethiobiotin synthase | *bmd_0829* | *bioD* | **3.22** | **5.68** |
| Adenosylmethionine-8-amino-7-oxononanoate transaminase | *bmd_0830* | *bioA* | **3.08** | **4.67** |
| Integral membrane protein | *bmd_0832* | | **2.13** | - |
| Iron(III)-citrate import ABC transporter, iron(III)-citrate-binding protein | *bmd_0872* | *yfmC* | 1.05 | - |
| 6-phospho-3-hexuloisomerase | *bmd_0890* | | - | **3.91** |
| 3-hexulose-6-phosphate synthase | *bmd_0891* | *hxlA* | - | **5.91** |
| HTH-type transcriptional activator hxlR | *bmd_0892* | | - | **3.04** |
| Hypothetical protein | *bmd_0893* | | - | 1.09 |
| Conserved hypothetical protein | *bmd_0894* | | - | 1.13 |
| Hypothetical protein | *bmd_0904* | | 1.67 | **2.55** |
| Transcriptional regulator, IclR family | *bmd_0911* | | - | **2.55** |
| Oxidoreductase, aldo/keto reductase family | *bmd_0912* | | - | **3.63** |
| 4-aminobutyrate aminotransferase | *bmd_0945* | | - | - |
| Hypothetical protein | *bmd_0971* | | 1.54 | **1.99** |
| Cold shock protein | *bmd_0987* | *cspB* | **4.27** | - |
| 2-cys peroxiredoxin | *bmd_0990* | | **2.07** | - |
| Capsule biosynthesis protein CapB | *bmd_1003* | *capB* | **2.16** | - |
| Capsule biosynthesis protein CapC | *bmd_1004* | *capC* | **1.98** | - |
| Capsule biosynthesis protein CapA | *bmd_1005* | *capA* | **2.21** | - |
| Putative gamma glutamyl transferase | *bmd_1006* | | **2.24** | - |
| Hypothetical protein | *bmd_1007* | | **2.14** | - |
| CsbD-like protein | *bmd_1013* | | - | **9.62** |
| Phosphoenolpyruvate-dependent sugar phosphotransferase system, EIIA 2 domain protein | *bmd_1027* | | - | - |
| PTS system, lactose/cellobiose specific IIB subunit family protein | *bmd_1028* | | - | - |
| Putative sugar-specific permease | *bmd_1029* | | - | - |
| Oxidoreductase, aldo/keto reductase family | *bmd_1041* | | - | **3.50** |
| Conserved hypothetical protein | *bmd_1042* | | 1.01 | **1.89** |
| Hypothetical protein | *bmd_1049* | | 1.48 | **1.87** |
| Glucose uptake protein glcU | *bmd_1053* | | **1.78** | 1.03 |
| Hypothetical protein | *bmd_1058* | | 1.51 | **1.90** |
| Hypothetical protein | *bmd_1059* | | 1.14 | **2.00** |
| Proton/sodium-glutamate symport protein | *bmd_1062* | | - | - |
| O-succinylbenzoic acid (OSB) synthetase | *bmd_1072* | *menC* | - | **1.81** |
| Gamma-glutamyltransferase | *bmd_1095* | *ggt* | - | - |
| Glycosyl transferase, family 2 | *bmd_1118* | | - | - |
| Glycosyl transferase, group 1 | *bmd_1119* | | - | - |
| Pyruvate oxidase | *bmd_1131* | | - | **3.47** |
| Flavoenzyme | *bmd_1132* | *yerD* | - | **2.06** |
| Fructokinase | *bmd_1144* | | - | - |
| Glucose uptake protein | *bmd_1145* | *glcU* | - | - |
| Hypothetical protein | *bmd_1186* | | 1.14 | **2.24** |

| Gene product | Gene ID | Gene symbol | 15°C | 45°C |
|---|---|---|---|---|
| Peptide methionine sulfoxide reductase MsrA/MsrB | *bmd_1201* | *msrAB* | - | **2.91** |
| Polyhydroxyalkanoic acid inclusion protein PhaP | *bmd_1211* | *phaP* | **1.94** | - |
| Poly-beta-hydroxybutyrate-responsive repressor | *bmd_1212* | *phaQ* | **1.94** | 1.54 |
| Putative iron-sulfur heterodisulfide reductase | *bmd_1224* | | 1.23 | **6.37** |
| Iron-sulfur cluster binding protein | *bmd_1225* | | 1.16 | **8.28** |
| Conserved hypothetical protein | *bmd_1226* | | 1.16 | **7.12** |
| NADH dehydrogenase | *bmd_1241* | | - | **4.02** |
| ATP-dependent Clp protease, ATP-binding subunit ClpE | *bmd_1249* | *clpE* | - | **2.73** |
| Putative Na+/H+ antiporter NhaC | *bmd_1250* | *nhaC* | 1.10 | - |
| Hypothetical protein | *bmd_1264* | | 1.15 | **1.81** |
| PTS system, glucose-specific IIBC component | *bmd_1282* | *ptsG* | - | - |
| Phosphocarrier protein HPr | *bmd_1283* | *ptsH* | - | - |
| Phosphotransferase system (PTS) enzyme I | *bmd_1284* | *ptsI* | - | - |
| Conserved hypothetical protein | *bmd_1285* | | **1.93** | - |
| Protein of unknown function (DUF1797) | *bmd_1307* | | **4.79** | - |
| Putative 2-cys peroxiredoxin | *bmd_1314* | | - | **1.82** |
| Thiol-disulfide isomerase | *bmd_1315* | | - | 1.24 |
| Arginine decarboxylase | *bmd_1333* | *speA* | - | - |
| GTPase | *bmd_1340* | *bipA* | **2.02** | - |
| Protein of unknown function (DUF1507) | *bmd_1348* | | **1.77** | - |
| Zn-dependent protease | *bmd_1362* | | - | **1.79** |
| Aspartate aminotransferase | *bmd_1378* | *aspB* | - | 1.06 |
| Cold shock protein | *bmd_1404* | *cspA* | - | - |
| Conserved hypothetical protein | *bmd_1408* | | 1.03 | **2.07** |
| Conserved hypothetical protein | *bmd_1412* | | - | - |
| Hypothetical protein | *bmd_1445* | | **1.83** | - |
| Cold shock protein | *bmd_1450* | *cspD* | - | **3.91** |
| Conserved hypothetical protein | *bmd_1451* | | - | **2.41** |
| Fatty acid desaturase | *bmd_1474* | *des* | **2.88** | - |
| 2,5-diketo-D-gluconic acid reductase B | *bmd_1514* | | **1.79** | 1.51 |
| Ferritin-like domain protein | *bmd_1538* | | - | 1.35 |
| Glucose starvation-inducible protein B | *bmd_1557* | | - | 1.50 |
| Hypothetical protein | *bmd_1594* | | 1.30 | - |
| 2,5-diketo-D-gluconic acid reductase A | *bmd_1595* | | 1.36 | - |
| Cold shock protein | *bmd_1682* | *cspA* | - | **2.60** |
| Dihydrodipicolinate synthase | *bmd_1694* | *dapA* | - | **2.05** |
| Nickel import ABC transporter, nickel-binding protein NikA | *bmd_1702* | *nikA* | - | - |
| Nickel import ABC transporter, permease subunit NikB | *bmd_1703* | *nikB* | - | - |
| Nickel import ABC transporter, permease subunit NikC | *bmd_1704* | *nikC* | - | - |
| Nickel import ABC transporter, ATP-binding protein NikD | *bmd_1705* | *nikD* | - | - |
| Nickel import ABC transporter, ATP-binding protein NikE | *bmd_1706* | *nikE* | - | - |
| Cold shock protein | *bmd_1730* | *cspC* | **9.75** | - |
| Hypothetical protein | *bmd_1733* | | **1.99** | 1.25 |
| Conserved hypothetical protein | *bmd_1761* | | - | - |
| Glucose starvation-inducible protein B (General stress protein B) | *bmd_1781* | | - | 1.28 |
| Hypothetical protein | *bmd_1790* | | - | **1.92** |
| Hypothetical protein | *bmd_1795* | | - | **1.80** |
| Glucose 1-dehydrogenase | *bmd_1796* | | 1.20 | **2.04** |
| Branched-chain amino acid transport system II carrier protein | *bmd_1825* | *brnQ* | - | - |
| Cytochrome P450 | *bmd_1855* | | - | **5.17** |
| Conserved hypothetical protein | *bmd_1890* | | - | **2.09** |
| Universal stress protein family | *bmd_1891* | | - | **2.74** |
| Putative peptidoglycan binding domain protein | *bmd_1902* | | **2.14** | - |
| Methyltransferase | *bmd_1924* | | **1.81** | - |
| Conserved hypothetical protein | *bmd_1925* | | **1.86** | - |
| Helix-turn-helix domain of resolvase | *bmd_1926* | | - | - |
| Homoserine O-succinyltransferase | *bmd_1937* | *metA* | - | - |
| Glutathione peroxidase family protein | *bmd_1940* | | 1.09 | **2.05** |
| Putative metal ABC transporter, metal-binding protein | *bmd_1949* | | - | - |
| Transition state regulatory protein abrb | *bmd_1974* | *abrB* | 1.01 | - |
| 3-oxoacyl-[acyl-carrier protein] reductase | *bmd_1976* | | - | **1.83** |
| Amino acid/peptide transporter (Peptide:H+ symporter) | *bmd_2012* | *dtpT* | - | - |
| Conserved hypothetical protein | *bmd_2029* | | - | - |
| Malate dehydrogenase | *bmd_2037* | | - | - |
| Hypothetical protein | *bmd_2044* | | 1.27 | **2.39** |
| Glutamate synthase, large subunit | *bmd_2055* | *gltA* | - | - |
| Glutamate synthase, small subunit | *bmd_2056* | *gltB* | - | - |
| 3-oxoacyl-[acyl-carrier-protein] synthase III protein 1 | *bmd_2082* | | **1.77** | - |
| conserved hypothetical protein | *bmd_2098* | | - | **1.95** |
| Transcriptional regulator, Tetr family | *bmd_2113* | | - | **1.85** |
| Multidrug resistance protein, major facilitator (mfs) superfamily | *bmd_2114* | | - | **1.95** |
| General stress protein | *bmd_2117* | | - | **6.94** |
| S1 RNA binding domain protein | *bmd_2164* | | 1.06 | - |
| Protease | *bmd_2165* | | - | - |
| Conserved hypothetical protein | *bmd_2177* | | - | **2.03** |
| Hypothetical protein | *bmd_2185* | | **1.82** | - |
| NADH dehydrogenase | *bmd_2191* | | - | **69.4** |
| Organic hydroperoxide resistance protein | *bmd_2231* | *ohrB* | - | - |

| Gene product | Gene ID | Gene symbol | 15°C | 45°C |
|---|---|---|---|---|
| Peptidoglycan-binding protein | *bmd_2238* | | 1.12 | - |
| Pyrroline-5-carboxylate reductase | *bmd_2243* | *proH* | - | - |
| Gamma-glutamyl phosphate reductase | *bmd_2245* | *proA* | - | - |
| Conserved hypothetical protein | *bmd_2246* | | **2.66** | 1.05 |
| Glyoxalase family protein | *bmd_2247* | | **3.08** | 1.05 |
| Conserved hypothetical protein | *bmd_2250* | | 1.09 | **1.76** |
| Carboxylesterase | *bmd_2256* | | 1.15 | **1.91** |
| Fumarate hydratase, class II | *bmd_2279* | *fumC* | - | - |
| Conserved hypothetical protein | *bmd_2282* | | - | 1.30 |
| Bacillolysin precursor (neutral protease) | *bmd_2285* | *nprM* | **2.96** | - |
| Hypothetical protein | *bmd_2299* | | - | **2.18** |
| Putative proton glutamate symport protein | *bmd_2307* | | - | **1.91** |
| Diaminopimelate decarboxylase | *bmd_2308* | *lysA* | - | **2.76** |
| Acyl-coa dehydrogenase | *bmd_2315* | | - | **1.96** |
| Fructoselysine-6-P-deglycase | *bmd_2368* | *frlB* | - | **1.89** |
| Rhodanese Domain Protein | *bmd_2379* | | - | - |
| Chaperone protein HtpG | *bmd_2385* | *htpG* | - | **2.49** |
| Putative cation transporter regulator | *bmd_2410* | | - | **7.79** |
| NAD dependent epimerase/dehydratase family | *bmd_2433* | | - | **1.91** |
| Cell wall-associated protease | *bmd_2442* | | - | - |
| Secreted cell wall DL-endopeptidase | *bmd_2460* | *cwlO* | - | - |
| Acetyltransferase, GNAT family | *bmd_2481* | | - | **1.97** |
| Manganese-dependent inorganic pyrophosphatase | *bmd_2499* | *ppaC* | - | - |
| HAD superfamily hydrolase | *bmd_2513* | | - | - |
| MarR family | *bmd_2514* | | - | - |
| Carbonic anhydrase | *bmd_2585* | | **2.16** | 1.13 |
| CbiET protein | *bmd_2601* | *cbiET* | 1.58 | **1.80** |
| Cobalamin biosynthesis protein CbiD | *bmd_2602* | *cbiD* | **2.25** | **2.09** |
| Precorrin-8X methylmutase CbiC | *bmd_2603* | *cbiC* | **2.41** | **2.32** |
| Precorrin-6x reductase | *bmd_2604* | *cbiJ* | **2.29** | **2.26** |
| Sirohydrochlorin cobaltochelatase | *bmd_2605* | *cbiX* | **2.07** | **2.17** |
| Precorrin 3 methylase | *bmd_2606* | *cbiH* | **2.32** | **2.11** |
| Cobalamin biosynthesis protein | *bmd_2607* | *cbiW* | **2.00** | **1.81** |
| Branched-chain amino acid uptake carrier | *bmd_2611* | *brnQ* | - | - |
| IDEAL domain protein | *bmd_2614* | | 1.19 | **2.45** |
| Conserved hypothetical protein | *bmd_2617* | | 1.12 | **3.86** |
| NADH dehydrogenase Ndh | *bmd_2618* | *ndh* | 1.01 | **3.56** |
| Malate permease | *bmd_2629* | | 1.04 | - |
| Conserved hypothetical protein | *bmd_2630* | | - | **1.76** |
| Intracellular protease, PfpI family | *bmd_2637* | | - | - |
| Conserved hypothetical protein | *bmd_2648* | | - | **3.08** |
| Acetyltransferase, GNAT family | *bmd_2650* | | - | - |
| Conserved hypothetical protein | *bmd_2669* | | - | 1.04 |
| Bacillus transposase family protein | *bmd_2670* | | - | - |
| Conserved hypothetical protein | *bmd_2671* | | - | - |
| Conserved hypothetical protein | *bmd_2672* | | - | - |
| 2',3'-cyclic-nucleotide 2'-phosphodiesterase | *bmd_2688* | *yfkN* | - | - |
| Cold shock protein | *bmd_2695* | *cspC* | **4.53** | - |
| Cold shock protein | *bmd_2698* | *cspC* | **4.55** | - |
| Hypothetical protein | *bmd_2701* | | **1.80** | - |
| Acetyl-CoA hydrolase/transferase family protein | *bmd_2706* | | - | - |
| Conserved hypothetical protein | *bmd_2710* | | - | - |
| Cold shock protein | *bmd_2791* | *cspC* | - | **2.26** |
| Cold shock protein | *bmd_2794* | *cspC* | **5.48** | - |
| Na+/H+ antiporter, bacterial form | *bmd_2858* | | 1.02 | **2.11** |
| Hypothetical protein | *bmd_2885* | | - | - |
| Conserved hypothetical protein | *bmd_2897* | | - | - |
| Spore germination protein PF | *bmd_2907* | | 1.18 | - |
| Hypothetical protein | *bmd_2908* | | 1.23 | - |
| Hydrolase, alpha/beta fold family | *bmd_2949* | | - | **1.81** |
| Hypothetical protein | *bmd_2977* | | - | - |
| ThiJ/PfpI family protein | *bmd_3006* | | - | **2.02** |
| Hypothetical protein | *bmd_3026* | | **1.81** | - |
| 3-phosphoshikimate 1-carboxyvinyltransferase | *bmd_3027* | *aroE* | - | - |
| Prephenate dehydrogenase | *bmd_3028* | *tyrA* | - | - |
| Chorismate synthase | *bmd_3029* | *aroF* | - | - |
| Cell wall endopeptidase | *bmd_3039* | *lytF* | - | - |
| Hypothetical protein | *bmd_3041* | | - | - |
| Conserved hypothetical protein | *bmd_3047* | | - | - |
| Nicotinate-nucleotide--dimethylbenzimidazole phosphoribosyltransferase | *bmd_3069* | *cobT* | - | - |
| Conserved hypothetical protein | *bmd_3090* | | - | **2.70** |
| Hypothetical protein | *bmd_3095* | | - | **1.94** |
| ATP-dependent Clp protease, proteolytic subunit ClpP | *bmd_3096* | *clpP* | - | **1.97** |
| Hypothetical protein | *bmd_3097* | | - | **1.81** |
| Putative lipoprotein | *bmd_3111* | | - | **1.96** |
| Malate dehydrogenase | *bmd_3115* | | - | - |
| Putative aminoglycoside N3'-acetyltransferase | *bmd_3116* | | - | 1.22 |

| Gene product | Gene ID | Gene symbol | 15°C | 45°C |
|---|---|---|---|---|
| Hypothetical protein | *bmd_3145* | | - | **5.52** |
| Cytochrome aa3 quinol oxidase, subunit IV | *bmd_3153* | *qoxD* | - | **2.07** |
| Cytochrome aa3 quinol oxidase, subunit III | *bmd_3154* | *qoxC* | - | **2.19** |
| Cytochrome aa3 quinol oxidase, subunit I | *bmd_3155* | *qoxB* | - | **2.21** |
| Cytochrome aa3 quinol oxidase, subunit II | *bmd_3156* | *qoxA* | - | **2.07** |
| Conserved hypothetical protein | *bmd_3167* | | - | **1.85** |
| Hypothetical protein | *bmd_3173* | | 1.26 | **3.37** |
| LPXTG-motif cell wall anchor domain protein | *bmd_3174* | | - | - |
| Putative Membrane Protein | *bmd_3179* | | - | - |
| Thiol-disulfide oxidoreductase BdbC | *bmd_3189* | *bdbC* | - | **1.83** |
| Thiol-disulfide oxidoreductase BdbD | *bmd_3190* | *bdbD* | - | **2.40** |
| Peptidase, M56 domain protein | *bmd_3191* | | - | **1.87** |
| Conserved hypothetical protein | *bmd_3192* | | - | **1.82** |
| Hypothetical protein | *bmd_3197* | | - | 1.13 |
| Putative ferrichrome ABC transporter, ferrichrome-binding protein | *bmd_3216* | *yclQ* | - | - |
| Putative ferrichrome ABC transporter, ATP-binding protein | *bmd_3217* | *yclP* | - | - |
| Putative ferrichrome ABC transporter, permease protein | *bmd_3218* | *yclO* | - | - |
| Putative ferrichrome ABC transporter, permease protein | *bmd_3219* | *yclN* | - | - |
| Hypothetical protein | *bmd_3242* | | - | - |
| ABC transporter, ATP-binding protein | *bmd_3273* | | **2.64** | 1.07 |
| ABC transporter, permease protein | *bmd_3274* | | **2.05** | 1.07 |
| Aldehyde dehydrogenase (NAD) Family Protein | *bmd_3376* | | - | **1.93** |
| Cold shock protein | *bmd_3402* | *cspC* | **5.78** | - |
| Cold shock protein | *bmd_3404* | *cspC* | **17.9** | - |
| 5-methyltetrahydropteroyltriglutamate--homocysteine S-methyltransferase | *bmd_3527* | *metE* | 1.70 | **4.00** |
| Putative protease, NlpC/P60 family | *bmd_3550* | | - | - |
| 8-amino-7-oxononanoate synthase | *bmd_3693* | *bioF* | **2.26** | **2.33** |
| Biotin biosynthesis protein BioH | *bmd_3694* | *bioH* | 1.67 | **1.87** |
| Biotin biosynthesis protein BioC | *bmd_3695* | *bioC* | **1.75** | 1.72 |
| Putative membrane protein | *bmd_3699* | | - | **2.04** |
| Conserved hypothetical protein | *bmd_3787* | | - | **3.54** |
| RNA polymerase sigma-H factor | *bmd_3805* | *sigH* | 1.18 | - |
| Cold shock protein | *bmd_3807* | | **11.6** | - |
| Hypothetical protein | *bmd_3853* | | - | - |
| Inner membrane protein yccS | *bmd_3865* | | 1.05 | **1.96** |
| Protease production regulatory protein | *bmd_3883* | *hpr* | - | - |
| Putative serine proteinase | *bmd_3899* | | - | - |
| Drug resistance MFS transporter, drug:H+ antiporter-1 (14 Spanner) (DHA2) family | *bmd_3918* | | 1.13 | **3.49** |
| Amino acid carrier protein | *bmd_3967* | | - | - |
| Universal stress protein family | *bmd_3975* | | 1.42 | **1.82** |
| Sucrose utilization operon antiterminator | *bmd_4003* | *sacT* | - | - |
| Sugar phosphotransferase system, glucose subfamily, IIA component -PTS system | *bmd_4004* | *ptbA* | - | - |
| Hypothetical protein | *bmd_4014* | | - | 1.42 |
| Transketolase | *bmd_4073* | *tkt* | **1.89** | - |
| Glutamine synthetase, type I | *bmd_4086* | *glnA* | - | - |
| Glutamine synthetase repressor | *bmd_4087* | *glnR* | 1.09 | - |
| 2-oxoglutarate ferredoxin oxidoreductase subunit beta | *bmd_4100* | | - | - |
| 2-oxoglutarate ferredoxin oxidoreductase subunit alpha | *bmd_4101* | | - | - |
| Peptidase, M16 family protein | *bmd_4113* | | - | **1.87** |
| Transcriptional regulator, GntR family | *bmd_4119* | | - | - |
| Ribosome recycling factor | *bmd_4149* | *frr* | 1.11 | - |
| Uridylate kinase | *bmd_4150* | *pyrH* | 1.14 | - |
| 30S ribosomal protein S2 | *bmd_4152* | *rpsB* | 1.18 | - |
| Tyrosine recombinase XerC | *bmd_4187* | *xerC* | 1.06 | - |
| Succinate-CoA ligase, alpha subunit | *bmd_4191* | *sucD* | - | 1.72 |
| Succinate-CoA ligase, beta subunit | *bmd_4192* | *sucC* | - | 1.52 |
| Conserved hypothetical protein | *bmd_4200* | | 1.36 | - |
| 30S ribosomal protein S16 | *bmd_4201* | *rpsP* | 1.18 | - |
| Signal recognition particle protein | *bmd_4202* | *ffh* | **1.98** | - |
| Signal recognition particle associated protein | *bmd_4203* | | **2.35** | - |
| Orotate phosphoribosyltransferase | *bmd_4236* | *pyrE* | - | - |
| Orotidine 5'-phosphate decarboxylase | *bmd_4237* | *pyrF* | - | - |
| Dihydroorotate dehydrogenase, catalytic subunit | *bmd_4238* | *pyrD* | - | - |
| Dihydroorotate dehydrogenase, electron transfer subunit | *bmd_4239* | *pyrK* | - | - |
| Carbamoyl-phosphate synthase, large subunit | *bmd_4240* | *pyrAB* | - | - |
| Carbamoyl-phosphate synthase, small subunit | *bmd_4241* | *pyrAA* | - | - |
| Dihydroorotase | *bmd_4242* | *pyrC* | - | - |
| Aspartate carbamoyltransferase | *bmd_4243* | *pyrB* | - | - |
| Cell division protein FtsL | *bmd_4270* | *ftsL* | 1.10 | **1.95** |
| Acetyltransferase, GNAT family | *bmd_4278* | | - | **1.96** |
| 50S ribosomal protein L32 | *bmd_4281* | *rpmF* | 1.52 | - |
| Conserved Hypothetical Protein | *bmd_4282* | | **1.91** | - |
| nucleoside diphosphate kinase | *bmd_4314* | *ndk* | 1.55 | - |
| NAD-dependent glycerol-3-phosphate dehydrogenase | *bmd_4324* | *gpsA* | 1.10 | - |
| GTP-binding protein EngA | *bmd_4325* | *EngA* | 1.12 | - |
| Negative regulator of genetic competence | *bmd_4341* | *mecB* | **4.13** | - |
| D-3-phosphoglycerate dehydrogenase | *bmd_4351* | *serA* | - | - |
| Two-component sensor histidine kinase ResE | *bmd_4353* | *resE* | - | **2.05** |

| Gene product | Gene ID | Gene symbol | 15°C | 45°C |
|---|---|---|---|---|
| Two-component response regulator ResD | bmd_4354 | resD | - | 2.33 |
| Pseudouridine synthase | bmd_4358 | rluB | 1.83 | - |
| Oxidoreductase, aldo/keto reductase family | bmd_4389 | | - | 2.64 |
| Acetyl-coa acetyltransferase | bmd_4393 | | 1.63 | - |
| Arginine ABC transporter, ATP-binding protein ArtM | bmd_4416 | artM | - | - |
| Arginine ABC transporter, permease protein ArtQ | bmd_4417 | artQ | - | 2.21 |
| Arginine ABC transporter, arginine-binding protein ArtP | bmd_4418 | artP | - | - |
| Protein of unknown function (DUF1094) | bmd_4419 | | 1.50 | 2.01 |
| Amino acid/peptide transporter (Peptide:H+ symporter) | bmd_4434 | | - | 1.15 |
| Regulatory protein Spx | bmd_4482 | spxA | 1.80 | 1.25 |
| Superoxide dismutase (Mn) | bmd_4502 | sodA | - | 3.29 |
| Phosphate starvation-induced protein PhoH | bmd_4539 | phoH | 1.84 | 1.10 |
| Chaperone protein DnaK | bmd_4551 | dnaK | - | 1.60 |
| Co-Chaperone GrpE | bmd_4552 | grpE | - | 1.57 |
| Heat-inducible transcription repressor HrcA | bmd_4553 | hrcA | - | 1.49 |
| Transcription elongation factor GreA | bmd_4588 | greA | 1.31 | - |
| Alanyl-tRNA synthetase | bmd_4597 | alaS | - | - |
| Aspartyl-tRNA synthetase | bmd_4612 | aspS | - | - |
| Histidyl-tRNA synthetase | bmd_4613 | hisS | - | - |
| Conserved hypothetical protein | bmd_4632 | | - | 1.98 |
| Cysteine desulfurase | bmd_4639 | nifS | - | - |
| Septum site-determining protein MinD | bmd_4651 | minD | 1.36 | - |
| Septum site-determining protein MinC | bmd_4652 | minC | 1.63 | - |
| Protein of unknown function (DUF420) | bmd_4661 | | - | 2.44 |
| Glutamate-1-semialdehyde-2,1-aminomutase | bmd_4667 | hemL | - | 2.14 |
| Delta-aminolevulinic acid dehydratase | bmd_4668 | hemB | - | 1.91 |
| Uroporphyrinogen-III synthase | bmd_4669 | hemD | - | 1.82 |
| Porphobilinogen deaminase | bmd_4670 | hemC | - | 2.35 |
| Uroporphyrin-III C-methyltransferase | bmd_4671 | hemX | - | 1.97 |
| Glutamyl-tRNA reductase | bmd_4672 | hemA | - | 2.39 |
| Trigger factor | bmd_4678 | tig | 1.12 | - |
| 3-isopropylmalate dehydratase, large subunit | bmd_4681 | leuC | - | - |
| Aspartate kinase | bmd_4713 | lysC | - | 3.38 |
| Thioredoxin | bmd_4715 | trx | 1.28 | 3.60 |
| S-adenosylmethionine decarboxylase | bmd_4745 | speH | 1.17 | - |
| FxsA cytoplasmic membrane protein | bmd_4759 | | 1.82 | - |
| Argininosuccinate lyase | bmd_4775 | argH | - | - |
| Argininosuccinate synthase | bmd_4776 | argG | - | - |
| ATP-NAD kinase | bmd_4786 | ppnK | - | 1.16 |
| Conserved hypothetical protein | bmd_4806 | | 1.15 | 1.92 |
| Conserved hypothetical protein | bmd_4807 | | - | 2.69 |
| Protein of unknown function (DUF948) | bmd_4808 | | - | 1.96 |
| Transcriptional regulator (DeoR family) | bmd_4828 | | 1.16 | 3.12 |
| S-adenosylmethionine synthetase | bmd_4847 | metK | - | - |
| DNA-protecting protein | bmd_4857 | dps | - | 5.58 |
| Ribonucleoside-diphosphate reductase, beta subunit | bmd_4871 | nrdF | 1.29 | 3.01 |
| Ribonucleoside-diphosphate reductase, alpha subunit | bmd_4872 | nrdE | 1.32 | 2.57 |
| Glycogen phosphorylases | bmd_4881 | glgP | - | - |
| Glycogen synthase | bmd_4882 | glgA | - | - |
| Glucose-1-phosphate adenylyltransferase, GlgD subunit | bmd_4883 | glgD | - | - |
| Glucose-1-phosphate adenylyltransferase, GlgC subunit | bmd_4884 | glgC | - | - |
| 1,4-alpha-glucan branching enzyme | bmd_4885 | glgB | 1.02 | - |
| Sirohydrochlorin ferrochelatase | bmd_4913 | sirB | - | 1.78 |
| Uroporphyrin-III C-methyltransferase | bmd_4914 | sirA | - | 2.30 |
| Adenylylsulfate kinase | bmd_4915 | cysC | - | 2.48 |
| Sulfate adenylyltransferase | bmd_4916 | sat | - | 2.33 |
| Sulfate permease | bmd_4917 | cysP | 1.05 | 2.22 |
| S1 RNA binding domain-containing protein - general stress protein 13 | bmd_4933 | | 2.53 | 1.00 |
| Aminotransferase | bmd_4937 | patB | - | 1.75 |
| Metal-dependent phosphohydrolase | bmd_4944 | | - | 1.84 |
| Iron-sulfur cluster assembly accessory protein | bmd_4954 | | - | 2.10 |
| NifU-like domain protein | bmd_4959 | | 1.24 | 1.86 |
| SUF system FeS assembly protein | bmd_4977 | iscU | 1.39 | - |
| Cysteine desulfurase SufS | bmd_4978 | sufS | 1.37 | - |
| FeS assembly protein SufD | bmd_4979 | sufD | 1.34 | - |
| FeS assembly ATPase SufC | bmd_4980 | sufC | 1.42 | - |
| Methionine import ABC transporter, methionine-binding protein MetQ | bmd_4982 | metQ | - | - |
| Putative ferrichrome import ABC transporter, ferrichrome-binding protein | bmd_5000 | yfiY | 1.32 | - |
| ATP-dependent Clp protease, proteolytic subunit ClpP | bmd_5044 | clpP | 1.82 | 2.10 |
| Putative triphosphate pyrophosphate hydrolase | bmd_5049 | YvcI | - | 1.75 |
| Thioredoxin-disulfide reductase | bmd_5050 | trxB | - | 1.77 |
| Sigma 54 modulation protein / S30EA ribosomal protein | bmd_5086 | | 1.54 | 3.25 |
| UDP-N-acetylglucosamine 1-carboxyvinyltransferase | bmd_5130 | murA | 1.34 | - |
| Integral membrane protein (DUF1779) | bmd_5131 | | 2.01 | - |
| Integral membrane protein (DUF1146) | bmd_5132 | | 1.39 | - |
| ATP synthase F0, C subunit | bmd_5139 | atpE | - | - |
| ATP synthase F0, A subunit | bmd_5140 | atpB | - | - |
| Thymidine kinase | bmd_5156 | tdk | 1.08 | - |

| Gene product | Gene ID | Gene symbol | 15°C | 45°C |
|---|---|---|---|---|
| UDP-N-acetylglucosamine 1-carboxyvinyltransferase 2 | *bmd_5159* | *murAB* | **1.78** | - |
| Transaldolase | *bmd_5160* | *tal* | 1.67 | - |
| CTP synthase | *bmd_5164* | *pyrG* | 1.21 | - |
| DNA-directed RNA polymerase, delta subunit | *bmd_5165* | *rpoE* | 1.05 | - |
| Agmatinase | *bmd_5177* | *speB* | - | - |
| Spermidine synthase | *bmd_5178* | *speE* | - | - |
| Protein of unknown function (UPF0447) | *bmd_5189* | | - | **3.26** |
| Conserved hypothetical protein | *bmd_5193* | | - | **1.77** |
| ABC transporter, CydDC cysteine exporter (CydDC-E) family, permease/ATP-binding protein CydC | *bmd_5214* | *cydC* | 1.10 | **5.71** |
| ABC transporter, CydDC cysteine exporter (CydDC-E) family, permease/ATP-binding protein CydD | *bmd_5215* | *cydD* | 1.07 | **6.94** |
| Cytochrome d ubiquinol oxidase, subunit II | *bmd_5216* | *cydB* | 1.11 | **10.9** |
| Cytochrome d ubiquinol oxidase, subunit I | *bmd_5217* | *cydA* | 1.07 | **7.17** |
| Gamma-glutamyl phosphate reductase | *bmd_5223* | *proA* | - | - |
| Glutamate 5-kinase | *bmd_5224* | *proB* | - | - |
| Alpha-amylase | *bmd_5229* | *amyL* | - | **3.54** |
| Transporter, divalent anion:Na+ symporter (DASS) family protein | *bmd_5230* | | 1.03 | **2.18** |
| GTP-binding protein EngD | *bmd_5258* | *EngD* | 1.37 | - |
| Jag sporulation protein | *bmd_5269* | *jag* | 1.09 | - |
| Membrane protein OxaA | *bmd_5270* | *oxaA* | 1.14 | - |
| Ribonuclease P protein component | *bmd_5271* | *rnpA* | 1.22 | - |

**Table A.5: Modification of intracellular protein concentrations in *B. megaterium* DSM 319 grown at 45°C compared to 37°C.** Data are given as fold change (FC) of protein concentrations compared to their values at 37°C. They were obtained from LC-IMS$^e$-measurements carried out using four biological replicates for each cultivation condition. Only proteins that were identified in at least 2 out of 3 technical replicates and 2 out of 4 biological replicates were considered for analysis. Furthermore, only those whose concentration was at least 1.75-fold up- (**red**) or down-regulated (**blue**) were considered as significantly regulated and listed. Analysis of variance (ANOVA) was also applied to find proteins whose production is significantly modified under heat stress (indicated by bold writing).

| Protein Name | Protein ID | Protein Symbol | 45°C |
|---|---|---|---|
| Glycine/betaine ABC transporter, ATP-binding protein OpuAA | BMD_0860 | opuAA | **2.17** |
| Glycine/betaine ABC transporter, glycine/betaine-binding protein OpuAC | BMD_0861 | opuAC | **2.49** |
| Oligopeptide ABC transporter, oligopeptide-binding protein | BMD_1832 | | **-5.70** |
| Amino acid transporter | BMD_4096 | | **-4.68** |
| Phosphocarrier protein HPr | BMD_1283 | ptsH | **-5.40** |
| Putative metal ABC transporter, metal-binding protein | BMD_1949 | | **-7.55** |
| Putative ferrichrome import ABC transporter, ferrichrome-binding protein | BMD_5000 | yfiY | **-2.13** |
| ATP-binding Mrp protein | BMD_0170 | mrp | **-2.35** |
| Putative ABC transporter, ATP-binding protein | BMD_0254 | ydiF | **3.37** |
| Putative efflux ABC transporter, ATP-binding protein | BMD_0361 | yfmM | **-4.96** |
| Cell division initiation protein DivIVA | BMD_4250 | divIVA | **-2.50** |
| GTP-binding protein Era | BMD_4534 | era | **-1.85** |
| Septation ring formation regulator EzrA | BMD_4791 | ezrA | **-7.67** |
| Sporulation-control protein Spo0M | BMD_3021 | spo0M | **-1.85** |
| Sporulation-control protein Spo0M | BMD_4015 | spo0M | **2.50** |
| Sporulation initiation phosphotransferase F (response regulator) | BMD_5162 | spo0F | **-8.87** |
| Monooxygenase | BMD_0599 | | **2.87** |
| Tellurium resistance protein terD,TerD family | BMD_2686 | | **2.22** |
| Small heat shock protein | BMD_0077 | | **2.08** |
| Heat shock - Cstr acitivity | BMD_0104 | mcsB | **11.64** |
| 2-cys peroxiredoxin | BMD_0990 | | **-2.23** |
| GTPase | BMD_1340 | bipA | **-3.31** |
| Cold shock protein | BMD_1404 | cspA | **-2.26** |
| Ferritin-like domain protein | BMD_1538 | | **1.75** |
| General stress protein 17M | BMD_2208 | | **-4.00** |
| Succinate-semialdehyde dehydrogenase (NADP+) - general stress protein | BMD_4061 | | **2.85** |
| DNA-protecting protein | BMD_4857 | dps | **11.25** |
| Tyrosine-protein kinase capB | BMD_1124 | | **-1.88** |
| pur operon repressor | BMD_0064 | purR | **-2.58** |
| LexA repressor | BMD_4077 | lexA | **1.87** |
| GTP-binding protein Era | BMD_4534 | era | **-1.85** |
| ATP-dependent Clp protease ATP-binding subunit ClpC | BMD_0105 | clpC | **3.14** |
| NAD+ synthetase | BMD_1223 | nadE | **-1.88** |
| YkvE - MarR-type repressor/ transcriptional regulator | BMD_1245 | | **2.43** |
| Transcriptional regulator | BMD_1920 | | **-3.79** |
| Uracil phosphoribosyl transferase/pyrimidine operon regulatory protein | BMD_4245 | pyrR | **1.88** |
| Glutamate synthase, large subunit | BMD_2055 | gltA | **-2.07** |
| Glycine cleavage system P protein | BMD_4469 | gcvPB | **-2.53** |
| ATP synthase F1, gamma subunit | BMD_5135 | atpG | **-1.81** |
| ATP synthase F1, delta subunit | BMD_5137 | atpH | **-1.84** |
| NADH dehydrogenase Ndh | BMD_2618 | ndh | **2.16** |
| Cytochrome aa3 quinol oxidase, subunit II | BMD_3156 | qoxA | **2.04** |

| Protein Name | Protein ID | Protein Symbol | 45°C |
|---|---|---|---|
| Thioredoxin | BMD_4715 | trx | 1.76 |
| Thioredoxin | BMD_4815 | | 2.40 |
| Thioredoxin-disulfide reductase | BMD_5050 | trxB | 1.76 |
| Acetate kinase | BMD_4779 | ackA | 1.97 |
| Alpha-phosphoglucomutase | BMD_0536 | pgcA | -2.86 |
| Fructose-1,6-bisphosphatase | BMD_3400 | fbp | 2.53 |
| Transketolase | BMD_4073 | tkt | -1.90 |
| Transaldolase | BMD_5160 | tal | -3.90 |
| 6-phosphogluconate dehydrogenase, decarboxylating | BMD_5197 | gnd | -2.34 |
| Gluconate kinase | BMD_0754 | gntK | 2.12 |
| Fructokinase | BMD_1144 | | -2.09 |
| Inositol monophosphatase | BMD_1338 | suhB | 2.59 |
| NAD dependent epimerase/dehydratase family | BMD_2433 | | -3.75 |
| Scyllo-inositol dehydrogenase (NADP+) | BMD_2681 | | 5.85 |
| Sucrose-6-phosphate hydrolase | BMD_3852 | | -4.58 |
| Fumarate hydratase, class I | BMD_0387 | | -4.45 |
| Fumarate hydratase, class II | BMD_2279 | fumC | -1.80 |
| Aconitate hydratase 1 | BMD_2546 | acnA | -1.78 |
| Malate:quinone-oxidoreductase | BMD_2731 | mqo | -2.59 |
| 2-oxoglutarate dehydrogenase, E1 component | BMD_2926 | odhA | -6.34 |
| Malate dehydrogenase | BMD_3115 | | 1.90 |
| Malate dehydrogenase | BMD_4764 | | 3.91 |
| Glycogen synthase | BMD_4882 | glgA | -3.34 |
| Glucose-1-phosphate adenylyltransferase, GlgD subunit | BMD_4883 | glgD | -3.50 |
| 4-aminobutyrate aminotransferase | BMD_0945 | | -4.16 |
| Aldehyde dehydrogenase (NAD) Family Protein | BMD_1546 | | -2.01 |
| Cyanophycinase domain protein | BMD_1604 | | 4.21 |
| 4-hydroxy 2-oxovalerate aldolase | BMD_1715 | | 2.26 |
| Succinate-semialdehyde dehydrogenase (NADP+) - GABA utilization | BMD_4061 | | 2.85 |
| 4-oxalocrotonate tautomerase | BMD_5182 | | -4.54 |
| Signal recognition particle protein | BMD_4202 | ffh | 5.74 |
| Protein-export membrane protein SecDF | BMD_4620 | secDF | 3.20 |
| Lipoyltransferase and lipoate-protein ligase | BMD_0611 | | 1.76 |
| Peptidase, M16 family protein | BMD_4113 | | -2.51 |
| Zinc protease | BMD_4130 | mlpA | -2.13 |
| Lipoate protein ligase | BMD_4467 | | 1.88 |
| 10 kDa chaperonin | BMD_0260 | groES | 2.53 |
| 60 kDa chaperonin | BMD_0261 | groEL | 2.40 |
| ATP-dependent chaperone ClpB | BMD_0687 | clpB | 3.11 |
| Chaperone protein HtpG | BMD_2385 | htpG | 3.34 |
| Heat shock protein HslVU, ATPase subunit HslU | BMD_4185 | hslU | 1.82 |
| Chaperone protein DnaK | BMD_4551 | dnaK | 1.92 |
| Co-chaperone GrpE | BMD_4552 | grpE | 2.69 |
| D-alanyl-D-alanine carboxypeptidase | BMD_0014 | dacA | -2.60 |
| Amidohydrolase | BMD_0337 | | -2.70 |
| Intracellular protease, PfpI family | BMD_0368 | | 6.48 |
| Oligoendopeptidase F | BMD_0722 | pepF | -1.77 |
| ATP-dependent Clp protease, ATP-binding subunit ClpE | BMD_1249 | clpE | 2.85 |
| Immune inhibitor A metalloprotease | BMD_2278 | inhA | -2.25 |
| Aminopeptidase pepS (M29 family) | BMD_2887 | pepS | -2.83 |
| Cell wall endopeptidase | BMD_3039 | lytF | 1.79 |
| RIP metalloprotease RseP | BMD_4145 | rseP | 19.72 |
| Proline dipeptidase | BMD_4459 | | -3.46 |
| M42 glutamyl aminopeptidase | BMD_4732 | | -2.07 |
| ATP-dependent Clp protease, proteolytic subunit ClpP | BMD_5044 | clpP | 2.41 |
| Biotin synthase | BMD_0460 | bioB | -2.72 |
| Dethiobiotin synthase | BMD_0829 | bioD | 2.57 |
| Adenosylmethionine-8-amino-7-oxononanoate transaminase | BMD_0830 | bioA | 2.06 |
| 8-amino-7-oxononanoate synthase | BMD_3693 | bioF | 2.48 |
| Glutamate-1-semialdehyde-2,1-aminomutase | BMD_0411 | gsaB | -2.91 |
| Oxygen-independent coproporphyrinogen III oxidase 2 | BMD_0573 | | -3.31 |
| Nitroreductase family protein | BMD_2595 | cbiY | -2.19 |
| Precorrin-2 C20-methyltransferase | BMD_2600 | cbiL | -2.19 |
| Sirohydrochlorin cobaltochelatase | BMD_2605 | cbiX | 2.66 |
| Cobalamin biosynthesis protein | BMD_2607 | cbiW | -2.15 |
| Delta-aminolevulinic acid dehydratase | BMD_4668 | hemB | 2.44 |
| Sirohydrochlorin ferrochelatase | BMD_4913 | sirB | -1.84 |
| Menaquinone methyltransferase | BMD_4316 | menH | -1.84 |
| 3,4-dihydroxy-2-butanone 4-phosphate synthase/GTP cyclohydrolase II | BMD_1278 | ribAB | -1.94 |
| 6,7-dimethyl-8-ribityllumazine synthase | BMD_1279 | ribH | -2.66 |
| Thiamine biosynthesis protein ThiC | BMD_0450 | thiC | -1.80 |
| Glycine oxidase ThiO | BMD_0552 | thiO | 1.80 |
| Thiamine biosynthesis protein ThiS | BMD_0553 | thiS | -8.19 |
| Thiazole biosynthesis protein ThiG | BMD_0554 | thiG | 2.50 |
| Thiamine-phosphate pyrophosphorylase | BMD_2116 | thiE | -4.27 |
| Thiamine biosynthesis/tRNA modification protein ThiI | BMD_4789 | thiI | 3.43 |
| Cysteine desulfurase | BMD_4790 | iscS | -1.88 |
| Phosphomethylpyrimidine kinase | BMD_5201 | thiD | 2.05 |

| Protein Name | Protein ID | Protein Symbol | 45°C |
|---|---|---|---|
| NAD+ synthase | BMD_2163 | nadE | 2.05 |
| 2,5-diketo-D-gluconic acid reductase A | BMD_1595 | | -10.75 |
| 1-deoxy-D-xylulose 5-phosphate reductoisomerase | BMD_4146 | dxr | -1.89 |
| 4-hydroxy-3-methylbut-2-en-1-yl diphosphate synthase | BMD_4513 | ispG | 3.57 |
| Tryptophanyl-tRNA synthetase | BMD_0705 | trpS | -2.10 |
| Phenylalanyl-tRNA synthetase, beta subunit | BMD_4728 | pheT | -1.89 |
| Phenylalanyl-tRNA synthetase, alpha subunit | BMD_4729 | pheS | -1.79 |
| Leucyl-tRNA synthetase | BMD_4834 | leuS | -2.71 |
| Arginyl-tRNA synthetase | BMD_5175 | argS | -1.89 |
| 50S ribosomal protein L25/general stress protein Ctc | BMD_0069 | ctc | 11.70 |
| 50S ribosomal protein L22 | BMD_0139 | rplV | -1.84 |
| 50S ribosomal protein L17 | BMD_0161 | rplQ | 1.77 |
| 50S ribosomal protein L32 | BMD_4281 | rpmF | -2.44 |
| 30S ribosomal protein S20 | BMD_4558 | rpsT | -2.28 |
| 50S ribosomal protein L9 | BMD_5252 | rplI | 1.93 |
| Dimethyladenosine transferase | BMD_0058 | ksgA | 2.62 |
| RNA methyltransferase, TrmH family, group 2 | BMD_0443 | | 2.20 |
| Pseudouridine synthase | BMD_4246 | rluD | -2.19 |
| tRNA (5-methylaminomethyl-2-thiouridylate)-methyltransferase | BMD_4604 | trmU | -1.81 |
| Thiamine biosynthesis/tRNA modification protein ThiI | BMD_4789 | thiI | 3.43 |
| Dihydrouridine synthase (Dus) | BMD_5237 | | -1.80 |
| Translation initiation factor IF-1 | BMD_0157 | infA | -4.65 |
| GTPase | BMD_1340 | bipA | -3.31 |
| Sigma 54 modulation protein / S30EA ribosomal protein | BMD_5086 | | 4.47 |
| Peptidyl-tRNA hydrolase | BMD_0070 | pth | -1.82 |
| Anthranilate phosphoribosyltransferase | BMD_2992 | | -2.33 |
| 3-phosphoshikimate 1-carboxyvinyltransferase | BMD_3027 | aroE | 1.96 |
| 3-phosphoshikimate 1-carboxyvinyltransferase | BMD_4302 | aroE | -1.93 |
| Tryptophan synthase, alpha subunit | BMD_4305 | trpA | -1.75 |
| Anthranilate synthase component I | BMD_4310 | trpE | -2.24 |
| 3-dehydroquinate synthase | BMD_4311 | aroB | -2.13 |
| Chorismate synthase | BMD_4312 | aroF | -2.08 |
| Homocysteine S-methyltransferase | BMD_0849 | ybgG | -2.64 |
| Methylthioribose-1-phosphate isomerase | BMD_1230 | mtnA | 1.92 |
| Transaminase | BMD_1233 | mtnE | 2.36 |
| 2,3-diketo-5-methylthiopentyl-1-phosphate enolase | BMD_1234 | mtnW | 2.33 |
| Methionine synthase, vitamin-B12 dependent | BMD_1273 | metH | -4.00 |
| N-acetyldiaminopimelate deacetylase | BMD_1311 | dapL | -2.33 |
| Diaminopimelate decarboxylase | BMD_2308 | lysA | 1.98 |
| 5-methyltetrahydropteroyltriglutamate--homocysteine S-methyltransferase | BMD_3527 | metE | 19.08 |
| Diaminopimelate decarboxylase | BMD_4369 | lysA | -2.47 |
| 5'-methylthioadenosine/S-adenosylhomocysteine nucleosidase | BMD_4582 | mtnN | -2.70 |
| Aspartate kinase | BMD_4713 | lysC | 1.82 |
| N-acetyl-gamma-glutamyl-phosphate reductase | BMD_0678 | argC | -2.14 |
| Arginine biosynthesis bifunctional protein ArgJ | BMD_0679 | argJ | -2.52 |
| Acetylglutamate kinase | BMD_0680 | argB | -2.04 |
| Glutamate synthase, large subunit | BMD_2055 | gltA | -2.07 |
| Glutamate synthase, small subunit | BMD_2056 | gltB | -1.88 |
| Argininosuccinate lyase | BMD_4775 | argH | -2.35 |
| Gamma-glutamyl phosphate reductase | BMD_5223 | proA | 3.27 |
| Dihydroxy-acid dehydratase | BMD_2497 | ilvD | -1.78 |
| 3-isopropylmalate dehydratase, large subunit | BMD_4681 | leuC | -1.76 |
| O-acetylhomoserine sulfhydrylase | BMD_0817 | | 1.81 |
| D-3-phosphoglycerate dehydrogenase | BMD_4351 | serA | -10.81 |
| Putative cysteine synthase A | BMD_4826 | ytkP | 2.20 |
| Aminotransferase | BMD_4937 | patB | 1.98 |
| Histidine biosynthesis bifunctional protein HisI | BMD_5052 | hisI | -2.07 |
| Phosphoribosylformimino-5-aminoimidazole carboxamide ribotide isomerase | BMD_5054 | hisA | -1.83 |
| Aldehyde dehydrogenase (NAD) Family Protein | BMD_1546 | | -2.01 |
| Penicillin-binding protein | BMD_4500 | pbpA | -2.79 |
| Rod shape-determining protein MreC | BMD_4654 | mreC | -3.00 |
| UDP-N-acetylmuramate--alanine ligase | BMD_4810 | murC | -1.87 |
| UDP-N-acetylglucosamine 1-carboxyvinyltransferase 2 | BMD_5159 | murAB | -5.10 |
| Glycosyl transferase, family 2 | BMD_1117 | | -1.84 |
| UTP-glucose-1-phosphate uridylyltransferase | BMD_1126 | galU | 2.55 |
| Glycosyl transferase, family 2 | BMD_5207 | | 1.95 |
| Transcription-repair coupling factor | BMD_0072 | mfd | 1.91 |
| ATP-dependent DNA helicase PcrA | BMD_0288 | pcrA | -2.02 |
| DNA topoisomerase III | BMD_2189 | topB | 7.13 |
| LexA repressor | BMD_4077 | lexA | 1.87 |
| DNA polymerase III, alpha subunit | BMD_4143 | polC | 1.80 |
| DNA topoisomerase I | BMD_4189 | topA | 4.96 |
| Holliday junction DNA helicase RuvA | BMD_4630 | ruvA | 2.61 |
| DNA mismatch repair protein MutS | BMD_4723 | mutS | 1.78 |
| DNA-directed DNA polymerase X | BMD_4724 | polX | 2.76 |
| Excinuclease ABC, A subunit | BMD_5068 | uvrA | 2.65 |
| DNA-binding protein HU | BMD_2784 | | -1.78 |
| Tena/thi-4 family domain protein | BMD_0885 | | 2.70 |

| Protein Name | Protein ID | Protein Symbol | 45°C |
|---|---|---|---|
| Tryptophan RNA-binding attenuator protein | BMD_4318 | mtrB | -2.45 |
| RNA polymerase sigma factor | BMD_4528 | sigA | -2.47 |
| Transcription elongation factor GreA | BMD_4588 | greA | -1.89 |
| Transcriptional repressor of de novo NAD biosynthesis NadR | BMD_4640 | nadR | -3.38 |
| ATP-dependent RNA helicase | BMD_0215 | | -2.88 |
| Alpha-phosphoglucomutase | BMD_0536 | pgcA | -2.86 |
| 3-oxoacyl-(acyl-carrier-protein) synthase III | BMD_0696 | fabH | -1.93 |
| Polyhydroxyalkanoic acid synthase, PhaR subunit | BMD_1214 | phaR | -3.27 |
| Acetoacetyl-CoA reductase | BMD_1215 | phaB | -4.06 |
| Polyhydroxyalkanoic acid synthase, PhaC subunit | BMD_1216 | phaC | -2.48 |
| 3-oxoacyl-[acyl-carrier protein] reductase | BMD_1253 | | 1.81 |
| Acyl carrier protein | BMD_4207 | acpP | -1.76 |
| Glycerol-3-phosphate acyltransferase PlsX | BMD_4210 | plsX | 2.30 |
| Lipoamide acyltransferase E2 component of branched-chain alpha-keto acid dehydrogenase | BMD_4423 | bkdB | -2.21 |
| 2-oxoisovalerate dehydrogenase E1 component beta subunit | BMD_4424 | bkdAB | -1.87 |
| 2-oxoisovalerate dehydrogenase E1 component alpha subunit | BMD_4425 | bkdAA | -2.15 |
| Acyl-CoA dehydrogenase | BMD_2954 | | 2.17 |
| Glycerophosphoryl diester phosphodiesterase | BMD_4432 | | 1.85 |
| Polyhydroxyalkanoic acid inclusion protein PhaP | BMD_1211 | phaP | -2.91 |
| Aldehyde dehydrogenase (NAD) Family Protein | BMD_1546 | | -2.01 |
| acetyl-CoA acetyltransferase | BMD_4393 | | - |
| Ribonucleoside-diphosphate reductase, beta subunit | BMD_4871 | nrdF | 3.70 |
| Adenylate kinase | BMD_0155 | adk | -1.83 |
| Polynucleotide phosphorylase | BMD_4132 | pnp | -3.87 |
| Guanylate kinase | BMD_4231 | gmk | -2.19 |
| pur operon repressor | BMD_0064 | purR | -2.58 |
| Amidophosphoribosyltransferase | BMD_0278 | purF | -2.03 |
| Formyltetrahydrofolate deformylase | BMD_4046 | purU | -4.72 |
| Carbamoyl-phosphate synthase, small subunit | BMD_4241 | pyrAA | -1.87 |
| Purine nucleoside phosphorylase | BMD_4010 | deoD | -2.06 |
| Polynucleotide phosphorylase | BMD_4132 | pnp | -3.87 |
| Cytidine deaminase | BMD_4535 | cdd | 2.73 |
| 5'-methylthioadenosine/S-adenosylhomocysteine nucleosidase | BMD_4582 | mtnN | -2.70 |
| Phosphopentomutase | BMD_4382 | drm | 7.18 |
| HAD superfamily hydrolase | BMD_2513 | | -5.49 |
| Agmatinase | BMD_5177 | speB | -4.85 |
| Spermidine synthase | BMD_5178 | speE | 2.57 |
| Sulfite reductase (NADPH) hemoprotein, beta-component | BMD_3121 | cysI | -2.06 |
| Putative cysteine synthase A | BMD_4826 | ytkP | 2.20 |
| S-adenosylmethionine synthetase | BMD_4847 | metK | -1.87 |
| Bacillus transposase family protein | BMD_2670 | | -2.06 |
| ATP-dependent RNA helicase | BMD_0345 | | -2.18 |
| Putative quinone oxidoreductase, YhdH/YhfP family | BMD_0543 | | 3.67 |
| Putative esterase | BMD_0748 | | -3.52 |
| Oxidoreductase, aldo/keto reductase family | BMD_0912 | | 5.60 |
| Nitrilotriacetate monooxygenase component B | BMD_0928 | | 4.32 |
| Oxidoreductase, aldo/keto reductase family | BMD_1041 | | 2.13 |
| Nitroreductase family protein | BMD_1291 | | 2.69 |
| NADH-dependent dehydrogenase | BMD_2104 | | -2.86 |
| Serine/threonine protein phosphatase | BMD_2286 | | 1.88 |
| Acetyltransferase, GNAT family | BMD_2481 | | 1.96 |
| DinB family protein | BMD_3065 | | 2.72 |
| Oxidoreductase, zinc-binding dehydrogenase family | BMD_3180 | | 2.14 |
| Oxidoreductase, aldo/keto reductase family | BMD_3288 | | 2.42 |
| Aminotransferase family protein | BMD_3340 | | -2.75 |
| Flavodoxin-like fold family protein | BMD_3911 | | 3.64 |
| Ribosome biogenesis GTPase A | BMD_4194 | RbgA | -3.03 |
| Radical SAM enzyme, Cfr family | BMD_4224 | | -4.43 |
| Oxidoreductase, aldo/keto reductase family | BMD_4389 | | 4.75 |
| FAD/FMN-binding oxidoreductase | BMD_4401 | | 7.30 |
| HAD superfamily (subfamily IIIA) phosphatase, TIGR01668 | BMD_4572 | YqeG | -1.76 |
| Putative triphosphate pyrophosphate hydrolase | BMD_5049 | YvcI | 2.24 |
| Protein-tyrosine phosphatase | BMD_5149 | | 22.88 |
| Methyltransferase (glucose inhibited division protein) GidB | BMD_5266 | GidB | -1.90 |
| Geranylgeranylglyceryl phosphate synthase family protein | BMD_0287 | | 2.13 |
| Conserved hypothetical protein | BMD_0295 | | 2.42 |
| YhgE/Pip-like protein | BMD_0899 | | 3.62 |
| Putative RNA methylase protein family (UPF0020) | BMD_1421 | | -2.00 |
| S1 RNA binding domain protein | BMD_2164 | | -3.08 |
| ThiJ/PfpI family protein | BMD_3006 | | 4.93 |
| Putative metal-dependent hydrolase | BMD_3772 | | -3.06 |
| TPR-repeat-containing protein | BMD_4301 | | -2.00 |
| GTP-binding protein EngA | BMD_4325 | EngA | -1.86 |
| Protein of unknown function (DUF1094) | BMD_4419 | | -2.27 |
| Protein of unknown function (DUF322) | BMD_4446 | | 1.92 |
| Putative RNA-binding protein | BMD_4569 | | -10.82 |
| GTP-binding protein | BMD_4571 | | -2.67 |
| Protein of unknown function (DUF948) | BMD_4808 | | 3.92 |

| Protein Name | Protein ID | Protein Symbol | 45°C |
|---|---|---|---|
| Protein of unknown function (DUF1444) | BMD_4814 | | -1.97 |
| GTP-binding protein EngD | BMD_5258 | EngD | -1.84 |
| Hypothetical protein | BMD_1166 | | -2.13 |
| Hypothetical protein | BMD_1845 | | -3.97 |
| Hypothetical protein | BMD_3479 | | -3.32 |
| Conserved hypothetical protein | BMD_0003 | | -1.97 |
| Conserved hypothetical protein | BMD_0194 | | 2.04 |
| Conserved hypothetical protein | BMD_0371 | | -2.07 |
| Conserved hypothetical protein | BMD_0668 | | -1.90 |
| Conserved hypothetical protein | BMD_0695 | | 1.78 |
| Conserved hypothetical protein | BMD_0757 | | 2.84 |
| Conserved hypothetical protein | BMD_1376 | | 1.81 |
| Conserved hypothetical protein | BMD_1761 | | -3.29 |
| Conserved hypothetical protein | BMD_1799 | | -6.16 |
| Putative lipoprotein | BMD_1898 | | -1.81 |
| Conserved hypothetical protein | BMD_1966 | | 2.35 |
| Conserved hypothetical protein | BMD_2103 | | 2.86 |
| Conserved hypothetical protein | BMD_2122 | | 2.02 |
| Conserved hypothetical protein | BMD_2177 | | 1.86 |
| Conserved hypothetical protein | BMD_2425 | | 2.53 |
| Conserved hypothetical protein | BMD_3480 | | -2.72 |
| Conserved hypothetical protein | BMD_4272 | | 2.70 |
| Conserved hypothetical protein | BMD_4593 | | -2.33 |
| Conserved hypothetical protein | BMD_4694 | | -2.03 |
| Conserved hypothetical protein | BMD_4807 | | 1.99 |
| Conserved hypothetical protein | BMD_5066 | | 2.24 |

**Table A.6: Concentrations of intracellular proteinogenic amino acids in *B. megaterium* DSM319.** For all conditions, cell suspensions taken from three biological replicates at optical densities ($OD_{600nm}$) between 2 and 6 were fast filtered and intracellular amino acids extracted in aminobutyric acid (ABU) as described by Krömer et al. [281]. Amino acids were then quantified by HPLC using ABU as internal standard.

| | | Concentration [µmol/$g_{CDW}$] | | | | | | | |
|---|---|---|---|---|---|---|---|---|---|
| | NaCl [M] | 15°C | 37°C | 45°C | 0.3 M NaCl | 0.6 M NaCl | 0.9 M NaCl | 1.2 M NaCl | 1.8 M NaCl |
| Alanine | Mean [µmol/g] | 5.4 | 14.2 | 49.0 | 19.6 | 21.9 | 25.8 | 24.4 | 17.0 |
| | Standard deviation [µmol/g] | 0.5 | 1.2 | 6.0 | 1.8 | 2.4 | 3.1 | 1.7 | 1.6 |
| Arginine | Mean [µmol/g] | 4.4 | 5.9 | 7.5 | 6.1 | 7.3 | 8.3 | 8.0 | 3.0 |
| | Standard deviation [µmol/g] | 0.4 | 0.5 | 0.9 | 1.0 | 0.9 | 0.9 | 1.1 | 0.3 |
| Asparagine | Mean [µmol/g] | 1.3 | 4.3 | 25.2 | 4.0 | 4.5 | 6.0 | 5.8 | 1.3 |
| | Standard deviation [µmol/g] | 0.2 | 0.5 | 2.6 | 0.4 | 0.7 | 0.7 | 0.6 | 0.2 |
| Aspartate | Mean [µmol/g] | 10.0 | 5.2 | 6.1 | 4.5 | 5.7 | 6.3 | 6.7 | 15.3 |
| | Standard deviation [µmol/g] | 1.5 | 0.7 | 0.9 | 0.4 | 1.0 | 0.9 | 0.6 | 1.6 |
| Cysteine | Mean [µmol/g] | 2.3 | 11.7 | 10.0 | 4.8 | 6.4 | 6.5 | 4.4 | 4.4 |
| | Standard deviation [µmol/g] | 0.3 | 1.4 | 64.8 | 0.6 | 1.2 | 1.1 | 0.8 | 0.8 |
| Glutamate | Mean [µmol/g] | 439.3 | 440.8 | 508.1 | 594.0 | 690.6 | 636.8 | 465.6 | 544.1 |
| | Standard deviation [µmol/g] | 43.1 | 37.2 | 54.8 | 39.8 | 56.7 | 42.6 | 39.9 | 1.6 |
| Glutamine | Mean [µmol/g] | 8.8 | 4.7 | 7.3 | 3.5 | 6.7 | 10.0 | 10.4 | 15.3 |
| | Standard deviation [µmol/g] | 1.1 | 0.5 | 0.9 | 0.4 | 1.0 | 1.0 | 1.5 | 29.2 |
| Glycine | Mean [µmol/g] | 18.3 | 12.5 | 1.8 | 22.0 | 25.5 | 27.1 | 27.2 | 8.4 |
| | Standard deviation [µmol/g] | 2.0 | 1.7 | 0.2 | 1.8 | 2.8 | 1.9 | 2.2 | 0.8 |
| Histidine | Mean [µmol/g] | 1.5 | 3.7 | 18.7 | 3.2 | 3.8 | 3.8 | 4.5 | 1.6 |
| | Standard deviation [µmol/g] | 0.2 | 0.9 | 1.4 | 0.5 | 1.0 | 0.5 | 0.5 | 0.2 |
| Isoleucine | Mean [µmol/g] | 5.5 | 6.8 | 4.2 | 7.0 | 8.0 | 8.1 | 7.4 | 4.7 |
| | Standard deviation [µmol/g] | 0.8 | 0.5 | 0.4 | 0.8 | 0.8 | 1.1 | 0.8 | 0.5 |
| Leucine | Mean [µmol/g] | 2.7 | 7.1 | 12.7 | 7.1 | 8.9 | 7.0 | 6.0 | 4.4 |
| | Standard deviation [µmol/g] | 0.2 | 0.7 | 1.4 | 1.2 | 0.7 | 0.8 | 0.5 | 0.4 |
| Lysine | Mean [µmol/g] | 4.2 | 18.9 | 7.8 | 4.7 | 7.4 | 5.6 | 5.5 | 3.9 |
| | Standard deviation [µmol/g] | 0.4 | 2.5 | 1.2 | 0.4 | 1.3 | 0.4 | 0.4 | 0.3 |
| Methionine | Mean [µmol/g] | 2.8 | 4.4 | 14.4 | 3.8 | 5.3 | 5.2 | 5.1 | 0.8 |
| | Standard deviation [µmol/g] | 0.3 | 0.6 | 1.5 | 0.3 | 0.6 | 0.8 | 0.5 | 0.1 |
| Phenylalanine | Mean [µmol/g] | 1.3 | 5.4 | 4.8 | 4.5 | 5.8 | 6.5 | 6.6 | 2.8 |
| | Standard deviation [µmol/g] | 0.2 | 0.6 | 0.5 | 0.4 | 1.0 | 0.9 | 0.8 | 0.3 |
| Proline | Mean [µmol/g] | 33.8 | 33.8 | 33.8 | 181.5 | 921.8 | 1316.3 | 1339.0 | 2180.0 |
| | Standard deviation [µmol/g] | 5.0 | 5.0 | 5.0 | 29.2 | 109.3 | 122.2 | 151.2 | 168.2 |
| Serine | Mean [µmol/g] | 5.1 | 9.8 | 9.9 | 24.5 | 28.3 | 31.5 | 33.7 | 9.5 |
| | Standard deviation [µmol/g] | 1.0 | 0.9 | 1.1 | 2.6 | 3.4 | 3.7 | 2.9 | 1.1 |
| Threonine | Mean [µmol/g] | 3.4 | 7.1 | 10.8 | 7.0 | 9.2 | 8.4 | 6.5 | 4.1 |
| | Standard deviation [µmol/g] | 0.4 | 0.7 | 0.9 | 1.5 | 0.8 | 0.7 | 0.3 | 0.4 |
| Tryptophan | Mean [µmol/g] | 1.2 | 4.4 | 3.7 | 3.7 | 5.9 | 6.0 | 5.3 | 1.0 |
| | Standard deviation [µmol/g] | 0.2 | 0.6 | 0.3 | 0.4 | 0.7 | 0.7 | 0.8 | 0.1 |
| Tyrosine | Mean [µmol/g] | 0.7 | 1.9 | 2.0 | 2.1 | 2.8 | 2.8 | 2.8 | 1.4 |
| | Standard deviation [µmol/g] | 0.1 | 0.3 | 0.2 | 0.2 | 0.3 | 0.3 | 0.2 | 0.2 |
| Valine | Mean [µmol/g] | 15.3 | 18.0 | 3.7 | 22.7 | 24.9 | 25.1 | 28.0 | 18.9 |
| | Standard deviation [µmol/g] | 2.9 | 2.0 | 0.4 | 2.0 | 2.8 | 2.7 | 2.4 | 2.1 |

**Table A.7: Flux distributions obtained when labelling data from experiments with 1-$^{13}$C glucose and a mixture of 50 % U-$^{12}$C / 50 % U-$^{13}$C-glucose as substrate are combined for simulating metabolic fluxes in *B. megaterium* DSM319 growing at 15°C, 45°C and 37°C in presence of 0, 0.6 and 1.2 M NaCl.** Model from Tab. A.3 was used for simulation with OpenFlux and confidence intervals were calculated using the Monte-Carlo algorithm.

| | 37°C / 0 M NaCl | | | | 0.6 M NaCl | | | | 1.2 M NaCl | | | | 15°C | | | | 45°C | | | |
|---|---|---|---|---|---|---|---|---|---|---|---|---|---|---|---|---|---|---|---|---|
| | opt. | low | high | Δ | opt. | low | high | Δ | opt. | low | high | Δ | opt. | low | high | Δ | opt. | low | high | Δ |
| GLC6P <=> F6P | 58.3 | 58.0 | 58.6 | 0.3 | 53.2 | 52.7 | 54.0 | 0.6 | 46.8 | 45.6 | 48.5 | 1.5 | 57.3 | 56.7 | 59.3 | 1.3 | 56.6 | 56.3 | 56.8 | 0.3 |
| F6P = F16BP | 78.8 | 78.7 | 78.8 | 0.0 | 79.5 | 79.3 | 79.7 | 0.2 | 78.4 | 78.0 | 79.0 | 0.5 | 78.1 | 77.9 | 78.8 | 0.4 | 81.4 | 81.3 | 81.5 | 0.1 |
| F16BP = DHAP + G3P | 78.8 | 78.7 | 78.8 | 0.0 | 79.5 | 79.3 | 79.7 | 0.2 | 78.4 | 78.0 | 79.0 | 0.5 | 78.1 | 77.9 | 78.8 | 0.4 | 81.4 | 81.3 | 81.5 | 0.1 |
| DHAP = G3P | 78.8 | 78.7 | 78.8 | 0.0 | 79.5 | 79.3 | 79.7 | 0.2 | 78.4 | 78.0 | 79.0 | 0.5 | 78.1 | 77.9 | 78.8 | 0.4 | 81.4 | 81.3 | 81.5 | 0.1 |
| GLC6P = P5P + CO2 | 39.1 | 38.8 | 39.4 | 0.3 | 46.0 | 45.2 | 46.5 | 0.6 | 52.5 | 50.9 | 53.8 | 1.5 | 38.9 | 36.9 | 39.5 | 1.3 | 42.6 | 42.4 | 42.9 | 0.3 |
| P5P + P5P <=> S7P + G3P | 11.5 | 11.4 | 11.6 | 0.1 | 14.1 | 13.9 | 14.3 | 0.2 | 16.5 | 16.0 | 16.9 | 0.4 | 11.5 | 10.9 | 11.7 | 0.4 | 13.5 | 13.4 | 13.5 | 0.0 |
| S7P + G3P <=> E4P + F6P | 11.5 | 11.4 | 11.6 | 0.1 | 14.1 | 13.9 | 14.3 | 0.2 | 16.5 | 16.0 | 16.9 | 0.4 | 11.5 | 10.9 | 11.7 | 0.4 | 13.5 | 13.4 | 13.5 | 0.0 |
| E4P + P5P = F6P + G3P | 9.7 | 9.6 | 9.8 | 0.1 | 12.9 | 12.7 | 13.1 | 0.2 | 15.7 | 15.1 | 16.1 | 0.5 | 10.2 | 9.5 | 10.4 | 0.4 | 12.1 | 12.1 | 12.2 | 0.0 |
| G3P <=>3PG | 166.0 | 165.0 | 166.0 | 0.5 | 170.0 | 170.0 | 170.0 | 0.0 | 171.0 | 171.0 | 172.0 | 0.5 | 165.0 | 164.0 | 165.0 | 0.5 | 173.0 | 173.0 | 174.0 | 0.5 |
| 3PG = PEP | 158.0 | 158.0 | 159.0 | 0.5 | 165.0 | 165.0 | 166.0 | 0.5 | 168.0 | 167.0 | 168.0 | 0.5 | 159.0 | 159.0 | 159.0 | 0.0 | 169.0 | 169.0 | 169.0 | 0.0 |
| PEP = PYR | 122.0 | 121.0 | 124.0 | 1.5 | 130.0 | 128.0 | 134.0 | 3.0 | 138.0 | 137.0 | 139.0 | 1.0 | 165.0 | 162.0 | 168.0 | 3.0 | 133.0 | 131.0 | 135.0 | 0.5 |
| PYR = ACCOA + CO2 | 108.0 | 108.0 | 108.0 | 0.0 | 122.0 | 122.0 | 123.0 | 0.5 | 131.0 | 130.0 | 131.0 | 0.5 | 102.0 | 101.0 | 102.0 | 0.5 | 125.0 | 124.0 | 125.0 | 0.1 |
| ACCOA + OAA = AKG + CO2 | 25.4 | 25.3 | 25.5 | 0.1 | 42.4 | 42.2 | 42.6 | 0.2 | 59.9 | 59.5 | 60.5 | 0.5 | 53.0 | 52.8 | 53.7 | 0.5 | 27.7 | 27.7 | 27.8 | 0.0 |
| AKG = 0.5 SUC + 0.5 SUC + CO2 | 18.0 | 17.9 | 18.1 | 0.1 | 28.9 | 28.7 | 29.1 | 0.2 | 45.7 | 45.3 | 46.3 | 0.5 | 41.8 | 41.6 | 42.5 | 0.4 | 21.4 | 21.3 | 21.4 | 0.0 |
| SUC = MAL | 11.6 | 11.5 | 11.7 | 0.1 | 25.9 | 25.7 | 26.1 | 0.2 | 43.7 | 43.3 | 44.2 | 0.5 | 41.5 | 41.2 | 42.1 | 0.4 | 11.0 | 11.0 | 11.1 | 1.9 |
| MAL = OAA | 6.0 | 4.6 | 7.5 | 1.5 | 19.0 | 16.3 | 22.3 | 3.0 | 38.9 | 37.9 | 40.0 | 1.1 | 32.7 | 32.0 | 33.8 | 0.9 | 3.6 | 1.8 | 5.6 | 0.0 |
| PYR + CO2 = OAA | 0.0 | 0.0 | 0.0 | 0.0 | 0.0 | 0.0 | 0.0 | 0.0 | 0.0 | 0.0 | 0.0 | 0.0 | 38.9 | 37.2 | 41.3 | 2.1 | 0.0 | 0.0 | 0.0 | 1.8 |
| MAL = PYR + CO2 | 5.6 | 4.2 | 6.9 | 1.4 | 6.9 | 3.8 | 9.4 | 2.8 | 4.8 | 4.3 | 5.4 | 0.6 | 8.8 | 8.3 | 9.3 | 0.5 | 7.5 | 5.6 | 9.2 | 1.8 |
| OAA <=> PEP + CO2 | -32.9 | -34.3 | -31.6 | 1.4 | -32.1 | -34.5 | -29.0 | 2.8 | -27.3 | -27.9 | -26.8 | 0.5 | 8.3 | 6.1 | 11.2 | 2.5 | -33.5 | -35.2 | -31.6 | 2.0 |
| CO2 = CO2_EX | 163.0 | 163.0 | 163.0 | 0.0 | 214.0 | 214.0 | 214.0 | 0.0 | 266.0 | 266.0 | 266.0 | 0.0 | 214.0 | 214.0 | 214.0 | 0.0 | 190.0 | 190.0 | 190.0 | 0.0 |

**Table A.8: Flux distributions obtained when only labelling data from experiments with 1-$^{13}$C glucose as substrate are used for simulating metabolic fluxes in *B. megaterium* DSM319 growing at 15°C, 45°C and 37°C in presence up to 1.8 M NaCl.** Simulation with OpenFlux was performed using a modified version of model from Tab. A.3 where pyruvate and phosphoenolpyruvate as well as malate and oxaloacetate were considered as global pools.

| | 37°C / 0 M NaCl | | | | 0.3 M NaCl | | | | 0.6 M NaCl | | | | 0.9 M NaCl | | | | 1.2 M NaCl | | | | 1.8 M NaCl | | | |
|---|---|---|---|---|---|---|---|---|---|---|---|---|---|---|---|---|---|---|---|---|---|---|---|---|
| | opt | low | high | Δ | opt | low | high | Δ | opt | low | high | Δ | opt | low | high | Δ | opt | low | high | Δ | opt | low | high | Δ |
| GLC6P <=> F6P | 54.7 | 54.0 | 55.6 | 0.8 | 53.9 | 53.6 | 54.5 | 0.4 | 52.1 | 51.6 | 52.8 | 0.6 | 49.9 | 49.6 | 50.3 | 0.3 | 47.4 | 47.1 | 48.0 | 0.4 | 46.5 | 46.3 | 46.7 | 0.2 |
| F6P = F16BP | 76.7 | 76.4 | 77.0 | 0.3 | 78.4 | 78.3 | 78.6 | 0.1 | 78.5 | 78.3 | 78.7 | 0.2 | 78.8 | 78.7 | 78.9 | 0.1 | 78.3 | 78.2 | 78.5 | 0.1 | 79.4 | 79.4 | 79.5 | 0.0 |
| F16BP = DHAP + G3P | 76.7 | 76.4 | 77.0 | 0.3 | 78.4 | 78.3 | 78.6 | 0.1 | 78.5 | 78.3 | 78.7 | 0.2 | 78.8 | 78.7 | 78.9 | 0.1 | 78.3 | 78.2 | 78.5 | 0.1 | 79.4 | 79.4 | 79.5 | 0.0 |
| DHAP = G3P | 76.7 | 76.4 | 77.0 | 0.3 | 78.4 | 78.3 | 78.6 | 0.1 | 78.5 | 78.3 | 78.7 | 0.2 | 78.8 | 78.7 | 78.9 | 0.1 | 78.3 | 78.2 | 78.5 | 0.1 | 79.4 | 79.4 | 79.5 | 0.0 |
| GLC6P = P5P + CO2 | 42.0 | 41.1 | 42.7 | 0.8 | 44.2 | 43.6 | 44.6 | 0.5 | 47 | 46.3 | 47.5 | 0.6 | 49.4 | 49.0 | 49.7 | 0.4 | 51.9 | 51.4 | 52.3 | 0.4 | 52.9 | 52.7 | 53.0 | 0.1 |
| P5P + P5P <=> S7P + G3P | 12.2 | 11.9 | 12.4 | 0.3 | 13.4 | 13.2 | 13.5 | 0.2 | 14.3 | 14 | 14.5 | 0.25 | 15.4 | 15.2 | 15.4 | 0.1 | 16.2 | 16.0 | 16.3 | 0.2 | 17.0 | 16.9 | 17.0 | 0.1 |
| S7P + G3P <=> E4P + F6P | 12.2 | 11.9 | 12.4 | 0.3 | 13.4 | 13.2 | 13.5 | 0.2 | 14.3 | 14 | 14.5 | 0.25 | 15.4 | 15.2 | 15.4 | 0.1 | 16.2 | 16.0 | 16.3 | 0.2 | 17.0 | 16.9 | 17.0 | 0.1 |
| E4P + P5P = F6P + G3P | 10.6 | 10.3 | 10.8 | 0.3 | 11.8 | 11.6 | 12.0 | 0.2 | 13 | 12.8 | 13.2 | 0.2 | 14.2 | 14.1 | 14.3 | 0.1 | 15.4 | 15.2 | 15.5 | 0.2 | 16.6 | 16.6 | 16.7 | 0.0 |
| G3P <=>3PG | 162.0 | 162.0 | 163.0 | 0.5 | 167.0 | 167.0 | 167.0 | 0.0 | 168 | 168 | 169 | 0.5 | 170.0 | 170.0 | 171.0 | 0.5 | 171.0 | 171.0 | 171.0 | 0.0 | 174.0 | 174.0 | 174.0 | 0.0 |
| 3PG = PYR | 156.0 | 155.0 | 156.0 | 0.5 | 160.0 | 160.0 | 161.0 | 0.5 | 163 | 162 | 163 | 0.5 | 166.0 | 166.0 | 166.0 | 0.0 | 167.0 | 167.0 | 167.0 | 0.0 | 172.0 | 172.0 | 172.0 | 0.0 |
| PYR = ACCOA + CO2 | 103.0 | 102.0 | 103.0 | 0.5 | 113.0 | 113.0 | 113.0 | 0.0 | 118 | 117 | 118 | 0.5 | 128.0 | 128.0 | 128.0 | 0.0 | 129.0 | 129.0 | 129.0 | 0.0 | 142.0 | 142.0 | 142.0 | 0.0 |
| ACCOA + OAA = AKG + CO2 | 29.4 | 29.2 | 29.7 | 0.3 | 25.7 | 25.5 | 25.9 | 0.2 | 35.6 | 35.4 | 35.8 | 0.2 | 45.0 | 44.9 | 45.2 | 0.2 | 45.7 | 45.6 | 45.9 | 0.1 | 59.7 | 59.6 | 59.7 | 0.1 |
| AKG = 0.5 SUC + 0.5 SUC + CO2 | 22.7 | 22.5 | 23.0 | 0.3 | 12.0 | 11.9 | 12.2 | 0.1 | 20.1 | 19.9 | 20.3 | 0.2 | 30.3 | 30.2 | 30.4 | 0.1 | 31.1 | 31.0 | 31.3 | 0.2 | 39.9 | 39.8 | 39.9 | 0.1 |
| SUC = OAA | 16.4 | 16.2 | 16.7 | 0.3 | 9.8 | 9.7 | 10.0 | 0.2 | 17.3 | 17.2 | 17.6 | 0.2 | 28.9 | 28.8 | 29.0 | 0.1 | 29.2 | 29.1 | 29.4 | 0.1 | 39.3 | 39.2 | 39.3 | 0.0 |
| PYR + CO2 <=> OAA | 27.8 | 27.8 | 27.8 | 0.0 | 26.9 | 26.9 | 26.9 | 0.0 | 26.4 | 26.4 | 26.4 | 0 | 22.9 | 22.9 | 22.9 | 0.0 | 22.1 | 22.1 | 22.1 | 0.0 | 21.5 | 21.5 | 21.5 | 0.0 |
| CO2 = CO2_EX | 169.0 | 169.0 | 169.0 | 0.0 | 168.0 | 168.0 | 168.0 | 0.0 | 194 | 194 | 194 | 0 | 230.0 | 230.0 | 230.0 | 0.0 | 236.0 | 236.0 | 236.0 | 0.0 | 273.0 | 273.0 | 273.0 | 0.0 |

**Table A.9: Comparison between measured and simulated labelling patterns of proteinogenic amino acids and intracellular polyhydroxybutyric acid when labelling data from tracer experiments with 1-$^{13}$C glucose and a mixture of 50 % U-$^{12}$C / 50 % U-$^{13}$C as substrates are used for simulation of metabolic fluxes in cells growing at 15°C, 45°C and 37°C in presence of 0 M, 0.6 M and 1.2 M NaCl**
Model from Tab. A.3 was used for simulation with OpenFlux.

| | | | 37°C / 0 M NaCl | | 15°C | | 45°C | | 0.6 M NaCl | | 1.2 M NaCl | |
|---|---|---|---|---|---|---|---|---|---|---|---|---|
| | | | Sim | Exp | Sim | Exp | Sim | Exp | Sim | Exp | Sim | Exp |
| 1-$^{13}$C labelling | Ala 260 | m+0 | 0.502 | 0.507 | 0.500 | 0.507 | 0.513 | 0.520 | 0.522 | 0.526 | 0.546 | 0.548 |
| | | m+1 | 0.362 | 0.362 | 0.362 | 0.363 | 0.355 | 0.352 | 0.347 | 0.347 | 0.329 | 0.329 |
| | | m+2 | 0.105 | 0.102 | 0.107 | 0.101 | 0.103 | 0.099 | 0.102 | 0.099 | 0.099 | 0.096 |
| | | m+3 | 0.031 | 0.030 | 0.031 | 0.030 | 0.030 | 0.029 | 0.029 | 0.028 | 0.027 | 0.026 |
| | Ala 232 | m+0 | 0.536 | 0.529 | 0.534 | 0.530 | 0.544 | 0.541 | 0.552 | 0.548 | 0.574 | 0.571 |
| | | m+1 | 0.365 | 0.371 | 0.365 | 0.370 | 0.358 | 0.361 | 0.350 | 0.355 | 0.331 | 0.335 |
| | | m+2 | 0.100 | 0.100 | 0.101 | 0.099 | 0.098 | 0.098 | 0.098 | 0.097 | 0.095 | 0.095 |
| | Val 288 | m+0 | 0.334 | 0.333 | 0.332 | 0.332 | 0.347 | 0.348 | 0.359 | 0.357 | 0.391 | 0.390 |
| | | m+1 | 0.404 | 0.406 | 0.403 | 0.406 | 0.401 | 0.402 | 0.397 | 0.398 | 0.385 | 0.386 |
| | | m+2 | 0.190 | 0.191 | 0.191 | 0.191 | 0.183 | 0.183 | 0.178 | 0.179 | 0.163 | 0.164 |
| | | m+3 | 0.056 | 0.055 | 0.057 | 0.055 | 0.054 | 0.053 | 0.052 | 0.052 | 0.048 | 0.047 |
| | | m+4 | 0.014 | 0.013 | 0.014 | 0.014 | 0.013 | 0.013 | 0.012 | 0.012 | 0.011 | 0.011 |
| | | m+5 | 0.002 | 0.002 | 0.002 | 0.002 | 0.002 | 0.002 | 0.002 | 0.002 | 0.002 | 0.002 |
| | Val 260 | m+0 | 0.348 | 0.338 | 0.346 | 0.338 | 0.359 | 0.352 | 0.370 | 0.363 | 0.403 | 0.396 |
| | | m+1 | 0.406 | 0.408 | 0.406 | 0.408 | 0.403 | 0.404 | 0.398 | 0.400 | 0.385 | 0.387 |
| | | m+2 | 0.182 | 0.188 | 0.184 | 0.188 | 0.176 | 0.181 | 0.172 | 0.176 | 0.157 | 0.161 |
| | | m+3 | 0.052 | 0.053 | 0.052 | 0.053 | 0.050 | 0.051 | 0.049 | 0.049 | 0.045 | 0.045 |
| | | m+4 | 0.012 | 0.013 | 0.012 | 0.013 | 0.012 | 0.012 | 0.011 | 0.011 | 0.010 | 0.010 |
| | Thr 404 | m+0 | 0.340 | 0.345 | 0.337 | 0.345 | 0.349 | 0.351 | 0.347 | 0.351 | 0.360 | 0.364 |
| | | m+1 | 0.378 | 0.378 | 0.377 | 0.378 | 0.376 | 0.376 | 0.374 | 0.374 | 0.368 | 0.368 |
| | | m+2 | 0.191 | 0.189 | 0.193 | 0.189 | 0.187 | 0.186 | 0.190 | 0.187 | 0.185 | 0.183 |
| | | m+3 | 0.070 | 0.069 | 0.072 | 0.070 | 0.069 | 0.068 | 0.070 | 0.069 | 0.068 | 0.066 |
| | | m+4 | 0.020 | 0.019 | 0.021 | 0.019 | 0.019 | 0.019 | 0.020 | 0.019 | 0.019 | 0.019 |
| | Thr 376 | m+0 | 0.370 | 0.374 | 0.375 | 0.378 | 0.372 | 0.376 | 0.382 | 0.383 | 0.395 | 0.398 |
| | | m+1 | 0.382 | 0.383 | 0.380 | 0.381 | 0.380 | 0.381 | 0.376 | 0.377 | 0.369 | 0.369 |
| | | m+2 | 0.183 | 0.179 | 0.180 | 0.177 | 0.182 | 0.179 | 0.179 | 0.177 | 0.175 | 0.173 |
| | | m+3 | 0.066 | 0.064 | 0.065 | 0.063 | 0.065 | 0.064 | 0.064 | 0.063 | 0.062 | 0.061 |
| | Asp 418 | m+0 | 0.339 | 0.346 | 0.336 | 0.344 | 0.348 | 0.351 | 0.346 | 0.351 | 0.360 | 0.364 |
| | | m+1 | 0.378 | 0.376 | 0.376 | 0.377 | 0.375 | 0.374 | 0.373 | 0.373 | 0.368 | 0.367 |
| | | m+2 | 0.191 | 0.188 | 0.194 | 0.189 | 0.188 | 0.186 | 0.190 | 0.187 | 0.185 | 0.183 |
| | | m+3 | 0.071 | 0.070 | 0.073 | 0.070 | 0.069 | 0.069 | 0.071 | 0.069 | 0.068 | 0.067 |
| | | m+4 | 0.020 | 0.020 | 0.021 | 0.020 | 0.020 | 0.019 | 0.020 | 0.020 | 0.019 | 0.019 |
| | Asp 390 | m+0 | 0.369 | 0.374 | 0.375 | 0.377 | 0.371 | 0.375 | 0.381 | 0.383 | 0.394 | 0.397 |
| | | m+1 | 0.381 | 0.382 | 0.379 | 0.381 | 0.380 | 0.380 | 0.375 | 0.376 | 0.368 | 0.368 |
| | | m+2 | 0.183 | 0.180 | 0.181 | 0.178 | 0.183 | 0.180 | 0.179 | 0.178 | 0.175 | 0.173 |
| | | m+3 | 0.066 | 0.065 | 0.066 | 0.064 | 0.066 | 0.065 | 0.065 | 0.064 | 0.063 | 0.062 |
| | Asp 316 | m+0 | 0.406 | 0.408 | 0.412 | 0.412 | 0.408 | 0.409 | 0.419 | 0.417 | 0.434 | 0.433 |
| | | m+1 | 0.390 | 0.386 | 0.387 | 0.386 | 0.388 | 0.385 | 0.382 | 0.380 | 0.373 | 0.370 |
| | | m+2 | 0.158 | 0.154 | 0.155 | 0.153 | 0.158 | 0.156 | 0.154 | 0.153 | 0.149 | 0.148 |
| | | m+3 | 0.047 | 0.051 | 0.046 | 0.050 | 0.046 | 0.050 | 0.045 | 0.050 | 0.044 | 0.049 |
| | Glu 432 | m+0 | 0.242 | 0.247 | 0.245 | 0.245 | 0.247 | 0.252 | 0.258 | 0.260 | 0.278 | 0.281 |
| | | m+1 | 0.367 | 0.368 | 0.367 | 0.369 | 0.367 | 0.367 | 0.367 | 0.367 | 0.366 | 0.365 |
| | | m+2 | 0.244 | 0.241 | 0.242 | 0.242 | 0.241 | 0.239 | 0.235 | 0.234 | 0.225 | 0.224 |
| | | m+3 | 0.104 | 0.102 | 0.103 | 0.102 | 0.103 | 0.101 | 0.100 | 0.098 | 0.094 | 0.093 |
| | | m+4 | 0.034 | 0.033 | 0.034 | 0.033 | 0.034 | 0.033 | 0.032 | 0.032 | 0.030 | 0.030 |
| | | m+5 | 0.009 | 0.009 | 0.009 | 0.009 | 0.009 | 0.008 | 0.008 | 0.008 | 0.008 | 0.008 |

**Table A.9 (continued)**

| | | | 37°C / 0 M NaCl | | 15°C | | 45°C | | 0.6 M NaCl | | 1.2 M NaCl | |
|---|---|---|---|---|---|---|---|---|---|---|---|---|
| | | | Sim | Exp | Sim | Exp | Sim | Exp | Sim | Exp | Sim | Exp |
| 1-$^{13}$C labelling | Glu 330 | m+0 | 0.331 | 0.323 | 0.322 | 0.320 | 0.343 | 0.341 | 0.346 | 0.343 | 0.377 | 0.371 |
| | | m+1 | 0.402 | 0.402 | 0.400 | 0.402 | 0.400 | 0.399 | 0.395 | 0.396 | 0.385 | 0.386 |
| | | m+2 | 0.193 | 0.199 | 0.199 | 0.200 | 0.187 | 0.188 | 0.187 | 0.189 | 0.173 | 0.176 |
| | | m+3 | 0.059 | 0.061 | 0.063 | 0.062 | 0.056 | 0.057 | 0.058 | 0.059 | 0.053 | 0.054 |
| | | m+4 | 0.014 | 0.015 | 0.016 | 0.016 | 0.014 | 0.014 | 0.014 | 0.015 | 0.013 | 0.013 |
| | Ser 390 | m+0 | 0.440 | 0.448 | 0.441 | 0.445 | 0.450 | 0.457 | 0.460 | 0.465 | 0.480 | 0.482 |
| | | m+1 | 0.365 | 0.363 | 0.364 | 0.364 | 0.359 | 0.356 | 0.353 | 0.351 | 0.339 | 0.338 |
| | | m+2 | 0.144 | 0.141 | 0.144 | 0.141 | 0.142 | 0.139 | 0.140 | 0.138 | 0.136 | 0.135 |
| | | m+3 | 0.051 | 0.049 | 0.051 | 0.049 | 0.049 | 0.048 | 0.048 | 0.047 | 0.045 | 0.045 |
| | Ser 362 | m+0 | 0.475 | 0.476 | 0.476 | 0.475 | 0.482 | 0.485 | 0.491 | 0.493 | 0.510 | 0.512 |
| | | m+1 | 0.379 | 0.380 | 0.379 | 0.381 | 0.374 | 0.373 | 0.367 | 0.366 | 0.352 | 0.352 |
| | | m+2 | 0.145 | 0.144 | 0.145 | 0.144 | 0.144 | 0.142 | 0.142 | 0.141 | 0.138 | 0.137 |
| | Ser 288 | m+0 | 0.515 | 0.515 | 0.516 | 0.514 | 0.523 | 0.524 | 0.532 | 0.534 | 0.554 | 0.554 |
| | | m+1 | 0.373 | 0.374 | 0.373 | 0.375 | 0.367 | 0.366 | 0.359 | 0.358 | 0.341 | 0.341 |
| | | m+2 | 0.111 | 0.111 | 0.111 | 0.111 | 0.110 | 0.110 | 0.108 | 0.108 | 0.104 | 0.105 |
| | Phe 234 | m+0 | 0.325 | 0.334 | 0.313 | 0.321 | 0.352 | 0.365 | 0.354 | 0.360 | 0.390 | 0.391 |
| | | m+1 | 0.413 | 0.411 | 0.411 | 0.411 | 0.413 | 0.409 | 0.410 | 0.405 | 0.400 | 0.396 |
| | | m+2 | 0.199 | 0.192 | 0.206 | 0.202 | 0.182 | 0.175 | 0.181 | 0.178 | 0.163 | 0.163 |
| | | m+3 | 0.052 | 0.048 | 0.057 | 0.053 | 0.044 | 0.041 | 0.045 | 0.044 | 0.039 | 0.040 |
| | | m+4 | 0.010 | 0.010 | 0.011 | 0.011 | 0.008 | 0.008 | 0.008 | 0.009 | 0.007 | 0.008 |
| | | m+5 | 0.001 | 0.002 | 0.002 | 0.002 | 0.001 | 0.001 | 0.001 | 0.002 | 0.001 | 0.002 |
| | | m+6 | 0.000 | 0.001 | 0.000 | 0.000 | 0.000 | 0.000 | 0.000 | 0.000 | 0.000 | 0.000 |
| | | m+7 | 0.000 | 0.000 | 0.000 | 0.000 | 0.000 | 0.000 | 0.000 | 0.000 | 0.000 | 0.000 |
| | | m+8 | 0.000 | 0.000 | 0.000 | 0.000 | 0.000 | 0.000 | 0.000 | 0.000 | 0.000 | 0.001 |
| | Phe 302 | m+0 | 0.724 | 0.732 | 0.720 | 0.732 | 0.728 | 0.734 | 0.730 | 0.731 | 0.722 | 0.729 |
| | | m+1 | 0.200 | 0.194 | 0.203 | 0.194 | 0.197 | 0.192 | 0.195 | 0.194 | 0.201 | 0.196 |
| | | m+2 | 0.076 | 0.074 | 0.077 | 0.075 | 0.076 | 0.074 | 0.075 | 0.074 | 0.077 | 0.075 |
| | Gly 246 | m+0 | 0.754 | 0.759 | 0.754 | 0.758 | 0.758 | 0.761 | 0.760 | 0.759 | 0.762 | 0.758 |
| | | m+1 | 0.175 | 0.171 | 0.174 | 0.172 | 0.171 | 0.170 | 0.169 | 0.171 | 0.168 | 0.171 |
| | | m+2 | 0.071 | 0.070 | 0.071 | 0.070 | 0.071 | 0.070 | 0.070 | 0.070 | 0.070 | 0.070 |
| | Gly 218 | m+0 | 0.829 | 0.828 | 0.829 | 0.828 | 0.829 | 0.827 | 0.829 | 0.828 | 0.829 | 0.827 |
| | | m+1 | 0.171 | 0.172 | 0.171 | 0.172 | 0.171 | 0.173 | 0.171 | 0.172 | 0.171 | 0.173 |
| | Tyr 466 | m+0 | 0.244 | 0.257 | 0.235 | 0.245 | 0.266 | 0.276 | 0.269 | 0.278 | 0.295 | 0.298 |
| | | m+1 | 0.365 | 0.368 | 0.361 | 0.366 | 0.370 | 0.373 | 0.369 | 0.367 | 0.366 | 0.364 |
| | | m+2 | 0.240 | 0.231 | 0.245 | 0.240 | 0.229 | 0.223 | 0.228 | 0.221 | 0.215 | 0.211 |
| | | m+3 | 0.104 | 0.094 | 0.109 | 0.102 | 0.095 | 0.089 | 0.095 | 0.089 | 0.088 | 0.084 |
| | | m+4 | 0.035 | 0.033 | 0.037 | 0.034 | 0.031 | 0.029 | 0.030 | 0.031 | 0.028 | 0.029 |
| | | m+5 | 0.009 | 0.009 | 0.010 | 0.009 | 0.008 | 0.007 | 0.008 | 0.008 | 0.007 | 0.008 |
| | | m+6 | 0.002 | 0.003 | 0.002 | 0.002 | 0.002 | 0.002 | 0.002 | 0.003 | 0.001 | 0.002 |
| | | m+7 | 0.000 | 0.001 | 0.000 | 0.001 | 0.000 | 0.001 | 0.000 | 0.001 | 0.000 | 0.001 |
| | | m+8 | 0.000 | 0.001 | 0.000 | 0.000 | 0.000 | 0.001 | 0.000 | 0.001 | 0.000 | 0.001 |
| | | m+9 | 0.000 | 0.001 | 0.000 | 0.000 | 0.000 | 0.000 | 0.000 | 0.001 | 0.000 | 0.001 |
| | Tyr 302 | m+0 | 0.724 | 0.732 | 0.720 | 0.732 | 0.728 | 0.735 | 0.730 | 0.732 | 0.722 | 0.731 |
| | | m+1 | 0.200 | 0.193 | 0.203 | 0.193 | 0.197 | 0.191 | 0.195 | 0.194 | 0.201 | 0.195 |
| | | m+2 | 0.076 | 0.074 | 0.077 | 0.075 | 0.076 | 0.073 | 0.075 | 0.074 | 0.077 | 0.075 |
| | Lys 431 | m+0 | 0.230 | 0.240 | 0.230 | 0.236 | 0.238 | 0.247 | 0.244 | 0.254 | 0.265 | 0.274 |
| | | m+1 | 0.364 | 0.363 | 0.362 | 0.363 | 0.365 | 0.364 | 0.364 | 0.362 | 0.364 | 0.362 |
| | | m+2 | 0.250 | 0.245 | 0.250 | 0.247 | 0.246 | 0.241 | 0.242 | 0.238 | 0.232 | 0.227 |
| | | m+3 | 0.109 | 0.105 | 0.110 | 0.107 | 0.106 | 0.103 | 0.105 | 0.102 | 0.098 | 0.095 |
| | | m+4 | 0.036 | 0.035 | 0.037 | 0.036 | 0.035 | 0.034 | 0.035 | 0.033 | 0.032 | 0.031 |
| | | m+5 | 0.009 | 0.009 | 0.010 | 0.010 | 0.009 | 0.009 | 0.009 | 0.009 | 0.008 | 0.008 |
| | | m+6 | 0.002 | 0.003 | 0.002 | 0.002 | 0.002 | 0.002 | 0.002 | 0.002 | 0.002 | 0.002 |

**Table A.9 (continued)**

| | | | 37°C / 0 M NaCl | | 15°C | | 45°C | | 0.6 M NaCl | | 1.2 M NaCl | |
|---|---|---|---|---|---|---|---|---|---|---|---|---|
| | | | Sim | Exp | Sim | Exp | Sim | Exp | Sim | Exp | Sim | Exp |
| | Lys 329 | m+0 | 0.269 | 0.272 | 0.272 | 0.266 | 0.275 | 0.275 | 0.287 | 0.288 | 0.309 | 0.310 |
| | | m+1 | 0.390 | 0.383 | 0.390 | 0.387 | 0.389 | 0.386 | 0.388 | 0.382 | 0.386 | 0.377 |
| | | m+2 | 0.232 | 0.234 | 0.230 | 0.233 | 0.229 | 0.230 | 0.222 | 0.224 | 0.210 | 0.213 |
| | | m+3 | 0.083 | 0.083 | 0.082 | 0.085 | 0.081 | 0.082 | 0.078 | 0.079 | 0.073 | 0.074 |
| | | m+4 | 0.022 | 0.023 | 0.022 | 0.024 | 0.021 | 0.022 | 0.021 | 0.022 | 0.019 | 0.020 |
| | | m+5 | 0.004 | 0.005 | 0.004 | 0.005 | 0.004 | 0.005 | 0.004 | 0.005 | 0.004 | 0.005 |
| | HB_255 | m+0 | - | - | - | - | - | - | 0.370 | 0.364 | 0.402 | 0.399 |
| | | m+1 | - | - | - | - | - | - | 0.397 | 0.399 | 0.384 | 0.386 |
| | | m+2 | - | - | - | - | - | - | 0.172 | 0.175 | 0.158 | 0.159 |
| | | m+3 | - | - | - | - | - | - | 0.050 | 0.050 | 0.046 | 0.046 |
| | | m+4 | - | - | - | - | - | - | 0.012 | 0.012 | 0.010 | 0.010 |
| | HB_233 | m+0 | - | - | - | - | - | - | 0.553 | 0.549 | 0.575 | 0.573 |
| | | m+1 | - | - | - | - | - | - | 0.349 | 0.354 | 0.329 | 0.333 |
| | | m+2 | - | - | - | - | - | - | 0.098 | 0.097 | 0.095 | 0.094 |
| 50 % U-$^{12}$C / 50% U-$^{13}$C labelling | Ala 260 | m+0 | 0.370 | 0.380 | 0.365 | 0.377 | 0.371 | 0.376 | 0.366 | 0.372 | 0.360 | 0.371 |
| | | m+1 | 0.133 | 0.128 | 0.137 | 0.128 | 0.133 | 0.128 | 0.136 | 0.134 | 0.141 | 0.134 |
| | | m+2 | 0.105 | 0.113 | 0.109 | 0.118 | 0.103 | 0.114 | 0.108 | 0.121 | 0.115 | 0.119 |
| | | m+3 | 0.392 | 0.379 | 0.389 | 0.378 | 0.393 | 0.382 | 0.389 | 0.372 | 0.384 | 0.376 |
| | Ala 232 | m+0 | 0.415 | 0.418 | 0.414 | 0.416 | 0.417 | 0.417 | 0.410 | 0.414 | 0.409 | 0.413 |
| | | m+1 | 0.126 | 0.140 | 0.128 | 0.142 | 0.123 | 0.136 | 0.134 | 0.148 | 0.136 | 0.145 |
| | | m+2 | 0.459 | 0.443 | 0.459 | 0.442 | 0.461 | 0.447 | 0.456 | 0.439 | 0.455 | 0.442 |
| | Val 288 | m+0 | 0.166 | 0.180 | 0.163 | 0.179 | 0.167 | 0.179 | 0.162 | 0.175 | 0.159 | 0.173 |
| | | m+1 | 0.078 | 0.081 | 0.080 | 0.081 | 0.076 | 0.078 | 0.082 | 0.086 | 0.084 | 0.086 |
| | | m+2 | 0.219 | 0.221 | 0.219 | 0.222 | 0.220 | 0.222 | 0.219 | 0.221 | 0.219 | 0.220 |
| | | m+3 | 0.241 | 0.237 | 0.241 | 0.237 | 0.241 | 0.239 | 0.239 | 0.236 | 0.239 | 0.237 |
| | | m+4 | 0.102 | 0.096 | 0.104 | 0.096 | 0.100 | 0.094 | 0.106 | 0.101 | 0.109 | 0.102 |
| | | m+5 | 0.195 | 0.185 | 0.193 | 0.185 | 0.196 | 0.188 | 0.192 | 0.181 | 0.189 | 0.182 |
| | Val 260 | m+0 | 0.184 | 0.196 | 0.184 | 0.195 | 0.186 | 0.196 | 0.180 | 0.192 | 0.179 | 0.190 |
| | | m+1 | 0.076 | 0.085 | 0.078 | 0.086 | 0.073 | 0.080 | 0.083 | 0.092 | 0.085 | 0.091 |
| | | m+2 | 0.395 | 0.392 | 0.394 | 0.392 | 0.398 | 0.397 | 0.389 | 0.386 | 0.388 | 0.387 |
| | | m+3 | 0.119 | 0.115 | 0.120 | 0.114 | 0.116 | 0.111 | 0.125 | 0.121 | 0.127 | 0.122 |
| | | m+4 | 0.225 | 0.212 | 0.225 | 0.213 | 0.227 | 0.217 | 0.222 | 0.209 | 0.221 | 0.210 |
| | Thr 404 | m+0 | 0.184 | 0.193 | 0.180 | 0.202 | 0.180 | 0.193 | 0.168 | 0.180 | 0.156 | 0.167 |
| | | m+1 | 0.195 | 0.199 | 0.177 | 0.181 | 0.209 | 0.212 | 0.185 | 0.191 | 0.190 | 0.190 |
| | | m+2 | 0.172 | 0.172 | 0.204 | 0.190 | 0.154 | 0.150 | 0.205 | 0.204 | 0.212 | 0.219 |
| | | m+3 | 0.237 | 0.232 | 0.243 | 0.238 | 0.235 | 0.235 | 0.231 | 0.227 | 0.228 | 0.227 |
| | | m+4 | 0.213 | 0.204 | 0.195 | 0.188 | 0.222 | 0.210 | 0.211 | 0.198 | 0.214 | 0.197 |
| | Thr 376 | m+0 | 0.207 | 0.223 | 0.208 | 0.232 | 0.202 | 0.227 | 0.193 | 0.210 | 0.182 | 0.199 |
| | | m+1 | 0.235 | 0.238 | 0.234 | 0.231 | 0.238 | 0.234 | 0.244 | 0.248 | 0.252 | 0.254 |
| | | m+2 | 0.305 | 0.289 | 0.320 | 0.305 | 0.296 | 0.279 | 0.306 | 0.296 | 0.303 | 0.298 |
| | | m+3 | 0.254 | 0.251 | 0.238 | 0.232 | 0.263 | 0.260 | 0.257 | 0.246 | 0.263 | 0.248 |
| | Asp 418 | m+0 | 0.183 | 0.193 | 0.180 | 0.203 | 0.180 | 0.192 | 0.168 | 0.181 | 0.155 | 0.167 |
| | | m+1 | 0.194 | 0.200 | 0.177 | 0.183 | 0.209 | 0.213 | 0.184 | 0.193 | 0.190 | 0.192 |
| | | m+2 | 0.172 | 0.173 | 0.204 | 0.192 | 0.154 | 0.153 | 0.206 | 0.204 | 0.212 | 0.219 |
| | | m+3 | 0.237 | 0.231 | 0.244 | 0.237 | 0.235 | 0.233 | 0.231 | 0.226 | 0.228 | 0.226 |
| | | m+4 | 0.214 | 0.203 | 0.195 | 0.187 | 0.222 | 0.209 | 0.211 | 0.196 | 0.214 | 0.195 |
| | Asp 390 | m+0 | 0.206 | 0.224 | 0.208 | 0.232 | 0.202 | 0.228 | 0.193 | 0.211 | 0.181 | 0.200 |
| | | m+1 | 0.234 | 0.237 | 0.234 | 0.231 | 0.238 | 0.234 | 0.244 | 0.247 | 0.252 | 0.253 |
| | | m+2 | 0.305 | 0.286 | 0.320 | 0.302 | 0.296 | 0.276 | 0.306 | 0.294 | 0.303 | 0.297 |
| | | m+3 | 0.254 | 0.253 | 0.238 | 0.235 | 0.264 | 0.262 | 0.257 | 0.248 | 0.263 | 0.249 |

**Table A.9 (continued)**

| | | | 37°C / 0 M NaCl | | 15°C | | 45°C | | 0.6 M NaCl | | 1.2 M NaCl | |
|---|---|---|---|---|---|---|---|---|---|---|---|---|
| | | | Sim | Exp | Sim | Exp | Sim | Exp | Sim | Exp | Sim | Exp |
| 50 % U-$^{12}$C / 50% U-$^{13}$C labelling | Asp 316 | m+0 | 0.221 | 0.239 | 0.223 | 0.248 | 0.216 | 0.242 | 0.207 | 0.227 | 0.195 | 0.215 |
| | | m+1 | 0.235 | 0.238 | 0.234 | 0.232 | 0.239 | 0.235 | 0.246 | 0.249 | 0.256 | 0.256 |
| | | m+2 | 0.302 | 0.282 | 0.318 | 0.300 | 0.292 | 0.271 | 0.303 | 0.290 | 0.299 | 0.292 |
| | | m+3 | 0.242 | 0.241 | 0.224 | 0.221 | 0.252 | 0.252 | 0.244 | 0.234 | 0.251 | 0.236 |
| | Glu 432 | m+0 | 0.092 | 0.105 | 0.093 | 0.107 | 0.090 | 0.108 | 0.085 | 0.096 | 0.080 | 0.091 |
| | | m+1 | 0.115 | 0.123 | 0.115 | 0.123 | 0.115 | 0.122 | 0.119 | 0.129 | 0.122 | 0.130 |
| | | m+2 | 0.240 | 0.239 | 0.248 | 0.247 | 0.234 | 0.237 | 0.234 | 0.236 | 0.228 | 0.233 |
| | | m+3 | 0.233 | 0.231 | 0.227 | 0.225 | 0.238 | 0.233 | 0.239 | 0.236 | 0.245 | 0.239 |
| | | m+4 | 0.188 | 0.174 | 0.193 | 0.177 | 0.185 | 0.170 | 0.190 | 0.178 | 0.189 | 0.179 |
| | | m+5 | 0.133 | 0.127 | 0.124 | 0.120 | 0.137 | 0.131 | 0.133 | 0.126 | 0.136 | 0.127 |
| | Glu 330 | m+0 | 0.163 | 0.176 | 0.145 | 0.166 | 0.173 | 0.187 | 0.144 | 0.158 | 0.141 | 0.149 |
| | | m+1 | 0.105 | 0.119 | 0.135 | 0.135 | 0.090 | 0.101 | 0.135 | 0.146 | 0.139 | 0.158 |
| | | m+2 | 0.364 | 0.358 | 0.337 | 0.344 | 0.378 | 0.374 | 0.337 | 0.334 | 0.334 | 0.324 |
| | | m+3 | 0.155 | 0.152 | 0.184 | 0.166 | 0.139 | 0.135 | 0.184 | 0.177 | 0.188 | 0.189 |
| | | m+4 | 0.213 | 0.196 | 0.200 | 0.189 | 0.220 | 0.203 | 0.199 | 0.185 | 0.198 | 0.180 |
| | Ser 390 | m+0 | 0.303 | 0.317 | 0.289 | 0.300 | 0.276 | 0.287 | 0.280 | 0.290 | 0.286 | 0.297 |
| | | m+1 | 0.182 | 0.176 | 0.191 | 0.185 | 0.198 | 0.196 | 0.196 | 0.194 | 0.192 | 0.191 |
| | | m+2 | 0.160 | 0.155 | 0.175 | 0.171 | 0.188 | 0.187 | 0.184 | 0.184 | 0.178 | 0.178 |
| | | m+3 | 0.354 | 0.351 | 0.345 | 0.344 | 0.337 | 0.330 | 0.340 | 0.331 | 0.344 | 0.335 |
| | Ser 362 | m+0 | 0.345 | 0.354 | 0.332 | 0.337 | 0.316 | 0.324 | 0.319 | 0.329 | 0.330 | 0.336 |
| | | m+1 | 0.222 | 0.220 | 0.243 | 0.243 | 0.267 | 0.270 | 0.263 | 0.263 | 0.245 | 0.252 |
| | | m+2 | 0.433 | 0.426 | 0.425 | 0.420 | 0.416 | 0.406 | 0.418 | 0.408 | 0.424 | 0.412 |
| | Ser 288 | m+0 | 0.364 | 0.375 | 0.350 | 0.357 | 0.334 | 0.343 | 0.336 | 0.348 | 0.349 | 0.356 |
| | | m+1 | 0.207 | 0.206 | 0.230 | 0.232 | 0.258 | 0.260 | 0.253 | 0.253 | 0.233 | 0.240 |
| | | m+2 | 0.428 | 0.419 | 0.419 | 0.411 | 0.408 | 0.396 | 0.410 | 0.398 | 0.418 | 0.403 |
| | Phe 234 | m+0 | 0.080 | 0.090 | 0.075 | 0.085 | 0.087 | 0.094 | 0.079 | 0.089 | 0.076 | 0.088 |
| | | m+1 | 0.040 | 0.056 | 0.043 | 0.063 | 0.034 | 0.052 | 0.040 | 0.058 | 0.045 | 0.058 |
| | | m+2 | 0.174 | 0.178 | 0.166 | 0.173 | 0.185 | 0.186 | 0.173 | 0.176 | 0.170 | 0.178 |
| | | m+3 | 0.094 | 0.095 | 0.105 | 0.108 | 0.078 | 0.085 | 0.095 | 0.097 | 0.098 | 0.099 |
| | | m+4 | 0.189 | 0.181 | 0.184 | 0.178 | 0.197 | 0.188 | 0.189 | 0.180 | 0.186 | 0.182 |
| | | m+5 | 0.097 | 0.092 | 0.108 | 0.104 | 0.080 | 0.083 | 0.097 | 0.094 | 0.100 | 0.096 |
| | | m+6 | 0.183 | 0.167 | 0.176 | 0.160 | 0.194 | 0.177 | 0.183 | 0.165 | 0.179 | 0.168 |
| | | m+7 | 0.053 | 0.053 | 0.057 | 0.057 | 0.048 | 0.050 | 0.054 | 0.055 | 0.059 | 0.055 |
| | | m+8 | 0.091 | 0.077 | 0.086 | 0.072 | 0.098 | 0.084 | 0.090 | 0.076 | 0.088 | 0.077 |
| | Phe 302 | m+0 | 0.381 | 0.399 | 0.378 | 0.394 | 0.381 | 0.395 | 0.382 | 0.394 | 0.376 | 0.392 |
| | | m+1 | 0.180 | 0.180 | 0.184 | 0.187 | 0.180 | 0.183 | 0.178 | 0.189 | 0.188 | 0.188 |
| | | m+2 | 0.439 | 0.422 | 0.438 | 0.419 | 0.439 | 0.422 | 0.440 | 0.417 | 0.436 | 0.419 |
| | Gly 246 | m+0 | 0.390 | 0.399 | 0.388 | 0.394 | 0.390 | 0.394 | 0.391 | 0.395 | 0.386 | 0.393 |
| | | m+1 | 0.168 | 0.176 | 0.171 | 0.187 | 0.168 | 0.181 | 0.166 | 0.185 | 0.174 | 0.184 |
| | | m+2 | 0.442 | 0.425 | 0.441 | 0.420 | 0.442 | 0.425 | 0.443 | 0.421 | 0.440 | 0.423 |
| | Gly 218 | m+0 | 0.455 | 0.478 | 0.455 | 0.481 | 0.455 | 0.478 | 0.455 | 0.480 | 0.455 | 0.477 |
| | | m+1 | 0.545 | 0.522 | 0.545 | 0.519 | 0.545 | 0.522 | 0.545 | 0.520 | 0.545 | 0.523 |
| | Tyr 466 | m+0 | 0.057 | 0.067 | 0.053 | 0.061 | 0.062 | 0.071 | 0.057 | 0.065 | 0.054 | 0.065 |
| | | m+1 | 0.044 | 0.050 | 0.045 | 0.053 | 0.042 | 0.047 | 0.044 | 0.051 | 0.046 | 0.051 |
| | | m+2 | 0.088 | 0.096 | 0.086 | 0.094 | 0.091 | 0.099 | 0.088 | 0.096 | 0.089 | 0.096 |
| | | m+3 | 0.126 | 0.126 | 0.128 | 0.126 | 0.124 | 0.125 | 0.126 | 0.126 | 0.125 | 0.127 |
| | | m+4 | 0.135 | 0.136 | 0.136 | 0.138 | 0.133 | 0.134 | 0.135 | 0.137 | 0.136 | 0.137 |
| | | m+5 | 0.138 | 0.137 | 0.140 | 0.141 | 0.136 | 0.135 | 0.138 | 0.138 | 0.140 | 0.138 |
| | | m+6 | 0.145 | 0.136 | 0.147 | 0.138 | 0.141 | 0.134 | 0.145 | 0.136 | 0.143 | 0.137 |
| | | m+7 | 0.120 | 0.113 | 0.119 | 0.112 | 0.123 | 0.116 | 0.120 | 0.113 | 0.120 | 0.113 |
| | | m+8 | 0.067 | 0.063 | 0.069 | 0.066 | 0.064 | 0.060 | 0.067 | 0.064 | 0.070 | 0.064 |
| | | m+9 | 0.080 | 0.074 | 0.077 | 0.071 | 0.085 | 0.078 | 0.080 | 0.073 | 0.078 | 0.073 |

**Table A.9 (continued)**

| | | | 37°C / 0 M NaCl | | 15°C | | 45°C | | 0.6 M NaCl | | 1.2 M NaCl | |
|---|---|---|---|---|---|---|---|---|---|---|---|---|
| | | | Sim | Exp | Sim | Exp | Sim | Exp | Sim | Exp | Sim | Exp |
| 50 % U-$^{12}$C / 50% U-$^{13}$C labelling | Tyr 302 | m+0 | 0.381 | 0.395 | 0.378 | 0.391 | 0.381 | 0.392 | 0.382 | 0.390 | 0.376 | 0.389 |
| | | m+1 | 0.180 | 0.180 | 0.184 | 0.187 | 0.180 | 0.183 | 0.178 | 0.189 | 0.188 | 0.188 |
| | | m+2 | 0.439 | 0.425 | 0.438 | 0.422 | 0.439 | 0.425 | 0.440 | 0.421 | 0.436 | 0.423 |
| | Lys 431 | m+0 | 0.083 | 0.095 | 0.082 | 0.099 | 0.081 | 0.095 | 0.076 | 0.089 | 0.070 | 0.082 |
| | | m+1 | 0.102 | 0.112 | 0.099 | 0.107 | 0.106 | 0.113 | 0.101 | 0.112 | 0.103 | 0.111 |
| | | m+2 | 0.160 | 0.163 | 0.171 | 0.173 | 0.154 | 0.155 | 0.165 | 0.169 | 0.163 | 0.171 |
| | | m+3 | 0.212 | 0.213 | 0.209 | 0.211 | 0.215 | 0.218 | 0.207 | 0.209 | 0.208 | 0.208 |
| | | m+4 | 0.176 | 0.170 | 0.180 | 0.168 | 0.175 | 0.166 | 0.186 | 0.178 | 0.190 | 0.183 |
| | | m+5 | 0.154 | 0.143 | 0.156 | 0.145 | 0.153 | 0.144 | 0.153 | 0.143 | 0.153 | 0.143 |
| | | m+6 | 0.113 | 0.104 | 0.104 | 0.096 | 0.117 | 0.108 | 0.112 | 0.101 | 0.113 | 0.101 |
| | Lys 329 | m+0 | 0.100 | 0.117 | 0.101 | 0.122 | 0.098 | 0.119 | 0.093 | 0.109 | 0.087 | 0.104 |
| | | m+1 | 0.118 | 0.130 | 0.118 | 0.127 | 0.119 | 0.127 | 0.123 | 0.135 | 0.127 | 0.137 |
| | | m+2 | 0.249 | 0.249 | 0.258 | 0.263 | 0.242 | 0.247 | 0.243 | 0.247 | 0.236 | 0.244 |
| | | m+3 | 0.232 | 0.225 | 0.225 | 0.215 | 0.238 | 0.226 | 0.239 | 0.229 | 0.245 | 0.234 |
| | | m+4 | 0.179 | 0.163 | 0.184 | 0.168 | 0.175 | 0.160 | 0.180 | 0.166 | 0.179 | 0.167 |
| | | m+5 | 0.122 | 0.116 | 0.113 | 0.106 | 0.127 | 0.121 | 0.122 | 0.113 | 0.125 | 0.113 |
| | HB_255 | m+0 | - | - | - | - | - | - | 0.180 | 0.194 | 0.179 | 0.190 |
| | | m+1 | - | - | - | - | - | - | 0.082 | 0.095 | 0.084 | 0.094 |
| | | m+2 | - | - | - | - | - | - | 0.390 | 0.385 | 0.388 | 0.385 |
| | | m+3 | - | - | - | - | - | - | 0.124 | 0.118 | 0.126 | 0.120 |
| | | m+4 | - | - | - | - | - | - | 0.223 | 0.208 | 0.223 | 0.211 |
| | HB_233 | m+0 | - | - | - | - | - | - | 0.410 | 0.421 | 0.409 | 0.417 |
| | | m+1 | - | - | - | - | - | - | 0.133 | 0.141 | 0.135 | 0.141 |
| | | m+2 | - | - | - | - | - | - | 0.457 | 0.438 | 0.456 | 0.442 |

**Table A.10: Comparison between measured and simulated labelling patterns of proteinogenic amino acids and intracellular polyhydroxybutyric acid when only labelling data from tracer experiments with 1-$^{13}$C glucose as substrate are used for simulation of metabolic fluxes in cells growing at 15°C, 45°C and 37°C in presence of 0 M, 0.6 M and 1.2 M NaCl.** Simulation with OpenFlux was performed using a modified version of model from Tab. A.3 where pyruvate and phosphoenolpyruvate as well as malate and oxaloacetate were considered as global pools.

| | | 0 M NaCl | | 0.3 M NaCl | | 0.6 M NaCl | | 0.9 M NaCl | | 1.2 M NaCl | | 1.8 M NaCl | | 15°C | |
|---|---|---|---|---|---|---|---|---|---|---|---|---|---|---|---|
| | | Sim | Exp | Sim | Exp | Sim | Exp | Sim | Exp | Sim | Exp | Sim | Exp | Sim | Exp |
| Ala 260 | m+0 | 0.508 | 0.507 | 0.516 | 0.516 | 0.526 | 0.526 | 0.536 | 0.535 | 0.548 | 0.548 | 0.553 | 0.552 | 0.508 | 0.507 |
| | m+1 | 0.361 | 0.362 | 0.355 | 0.355 | 0.347 | 0.347 | 0.339 | 0.340 | 0.329 | 0.329 | 0.324 | 0.326 | 0.359 | 0.363 |
| | m+2 | 0.101 | 0.102 | 0.100 | 0.100 | 0.099 | 0.099 | 0.098 | 0.098 | 0.096 | 0.096 | 0.096 | 0.095 | 0.103 | 0.101 |
| Ala 232 | m+0 | 0.531 | 0.529 | 0.539 | 0.538 | 0.549 | 0.548 | 0.559 | 0.557 | 0.573 | 0.571 | 0.576 | 0.573 | 0.532 | 0.530 |
| | m+1 | 0.369 | 0.371 | 0.362 | 0.364 | 0.353 | 0.355 | 0.345 | 0.347 | 0.332 | 0.335 | 0.330 | 0.332 | 0.368 | 0.370 |
| Val 288 | m+0 | 0.336 | 0.333 | 0.346 | 0.344 | 0.360 | 0.357 | 0.373 | 0.370 | 0.393 | 0.390 | 0.399 | 0.395 | 0.336 | 0.332 |
| | m+1 | 0.406 | 0.406 | 0.403 | 0.403 | 0.399 | 0.398 | 0.394 | 0.394 | 0.387 | 0.386 | 0.384 | 0.385 | 0.404 | 0.406 |
| | m+2 | 0.188 | 0.191 | 0.183 | 0.185 | 0.176 | 0.179 | 0.170 | 0.173 | 0.161 | 0.164 | 0.159 | 0.161 | 0.189 | 0.191 |
| Val 260 | m+0 | 0.342 | 0.338 | 0.353 | 0.349 | 0.366 | 0.363 | 0.380 | 0.376 | 0.401 | 0.396 | 0.406 | 0.400 | 0.343 | 0.338 |
| | m+1 | 0.409 | 0.408 | 0.405 | 0.405 | 0.401 | 0.400 | 0.395 | 0.396 | 0.387 | 0.387 | 0.385 | 0.386 | 0.407 | 0.408 |
| | m+2 | 0.185 | 0.188 | 0.180 | 0.183 | 0.173 | 0.176 | 0.167 | 0.169 | 0.157 | 0.161 | 0.156 | 0.159 | 0.185 | 0.188 |
| Thr 404 | m+0 | 0.346 | 0.345 | 0.345 | 0.344 | 0.352 | 0.351 | 0.351 | 0.354 | 0.360 | 0.364 | 0.358 | 0.359 | 0.335 | 0.345 |
| | m+1 | 0.377 | 0.378 | 0.376 | 0.377 | 0.373 | 0.374 | 0.371 | 0.372 | 0.368 | 0.368 | 0.368 | 0.369 | 0.374 | 0.378 |
| | m+2 | 0.188 | 0.189 | 0.189 | 0.190 | 0.187 | 0.187 | 0.188 | 0.187 | 0.185 | 0.183 | 0.186 | 0.185 | 0.195 | 0.189 |
| Thr 376 | m+0 | 0.374 | 0.374 | 0.376 | 0.375 | 0.384 | 0.383 | 0.389 | 0.387 | 0.398 | 0.398 | 0.395 | 0.394 | 0.376 | 0.378 |
| | m+1 | 0.382 | 0.383 | 0.380 | 0.381 | 0.376 | 0.377 | 0.372 | 0.375 | 0.367 | 0.369 | 0.368 | 0.370 | 0.379 | 0.381 |
| | m+2 | 0.180 | 0.179 | 0.180 | 0.179 | 0.177 | 0.177 | 0.176 | 0.176 | 0.173 | 0.173 | 0.175 | 0.174 | 0.180 | 0.177 |
| Asp 418 | m+0 | 0.345 | 0.346 | 0.344 | 0.345 | 0.351 | 0.351 | 0.351 | 0.354 | 0.359 | 0.364 | 0.357 | 0.360 | 0.334 | 0.344 |
| | m+1 | 0.377 | 0.376 | 0.375 | 0.376 | 0.373 | 0.373 | 0.370 | 0.371 | 0.367 | 0.367 | 0.367 | 0.369 | 0.373 | 0.377 |
| | m+2 | 0.189 | 0.188 | 0.190 | 0.190 | 0.187 | 0.187 | 0.189 | 0.187 | 0.185 | 0.183 | 0.186 | 0.184 | 0.195 | 0.189 |
| Asp 390 | m+0 | 0.374 | 0.374 | 0.376 | 0.376 | 0.383 | 0.383 | 0.388 | 0.386 | 0.397 | 0.397 | 0.395 | 0.395 | 0.375 | 0.377 |
| | m+1 | 0.381 | 0.382 | 0.379 | 0.380 | 0.375 | 0.376 | 0.371 | 0.374 | 0.367 | 0.368 | 0.367 | 0.368 | 0.378 | 0.381 |
| | m+2 | 0.180 | 0.180 | 0.180 | 0.180 | 0.178 | 0.178 | 0.177 | 0.177 | 0.174 | 0.173 | 0.175 | 0.174 | 0.180 | 0.178 |
| Asp 316 | m+0 | 0.411 | 0.408 | 0.413 | 0.409 | 0.421 | 0.417 | 0.427 | 0.421 | 0.437 | 0.433 | 0.434 | 0.433 | 0.413 | 0.412 |
| | m+1 | 0.389 | 0.386 | 0.386 | 0.384 | 0.382 | 0.380 | 0.377 | 0.377 | 0.371 | 0.370 | 0.372 | 0.371 | 0.385 | 0.386 |
| | m+2 | 0.154 | 0.154 | 0.155 | 0.155 | 0.152 | 0.153 | 0.151 | 0.152 | 0.148 | 0.148 | 0.149 | 0.149 | 0.155 | 0.153 |
| Glu 432 | m+0 | 0.243 | 0.247 | 0.248 | 0.250 | 0.258 | 0.260 | 0.266 | 0.267 | 0.280 | 0.281 | 0.279 | 0.279 | 0.244 | 0.245 |
| | m+1 | 0.369 | 0.368 | 0.368 | 0.367 | 0.368 | 0.367 | 0.367 | 0.367 | 0.366 | 0.365 | 0.366 | 0.366 | 0.367 | 0.369 |
| | m+2 | 0.243 | 0.241 | 0.240 | 0.239 | 0.235 | 0.234 | 0.231 | 0.231 | 0.224 | 0.224 | 0.224 | 0.224 | 0.242 | 0.242 |
| Glu 330 | m+0 | 0.322 | 0.323 | 0.330 | 0.330 | 0.342 | 0.343 | 0.346 | 0.354 | 0.365 | 0.371 | 0.370 | 0.372 | 0.307 | 0.320 |
| | m+1 | 0.404 | 0.402 | 0.401 | 0.399 | 0.397 | 0.396 | 0.393 | 0.392 | 0.387 | 0.386 | 0.385 | 0.385 | 0.399 | 0.402 |
| | m+2 | 0.198 | 0.199 | 0.194 | 0.195 | 0.188 | 0.189 | 0.187 | 0.183 | 0.179 | 0.176 | 0.177 | 0.175 | 0.208 | 0.200 |
| Ser 390 | m+0 | 0.442 | 0.448 | 0.449 | 0.454 | 0.458 | 0.465 | 0.467 | 0.471 | 0.477 | 0.482 | 0.483 | 0.485 | 0.445 | 0.445 |
| | m+1 | 0.365 | 0.363 | 0.360 | 0.359 | 0.354 | 0.351 | 0.348 | 0.346 | 0.341 | 0.338 | 0.337 | 0.337 | 0.363 | 0.364 |
| | m+2 | 0.143 | 0.141 | 0.141 | 0.140 | 0.140 | 0.138 | 0.138 | 0.137 | 0.136 | 0.135 | 0.135 | 0.134 | 0.142 | 0.141 |
| Ser 362 | m+0 | 0.471 | 0.476 | 0.478 | 0.482 | 0.487 | 0.493 | 0.495 | 0.500 | 0.508 | 0.512 | 0.511 | 0.514 | 0.474 | 0.475 |
| | m+1 | 0.383 | 0.380 | 0.377 | 0.375 | 0.370 | 0.366 | 0.364 | 0.361 | 0.354 | 0.352 | 0.351 | 0.350 | 0.381 | 0.381 |
| Ser 288 | m+0 | 0.511 | 0.515 | 0.518 | 0.521 | 0.528 | 0.534 | 0.538 | 0.541 | 0.552 | 0.554 | 0.555 | 0.557 | 0.513 | 0.514 |
| | m+1 | 0.377 | 0.374 | 0.371 | 0.368 | 0.363 | 0.358 | 0.355 | 0.352 | 0.344 | 0.341 | 0.341 | 0.338 | 0.375 | 0.375 |
| Phe 234 | m+0 | 0.334 | 0.334 | 0.346 | 0.345 | 0.359 | 0.360 | 0.378 | 0.373 | 0.394 | 0.391 | 0.388 | 0.387 | 0.320 | 0.321 |
| | m+1 | 0.419 | 0.411 | 0.416 | 0.408 | 0.412 | 0.405 | 0.408 | 0.402 | 0.401 | 0.396 | 0.400 | 0.398 | 0.415 | 0.411 |
| | m+2 | 0.192 | 0.192 | 0.185 | 0.185 | 0.178 | 0.178 | 0.167 | 0.172 | 0.160 | 0.163 | 0.164 | 0.165 | 0.201 | 0.202 |
| Phe 302 | m+0 | 0.731 | 0.732 | 0.730 | 0.732 | 0.731 | 0.731 | 0.730 | 0.730 | 0.729 | 0.729 | 0.729 | 0.729 | 0.724 | 0.732 |
| | m+1 | 0.194 | 0.194 | 0.194 | 0.194 | 0.194 | 0.194 | 0.195 | 0.195 | 0.196 | 0.196 | 0.196 | 0.196 | 0.199 | 0.194 |
| Gly 246 | m+0 | 0.764 | 0.759 | 0.763 | 0.756 | 0.763 | 0.759 | 0.764 | 0.759 | 0.761 | 0.758 | 0.764 | 0.760 | 0.764 | 0.758 |
| | m+1 | 0.166 | 0.171 | 0.167 | 0.173 | 0.167 | 0.171 | 0.166 | 0.171 | 0.169 | 0.171 | 0.166 | 0.169 | 0.166 | 0.172 |

**Table A.10 (continued)**

| | | 0 M NaCl | | 0.3 M NaCl | | 0.6 M NaCl | | 0.9 M NaCl | | 1.2 M NaCl | | 1.8 M NaCl | | 15°C | |
|---|---|---|---|---|---|---|---|---|---|---|---|---|---|---|---|
| | | Sim | Exp | Sim | Exp | Sim | Exp | Sim | Exp | Sim | Exp | Sim | Exp | Sim | Exp |
| Gly 218 | m+0 | 0.829 | 0.828 | 0.829 | 0.825 | 0.829 | 0.828 | 0.829 | 0.828 | 0.829 | 0.827 | 0.829 | 0.829 | 0.829 | 0.828 |
| | m+1 | 0.171 | 0.172 | 0.171 | 0.175 | 0.171 | 0.172 | 0.171 | 0.172 | 0.171 | 0.173 | 0.171 | 0.171 | 0.171 | 0.172 |
| Tyr 466 | m+0 | 0.255 | 0.257 | 0.264 | 0.262 | 0.274 | 0.278 | 0.288 | 0.287 | 0.299 | 0.298 | 0.296 | 0.295 | 0.244 | 0.245 |
| | m+1 | 0.372 | 0.368 | 0.372 | 0.364 | 0.371 | 0.367 | 0.370 | 0.368 | 0.368 | 0.364 | 0.366 | 0.364 | 0.366 | 0.366 |
| | m+2 | 0.235 | 0.231 | 0.230 | 0.224 | 0.225 | 0.221 | 0.218 | 0.217 | 0.213 | 0.211 | 0.215 | 0.213 | 0.241 | 0.240 |
| Tyr 302 | m+0 | 0.731 | 0.732 | 0.730 | 0.732 | 0.731 | 0.732 | 0.730 | 0.732 | 0.729 | 0.731 | 0.729 | 0.731 | 0.724 | 0.732 |
| | m+1 | 0.194 | 0.193 | 0.194 | 0.194 | 0.194 | 0.194 | 0.195 | 0.194 | 0.196 | 0.195 | 0.196 | 0.194 | 0.199 | 0.193 |
| Lys 431 | m+0 | 0.234 | 0.240 | 0.238 | 0.244 | 0.247 | 0.254 | 0.253 | 0.261 | 0.266 | 0.274 | 0.266 | 0.268 | 0.230 | 0.236 |
| | m+1 | 0.366 | 0.363 | 0.365 | 0.361 | 0.366 | 0.362 | 0.364 | 0.363 | 0.364 | 0.362 | 0.364 | 0.362 | 0.361 | 0.363 |
| | m+2 | 0.248 | 0.245 | 0.246 | 0.243 | 0.241 | 0.238 | 0.237 | 0.234 | 0.231 | 0.227 | 0.231 | 0.230 | 0.249 | 0.247 |
| Lys 329 | m+0 | 0.270 | 0.272 | 0.276 | 0.275 | 0.287 | 0.288 | 0.296 | 0.295 | 0.312 | 0.310 | 0.311 | 0.306 | 0.271 | 0.266 |
| | m+1 | 0.392 | 0.383 | 0.390 | 0.381 | 0.390 | 0.382 | 0.388 | 0.381 | 0.386 | 0.377 | 0.385 | 0.382 | 0.389 | 0.387 |
| | m+2 | 0.231 | 0.234 | 0.228 | 0.232 | 0.222 | 0.224 | 0.217 | 0.221 | 0.209 | 0.213 | 0.209 | 0.212 | 0.230 | 0.233 |
| HB 275 | m+0 | - | - | 0.352 | 0.351 | 0.366 | 0.364 | 0.380 | 0.378 | 0.401 | 0.399 | 0.405 | 0.403 | - | - |
| | m+1 | - | - | 0.404 | 0.404 | 0.399 | 0.399 | 0.394 | 0.395 | 0.386 | 0.386 | 0.383 | 0.386 | - | - |
| | m+2 | - | - | 0.180 | 0.181 | 0.173 | 0.175 | 0.167 | 0.168 | 0.158 | 0.159 | 0.156 | 0.156 | - | - |
| HB 233 | m+0 | - | - | 0.540 | 0.539 | 0.550 | 0.549 | 0.560 | 0.559 | 0.575 | 0.573 | 0.577 | 0.576 | - | - |
| | m+1 | - | - | 0.361 | 0.363 | 0.352 | 0.354 | 0.344 | 0.345 | 0.331 | 0.333 | 0.328 | 0.330 | - | - |

**Table A.11: Gene set enrichment analysis (GSEA) for *B. megaterium* growing at 15°C, 45°C and under severe osmotic stress (NaCl > 0.6 M).** Fold change (FC) of transcript concentrations compared to their values in cells grown at 37°C without additional NaCl was used for the analysis (http://www.broadinstitute.org/gsea/index.jsp).

| Name | Size | ES | NES | NOM p-val | FDR q-val | FWER p-val | Rank at max | Leading edge |
|---|---|---|---|---|---|---|---|---|
| **15°C up-regulated** | | | | | | | | |
| Biosynthesis of cofactors, prosthetic groups, carriers and vitamins - biotin | 10 | 0.85 | 1.80 | 0.00 | 0.05 | 0.01 | 175 | tags=60%, list=3%, signal=62% |
| Transcription - rna processing | 22 | 0.52 | 1.69 | 0.11 | 0.18 | 0.32 | 566 | tags=36%, list=11%, signal=41% |
| **15°C down-regulated** | | | | | | | | |
| Cell envelope - biosynthesis and degradation of surface polysaccharides and lipopolysaccharides | 38 | -0.59 | -2.07 | 0.00 | 0.02 | 0.00 | 679 | tags=34%, list=13%, signal=39% |
| Central intermediary metabolism - phosphorus compounds | 6 | -0.79 | -2.01 | 0.00 | 0.02 | 0.02 | 225 | tags=17%, list=4%, signal=17% |
| Amino acid biosynthesis - histidine family | 15 | -0.76 | -2.00 | 0.00 | 0.02 | 0.02 | 684 | tags=67%, list=13%, signal=77% |
| Amino acid biosynthesis - glutamate family | 23 | -0.73 | -1.86 | 0.00 | 0.02 | 0.02 | 505 | tags=52%, list=10%, signal=58% |
| Purines, pyrimidines, nucleosides, and nucleotides - pyrimidine ribonucleotide biosynthesis | 16 | -0.71 | -1.80 | 0.00 | 0.02 | 0.03 | 707 | tags=63%, list=14%, signal=72% |
| Protein fate - protein folding and stabilization | 16 | -0.66 | -1.72 | 0.00 | 0.04 | 0.16 | 45 | tags=31%, list=1%, signal=31% |
| Biosynthesis of cofactors, prosthetic groups, carriers and vitamins - thiamine | 16 | -0.60 | -1.70 | 0.00 | 0.05 | 0.25 | 814 | tags=63%, list=16%, signal=74% |
| Biosynthesis of cofactors, prosthetic groups, carriers and vitamins - pyridoxine | 6 | -0.81 | -1.67 | 0.00 | 0.05 | 0.31 | 137 | tags=67%, list=3%, signal=68% |
| Amino acid biosynthesis - aromatic amino acid family | 37 | -0.49 | -1.67 | 0.00 | 0.05 | 0.31 | 779 | tags=38%, list=15%, signal=44% |
| Energy metabolism - tca cycle | 27 | -0.74 | -1.64 | 0.00 | 0.05 | 0.31 | 936 | tags=70%, list=18%, signal=86% |
| Central intermediary metabolism - polyamine biosynthesis | 9 | -0.73 | -1.59 | 0.00 | 0.10 | 0.37 | 631 | tags=44%, list=12%, signal=51% |
| Amino acid biosynthesis - other | 6 | -0.66 | -1.59 | 0.00 | 0.09 | 0.37 | 1105 | tags=50%, list=22%, signal=64% |
| Biosynthesis of cofactors, prosthetic groups, carriers and vitamins - pantothenate and coenzyme a | 9 | -0.73 | -1.54 | 0.00 | 0.10 | 0.46 | 500 | tags=44%, list=10%, signal=49% |
| Amino acid biosynthesis - pyruvate family | 15 | -0.67 | -1.52 | 0.20 | 0.15 | 0.66 | 898 | tags=67%, list=18%, signal=81% |
| Amino acid biosynthesis - serine family | 18 | -0.70 | -1.52 | 0.00 | 0.14 | 0.66 | 903 | tags=44%, list=18%, signal=54% |
| Protein synthesis - trna aminoacylation | 25 | -0.66 | -1.49 | 0.13 | 0.19 | 0.85 | 1045 | tags=76%, list=20%, signal=95% |
| Energy metabolism - glycolysis/gluconeogenesis | 34 | -0.44 | -1.48 | 0.12 | 0.18 | 0.85 | 1151 | tags=44%, list=22%, signal=57% |
| Amino acid biosynthesis - aspartate family | 42 | -0.63 | -1.47 | 0.00 | 0.19 | 0.94 | 1065 | tags=55%, list=21%, signal=69% |
| **45°C up-regulated** | | | | | | | | |
| Energy metabolism - electron transport | 69 | 0.62 | 1.92 | 0.00 | 0.13 | 0.10 | 778 | tags=39%, list=15%, signal=46% |
| Biosynthesis of cofactors, prosthetic groups, carriers and vitamins - biotin | 10 | 0.88 | 1.88 | 0.00 | 0.08 | 0.12 | 197 | tags=70%, list=4%, signal=73% |
| Biosynthesis of cofactors, prosthetic groups, carriers and vitamins - thiamine | 16 | 0.79 | 1.83 | 0.00 | 0.09 | 0.20 | 302 | tags=44%, list=6%, signal=46% |
| Cellular processes - adaptations to atypical conditions | 72 | 0.55 | 1.82 | 0.00 | 0.07 | 0.20 | 782 | tags=46%, list=15%, signal=53% |
| Protein fate - protein folding and stabilization | 16 | 0.67 | 1.73 | 0.00 | 0.08 | 0.29 | 354 | tags=50%, list=7%, signal=54% |
| Biosynthesis of cofactors, prosthetic groups, carriers and vitamins - menaquinone and ubiquinone | 15 | 0.56 | 1.60 | 0.00 | 0.19 | 0.46 | 566 | tags=40%, list=11%, signal=45% |
| **45°C down-regulated** | | | | | | | | |
| Amino acid biosynthesis - glutamate family | 23 | -0.81 | -2.06 | 0.00 | 0.02 | 0.00 | 334 | tags=61%, list=7%, signal=65% |
| Central intermediary metabolism - polyamine biosynthesis | 9 | -0.78 | -1.95 | 0.00 | 0.06 | 0.10 | 412 | tags=44%, list=8%, signal=48% |
| Cell envelope - biosynthesis of murein sacculus and peptidoglycan | 55 | -0.59 | -1.84 | 0.00 | 0.06 | 0.11 | 613 | tags=38%, list=12%, signal=43% |
| Protein synthesis - trna and rrna base modification | 33 | -0.62 | -1.75 | 0.00 | 0.08 | 0.20 | 1226 | tags=61%, list=24%, signal=79% |
| Purines, pyrimidines, nucleosides, and nucleotides - nucleotide and nucleoside interconversions | 10 | -0.87 | -1.71 | 0.00 | 0.08 | 0.29 | 603 | tags=90%, list=12%, signal=102% |
| Protein synthesis - trna aminoacylation | 25 | -0.69 | -1.69 | 0.00 | 0.07 | 0.29 | 535 | tags=56%, list=10%, signal=62% |
| Transport and binding proteins - cations and iron carrying compounds | 92 | -0.55 | -1.61 | 0.00 | 0.12 | 0.38 | 1095 | tags=50%, list=21%, signal=62% |
| Protein synthesis - ribosomal proteins: synthesis and modification | 64 | -0.70 | -1.56 | 0.00 | 0.19 | 0.55 | 768 | tags=61%, list=15%, signal=71% |

**Tab A.11 (continued)**

| Name | Size | ES | NES | NOM p-val | FDR q-val | FWER p-val | Rank at max | Leading edge |
|---|---|---|---|---|---|---|---|---|
| Transcription - rna processing | 22 | -0.58 | -1.55 | 0.00 | 0.18 | 0.55 | 556 | tags=36%, list=11%, signal=41% |
| Purines, pyrimidines, nucleosides, and nucleotides - other | 8 | -0.64 | -1.53 | 0.16 | 0.18 | 0.55 | 482 | tags=38%, list=9%, signal=41% |
| Purines, pyrimidines, nucleosides, and nucleotides - purine ribonucleotide biosynthesis | 28 | -0.67 | -1.51 | 0.30 | 0.20 | 0.62 | 1029 | tags=57%, list=20%, signal=71% |
| Purines, pyrimidines, nucleosides, and nucleotides - pyrimidine ribonucleotide biosynthesis | 16 | -0.64 | -1.41 | 0.17 | 0.24 | 0.77 | 749 | tags=63%, list=15%, signal=73% |
| Protein fate - protein and peptide secretion and trafficking | 20 | -0.66 | -1.41 | 0.00 | 0.25 | 0.83 | 916 | tags=65%, list=18%, signal=79% |
| **High salt concentrations up-regulated** | | | | | | | | |
| Fatty acid and phospholipid metabolism - other | 11 | 0.75 | 1.75 | 0.00 | 0.20 | 0.19 | 632 | tags=55%, list=12%, signal=62% |
| Cellular processes - chemotaxis and motility | 46 | 0.65 | 1.72 | 0.02 | 0.18 | 0.29 | 765 | tags=59%, list=15%, signal=68% |
| Amino acid biosynthesis - other | 6 | 0.67 | 1.65 | 0.02 | 0.18 | 0.42 | 632 | tags=50%, list=12%, signal=57% |
| Energy metabolism - tca cycle | 27 | 0.63 | 1.64 | 0.00 | 0.15 | 0.43 | 641 | tags=56%, list=13%, signal=63% |
| Unknown function - general | 296 | 0.30 | 1.61 | 0.00 | 0.14 | 0.46 | 948 | tags=27%, list=19%, signal=31% |
| Energy metabolism - pentose phosphate pathway | 31 | 0.56 | 1.60 | 0.00 | 0.14 | 0.50 | 721 | tags=42%, list=14%, signal=49% |
| Energy metabolism - electron transport | 69 | 0.45 | 1.59 | 0.00 | 0.14 | 0.57 | 1051 | tags=35%, list=21%, signal=43% |
| Amino acid biosynthesis - aromatic amino acid family | 37 | 0.38 | 1.58 | 0.00 | 0.14 | 0.59 | 970 | tags=32%, list=19%, signal=40% |
| Cellular processes - adaptations to atypical conditions | 72 | 0.54 | 1.56 | 0.00 | 0.14 | 0.61 | 982 | tags=46%, list=19%, signal=56% |
| Transport and binding proteins - cations and iron carrying compounds | 92 | 0.38 | 1.53 | 0.13 | 0.16 | 0.69 | 1020 | tags=35%, list=20%, signal=43% |
| Energy metabolism - fermentation | 23 | 0.56 | 1.52 | 0.06 | 0.16 | 0.71 | 560 | tags=30%, list=11%, signal=34% |
| Cellular processes - detoxification | 12 | 0.45 | 1.52 | 0.06 | 0.15 | 0.73 | 785 | tags=42%, list=15%, signal=49% |
| Cellular processes - toxin production and resistance | 57 | 0.36 | 1.50 | 0.04 | 0.16 | 0.76 | 729 | tags=23%, list=14%, signal=26% |
| Cellular processes - dna transformation | 23 | 0.48 | 1.48 | 0.00 | 0.17 | 0.80 | 416 | tags=17%, list=8%, signal=19% |
| Biosynthesis of cofactors, prosthetic groups, carriers and vitamins - biotin | 10 | 0.76 | 1.47 | 0.00 | 0.16 | 0.81 | 918 | tags=80%, list=18%, signal=97% |
| Energy metabolism - other | 42 | 0.39 | 1.41 | 0.05 | 0.23 | 0.92 | 890 | tags=36%, list=17%, signal=43% |
| Fatty acid and phospholipid metabolism - degradation | 56 | 0.42 | 1.41 | 0.11 | 0.21 | 0.92 | 1265 | tags=38%, list=25%, signal=49% |
| Biosynthesis of cofactors, prosthetic groups, carriers and vitamins - other | 18 | 0.50 | 1.40 | 0.11 | 0.22 | 0.95 | 628 | tags=39%, list=12%, signal=44% |
| **High salt concentrations down-regulated** | | | | | | | | |
| Purines, pyrimidines, nucleosides, and nucleotides - purine ribonucleotide biosynthesis | 28 | -0.78 | -1.98 | 0.00 | 0.01 | 0.01 | 323 | tags=50%, list=6%, signal=53% |
| Amino acid biosynthesis - histidine family | 15 | -0.76 | -1.97 | 0.00 | 0.00 | 0.01 | 215 | tags=53%, list=4%, signal=56% |
| Amino acid biosynthesis - glutamate family | 23 | -0.51 | -1.67 | 0.08 | 0.14 | 0.31 | 416 | tags=48%, list=8%, signal=52% |
| Transport and binding proteins - nucleosides, purines and pyrimidines | 5 | -0.92 | -1.61 | 0.00 | 0.17 | 0.45 | 155 | tags=60%, list=3%, signal=62% |
| Purines, pyrimidines, nucleosides, and nucleotides - salvage of nucleosides and nucleotides | 17 | -0.47 | -1.57 | 0.00 | 0.20 | 0.54 | 511 | tags=29%, list=10%, signal=33% |
| Biosynthesis of cofactors, prosthetic groups, carriers and vitamins - folic acid | 15 | -0.57 | -1.57 | 0.00 | 0.18 | 0.54 | 957 | tags=33%, list=19%, signal=41% |
| Purines, pyrimidines, nucleosides, and nucleotides - pyrimidine ribonucleotide biosynthesis | 16 | -0.67 | -1.53 | 0.10 | 0.21 | 0.72 | 611 | tags=75%, list=12%, signal=85% |
| Central intermediary metabolism - polyamine biosynthesis | 9 | -0.66 | -1.52 | 0.00 | 0.20 | 0.72 | 556 | tags=44%, list=11%, signal=50% |
| Transport and binding proteins - other | 27 | -0.57 | -1.49 | 0.00 | 0.21 | 0.77 | 858 | tags=41%, list=17%, signal=49% |
| Transport and binding proteins - amino acids, peptides and amines | 112 | -0.44 | -1.48 | 0.00 | 0.21 | 0.78 | 391 | tags=24%, list=8%, signal=26% |
| Cell envelope - biosynthesis of murein sacculus and peptidoglycan | 55 | -0.46 | -1.48 | 0.00 | 0.19 | 0.78 | 999 | tags=38%, list=19%, signal=47% |
| Purines, pyrimidines, nucleosides, and nucleotides - other | 8 | -0.62 | -1.48 | 0.00 | 0.18 | 0.79 | 131 | tags=25%, list=3%, signal=26% |
| Central intermediary metabolism - phosphorus compounds | 6 | -0.55 | -1.47 | 0.00 | 0.18 | 0.81 | 423 | tags=33%, list=8%, signal=36% |
| Transcription - rna processing | 22 | -0.48 | -1.46 | 0.07 | 0.18 | 0.82 | 923 | tags=45%, list=18%, signal=55% |
| Cell envelope - other | 27 | -0.45 | -1.44 | 0.02 | 0.19 | 0.84 | 984 | tags=44%, list=19%, signal=55% |
| Biosynthesis of cofactors, prosthetic groups, carriers and vitamins - menaquinone and ubiquinone | 15 | -0.51 | -1.43 | 0.02 | 0.19 | 0.85 | 985 | tags=40%, list=19%, signal=49% |
| Cell envelope - biosynthesis and degradation of surface polysaccharides and lipopolysaccharides | 38 | -0.51 | -1.39 | 0.09 | 0.24 | 0.91 | 795 | tags=34%, list=16%, signal=40% |

**TableA.12: Gene expression levels in *B. megaterium* DSM319 grown at 37°C with 0.6, 1.2 and 1.8 M NaCl, respectively.** Data are given as fold change (FC) of transcript concentrations compared to their values in cells grown without additional NaCl supplementation. They were obtained from microarray experiments carried out using four biological replicates for each cultivation condition. Only genes whose expression was at least 1.75-fold up- (**red**) or down-regulated (**blue**) with a p-value < 0.05 at 0.6, 1.2 and/or 1.8 M NaCl were considered as significantly regulated and listed.

| Gene product | Gene_id | Gene symbol | 0.6 M | 1.2 M | 1.8 M |
|---|---|---|---|---|---|
| Sigma-F transcribed protein CsfB | *bmd_0044* | *csfB* | -1.43 | **-2.45** | **-1.87** |
| Transition state regulatory protein AbrB | *bmd_0054* | *abrB* | -1.39 | **-2.07** | -1.45 |
| Control of biofilm formation | *bmd_0061* | *veg* | 1.09 | 1.51 | **2.26** |
| 50S ribosomal protein L25/general stress protein Ctc | *bmd_0069* | *ctc* | -1.37 | **3.51** | **3.26** |
| Conserved hypothetical protein | *bmd_0108* | | 1.01 | **1.84** | -1.02 |
| KinB sporulation signaling pathway activation protein | *bmd_0173* | *kbaA* | 1.28 | 1.68 | **1.85** |
| Hypothetical protein | *bmd_0186* | | -1.32 | **1.88** | **2.45** |
| RNA polymerase sigma-W factor | *bmd_0187* | *sigW* | -1.07 | **1.93** | 1.05 |
| Anti-sigma-W factor | *bmd_0188* | *rsiW* | -1.01 | **1.83** | -1.04 |
| Putative membrane protein | *bmd_0208* | | 1.37 | **1.80** | 1.51 |
| Anti-sigma B factor antagonist | *bmd_0227* | *rsbV* | -1.22 | **1.75** | **1.91** |
| Serine-protein kinase RsbW (anti-sigma B factor) | *bmd_0228* | *rsbW* | -1.19 | **1.84** | 1.66 |
| RNA polymerase sigma-B factor | *bmd_0229* | *sigB* | -1.17 | **1.88** | 1.71 |
| Phosphoserine phosphatase RsbX | *bmd_0230* | *rsbX* | -1.13 | **1.75** | 1.68 |
| Putative Redox-sensing transcriptional repressor rex | *bmd_0255* | | 1.35 | **1.87** | 1.27 |
| Twin arginine-targeting protein translocase, TatA/E family protein | *bmd_0256* | *tatA* | 1.27 | **1.88** | 1.33 |
| Hypoxanthine/guanine permease | *bmd_0266* | *pbuG* | -1.31 | **-5.31** | **-3.53** |
| Phosphoribosylaminoimidazole carboxylase, catalytic subunit | *bmd_0271* | *purE* | 1.24 | **-3.25** | **-2.72** |
| Phosphoribosylaminoimidazole carboxylase, ATPase subunit | *bmd_0272* | *purK* | 1.39 | **-2.79** | **-2.54** |
| Adenylosuccinate lyase | *bmd_0273* | *purB* | 1.48 | **-2.30** | **-2.35** |
| Phosphoribosylaminoimidazole-succinocarboxamide synthase | *bmd_0274* | *purC* | 1.33 | **-2.46** | **-2.32** |
| Phosphoribosylformylglycinamidine synthase, purS protein | *bmd_0275* | *purS* | 1.44 | **-2.48** | **-2.44** |
| Phosphoribosylformylglycinamidine synthase I | *bmd_0276* | *purQ* | 1.45 | **-2.22** | **-1.97** |
| Phosphoribosylformylglycinamidine synthase II | *bmd_0277* | *purL* | 1.53 | **-2.16** | **-2.57** |
| Amidophosphoribosyltransferase | *bmd_0278* | *purF* | 1.49 | **-2.14** | **-2.23** |
| Phosphoribosylformylglycinamidine cyclo-ligase | *bmd_0279* | *purM* | 1.54 | **-2.11** | **-2.11** |
| Phosphoribosylglycinamide formyltransferase | *bmd_0280* | *purN* | 1.39 | **-2.23** | **-2.25** |
| Bifunctional purine biosynthesis protein PurH | *bmd_0281* | *purH* | 1.39 | **-2.16** | **-2.10** |
| Phosphoribosylamine--glycine ligase | *bmd_0282* | *purD* | 1.41 | **-2.13** | **-2.09** |
| TrpR like protein, YerC/YecD | *bmd_0285* | | -1.28 | **-1.99** | -1.71 |
| Conserved hypothetical protein | *bmd_0309* | | -1.01 | **1.83** | **-1.96** |
| Amino acid permease | *bmd_0315* | | -1.37 | **-2.04** | **-1.97** |
| Conserved hypothetical protein | *bmd_0317* | | 1.17 | **4.41** | **3.96** |
| Conserved hypothetical protein | *bmd_0318* | | 1.26 | **2.51** | **2.23** |
| Intracellular protease, PfpI family | *bmd_0331* | | 1.21 | **1.95** | 1.48 |
| Conserved hypothetical protein | *bmd_0333* | | 1.06 | **2.48** | 1.26 |
| Conserved hypothetical protein | *bmd_0364* | | **2.30** | **25.11** | **51.61** |
| Intracellular protease, PfpI family | *bmd_0368* | | -1.40 | 1.69 | **2.35** |
| Conserved hypothetical protein | *bmd_0376* | | -1.48 | **-1.99** | -1.66 |
| Conserved hypothetical protein | *bmd_0394* | | **-1.96** | **-2.55** | -1.64 |
| Membrane-bound metal-dependent hydrolase (DUF457) | *bmd_0402* | | 1.13 | **2.23** | 1.69 |
| Undecaprenol kinase | *bmd_0452* | *uppP* | -1.19 | **-2.01** | -1.74 |
| Proton/sodium-glutamate symport protein | *bmd_0453* | | **2.04** | **2.48** | **1.88** |
| Biotin synthase | *bmd_0460* | *bioB* | 1.33 | **1.87** | **2.25** |
| Putative exported cell wall-binding protein | *bmd_0478* | *yocH* | 1.01 | **-3.34** | -1.75 |
| Hypothetical protein | *bmd_0485* | | -1.13 | **1.92** | **1.80** |
| Conserved hypothetical protein | *bmd_0515* | | 1.00 | 1.13 | **-1.79** |
| Conserved hypothetical protein | *bmd_0521* | | -1.12 | **3.66** | **2.52** |
| Glycerol uptake facilitator protein | *bmd_0533* | *glpF* | 1.06 | **2.04** | 1.31 |
| Glycerol kinase | *bmd_0534* | *glpK* | 1.09 | **2.17** | 1.23 |
| L-cystine import ABC transporter, ATP-binding protein TcyC | *bmd_0545* | *tcyC* | -1.29 | **-1.85** | **-2.02** |
| L-cystine import ABC transporter, permease protein TcyB | *bmd_0546* | *tcyB* | -1.27 | **-2.04** | **-2.03** |
| L-cystine import ABC transporter, L-cystine-binding protein TcyA | *bmd_0547* | *tcyA* | -1.38 | **-2.30** | **-2.62** |
| Conserved hypothetical protein | *bmd_0577* | | -1.29 | **-1.88** | -1.06 |
| O-acetyltransferase | *bmd_0591* | | 1.02 | **2.46** | 1.67 |
| PAP2 family protein | *bmd_0597* | | -1.11 | **-1.82** | -1.66 |
| Monooxygenase | *bmd_0599* | | -1.04 | **1.75** | 1.27 |
| Extracellular solute-binding protein | *bmd_0606* | | 1.21 | **2.08** | 1.46 |
| Conserved hypothetical protein | *bmd_0638* | | 1.31 | **2.10** | **1.94** |
| Conserved hypothetical protein | *bmd_0676* | | 1.15 | **2.39** | **2.04** |
| N-acetyl-gamma-glutamyl-phosphate reductase | *bmd_0678* | *argC* | -1.39 | **-2.50** | -1.70 |
| Arginine biosynthesis bifunctional protein ArgJ | *bmd_0679* | *argJ* | -1.38 | **-2.28** | -1.71 |
| Acetylglutamate kinase | *bmd_0680* | *argB* | -1.21 | **-2.07** | -1.48 |
| Acetylornithine aminotransferase | *bmd_0681* | *argD* | -1.28 | **-1.96** | -1.73 |
| NAD dependent epimerase/dehydratase | *bmd_0685* | | -1.37 | **2.69** | **2.02** |
| Oligopeptide ABC transporter, ATP-binding protein AppF | *bmd_0700* | *appF* | 1.37 | **2.06** | **1.87** |
| Oligopeptide ABC transporter, oligopeptide-binding protein AppA | *bmd_0701* | *appA* | 1.53 | **3.12** | **2.03** |

| Gene product | Gene_id | Gene symbol | 0.6 M | 1.2 M | 1.8 M |
|---|---|---|---|---|---|
| Oligopeptide ABC transporter, permease protein AppB | *bmd_0702* | *appB* | 1.47 | **2.38** | **2.02** |
| Oligopeptide ABC transporter, permease protein AppC | *bmd_0703* | *appC* | 1.21 | **1.89** | 1.74 |
| Amino acid permease | *bmd_0712* | | 1.03 | -1.39 | **-2.05** |
| Arginine/ornithine antiporter | *bmd_0713* | *arcD* | -1.15 | **-2.31** | **-1.82** |
| Competence-associated adapter protein | *bmd_0719* | *mecA* | -1.08 | **1.96** | 1.28 |
| 6-phosphogluconate dehydrogenase (decarboxylating) | *bmd_0753* | *gnd* | 1.29 | **2.14** | 1.16 |
| Gluconate kinase | *bmd_0754* | *gntK* | 1.37 | **2.28** | 1.51 |
| Transporter, gluconate:H+ symporter (GntP) family | *bmd_0756* | | **2.00** | **3.86** | **1.86** |
| Conserved hypothetical protein | *bmd_0757* | | 1.43 | **1.97** | 1.49 |
| Amino acid permease | *bmd_0809* | | -1.54 | **-3.03** | -1.46 |
| Nucleoside transporter, NupC family | *bmd_0826* | | -1.24 | **-2.43** | -1.73 |
| Integral membrane protein | *bmd_0832* | | -1.13 | **-1.89** | -1.36 |
| Homocysteine S-methyltransferase | *bmd_0849* | *ybgG* | 1.22 | **2.03** | 1.24 |
| Hypothetical protein | *bmd_0893* | | -1.38 | **3.23** | **2.49** |
| Conserved hypothetical protein | *bmd_0894* | | -1.45 | **3.14** | **2.54** |
| Conserved hypothetical protein | *bmd_0895* | | -1.09 | **2.16** | **1.93** |
| Ferrous iron transport protein B | *bmd_0896* | *feoB* | -1.14 | **1.84** | **1.84** |
| Transporter, solute:sodium symporter (SSS) family | *bmd_0908* | | 1.15 | **1.79** | 1.56 |
| Transcriptional regulator, IclR family | *bmd_0911* | | -1.19 | **2.30** | 1.39 |
| Oxidoreductase, aldo/keto reductase family | *bmd_0912* | | -1.21 | **2.58** | 1.73 |
| 4-aminobutyrate aminotransferase | *bmd_0945* | | -1.62 | **-3.43** | **-2.85** |
| Allophanate hydrolase subunit 1 | *bmd_0960* | | 1.52 | **2.53** | 1.51 |
| Allophanate hydrolase subunit 2 | *bmd_0961* | | **1.95** | **3.05** | 1.51 |
| LamB/YcsF family protein | *bmd_0962* | | **1.93** | **3.03** | 1.71 |
| Uncharacterized membrane protein ycsG | *bmd_0963* | | **1.87** | **3.10** | 1.60 |
| Amidohydrolase | *bmd_0986* | | -1.19 | **-2.48** | **-2.03** |
| Cold shock protein | *bmd_0987* | *cspB* | -1.38 | **-2.83** | **-1.80** |
| Antioxidant, AhpC/TSA family | *bmd_0991* | | 1.21 | 1.34 | **1.84** |
| Capsule biosynthesis protein CapB | *bmd_1003* | *capB* | **2.48** | **4.53** | **3.16** |
| Capsule biosynthesis protein CapC | *bmd_1004* | *capC* | **2.17** | **3.81** | **2.90** |
| Capsule biosynthesis protein CapA | *bmd_1005* | *capA* | **2.43** | **4.79** | **2.84** |
| Putative gamma glutamyl transferase | *bmd_1006* | | **2.36** | **4.23** | **3.08** |
| Hypothetical protein | *bmd_1007* | | **2.19** | **3.78** | **2.78** |
| CsbD-like protein | *bmd_1013* | | -1.55 | **2.14** | **3.34** |
| Phosphoenolpyruvate-dependent sugar phosphotransferase system, EIIA 2 domain | *bmd_1027* | | 1.60 | **1.75** | **-2.04** |
| PTS system, lactose/cellobiose specific IIB subunit family protein | *bmd_1028* | | 1.66 | 1.68 | **-2.17** |
| Oxidoreductase, aldo/keto reductase family | *bmd_1041* | | 1.31 | **2.99** | 1.73 |
| Hypothetical protein | *bmd_1059* | | 1.39 | **2.17** | **1.76** |
| Proton/sodium-glutamate symport protein | *bmd_1062* | | -1.57 | **-2.27** | **-3.69** |
| Endopeptidase LytE | *bmd_1065* | *lytE* | -1.16 | **-2.04** | **-1.78** |
| Hypothetical protein | *bmd_1070* | | 1.10 | **2.41** | **2.39** |
| Capsule biosynthesis protein CapB | *bmd_1092* | *capB* | -1.74 | **-3.56** | **-2.45** |
| Capsule biosynthesis protein CapC | *bmd_1093* | *capC* | -1.66 | **-3.51** | **-2.81** |
| Capsule biosynthesis protein CapA | *bmd_1094* | *capA* | -1.74 | **-2.87** | **-2.00** |
| Gamma-glutamyltransferase | *bmd_1095* | *ggt* | **-1.78** | **-3.07** | **-2.50** |
| Putative peptidoglycan binding domain protein | *bmd_1096* | | **-2.03** | **-3.76** | **-2.49** |
| Conserved hypothetical protein | *bmd_1102* | | -1.21 | -1.58 | -1.48 |
| Conserved hypothetical protein | *bmd_1104* | | -1.16 | **-1.87** | -1.33 |
| UTP-glucose-1-phosphate uridylyltransferase | *bmd_1114* | *galU* | -1.44 | **-2.85** | **-1.91** |
| Galactosyl transferase cpsE | *bmd_1115* | | -1.39 | **-2.17** | -1.58 |
| Putative membrane protein | *bmd_1116* | | -1.34 | **-2.01** | -1.52 |
| Glycosyl transferase, family 2 | *bmd_1117* | | -1.34 | **-2.28** | -1.64 |
| Glycosyl transferase, family 2 | *bmd_1118* | | -1.38 | **-2.27** | -1.67 |
| Glycosyl transferase, group 1 | *bmd_1119* | | -1.43 | **-2.07** | -1.73 |
| Glycosyl transferase, group 1 | *bmd_1120* | | -1.36 | **-2.43** | **-1.75** |
| Polysaccharide biosynthesis protein | *bmd_1121* | | -1.41 | **-2.57** | **-2.01** |
| UDPglucose 6-dehydrogenase | *bmd_1122* | | -1.39 | **-2.16** | **-2.18** |
| Chain length determinant family protein | *bmd_1123* | | -1.33 | **-1.77** | -1.49 |
| Tyrosine-protein phosphatase capC | *bmd_1125* | | 1.09 | **1.97** | 1.72 |
| UTP-glucose-1-phosphate uridylyltransferase | *bmd_1126* | *galU* | 1.09 | 1.74 | 1.47 |
| Membrane-bound protein lytR | *bmd_1127* | | -1.21 | **-1.85** | -1.64 |
| Tyrosine-protein phosphatase | *bmd_1129* | *ywqE* | -1.06 | -1.73 | -1.50 |
| Pyruvate oxidase | *bmd_1131* | | -1.20 | **2.41** | **2.26** |
| Flavoenzyme | *bmd_1132* | *yerD* | -1.06 | **1.77** | 1.56 |
| Hypothetical protein | *bmd_1154* | | 1.30 | **2.16** | **1.81** |
| Lactoylglutathione lyase | *bmd_1173* | | 1.20 | **3.05** | **2.02** |
| Conserved hypothetical protein | *bmd_1174* | | 1.27 | **3.25** | **2.13** |
| Conserved hypothetical protein | *bmd_1178* | | -1.54 | **2.45** | **1.94** |
| Hypothetical protein | *bmd_1185* | | 1.02 | **-2.55** | -1.65 |
| Hypothetical protein | *bmd_1186* | | -1.16 | **-2.06** | -1.45 |
| Hypoxanthine/guanine permease | *bmd_1193* | *pbuO* | -1.39 | **-3.12** | **-1.91** |
| Transcriptional regulator, MarR family | *bmd_1200* | | -1.23 | **-1.84** | -1.42 |
| Polyhydroxyalkanoic acid inclusion protein PhaP | *bmd_1211* | *phaP* | 1.29 | **2.17** | **2.16** |
| Poly-beta-hydroxybutyrate-responsive repressor | *bmd_1212* | *phaQ* | 1.12 | **1.79** | 1.42 |
| NAD+ synthetase | *bmd_1223* | *nadE* | -1.18 | -1.48 | **-1.77** |
| 5-methylthioribose kinase | *bmd_1231* | *mtnK* | 1.07 | **-1.83** | -1.66 |

| Gene product | Gene ID | Gene symbol | 0.6 M | 1.2 M | 1.8 M |
|---|---|---|---|---|---|
| 2,3-diketo-5-methylthiopentyl-1-phosphate enolase | *bmd_1234* | *mtnW* | 1.03 | -1.99 | -1.75 |
| 2-hydroxy-3-keto-5-methylthiopentenyl-1- phosphate phosphatase | *bmd_1235* | *mtnX* | -1.03 | -2.00 | -1.76 |
| Methylthioribulose-1-phosphate dehydratase | *bmd_1236* | *mtnB* | -1.04 | -1.99 | -1.79 |
| 1,2-dihydroxy-3-keto-5-methylthiopentene dioxygenase | *bmd_1237* | *mtnD* | -1.05 | -2.17 | -1.79 |
| Ribose ABC transporter, ribose-binding protein RbsB | *bmd_1238* | *rbsB* | -1.14 | -2.73 | -2.38 |
| Ribose ABC transporter, ATP-binding protein RbsA | *bmd_1239* | *rbsA* | -1.27 | -3.01 | -1.93 |
| Ribose ABC transporter, permease protein RbsC | *bmd_1240* | *rbsC* | -1.27 | -2.33 | -1.56 |
| ATP-dependent Clp protease, ATP-binding subunit ClpE | *bmd_1249* | *clpE* | -1.27 | 1.97 | 1.35 |
| Putative Na+/H+ antiporter NhaC | *bmd_1250* | *nhaC* | -1.35 | -2.62 | -2.71 |
| Conserved hypothetical protein | *bmd_1259* | | -1.52 | -2.19 | -1.24 |
| Conserved hypothetical protein | *bmd_1261* | | 1.73 | 3.53 | 2.17 |
| Phosphotransferase system (PTS) enzyme I | *bmd_1284* | *ptsI* | 1.15 | 1.92 | 1.28 |
| Conserved hypothetical protein | *bmd_1285* | | -1.42 | -2.75 | -1.46 |
| LrgA family protein | *bmd_1286* | | -1.41 | -2.46 | -1.55 |
| Conserved hypothetical protein | *bmd_1288* | | -1.43 | -2.62 | -1.59 |
| Mechanosensitive ion channel | *bmd_1313* | | -1.03 | 1.84 | 1.37 |
| 6-phosphogluconate dehydrogenase, decarboxylating | *bmd_1316* | *gnd* | -1.25 | -2.39 | -2.14 |
| Arginine decarboxylase | *bmd_1333* | *speA* | -1.55 | -3.18 | -2.17 |
| Conserved hypothetical protein | *bmd_1358* | | 1.21 | 1.91 | 1.87 |
| Penicillin-binding protein 1A/1B | *bmd_1383* | *ponA* | -1.36 | -1.61 | -1.77 |
| Conserved hypothetical protein | *bmd_1389* | | -1.35 | -1.92 | -1.29 |
| Conserved hypothetical protein | *bmd_1399* | | 1.21 | 1.73 | 1.58 |
| Sodium/proline symporter, frameshift | *bmd_1401* | | 1.84 | 3.20 | 2.39 |
| Conserved hypothetical protein | *bmd_1412* | | -1.35 | -2.16 | -1.79 |
| Modulator of lia operon expression | *bmd_1416* | | 1.06 | 1.87 | 1.04 |
| Putative RNA methylase protein family (UPF0020) | *bmd_1421* | | 1.04 | 1.77 | 1.55 |
| Carboxypeptidase Taq (M32) metallopeptidase | *bmd_1431* | | 1.38 | 2.01 | 2.14 |
| Xanthine phosphoribosyltransferase | *bmd_1432* | *xpt* | 1.08 | -1.91 | -1.55 |
| Xanthine permease | *bmd_1433* | | 1.09 | -1.97 | -1.44 |
| Succinate-semialdehyde dehydrogenase (NADP+) - general stress protein | *bmd_1435* | | 1.35 | 2.79 | 2.28 |
| Succinate-semialdehyde dehydrogenase (NADP+) - GABA utilization | *bmd_1435* | | 1.35 | 2.79 | 2.28 |
| Conserved hypothetical protein | *bmd_1442* | | -1.17 | -1.80 | -1.65 |
| Hypothetical protein | *bmd_1443* | | -1.10 | -1.80 | -1.60 |
| Cold shock protein | *bmd_1450* | *cspD* | 1.32 | 1.65 | 2.01 |
| Acetyltransferase, GNAT family | *bmd_1466* | | -1.26 | -1.77 | -1.57 |
| Major facilitator transporter family protein (putative permease) | *bmd_1484* | | -1.27 | -2.13 | -1.46 |
| Amidohydrolase | *bmd_1487* | | 1.31 | 1.99 | 1.40 |
| L-seryl-tRNA(Sec) selenium transferase | *bmd_1488* | *selA* | 1.48 | 1.97 | 1.33 |
| Conserved hypothetical protein | *bmd_1489* | | 1.40 | 2.23 | 1.55 |
| 2-dehydro-3-deoxygluconokinase | *bmd_1490* | | 1.48 | 1.99 | 1.28 |
| Transcriptional regulator, GntR family | *bmd_1491* | | 1.21 | 1.88 | 1.38 |
| Transporter, gluconate:H+ symporter (GntP) family | *bmd_1492* | | 1.14 | 2.22 | 1.65 |
| Conserved hypothetical protein | *bmd_1493* | | 1.23 | 2.25 | 1.65 |
| Conserved hypothetical protein | *bmd_1494* | | 1.31 | 2.46 | 1.77 |
| Ferrichrome import ABC transporter, ferrichrome-binding protein FhuD | *bmd_1509* | *fhuD* | -1.33 | 1.97 | 1.17 |
| Ferrichrome import ABC transporter, ATP-binding protein FhuC | *bmd_1510* | *fhuC* | -1.31 | 2.03 | 1.18 |
| Putative Drug Resistance Transporter Family | *bmd_1513* | | -1.51 | -1.23 | 2.27 |
| 2,5-diketo-D-gluconic acid reductase B | *bmd_1514* | | 1.00 | 2.06 | 2.34 |
| HTH-type transcriptional activator hxlR | *bmd_1518* | | 1.26 | 2.03 | 1.41 |
| 3-hexulose-6-phosphate synthase | *bmd_1519* | *hxlA* | 1.17 | 1.78 | 1.27 |
| Two-component sensor histidine kinase/response regulator | *bmd_1527* | | -1.20 | -1.95 | -1.85 |
| Methyltransferase, CheR family | *bmd_1528* | | -1.25 | -1.80 | -1.53 |
| Ferritin-like domain protein | *bmd_1538* | | -1.30 | 2.81 | 3.37 |
| Aldehyde dehydrogenase (NAD) Family Protein | *bmd_1546* | | -1.31 | 3.76 | 3.32 |
| Glucose starvation-inducible protein B | *bmd_1557* | | 1.37 | 5.46 | 12.05 |
| Putative methionine import ABC transporter, methionine-binding protein Met | *bmd_1578* | *met* | -1.20 | -2.03 | -1.86 |
| Methionine import ABC transporter, ATP-binding protein MetN | *bmd_1579* | *metN* | -1.25 | -2.16 | -1.67 |
| Putative methionine import ABC transporter, permease protein Met | *bmd_1580* | *met* | -1.27 | -2.16 | -1.86 |
| 2,5-diketo-D-gluconic acid reductase A | *bmd_1595* | | -1.23 | -1.78 | -1.60 |
| Endopeptidase LytF (cell wall hydrolase) | *bmd_1625* | *lytF* | -1.97 | -4.29 | -3.02 |
| Conserved hypothetical protein | *bmd_1626* | | -1.72 | -1.88 | -1.37 |
| Methylmalonate-semialdehyde dehydrogenase (acylating) | *bmd_1655* | *mmsA* | 1.19 | 1.78 | 1.33 |
| Conserved hypothetical protein | *bmd_1667* | | -1.01 | 3.07 | 2.81 |
| Spore coat protein F | *bmd_1668* | *cotF* | 1.01 | 3.03 | 2.82 |
| Hypothetical protein | *bmd_1681* | | 1.34 | 2.75 | 2.01 |
| Cold shock protein | *bmd_1682* | *cspA* | -1.30 | 1.62 | 2.50 |
| CBS domain pair family protein | *bmd_1697* | | -1.02 | 2.25 | 2.42 |
| Glutamate dehydrogenase | *bmd_1700* | | -2.35 | -3.76 | -1.37 |
| 4-hydroxy 2-oxovalerate aldolase | *bmd_1715* | | -1.05 | -2.22 | -2.19 |
| Conserved hypothetical protein | *bmd_1761* | | -1.34 | 2.81 | 2.10 |
| hut operon positive regulatory protein | *bmd_1769* | | 1.23 | 2.20 | 1.47 |
| Spore coat protein F | *bmd_1779* | *cotF* | -1.03 | 3.89 | 3.39 |
| Hypothetical protein | *bmd_1780* | | -1.04 | 3.94 | 3.02 |
| Glucose starvation-inducible protein B (General stress protein B) | *bmd_1781* | | -1.05 | 4.11 | 3.97 |
| Stress response protein YsnF | *bmd_1782* | *ysnF* | -1.23 | 2.75 | 1.71 |
| CBS domain pair family protein | *bmd_1800* | | -1.08 | 2.46 | 2.51 |

| Gene product | Gene ID | Gene symbol | 0.6 M | 1.2 M | 1.8 M |
|---|---|---|---|---|---|
| Protein of unknown funtion (DUF77) | *bmd_1801* | | -1.22 | **2.43** | **2.22** |
| Hypothetical protein | *bmd_1802* | | -1.11 | **3.25** | **3.01** |
| Oligopeptide ABC transporter, oligopeptide-binding protein | *bmd_1832* | | 1.38 | -1.66 | **-2.17** |
| Glyceraldehyde-3-phosphate dehydrogenase (NADP) | *bmd_1844* | *gapN* | -1.31 | **-2.87** | -1.54 |
| Conserved hypothetical protein | *bmd_1890* | | -1.02 | **1.82** | **1.97** |
| ***Two-component sensor histidine kinase*** | *bmd_1892* | | **3.86** | -1.37 | **-1.87** |
| ***Two-component response regulator*** | *bmd_1893* | | **4.38** | -1.23 | **-1.94** |
| ***Conserved hypothetical protein*** | *bmd_1894* | | **2.60** | -1.02 | -1.08 |
| ***Copper chaperone CopZ (copper-ion-binding protein)*** | *bmd_1895* | *copZ* | **2.60** | -1.03 | -1.33 |
| Putative lipoprotein | *bmd_1898* | | **3.05** | **-2.01** | **-3.73** |
| Putative peptidoglycan binding domain protein | *bmd_1902* | | 1.21 | **2.68** | 1.36 |
| Transcriptional regulator, GntR family | *bmd_1914* | | -1.41 | **-1.80** | -1.28 |
| Tartrate dehydrogenase/decarboxylase | *bmd_1915* | *ycsA* | **2.06** | **3.94** | 1.73 |
| Hypothetical protein | *bmd_1921* | | -1.64 | -1.23 | **-2.24** |
| Putative metal ABC transporter, metal-binding protein | *bmd_1949* | | -1.38 | **-3.23** | **-2.73** |
| Putative phosphatase | *bmd_1982* | | -1.06 | **2.17** | 1.22 |
| Tellurite resistance protein,putative | *bmd_1983* | | -1.07 | **2.07** | 1.33 |
| Sodium:dicarboxylate symporter | *bmd_1992* | | 1.19 | **-1.82** | **-1.93** |
| Phenylacetaldehyde dehydrogenase | *bmd_1994* | | 1.39 | **4.00** | **2.39** |
| Foldase protein PrsA | *bmd_2008* | *prsA* | 1.26 | **1.79** | -1.67 |
| Amino acid/peptide transporter (Peptide:H+ symporter) | *bmd_2012* | *dtpT* | -1.34 | **-2.04** | **-2.21** |
| Cytochrome P450 | *bmd_2035* | | 1.12 | **3.10** | **1.97** |
| Malate dehydrogenase | *bmd_2037* | | 1.44 | **3.78** | **1.86** |
| Glutamate synthase, large subunit | *bmd_2055* | *gltA* | 1.00 | **-1.80** | -1.37 |
| Glutamate synthase, small subunit | *bmd_2056* | *gltB* | 1.01 | **-1.80** | -1.60 |
| Tetrahydrofolate dehydrogenase/cyclohydrolase domain protein | *bmd_2060* | | 1.49 | **-2.11** | **-1.88** |
| Protein of unknown function (DUF161) | *bmd_2083* | | -1.39 | **-2.62** | **-1.76** |
| Putative lipoprotein | *bmd_2090* | | -1.15 | **-1.83** | -1.50 |
| Hypothetical protein | *bmd_2099* | | -1.48 | **2.20** | **2.41** |
| DNA-3-methyladenine glycosylase family protein | *bmd_2107* | | 1.11 | **1.77** | 1.41 |
| Conserved hypothetical protein | *bmd_2128* | | 1.01 | 1.74 | **1.90** |
| Hypothetical protein | *bmd_2153* | | 1.12 | **2.31** | 1.53 |
| S1 RNA binding domain protein | *bmd_2164* | | -1.27 | **-2.19** | **-1.82** |
| 3-hydroxybutyrate dehydrogenase | *bmd_2166* | | 1.11 | **2.77** | **1.76** |
| NADH dehydrogenase | *bmd_2191* | | **2.71** | **2.23** | **-4.49** |
| General stress protein 17M | *bmd_2208* | | -1.37 | **3.32** | **3.56** |
| 1,4-dihydroxy-2-naphthoate octaprenyltransferase | *bmd_2219* | *menA* | -1.19 | **-1.79** | -1.38 |
| Protein of unknown function (DUF1696) | *bmd_2222* | | 1.19 | 1.57 | **2.12** |
| Major Facilitator Superfamily protein | *bmd_2223* | | -1.04 | 1.23 | **1.83** |
| Conserved hypothetical protein | *bmd_2227* | | -1.33 | **-2.03** | -1.08 |
| RNA polymerase sigma factor, sigma-70 family | *bmd_2228* | | -1.38 | **-1.96** | -1.23 |
| Organic hydroperoxide resistance protein | *bmd_2231* | *ohrB* | **-1.91** | 1.05 | 1.37 |
| Peptidoglycan-binding protein | *bmd_2238* | | 1.21 | **-2.48** | -1.67 |
| Pyrroline-5-carboxylate reductase | *bmd_2243* | *proH* | **3.94** | **10.63** | **6.44** |
| Glutamate 5-kinase | *bmd_2244* | *proJ* | **3.97** | **10.56** | **5.90** |
| Gamma-glutamyl phosphate reductase | *bmd_2245* | *proA* | **3.18** | **8.75** | **4.88** |
| Conserved hypothetical protein | *bmd_2250* | | 1.07 | **1.83** | 1.09 |
| Immune inhibitor A metalloprotease | *bmd_2278* | *inhA* | -1.21 | **-2.33** | **-2.83** |
| Fumarate hydratase, class II | *bmd_2279* | *fumC* | -1.14 | **-2.43** | **-2.52** |
| Conserved hypothetical protein | *bmd_2282* | | -1.60 | 1.32 | **1.89** |
| Bacillolysin precursor (neutral protease) | *bmd_2285* | *nprM* | 1.46 | **6.63** | **3.15** |
| Amino acid permease family protein | *bmd_2362* | | 1.29 | **2.48** | 1.63 |
| ***Fructoselysine-6-P-deglycase*** | *bmd_2368* | *frlB* | **2.46** | 1.60 | -1.29 |
| Putative cation transporter regulator | *bmd_2410* | | -1.19 | **1.85** | **1.81** |
| Nitroreductase family protein | *bmd_2414* | | -1.02 | **1.92** | 1.34 |
| NAD dependent epimerase/dehydratase family | *bmd_2433* | | 1.23 | **3.10** | **2.18** |
| Conserved hypothetical protein | *bmd_2439* | | -1.38 | **-1.79** | -1.34 |
| Cell wall-associated protease | *bmd_2442* | | **-2.01** | **-3.66** | **-2.76** |
| Secreted cell wall DL-endopeptidase | *bmd_2460* | *cwlO* | -1.38 | **-5.46** | **-2.56** |
| Dihydroxy-acid dehydratase | *bmd_2497* | *ilvD* | 1.39 | **2.16** | **2.75** |
| Lysine-specific permease | *bmd_2525* | | -1.21 | **-2.66** | -1.74 |
| GNAT family acetyltransferase | *bmd_2527* | | -1.40 | **-2.25** | -1.47 |
| Carbonic anhydrase | *bmd_2585* | | 1.25 | **5.46** | **2.57** |
| Putative sulfate transport protein (permease activity) | *bmd_2586* | | 1.15 | **2.93** | **1.98** |
| CbiET protein | *bmd_2601* | *cbiET* | 1.10 | 1.01 | **1.85** |
| Cobalamin biosynthesis protein CbiD | *bmd_2602* | *cbiD* | 1.04 | -1.03 | **2.17** |
| Precorrin-8X methylmutase CbiC | *bmd_2603* | *cbiC* | 1.06 | 1.07 | **2.19** |
| Precorrin-6x reductase | *bmd_2604* | *cbiJ* | 1.06 | 1.01 | **2.13** |
| Sirohydrochlorin cobaltochelatase | *bmd_2605* | *cbiX* | 1.05 | 1.05 | **2.20** |
| Precorrin 3 methylase | *bmd_2606* | *cbiH* | 1.01 | 1.06 | **2.25** |
| Cobalamin biosynthesis protein | *bmd_2607* | *cbiW* | -1.02 | 1.04 | **1.96** |
| IDEAL domain protein | *bmd_2614* | | 1.33 | **1.92** | **2.05** |
| Ammonium transporter | *bmd_2615* | *amt* | -1.25 | **-2.45** | -1.56 |
| Hypothetical protein | *bmd_2616* | | -1.23 | **-2.17** | -1.56 |
| Malate permease | *bmd_2629* | | -1.37 | **-2.31** | -1.45 |
| Conserved hypothetical protein | *bmd_2648* | | -1.04 | **4.11** | **2.40** |

| Gene product | Gene ID | Gene symbol | 0.6 M | 1.2 M | 1.8 M |
|---|---|---|---|---|---|
| Acetyltransferase, GNAT family | *bmd_2650* | | -1.45 | **-1.91** | -1.05 |
| Endonuclease V | *bmd_2656* | | -1.21 | **-1.82** | -1.53 |
| MATE efflux family protein | *bmd_2674* | | -1.27 | **-2.06** | **-1.76** |
| Tellurium resistance protein, TerD family | *bmd_2685* | | 1.22 | **2.01** | 1.71 |
| Tellurium resistance protein terD,TerD family | *bmd_2686* | | 1.26 | **2.01** | 1.67 |
| Probable tellurium resistance protein, TerD family | *bmd_2687* | | 1.14 | **2.03** | **1.80** |
| 2',3'-cyclic-nucleotide 2'-phosphodiesterase | *bmd_2688* | *yfkN* | -1.19 | **-2.48** | **-2.39** |
| Cold shock protein | *bmd_2698* | *cspC* | -1.16 | -1.68 | 1.13 |
| Conserved hypothetical protein | *bmd_2710* | | **-2.38** | **-6.73** | **-4.45** |
| Hypothetical protein | *bmd_2714* | | -1.55 | 1.52 | **1.78** |
| Hypothetical protein | *bmd_2753* | | -1.37 | 1.59 | **2.14** |
| Conserved hypothetical protein | *bmd_2757* | | -1.32 | **-2.01** | -1.35 |
| Cold shock protein | *bmd_2791* | *cspC* | -1.23 | 1.39 | **2.16** |
| Hypothetical protein | *bmd_2822* | | -1.33 | **-1.79** | -1.32 |
| Peptidase M48 | *bmd_2826* | | -1.01 | **2.30** | 1.08 |
| Conserved hypothetical protein | *bmd_2897* | | -1.48 | **2.60** | **4.50** |
| Conserved hypothetical protein | *bmd_2910* | | 1.16 | **-1.88** | **-1.85** |
| Monoacylglycerol lipase | *bmd_2911* | | 1.67 | -1.49 | **-2.11** |
| 2-oxoglutarate dehydrogenase, E2 component (dihydrolipoamide succinyltransferase) | *bmd_2925* | *odhB* | 1.29 | **3.20** | **3.40** |
| 2-oxoglutarate dehydrogenase, E1 component | *bmd_2926* | *odhA* | 1.19 | **2.43** | **2.36** |
| NAD dependent epimerase/dehydratase family | *bmd_2930* | | 1.23 | **1.99** | **2.32** |
| Amino acid permease | *bmd_2966* | | 1.57 | **3.66** | **2.36** |
| Hypothetical protein | *bmd_2977* | | -1.12 | **-1.79** | -1.32 |
| Endopeptidase | *bmd_2993* | | -1.66 | **-2.20** | **-1.96** |
| ThiJ/PfpI family protein | *bmd_3006* | | -1.42 | **3.68** | **4.07** |
| Copper resistance protein | *bmd_3010* | *copC* | 1.00 | 1.02 | **-1.98** |
| ***Cell wall endopeptidase*** | *bmd_3039* | *lytF* | **1.75** | 1.39 | 1.13 |
| Conserved hypothetical protein | *bmd_3050* | | 1.22 | **-1.99** | **-2.21** |
| Bacterial regulatory protein, arsR family | *bmd_3056* | | 1.03 | 1.21 | **1.79** |
| Conserved hypothetical protein | *bmd_3061* | | 1.37 | **2.03** | 1.69 |
| Ribosomal protein S14 | *bmd_3063* | | 1.13 | **2.28** | 1.74 |
| Transition state regulator, domain protein | *bmd_3064* | | -1.26 | **-4.53** | **-2.10** |
| DinB family protein | *bmd_3065* | | -1.23 | **-1.84** | -1.48 |
| Nicotinate-nucleotide--dimethylbenzimidazole phosphoribosyltransferase | *bmd_3069* | *cobT* | -1.22 | **-2.13** | **-1.79** |
| Hypothetical protein | *bmd_3082* | | 1.22 | **2.60** | **2.77** |
| B12 binding domain protein | *bmd_3083* | | 1.27 | **2.62** | **2.63** |
| Conserved hypothetical protein | *bmd_3090* | | -1.65 | 1.58 | **1.95** |
| Malate dehydrogenase | *bmd_3115* | | 1.28 | **2.31** | 1.48 |
| Putative aminoglycoside N3'-acetyltransferase | *bmd_3116* | | 1.33 | **3.07** | **1.90** |
| Drug resistance MFS transporter, drug:H+ antiporter-1 (14 Spanner) (DHA2) family | *bmd_3125* | | -1.32 | **-1.88** | -1.47 |
| Transcriptional regulator, MarR family | *bmd_3126* | | -1.29 | **-1.87** | -1.49 |
| UDP-glucuronosyltransferase, macrolide glycosyltransferase Family | *bmd_3136* | | 1.27 | **2.10** | 1.39 |
| Hypothetical protein | *bmd_3145* | | -1.52 | **2.41** | **2.05** |
| Hypothetical protein | *bmd_3147* | | -1.55 | **-2.58** | **-1.99** |
| Aminoglycoside N(6')-acetyltransferase, GNAT family | *bmd_3149* | | 1.26 | **1.92** | **2.10** |
| Conserved hypothetical protein | *bmd_3167* | | -1.21 | **2.83** | **2.99** |
| LPXTG-motif cell wall anchor domain protein | *bmd_3174* | | **-1.84** | **-4.06** | **-2.41** |
| Sortase family protein | *bmd_3175* | | -1.49 | **-2.14** | -1.62 |
| Putative membrane protein | *bmd_3179* | | -1.24 | **-3.03** | **-2.32** |
| Small multidrug resistance (SMR) family protein | *bmd_3202* | | -1.36 | **-1.79** | -1.49 |
| Cold shock protein | *bmd_3204* | *cspB* | -1.21 | **-1.84** | -1.38 |
| Manganese catalase | *bmd_3215* | | 1.01 | **4.14** | **4.20** |
| Putative ferrichrome ABC transporter, ferrichrome-binding protein | *bmd_3216* | *yclQ* | 1.04 | **3.16** | 1.64 |
| Putative ferrichrome ABC transporter, ATP-binding protein | *bmd_3217* | *yclP* | 1.04 | **2.99** | 1.65 |
| Putative ferrichrome ABC transporter, permease protein | *bmd_3218* | *yclO* | 1.00 | **2.45** | 1.26 |
| Putative ferrichrome ABC transporter, permease protein | *bmd_3219* | *yclN* | -1.04 | **3.05** | 1.61 |
| Hypothetical protein | *bmd_3222* | | -1.12 | **2.95** | **2.75** |
| Hypothetical protein | *bmd_3242* | | **-1.89** | 1.23 | **2.05** |
| Hypothetical protein | *bmd_3262* | | -1.60 | **-2.85** | **-1.80** |
| Conserved hypothetical protein | *bmd_3307* | | -1.01 | **1.88** | 1.57 |
| Conserved hypothetical protein | *bmd_3373* | | 1.06 | **2.25** | 1.28 |
| Cold shock protein | *bmd_3404* | *cspC* | 1.22 | 1.35 | **1.76** |
| Osmoprotectant transporter gene ousA | *bmd_3405* | | 1.53 | **3.29** | **2.39** |
| Threonine synthase | *bmd_3406* | *thrC* | 1.48 | -1.67 | **-2.44** |
| Proton/ glutamate symport protein | *bmd_3407* | | 1.41 | **-2.43** | **-2.19** |
| Hypothetical protein | *bmd_3408* | | 1.34 | **-2.39** | **-2.61** |
| Sulfate transporter family protein | *bmd_3416* | | -1.04 | 1.72 | **1.86** |
| ***Two-component response regulator*** | *bmd_3443* | | **2.00** | -1.08 | -1.30 |
| ***Putative membrane protein*** | *bmd_3444* | | **2.62** | -1.03 | -1.21 |
| ***Putative membrane protein*** | *bmd_3445* | | **2.41** | 1.02 | -1.18 |
| ***Putative ABC transporter, ATP-binding protein*** | *bmd_3446* | | **2.69** | 1.06 | -1.16 |
| Positive regulator of sigma-B activity | *bmd_3481* | *rsbR* | -1.34 | **-2.28** | **-1.87** |
| Hypothetical protein | *bmd_3488* | | -1.23 | **2.58** | **2.26** |
| Hypothetical protein | *bmd_3489* | | -1.18 | **2.39** | **2.19** |
| Conserved hypothetical protein | *bmd_3492* | | -1.29 | **3.73** | **2.52** |

| Gene product | Gene ID | Gene symbol | 0.6 M | 1.2 M | 1.8 M |
|---|---|---|---|---|---|
| Oxidoreductase, short chain dehydrogenase/reductase family protein | *bmd_3493* | | -1.15 | **4.50** | **3.22** |
| Conserved hypothetical protein | *bmd_3494* | | -1.15 | **1.96** | **2.16** |
| 5-methyltetrahydropteroyltriglutamate--homocysteine S-methyltransferase | *bmd_3527* | *metE* | -1.01 | -1.05 | **2.48** |
| Putative protease, NlpC/P60 family | *bmd_3550* | | 1.64 | 1.34 | **1.83** |
| 8-amino-7-oxononanoate synthase | *bmd_3693* | *bioF* | 1.59 | **1.88** | 1.31 |
| Conserved hypothetical protein | *bmd_3711* | | -1.36 | **2.11** | 1.63 |
| CAAX amino terminal protease family protein | *bmd_3728* | | 1.07 | **3.58** | 1.53 |
| Hypothetical protein | *bmd_3729* | | -1.02 | **3.10** | 1.53 |
| Conserved hypothetical protein | *bmd_3744* | | -1.23 | 1.69 | **1.81** |
| Malate dehydrogenase | *bmd_3745* | | 1.00 | **1.84** | **2.18** |
| Oxidoreductase molybdopterin binding domain protein | *bmd_3784* | | -1.13 | **-2.36** | -1.73 |
| Conserved hypothetical protein | *bmd_3787* | | 1.20 | **3.32** | **2.67** |
| Putative 1-pyrroline-5-carboxylate dehydrogenase | *bmd_3813* | *putC* | **4.38** | **5.58** | **3.49** |
| Proline oxidase | *bmd_3814* | *putB* | **1.80** | **1.83** | **1.84** |
| Hypothetical protein | *bmd_3855* | | -1.21 | 1.06 | **1.96** |
| Hypothetical protein | *bmd_3856* | | -1.02 | **2.00** | 1.74 |
| Sporulation-specific extracellular nuclease | *bmd_3867* | *nucB* | -1.21 | **1.85** | 1.57 |
| Putative lipoprotein | *bmd_3898* | | -1.46 | **-3.16** | -1.55 |
| Putative serine proteinase | *bmd_3899* | | -1.33 | **-2.99** | -1.66 |
| Hypothetical protein | *bmd_3908* | | 1.14 | 1.54 | **1.79** |
| NADH-dependent flavin oxidoreductase | *bmd_3933* | | -1.39 | **-2.07** | -1.56 |
| GABA permease (4-amino butyrate transport carrier) | *bmd_3936* | | -1.24 | **-2.11** | -1.40 |
| NAD dependent epimerase/dehydratase family | *bmd_3943* | | -1.23 | **1.95** | **1.99** |
| Endopeptidase | *bmd_3978* | *lytF* | **-1.95** | **-3.73** | **-2.32** |
| Conserved hypothetical protein | *bmd_3982* | | 1.21 | **1.85** | 1.74 |
| Hypothetical protein | *bmd_4014* | | -1.10 | **1.77** | 1.30 |
| Sporulation-control protein Spo0M | *bmd_4015* | *spo0M* | -1.12 | **2.06** | 1.09 |
| Serine/threonine protein kinase | *bmd_4016* | *prkC* | -1.21 | **2.13** | 1.15 |
| Hypothetical protein | *bmd_4017* | | -1.20 | **1.78** | 1.12 |
| D-amino acid aminotransferase | *bmd_4023* | *dat* | 1.29 | **2.64** | 1.72 |
| Conserved hypothetical protein | *bmd_4042* | | -1.48 | **-2.20** | -1.53 |
| Siderophore biosynthesis protein | *bmd_4048* | | 1.01 | **9.99** | **2.62** |
| Transporter (Major facilitator Superfamily) | *bmd_4049* | | -1.01 | **13.74** | **3.14** |
| Putative L-lysine 6-monooxygenase (NADPH) | *bmd_4050* | | 1.00 | **10.56** | **3.05** |
| Siderophore biosynthesis protein | *bmd_4051* | | 1.04 | **13.09** | **3.86** |
| Siderophore biosynthesis protein | *bmd_4052* | | 1.07 | **15.03** | **4.11** |
| L-2,4-diaminobutyrate decarboxylase | *bmd_4053* | | 1.14 | **19.70** | **4.93** |
| 2,4-diaminobutyrate 4-transaminase | *bmd_4054* | | 1.21 | **16.56** | **4.75** |
| Putative membrane protein | *bmd_4090* | | -1.33 | **-2.41** | -1.59 |
| 2-oxoglutarate ferredoxin oxidoreductase subunit beta | *bmd_4100* | | -1.35 | **-1.85** | -1.50 |
| 2-oxoglutarate ferredoxin oxidoreductase subunit alpha | *bmd_4101* | | -1.28 | **-1.80** | -1.72 |
| Peptidase, M16 family protein | *bmd_4113* | | 1.19 | **2.39** | 1.57 |
| Putative Zn-protease | *bmd_4114* | | 1.05 | **1.77** | 1.31 |
| Polynucleotide phosphorylase | *bmd_4132* | *pnp* | -1.07 | -1.56 | **-1.93** |
| Flagellar motor switch protein FliN | *bmd_4168* | *fliN* | 1.14 | **1.89** | 1.53 |
| Flagellar motor switch protein FliM | *bmd_4169* | *fliM* | 1.15 | **1.91** | 1.62 |
| Flagellar basal body-associated protein FliL | *bmd_4170* | *fliL* | 1.10 | **2.03** | 1.54 |
| Flagellar protein FlbD | *bmd_4171* | *flbD* | 1.25 | **1.88** | 1.50 |
| Flagellar hook protein FlgE | *bmd_4172* | *flgE* | 1.16 | **1.83** | 1.55 |
| Flagellar hook-length control protein | *bmd_4174* | *flik* | 1.15 | **2.19** | 1.75 |
| Conserved hypothetical protein | *bmd_4175* | | 1.15 | **1.97** | 1.69 |
| Flagellar export protein FliJ | *bmd_4176* | *fliJ* | 1.20 | **2.00** | **1.78** |
| Flagellum-specific ATP synthase | *bmd_4177* | *fliI* | 1.24 | **2.10** | 1.69 |
| Flagellar assembly protein FliH | *bmd_4178* | *fliH* | 1.13 | **1.79** | 1.60 |
| Dihydroorotate dehydrogenase, electron transfer subunit | *bmd_4239* | *pyrK* | 1.17 | -1.46 | **-1.85** |
| Carbamoyl-phosphate synthase, large subunit | *bmd_4240* | *pyrAB* | 1.14 | -1.52 | **-2.17** |
| Carbamoyl-phosphate synthase, small subunit | *bmd_4241* | *pyrAA* | 1.20 | -1.55 | **-2.27** |
| Dihydroorotase | *bmd_4242* | *pyrC* | 1.21 | -1.61 | **-1.89** |
| Uracil permease | *bmd_4244* | *pyrP* | -1.02 | **-1.95** | **-1.94** |
| Uracil phosphoribosyl transferase/pyrimidine operon regulatory protein | *bmd_4245* | *pyrR* | -1.17 | **-2.25** | -1.51 |
| Nucleoside diphosphate kinase | *bmd_4314* | *ndk* | 1.34 | **2.17** | **1.86** |
| 1-acyl-sn-glycerol-3-phosphate acyltransferase | *bmd_4331* | *plsC* | -1.26 | -1.73 | **-1.78** |
| FMN permease | *bmd_4350* | *fmnP* | -1.25 | **-2.14** | -1.43 |
| Protein of unknown function (DUF1002) | *bmd_4368* | | -1.73 | -1.43 | **-1.81** |
| Diaminopimelate decarboxylase | *bmd_4369* | *lysA* | 1.18 | 1.60 | **1.83** |
| Oxidoreductase, aldo/keto reductase family | *bmd_4389* | | 1.09 | **1.95** | 1.34 |
| Conserved hypothetical protein | *bmd_4390* | | 1.09 | 1.65 | **1.87** |
| 3-oxoacid CoA-transferase subunit B | *bmd_4391* | *scoB* | 1.34 | **2.00** | 1.52 |
| 3-oxoacid CoA-transferase subunit A | *bmd_4392* | *scoA* | 1.34 | **1.78** | 1.44 |
| Conserved hypothetical protein | *bmd_4397* | | -1.18 | **-2.17** | -1.45 |
| Methylmalonate-semialdehyde dehydrogenase | *bmd_4404* | *mmsA* | 1.16 | 1.39 | **1.87** |
| Hypothetical protein | *bmd_4407* | | 1.23 | 1.58 | **1.77** |
| Arginine ABC transporter, ATP-binding protein ArtM | *bmd_4416* | *artM* | -1.25 | **-1.87** | **-1.90** |
| Arginine ABC transporter, permease protein ArtQ | *bmd_4417* | *artQ* | -1.23 | **-1.82** | **-1.82** |
| Arginine ABC transporter, arginine-binding protein ArtP | *bmd_4418* | *artP* | -1.21 | **-1.88** | **-1.82** |
| Amino acid/peptide transporter (Peptide:H+ symporter) | *bmd_4434* | | -1.25 | **-3.43** | **-2.78** |

| Gene product | Gene ID | Gene symbol | 0.6 M | 1.2 M | 1.8 M |
|---|---|---|---|---|---|
| Glycine cleavage system T protein | *bmd_4471* | *gcvT* | -1.15 | **-2.25** | -1.21 |
| Conserved hypothetical protein | *bmd_4483* | | 1.35 | **2.25** | **1.95** |
| 50S ribosomal protein L33 | *bmd_4493* | *rpmG* | -1.22 | **-1.84** | -1.36 |
| Hypothetical protein | *bmd_4496* | | -1.21 | **-1.83** | -1.24 |
| Conserved hypothetical protein | *bmd_4542* | | 1.37 | **1.95** | 1.12 |
| Conserved hypothetical protein | *bmd_4543* | | 1.39 | **2.08** | -1.08 |
| Putative membrane protein | *bmd_4544* | | 1.31 | **1.96** | -1.06 |
| Conserved hypothetical protein | *bmd_4560* | | -1.01 | 1.43 | **1.93** |
| Hypothetical protein | *bmd_4598* | | -1.17 | 1.34 | **1.89** |
| Conserved hypothetical protein | *bmd_4632* | | -1.22 | **2.60** | **2.83** |
| Phosphate transporter | *bmd_4695* | *pit* | -1.31 | **-1.78** | -1.45 |
| Protein of unknown function (DUF47) | *bmd_4696* | | -1.35 | **-1.82** | -1.37 |
| Succinate dehydrogenase, iron-sulfur protein | *bmd_4709* | *sdhB* | 1.20 | **1.89** | 1.74 |
| Succinate dehydrogenase, flavoprotein subunit | *bmd_4710* | *sdhA* | 1.26 | **2.04** | **1.99** |
| Succinate dehydrogenase, cytochrome b558 subunit | *bmd_4711* | *sdhC* | 1.25 | **1.80** | **1.77** |
| Aspartate kinase | *bmd_4713* | *lysC* | 1.39 | 1.30 | **2.02** |
| Electron transfer flavoprotein, alpha subunit | *bmd_4716* | *etfA* | 1.48 | **2.69** | **1.75** |
| Electron transfer flavoprotein, beta subunit | *bmd_4717* | *etfB* | 1.34 | **2.25** | 1.37 |
| Malate dehydrogenase, NAD-dependent | *bmd_4754* | *mdh* | 1.47 | **2.10** | **2.01** |
| Isocitrate dehydrogenase, NADP-dependent | *bmd_4755* | *icd* | 1.49 | **2.08** | **2.02** |
| Citrate synthase II | *bmd_4756* | *citZ* | 1.52 | **2.39** | **2.24** |
| ATP-NAD kinase | *bmd_4786* | *ppnK* | 1.28 | **1.75** | **1.82** |
| Acetyl-coenzyme A synthetase | *bmd_4798* | *acsA* | 1.58 | **2.57** | **1.93** |
| Conserved hypothetical protein | *bmd_4807* | | -1.25 | **2.28** | **2.06** |
| Protein of unknown function (DUF948) | *bmd_4808* | | -1.33 | **2.22** | **2.15** |
| Aminopeptidase | *bmd_4809* | | -1.06 | -1.51 | **-1.79** |
| M42 glutamyl aminopeptidase | *bmd_4817* | | 1.26 | **1.83** | 1.58 |
| Conserved hypothetical protein | *bmd_4849* | | 1.13 | 1.26 | **1.88** |
| DNA-protecting protein | *bmd_4857* | *dps* | -1.55 | 1.45 | **2.10** |
| 50S ribosomal protein L31 | *bmd_4863* | *rpmE* | -1.06 | **1.85** | 1.23 |
| Flavodoxin | *bmd_4866* | *fldA* | -1.07 | **3.92** | **2.09** |
| Conserved hypothetical protein | *bmd_4867* | | -1.07 | **2.50** | 1.73 |
| Conserved hypothetical protein | *bmd_4868* | | -1.03 | **3.68** | **2.52** |
| 2-succinyl-6-hydroxy-2,4-cyclohexadiene-1-carboxylate synthase | *bmd_4876* | | -1.11 | -1.48 | **-1.95** |
| Metal-dependent phosphohydrolase | *bmd_4944* | | 1.12 | **2.95** | **2.47** |
| NADH dehydrogenase YutJ | *bmd_4957* | *yutJ* | 1.13 | **2.10** | **2.32** |
| FeS assembly protein SufB | *bmd_4976* | *sufB* | 1.04 | 1.71 | **1.92** |
| SUF system FeS assembly protein | *bmd_4977* | *iscU* | 1.13 | **1.92** | **2.07** |
| Cysteine desulfurase SufS | *bmd_4978* | *sufS* | 1.13 | **1.77** | **2.06** |
| FeS assembly protein SufD | *bmd_4979* | *sufD* | 1.12 | 1.60 | **1.96** |
| FeS assembly ATPase SufC | *bmd_4980* | *sufC* | 1.06 | 1.49 | **1.77** |
| Methionine import ABC transporter, methionine-binding protein MetQ | *bmd_4982* | *metQ* | -1.28 | **-2.68** | **-2.13** |
| Methionine import ABC transporter, permease protein MetP | *bmd_4983* | *metP* | -1.26 | **-2.68** | **-1.99** |
| Methionine import ABC transporter, ATP-binding protein MetN | *bmd_4984* | *metN* | -1.25 | **-2.41** | **-2.19** |
| Conserved hypothetical protein | *bmd_4995* | | 1.11 | **2.62** | **2.16** |
| Conserved hypothetical protein | *bmd_4996* | | 1.16 | **2.71** | **2.01** |
| Putative ferrichrome import ABC transporter, ATP-binding protein | *bmd_4997* | *yusV* | 1.11 | **2.95** | **2.04** |
| Putative ferrichrome import ABC transporter, permease protein | *bmd_4998* | *yfhA* | 1.15 | **2.95** | **2.27** |
| Putative ferrichrome import ABC transporter, permease protein | *bmd_4999* | *yfiZ* | 1.01 | **2.53** | **2.00** |
| Putative ferrichrome import ABC transporter, ferrichrome-binding protein | *bmd_5000* | *yfiY* | -1.36 | **3.84** | **1.85** |
| Short chain dehydrogenase | *bmd_5005* | | -1.31 | **2.00** | 1.63 |
| Major facilitator family transporter | *bmd_5006* | *yceI* | -1.28 | **-2.10** | **-1.79** |
| Phosphoglycerate kinase | *bmd_5037* | *pgk* | -1.07 | -1.27 | **-1.77** |
| Conserved hypothetical protein | *bmd_5040* | | 1.17 | **1.85** | 1.28 |
| Histidine biosynthesis bifunctional protein HisI | *bmd_5052* | *hisI* | -1.09 | **-2.04** | -1.74 |
| Imidazole glycerol phosphate synthase, cyclase subunit | *bmd_5053* | *hisF* | 1.05 | **-1.79** | -1.63 |
| Phosphoribosylformimino-5-aminoimidazole carboxamide ribotide isomerase | *bmd_5054* | *hisA* | -1.01 | **-1.87** | **-1.97** |
| Imidazole glycerol phosphate synthase, glutamine amidotransferase subunit | *bmd_5055* | *hisH* | -1.04 | **-1.99** | -1.67 |
| Imidazoleglycerol-phosphate dehydratase | *bmd_5056* | *hisB* | -1.04 | **-1.95** | -1.75 |
| Histidinol dehydrogenase | *bmd_5057* | *hisD* | -1.04 | **-1.97** | **-1.93** |
| ATP phosphoribosyltransferase, catalytic subunit | *bmd_5058* | *hisG* | -1.06 | **-2.04** | **-1.77** |
| ATP phosphoribosyltransferase, regulatory subunit | *bmd_5059* | *hisZ* | -1.04 | **-2.03** | -1.67 |
| Integral membrane protein | *bmd_5064* | | -1.21 | **2.51** | 1.39 |
| Regulator (stress mediated) | *bmd_5065* | | -1.13 | **2.62** | 1.28 |
| Conserved hypothetical protein | *bmd_5066* | | -1.27 | **2.41** | 1.35 |
| Sigma-54 dependent transcriptional regulator | *bmd_5070* | | 1.36 | **2.03** | 1.49 |
| Proline dehydrogenase | *bmd_5071* | | 1.21 | **1.93** | **1.95** |
| Sigma 54 modulation protein / S30EA ribosomal protein | *bmd_5086* | | 1.19 | **3.61** | **3.62** |
| Sodium:solute symporter family protein | *bmd_5092* | | **1.92** | **3.39** | 1.68 |
| Betaine aldehyde dehydrogenase | *bmd_5093* | *gbsA* | 1.74 | **3.39** | **2.25** |
| Alcohol dehydrogenase | *bmd_5094* | *gbsB* | 1.59 | **2.99** | **2.17** |
| Flotillin-like protein | *bmd_5114* | | 1.08 | **2.22** | 1.27 |
| Endopeptidase LytF | *bmd_5120* | *lytF* | -1.38 | **-2.07** | **-2.02** |
| Serine hydroxymethyltransferase | *bmd_5146* | *glyA* | 1.04 | **-1.91** | -1.65 |
| Thymidine kinase | *bmd_5156* | *tdk* | -1.18 | **-2.04** | **-1.89** |
| 50S ribosomal protein L31 | *bmd_5157* | *rpmE* | -1.09 | **-1.83** | -1.45 |

| Gene product | Gene ID | Gene symbol | 0.6 M | 1.2 M | 1.8 M |
|---|---|---|---|---|---|
| UDP-N-acetylglucosamine 1-carboxyvinyltransferase 2 | *bmd_5159* | *murAB* | 1.43 | **2.38** | 1.49 |
| Transaldolase | *bmd_5160* | *tal* | 1.48 | **2.51** | **1.97** |
| CTP synthase | *bmd_5164* | *pyrG* | -1.29 | **-1.75** | **-1.93** |
| Agmatinase | *bmd_5177* | *speB* | -1.67 | **-2.17** | -1.74 |
| Protein of unknown function (UPF0447) | *bmd_5189* | | 1.19 | **1.75** | 1.47 |
| Transcriptional regulator, LacI family | *bmd_5220* | | 1.05 | **1.80** | 1.63 |
| Esterase | *bmd_5221* | | 1.12 | **2.23** | **1.86** |
| Arabinose-proton symporter | *bmd_5222* | *araE* | 1.47 | **2.13** | 1.69 |
| Gamma-glutamyl phosphate reductase | *bmd_5223* | *proA* | -1.55 | **-3.18** | **-2.69** |
| Glutamate 5-kinase | *bmd_5224* | *proB* | -1.54 | **-3.25** | **-2.49** |

**Table A.13: Modification of intracellular protein concentrations in *B. megaterium* DSM319 grown at 37°C with 0.6, 1.2 and 1.8 M NaCl, respectively.** Data are given as fold change (FC) of protein concentrations compared to their values in cells grown without additional NaCl supplementation. They were obtained from LC-IMS$^e$-measurements carried out using four biological replicates for each cultivation condition. Only proteins that were identified in at least 2 out of 3 technical replicates and 2 out of 4 biological replicates were considered for analysis. Furthermore, only those whose concentration was at least 1.75-fold up- (**red**) or down-regulated (**blue**) at 0.6, 1.2 and/or 1.8 M NaCl were considered as significantly regulated and listed. Analysis of variance (ANOVA) was also applied to find proteins whose production is significantly modified at all three NaCl concentrations (indicated b bold writing).

| Protein function | ID | Protein Symbol | 0.6 M | 1.2 M | 1.8 M |
|---|---|---|---|---|---|
| Chromosomal replication initiator protein DnaA | BMD_0001 | DnaA | -1.01 | -1.42 | **1.86** |
| Conserved hypothetical protein | BMD_0003 | | -1.48 | -1.36 | **-1.92** |
| Recombination protein RecR | BMD_0026 | RecR | 1.12 | **1.87** | **2.65** |
| Dimethyladenosine transferase | BMD_0058 | KsgA | 1.39 | 1.11 | **1.79** |
| 50S ribosomal protein L25/general stress protein Ctc | BMD_0069 | Ctc | **3.21** | **6.46** | **10.73** |
| Transcription-repair coupling factor | BMD_0072 | Mfd | -1.05 | -1.05 | **-1.92** |
| Heat shock - Cstr acitivity | BMD_0104 | McsB | -1.01 | 1.48 | **3.19** |
| 23S rRNA methyltransferase | BMD_0115 | RlmB | **-2.17** | -1.32 | -1.39 |
| 50S ribosomal protein L1 | BMD_0122 | RplA | -1.26 | **-1.77** | -1.48 |
| 30S ribosomal protein S7 | BMD_0130 | RpsG | -1.30 | -1.29 | **-2.00** |
| 50S ribosomal protein L23 | BMD_0136 | RplW | **-2.17** | **-2.07** | **-2.05** |
| 30S ribosomal protein S19 | BMD_0138 | RpsS | -1.21 | -1.63 | **-2.12** |
| 50S ribosomal protein L22 | BMD_0139 | RplV | **-1.77** | -1.38 | **-2.07** |
| 50S ribosomal protein L16 | BMD_0141 | RplP | **-2.07** | -1.73 | -1.33 |
| 50S ribosomal protein L29 | BMD_0142 | RpmC | -1.49 | -1.46 | **-2.00** |
| 50S ribosomal protein L24 | BMD_0145 | RplX | -1.03 | -1.23 | **-2.28** |
| 30S ribosomal protein S14 | BMD_0147 | RpsN | -1.62 | **-1.87** | **-2.24** |
| 30S ribosomal protein S5 | BMD_0151 | RpsE | -1.39 | -1.29 | **-1.94** |
| 50S ribosomal protein L15 | BMD_0153 | RplO | -1.11 | -1.25 | **-1.93** |
| Translation initiation factor IF-1 | BMD_0157 | InfA | -1.35 | -1.34 | **-2.36** |
| 50S ribosomal protein L13 | BMD_0166 | RplM | -1.34 | -1.62 | **-1.92** |
| Glucosamine--fructose-6-phosphate aminotransferase, isomerizing | BMD_0192 | GlmS | -1.37 | **-2.02** | **-2.34** |
| D-alanine-D-alanine ligase | BMD_0213 | Ddl | -1.51 | -1.53 | **-1.97** |
| ATP-dependent RNA helicase | BMD_0215 | | -1.14 | -1.28 | **-1.93** |
| Anti-sigma B factor antagonist | BMD_0227 | RsbV | -1.42 | 1.29 | **2.68** |
| RNA polymerase sigma-B factor | BMD_0229 | SigB | 1.10 | 1.11 | **2.90** |
| S1 RNA binding domain protein | BMD_0231 | | 1.09 | 1.52 | **2.94** |
| Putative Redox-sensing transcriptional repressor rex | BMD_0255 | | 1.51 | **2.10** | 1.68 |
| 10 kDa chaperonin | BMD_0260 | GroES | -1.00 | 1.10 | **1.76** |
| GMP synthase [glutamine-hydrolyzing] | BMD_0265 | | 1.05 | -1.28 | **-2.48** |
| Phosphoribosylaminoimidazole carboxylase, catalytic subunit | BMD_0271 | PurE | 1.01 | **-2.49** | **-4.28** |
| Phosphoribosylaminoimidazole carboxylase, ATPase subunit | BMD_0272 | PurK | 1.21 | **-1.88** | **-4.34** |
| Adenylosuccinate lyase | BMD_0273 | PurB | -1.00 | **-1.94** | **-3.75** |
| Phosphoribosylaminoimidazole-succinocarboxamide synthase | BMD_0274 | PurC | 1.04 | **-1.85** | **-3.34** |
| Phosphoribosylformylglycinamidine synthase, purS protein | BMD_0275 | PurS | 1.34 | -1.52 | **-4.00** |
| Phosphoribosylformylglycinamidine synthase I | BMD_0276 | PurQ | 1.07 | **-2.12** | **-3.84** |
| Phosphoribosylformylglycinamidine synthase II | BMD_0277 | PurL | -1.06 | -1.63 | **-2.54** |
| Amidophosphoribosyltransferase | BMD_0278 | PurF | 1.04 | **-2.05** | **-5.24** |
| Phosphoribosylformylglycinamidine cyclo-ligase | BMD_0279 | PurM | -1.03 | **-2.29** | **-6.67** |
| Bifunctional purine biosynthesis protein PurH | BMD_0281 | PurH | 1.08 | **-1.87** | **-3.44** |
| Phosphoribosylamine--glycine ligase | BMD_0282 | PurD | 1.11 | **-3.05** | **-8.83** |
| Methionine aminopeptidase, type I | BMD_0304 | Map | 1.26 | 1.36 | **3.19** |
| Intracellular protease, PfpI family | BMD_0331 | | **1.93** | **2.25** | **3.28** |
| Putative efflux ABC transporter, ATP-binding protein | BMD_0361 | YfmM | -1.28 | **-1.77** | **-3.35** |
| Intracellular protease, PfpI family | BMD_0368 | | 1.17 | 1.60 | **7.51** |
| Conserved hypothetical protein | BMD_0371 | | -1.23 | -1.48 | **-2.24** |
| Conserved hypothetical protein | BMD_0401 | | **-2.88** | -1.51 | -1.12 |
| Glutamate-1-semialdehyde-2,1-aminomutase | BMD_0411 | GsaB | **1.87** | **2.25** | **2.12** |
| Peroxide operon regulator | BMD_0417 | PerR | 1.37 | **2.57** | **4.64** |
| Conserved hypothetical protein | BMD_0419 | | 1.12 | -1.40 | **-1.81** |
| Conserved hypothetical protein | BMD_0440 | | 1.36 | **2.80** | **2.59** |
| RNA methyltransferase, TrmH family, group 2 | BMD_0443 | | -1.59 | **-1.76** | -1.08 |
| Proton/sodium-glutamate symport protein | BMD_0453 | | 1.48 | 1.71 | **1.89** |
| Biotin synthase | BMD_0460 | BioB | 1.10 | **1.85** | **2.11** |
| Putative exported cell wall-binding protein | BMD_0478 | YocH | **2.50** | **11.03** | **19.44** |
| Cell division protein FtsZ | BMD_0511 | FtsZ | **1.89** | **2.67** | **3.09** |
| Glycerol kinase | BMD_0534 | GlpK | 1.33 | 1.19 | **1.83** |
| Putative quinone oxidoreductase, YhdH/YhfP family | BMD_0543 | | 1.30 | 1.32 | **3.02** |
| L-cystine import ABC transporter, L-cystine-binding protein TcyA | BMD_0547 | TcyA | **-2.12** | **-4.49** | **-2.37** |
| Thiamine biosynthesis protein ThiS | BMD_0553 | ThiS | -1.49 | **-3.38** | **-2.89** |
| Phosphomethylpyrimidine kinase | BMD_0556 | ThiD | 1.70 | **1.75** | **1.81** |
| Conserved hypothetical protein | BMD_0570 | | 1.58 | **1.78** | **1.81** |
| DNA-binding protein HU | BMD_0576 | | -1.63 | **-1.90** | -1.23 |
| Protease production transcriptional regulator Hpr | BMD_0585 | Hpr | -1.03 | **-1.92** | **-2.28** |

| Protein function | ID | Protein Symbol | 0.6 M | 1.2 M | 1.8 M |
|---|---|---|---|---|---|
| Monooxygenase | BMD_0599 | | 1.45 | 2.16 | 2.39 |
| Ferrochelatase | BMD_0602 | HemH | -1.25 | -1.73 | -4.53 |
| Nuclease SbcCD, C subunit | BMD_0645 | SbcC | -2.25 | -2.12 | -5.11 |
| Conserved hypothetical protein | BMD_0668 | | 1.29 | 1.54 | 2.10 |
| Conserved hypothetical protein | BMD_0669 | | 1.68 | 1.32 | 2.81 |
| N-acetyl-gamma-glutamyl-phosphate reductase | BMD_0678 | ArgC | -1.42 | -2.15 | -2.27 |
| Arginine biosynthesis bifunctional protein ArgJ | BMD_0679 | ArgJ | -1.58 | -2.33 | -4.02 |
| Acetylglutamate kinase | BMD_0680 | ArgB | -1.10 | -1.73 | -2.75 |
| Acetylornithine aminotransferase | BMD_0681 | ArgD | -1.05 | -1.48 | -1.92 |
| Carbamoyl-phosphate synthase, small subunit | BMD_0682 | CarA | -1.41 | -2.12 | -1.93 |
| Carbamoyl-phosphate synthase, large subunit | BMD_0683 | CarB | -1.39 | -2.01 | -1.67 |
| ATP-dependent chaperone ClpB | BMD_0687 | ClpB | -1.45 | -2.15 | -1.24 |
| Oxidoreductase family protein | BMD_0691 | | -1.14 | -1.61 | -2.04 |
| 3-oxoacyl-(acyl-carrier-protein) synthase III | BMD_0696 | FabH | -1.21 | -1.74 | -2.48 |
| Oligopeptide ABC transporter, ATP-binding protein AppF | BMD_0700 | AppF | -2.46 | 1.23 | 1.40 |
| Oligopeptide ABC transporter, oligopeptide-binding protein AppA | BMD_0701 | AppA | 1.06 | 3.40 | 3.14 |
| Oligopeptide ABC transporter, permease protein OppB | BMD_0707 | OppB | -2.59 | -3.02 | -4.31 |
| Oligopeptide ABC transporter, ATP-binding protein OppF | BMD_0710 | OppF | -1.64 | -1.40 | -2.06 |
| Gluconate kinase | BMD_0754 | GntK | 2.24 | 3.14 | 2.35 |
| Conserved hypothetical protein | BMD_0757 | | 2.44 | 2.83 | 2.35 |
| O-acetylhomoserine sulfhydrylase | BMD_0817 | | 1.34 | 1.29 | -2.55 |
| Glycine/betaine ABC transporter, ATP-binding protein OpuAA | BMD_0860 | OpuAA | 1.15 | 2.04 | 2.79 |
| Iron(III)-citrate import ABC transporter, iron(III)-citrate-binding protein | BMD_0872 | YfmC | -2.31 | -1.55 | -4.20 |
| 3-hexulose-6-phosphate synthase | BMD_0891 | HxlA | -1.11 | 1.53 | 2.80 |
| Hypothetical protein | BMD_0893 | | 1.03 | 1.75 | 9.93 |
| Oxidoreductase, aldo/keto reductase family | BMD_0912 | | 1.77 | 2.44 | 3.87 |
| Nitrilotriacetate monooxygenase component B | BMD_0928 | | 1.13 | 1.24 | 3.53 |
| 4-aminobutyrate aminotransferase | BMD_0945 | | -1.88 | -4.11 | -8.67 |
| Shikimate kinase | BMD_0952 | AroK | -1.16 | -1.68 | -2.60 |
| Cob(II)yrinic acid a,c-diamide reductase | BMD_0969 | BluB | 1.77 | 1.79 | 1.19 |
| Oxidoreductase, Gfo/Idh/MocA family (NAD-binding Rossmann fold) | BMD_0989 | | 1.81 | 2.77 | 1.76 |
| 2-cys peroxiredoxin | BMD_0990 | | 1.24 | 1.95 | 1.88 |
| Oxidoreductase, aldo/keto reductase family | BMD_1041 | | 2.22 | 3.22 | 3.01 |
| UDP-glucose 4-epimerase, galE | BMD_1046 | GalE | 1.89 | 1.86 | 2.16 |
| UTP-glucose-1-phosphate uridylyltransferase | BMD_1114 | GalU | -1.52 | -2.35 | -3.05 |
| Glycosyl transferase, family 2 | BMD_1117 | | -2.22 | -3.50 | -8.20 |
| Glycosyl transferase, family 2 | BMD_1118 | | -1.53 | -1.53 | -4.03 |
| UDPglucose 6-dehydrogenase | BMD_1122 | | -1.43 | -2.42 | -3.62 |
| Tyrosine-protein kinase capB | BMD_1124 | | -1.41 | -1.77 | -6.42 |
| Tyrosine-protein phosphatase capC | BMD_1125 | | 1.25 | 1.87 | 1.79 |
| UTP-glucose-1-phosphate uridylyltransferase | BMD_1126 | GalU | 1.17 | 1.70 | 1.83 |
| Fructokinase | BMD_1144 | | -1.18 | -1.55 | -2.37 |
| Hypothetical protein | BMD_1166 | | -1.48 | -2.06 | -1.92 |
| Putative membrane protein | BMD_1170 | | -6.55 | -7.80 | -2.60 |
| Conserved hypothetical protein | BMD_1181 | | -1.16 | 1.11 | 1.83 |
| Polyhydroxyalkanoic acid inclusion protein PhaP | BMD_1211 | PhaP | 1.32 | 1.81 | 2.15 |
| Polyhydroxyalkanoic acid synthase, PhaR subunit | BMD_1214 | PhaR | 1.66 | 2.24 | 2.22 |
| Polyhydroxyalkanoic acid synthase, PhaC subunit | BMD_1216 | PhaC | 1.35 | 1.32 | 1.81 |
| Methylthioribose-1-phosphate isomerase | BMD_1230 | MtnA | 1.34 | 1.14 | -1.92 |
| 5-methylthioribose kinase | BMD_1231 | MtnK | 1.02 | -1.89 | -2.97 |
| Transaminase | BMD_1233 | MtnE | -1.21 | -1.45 | -3.29 |
| 2,3-diketo-5-methylthiopentyl-1-phosphate enolase | BMD_1234 | MtnW | 1.13 | -1.26 | -1.92 |
| YkvE - MarR-type repressor/ transcriptional regulator | BMD_1245 | | 1.18 | 1.35 | 1.92 |
| ATP-dependent Clp protease, ATP-binding subunit ClpE | BMD_1249 | ClpE | -2.12 | -1.34 | -1.34 |
| Homocysteine S-methyltransferase/5,10-methylenetetrahydrofolate reductase | BMD_1274 | YitJ | -1.06 | -1.55 | -1.79 |
| PTS system, glucose-specific IIBC component | BMD_1282 | PtsG | 1.42 | 1.95 | 1.35 |
| Phosphocarrier protein HPr | BMD_1283 | PtsH | -1.15 | 1.15 | -2.65 |
| Protein of unknown function (DUF1797) | BMD_1307 | | -1.06 | -1.36 | -2.56 |
| Conserved hypothetical protein | BMD_1321 | | 1.30 | 1.23 | 1.95 |
| Conserved hypothetical protein | BMD_1334 | | 1.59 | 1.21 | 2.05 |
| Inositol monophosphatase | BMD_1338 | SuhB | 1.66 | 2.55 | 5.94 |
| GTPase | BMD_1340 | BipA | -1.79 | -2.08 | -3.93 |
| 3-methyl-2-oxobutanoate hydroxymethyltransferase | BMD_1371 | PanB | 3.49 | 5.93 | 5.47 |
| Pantoate--beta-alanine ligase | BMD_1372 | PanC | 2.53 | 2.65 | 1.91 |
| Aspartate aminotransferase | BMD_1378 | AspB | -1.03 | -1.27 | -2.68 |
| Penicillin-binding protein 1A/1B | BMD_1383 | PonA | -1.31 | -2.10 | -1.84 |
| Cell division protein | BMD_1414 | GpsB | -1.58 | -1.02 | 2.02 |
| Carboxypeptidase Taq (M32) metallopeptidase | BMD_1431 | | 1.63 | 2.63 | 3.09 |
| Xanthine phosphoribosyltransferase | BMD_1432 | Xpt | -1.15 | -3.00 | -6.05 |
| Putative GTPase | BMD_1440 | | -1.90 | -2.30 | -4.65 |
| Ferrichrome import ABC transporter, ATP-binding protein FhuC | BMD_1510 | FhuC | 2.20 | 5.70 | 12.52 |
| Ferritin-like domain protein | BMD_1538 | | 1.86 | 2.13 | 7.42 |
| Aldehyde dehydrogenase (NAD) Family Protein | BMD_1546 | | 1.68 | 4.91 | 32.91 |
| 2,5-diketo-D-gluconic acid reductase A | BMD_1595 | | -1.12 | -2.13 | -3.04 |
| Conserved hypothetical protein | BMD_1629 | | -1.01 | -1.41 | -3.20 |
| Nickel import ABC transporter, nickel-binding protein NikA | BMD_1702 | NikA | -2.49 | -2.66 | -2.46 |

| Protein function | ID | Protein Symbol | 0.6 M | 1.2 M | 1.8 M |
|---|---|---|---|---|---|
| 4-hydroxy 2-oxovalerate aldolase | BMD_1715 | | -1.03 | -1.73 | -3.23 |
| RecA1 protein | BMD_1726 | RecA1 | 1.01 | -1.06 | 1.97 |
| Conserved hypothetical protein | BMD_1761 | | -1.10 | -1.20 | 2.52 |
| hut operon positive regulatory protein | BMD_1769 | | 2.11 | 3.05 | 3.26 |
| Stress response protein YsnF | BMD_1782 | YsnF | -1.29 | -1.18 | 3.48 |
| Conserved hypothetical protein | BMD_1799 | | -2.05 | -1.76 | 1.43 |
| Oligopeptide ABC transporter, oligopeptide-binding protein | BMD_1832 | | -1.16 | -1.19 | -3.76 |
| Hypothetical protein | BMD_1845 | | 1.57 | -1.73 | -6.95 |
| Aldose 1-epimerase | BMD_1850 | Mro | 1.98 | 1.43 | 1.78 |
| Copper chaperone CopZ (copper-ion-binding protein) | BMD_1895 | CopZ | 2.51 | 1.41 | -1.32 |
| Putative lipoprotein | BMD_1898 | | 3.82 | 2.19 | -1.90 |
| Tartrate dehydrogenase/decarboxylase | BMD_1915 | YcsA | 4.51 | 6.73 | 7.09 |
| Transcriptional regulator | BMD_1920 | | 1.76 | 1.87 | -1.15 |
| PBS lyase HEAT-like repeat family protein | BMD_1943 | | 1.61 | 2.72 | 2.82 |
| Putative metal ABC transporter, metal-binding protein | BMD_1949 | | -2.07 | -3.74 | - |
| Cobalamin synthesis protein/P47K family protein | BMD_1961 | | -1.98 | -1.39 | -1.35 |
| Amino acid/peptide transporter (Peptide:H+ symporter) | BMD_2012 | DtpT | -2.72 | -4.42 | -1.85 |
| Malate dehydrogenase | BMD_2037 | | 2.17 | 1.74 | 1.58 |
| Glutamate synthase, large subunit | BMD_2055 | GltA | -1.10 | -1.55 | -2.01 |
| Glutamate synthase, small subunit | BMD_2056 | GltB | -1.02 | -1.28 | -2.12 |
| Aspartate kinase | BMD_2089 | YclM | 1.01 | -1.38 | -1.90 |
| Conserved hypothetical protein | BMD_2103 | | -1.21 | -1.94 | 1.41 |
| NADH-dependent dehydrogenase | BMD_2104 | | -1.01 | -1.73 | -2.18 |
| Putative ABC transporter, ATP-binding protein | BMD_2131 | YlmA | -1.77 | 1.02 | 1.11 |
| Putative nicotinate phosphoribosyltransferase | BMD_2161 | | -1.01 | 1.01 | -2.23 |
| NAD+ synthase | BMD_2163 | NadE | 1.37 | 2.01 | 2.50 |
| S1 RNA binding domain protein | BMD_2164 | | -1.80 | -2.66 | -2.24 |
| General stress protein 17M | BMD_2208 | | 1.18 | 2.47 | 11.78 |
| Organic hydroperoxide resistance protein | BMD_2231 | OhrB | -2.19 | -2.68 | 1.85 |
| Gamma-glutamyl phosphate reductase | BMD_2245 | ProA | 8.83 | 14.81 | 19.77 |
| Conserved hypothetical protein | BMD_2246 | | 3.48 | 3.80 | 2.77 |
| Immune inhibitor A metalloprotease | BMD_2278 | InhA | -2.20 | 3.72 | 1.91 |
| Fumarate hydratase, class II | BMD_2279 | FumC | -1.17 | -3.10 | -3.03 |
| Chaperone protein HtpG | BMD_2385 | HtpG | -1.19 | -1.08 | -1.92 |
| Conserved hypothetical protein | BMD_2425 | | -1.78 | -1.71 | -1.18 |
| NAD dependent epimerase/dehydratase family | BMD_2433 | | 2.10 | 4.76 | 6.48 |
| Acetyltransferase, GNAT family | BMD_2481 | | 1.44 | 1.31 | 1.99 |
| Dihydroxy-acid dehydratase | BMD_2497 | IlvD | 1.19 | 1.43 | 2.20 |
| HAD superfamily hydrolase | BMD_2513 | | 1.26 | -1.08 | -3.09 |
| Conserved hypothetical protein | BMD_2538 | | 1.12 | 1.94 | 1.90 |
| Precorrin-4 C11-methyltransferase | BMD_2599 | CbiF | 1.93 | 1.64 | 1.89 |
| CbiET protein | BMD_2601 | CbiET | 1.48 | 1.45 | 1.75 |
| Precorrin-8X methylmutase CbiC | BMD_2603 | CbiC | 1.51 | 1.59 | 1.91 |
| Sirohydrochlorin cobaltochelatase | BMD_2605 | CbiX | 1.21 | 1.66 | 2.52 |
| Precorrin 3 methylase | BMD_2606 | CbiH | 1.38 | 1.75 | 1.91 |
| Malate dehydrogenase | BMD_2620 | | 3.91 | 1.20 | -1.02 |
| Scyllo-inositol dehydrogenase (NADP+) | BMD_2681 | | 1.88 | 3.18 | 3.82 |
| Tellurite resistance protein, putative | BMD_2683 | | 1.46 | 1.49 | 3.05 |
| Tellurium resistance protein terD,TerD family | BMD_2686 | | 1.37 | 3.21 | 4.99 |
| Probable tellurium resistance protein, TerD family | BMD_2687 | | -1.10 | 2.08 | 4.08 |
| Aminopeptidase pepS (M29 family) | BMD_2887 | PepS | 1.44 | 1.88 | 2.93 |
| Conserved hypothetical protein | BMD_2910 | | -1.32 | -1.06 | -1.77 |
| 2-oxoglutarate dehydrogenase, E2 component (dihydrolipoamide succinyltransferase) | BMD_2925 | OdhB | 1.30 | 1.95 | 2.32 |
| 2-oxoglutarate dehydrogenase, E1 component | BMD_2926 | OdhA | 1.38 | 1.75 | 2.95 |
| Acyl-CoA dehydrogenase | BMD_2954 | | 1.15 | 1.52 | 2.08 |
| Urease accessory protein UreG | BMD_2986 | UreG | 1.16 | -1.14 | -2.33 |
| Anthranilate phosphoribosyltransferase | BMD_2992 | | 2.05 | 1.48 | 2.14 |
| ThiJ/PfpI family protein | BMD_3006 | | -1.09 | 3.94 | 25.15 |
| Sporulation-control protein Spo0M | BMD_3021 | Spo0M | -2.15 | -1.73 | -1.71 |
| Cell wall endopeptidase | BMD_3039 | LytF | 9.59 | 13.22 | 23.85 |
| Undecaprenyldiphospho-muramoylpentapeptide beta-N-acetylglucosaminyltransferase | BMD_3054 | MurG | -1.16 | -1.34 | -2.42 |
| Aspartate ammonia-lyase | BMD_3099 | AnsB | -1.52 | -1.46 | -3.62 |
| Sulfite reductase (NADPH) hemoprotein, beta-component | BMD_3121 | CysI | 1.01 | -1.32 | -2.14 |
| Sulfite reductase (NADPH) flavoprotein alpha-component | BMD_3122 | | -1.02 | 1.00 | -2.09 |
| UDP-glucuronosyltransferase, macrolide glycosyltransferase Family | BMD_3136 | | 2.46 | 2.77 | 6.87 |
| Cytochrome aa3 quinol oxidase, subunit III | BMD_3154 | QoxC | -1.22 | -1.07 | -1.82 |
| Conserved hypothetical protein | BMD_3167 | | -1.69 | 1.51 | 29.09 |
| Oxidoreductase, zinc-binding dehydrogenase family | BMD_3180 | | -1.25 | -1.36 | 2.63 |
| Peptide chain release factor 3 | BMD_3203 | PrfC | -1.48 | -3.59 | -3.27 |
| Putative ferrichrome ABC transporter, ATP-binding protein | BMD_3217 | YclP | 1.59 | 1.84 | 2.93 |
| Oxidoreductase, aldo/keto reductase family | BMD_3288 | | 1.76 | 2.06 | 2.76 |
| Aminotransferase family protein | BMD_3340 | | 1.56 | 1.60 | 2.07 |
| Flavodoxin-like fold family protein | BMD_3384 | | 1.59 | 2.39 | 3.06 |
| Threonine synthase | BMD_3406 | ThrC | 1.05 | -1.76 | -1.98 |
| Hypothetical protein | BMD_3479 | | -1.07 | -1.68 | -2.72 |
| Conserved hypothetical protein | BMD_3480 | | -1.54 | -1.80 | -4.59 |

| Protein function | ID | Protein Symbol | 0.6 M | 1.2 M | 1.8 M |
|---|---|---|---|---|---|
| 5-methyltetrahydropteroyltriglutamate--homocysteine S-methyltransferase | BMD_3527 | MetE | 1.74 | 2.25 | 16.50 |
| 8-amino-7-oxononanoate synthase | BMD_3693 | BioF | 1.96 | 1.71 | -1.28 |
| Biotin biosynthesis protein BioC | BMD_3695 | BioC | 1.77 | 1.88 | -1.14 |
| Malate dehydrogenase | BMD_3745 | | -1.42 | -2.01 | 2.54 |
| Putative metal-dependent hydrolase | BMD_3772 | | 1.80 | 1.82 | 1.08 |
| Putative 1-pyrroline-5-carboxylate dehydrogenase | BMD_3813 | PutC | 23.06 | 23.81 | 36.79 |
| Xaa-Pro dipeptidase | BMD_3907 | PepQ | 1.75 | 1.80 | 2.51 |
| Flavodoxin-like fold family protein | BMD_3911 | | 1.60 | 2.47 | 1.99 |
| Sulfatase | BMD_3930 | | 1.18 | 3.01 | 2.56 |
| 6-phosphofructokinase | BMD_3977 | PfkA | 1.03 | -1.37 | -2.01 |
| D-amino acid aminotransferase | BMD_4023 | Dat | 2.71 | 3.83 | 5.32 |
| Siderophore biosynthesis protein | BMD_4048 | | 1.47 | 4.59 | 5.40 |
| Siderophore biosynthesis protein | BMD_4052 | | -2.29 | 1.25 | 1.67 |
| 2,4-diaminobutyrate 4-transaminase | BMD_4054 | | 1.10 | 3.28 | 5.84 |
| Succinate-semialdehyde dehydrogenase (NADP+) - general stress protein | BMD_4061 | | 1.37 | 2.47 | 4.27 |
| Succinate-semialdehyde dehydrogenase (NADP+) - GABA utilization | BMD_4061 | | 1.37 | 2.47 | 4.27 |
| LexA repressor | BMD_4077 | LexA | 1.76 | 1.49 | 1.01 |
| Glutamine synthetase repressor | BMD_4087 | GlnR | 1.25 | 1.82 | 2.73 |
| DNA mismatch repair protein MutS | BMD_4095 | MutS | -1.93 | -1.20 | -1.01 |
| Amino acid transporter | BMD_4096 | | -1.40 | -1.23 | -3.32 |
| 2-oxoglutarate ferredoxin oxidoreductase subunit alpha | BMD_4101 | | -2.35 | -2.13 | -2.64 |
| RecA2 protein | BMD_4106 | RecA2 | 1.09 | 1.64 | 2.56 |
| Competence/damage-inducible regulator | BMD_4107 | CinA | -1.32 | 1.18 | 2.16 |
| Hypothetical protein | BMD_4109 | | 1.04 | 1.70 | 1.92 |
| Peptidase, M16 family protein | BMD_4113 | | 1.38 | 1.82 | 1.60 |
| Putative Zn-protease | BMD_4114 | | 1.45 | 2.95 | 4.06 |
| Putative ABC transporter, ATP-binding protein | BMD_4117 | YufO | 1.00 | -1.21 | -2.14 |
| Transcriptional regulator, GntR family | BMD_4119 | | -1.19 | -1.43 | -2.79 |
| Polynucleotide phosphorylase | BMD_4132 | Pnp | -1.22 | -1.50 | -2.10 |
| 30S ribosomal protein S15 | BMD_4133 | RpsO | -2.10 | -2.45 | -2.40 |
| Translation initiation factor IF-2 | BMD_4138 | InfB | -1.08 | 1.46 | 1.86 |
| Conserved hypothetical protein | BMD_4142 | | -1.07 | 1.19 | 1.97 |
| Prolyl-tRNA synthetase | BMD_4144 | ProS | -1.12 | -1.26 | -1.87 |
| Uridylate kinase | BMD_4150 | PyrH | -1.33 | -2.12 | -2.16 |
| DNA topoisomerase I | BMD_4189 | TopA | 1.20 | 1.68 | 1.96 |
| Ribosome biogenesis GTPase A | BMD_4194 | RbgA | 1.17 | -1.22 | -2.16 |
| 50S ribosomal protein L19 | BMD_4196 | RplS | -1.49 | -1.47 | -1.78 |
| Signal recognition particle protein | BMD_4202 | Ffh | 1.17 | 1.74 | 2.24 |
| Putative phosphatase | BMD_4216 | | 1.34 | 1.75 | 2.11 |
| Ribosome small subunit-dependent GTPase A | BMD_4221 | RsgA | 1.06 | 1.59 | 1.90 |
| Radical SAM enzyme, Cfr family | BMD_4224 | | 1.54 | 1.45 | 1.88 |
| Methionyl-tRNA formyltransferase | BMD_4226 | Fmt | 1.31 | 1.43 | 3.05 |
| Guanylate kinase | BMD_4231 | Gmk | 1.06 | -1.47 | -1.95 |
| Orotidine 5'-phosphate decarboxylase | BMD_4237 | PyrF | 1.35 | -1.05 | -2.52 |
| Dihydroorotate dehydrogenase, catalytic subunit | BMD_4238 | PyrD | 1.02 | -1.04 | -1.87 |
| Dihydroorotate dehydrogenase, electron transfer subunit | BMD_4239 | PyrK | 1.21 | 1.11 | -2.13 |
| Carbamoyl-phosphate synthase, large subunit | BMD_4240 | PyrAB | -1.09 | -1.22 | -2.06 |
| Aspartate carbamoyltransferase | BMD_4243 | PyrB | -1.03 | -1.11 | -2.02 |
| Pseudouridine synthase | BMD_4246 | RluD | -1.36 | -2.09 | -2.57 |
| Cell division machinery factor | BMD_4253 | SepF | -1.23 | 2.05 | 1.62 |
| Cell division protein FtsZ | BMD_4260 | FtsZ | 1.41 | 1.38 | 1.90 |
| UDP-N-acetylenolpyruvoylglucosamine reductase | BMD_4263 | MurB | -1.17 | -1.77 | -2.38 |
| UDP-N-acetylmuramoylalanyl-D-glutamate--2,6- diaminopimelate ligase | BMD_4267 | MurE | -1.35 | -1.59 | -2.59 |
| Acetyltransferase, GNAT family | BMD_4278 | | -1.12 | -1.39 | -2.01 |
| 50S ribosomal protein L32 | BMD_4281 | RpmF | 1.08 | -1.19 | -2.12 |
| Conserved hypothetical protein | BMD_4282 | | 1.69 | 2.39 | 2.30 |
| Tryptophan synthase, alpha subunit | BMD_4305 | TrpA | 2.27 | 2.60 | 1.68 |
| Tryptophan synthase, beta subunit | BMD_4306 | TrpB | 1.70 | 1.79 | 2.25 |
| Indole-3-glycerol-phosphate synthase | BMD_4308 | TrpC | 1.84 | 2.62 | 2.69 |
| Anthranilate phosphoribosyltransferase | BMD_4309 | TrpD | -6.90 | -5.79 | -7.10 |
| Nucleoside diphosphate kinase | BMD_4314 | Ndk | 1.50 | 1.81 | 2.47 |
| Tryptophan RNA-binding attenuator protein | BMD_4318 | MtrB | -2.02 | -1.47 | -2.64 |
| NAD-dependent glycerol-3-phosphate dehydrogenase | BMD_4324 | GpsA | 1.06 | -1.04 | -1.87 |
| GTP-binding protein EngA | BMD_4325 | EngA | -1.43 | -1.92 | -1.86 |
| NAD-specific glutamate dehydrogenase | BMD_4340 | GudB | -2.57 | -2.19 | -1.65 |
| D-3-phosphoglycerate dehydrogenase | BMD_4351 | SerA | -1.68 | -2.05 | -2.90 |
| Pseudouridine synthase | BMD_4358 | RluB | -3.07 | -1.87 | 1.35 |
| Diaminopimelate decarboxylase | BMD_4369 | LysA | 1.23 | 1.78 | 1.87 |
| Nudix hydrolase, YffH family | BMD_4387 | | 1.63 | 2.84 | 3.33 |
| Oxidoreductase, aldo/keto reductase family | BMD_4389 | | 1.48 | 2.26 | 3.59 |
| Pyrroline-5-carboxylate reductase | BMD_4400 | ProI | -1.72 | -1.98 | -2.07 |
| FAD/FMN-binding oxidoreductase | BMD_4401 | | 1.22 | 1.10 | 3.03 |
| Arginine ABC transporter, ATP-binding protein ArtM | BMD_4416 | ArtM | 1.04 | -1.90 | -2.15 |
| Arginine ABC transporter, permease protein ArtQ | BMD_4417 | ArtQ | -1.39 | -2.10 | -2.69 |
| Arginine ABC transporter, arginine-binding protein ArtP | BMD_4418 | ArtP | -1.07 | -1.19 | -1.86 |
| Conserved hypothetical protein | BMD_4433 | | 1.01 | -1.54 | -2.39 |

| Protein function | ID | Protein Symbol | 0.6 M | 1.2 M | 1.8 M |
|---|---|---|---|---|---|
| Protein of unknown function (DUF322) | BMD_4446 | | -1.23 | 1.09 | 1.84 |
| Translation elongation factor P | BMD_4458 | Efp | 1.42 | 1.12 | 2.11 |
| Proline dipeptidase | BMD_4459 | | 1.55 | 1.98 | 1.01 |
| Lipoate protein ligase | BMD_4467 | | -2.17 | -3.08 | -1.32 |
| Rhodanese-like domain protein | BMD_4468 | | 1.08 | -1.50 | -1.93 |
| Glycine cleavage system T protein | BMD_4471 | GcvT | 1.29 | 1.77 | 3.11 |
| Metallo-beta-lactamase family protein | BMD_4484 | | 1.40 | 1.88 | 1.19 |
| Conserved hypothetical protein | BMD_4524 | | 1.50 | 2.39 | 3.93 |
| GTP-binding protein Era | BMD_4534 | Era | -1.83 | 1.74 | -1.37 |
| Conserved hypothetical protein | BMD_4537 | | -1.20 | 1.89 | 2.16 |
| GatB/Yqey domain protein | BMD_4545 | | 1.74 | 1.52 | 2.43 |
| 30S ribosomal protein S21 | BMD_4546 | RpsU | -1.04 | -1.23 | -4.11 |
| 30S ribosomal protein S20 | BMD_4558 | RpsT | -1.42 | -1.68 | -2.92 |
| GTP-binding protein | BMD_4571 | | -1.94 | -2.45 | -1.76 |
| 5'-methylthioadenosine/S-adenosylhomocysteine nucleosidase | BMD_4582 | MtnN | 1.16 | 1.04 | -1.90 |
| Protein of unknown function (DUF1510) | BMD_4585 | | 2.18 | 3.39 | 4.09 |
| Transcription elongation factor GreA | BMD_4588 | GreA | 1.42 | 1.77 | 1.70 |
| Cysteine desulfurase | BMD_4605 | IscS | -1.07 | 1.57 | 2.08 |
| Transcriptional regulator of cysteine biosynthesis | BMD_4606 | CymR | 1.28 | 1.23 | 2.69 |
| GTP pyrophosphokinase | BMD_4617 | RelA | 1.63 | 1.93 | 2.41 |
| Queuine tRNA-ribosyltransferase | BMD_4626 | Tgt | -1.10 | -1.38 | -3.08 |
| Holliday junction DNA helicase RuvA | BMD_4630 | RuvA | -1.16 | -1.77 | 1.10 |
| 50S ribosomal protein L27 | BMD_4645 | RpmA | -1.27 | -2.07 | -3.19 |
| Rod shape-determining protein MreC | BMD_4654 | MreC | -1.47 | -1.22 | -1.82 |
| Delta-aminolevulinic acid dehydratase | BMD_4668 | HemB | 1.21 | 1.52 | 2.03 |
| 3-isopropylmalate dehydrogenase | BMD_4682 | LeuB | -1.10 | -1.12 | -1.81 |
| Protein of unknown function (DUF47) | BMD_4696 | BMD_4 | -1.88 | -2.66 | -2.25 |
| Succinate dehydrogenase, flavoprotein subunit | BMD_4710 | SdhA | 1.23 | 1.59 | 2.32 |
| Succinate dehydrogenase, cytochrome b558 subunit | BMD_4711 | SdhC | 1.19 | 1.31 | 2.19 |
| DNA mismatch repair protein MutS | BMD_4723 | MutS | 1.74 | 3.06 | 2.26 |
| DNA-directed DNA polymerase X | BMD_4724 | PolX | -1.96 | -1.58 | 1.42 |
| 50S ribosomal protein L20 | BMD_4736 | RplT | -1.65 | -1.90 | -1.85 |
| DNA polymerase I | BMD_4750 | PolA | 1.09 | 1.48 | 2.45 |
| Malate dehydrogenase, NAD-dependent | BMD_4754 | Mdh | 1.43 | 1.56 | 1.94 |
| Malate dehydrogenase | BMD_4764 | | 1.53 | 1.83 | 2.77 |
| Thiamine biosynthesis/tRNA modification protein ThiI | BMD_4789 | ThiI | 1.21 | 1.29 | 2.41 |
| Cysteine desulfurase | BMD_4790 | IscS | -1.35 | -1.08 | 2.17 |
| GAF domain protein | BMD_4794 | | 1.18 | 1.37 | 1.99 |
| Conserved hypothetical protein | BMD_4807 | | 1.18 | 2.08 | 1.71 |
| Protein of unknown function (DUF948) | BMD_4808 | | -1.09 | 1.05 | 2.58 |
| Aminopeptidase | BMD_4809 | | -1.00 | -1.28 | -2.10 |
| DNA translocase FtsK (DNA translocase SpoIIIE) | BMD_4812 | FtsK | 1.08 | 1.53 | 1.82 |
| Protein of unknown function (DUF1444) | BMD_4814 | | 1.33 | 1.82 | 2.45 |
| Thioredoxin | BMD_4815 | | -1.35 | -1.26 | 2.50 |
| M42 glutamyl aminopeptidase | BMD_4817 | | 1.81 | 3.16 | 3.69 |
| Putative cysteine synthase A | BMD_4826 | YtkP | 2.40 | 3.84 | 4.15 |
| S-adenosylmethionine synthetase | BMD_4847 | MetK | -1.57 | -2.06 | -1.84 |
| Phosphoenolpyruvate carboxykinase (ATP) | BMD_4848 | PckA | 1.19 | 2.22 | 3.70 |
| DNA-protecting protein | BMD_4857 | Dps | -1.21 | 1.13 | 4.49 |
| S-ribosylhomocysteine lyase | BMD_4858 | LuxS | 1.49 | 1.84 | 1.24 |
| Ribonucleoside-diphosphate reductase, beta subunit | BMD_4871 | NrdF | 1.59 | 1.51 | 1.97 |
| Sirohydrochlorin ferrochelatase | BMD_4913 | SirB | 2.03 | 1.49 | 1.28 |
| NADH-dependent butanol dehydrogenase A | BMD_4931 | | -1.54 | -2.16 | -2.05 |
| S1 RNA binding domain-containing protein - general stress protein 13 | BMD_4933 | | 1.60 | 1.78 | 1.40 |
| Aminotransferase | BMD_4937 | PatB | 1.38 | 2.72 | 2.44 |
| Leucyl aminopeptidase | BMD_4947 | PepA | 1.34 | 1.68 | 2.41 |
| NADH dehydrogenase YutJ | BMD_4957 | YutJ | 2.78 | 4.28 | 9.24 |
| Homoserine kinase | BMD_4960 | ThrB | 1.39 | 1.82 | 1.85 |
| Conserved hypothetical protein | BMD_4968 | | 1.57 | 1.75 | 1.68 |
| SUF system FeS assembly protein | BMD_4977 | IscU | 1.43 | 1.93 | 2.09 |
| Cysteine desulfurase SufS | BMD_4978 | SufS | 1.73 | 2.14 | 3.26 |
| FeS assembly protein SufD | BMD_4979 | SufD | 1.12 | 1.39 | 1.79 |
| Methionine import ABC transporter, methionine-binding protein MetQ | BMD_4982 | MetQ | -1.42 | -2.03 | -3.42 |
| Methionine import ABC transporter, ATP-binding protein MetN | BMD_4984 | MetN | -1.33 | -1.56 | -2.64 |
| Conserved hypothetical protein | BMD_4989 | | -2.04 | 1.17 | -1.56 |
| Putative ferrichrome import ABC transporter, ferrichrome-binding protein | BMD_5000 | YfiY | -1.91 | 1.12 | 1.88 |
| Phosphoglycerate kinase | BMD_5037 | Pgk | -1.14 | -1.14 | -1.79 |
| Glyceraldehyde-3-phosphate dehydrogenase, type I | BMD_5038 | Gap | -1.11 | -1.39 | -1.81 |
| Conserved hypothetical protein | BMD_5046 | | 1.72 | 2.52 | 4.19 |
| Putative triphosphate pyrophosphate hydrolase | BMD_5049 | YvcI | 1.91 | -1.07 | -1.11 |
| Histidine biosynthesis bifunctional protein HisI | BMD_5052 | HisI | 1.16 | -1.11 | -2.27 |
| Imidazole glycerol phosphate synthase, cyclase subunit | BMD_5053 | HisF | -1.10 | -1.53 | -2.62 |
| Phosphoribosylformimino-5-aminoimidazole carboxamide ribotide isomerase | BMD_5054 | HisA | 1.14 | -1.48 | -2.55 |
| HPr(Ser) kinase/phosphatase | BMD_5063 | HprK | -1.43 | -1.74 | -1.85 |
| Excinuclease ABC, A subunit | BMD_5068 | UvrA | 2.54 | 2.21 | 2.11 |
| Peptide chain release factor 2 | BMD_5083 | PrfB | -1.28 | -1.70 | -1.91 |

| Protein function | ID | Protein Symbol | 0.6 M | 1.2 M | 1.8 M |
|---|---|---|---|---|---|
| Preprotein translocase, SecA subunit | BMD_5084 | SecA | -1.07 | 1.14 | 2.06 |
| Sigma 54 modulation protein / S30EA ribosomal protein | BMD_5086 | | 1.27 | 2.61 | 9.06 |
| UDP-N-acetylglucosamine 1-carboxyvinyltransferase | BMD_5130 | MurA | -1.85 | -1.61 | 1.24 |
| ATP synthase F1, gamma subunit | BMD_5135 | AtpG | -1.16 | -1.60 | -2.57 |
| Ribose 5-phosphate isomerase B | BMD_5148 | RpiB | -1.28 | -1.37 | -2.04 |
| Protein-tyrosine phosphatase | BMD_5149 | | 9.48 | 3.75 | 26.42 |
| Transaldolase | BMD_5160 | Tal | 1.66 | 2.69 | 3.75 |
| Sporulation initiation phosphotransferase F (response regulator) | BMD_5162 | Spo0F | -1.26 | -1.40 | -2.09 |
| CTP synthase | BMD_5164 | PyrG | -1.48 | -2.44 | -2.60 |
| Agmatinase | BMD_5177 | SpeB | -2.40 | -3.06 | -2.96 |
| Spermidine synthase | BMD_5178 | SpeE | -2.09 | -3.22 | -2.11 |
| 4-oxalocrotonate tautomerase | BMD_5182 | | 1.98 | 2.17 | -1.00 |
| Protein of unknown function (UPF0447) | BMD_5189 | | 1.16 | 1.85 | 2.20 |
| 6-phosphogluconate dehydrogenase, decarboxylating | BMD_5197 | Gnd | -1.43 | -1.82 | -2.46 |
| Conserved hypothetical protein | BMD_5198 | | 2.66 | 2.06 | 2.14 |
| Alanine dehydrogenase | BMD_5199 | Ald | 1.59 | 5.62 | 9.70 |
| Phosphomethylpyrimidine kinase | BMD_5201 | ThiD | 1.18 | 1.90 | 3.30 |
| Cof-like hydrolase | BMD_5202 | | 2.39 | 2.45 | 3.11 |
| Glycosyl transferase, family 2 | BMD_5207 | | -1.17 | -1.58 | -1.94 |
| Gamma-glutamyl phosphate reductase | BMD_5223 | ProA | -2.33 | -3.53 | -9.96 |
| Catalase | BMD_5226 | KatA | -1.14 | -1.85 | -3.14 |
| 50S ribosomal protein L9 | BMD_5252 | RplI | 1.06 | 1.31 | 1.98 |
| Single-strand binding protein | BMD_5256 | SsbA | 1.22 | -1.20 | -1.81 |
| GTP-binding protein EngD | BMD_5258 | EngD | -1.29 | -1.35 | -2.05 |
| tRNA uridine 5-carboxymethylaminomethyl modification enzyme GidA | BMD_5267 | GidA | 1.32 | 1.61 | 3.50 |
| tRNA modification GTPase TrmE | BMD_5268 | TrmE | -1.17 | 1.09 | 1.76 |

**Table A.14: Extracellular concentrations of proteinogenic amino acids in B. megaterium DSM319 grown with NaCl concentrations between 0 and 1.2 M NaCl.** Only amino acids whose extracellular concentration was higher than 5 µmol $g_{CDW}^{-1}$ are listed. For all conditions, samples were taken from three biological replicates at an $OD_{600nm}$ of 6 and culture supernatant was analysed by HPLC using aminobutyric acid (ABU) as internal standard [281].

| | | Concentration [µmol/$g_{CDW}$] | | | | |
|---|---|---|---|---|---|---|
| | NaCl [M] | 0 M NaCl | 0.3 M NaCl | 0.6 M NaCl | 0.9 M NaCl | 1.2 M NaCl |
| Alanine | Mean [µmol $g_{CDW}^{-1}$] | 15.49 | 11.47 | 9.05 | 10.14 | 7.32 |
| | Standard deviation | 2.79 | 0.98 | 0.09 | 0.82 | 0.15 |
| Glutamate | Mean [µmol $g_{CDW}^{-1}$] | 138.46 | 91.99 | 48.63 | 26.85 | 12.03 |
| | Standard deviation | 3.12 | 14.57 | 1.24 | 1.28 | 1.77 |
| Glycine | Mean [µmol $g_{CDW}^{-1}$] | 13.15 | 11.11 | 9.12 | 10.37 | 9.12 |
| | Standard deviation | 1.36 | 1.53 | 2.27 | 0.89 | 1.25 |
| Serine | Mean [µmol $g_{CDW}^{-1}$] | 15.75 | 13.90 | 11.94 | 15.67 | 13.99 |
| | Standard deviation | 1.21 | 1.36 | 1.90 | 1.31 | 0.57 |
| Tryptophan | Mean [µmol $g_{CDW}^{-1}$] | 13.06 | 10.13 | 4.54 | 15.59 | 8.91 |
| | Standard deviation | 1.08 | 1.00 | 5.48 | 4.12 | 0.30 |
| Valine | Mean [µmol $g_{CDW}^{-1}$] | 45.26 | 29.20 | 11.82 | 42.97 | 30.46 |
| | Standard deviation | 0.10 | 1.45 | 1.30 | 6.32 | 4.35 |

**Table A.15: Biochemical reaction network used for elementary flux mode analysis in *B. megaterium*.** Reactants that are specified as influx or efflux compounds are not considered for stoichiometric balancing

| | Reaction | Gene |
|---|---|---|
| **Influx** | '--> GLC[e]' | |
| | 'CO2[c] -->' | |
| | '--> O2[c]' | |
| | '--> NH3[c]' | |
| | '--> SO4[e]' | |
| **Efflux** | 'biomass[c] -->' | |
| | 'PHB[c] -->' | |
| | 'PRO[c] -->' | |
| | 'GLU[c] -->' | |
| | 'PYR[c] -->' | |
| | 'ACE[c] -->' | |
| | 'LAC[c] -->' | |
| | 'AKG[c] -->' | |
| | 'SUCC[c] -->' | |
| | 'ATPmaintenance[c] -->' | |
| | 'H2O2[c] -->' | |
| **Carbon assimilation** | 'PEP[c] + GLC[e] --> PYR[c] + G6P[c]' | |
| **Glycolysis / Gluconeogenesis** | 'G6P[c] <==> F6P[c]' | *pgi* |
| | 'ATP[c] + F6P[c] --> ADP[c] + F-16-BP[c]' | *pfkA* |
| | 'F-16-BP[c] --> F6P[c]' | *fbp* |
| | 'F-16-BP[c] <==> GA3P[c] + DHAP[c]' | *fba* |
| | 'DHAP[c] <==> GA3P[c]' | *tpiA* |
| | 'GA3P[c] + NAD[c] <==> 13-PG[c] + NADH[c]' | *gap* |
| | 'ADP[c] + 13-PG[c] --> ATP[c] + 3-PG[c]' | *pgk* |
| | '3-PG[c] <==> 2-PG[c]' | *gpmi* |
| | '2-PG[c] <==> PEP[c]' | *eno* |
| | 'PEP[c] + ADP[c] --> PYR[c] + ATP[c]' | *pyk* |
| **Pentose phosphate pathway** | 'G6P[c] + NADP[c] --> GLC-LAC[c] + NADPH[c]' | *zwf* |
| | 'GLC-LAC[c] --> 6-P-Gluconate[c]' | *bmd_0305* |
| | '6-P-Gluconate[c] + NADP[c] --> RIB-5P[c] + CO2[c] + NADPH[c]' | *gnd* |
| | 'RIB-5P[c] <==> XYL-5P[c]' | *rpe* |
| | 'RIB-5P[c] <==> RIBO-5P[c]' | *rpiA, rpiB* |
| | 'S7P[c] + GA3P[c] <==> RIBO-5P[c] + XYL-5P[c]' | *tkt* |
| | 'S7P[c] + GA3P[c] <==> E-4P[c] + F6P[c]' | *tal* |
| | 'F6P[c] + GA3P[c] <==> E-4P[c] + XYL-5P[c]' | *tkt* |
| **Tricarboxylic acid cycle** | 'PYR[c] + H-CoA[c] + NAD[c] --> AC-CoA[c] + NADH[c] + CO2[c]' | *pdha, pdhB, pdhC* |
| | 'AC-CoA[c] + OA[c] --> CIT[c] + H-CoA[c]' | *citA, citZ* |
| | 'CIT[c] <==> Cis-ACO[c]' | *acnA* |
| | 'Cis-ACO[c] <==> ICI[c]' | *acnA* |
| | 'ICI[c] + NADP[c] --> AKG[c] + CO2[c] + NADPH[c]' | *icd* |
| | 'AKG[c] + NAD[c] + H-CoA[c] --> SUCC-CoA[c] + NADH[c] + CO2[c]' | *odhA, odhB, pdhD* |
| | 'SUCC-CoA[c] + ADP[c] --> SUCC[c] + H-CoA[c] + ATP[c]' | *sucC, sucD, bmd_2706* |
| | 'SUCC[c] + MK[c] <==> FUM[c] + MKH2[c]' | *sdhA, sdhB, sdhC* |
| | 'FUM[c] <==> MAL[c]' | *fumC, bmd_0387* |
| | 'MAL[c] + NAD[c] --> OA[c] + NADH[c]' | *mdh, mqo* |

**Table A.15 (continued)**

| | | |
|---|---|---|
| **Organic acid production and assimilation** | 'PYR[c] + NADH[c] --> LAC[c] + NAD[c]' | *ldh* |
| | 'PYR[c] + O2[c] + ATP[c] --> ACE[c] + CO2[c] + H2O2[c]' | *bmd_1131, ackA* |
| | 'AC-CoA[c] + ADP[c] --> ACE[c] + H-CoA[c] + ATP[c]' | |
| | 'ATP[c] + ACE[c] + H-CoA[c] --> AC-CoA[c] + AMP[c]' | *acsA* |
| **PEP-PYR-OAA node** | 'OA[c] + ATP[c] --> PEP[c] + ADP[c] + CO2[c]' | *pckA* |
| | 'MAL[c] + NADP[c] --> PYR[c] + CO2[c] + NADPH[c]' | *malE* |
| | 'PYR[c] + ATP[c] + CO2[c] --> OA[c] + ADP[c]' | *pycA* |
| | 'PEP[c] + CO2[c] --> OA[c]' | *bmd_0812* |
| **PHB metabolism** | '(2) AC-CoA[c] --> ACE-CoA[c] + (1) H-CoA[c]' | *mmgA* |
| | 'ACE-CoA[c] + NADPH[c] --> PHB[c] + NADP[c] + (1) H-CoA[c]' | *phaB, phaC, phaR* |
| | 'PHB[c] + NAD[c] + SUCC-CoA[c] --> SUCC[c] + ACE-CoA[c]' | *phaZ, bmd_2166* |
| **Glutamate and proline metabolism** | 'AKG[c] + NADH[c] + NH3[c] <==> GLU[c] + NAD[c]' | *rocG, gudB, bmd_1700* |
| | 'GLU[c] + ATP[c] + NH3[c] --> GLN[c] + ADP[c]' | *glnA* |
| | 'AKG[c] + NADPH[c] + GLN[c] --> (2) GLU[c] + NADP[c]' | *gltA, gltB,bmd_4410* |
| | 'AKG[c] + NADH[c] + GLN[c] --> (2) GLU[c] + NAD[c]' | *gltA, gltB,bmd_4410* |
| | 'GLU[c] + ATP[c] --> ADP[c] + GLU5P[c]' | *proB, proJ* |
| | 'GLU5P[c] + NADPH[c] --> GLU5S[c] + NADP[c]' | *proA, proA** |
| | 'GLU5S[c] --> PYR5C[c]' | *spontaneous* |
| | 'PYR5C[c] + NADPH[c] --> PRO[c] + NADP[c]' | *proI, proH* |
| **Biomass formation** | '(7.575) NH3[c] + (0.076) H2S[c] + (0.109) G6P[c] + (0.108) F6P[c] + (0.709) RIBO-5P[c] + (0.174) E-4P[c] + (0.228) GA3P[c] + (0.727) 3-PG[c] + (0.373) PEP[c] + (1.829) PYR[c] + (3.706) AC-CoA[c] + (1.156) OA[c] + (1.877) AKG[c] + (12.646) NADPH[c] + (11.509) ATP[c] + (1.926) NAD[c] --> biomass[c] + (12.646) NADP[c] + (3.706) H-CoA[c] + (1.184) CO2[c] + (11.509) ADP[c] + (1.926) NADH[c]' | |
| **Cofactor and energy metabolism** | 'NADH[c] + (0.5) O2[c] + (2) ADP[c] --> NAD[c] + (2) ATP[c]' | |
| | 'MKH2[c] + (0.5) O2[c] + (2) ADP[c] --> MK[c] + (2) ATP[c]' | |
| | 'AMP[c] + ATP[c] --> (2) ADP[c]' | |
| | 'ATP[c] --> ADP[c] + ATPmaintenance[c]' | |
| **Sulfur metabolism** | 'SO4[e] + ATP[c] --> SO4[c] + ADP[c]' | |
| | 'SO4[c] + (2) ATP[c] + NADPH[c] --> H2SO3[c] + ADP[c] + AMP[c] + NADP[c]' | |
| | 'H2SO3[c] + (3) NADPH[c] --> H2S[c] + (3) NADP[c]' | |

## 9.2 Figures

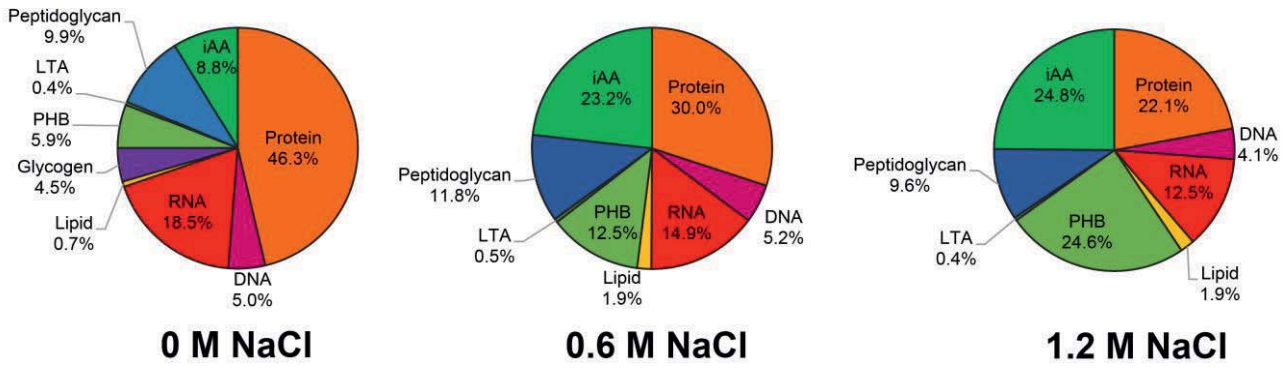


**Figure A.1: Macromolecular composition of *B. megaterium* DSM319 growing in M9 minimal medium supplemented with 0, 0.6 and 1.2 NaCl, respectively.** Protocols used for the determination of each cellular component are described in section 3.10. **DNA:** deoxyribonucleic acid, **iAA:** intracellular amino acids, **LTA:** lipoteichoic acids, **PHB:** polyhydroxybutyrate, **RNA:** ribonucleic acid.

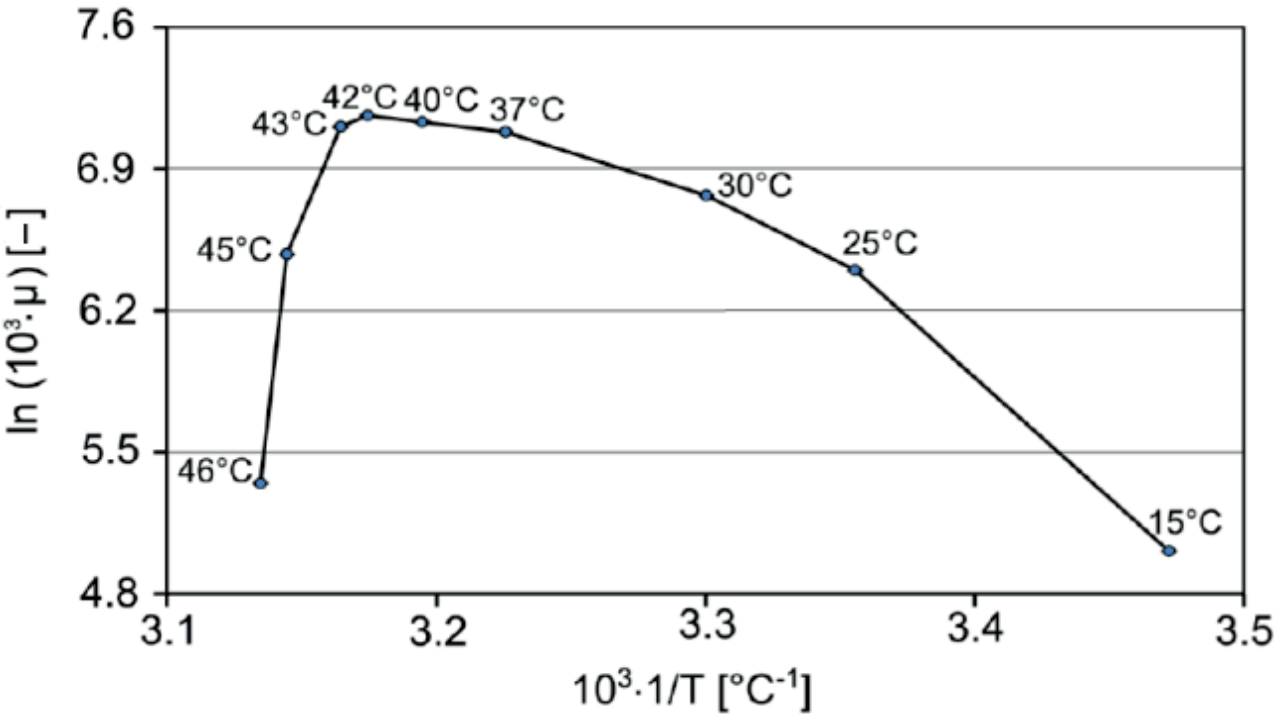


**Figure A.2: Arrhenius plot for *B. megaterium* DSM319 growing in M9 minimal medium.** Linear domain between 25°C and 42°C indicates physiological growth temperatures.

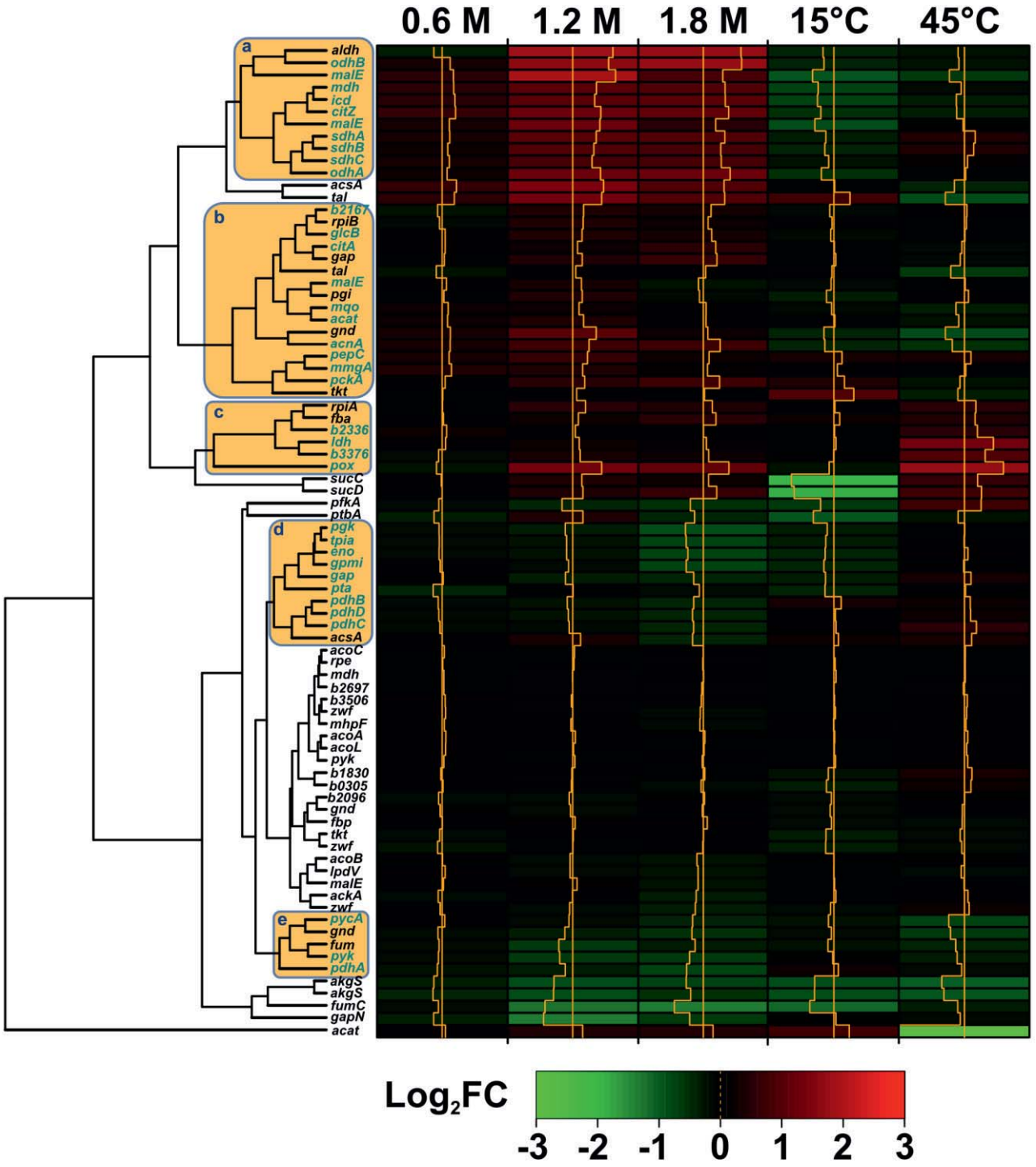


**Figure A.3: Hierarchical clustering of gene expression ratios of 82 selected genes of the central carbon metabolism of *B. megaterium* DSM319.** Expression is indicated as $\log_2$ fold change ($\log_2$ FC) compared to expression at 37°C. Five main regulation clusters can be identified: (a) genes from the tricarboxylic acid cycle, (b) gene from the tricarboxylic and pyruvate metabolisms, (c) genes involved in overflow metabolism, (d) genes from the glycolysis and (e) genes at the pyruvate node.

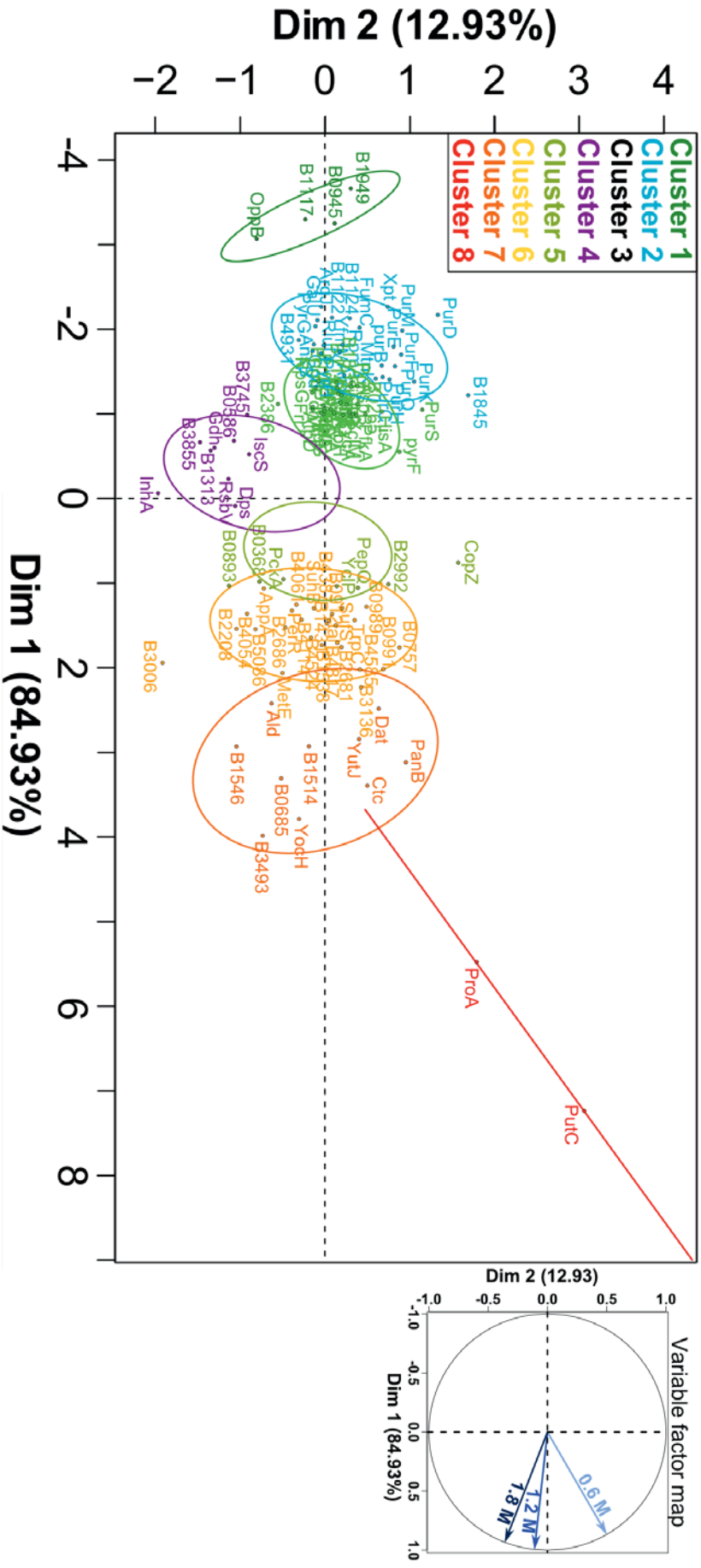


**Figure A.4: Principal component analysis (PCA) followed by hierarchical clustering (HCPC) on fold change between protein concentrations at 0.6, 1.2 and 1.8 M NaCl and their concentration in cells growing at 37°C without additional NaCl supplementation** – For more clarity, BMD was replaced by B in protein names and only the 125 proteins most relevant for the PCA construction are presented. Eight key clusters can be detected. Given the important weight of the first principal component (84.93 %) and the strong dependence of the three conditions to this dimension (> 0.8), clusters described from left to right the transition from proteins whose concentration is strongly reduced (**Cluster 1**) to those whose concentration is strongly increased under salt stress (**Cluster 8**).

*Schriftenreihe des Instituts für Bioverfahrenstechnik*
*der Technischen Universität Braunschweig*

**Band 1** **Sunder, Matthias**: Oxidation grundwasserrelevanter Spurenverunreinigungen mit Ozon und Wasserstoffperoxid im Rohrreaktor. 1996. FIT-Verlag · Paderborn, ISBN 3-932252-00-4

**Band 2** **Pack, Hubertus**: Schwermetalle in Abwasserströmen: Biosorption und Auswirkung auf eine schadstoffabbauende Bakterienkultur. 1996. FIT-Verlag · Paderborn, ISBN 3-932252-01-2

**Band 3** **Brüggenthies, Antje**: Biologische Reinigung EDTA-haltiger Abwässer. 1996. FIT-Verlag · Paderborn, ISBN 3-932252-02-0

**Band 4** **Liebelt, Uwe**: Anaerobe Teilstrombehandlung von Restflotten der Reaktivfärberei. 1997. FIT-Verlag · Paderborn, ISBN 3-932252-03-9

**Band 5** **Mann, Volker G.**: Optimierung und Scale up eines Suspensionsreaktorverfahrens zur biologischen Reinigung feinkörniger, kontaminierter Böden. 1997. FIT-Verlag · Paderborn, ISBN 3-932252-04-7

**Band 6** **Boll Marco**: Einsatz von Fuzzy-Control zur Regelung verfahrenstechnischer Prozesse. 1997. FIT-Verlag · Paderborn, ISBN 3-932252-06-3

**Band 7** **Büscher, Klaus**: Bestimmung von mechanischen Beanspruchungen in Zweiphasenreaktoren. 1997. FIT-Verlag · Paderborn, ISBN 3-932252-07-1

**Band 8** **Burghardt, Rudolf**: Alkalische Hydrolyse – Charakterisierung und Anwendung einer Aufschlußmethode für industrielle Belebtschlämme. 1998. FIT-Verlag · Paderborn, ISBN 3-932252-13-6

**Band 9** **Hemmi, Martin**: Biologisch-chemische Behandlung von Färbereiabwässern in einem Sequencing Batch Process. 1999. FIT-Verlag · Paderborn, ISBN 3-932252-14-4

**Band 10** **Dziallas, Holger**: Lokale Phasengehalte in zwei- und dreiphasig betriebenen Blasensäulenreaktoren. 2000. FIT-Verlag · Paderborn, ISBN 3-932252-15-2

**Band 11** **Scheminski, Anke**: Teiloxidation von Faulschlämmen mit Ozon. 2001. FIT-Verlag · Paderborn, ISBN 3-932252-16-0

**Band 12** **Mahnke, Eike Ulf**: Fluiddynamisch induzierte Partikelbeanspruchung in pneumatisch gerührten Mehrphasenreaktoren. 2002. FIT-Verlag · Paderborn, ISBN 3-932252-17-9

**Band 13** **Michele, Volker**: CDF modeling and measurement of liquid flow structure and phase holdup in two- and three-phase bubble columns. 2002. FIT-Verlag · Paderborn, ISBN 3-932252-18-7

**Band 14** **Wäsche, Stefan**: Einfluss der Wachstumsbedingungen auf Stoffübergang und Struktur von Biofilmsystemen. 2003. FIT-Verlag · Paderborn, ISBN 3-932252-19-5

**Band 15** **Krull Rainer**: Produktionsintegrierte Behandlung industrieller Abwässer zur Schließung von Stoffkreisläuren. 2003. FIT-Verlag · Paderborn, ISBN 3-932252-20-9

*Schriftenreihe des Instituts für Bioverfahrenstechnik*
*der Technischen Universität Braunschweig*

**Band 16** **Otto, Peter**: Entwicklung eines chemisch-biologischen Verfahrens zur Reinigung EDTA enthaltender Abwässer. 2003. FIT-Verlag · Paderborn, ISBN 3-932252-21-7

**Band 17** **Horn, Harald**: Modellierung von Stoffumsatz und Stofftransport in Biofilmsystemen. 2003. FIT-Verlag · Paderborn, ISBN 3-932252-22-5

**Band 18** **Mora Naranjo, Nelson**: Analyse und Modellierung anaerober Abbauprozesse in Deponien. 2004. FIT-Verlag · Paderborn, ISBN 3-932252-23-3

**Band 19** **Döpkens, Eckart**: Abwasserbehandlung und Prozesswasserrecycling in der Textilindustrie. 2004. FIT-Verlag · Paderborn, ISBN 3-932252-24-1

**Band 20** **Haarstrick, Andreas**: Modellierung millieugesteuerter biologischer Abbauprozesse in heterogenen problembelasteten Systemen. 2005. FIT-Verlag · Paderborn, ISBN 3-932252-27-6

**Band 21** **Baaß, Anne-Christina**: Mikrobieller Abbau der Polyaminopolycarbonsäuren Propylendiamintetraacetat (PDTA) und Diethylentriaminpentaacetat (DTPA). 2004. FIT-Verlag · Paderborn, ISBN 3-932252-26-8

**Band 22** **Staudt, Christian**: Entwicklung der Struktur von Biofilmen. 2006. FIT-Verlag · Paderborn, ISBN 3-932252-28-4

**Band 23** **Pilz, Roman Daniel**: Partikelbeanspruchung in mehrphasig betriebenen Airlift-Reaktoren. 2006. FIT-Verlag · Paderborn, ISBN 3-932252-29-2

**Band 24** **Schallenberg, Jörg**: Modellierung von zwei- und dreiphasigen Strömungen in Blasensäulenreaktoren. 2006. FIT-Verlag · Paderborn, ISBN 3-932252-30-6

**Band 25** **Enß, Jan Hendrik**: Einfluss der Viskosität auf Blasensäulenströmungen. 2006. FIT-Verlag · Paderborn, ISBN 3-932252-31-4

**Band 26** **Kelly, Sven**: Fluiddynamischer Einfluss auf die Morphogenese von Biopellets filamentöser Pilze. 2006. FIT-Verlag · Paderborn, ISBN 3-932252-32-2

**Band 27** **Grimm, Luis Hermann**: Sporenaggregationsmodell für die submerse Kultivierung koagulativer Myzelbildner. 2006. FIT-Verlag · Paderborn, ISBN 3-932252-33-0

**Band 28** **León Ohl, Andrés**: Wechselwirkungen von Stofftransport und Wachstum in Biofilsystemen. 2007. FIT-Verlag · Paderborn, ISBN 3-932252-34-9

**Band 29** **Emmler, Markus**: Freisetzung von Glucoamylase in Kultivierungen mit *Aspergillus niger*. 2007. FIT-Verlag · Paderborn, ISBN 3-932252-35-7

**Band 30** **Leonhäuser, Johannes**: Biotechnologische Verfahren zur Reinigung von quecksilberhaltigem Abwasser. 2007. FIT-Verlag · Paderborn, ISBN 3-932252-36-5

**Band 31** **Jungebloud, Anke**: Untersuchung der Genexpression in *Aspergillus niger* mittels Echtzeit-PCR. 1996. FIT-Verlag · Paderborn, ISBN 978-3-932252-37-2

**Band 32** **Hille, Andrea**: Stofftransport und Stoffumsatz in filamentösen Pilzpellets. 2008. FIT-Verlag · Paderborn, ISBN 978-3-932252-38-9

**Band 33** **Fürch, Tobias**: Metabolic characterization of recombinant protein production in *Bacillus megaterium*. 2008. FIT-Verlag · Paderborn, ISBN 978-3-932252-39-6

**Band 34** **Grote, Andreas Georg**: Datenbanksysteme und bioinformatische Werkzeuge zur Optimierung biotechnologischer Prozesse mit Pilzen. 2008. FIT-Verlag · Paderborn, ISBN 978-3-932252-40-120

**Band 35** **Möhle, Roland Bernhard**: An Analytic-Synthetic Approach Combining Mathematical Modeling and Experiments – Towards an Understanding of Biofilm Systems. 2008. FIT-Verlag · Paderborn, ISBN 978-3-932252-41-9

**Band 36** **Reichel, Thomas**: Modelle für die Beschreibung das Emissionsverhaltens von Siedlungsabfällen. 2008. FIT-Verlag · Paderborn, ISBN 978-3-932252-42-6

**Band 37** **Schultheiss, Ellen**: Charakterisierung des Exopolysaccharids PS-EDIV von *Sphingomonas pituitosa*. 2008. FIT-Verlag · Paderborn, ISBN 978-3-932252-43-3

**Band 38** **Dreger, Michael Andreas**: Produktion und Aufarbeitung des Exopolysaccharids PS-EDIV aus *Sphingomonas pituitosa*. 1996. FIT-Verlag · Paderborn, ISBN 978-3-932252-44-0

**Band 39** **Wiebels, Cornelia**: A Novel Bubble Size Measuring Technique for High Bubble Density Flows. 2009. FIT-Verlag · Paderborn, ISBN 978-3-932252-45-7

**Band 40** **Bohle, Kathrin**: Morphologie- und produktionsrelevante Gen- und Proteinexpression in submersen Kultivierungen von *Aspergillus niger*. 2009. FIT-Verlag · Paderborn, ISBN 978-3-932252-46-2

**Band 41** **Fallet, Claas**: Reaktionstechnische Untersuchungen der mikrobiellen Stressantwort und ihrer biotechnologischen Anwendungen. 2009. FIT-Verlag · Paderborn, ISBN 978-3-932252-47-1

**Band 42** **Vetter, Andreas**: Sequential Co-simulation as Method to Couple CFD and Biological Growth in a Yeast. 2009. FIT-Verlag · Paderborn, ISBN 978-3-932252-48-8

**Band 43** **Jung, Thomas**: Einsatz chemischer Oxidationsverfahren zur Behandlung industrieller Abwässer. 2010. FIT-Verlag · Paderborn, ISBN 978-3-932252-49-5

**Band 45** **Herrmann, Tim**: Transport von Proteinen in Partikeln der Hydrophoben Interaktions Chromatographie. 2010. FIT-Verlag · Paderborn, ISBN 978-3-932252-51-8

**Band 46** **Becker, Judith**: Systems Metabolic Engineering of Corynebacterium glutamicum towards improved Lysine Production. 2010. Cuvillier-Verlage · Göttingen, ISBN 978-3-86955-426-6

**Band 47** **Melzer, Guido**: Metabolic Network Analysis of the Cell Factory *Aspergillus niger*. 2010. Cuvillier-Verlag · Göttingen, ISBN 978-3-86955-456-3

**Band 48** **Bolten J., Christoph**: Bio-based Production of L-Methionine in *Corynebacterium glutamicum*. 2010. Cuvillier-Verlag · Göttingen, ISBN 978-3-86955-486-0

*Schriftenreihe des Instituts für Bioverfahrenstechnik*
*der Technischen Universität Braunschweig*

**Band 49** **Lüders, Svenja**: Prozess- und Proteomanalyse gestresster Mikroorganismen. 2010. Cuvillier-Verlag · Göttingen, ISBN 978-3-86955-435-8

**Band 50** **Wittmann, Christoph**: Entwicklung und Einsatz neuer Tools zur metabolischen Netzwerkanalyse des industriellen Aminosäure-Produzenten *Corynebacterium glutamicum*. 2010. Cuvillier-Verlag · Göttingen, ISBN 978-3-86955-445-7

**Band 51** **Edlich, Astrid**: Entwicklung eines Mikroreaktors als Screening-Instrument für biologische Prozesse. 2010. Cuvillier-Verlag · Göttingen, ISBN 978-3-86955-470-9

**Band 52** **Hage, Kerstin**: Bioprozessoptimierung und Metabolomanalyse zur Proteinproduktion in *Bacillus licheniformis*. 2010. Cuvillier-Verlag · Göttingen, ISBN 978-3-86955-578-2

**Band 53** **Kiep, Katina Andrea**: Einfluss von Kultivierungsparametern auf die Morphologie und Produktbildung von *Aspergillus niger*. 2010. Cuvillier-Verlag · Göttingen, ISBN 978-3-86955- 632-1

**Band 54** **Fischer, Nicole**: Experimental investigations on the influence of physico-chemical parameters on anaerobic degradation in MBT residual waste. 2011. Cuvillier-Verlag · Göttingen, ISBN 978-3-86955-679-6

**Band 55** **Schädel, Friederike**: Stressantwort von Mikroorganismen. 2011. Cuvillier-Verlag · Göttingen, ISBN 978-3-86955-746-5

**Band 56** **Wichter, Johannes**: Untersuchung der L-Cystein-Biosynthese in *Escherichia coli* mit Techniken der Metabolom- und $^{13}$C-Stoffflussanalyse. 2011. Cuvillier-Verlag · Göttingen, ISBN 978-3-86955-750-2

**Band 57** **Knappik, Irena Isabell**: Charakterisierung der biologischen und chemischen Reaktionsprozesse in Siedlungsabfällen. 2011. Cuvillier-Verlag · Göttingen, ISBN 978-3- 86955-760-1

**Band 58** **Driouch, Habib**: Systems biotechnology of recombinant protein production in *Aspergillus niger*. 2011. Cuvillier-Verlag Göttingen, ISBN 978-3-86955-808-0

**Band 59** **Gehder, Matthias:** Development and Validation of Indicators for the Production and Quality of Seed Cultures. 2011. Cuvillier-Verlag Göttingen, ISBN 978-3-86955-847-9

**Band 60** **Sommer, Becky:** Methodenentwicklung zur Charakterisierung sporenbildender Pilz-Seedingkulturen. 2011. Cuvillier-Verlag Göttingen, ISBN 978-3-86955-851-6

**Band 61** **Dohnt, Katrin:** Charakterisierung von *Pseudomonas aeruginosa*-Biofilmen in einem *in vitro*-Harnwegskathetersystem. 2011. Cuvillier-Verlag Göttingen, ISBN 978-3-86955-852-3

**Band 62** **Greis, Tillman:** Modelling the risk of chlorinated hydrocarbons in urban groundwater. 2011. Cuvillier-Verlag Göttingen, ISBN 978-3-86955-970-4

**Band 63** **David, Florian:** Holistic bioprocess engineering of antibody fragment secreting *Bacillus megaterium*. 2012. Cuvillier-Verlag Göttingen, ISBN 978-3-95404-115-2

**Band 64** **Palme, Wiebke:** Taxonomische Einordnung des Polyaminopolycarbonsäure-abbauenden Stammes BNC1 und Untersuchungen zum Abbau von 1,3 Propylendiamintetraacetat. 2012. Cuvillier-Verlag Göttingen, ISBN 978-3-95404-158-9

**Band 65** **Lin, Pey-Jin:** Effect of fluid dynamics on pellet morphology and product formation of *Aspergillus niger*. 2012. Cuvillier-Verlag Göttingen, ISBN 978-3-95404-181-7

**Band 66** **Kind, Stefanie:** Synthetic Metabolic Engineering of *Corynebacterium glutamicum* for Biobased Production of 1,5-Diaminopentane. 2012. Cuvillier-Verlag Göttingen, ISBN 978-3- 95404-264-7

**Band 67** **Wilk, Franziska:** Charakterisierung von Stoffströmen vorbehandelter Siedlungsabfälle in Deponiebioreaktoren. 2012. Cuvillier-Verlag Göttingen, ISBN 978-3-95404-281-4

**Band 68** **Korneli, Claudia:** Target-oriented Bioprocess Optimization for Recombinant Protein Production in *Bacillus megaterium*. 2012. Cuvillier-Verlag Göttingen, ISBN 978-3-95404-289-0

**Band 69** **Eslahpazir Esfandabadi, Manely:** Target-oriented Bioprocess Optimization for Recombinant Protein Production in *Bacillus megaterium*. 2012. Cuvillier-Verlag Göttingen, ISBN 978-3-95404-289-0

**Band 70** **Wucherpfennig, Thomas:** Cellular morphology : a novel process parameter for the cultivation of eukaryotic cells. 2013. Cuvillier-Verlage Göttingen, ISBN: 978-3-95404-456-6

**Band 71** **Buschke, Nele:** From Waste to Value - Bio-Nylon Monomers from Renewables using Corynebacterium glutamicum. 2013. Cuvillier-Verlage Göttingen, ISBN: 978-3-95404-457-3

**Band 72** **Bergmann, Sven:** Ectoine production by halotolerant microorganisms – Process optimization and characterization of cellular state. 2013. Cuvillier-Verlage Göttingen, ISBN: 978-3-95404-556-3

**Band 73** **Hellriegel, Jan:** Engineering a Biofilm - Imitating Physico-Chemical Properties to Improve Mechanical Characterization. 2014. Cuvillier-Verlag Göttingen, ISBN 978-3-95404-753-6

**Band 74** **Berger, Antje:** Metabolische Netzwerkanalyse uropathogener *Pseudomonas aeruginosa*-Isolate. 2014. Cuvillier-Verlag Göttingen, ISBN 978-3-95404-762-8

**Band 75** **Peterat, Gena:** Prozesstechnik und reaktionskinetische Analysen in einem mehrphasigen Mikrobioreaktorsystem. 2014. Cuvillier-Verlag Göttingen, ISBN 978-3-95404-887-8